Development of Pd-Catalysed C–H Bond Functionalisation Methodologies for the Accession of Molecular Complexity

Alan James Reay

PhD

University of York

Chemistry

April 2016

Abstract

This thesis describes the development of novel Pd-catalysed C–H bond functionalisation methodologies, with a view towards their application in sustainable chemical synthesis. The basis of this project focuses on the need for more efficient utilisation of precious metal catalysts, such as Pd, achieved by mechanistic understanding of the role of heterogeneous Pd nanoparticles (PdNPs) in such chemistry. An overview of observations from Pd-catalysed cross-coupling and C–H bond functionalisation chemistry is given initially, focusing on the mechanistic dichotomy between observed homogeneous and heterogeneous catalytic manifolds in these fields. The generation of potentially harmful stoichiometric byproducts in direct arylation methodologies is also examined for two classes of commonly-used electrophilic arylating agents, aryliodonium and aryldiazonium salts (Chapter 1).

The synthetic utility of C–H bond functionalisation chemistry has been exemplified through the development of complementary conditions for the direct arylation of the amino acid tryptophan (**I**) to form highly fluorescent 2-aryltryptophans (**II**), all of which have been evaluated using several key mass-based green metrics (Chapter 2). These conditions have also been shown to be effective for the functionalisation of tryptophan-containing peptides.
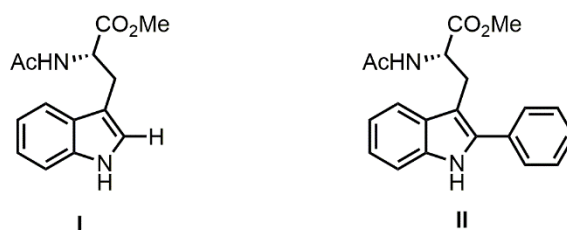
Initial rates kinetic analysis of the activity of several homogeneous and heterogeneous Pd catalysts in other direct arylation chemistry has highlighted remarkable similarities between apparently distinct catalysts, which suggests the formation of a comparable active catalyst phase. Heterogeneous Pd sources have also been successfully applied to the selective functionalisation of several biomolecules (Chapter 3).

The final part of this thesis describes fundamental studies on the nature of the ubiquitous Pd^0 catalyst $Pd_2(dba)_3$. The major and minor isomers of this catalyst were characterised both in solution and in the solid state, which revealed that dynamic exchange between these species and free ligand varies significantly as a function of temperature. Crucially, this catalyst has also been shown by NMR and MS studies to be a source of catalytically competent PdNPs under commonly-found experimental conditions (Chapter 4).

List of Contents

List of Figures

9

14

List of Schemes

List of Tables

Acknowledgements

I would like to extend my gratitude to my supervisor Ian Fairlamb, for giving me the wonderful opportunity to work within his group. I can honestly say that the last few years have been immensely enjoyable, and I really can't thank him enough for all the help, training and support he has offered through my studies. Under his guidance I have learned a great many new things, and I feel that it would be difficult to have gotten any more out of this project than I have. For this I am eternally grateful.

I have had the good fortune of working with several talented researchers, whose dedication and hard work are clearly demonstrated in their contributions to this thesis. Anders, Tom and Lydia have not only made significant contributions to this project, but are also all lovely people. Working with them has been a genuine pleasure. I also wish to thank Tom W for his research, which has provided inspiration for me through my project.

Now that I am at the end of my time in York, it seems appropriate to reflect on the people that I have worked with in the last few years within the Fairlamb group. All of these people have contributed in some way to my time here, and for that I wish to thank them. There are far too many to list them all here, but I do wish to specifically acknowledge the help and support of those people with whom I have spent a significant amount of time: Tom R (who really taught me a lot about everything), Josh (who I have known for many years now, and is as funny and kind now as he was in 2008), Lyndsay (for spending an awful lot of time hungover in various European hotels), George (for always being willing to see the latest superhero movie), Ben (one of the nicest people I have ever met) and Kate (who shares my love of the northeast coastline). Special thanks should also go to Ryan, Tim, Don and Chris W, friends who have all now moved onto pastures new. I also wish to thank Will and the rest of the Organics team; playing with you guys really was the highlight of each week.

The quality of technical support in York is unbelievably good, so I wish to acknowledge Heather Fish (NMR), Karl Heaton and Ed Bergstrom (MS), Adrian Whitwood (XRD), Graeme McAllister (CHN) and Meg Stark (TEM) for their invaluable assistance.

Finally, I want to thank my family for everything. During the course of this project I lost both my father and grandfather; I feel sure that they both knew how I felt about them, and how much they meant to me. Mum and Hannah are still providing their love and support.

Beck has been my best friend for 7 years now, I am sure she knows just how much she means to me. I think it's true to say that pretty much everything good I do is down to her.

Author's Declaration

The work presented in this thesis is my own except where referenced or clearly indicated in the body of the text. The work was carried out at the University of York between October 2012 and April 2016, and has not previously been presented for an award at this or any other university.

Parts of this work have been reproduced in published papers, copies of which can be found in Appendix 1:

Kapdi, A. R.; Whitwood, A. C.; Williamson, D. C.; Lynam, J. M.; Burns, M. J.; Williams, T. J.; Reay, A. J.; Holmes, J.; Fairlamb, I. J. S.; The elusive structure of $Pd_2(dba)_3$. Examination by isotopic labeling, NMR spectroscopy, and X-ray diffraction analysis: synthesis and characterization of $Pd_2(dba-Z)_3$ complexes, *J. Am. Chem. Soc.* **2013**, *135*, 8388–8399.

Williams, T. J.; Reay, A. J.; Whitwood, A. C.; Fairlamb, I. J. S.; A mild and selective Pd-mediated methodology for the synthesis of highly fluorescent 2-arylated tryptophans and tryptophan-containing peptides: a catalytic role for Pd^0 nanoparticles?, *Chem. Commun.* **2014**, *50*, 3052–3054.

Reay, A. J.; Williams, T. J.; Fairlamb, I. J. S.; Unified mild reaction conditions for C2-selective Pd-catalysed tryptophan arylation, including tryptophan-containing peptides, *Org. Biomol. Chem.* **2015**, *13*, 8298–8309.

Alan James Reay

April 2016

Chapter 1: Introduction

1.1 Pd-Catalysed C–X Bond Functionalisation

1.1.1 Background

Metal-catalysed cross-coupling reactions have increased in significance since their discovery to the point where these methods now underpin modern synthetic chemistry. A variety of transformations can be effected through the reaction of activated organohalides with organometallics including tin, silicon, zinc, boron and magnesium in the presence of transition metal catalysts such as palladium, ruthenium, nickel and copper.[1]

The use of palladium in particular has increased enormously in scope and synthetic applicability over the last fifty years so that it is now readily applied to many complex synthetic organic routes.[2] The importance of palladium in synthetic methodology has been further highlighted by the awarding of the 2010 Nobel Prize in Chemistry to Heck, Negishi and Suzuki for their pioneering work in this field.[3] Heck and co-workers are credited with developing aryl, benzyl or vinyl halide couplings to terminal alkenes using palladium(II) throughout the 1960s and 1970s, such as the coupling of iodobenzene **1** and styrene **2** in the presence of catalytic amounts of palladium to produce (*E*)-stilbene **3**.[4] This approach was also developed independently by Mizoroki and co-workers, who used palladium(II) chloride in an analogous system and found that the use of potassium acetate and higher temperatures (120 °C) allowed the yield to be increased to 90% (**Scheme 1**).[5] Importantly, the nature of the base used in these two systems appears to directly affect the efficiency of the reaction; with Mizoroki's use of an inorganic acetate base providing a higher yield (albeit at increased temperature) than Heck's use of an organic amine base.
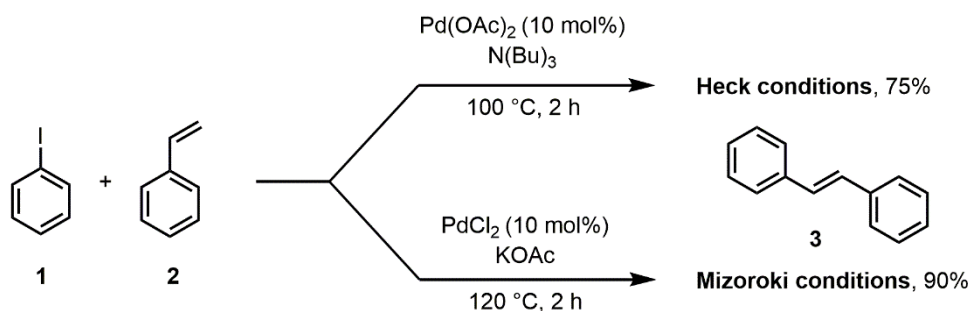
Scheme 1 Pd-catalysed formation of (*E*)–stilbene **3** from iodobenzene **1** and styrene **2**.

Since this pioneering work, many different approaches for the palladium-catalysed formation of new C–C bonds with a variety of coupling partners have been established. Notable

examples using halides or pseudohalides include, but are not limited to; the Stille (organotin reagents),[6-8] Suzuki–Miyaura (organoboronic acids),[9,10] Sonogashira (terminal alkynes),[11] Kumada–Corriu (Grignard reagents),[12,13] Hiyama (organosilanes),[14] and Negishi (organozinc reagents)[15] reactions (**Figure 1**). Note that some of these reactions require base whereas others require activating species such as fluoride.
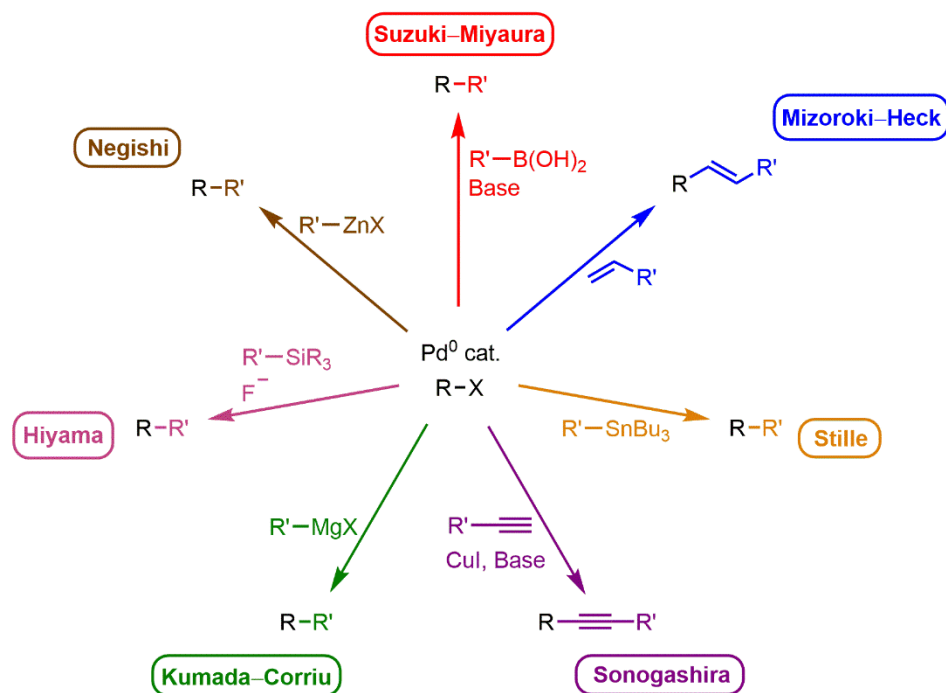
Figure 1 Selected examples of typical Pd-catalysed cross-coupling reactions.

These reactions offer a huge variety of chemoselective transformations that can be applied to the synthesis of complex natural products, such as the use of an intramolecular Mizoroki–Heck cyclisation in Danishefsky's total synthesis of the important anticancer compound Taxol **4** (**Scheme 2**).[16] Danishefsky's synthesis demonstrates that upon choice of a suitable base and palladium source (stoichiometric in this case), selective cross-coupling reactions can be performed in the presence of multiple functional groups. These types of reactions can also be used in a combinatorial fashion, exemplified by Stoltz's total synthesis of (+)–Dragmacidin F **5** (**Scheme 3**).[17]
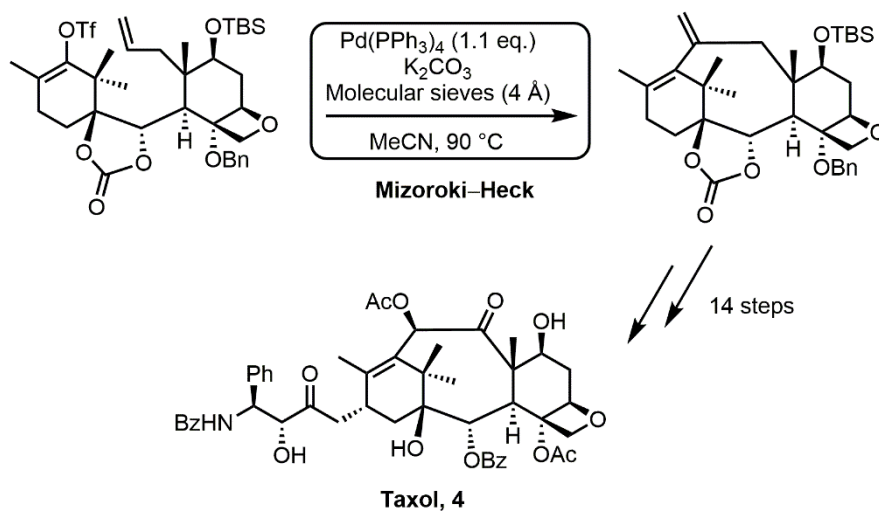
Scheme 2 Key Mizoroki–Heck cross-coupling used in Danishefsky's total synthesis of Taxol **4**.
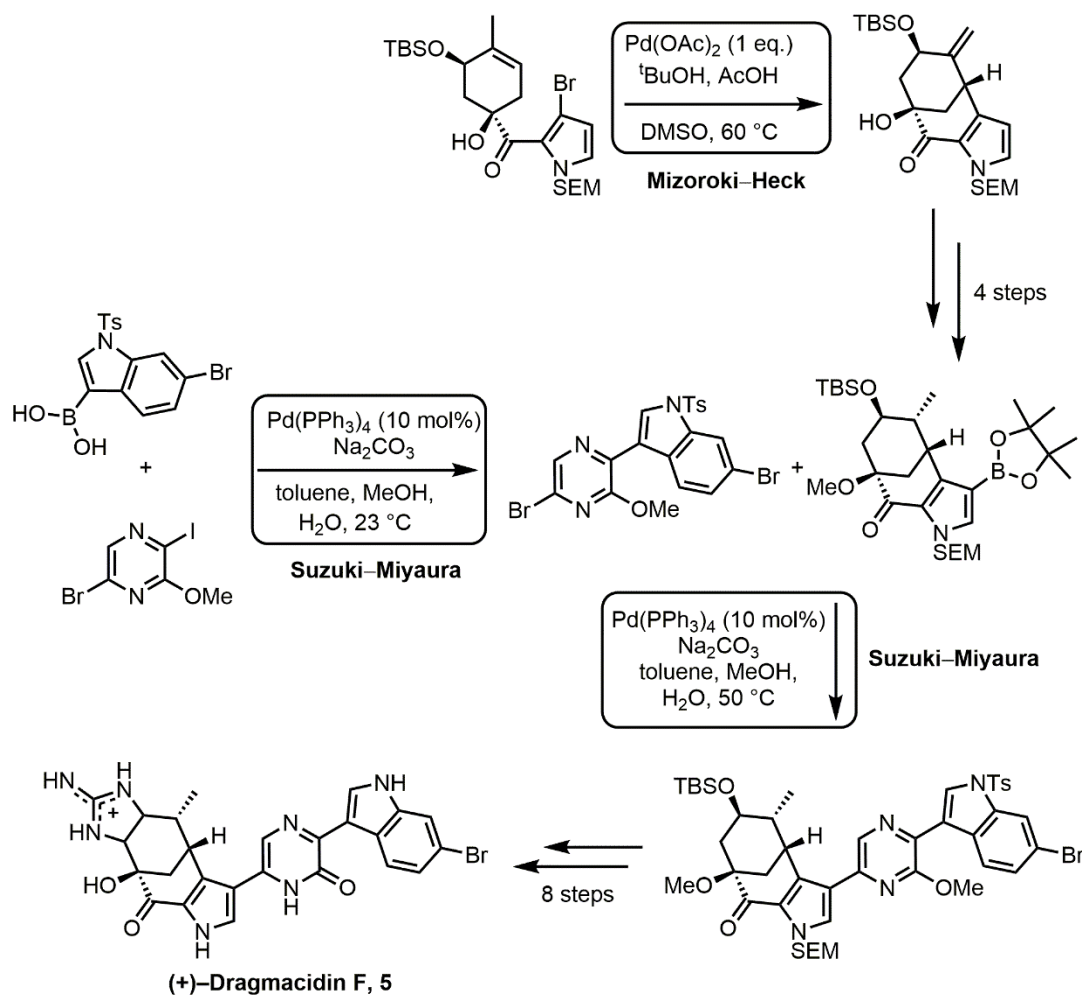
Scheme 3 Key Mizoroki–Heck and Suzuki–Miyaura cross-couplings used in Stolz's total synthesis of (+)–Dragmacidin F **5**.

34

Many mechanisms have been published in the area of palladium-catalysed C–X bond cross-coupling processes, particularly when concerning well-established and versatile reactions such as those highlighted above. Often these are homogeneous in nature, and revolve around the reaction of mononuclear Pd^0 precursors with alkyl halides to generate the oxidative addition products. The typical picture of palladium cross-coupling found in the literature is summarised in **Scheme 4**; a Pd^0 precursor undergoes oxidative addition across a C–X bond, followed by transmetallation with a second pre-functionalised substrate (e.g. boronic acid, organostanne etc.) and subsequent reductive elimination to provide the new C–C bond and regenerate the Pd^0 catalyst.
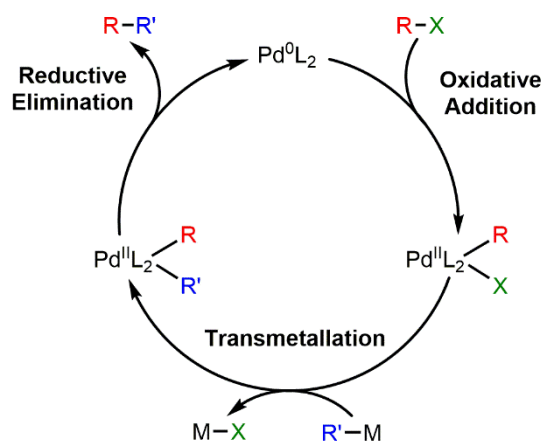
Scheme 4 Simplified mechanism for Pd-catalysed cross-coupling.

There is however a significant body of evidence to suggest that many cross-coupling processes could involve both homogeneous and heterogeneous Pd species. Common 'homogeneous' Pd precursors, such as $Pd(OAc)_2$, have been conclusively shown to aggregate to form higher-order Pd species. The likelihood is that such species can play an active role in catalysis instead of, or alongside, more typical homogeneous manifolds. Such aggregates could also act as a reservoir for catalytically active Pd, providing a measure of control over the quantity of catalyst active in any given cycle. Additionally, commercially obtained Pd catalysts like $Pd(OAc)_2$ can contain significant quantities of catalytically active impurities such as $Pd_3(OAc)_5(NO_2)$ and polymeric $[Pd(OAc)_2]_n$.[18,19] This holistic approach to the question of homogeneous versus heterogeneous catalysis can be represented as shown in **Figure 2**.
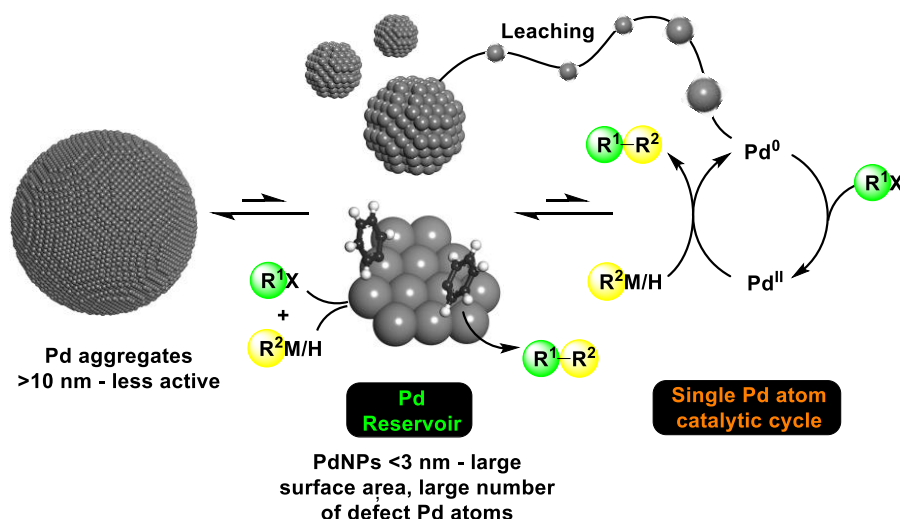
Figure 2 Schematic representation for the role of aggregated Pd in catalysis. Reproduced by permission of The Royal Society of Chemistry.[20]

1.1.2 Mizoroki–Heck and Sonogashira Cross-Couplings

Some of the first evidence for the existence of Pd reservoirs in cross-coupling chemistry was published by de Vries and co-workers, who discovered that the Mizoroki–Heck reaction of bromobenzene **6** with *n*-butylacrylate **7** in the presence of Pd(OAc)$_2$ to produce **8** exhibited an inverse relationship of catalyst activity, with respect to catalyst concentration (**Figure 3**).[21]
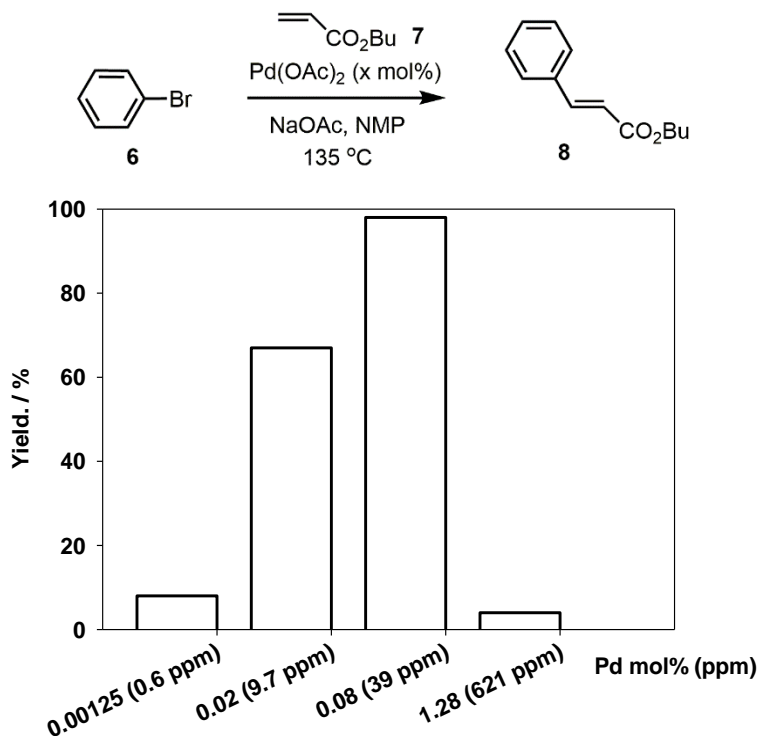
Figure 3 Inverse relationship between catalyst activity and concentration in a Mizoroki–Heck cross-coupling. Adapted with permission from *Org. Lett.* **2003**, *5*, 3285–3288.

For this reaction, the optimal catalyst loading was found to be 0.08 mol% (39 ppm), with higher or lower catalyst loadings resulting in decreased yields. This observation is attributable to the formation of Pd aggregates at higher catalyst loadings, often associated with the precipitation of Pd black. There is however a point at which the catalyst loading becomes so low that the reaction cannot effectively proceed. This inverse relationship provides evidence for catalytically relevant Pd colloids, but the structure of the catalyst in this reaction is unclear; ESI–MS data did however highlight the presence of $PdBr_3^-$ under working reaction conditions. These observations led both de Vries and Reetz to propose a unified mechanism for the Mizoroki–Heck reaction, which accounts for both homogeneous and heterogeneous manifolds (**Scheme 5**).[22] In this mechanism Pd^0 exists as both lower-order monomeric or dimeric catalytic species, as well as higher-order palladium species such as multinuclear colloids, all of which are capable of interconverting and performing the desired coupling transformation. Importantly however the shapes of these particles are poorly defined, size instead being relied upon to indicate the nature, and by extension activity, of these higher-order species.
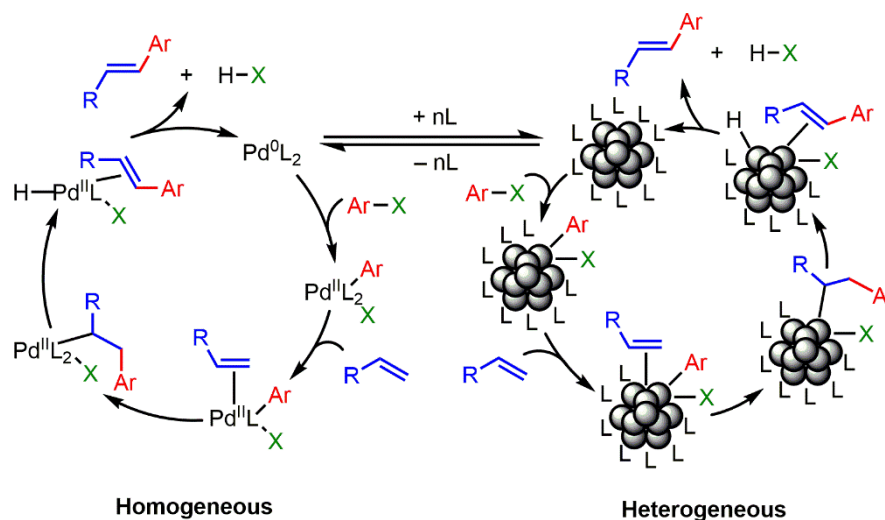
Scheme 5 A unified Mizoroki–Heck mechanism.

A similar inverse relationship was also observed in work conducted by the Fairlamb group, who studied the Sonogashira cross-coupling of 4-bromoacetophenone **9** with phenylacetylene **10** to produce **11**. In this reaction several palladacylic precatalysts proposed to act as Pd reservoirs were applied and their turnover frequencies (TOFs) studied as a function of catalyst loading, at either 0.1 mol% (orange), 0.01 mol% (purple) or 0.001 mol% (blue). In this reaction, 0.001 mol% (92 ppm) provided optimal TOFs (**Figure 4**).
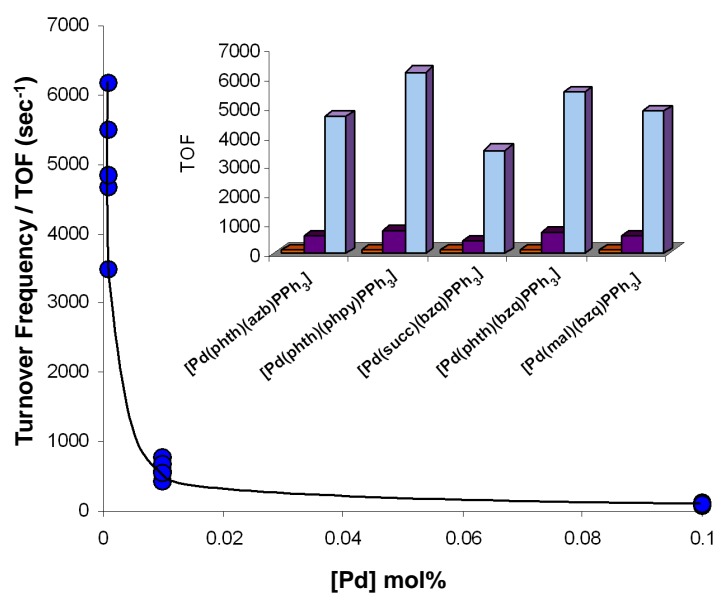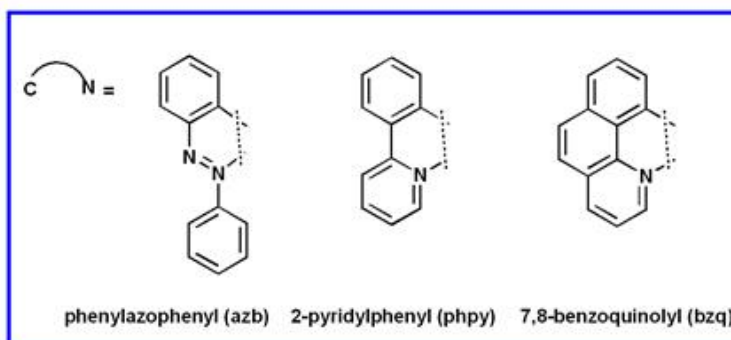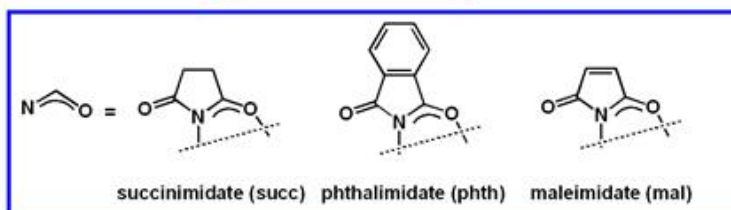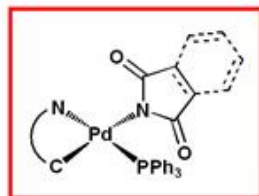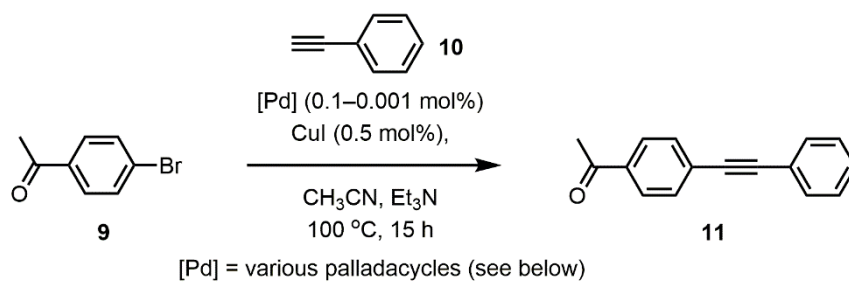
Figure 4 Inverse relationship between Pd loading and TOF in a Sonogashira cross-coupling. Figure prepared by Prof. I. J. S. Fairlamb.

As can be inferred from **Figure 2** and **Scheme 5**, in many cases these higher-order Pd aggregates are proposed to act as sources of mononuclear Pd, meaning that the active catalytic turnover of substrate can be considered homogeneous. Evidence for the leaching of catalytically active Pd from supported catalysts such as Pd/C, Pd/SiO_2 and $Pd/\gamma–Al_2O_3$ has been reported.[23,24] The mechanism of such leaching has been studied by Dupont and co-workers, who demonstrated that quaternary ammonium salts can stabilise higher order Pd species, facilitating the release of oxidised Pd^{II} species into solution (Jeffery conditions).[25] Rothenberg *et al*. utilised a reactor containing a membrane which could select for particles <5 nm in size in their efforts to demonstrate the leaching of Pd from larger Pd species (*ca.* 15 nm) under Mizoroki–Heck reaction conditions.[26] Later work from the same group also demonstrated the formation and subsequent growth of Pd clusters from several Pd^{II} precursors using UV–visible spectroscopy, which allowed for modelling of the reduction, including cluster growth and aggregation of such species.[27] Baiker and co-workers have also used *in situ* extended X-ray absorption fine structure (EXAFS) to analyse the Mizoroki–Heck reaction of bromobenzene **6** with styrene **2**, mediated by Pd/Al_2O_3 (**Scheme 6**).
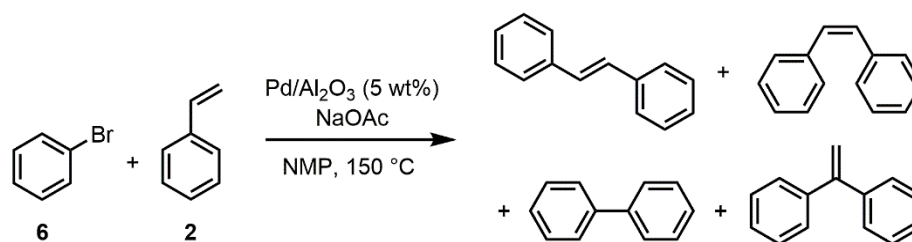
Scheme 6 Mizoroki–Heck cross-coupling mediated by Pd/Al_2O_3.

Baiker's study demonstrated the formation of higher-order Pd complexes *in situ*, assigned as Pd^0 colloids approximately 2 nm in diameter, which shortly preceded the formation of product. These complexes were observed throughout the reaction with very little change until complete conversion of the substrate at which point significant variations in the EXAFS data were seen. It was also proposed that the rate-determining step of this reaction was dissociation of mononuclear Pd^0 from these multinuclear Pd^0 colloids; hence these observed colloids are directly involved in the catalytic cycle and do not serve purely as a reservoir for mononuclear Pd species.[28]

1.1.3 Suzuki–Miyaura Cross-Couplings

Similar observations regarding the catalytic competence of higher-order Pd species have also been made in the Suzuki–Miyaura reaction. Fairlamb and co-workers tested well-defined PdNPs supported on a (poly)vinylpyrrolidone (PVP) polymer **12** (**Figure 5**), which is known to stabilise PdNPs and prevent their thermodynamically favourable agglomeration.[29-31]

12
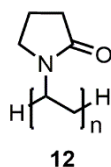
Figure 5 Monomer unit of (poly)vinylpyrrolidone (PVP) **12**.

A seeding method was used to synthesise PVP–Pd **13** with NPs of four different diameters, between 1.8 and 4.0 nm, which were then applied to the cross-coupling of phenylboronic acid **14** and iodoanisole **15** in methanol to produce **16**. The activity of each of these catalysts was then compared as a function of the TOF against the total number of surface Pd atoms, which demonstrated an inverse relationship *i.e.* higher activity for the smaller particles. If the TOF was normalised against only those Pd atoms contained within defect sites on the truncated cuboctahedral particles however, no difference was observed (**Figure 6**).[32,33] This strongly suggests that it is the abundance of surface defect sites which determines the activity of these particles; simply put, the more defect sites per particle, the more active the catalyst.
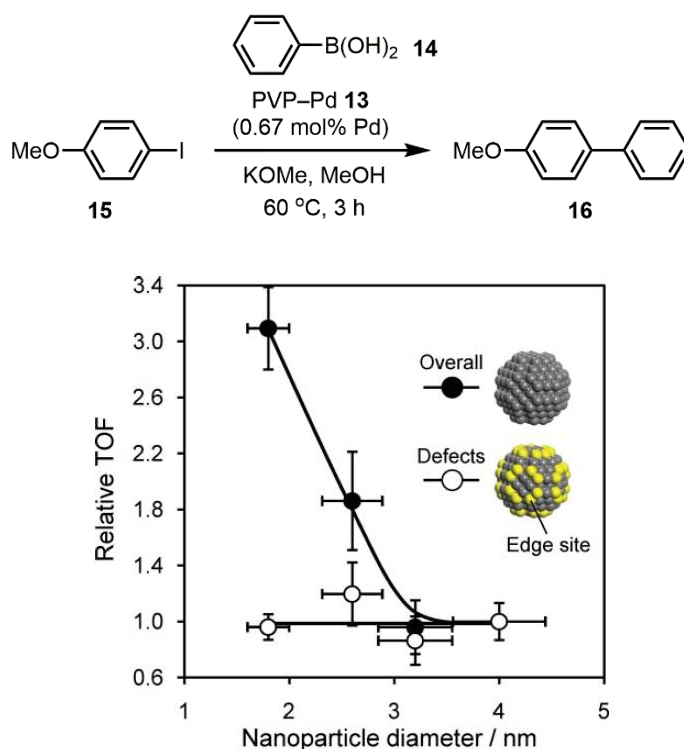
Figure 6 Relationship between TOF and particle size normalised to either total surface Pd atoms (●) or defect surface Pd atoms (○) in a Suzuki–Miyaura cross-coupling. Reproduced by permission of The Royal Society of Chemistry.[33]

This trend could however be observed if low-coordinate Pd species demonstrated preferential solubility, so *in operando* X-ray absorption spectroscopy was used to monitor the coordination environment of the PdNPs, to determine the heterogeneity of the reaction under normal working conditions (**Figure 7**).

40

These measurements indicated no sintering or leaching of the particles during the reaction, a result confirmed by EXAFS, X-ray photoelectron spectroscopy (XPS) and transmission electron microscopy (TEM) studies. Importantly no induction period was seen, which is consistent with the observation that nanoparticulate Pd is not simply acting as a pre-catalyst or Pd reservoir.
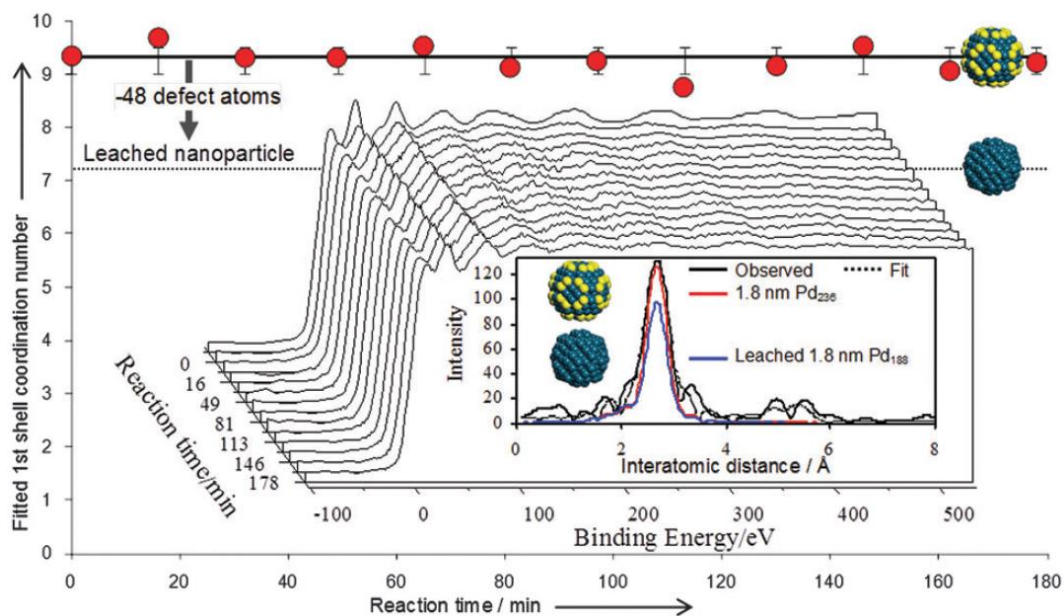
Figure 7 XAS spectra of PdNP coordination environment in a Suzuki–Miyaura cross-coupling. Reproduced with permission from *Angew. Chem. Int. Ed.* **2010**, *49*, 1820–1824. Copyright 2010 WILEY-VCH Verlag GmbH & Co.

Elemental mercury was administered to the reaction after a brief induction period (8 min) under normal working conditions, as mercury has been shown to inhibit surface reactions through poisoning of the catalyst; believed to occur as a result of surface amalgamation of the mercury with any heterogeneous particles present in the reaction mixture.[34,35] This poisoning test caused immediate cessation of catalytic activity and the resultant Pd core/Hg shell particles were successfully characterised by XPS, showing a 1:1 correlation between the surface Pd and Hg atoms. This emphatically demonstrated the lack of any Pd leaching in this system, confirming its heterogeneous nature. These results also provide strong evidence that the Suzuki–Miyaura reaction can also operate in a dual-phase catalytic system for common Pd^0 catalysts, e.g. $Pd(PPh_3)_4$ or $Pd_2(dba)_3$.

The relevance of surface defect sites to the catalytic activity of PdNPs was also discussed by Blackmond and co-workers during their study on a Mizoroki–Heck reaction. They correlated the ratio of defect sites to terrace sites in nanoparticles of varying sizes, obtained by the reduction of $Pd_2(dba)_3 \cdot dba$ with hydrogen in the presence of PVP **12** (**Figure 8**).[30]
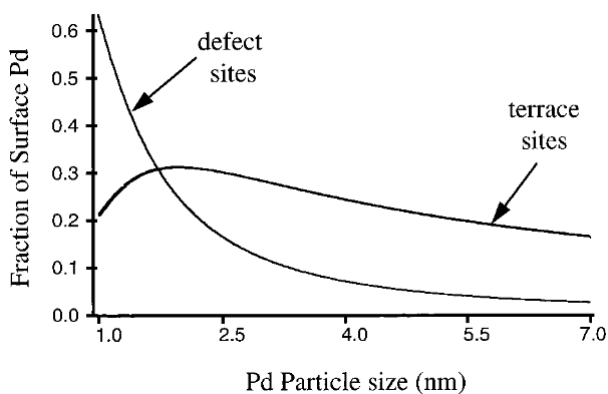
Figure 8 Ratio of defect sites to terrace sites in truncated cuboctahedral PdNPs. Adapted with permission from *Langmuir* **1999**, *15*, 7621–7625. Copyright 1999 American Chemical Society.

This builds upon work performed by Knight *et al*. which explored the number of atoms contained within the stable shell structures of sodium nanoparticles (**Figure 9**).[36]
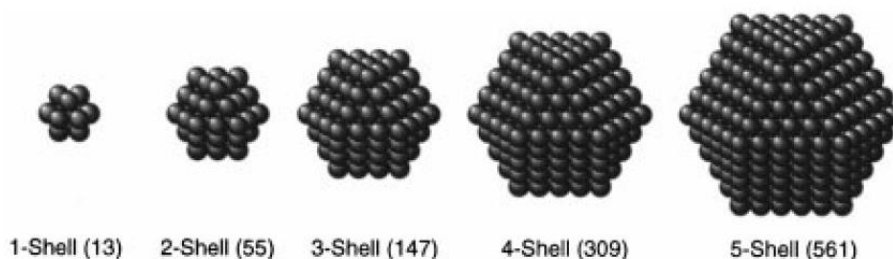
Figure 9 Stable closed-shell structures of metal nanoparticles.

The examples highlighted above serve to demonstrate the ability of nominally homogeneous Pd (pre)catalysts to serve as a source of heterogeneous Pd, either as a result of propagation to form catalytically competent PdNPs, or as a reservoir of Pd colloids which are slowly released into solution. There are also instances of supported Pd nanocatalysts which are prepared, purified and characterised independently, before being used in a range of Pd-mediated cross-coupling reactions.[37-40]

1.2 Pd-Catalysed C–H Bond Functionalisation

1.2.1 Background

While useful from a synthetic viewpoint, a significant drawback to C–X bond cross-coupling reactions is the need to pre-functionalise the substrate with activated functional groups such as boronic acids or organostannes, among others. This not only adds unwanted complexity and the potential for unwanted byproducts to the reaction but also increases the economic and environmental cost of syntheses employing such transformations. Removing substrate pre-functionalisation potentially allows for the minimisation of downstream chemical waste;

moreover, it eliminates the need for prior mandatory reaction steps that enable the installation of chemical functionality which is ultimately lost in the final and desired chemical transformation. Recent advances in direct C–H bond functionalisation have attempted to address this issue, as mild and selective methods can now be used to cleave and generate C–H bonds directly without the need for pre-functionalised starting materials, expanding the toolkit of the synthetic chemist.[41] These processes can include direct, oxidative or decarboxylative couplings, in addition to the classical cross-coupling of organometallic reagents highlighted above (**Figure 10**).
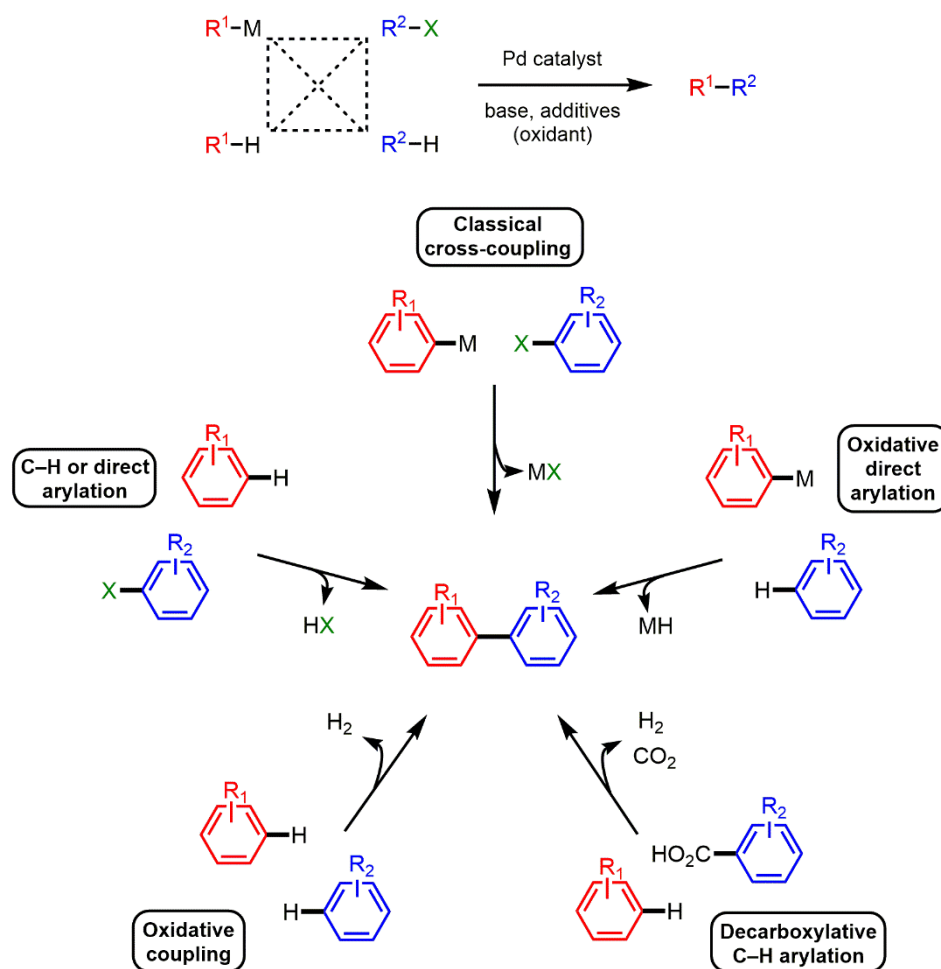
Figure 10 Overview of Pd-catalysed processes for the formation of new carbon–carbon bonds.

It is important at this point to note the difference in nomenclature as regards C–H bond activation and C–H bond functionalisation; C–H bond activation specifically refers to the activation of a C–H σ–bond by a metal centre while C–H bond functionalisation refers to the overall process by which a C–H fragment is coupled to another C–H or C–X fragment to generate a new C–C bond.

Despite its relative infancy, C–H bond functionalisation has gained a large amount of research interest, with an ever-increasing number of publications in this area. The ability to directly couple two fragments together without the need for pre-functionalisation is a particularly attractive prospect for the synthesis of natural products or pharmaceuticals.[42] One such example used on an industrial scale by Bristol-Myers Squibb is the synthesis of the potent antitumor agent Rebeccamycin Aglycone **17** (**Scheme 7**).[43]
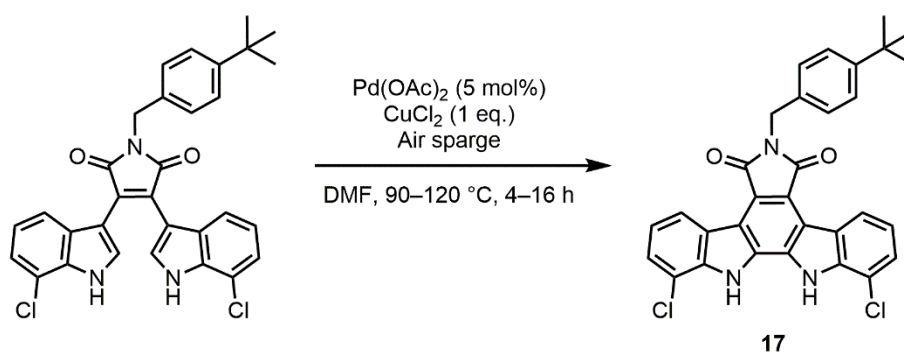
Scheme 7 Synthesis of Rebeccamycin Aglycone **17**.

The synthetic applicability of this type of methodology is demonstrated by examples of $C(sp^3)$–H bond functionalisations, which can be used to construct otherwise challenging motifs, such as the isolable aryl-cyclobutane intermediate **18** in the total synthesis of Coralydine **19** (**Scheme 8**).[44,45]
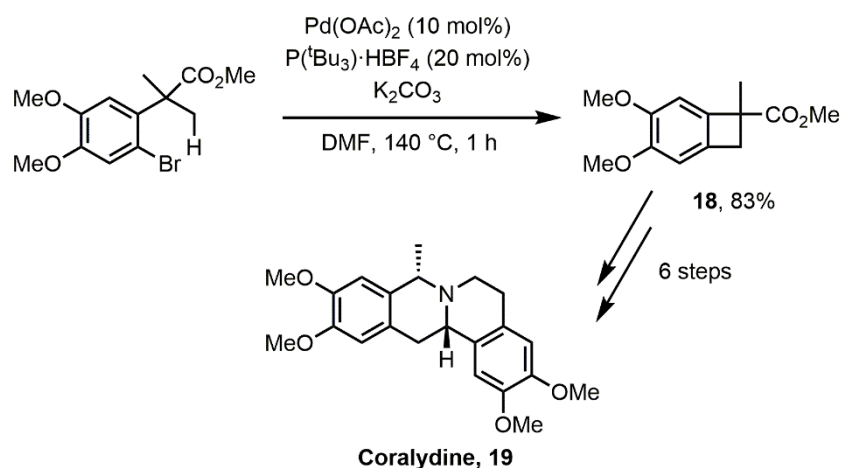
Scheme 8 Baudoin's synthesis of Coralydine **19**.

1.2.2 Mechanistic Interpretations of C–H Bond Functionalisation

Reported mechanistic investigations of C–H bond functionalisation processes typically focus on the concept of mononuclear Pd species mediating the catalytic cycle. Often these centre around variations on the key mechanism in this class of reactions, the concerted metalation–deprotonation (CMD) or ambiphilic metal–ligand activation (AMLA) process (**Scheme 9**), proposed independently by Fagnou (CMD)[46] and Davies/Macgregor (AMLA)[47] and co-workers.
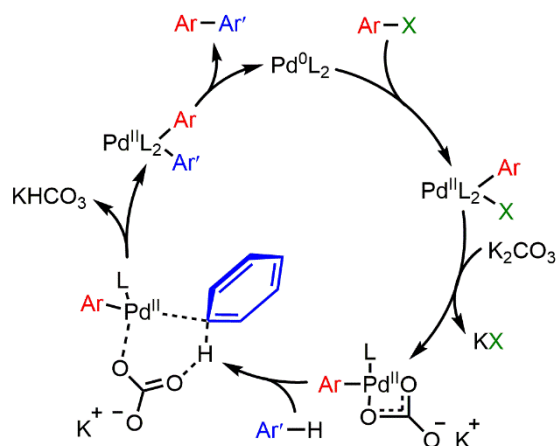
Scheme 9 CMD or AMLA-6 mechanism for direct C–H bond functionalisation.

Given the significant body of evidence within cross-coupling catalysis however, it should be expected that C–H bond functionalisations possess a capacity for complex, multistep reaction processes involving higher-order Pd species. It is important to recognise that common Pd (pre)catalysts can often act as Pd reservoirs for the subsequent generation of Pd^0 particles, or indeed as PdNP sources in their own right in this type of chemistry. Research conducted by Fairlamb and co-workers on the direct *C*8-arylation of adenosine mediated by $Pd(OAc)_2$ demonstrated the rapid formation of Pd agglomerates under the reaction conditions, with substrate turnover occurring concomitantly with the observation of Pd/Cu-containing nanoparticles.[48] Optimisation of this protocol for the functionalisation of the more sensitive 2′-deoxyadenosine **20** to form **21** demonstrated that these nanoparticles were critical to precatalyst activation, with the (pre)catalyst *trans*-$Pd(OAc)_2(piperidine)_2$ used in this reaction shown to degrade rapidly to form well-defined 1.7 nm PdNPs, *via* a $Pd(DMF)_2(piperidine)_2$ intermediate (**Scheme 10**).[49] Polar aprotic solvents such as DMF have been shown by Hii *et al*. to effect a rapid dissociation of $Pd(OAc)_2$, leading to speciation of PdNPs from this ubiquitous Pd precursor catalyst.[50]
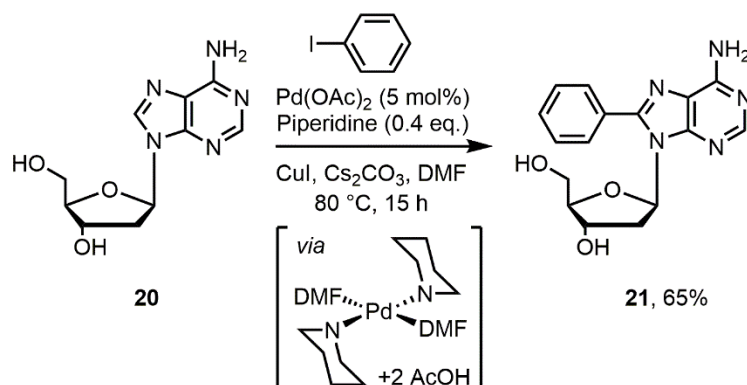
Scheme 10 Direct arylation of 2′-deoxyadenosine **20** catalysed by DMF–PdNPs.

While many examples exist of this type of speciation from common Pd precursors,[51-56] it is important to note that the multinuclear colloids proposed as sources of heterogeneous Pd[0] are often poorly defined, ranging from a few palladium atoms up to particles in the 5 nm range consisting of many thousands of palladium atoms. Importantly, this creates a significant physical difference between the surface, terrace site and bulk palladium atoms in the context of their catalytic activity. This, in addition to their specific morphology and other surface effects, must be kept in mind when attempting to demonstrate the heterogeneous nature of a given reaction. Such considerations regarding the activation of Pd(OAc)$_2$ and other related precursors to form well-defined PdNPs can be extended to many C–H bond functionalisation protocols, allowing for the activity of pre-synthesised PdNP catalysts to be independently tested and compared in these reactions.[57-64] The use of pre-supported PdNP catalysts such as PVP–Pd **13** allows for a greater degree of control over potentially complex catalytic manifolds, where a multi-ensemble of higher order Pd species often play a key role.[65,66]

The relevance of higher-order Pd species in C–H bond functionalisation processes and the activity of pre-synthesised supported PdNPs in this chemistry has recently been reviewed in detail (see Appendix 1).[20]

1.3 Arylating Agents for C–H Bond Functionalisations at Pd

1.3.1 Aryliodonium and Diaryliodonium Salts

One of the key features of many C–H bond functionalisation processes is the need for organohalides or organopseudohalides to act as the coupling partner for the desired C–H fragment (**Figure 10**). Choosing the appropriate coupling partner for a given methodology is far from trivial however, as several drawbacks exist. Iodoarenes for example are often employed preferentially due to the relatively weak C–I bond (*ca.* 240 kJ mol^{-1}), as compared to either bromoarenes (*ca.* 276 kJ mol^{-1}) or chloroarenes (*ca.* 339 kJ mol^{-1}). This is despite

the toxicity of iodine-containing waste streams, the decreased mass intensity of these reagents or their relatively higher cost. Furthermore, external oxidants can often be required either for regeneration of the active catalyst following substrate turnover, or transformation of the substrate into the desired target molecule (in an oxidative process, **Figure 10**). These considerations have led to significant developments in the use of hypervalent iodine(III) reagents as coupling partners for many C–H bond functionalisation processes, as they are both strong electrophiles and powerful oxidants.[67-70] Moreover, employing iodobenzene **1** as a leaving group (as opposed to I⁻ for example), means these species are typically more reactive than aryl halides.[71]

The reactivity of λ^3-iodanes has recently been explored in a computational study, which provides extensive detail on the impact of differing structural motifs on the reaction mechanisms which may be observed.[72] Unsurprisingly, it is the hypervalent nature of these compounds which gives rise to the wide range of synthetic applications in which they have been found to be effective (*vide infra)*. Perhaps most interestingly, the authors report that the unique electronic nature of λ^3-iodanes allows these species to isomerise through a pseudo Jahn-Teller effect. The iodine(III) acetates **22** and **23** for example are typically applied as terminal oxidants for catalytic processes, with their labile acetate groups allowing for facile metal binding and/or electron transfer (**Figure 11**).
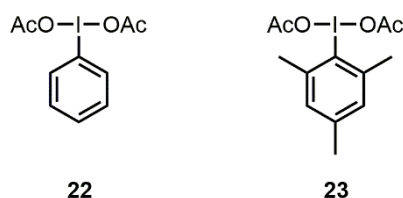
Figure 11 Structures of common hypervalent iodine(III) reagents.

The strongly oxidative nature of λ^3-iodanes can result in their acting in a non-innocent fashion, as studies on the ligand-directed, site-selective acetoxylation of arenes by Sanford *et al*. have shown (**Scheme 11**).[73] The steric demands of the iodine(III) oxidant used (**22** or **23**) in this case are proposed to be the source of the observed regioselectivity. It was also suggested that the acetate group donated to the substrate **24** is derived directly from these oxidants, although this claim is unsubstantiated by mechanistic evidence. It is equally likely that the acetate group is derived from the acetic acid/acetic anhydride solvent mixture used.
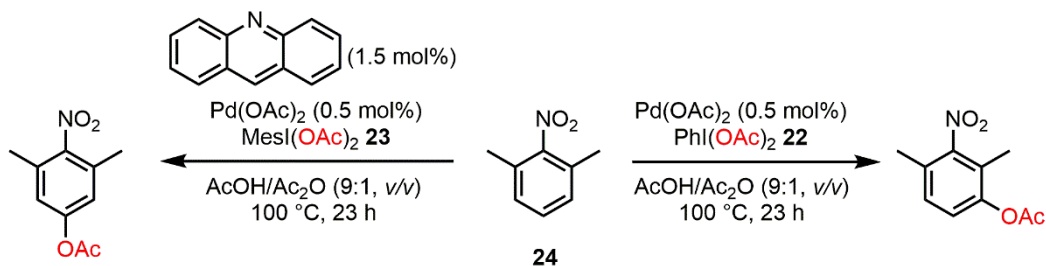
Scheme 11 Site-selective acetoxylation of arenes using iodine(III) reagents.

Qin and co-workers have also shown that **22** can be used facilitate the functionalisation of $C(sp^3)$–H bonds, with the reactivity of this species towards acetoxylation or arylation regulated simply by addition of carbonate base (**Scheme 11**).[74] In this system, the innate lack of reactivity in the C–H bond to be functionalised is overcome by decorating amide **25** with a proximal 8-aminoquinoline directing group, which also serves to provide the desired regioselectivity.
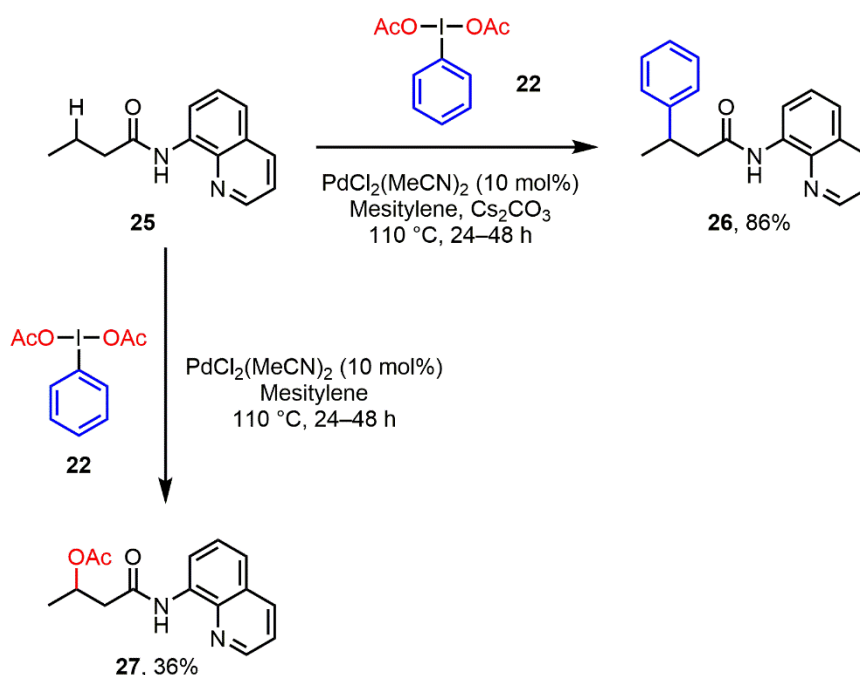
Scheme 12 Orthogonal arylation/acetoxylation using hypervalent iodine(III) reagents.

Exploratory mechanistic studies using (p-CO$_2$Me)PhI(OAc)$_2$ **28** indicated that decomposition of the iodine(III) species to form (p-CO$_2$Me)PhI **29** preceded product formation under the direct arylation conditions, suggesting that iodoarenes were the true arylating agents in this system. When **29** was used as the arylation agent in place of **28** however only 13% of the desired product was obtained, corresponding to approximately one catalyst turnover, signifying that the acetate anions generated from decomposition of **28** play a key role in this system (**Scheme 13**a). Replacement of Cs$_2$CO$_3$ with CsOAc under otherwise identical

conditions provided 87% of the desired product, proving that these acetate anions (or related complexes thereof) were effectively promoting the catalysis (**Scheme 13**b).
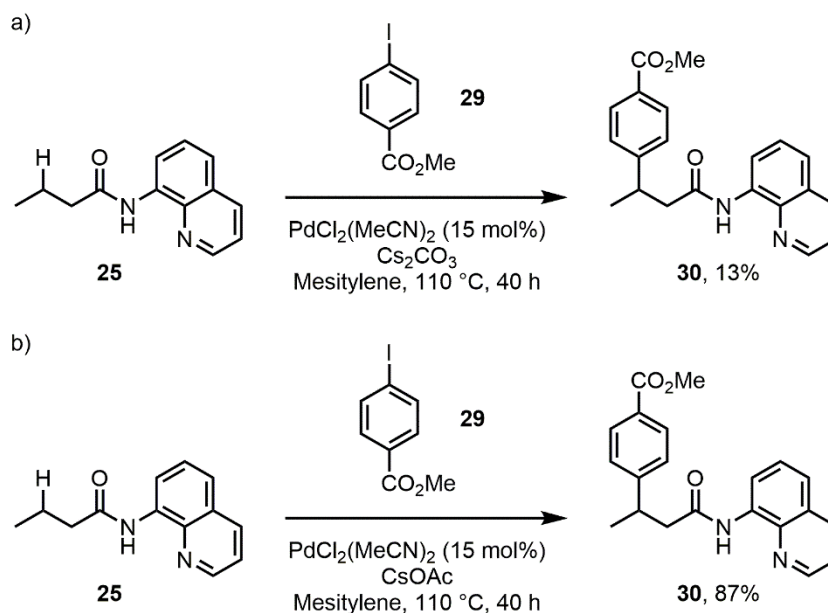
Scheme 13 Effect of acetate anion on direct arylation with iodoarenes.

These highly electrophilic species have even been demonstrated to selectively cleave the peptide bonds of asparagine residues in neutral aqueous media, *via* an elegantly designed Hofmann rearrangement.[75]
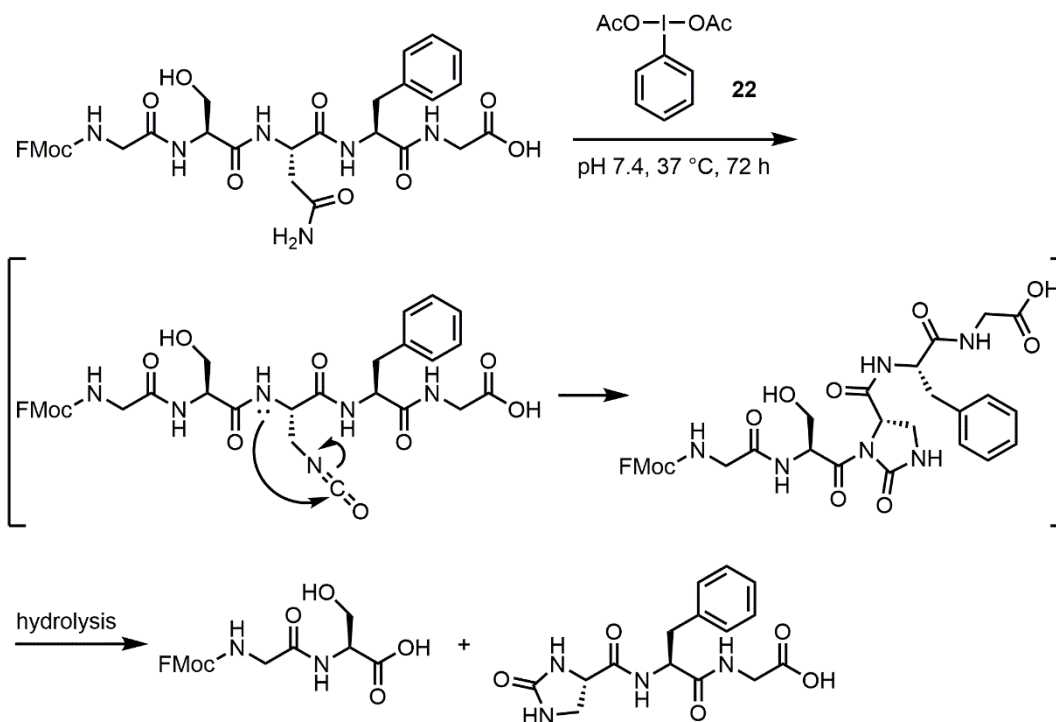
Scheme 14 Selective asparagine cleavage mediated by hypervalent iodine(III) reagent.

In addition to iodine(III) diacetates, diaryliodonium salts are the other prominent type of iodine(III) reagent primarily used in catalysis. These are notable because they are able to provide a synthetically broad range of coupling partners, typically synthesised in one-pot processes from the corresponding iodoarene. They are often employed in cross-coupling reactions such as the Suzuki–Miyaura, the first example of which was published by Bumagin and co-workers, who generated biaryls through the direct coupling of symmetric diaryliodonium salts with sodium tetraphenylborate **31** in the presence of PdCl$_2$ in water (**Scheme 15**).[76] These conditions are especially notable as up to four equivalents (w.r.t. iodonium salt) of product are obtained, representing a near-perfect incorporation of the aromatic groups.
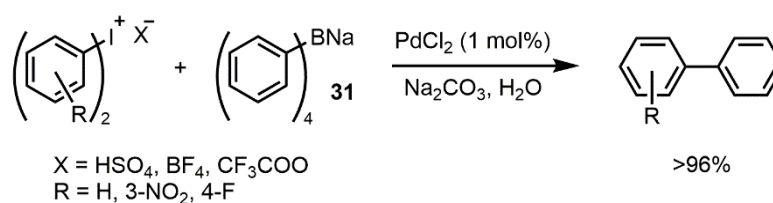
Scheme 15 Suzuki-Miyaura cross-coupling of diaryliodonium salts.

More recently, diaryliodonium salts have been applied to the emerging field of catalytic C–H bond functionalisation mediated by palladium. One of the key challenges of such chemistry is the need to direct the desired transformation to one C–H bond, in the presence of many other potentially competing C–H bonds. Often this is accomplished by using either introduced regioselectivity (e.g. directing group strategies) or taking advantage of innate regioselectivity, by targeting the most acidic or most electronically activated position in a given molecule. Sanford and co-workers used a range of 2-phenylpyridines, quinolines and other directing substrates to direct selectivity in their system, which describes a direct C(sp^2)–H arylation using symmetric and asymmetric diaryliodonium salts, mediated by Pd(OAc)$_2$ in AcOH (**Scheme 16**).[77] The key feature in all of their chosen substrates is the use of proximal nitrogen directing groups at either the 1,3 or 1,4 position, with respect to the C–H bond being functionalised.
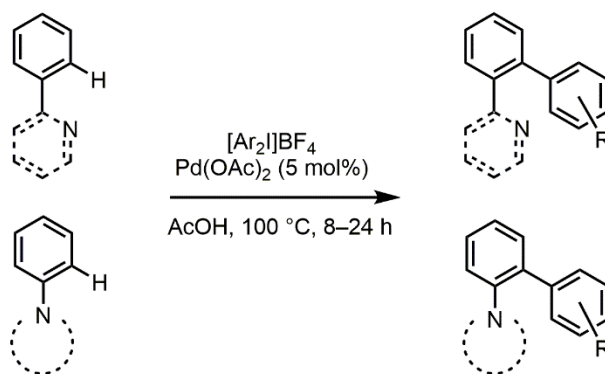
Scheme 16 Nitrogen-directed arylation using diaryliodonium salts.

Subsequent mechanistic investigation of this reaction led the authors to propose a key turnover-limiting step, involving oxidation of the Pd[II] dimer **32** by the strongly oxidising [Ar$_2$I]BF$_4$ (**Scheme 17**).[78] The resulting species could be considered a mixed Pd[II]/Pd[IV] or a Pd[III]/Pd[III] dimer.[79] In later work, it was shown that similar transformations could be effected *via* a radical-based mechanism, with a tandem Pd[II]–Ir[III]–visible light catalytic manifold.[80]
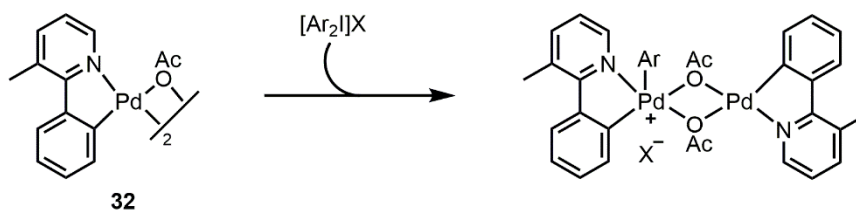
Scheme 17 Sanford's proposed high oxidation state bimetallic Pd intermediate.

In later work, the same group applied similar conditions to substrates with innate electronic reactivity, *N*-methylindoles, as opposed to the directing group approach used in **Scheme 16**. This proved extremely effective, as synthetically useful yields of the desired 2-arylindoles could be obtained from reactions conducted at room temperature, as opposed to the elevated temperature previously required (**Scheme 16**). Furthermore, when using *N*-methylindole **33**, Pd(OAc)$_2$ provided the desired arylation product **34** in 49% yield within 5 minutes; upon changing the catalyst to the carbene-ligated **35**, the desired product was obtained in 86%, but after a much longer reaction time (**Scheme 18**, 18 h).[81] The authors use this example to propose evidence of electrophilic palladation in the mechanism, in support of a proposed Pd[II]/Pd[IV] catalytic pathway (as for their previous work, **Scheme 17**).[78] It can however be argued that Pd(OAc)$_2$ and **35** are intrinsically different catalysts, therefore they do not necessarily operate *via* the same catalytic manifold. That said, conditions such as these are extremely likely to produce speciation to form higher-order Pd species *in* situ, thus the difference in rates and final yields obtained may result from Pd(OAc)$_2$ and **35** displaying varying tendencies towards this process.[20] Moreover, the authors of this work obtain similar

results by pre-mixing a solution of **22** and **14** prior to substrate addition, which they use as evidence for the *in situ* formation of diaryliodonium species (*vide infra*).
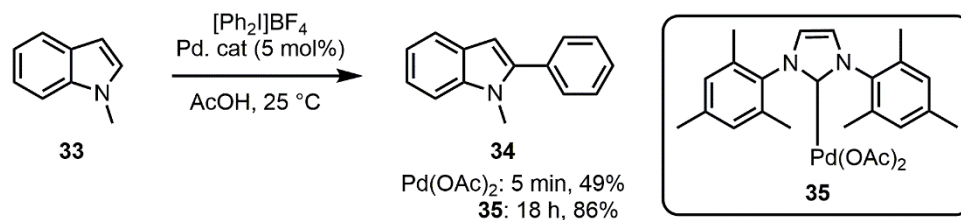
Scheme 18 Room temperature arylation of *N*-methylindole.

Daugulis and Zaitsev demonstrated that anilides were an effective directing group in the *ortho*-arylation of the simple arene **36** to produce **37** using diphenyliodonium salts, mediated by catalytic Pd(OAc)$_2$ in acetic acid (**Scheme 19**).[82] In an interesting parallel to the work by Qin and co-workers (**Scheme 12** and **Scheme 13**), they discovered that simple iodoarenes could be used in place of diaryliodonium salts if stoichiometric AgOAc was added, citing lack of commercial availability of the diaryliodonium salts as their reasons for this switch. No mention was made of the necessity of the silver cation in this reaction, hence it could be the case that the acetate anion is promoting the catalysis, as Qin *et al.* found many years later.[74]

Scheme 19 Anilide-directed *ortho*-arylation using diaryliodonium salts.

Liu and co-workers published the first reported stable complex of acyloxy-directed Pd-insertion into a C–H bond, allowing them to postulate that triflic acid (TfOH) might be a useful additive to tune the elecrophilicity of Pd^{II} in C–H bond functionalisation reactions, allowing for modification of previously unreactive motifs. They demonstrated that a combination of Pd(OAc)$_2$, catalytic TfOH and [Ph$_2$I]OTf **38** could effectively arylate a range of phenol esters such as **39** to produce **40**, in synthetically useful yields at low temperatures (**Scheme 20**). Interestingly, they also found that addition of Ac$_2$O to the reaction removed any sensitivity to moisture. Replacement of Pd(OAc)$_2$ and Ac$_2$O with Pd(OPiv)$_2$ and Piv$_2$O (Piv = pivaloyl), respectively, was found to increase the yields obtained for several examples.[83]
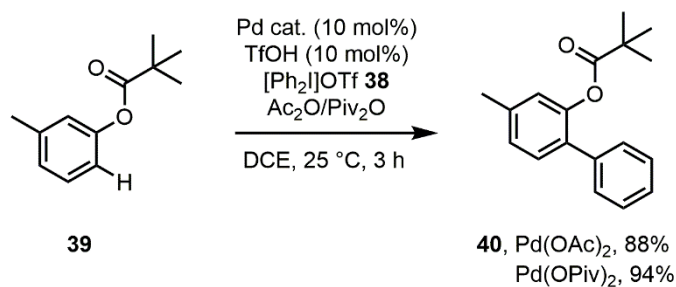
Scheme 20 Direct arylation of phenol esters using diaryliodonium salts.

Greaney and co-workers applied symmetric diaryliodonium salts to their work on the direct arylation of simple, unactivated arenes, in order to generate biaryls of value to the chemical industry. Lack of directing groups in their substrates (such as *p*-xylene, **41**) led to a corresponding problematic lack of selectivity in the C–H bond functionalised and product subsequently obtained. After extensive screening, they discovered that use of the Hermann–Beller palladacyle **42** was effective in directing arylation of **41** to a single site to produce **43** (**Scheme 21**). Furthermore, using trifluoroacetic acid (TFA) to tune the elecrophilicity of Pd^{II} improved the yields observed (as with the addition of TfOH in Liu's work, *vide supra*).[84]
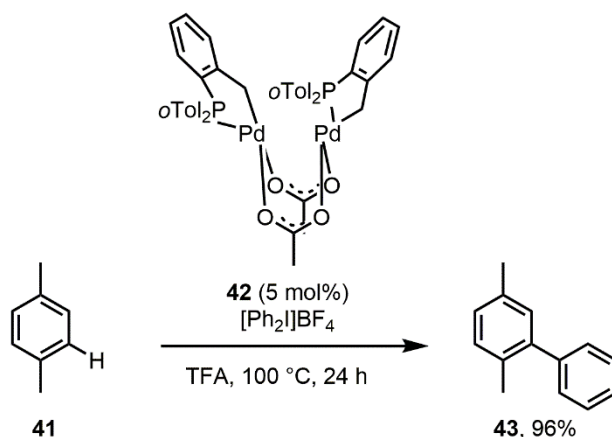
Scheme 21 Direct arylation of *p*-xylene **41** mediated by the Hermann–Beller palladacycle **42**.

In the examples utilising diaryliodonium salts highlighted above, a significant drawback lies in the fact that typically one or more equivalents of iodoarene are lost as waste, for each equivalent of substrate turned over. In terms of atom economy, sustainability and simple economics, this significantly reduces the appeal and versatility of transformations using these reagents. Bumagin's example (**Scheme 15**) is a rare instance of these reagents being used in an atom-efficient manner, yet even this requires a privileged substrate (tetraphenylborate **31**). Greaney and co-workers have attempted to address this issue by applying tandem Cu catalysis to functionalised indoles, where the "byproducts" of the initial C–H arylation (iodoarenes) are then captured by a second Cu centre and used to effect N–H arylation on the

same substrate. This overall transformation can be conducted in a single reaction vessel ("one-pot"), although this approach is so far limited to using the phenyldimethyluracil iodonium salt **44**, in order to provided differentiation between the two aromatic groups for each catalytic step (**Scheme 22**). Nevertheless, this example represents a current "best-in-class" approach to removing the stoichiometric iodoarene byproducts of such reactions.[85]
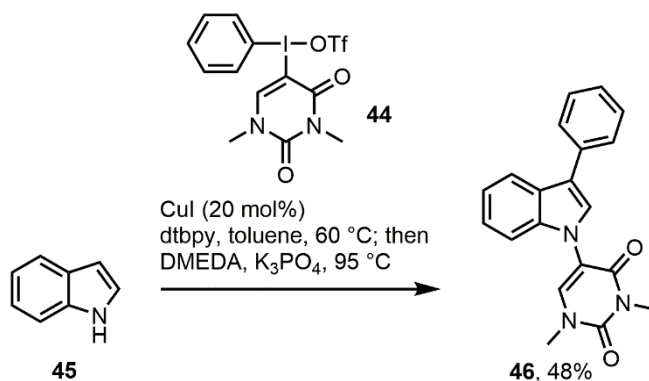
Scheme 22 Tandem C–H and N–H arylation of indoles.

Other approaches for the atom-efficient utilisation of diaryliodonium salts include supporting these reagents on ionic liquids,[86] polymers[87] or other solid supports,[88] allowing for their subsequent recovery and re-use.

1.3.2 Aryldiazonium Salts

These approaches go some way toward mitigating the disadvantages of diaryliodonium salts, but the fundamental limitation of these reagents is the presence of two aromatic groups. There is thus a need to seek alternative electrophilic reagents for Pd-catalysed direct arylation reactions, which can combine the generality of iodine(III) salts with more atom-efficient byproduct generation. Aryldiazonium salts present just such an alternative, as they bear some useful similarities to diaryliodonium salts in terms of their structure and reactivity, but importantly produce dinitrogen instead of iodoarenes as a major byproduct. It is however the case that despite the wide-ranging applications of iodine(III) species, investigations of their diazonium counterparts have largely been limited to certain Pd-catalysed cross-coupling reactions;[89] primarily they have been applied as a replacement for aryl halides in Sonogashira,[90] Suzuki–Miyaura[91] or Heck–Matsuda reactions.[92-94] This latter reaction was first reported by Matsuda in 1977 and combines Mizoroki–Heck palladium catalysis with aryldiazonium salts to generate the corresponding substituted alkenes. The reaction of phenyldiazonium chloride **47** with styrene **2** is shown in **Scheme 23**.[95] The use of $LiPdCl_3$ as a precatalyst is unusual and the likelihood is that the authors used a 1:1 mixture of $PdCl_2$ and Li_2PdCl_4 as their source of catalytic palladium.
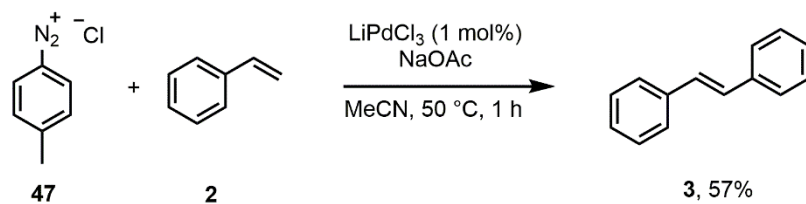
Scheme 23 Heck–Matsuda reaction in the synthesis of (*E*)-stilbene **3**.

Sigman and co-workers have demonstrated that a one-pot combination of the Suzuki–Miyaura and Heck–Matsuda cross-coupling reactions can be used to generate highly functionalised molecules in an elegant three-component synthesis, such as the reaction between phenyldiazonium **48**, alkene **49** and arylboronic acid **50** in the presence of a Pd^0 (pre)catalyst (**Scheme 24**).[96]
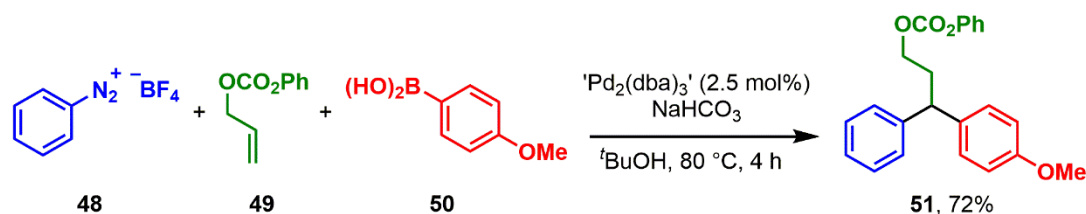
Scheme 24 One-pot combination of the Suzuki–Miyaura and Heck–Matsuda cross-couplings.

Wei and co-workers have demonstrated the efficacy of aryldiazonium salts in several cross-coupling reactions catalysed by the nanoparticulate Pd catalyst, $Pd/Al(OH)_3$, which consists of PdNPs approximately 2–3 nm in diameter. A Suzuki–Miyaura reaction between arylboronic acids and aryldiazonium salts in the presence of this catalyst was shown to proceed effectively at room temperature in methanol without any additional base or phosphine (note that the counter-ion of the aryldiazonium salt could act as a base), affording many derivatives in synthetically useful yields (**Scheme 25**).[97] A brief recycling experiment demonstrated that this catalyst rapidly decreased in efficiency over 2 recovery/re-use cycles, implying that leaching or at the very least sintering/agglomeration of the PdNPs was occurring under the reaction conditions.
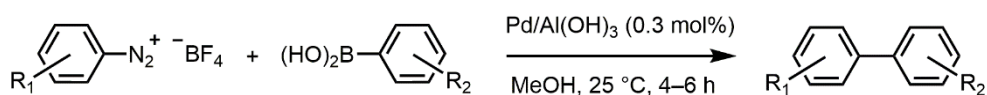
Scheme 25 Suzuki–Miyaura reaction of aryldiazonium salts catalysed by nanoparticulate Pd.

This catalyst was subsequently applied to a Heck–Matsuda reaction between aryldiazonium salts and terminal alkenes in ethanol; once again good to excellent yields of the desired cross-coupling products were obtained without the need for additional base or ligand (**Scheme 26**).[98]
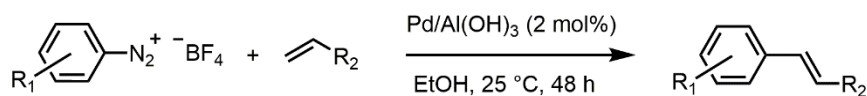
Scheme 26 Heck–Matsuda reaction of aryldiazonium salts catalysed by nanoparticulate Pd.

An analogous recycling experiment was performed and under these conditions the Pd/Al(OH)$_3$ catalyst demonstrated slightly better efficiency after 2 recovery/re-use cycles, although its performance rapidly deteriorated after this. For their recycling experiments however, the authors of this work used progressively increasing reaction times for each subsequent re-use in order to obtain similar yields, which strongly suggests that the catalyst is losing its catalytic efficiency and this fact is masked by the pursuit of isolated yield of product over actual comparison of catalytic activity. Structural studies on the recycled catalyst demonstrated that the Al(OH)$_3$ support displayed little change in either its surface area or pore size after several uses. Conversely, TEM images of the PdNPs displayed significant desorption and agglomeration had occurred under the reaction conditions. Inductively coupled plasma atomic emission spectroscopy (ICP–AES) demonstrated that substantial leaching of the Pd catalyst occurred, leading to the observed decrease in catalytic activity. This is certainly also occurring under the Suzuki–Miyaura reaction conditions detailed above (**Scheme 25**). The same group have also recently demonstrated the effective combination of aryldiazonium salts with this catalyst in a Stille cross-coupling of substituted tributylarylstannanes under mild conditions (**Scheme 27**).[99]
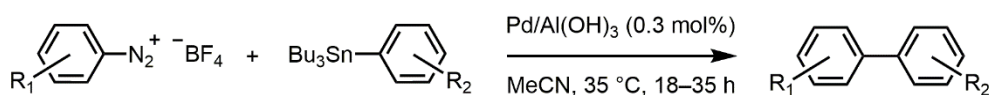
Scheme 27 Stille reaction of aryldiazonium salts catalysed by nanoparticulate Pd.

Despite the many examples of their useful application in Pd-catalysed cross-couplings, aryldiazonium salts are as yet vastly underexplored for direct C–H bond functionalisations. One notable exception combines the ruthenium-mediated visible-light photoredox catalysis pioneered by Macmillan *et al.*[100] with a Pd-mediated room temperature direct C–H arylation. As with this group's earlier work on Pd-mediated C–H bond functionalisations using diaryliodonium salts (**Scheme 16**),[77] a directing group strategy employing proximal nitrogen directing groups at either the 1,3 or 1,4 position was combined with electrophilic aryldiazonium salts to generate a range of arylated products in methanol at 25 °C (**Scheme 28**).[101] This process was proposed to proceed through an aryl radical intermediate, formed by one-electron reduction of the aryldiazonium salt by a photoexcited Ru(bpy)$_3^{2+*}$ transient species.
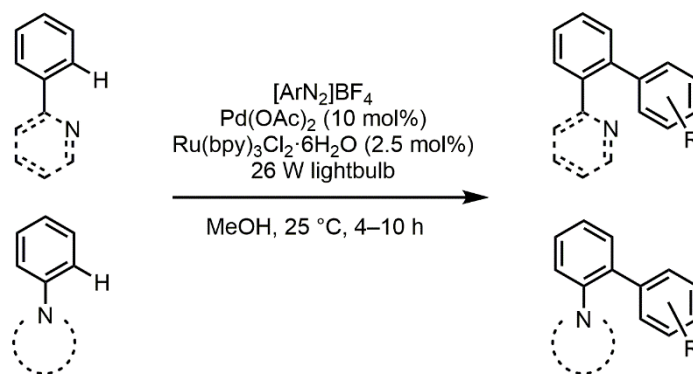
Scheme 28 Nitrogen-directed arylation using aryldiazonium salts.

Correia *et al*. have also shown that aryldiazonium salts can be used for the direct arylation of *N*-methylindole **33**, benzofuran **52** and benzothiophene **53** under mild conditions with typically short reaction times (**Scheme 29**).[102]
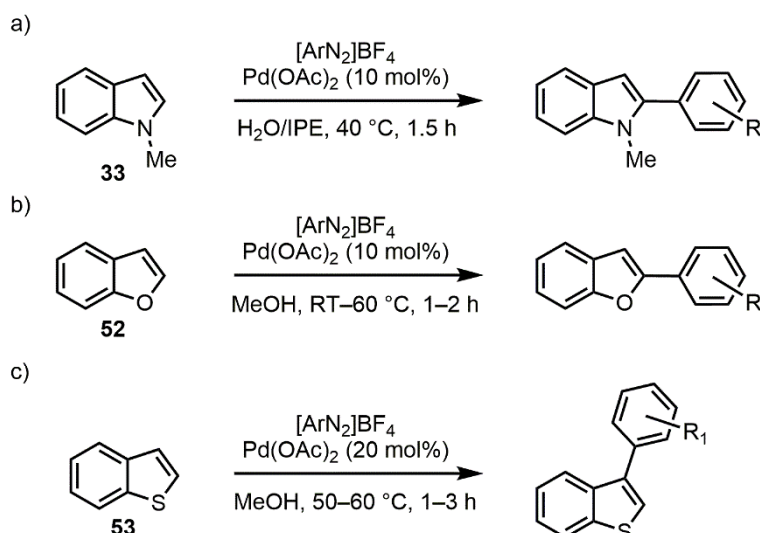
Scheme 29 Direct arylation using aryldiazonium salts of a) *N*-methylindole **33**, b) benzofuran **52** and c) benzothiophene **53**.

During the screening for this reaction, the authors originally found that when acetic acid was used as a solvent, moderate conversion of *N*-methylindole **33** was observed. They subsequently deduced that the major side product in this reaction was a diazo species, formed by nucleophilic attack of the arylindole formed under the reaction conditions on unreacted aryldiazonium salt starting material. To combat this issue, the reaction solvent was changed to a biphasic mixture in an attempt to separate the remaining aryldiazonium salt from the product; the use of a 2:1 H_2O/di-*iso*-propyl ether (IPE) solvent mixture allowed for good yields of the desired products to be obtained. When attempting this reaction with the electron-deficient 4-trifluoromethylbenzene diazonium salt **54**, no reaction was seen. It required *N*-Boc protection of the indole (**55**), an increase in catalyst loading, a change of solvent to *tert*-

butanol and a much increased reaction time in order to observe the desired arylation product **56** in good conversion (**Scheme 30**). It is evident that for these authors, room temperature must be at least 25 °C in order for the ^{t}BuOH solvent to exist as a liquid. The observation that the nucleophilicity of the substrates appeared to correlate with their reactivity led the authors to suggest that the mechanism for this process involves a nucleophilic attack on the palladium centre from the heteroaromatic substrates, as proposed by Zhao,[103] instead of the radical-based mechanism proposed by Sanford and co-workers (*vide supra*).
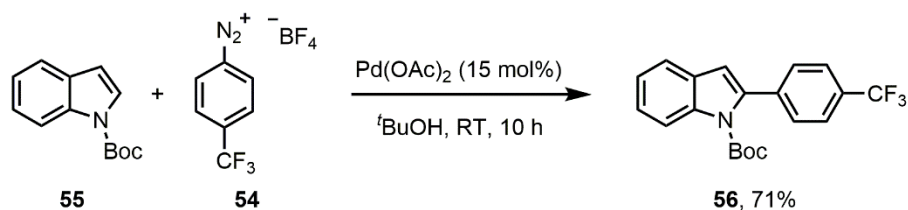
Scheme 30 Direct arylation of protected indole using electron-deficient aryldiazonium salt.

The stability of aryldiazonium reagents is one possible reason why these species have not yet found wider application in the important field of Pd-catalysed C–H bond functionalisation. They are often perceived to be highly explosive, although this particular risk can be mitigated through the use of flow technology, particularly in large scale reactions.[104,105] Additionally, the counter ion used has a large impact in this regard, with tetrafluoroborate and tosylate salts demonstrating greatly increased stability over halide anions.[93] Their safe use in many varied applications has been demonstrated extensively,[106] with *in situ* formation from the corresponding aniline a common approach used to limit handling of the crystalline salts of these species.[107,108]

1.4 Project Aim & Objectives

1.4.1 Aims

I.   Develop new synthetic methodology based on the application of catalytic C–H bond functionalisation chemistry to access molecular complexity.

II. Investigate the role of higher-order Pd species in catalytic C–H bond functionalisation reactions through the comparison of pre-synthesised heterogeneous nanocatalysts with those forming *in situ*.

III. Study the propagation of palladium nanoparticles and clusters from commonly used Pd (pre)catalysts.

1.4.2 Objectives

I.   To explore the use of electrophilic arylating agents such as diaryliodonium and aryldiazonium salts with a view to developing mild and sustainable C–H bond functionalisation processes, in order to allow the selective functionalisation of tryptophan and related biomolecules (Chapter 2).

II. To demonstrate and compare the activity of heterogeneous and homogeneous Pd catalysts in the direct arylation of heterocycles in order to elucidate mechanistic information about these processes, including the application of heterogeneous catalysis to the selective functionalisation of biomolecules (Chapter 3).

III. To characterise the Pd^0 precursor complex $Pd_2(dba)_3$ and related solvated compounds in solution and in the solid state, in particular studying its behaviour in dynamic systems and thus its potential for the formation of palladium nanoparticles and clusters (Chapter 4).

Chapter 2: Direct C–H Bond Functionalisation of Tryptophans and Peptides

2.1 Literature Syntheses of Arylated Tryptophans

2.1.1 Cross-Couplings

Tryptophan is a hydrophobic, indole-containing amino acid present in approximately 90% of proteins, which is known to alter the structure of proteins as well as providing a natural fluorescent marker.[109] These intrinsic photophysical properties can also be enhanced by extension of the aromatic π-system, such as that obtained by generation of aryl-substituted tryptophans *via* direct metal-mediated catalysis. Miller and co-workers have demonstrated that a Suzuki–Miyaura reaction between the commercially available borylated tryptophan derivative **57** and bromoindole **58** provides the desired *C*2-arylation product **59** in good yield, although the high temperature required potentially limit the applicability of this method for more complex substrates (**Scheme 31**).[110]
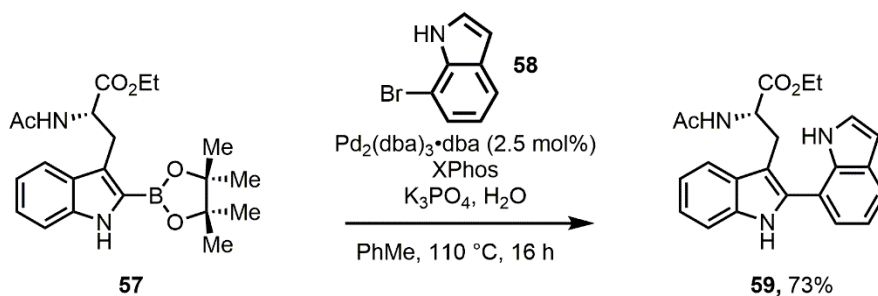
Scheme 31 Suzuki–Miyaura coupling to produce *C*2-tryptophan derivative **59**.

A similar approach by Meinke *et al.* utilised a Suzuki–Miyaura coupling to prepare several *C*2-functionalised derivatives of the tryptophan-containing natural product apicidin **60**, obtained by reaction of brominated precursor **61** with the appropriate arylboronic acid (**Scheme 32**).[111] The authors state that this reaction "provided good yields of the desired 2-arylindoles", although only an approximate yield of 65% was provided for all five analogues prepared (**62–66**).

60
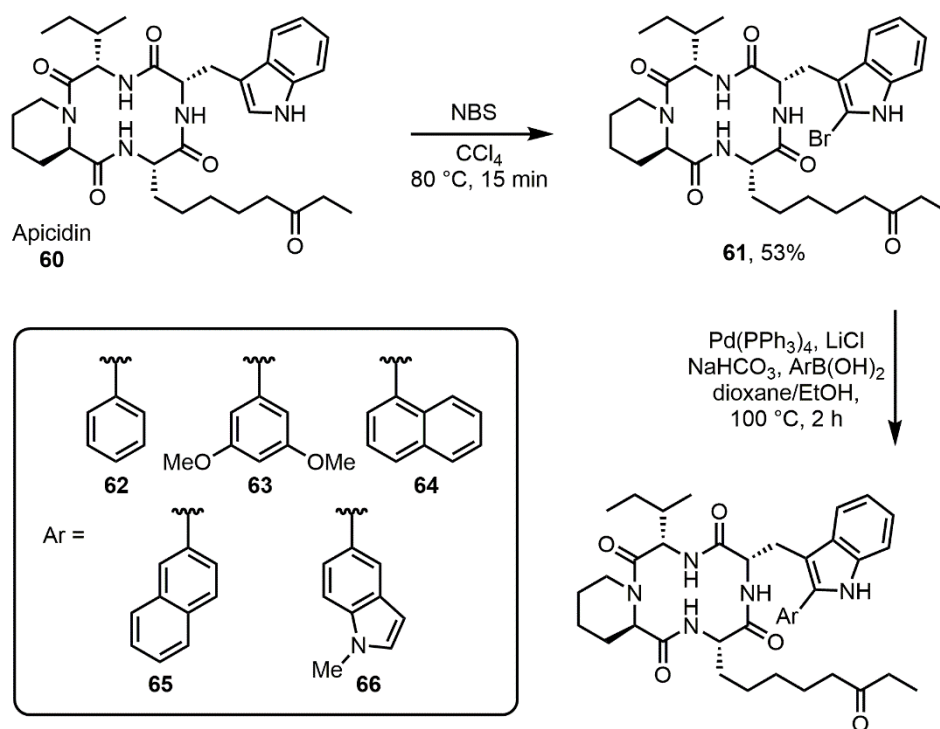
Scheme 32 Preparation of arylated apicidin analogues *via* a Suzuki–Miyaura coupling.

Winn and co-workers also selected the Suzuki–Miyaura reaction to selectively functionalise several unprotected 5- and 7-bromotryptophans in water (**Scheme 33**).[112]
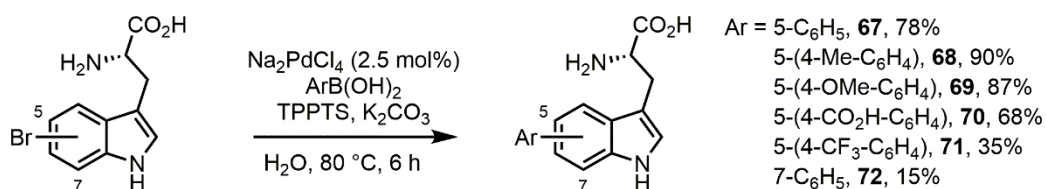
Scheme 33 Suzuki–Miyaura coupling of unprotected bromotryptophans in water.

The fluorescence properties of the arylated products obtained were evaluated and shown to provide stronger emission signals than that of the parent tryptophan compound **73** (**Table 1**, Entry 1). Importantly, the position and nature of the aromatic substituent used gave rise to varying emission signals and Stokes shifts; an electron-withdrawing carboxy group attached to the phenyl ring (**70**) produced the largest Stokes shift of those examples tested (**Table 1**, Entry 4), while 5-phenyltryptophan **67** (**Table 1**, Entry 2) was seen to be much more strongly fluorescent than its 7-phenyl regioisomer **72** (**Table 1**, Entry 5).

Table 1 Fluorescence spectroscopic properties for aryltryptophans.[a]

Entry	Compound	λ_{ex} / nm	λ_{em} / nm	Stokes shift / cm^{-1}
1	**73**	280	348	6978
2	**67**	254	370	12343
3	**69**	254	353	11041
4	**70**	254	411	15039
5	**72**	254	384	12703

[a] All spectra recorded in methanol.

2.1.2 Direct C–H Bond Functionalisations

While these approaches provide several facile routes to access aryltryptophans, they all suffer from the disadvantage of having to prepare pre-functionalised halogenated or borylated starting materials, as is usually the case for traditional cross-coupling processes. More recent developments in the field of metal-mediated C–H bond functionalisations provide a way to obviate this potential limitation, as the desired product(s) can be obtained from the direct reaction of an intrinsically reactive C–H bond within the indole moiety, thus increasing the atom economy and mass efficiency for the overall transformation required. Lavilla and co-workers adapted the Pd-mediated arylation conditions of Larossa *et al.*[113] to produce a range of *C*2-aryltryptophans directly from protected tryptophan derivative **74** in synthetically useful yields under microwave irradiation for 5 minutes. The arylating agents in this protocol are iodoarenes, with AgBF$_4$ and 2-nitrobenzoic acid used as stoichiometric additives (**Scheme 34**).[114]
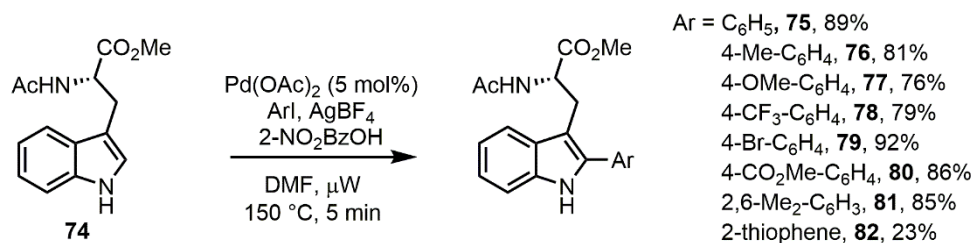
Scheme 34 Direct arylation of tryptophan **74** using a catalytic Pd/stoichiometric Ag system.

This methodology was also adapted to allow the selective modification of several tryptophan-containing peptides, where in phosphate buffer at pH 6.0 the temperature could be lowered to 80 °C while still allowing for high conversions to the desired products (**Scheme 35**). A

tenfold excess of aryl iodide was however required in these cases. Furthermore, those peptides with sulphur-containing amino acids in their sequence (**90**) proved unsuitable arylation substrates, due to selective hydrolysis of the peptide bond presumably caused by *in situ* palladium complex formation. The specific position of tryptophan within the peptide had no effect on the efficacy of this protocol.

Ac-Ala-**Trp**-Ala-OH, **$$**, 57%
Ac-**Trp**-Leu-Asp-Phe-OH, **$$**, 68%
Ac-Tyr-Pro-**Trp**-Phe-OH, **$$**, 75%
Ac-Arg-Gly-**Trp**-Ala-OH, **$$**, 94%
Ac-His-Gly-**Trp**-Ala-OH, **$$**, 51%
Ac-Lys-Gly-**Trp**-Ala-OH, **$$**, 95%
Ac-Ser-Gly-**Trp**-Ala-OH, **$$**, 62%
Ac-Met-Gly-**Trp**-Ala-OH, **$$**, 0%
Ac-Gln-Phe-Ala-**Trp**-OH, **$$**, 88%
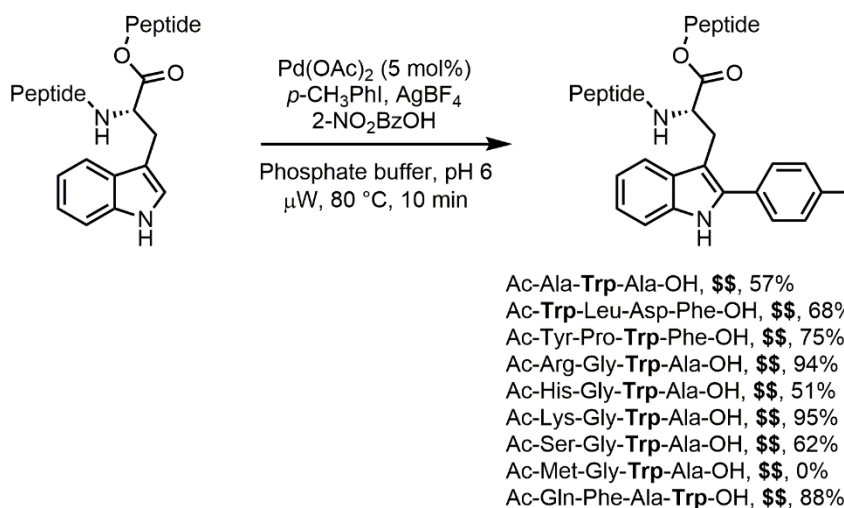
Scheme 35 Selective arylation of tryptophan-containing peptides.

One issue observed with the protocol developed on single tryptophan residues (**Scheme 34**) was that the nitrogen protecting group was critical in providing the desired products in synthetically useful yields. The acetyl protecting group used in this case has poor utility for masking amino functionality in peptide syntheses; to address this drawback later work from the same group explored the effect of acid additives on several tryptophan derivatives, as well as unprotected tryptophan itself.[115] Interestingly it was found that addition of stoichiometric TFA to the reaction allowed for quantitative conversion (at 90 °C in DMF) of unprotected tryptophan, in addition to *N*-Tfa (**92**) and *N*-Fmoc (**93**) tryptophans. As the Fmoc protecting group is readily compatible with solid-phase peptide synthesis it was selected to exemplify these new reaction conditions for a range of aryl iodides (**Scheme 36**).

Ar = C$_6$H$_5$, **94**, 56%
4-Me-C$_6$H$_4$, **95**, 81%
4-OMe-C$_6$H$_4$, **96**, 63%
4-Br-C$_6$H$_4$, **97**, 62%
4-CO$_2$Me-C$_6$H$_4$, **98**, 68%
4-NO$_2$-C$_6$H$_4$, **99**, 91%
3-CF$_3$-C$_6$H$_4$, **100**, 59%
1-pyrene, **101**, 66%
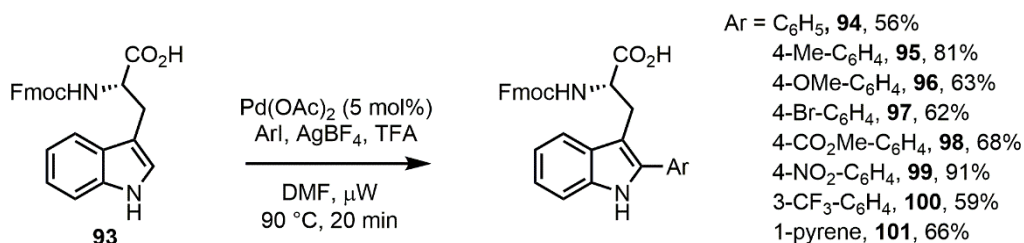
Scheme 36 Direct arylation of Fmoc-protected tryptophan **93** using a Pd/TFA system.

The aqueous conditions developed for short-chain peptides (**Scheme 35**) were also subsequently adapted in the post-synthetic modification of the natural product brevianamide **102**, which contains a masked tryptophan functionality (**Scheme 37**). This protocol was used to synthesise a range of novel *C*2-arylated analogues which displayed antitumoral activity distinct from that of the parent compound **102**.[116]

Ar = 4-Me-C_6H_4, **103**, 84%
4-OMe-C_6H_4, **104**, 86%
4-CF_3-C_6H_4, **105**, 73%
4-Cl-C_6H_4, **106**, 72%
4-I-C_6H_4, **107**, 7%
4-CO_2Me-C_6H_4, **108**, 95%
3-OMe-C_6H_4, **109**, 73%
3-CF_3-C_6H_4, **110**, 51%
3-Cl-C_6H_4, **111**, 71%
3-CO_2Me-C_6H_4, **112**, 40%
3,5-CF_3-C_6H_4, **113**, 13%
2-OMe-C_6H_4, **114**, 70%
2-CF_3-C_6H_4, **115**, 51%
2-Cl-C_6H_4, **116**, 54%
2-thiophene, **117**, 9%
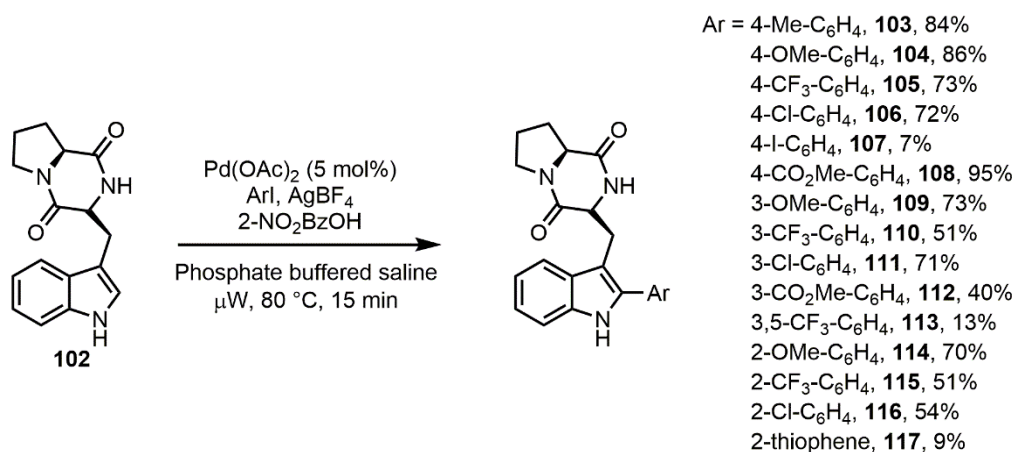
Scheme 37 Direct arylation of brevianamide using a Pd/Ag system.

The arylating conditions developed by this group shown in **Scheme 34** and **Scheme 36** were subsequently adapted to allow preparation of stapled tryptophan–tyrosine/phenylalanine peptides through an elegant *C*2-activation, allowing rapid access to complex macrocyclic peptide architectures.[117] One such product obtained from the intramolecular reaction of a tryptophan residue with a phenylalanine residue to produce a peptide containing the tumour-homing signalling sequence Asn-Gly-Arg is shown in **Scheme 38**.
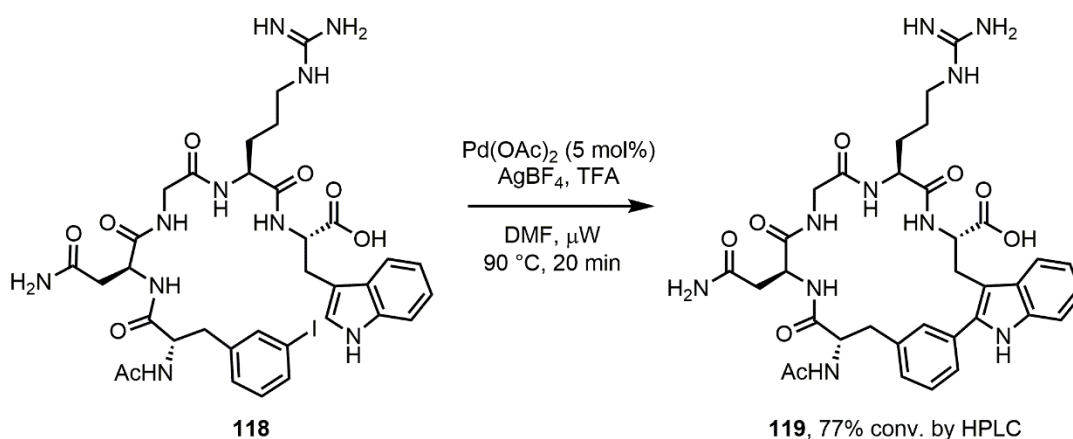
Scheme 38 Stapled bond formation of peptides through intramolecular *C*2-arylation of tryptophan.

The protocols described by Lavilla *et al.* were also adapted by James and co-workers in a sophisticated Pd-mediated peptidic macrocyclisation using an intramolecular *C*2-arylation of a derivatised tryptophan residue (**Scheme 39**).[118]
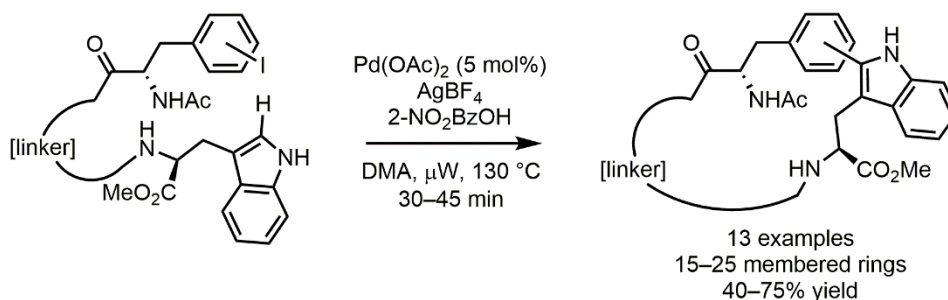
Scheme 39 Peptidic macrocyclisation utilising an intramolecular *C*2-arylation of tryptophan.

The major drawback in the application of direct C–H bond functionalisation to the modification of tryptophan derivatives in the examples highlighted above is the need for high temperatures and microwave irradiation. To address this issue, studies conducted in the Fairlamb group adapted Sanford's work on the room temperature direct arylation of indoles[81] to demonstrate the effective *C*2-arylation of tryptophan **74** under much milder conditions than had been previously achieved. This was accomplished through mixing of phenylboronic acid **14** and aryliodonium salt **22** in the presence of catalytic palladium and glacial acetic acid (**Scheme 40**).[119] Under these conditions it was proposed that **14** and **22** form a symmetric diphenyliodonium salt *in situ*.
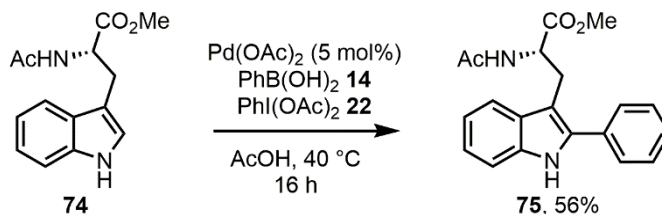
Scheme 40 Direct *C*2-arylation of tryptophan with **14** and **22**.

Replacing aryliodonium salt **22** with catalytic quantities of $Cu(OAc)_2$ allowed for moderate to high yields of the desired arylated products to be obtained when using a range of arylboronic acids (**Scheme 41**), while maintaining a mild reaction temperature. In this protocol atmospheric oxygen functions as the terminal oxidant for the copper(II) salt.
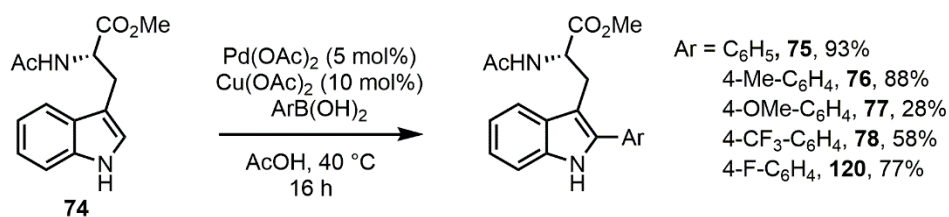
Scheme 41 Direct *C*2-arylation of tryptophan using a Pd/Cu catalytic system.

This latter methodology was also exemplified on two tryptophan-containing peptides, dipeptide **121** and hexapeptide **123**, affording excellent conversion to the desired arylation products under similarly mild conditions (**Scheme 42**).
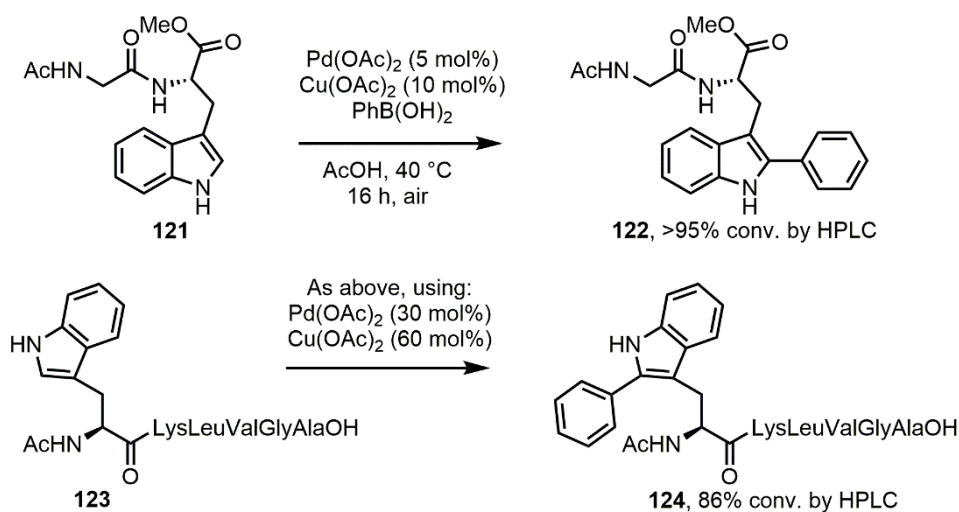
Scheme 42 Direct arylation of di- and hexapeptides using a Pd/Cu catalytic system.

More recently, Ackermann and co-workers have demonstrated the room temperature direct arylation of a protected Ala-Trp-Gly tripeptide **125** using a range of symmetric diaryliodonium salts, drawing comparisons with the *in situ* formation of such species in the methodology shown in **Scheme 40**. Application of catalytic Pd(OAc)$_2$ in glacial acetic acid facilitated generation of a series of functionalised tripeptides in moderate to high yields (**Scheme 43**). This protocol was exemplified with tryptophan-containing peptides to selectively install a phenyl group at the *C*2 position of the tryptophan residue. Interestingly the methodology described in **Scheme 43** was also shown to proceed effectively in water, albeit with reduced yields of the desired products, with a slightly extended reaction time (to 24 h).[120]
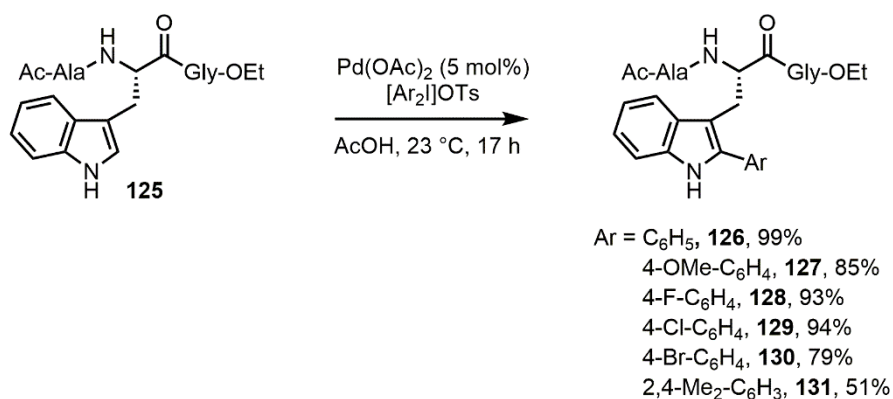
Scheme 43 Direct arylation of a tryptophan-containing tripeptide using a diaryliodonium salt.

Earlier work from the Ackermann group had demonstrated that the symmetric diaryliodonium salt **132** can function as an effective metal-free arylating reagent for engineered *C*3-substituted indoles incorporated within non-natural peptidic scaffolds. In DMF at 100 °C, *C*2-arylation of the synthetic indole proceeded with remarkably high selectivity in the presence of a tryptophan residue; this was ascribed to the relative proximity of the pivotal amide functionalities, *i.e.* the length of the carbon chain linker adjacent to the indole moiety. An example of this bioorthogonality was exemplified using hexapeptide **133** as outlined in **Scheme 44**.
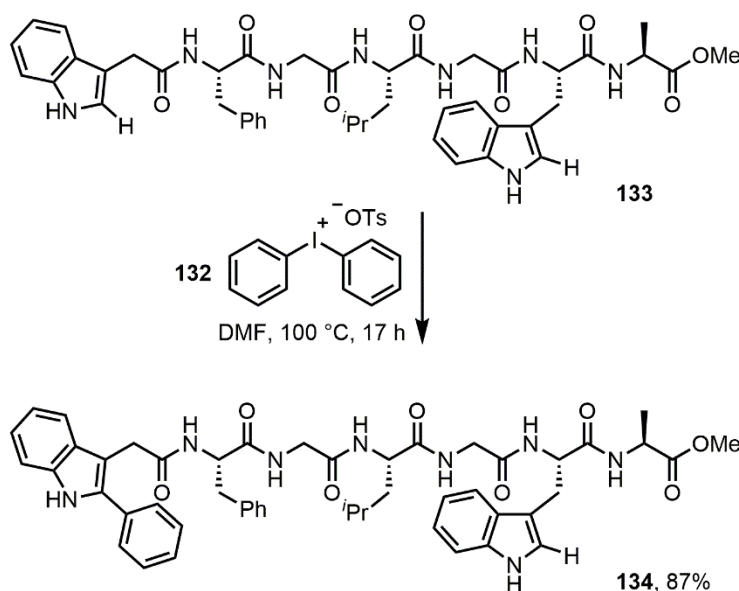
Scheme 44 Selective metal-free arylation of a synthetic *C*3-substituted indole.

2.2 Development of Diaryliodonium Salt Conditions

2.2.1 Method Development

The two sets of reaction conditions previously developed within the Fairlamb group[119] were the first demonstration of low temperature (40 °C) direct arylations of tryptophan, however despite the mild conditions and synthetically useful yields obtained, some potential drawbacks can be identified. Addition of multiple equivalents of boron- and iodine-containing arylating reagents severely impacts the atom economy and mass intensity of the process in **Scheme 40** (this can be quantified using green metrics, *vide infra*). Addition of a second transition metal (copper) in the conditions shown in **Scheme 41** is similarly undesirable. With these factors in mind, a focus was placed on investigating the role of the proposed oxidant in these systems, with the primary aim of identifying efficient and sustainable synthetic protocols. Protected tryptophan **74** was accessed in two high-yielding steps from commercially available L-tryptophan **73** using the method of Taylor and co-workers (**Scheme 45**).[121]
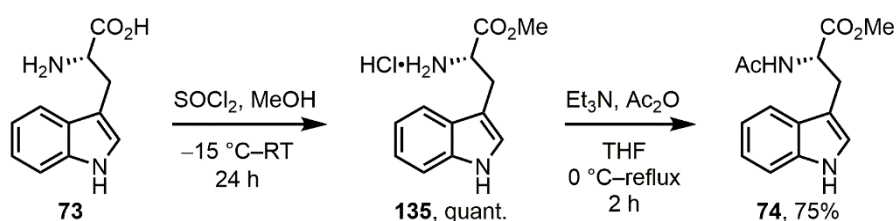
Scheme 45 Synthesis of *N*-Ac, *O*-Me tryptophan **74**.

^{1}H NMR spectroscopic analysis of **74** in CDCl$_3$ confirmed the presence of the C-terminus methyl ester at δ 3.70 ppm and N-terminus amide doublet at δ 6.03 ppm ($^3J_{H–H} = 8.0$ Hz) and singlet at δ 1.95 ppm. Retention of the indole NH is seen as a broad singlet due to exchange on the NMR timescale at δ 8.27 ppm. The C-2 proton at δ 6.97 ppm is observed as a doublet $^3J_{H–H} = 2.5$ Hz coupling to the indole NH; likely this coupling is not observed on the indole NH due to the aforementioned signal broadening. A doublet of triplets at δ 4.96 ppm can be assigned as the enantiomeric proton, which demonstrates $^3J_{H–H} = 8.0$ Hz coupling to the amide NH and $^3J_{H–H} = 5.0$ Hz coupling to the adjacent CH$_2$ group. These protons are inequivalent in their coupling to the enantiomeric proton however and so give rise to two diastereotopic signals, which overlap to give the misleading appearance of a complex multiplet, even more so due to the significant roofing observed. Correct assignment however shows a doublet of doublets at δ 3.35 ppm and another doublet of doublets at δ 3.30 ppm, each with $^3J_{H–H} = 5.0$ Hz and $^2J_{H–H} = 15.0$ Hz (**Figure 12**).
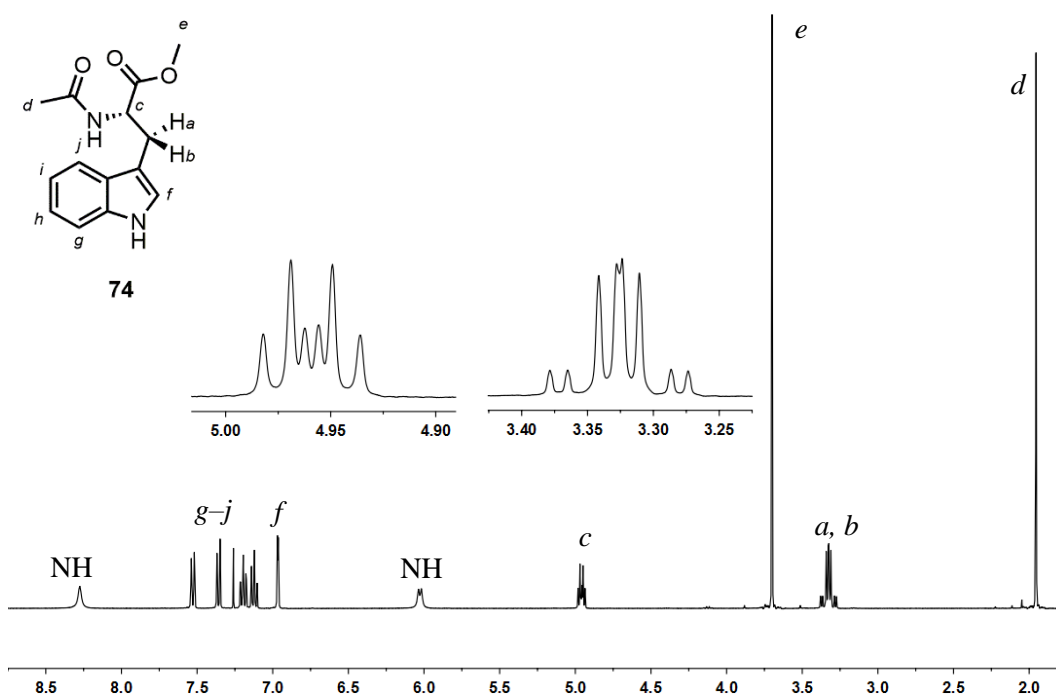
Figure 12 ^{1}H NMR spectrum of **74** (400 MHz, CDCl$_3$).

With **74** in hand, an analogous experiment to that shown in **Scheme 40** was performed using d_5-PhB(OH)$_2$ (d_5-**14**) to evaluate the nature of the arylating agent in this system *i.e.* whether this species was derived from PhB(OH)$_2$ **14**, PhI(OAc)$_2$ **22** or both. ESI–HRMS analysis of this reaction indicated an approximately 1:1 mixture of H- and D-labelled products were formed, providing convincing evidence for the formation of the proposed[81] symmetrical [Ph$_2$I]$^+$ species *in situ* (**Scheme 46**). Importantly this demonstrates the non-innocent role of PhI(OAc)$_2$ **22**, often proposed to act as a simple oxidant, in this system.
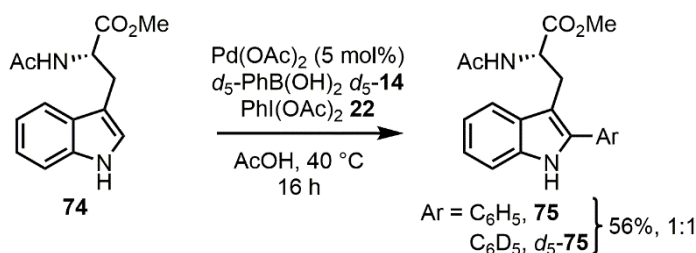
Scheme 46 Deuterium-labelling experiment in the direct arylation of tryptophan.

This non-selective donation presents an issue for the introduction of substituted aromatic groups, so an alternative arylation strategy was sought. Replacing **22** with Cu(OAc)$_2$ (**Scheme 41**)[119] circumvented this issue, but during attempts to functionalise peptides **136** and **138** significant quantities of aromatic oxidation were noted in this Pd/Cu catalytic system. HPLC–MS analysis of the reaction of tripeptide **136** under these conditions

demonstrated complete loss of starting material, but also revealed the formation of dihydroxylated and diarylated side products, in addition to the desired arylation product **137**. When these conditions were applied to tetrapeptide **138**, similar dihydroxylation side products were observed in addition to the desired arylation product **139** (**Scheme 47**). Copies of the HPLC–MS chromatograms are provided in Appendix 4.
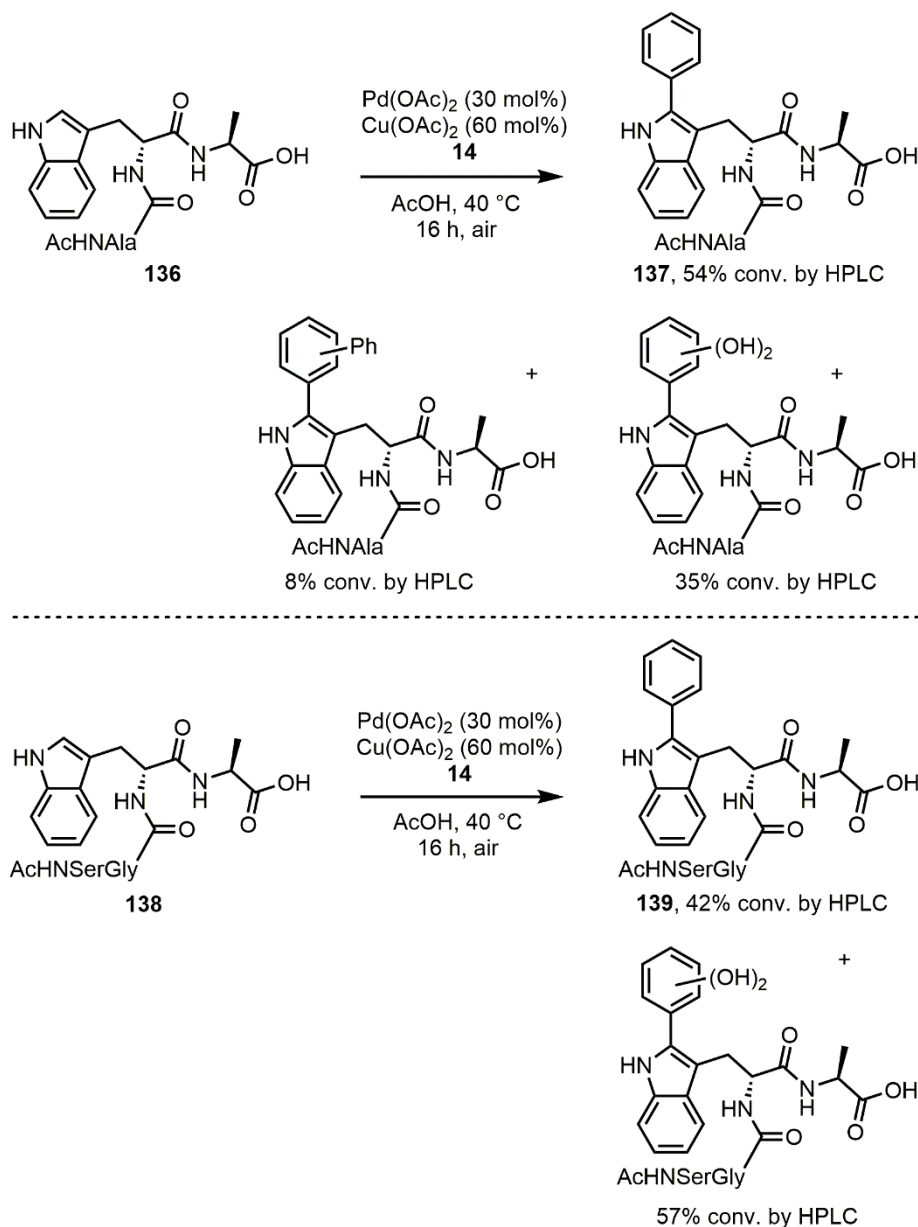
Scheme 47 Side product formation in peptides susceptible to aromatic oxidation.

Given the efficacy of this protocol for the selective functionalisation of other peptides (**Scheme 42**),[119] a terminal alanine residue neighbouring tryptophan was proposed to be crucial in affecting the selectivity of the reaction in **Scheme 47**, in conjunction with the use of copper(II).

Free *C*-terminus alanines have been shown to form stable complexes with copper (II),[122] while Delboni and co-workers have published the single crystal structure of a tryptophan-glycine copper(II) complex (**Figure 13**), which demonstrates the ability of free *C*-termini adjacent to tryptophan residues to coordinate copper(II).[123] It is proposed therefore that such species are responsible for the observed hydroxylation of the arylation products in **Scheme 47**.
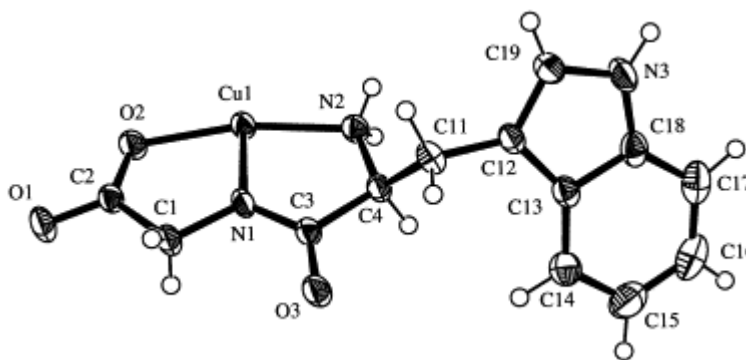
Figure 13 Crystal structure of (L-tryptophyl-glycinato) copper(II). Reprinted from *Inorg. Chim. Acta* **2001**, *312*, 133–138. Copyright 2001, with permission from Elsevier.

This over-oxidation confirms that while addition of copper(II) as a co-catalyst facilitates high conversion to the desired aryltryptophans, it has limitations when applied to more challenging substrates. It was hypothesised that the ability to utilise a single arylating agent without requiring additional transition metal co-catalysts would provide a suitable solution to the drawbacks outlined above. The observation that *in situ* [Ph$_2$I]$^+$ species can prove effective in this type of transformation (**Scheme 40**) led to examination of pre-synthesised asymmetric diaryliodonium salts, where a non-transferable 'dummy group' could be used to generate arene selectivity in the products (*vide supra*). The simple [PhMesI]OTf salt **140** was therefore synthesised in a high-yielding one-pot process from mesitylene **140** and **22** using the method reported by Gaunt and co-workers (**Scheme 48**).[124]
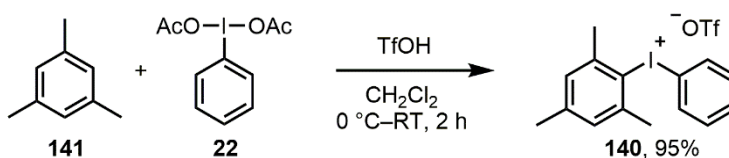
Scheme 48 Synthesis of [PhMesI]OTf salt **140**.

When **140** was applied to the arylation conditions shown in Scheme 40, in place of **14** and **22** the desired arylation product **75** was obtained with a yield of 65%. Optimisation of the reaction conditions demonstrated that full conversion of starting material **74** could be achieved after 16 h at 25 °C in ethyl acetate (**Table 5**, Entry 5). Other solvents demonstrated

to be incompatible with this chemistry were; acetonitrile, acetone, DCM, DMF, DMSO, 1,4-dioxane and water, all which provided no conversion to the desired product **75** (see Chapter 6 for details).

Table 2 Optimisation of direct arylation of tryptophan using [PhMesI]OTf **140**.[a]
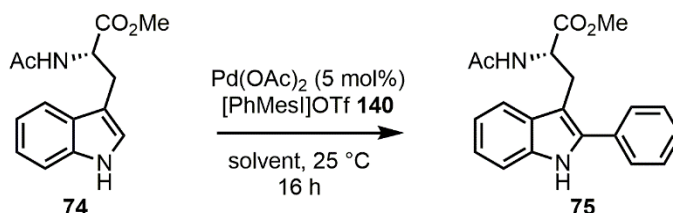
Entry	Solvent	Conv. to 75[b] (yield)[c] / %	Conv. to 142[b] (yield)[c] / %
1	AcOH[d]	70 (65)	0
2	MeOH	12	0
3	EtOH	15	0
4	*i*PrOH	47	3
5	EtOAc	91 (85)	9 (3)
6	EtOAc[e,f]	50	10

[a] All reactions conducted with **74** (50 mg, 0.192 mmol, 1 eq.), **140** (181 mg, 0.384 mmol, 2 eq.), Pd(OAc)$_2$ (2 mg, 9.6 µmol, 5 mol%) and solvent (5 mL), unless otherwise specified. [b] As determined by ^{1}H NMR spectroscopic analysis of the crude reaction mixture following an aqueous workup. [c] Following purification by silica gel flash column chromatography. [d] Reaction conducted at 40 °C. [e] Using **143** (0.384 mmol, 2 eq.) in place of **140**. [f] 40% remaining starting material.

Removal of the acidic conditions previously required, in addition to complete substrate conversion at 25 °C, meant that this protocol (**Table 2**, Entry 5) provided distinct benefits over the previous methodologies for generation of 2-phenyltryptophan **75**. In addition to the desired phenylated product **75** however, a small quantity of mesityled product **142** was formed from partial addition of the sterically-hindered mesityl component of iodonium salt **140**. Attempts to improve upon this through use of the more sterically-demanding tri-*iso*-propylphenyl (TRIP) dummy group (**143**) failed however, as this substrate lowered both the reactivity of the system and selectivity for the desired product **75** (**Table 2**, Entry 6). A small counter-ion screen was also performed which confirmed the efficacy of the triflate counter-ion used above (**Table 3**).

Table 3 Counter-ion screen for asymmetric [PhMesI]X salts in the direct arylation of tryptophan **74**.[a]
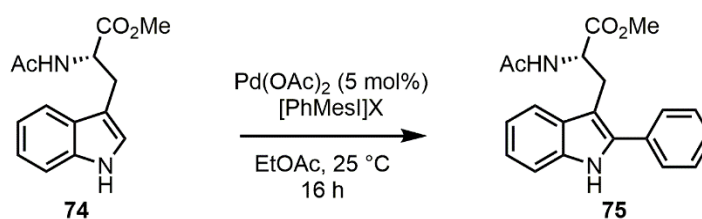
Entry	Counter-ion (X)	Conv. to 75[b] / %	Conv. to 142[b] / %
1	⁻OTf (**140**)	91	9
2	⁻BF$_4$ (**144**)	Trace	Trace
3	⁻PF$_6$ (**145**)	65	13
4	⁻SbF$_6$ (**146**)	64	10

[a] All reactions conducted with **74** (50 mg, 0.192 mmol, 1 eq.), [PhMesI]X (0.384 mmol, 2 eq.), Pd(OAc)$_2$ (2 mg, 9.6 μmol, 5 mol%) and EtOAc (5 mL). [b] As determined by ^{1}H NMR spectroscopic analysis of the crude reaction mixture following an aqueous workup.

It was during development of these conditions that the selective metal-free arylation protocol of non-natural indoles in the presence of tryptophan residues using [Ar$_2$I]$^+$ salts (Scheme 44) was published by Ackermann and co-workers.[125] Several experiments were performed to evaluate these conditions when applied to tryptophan **74**, in the presence and absence of Pd and/or air (**Table 4**). These tests established that no reaction is observed without addition of Pd(OAc)$_2$ (5 mol%) and that air has no appreciable effect on this reaction, which correlates with the observations of Ackermann *et al.*

Table 4 Evaluation of Ackermann conditions[125] in the direct arylation of tryptophan.[a]
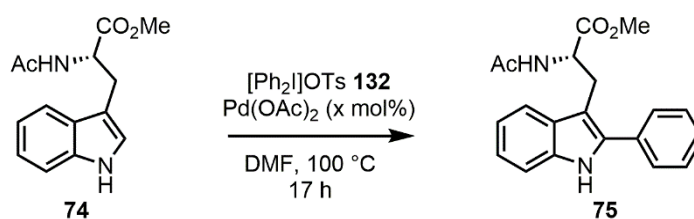
Entry	Pd(OAc)$_2$ / mol%	Air	Conv.[b] / %
1	0	No	0
2	0	Yes	0
3	5	No	93
4	5	Yes	93

[a] All reactions conducted with **74** (65 mg, 0.25 mmol, 1 eq.), **132** (170 mg, 0.375 mmol, 1.5 eq.) and DMF (2 mL). Where indicated, Pd(OAc)$_2$ (2 mg, 9.6 μmol, 5 mol%) was added. [b] As determined by ^{1}H NMR spectroscopic analysis of the crude reaction mixture following an aqueous workup.

2.2.2 Application to Peptides

With these optimised arylation conditions (**Table 2**, Entry 12) in hand, more complex, biologically or medicinally relevant substrates were investigated in order to demonstrate the applicability of this methodology. Second-generation derivatives of the potent anti-cancer compound Sansalvamide A were thus identified, as this macrocyclic pentapeptide has unique reactivity against several different forms of cancer. It also displays interesting configurational requirements for biological activity, as modification of the side chains and optical configurations of the amino acid residues in this compound allows for targeting of specific chemotherapeutic benefits, for different mutagenic cell lines.[126] Following the method of McAlpine and co-workers, a simple *N*-Boc protection/deprotection strategy was employed to synthesise the linear tryptophan-containing pentapeptide Boc-LeuLeuValLeuTrp-OMe **158**, itself a precursor to the macrocyclic final product **147** shown in **Figure 14**. This was accomplished by first preparing the free-amine tripeptide H$_2$N-ValLeuTrp-OMe **153** (**Scheme 49**) and free-acid dipeptide Boc-LeuLeu-OH **157** (**Scheme 50**), before a final coupling reaction to generate **158** in synthetically useful yields (**Scheme 51**).
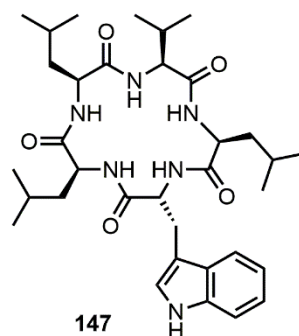
Figure 14 Tryptophan-containing Sansalvamide A derivative **147**.
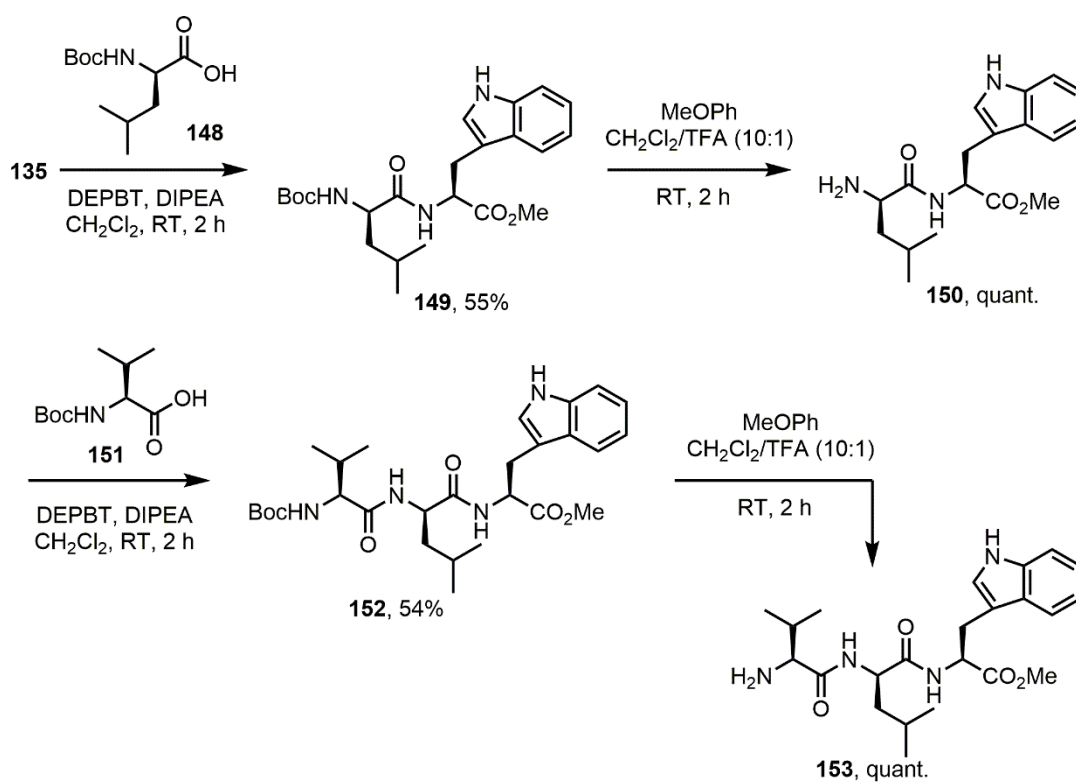
Scheme 49 Synthesis of free-amine tripeptide precursor **153**.

75
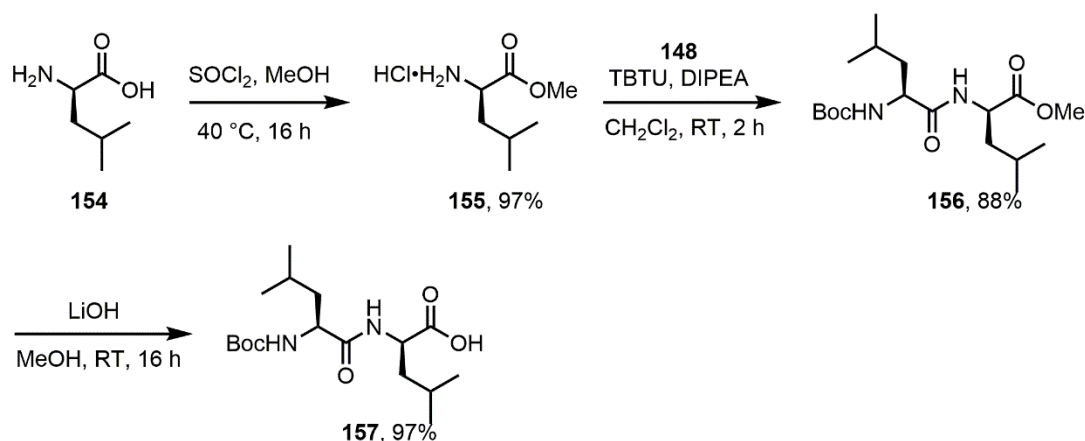
Scheme 50 Synthesis of free-acid dipeptide precursor **157**.
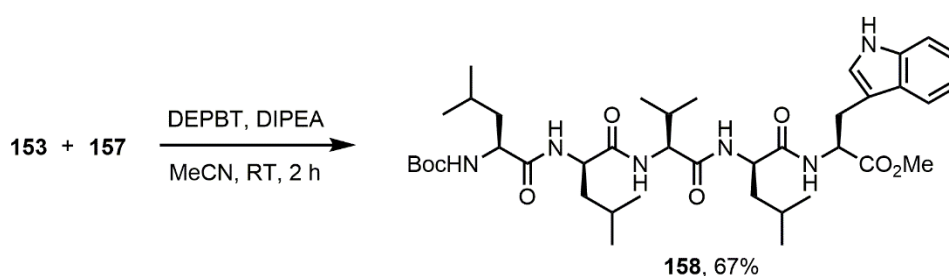
Scheme 51 Amide coupling to generate linear pentapeptide **158**.

The optimised arylation conditions shown in **Table 2**, Entry 12 were then applied to **158** in an attempt to generate the arylated pentapeptide product **159** (Scheme 52). Note that for this complex peptide the Pd catalyst loading was increased to 30 mol%.
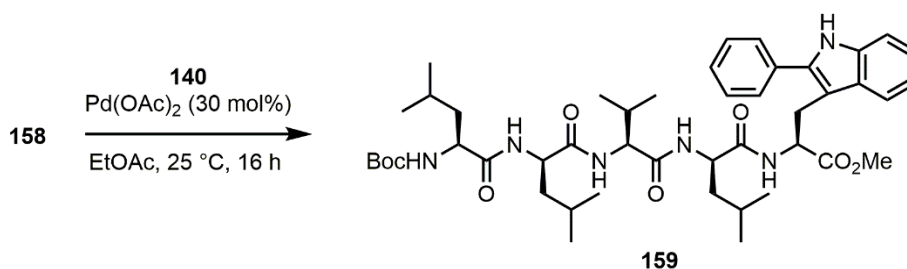
Scheme 52 Direct arylation of linear pentapeptide **158**.

TLC analysis of the crude mixture from this reaction indicated some conversion, attempts at purification were however unsuccessful, although ESI–HRMS analysis of the crude mixture did confirm approximately 20% conversion to the desired arylation product **159** ([M+Na]$^+$ 855.4980). Due to the purification difficulties of this complex peptide, it was decided to first apply the arylation methodology to more modest peptide targets as a proof of principle. With this in mind the intermediate dipeptide **149** was subjected to the previously optimised Cu^{II}

co-catalysed conditions shown in **Scheme 41**, which had been proven to work effectively on other peptides (**Scheme 53**).
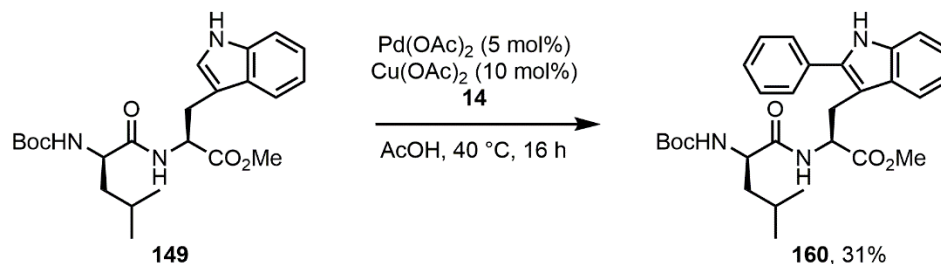
Scheme 53 Direct arylation of Boc-dipeptide **149** using Cu^{II} co-catalysis.

Surprisingly, only 31% of the desired arylation product **160** could be obtained, contrasting with the complete conversion seen when using **74** as a substrate. It was hypothesised that the change in protecting group (*N*–Boc for *N*–Ac) may have been the cause of this discrepancy, so the analogous *N*–Boc, *O*–Me protected tryptophan **161** was synthesised, before being tested under the optimised conditions shown in **Table 2**, Entry 12 (**Scheme 54**).
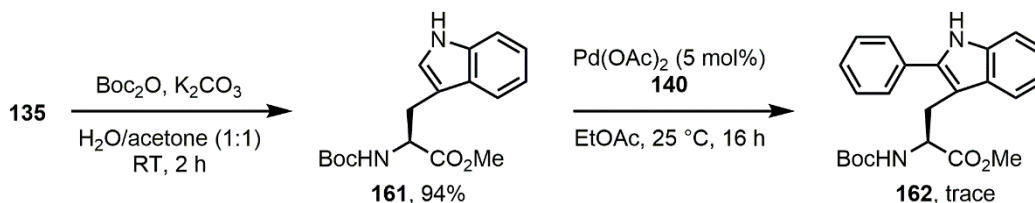
Scheme 54 Synthesis and attempted direct arylation of *N*–Boc tryptophan **161**.

As **Scheme 54** shows, under these conditions only a trace of the desired arylation product **162** could be observed by TLC or ESI–HRMS and this could not be isolated, effectively demonstrating the pronounced effect of the change in protecting group on the efficiency of the arylation protocol; it is likely that this is rooted in steric effects due to the increased size of *N*–Boc over *N*–Ac. The synthesis of the *N*–Ac analogue of dipeptide **149** was thus attempted from **154** and **135** (**Scheme 55**).
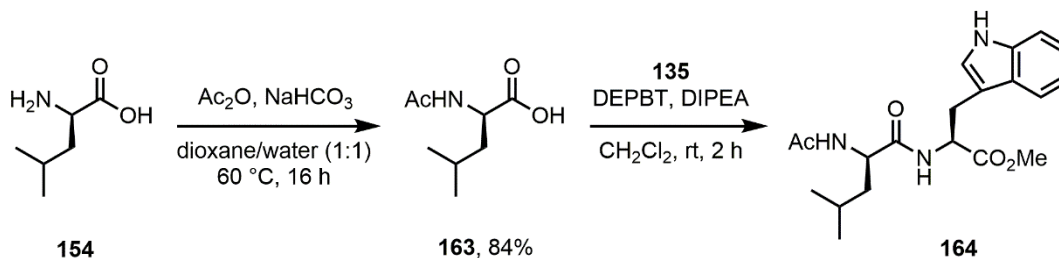
Scheme 55 Synthesis of *N*–Ac Leu–Trp dipeptide **164**.

While the initial *N*–Ac protection of ʟ–Leucine **154** proceeded in good yield, attempts at coupling this to **135** resulted in an inseparable mixture of **135** and **164**. While significant effort was expended to resolve this issue, unfortunately the desired dipeptide **164** could not be purified. It was therefore decided to switch the protecting group from *N*–Ac to *N*–Tfa, which satisfies the steric requirements, provides a useful ^{19}F NMR handle and is easily removed by aqueous sodium hydroxide.[127] This switch to *N*–Tfa produced none of the synthetic difficulties found with the *N*–Ac protecting group and three substrates were protected according to literature procedures (**Scheme 56**).[128]
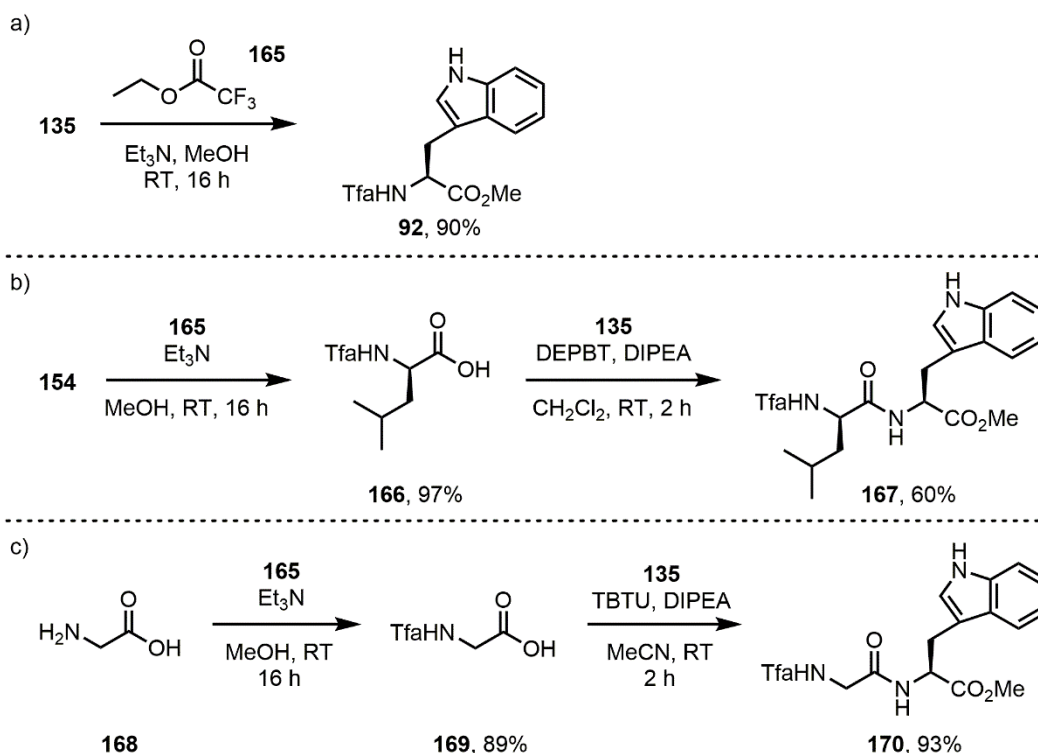
Scheme 56 Synthesis of: a) *N*–Tfa tryptophan **92**, b) Tfa Leu–Trp **167**, c) Tfa Gly–Trp **170**.

The substrates shown in **Scheme 56** were then subjected to the arylation conditions outlined in **Table 2**, Entry 12. This provided the desired arylation products in moderate to good yields, thus demonstrating the utility of this protocol when applied to small tryptophan-containing peptides (**Scheme 57**). These conditions were also successfully applied to peptides **136** and **138**, which had proven problematic with the Cu-containing conditions shown in **Scheme 41**, affording the desired arylation products **137** and **139** in useful conversions (**Scheme 58**).
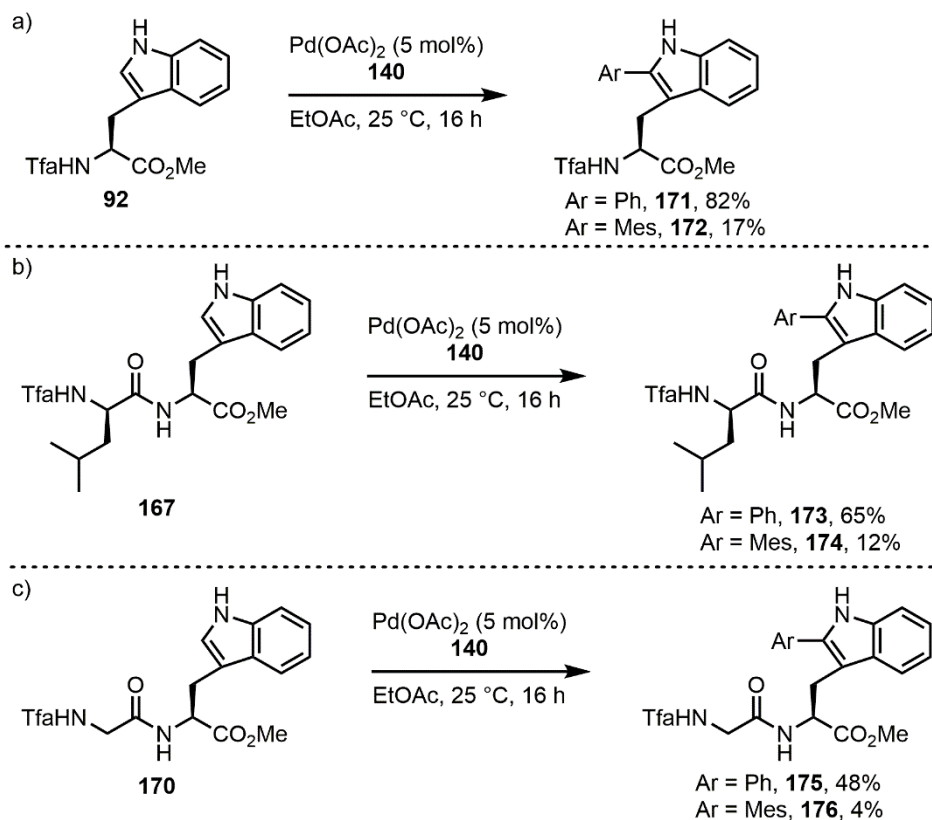
Scheme 57 Arylation of a) *N*–Tfa tryptophan **92**, b) Tfa Leu–Trp **167**, c) Tfa Gly–Trp **170**.
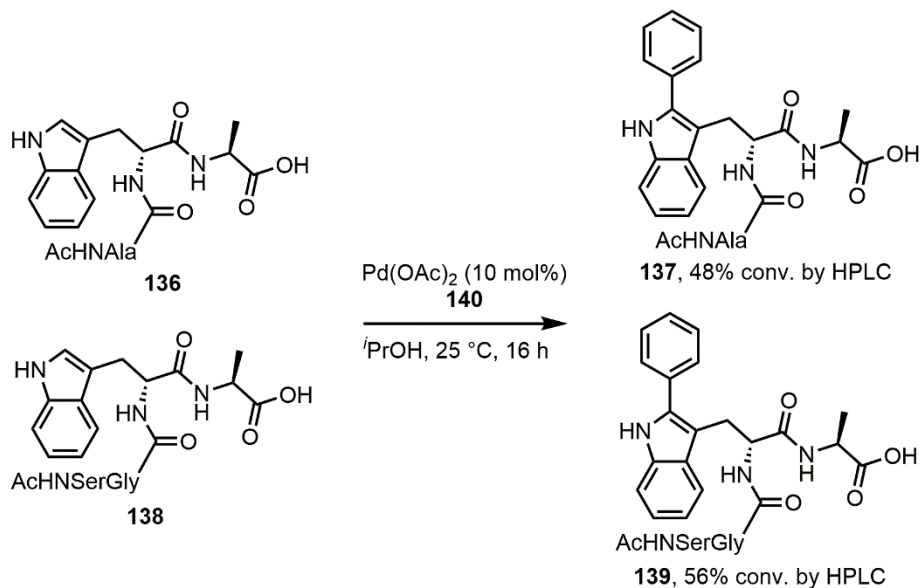
Scheme 58 Arylation of peptides susceptible to dihydroxylation using a diaryliodonium salt.

2.3 Development of Aryldiazonium Salt Conditions

2.3.1 Method Development and Scope

Despite the general applicability of these methods for the generation of 2-aryltryptophans, the limitations highlighted above meant that efforts were redirected towards identifying alternative arylating conditions. Furthermore, the generation of stoichiometric byproducts such as iodoarenes complicates product purification, hugely limits the efficiency and increases the mass intensity of any given process. With these factors in mind, it was hypothesised that a substrate containing a single aryl group, which can be readily functionalised with a range of chemical moieties, would provide an ideal coupling partner. The use of aryldiazonium salts was therefore investigated as these bear some useful similarities to diaryliodonium salts, in terms of both their structure and reactivity (see Chapter 1).[91] To begin these studies, several aryldiazonium tetrafluoroborate salts were readily synthesised in an oxidative process from the corresponding commercially available anilines,[129] accessing the desired products in low to moderate yields (**Table 5**a). Following a subsequent review of the literature, an improved synthesis of these salts published by Goossen and co-workers was found, which provided access to the same salts in excellent yields (**Table 5**b).[130]

SAFETY NOTE: Aryldiazonium salts can display both thermal and shock sensitivity which can result in violent explosion, driven by the entropically favourable loss of dinitrogen. Extreme care must therefore be taken when considering syntheses either generating or employing such reagents. The nature of the counter anion used is critical to the stability of these species; halide anions which are often found in the literature should be avoided at all costs as these display very poor stability. Tetrafluoroborate and tosylate anions such as those used in the entirety of this project display vastly increased thermal and shock sensitivity.[93] All of the aryldiazonium salts used in this project and others[131,132] were stored at −18 °C over a period of many months and no decomposition was ever observed. The safe use of aryldiazonium salts has been demonstrated extensively,[106] with in situ formation from the corresponding anilines,[107,108] often coupled with flow technology,[104,105] a common approach used to limit handling of the crystalline salts of these species.

Table 5 Synthesis of aryldiazonium tetrafluoroborates.
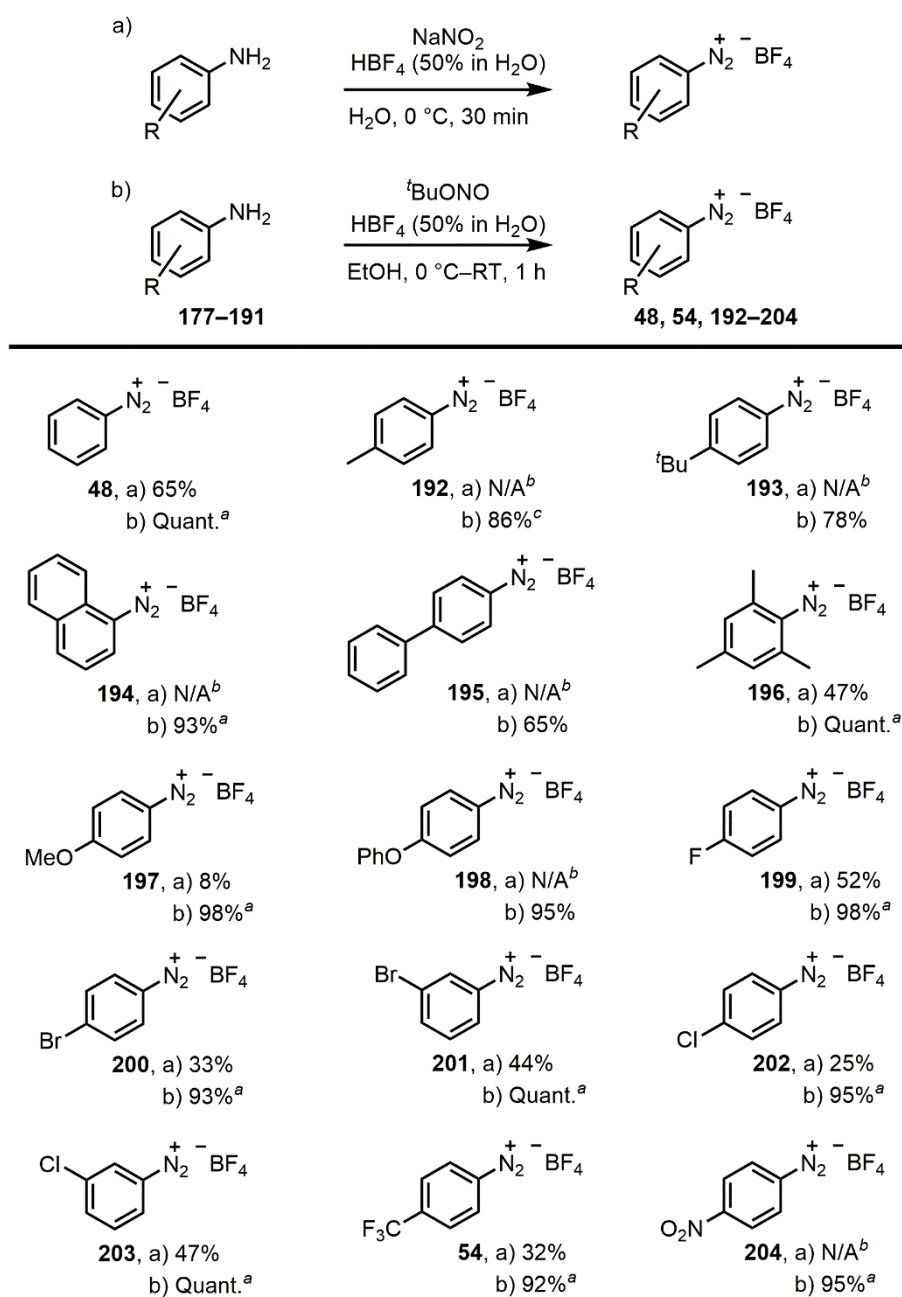
a Reaction performed by A. Hammarback. *b* Reaction not performed. *c* Reaction performed by T. Sheridan.

When tryptophan **74** was treated with one equivalent of benzenediazonium salt **48**, in the presence of catalytic Pd(OAc)$_2$ in ethyl acetate, the desired arylation product **75** was obtained in quantitative yield after 16 h at room temperature (typically 20 °C). These conditions were then extended across the range of diazonium salts shown in **Table 5**, to generate several functionalised 2-aryltryptophans, the results of which are shown in **Table 6**.

Table 6 Scope of aryldiazonium tetrafluoroborate salts for the direct arylation of tryptophan **74**.[a]

75, quant.   76, quant.   205, quant.

206, quant.   207, quant.   142, 83%[b]

77, quant.[b]   208, quant.   120, quant.

79, quant.   209, quant.   210, 73%

211, 63%   78, 0%   212, 0%
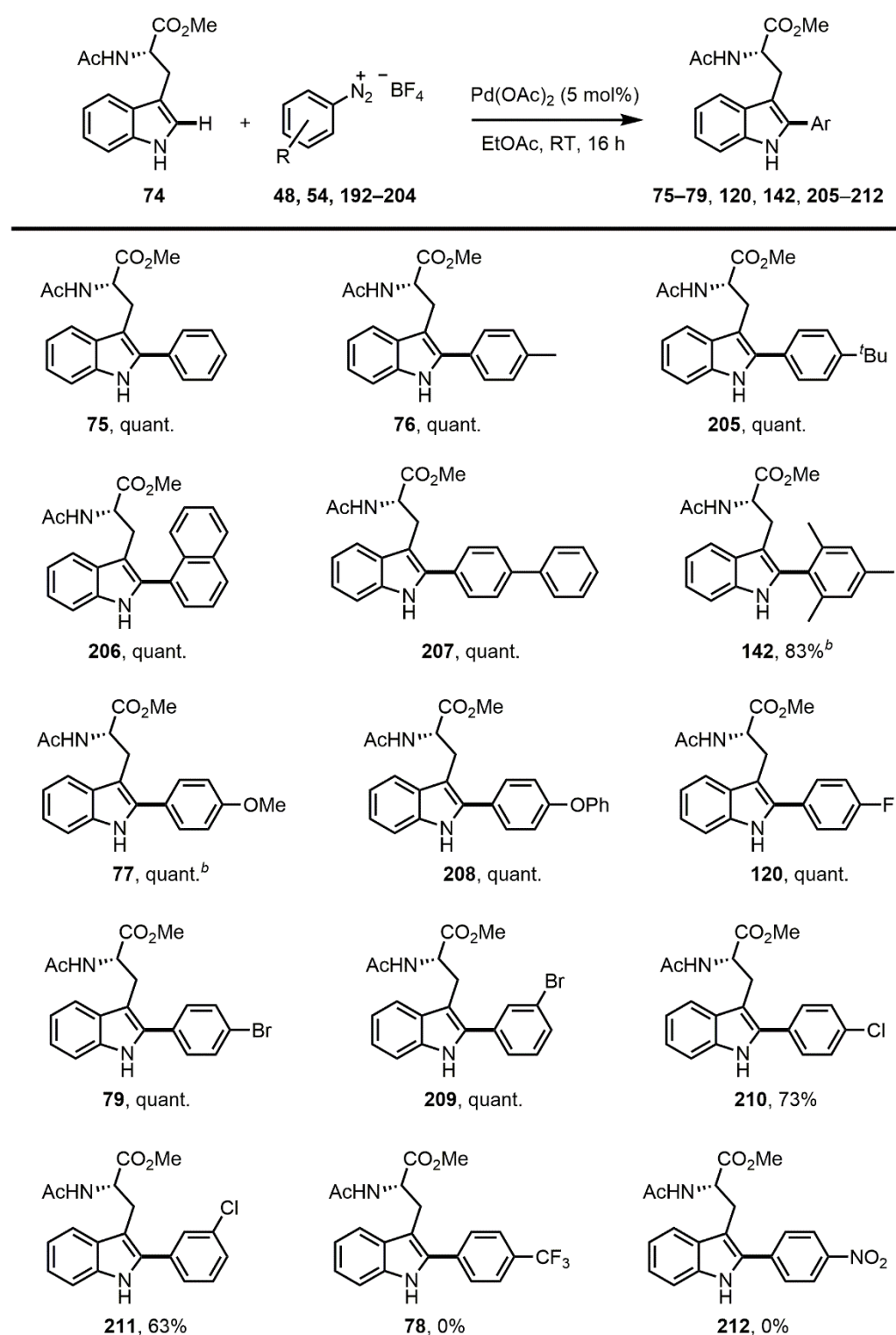
[a] All reactions conducted with **74** (50 mg, 0.192 mmol, 1 eq.), aryldiazonium salt (0.192 mmol, 1 eq.), Pd(OAc)$_2$ (2.2 mg, 9.6 μmol, 5 mol%) and EtOAc (5 mL) at RT (*ca.* 16–23 °C). [b] Reaction time extended to 24 h.

Alkylated, electron-donating and halide-containing examples provided good to excellent yields, while the sterically encumbered 1-napthyl and 2,4,6-trimethylphenyl salts also proved

effective (giving **206** and **142**, respectively). The quantitative synthesis of the biphenyl-substituted product **207** provided access to a product exhibiting fluorescence at long-wave UV light (excitation at 365 nm), markedly distinct from that of the single arene-containing examples or the parent compound **74**. Additionally, the tolerance of the synthetic protocol towards halogenated arenes provides a useful orthogonality to further functionalisation to produce, for example, other biaryl derivatives. It is important to note that aryldiazonium salts containing strongly electron-withdrawing substituents (**54** and **204**) were not tolerated by this arylation protocol, an observation also made by Correia and co-workers[102] who describe the formation of a diazo side product generated by the nucleophilic attack of a *C2*-arylated indole on electron-deficient aryldiazonium salts.

Peptides **136** and **138** which had previously demonstrated oxidative sensitivity to the Cu^{II}-mediated reaction conditions (**Scheme 47**) were also subjected to the optimised aryldiazonium salts conditions, affording the desired arylation products **137** and **139** in excellent conversion, with no evidence of the undesired aromatic dihydroxylation (**Scheme 59**). The solvent was switched to *iso*-propanol and the catalyst loading increased to ensure quantitative conversion of these challenging polar substrates.
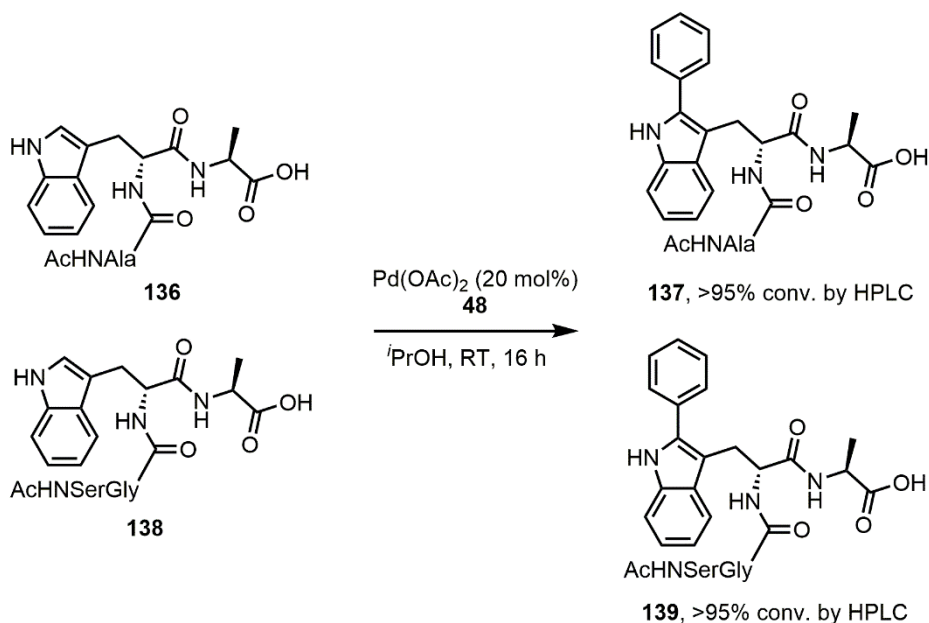
Scheme 59 Selective functionalisation of peptides using aryldiazonium salts.

During investigation of the mechanism for this reaction in a related project,[131] it was found that addition of catalytic quantities of acid had a profound impact, removing the observed induction period and thus accelerating conversion to product. When using 5 mol% of *p*-toluenesulfonic acid (TsOH), the reaction reached completion within *ca.* one hour at 37 °C, compared to two hours without acid (at 37 °C). As catalytically active cyclometallated Pd–

OTs complexes have been reported by both Brown[133] and Bedford[134] *et al*. (**Figure 15**), complex **215** was prepared according to literature procedures (**Scheme 60**).
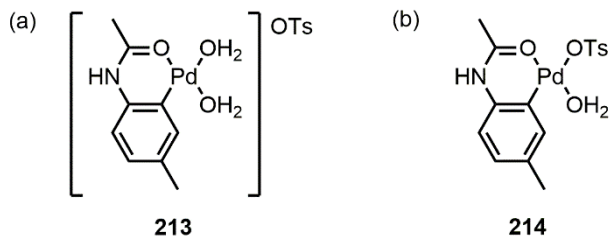
Figure 15 Cyclometallated Pd–OTs complexes reported by (a) Brown *et al*. and (b) Bedford *et al*.
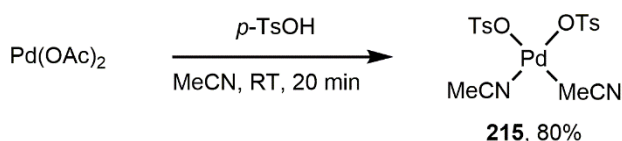
Scheme 60 Synthesis of Pd(OTs)$_2$(MeCN)$_2$ **215**.

Complex **215** was then tested in the arylation protocol detailed above in place of Pd(OAc)$_2$ (**Table 6**), where it was found that the catalyst loading could be decreased to 1 mol%, and still provide the desired arylation product **75** in quantitative yield after 16 h at room temperature (**Scheme 61**).
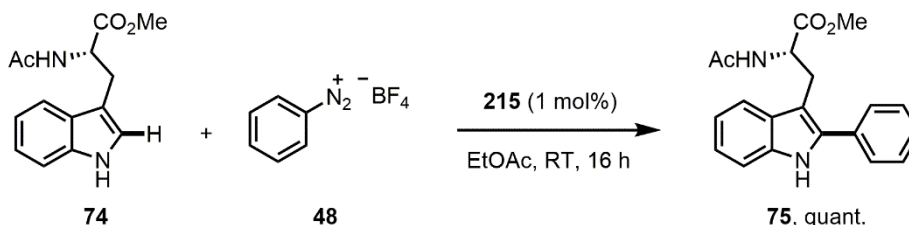
Scheme 61 Direct arylation of tryptophan **74** at 1 mol% Pd loading.

An experiment was also performed to demonstrate that sub-stoichiometric quantities of MeCN were not inhibiting the reaction (**Scheme 62**).
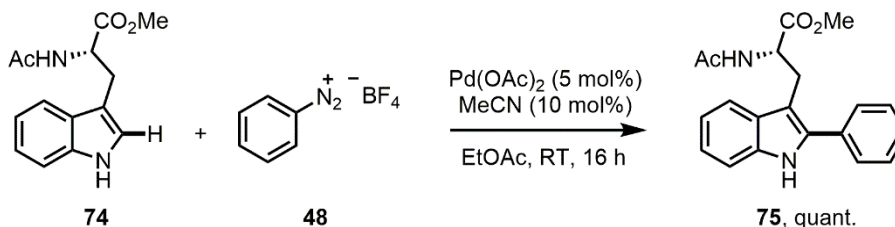
Scheme 62 Effect of MeCN on direct arylation of tryptophan **74** using aryldiazonium salts.

The scope of the arylation protocol using this catalytic system was also explored (**Table 7**).

Table 7 Scope of aryldiazonium tetrafluoroborate salts for the direct arylation of tryptophan **74** using a Pd–OTs catalytic system.[a]

75, quant.[c]	**76**, quant.	**205**, quant.
206, quant.	**207**, quant.	**142**, 75% (72%,[b] 45%[c])
77, quant. (49%,[b] 40%[c])	**208**, quant.	**120**, quant.
79, quant.	**209**, 69%	**210**, 80%
211, 80%	**78**, 0%	**212**, 0%
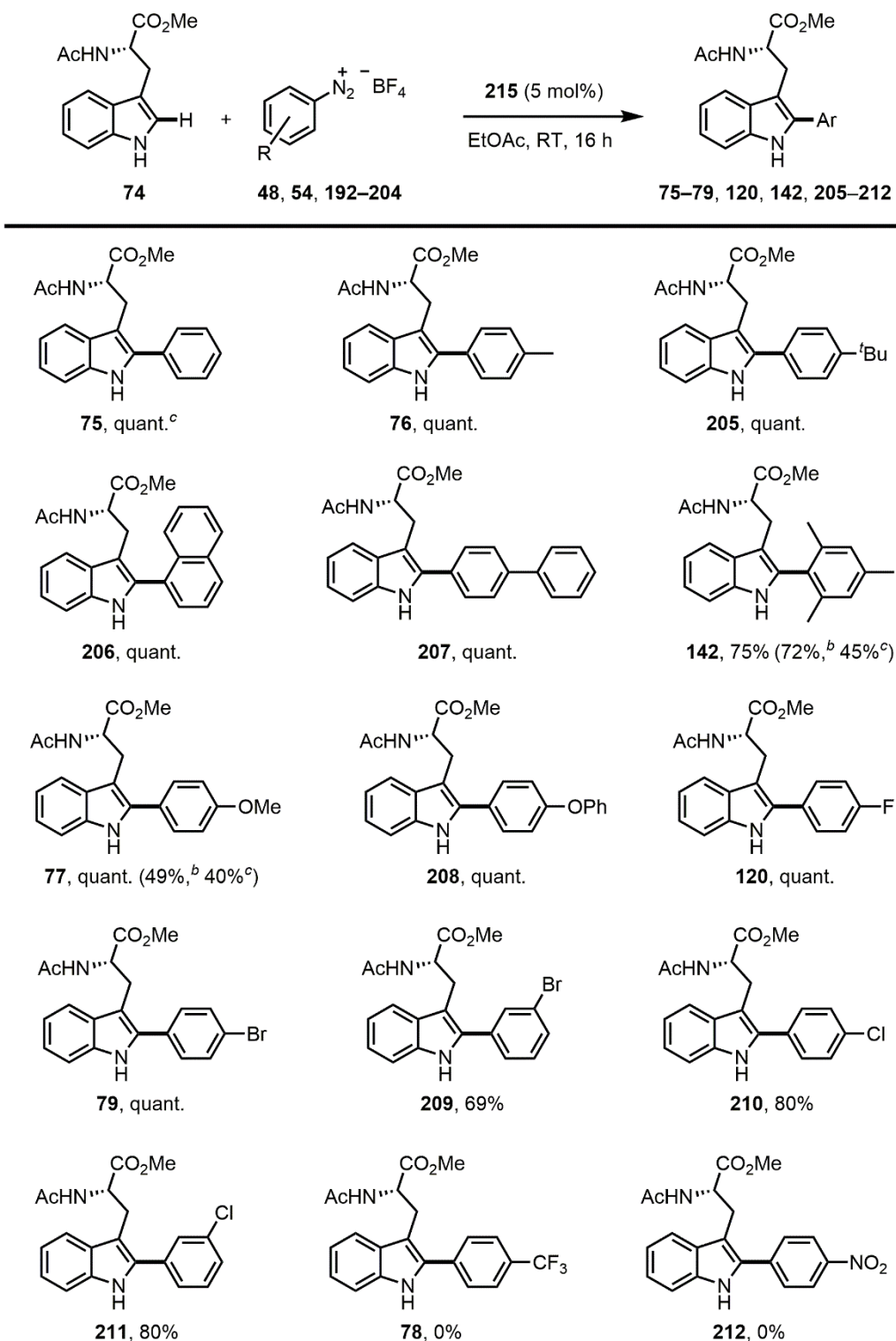
[a] All reactions conducted with **74** (50 mg, 0.192 mmol, 1 eq.), aryldiazonium salt (0.192 mmol), Pd(OTs)$_2$(MeCN)$_2$ (5.1 mg, 9.6 µmol, 5 mol%) and EtOAc (5 mL) at RT (*ca.* 16–23 °C). [b] Conversion when using 2.5 mol% catalyst, as determined by ^{1}H NMR spectroscopic analysis of the crude reaction mixture following an aqueous workup. [c] Conversion when using 1 mol% catalyst, as determined by ^{1}H NMR spectroscopic analysis of the crude reaction mixture following an aqueous workup.

The scope of the arylation protocol using the catalytic system in Scheme 61 was explored initially (1 mol% Pd), however several analogues displayed decreased activity at catalyst loadings below 5 mol%, so 5 mol% Pd and a reaction time of 16 hours was used for the majority of substrates tested (Table 7). This provided the desired products in isolated yields comparable to those obtained using the previous reaction conditions (Table 6).

2.4 Product Characterisation

^{1}H NMR spectroscopic analysis of **75** in CDCl$_3$ confirmed the loss of the diagnostic *C*-2 proton from δ 6.97 ppm, with retention of the indole NH as a broad singlet at δ 8.20 ppm. The additional aromatic signals are observed as several unresolvable multiplets between δ 7.60–7.34 ppm. The C-terminus methyl ester has undergone an upfield shift from δ 3.70 ppm to δ 3.29 ppm, as has the *N*-terminus amide doublet at δ 5.79 ppm ($^3J_{H–H} = 8.0$ Hz) and singlet at δ 1.66 ppm. A similar upfield shift of the enantiomeric proton at δ 4.84 ppm (dt, $^3J_{H–H} = 8.0, 5.0$ Hz) can also be observed. Conversely, the two diastereotopic protons have undergone a downfield shift, to δ 3.55 ppm and δ 3.52 ppm. These signals are even more misleading than before due to a substantial roofing effect, resulting from a small difference in chemical shift ($δ_a − δ_b = 0.03$ ppm), rendering the $^2J_{H–H} = 15.0$ Hz coupling almost impossible to observe (**Figure 16**).
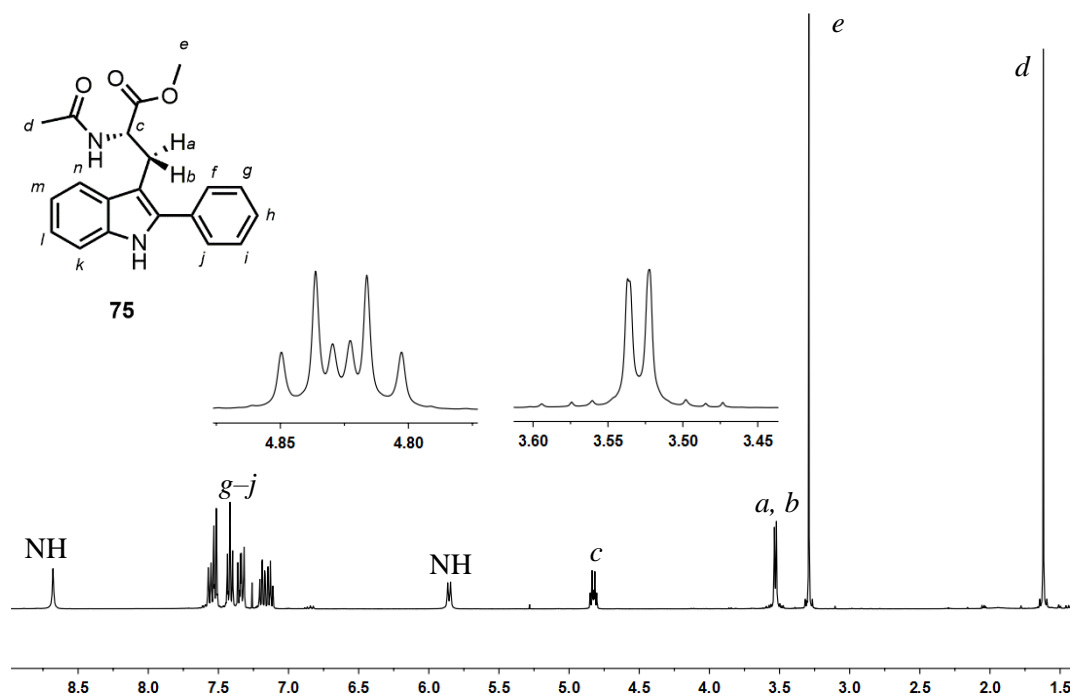
Figure 16 ^{1}H NMR spectrum of **75** (400 MHz, CDCl$_3$).

86

Single crystal X-ray diffraction structures of **75**, **142** and **210** were obtained (**Figure 17**–**Figrre 19**); the absolute stereochemistry of **210** was determined and the product confirmed as *S* (identical stereochemistry to the L-tryptophan starting material **74**). These structures all demonstrate that the installed aromatic group lies orthogonal to the indole ring in the solid state, which is presumably the ground-state configuration given that the single crystals grown to provide these structures were obtained by simple evaporation under ambient conditions. Presumably the aromaticity of these compounds is lessened as a result of the out-of-plane configuration across their conjugated ring systems.
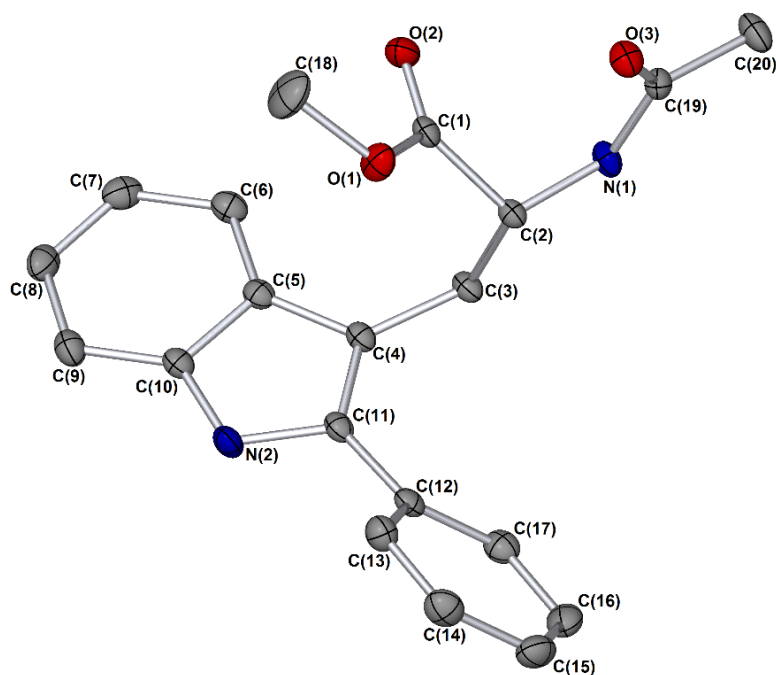
Figure 17 Single crystal X-ray diffraction structure of **75**. Thermal ellipsoids shown with 50% probability and hydrogen atoms removed for clarity. Selected bond lengths (Å): C(3)–C(4): 1.500(3), C(4)–C(11): 1.375(3), N(2)–C(11): 1.388(2), C(11)–C(12): 1.475(3). Selected bond angles (°): C(4)–C(11)–C(12): 131.75(18), N(2)–C(11)–C(12): 118.71(17).
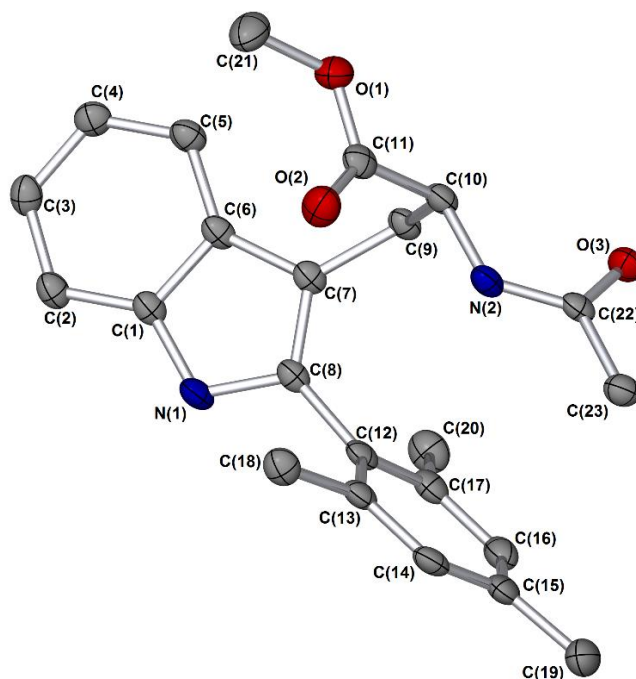
Figure 18 Single crystal X-ray diffraction structure of **142**. Thermal ellipsoids shown with 50% probability and hydrogen atoms removed for clarity. Selected bond lengths (Å): C(7)–C(9): 1.506(3), C(7)–C(8): 1.378(3), N(1)–C(8): 1.378(3), C(8)–C(12): 1.484(3). Selected bond angles (°): C(7)–C(8)–C(12): 128.9(2), N(1)–C(8)–C(12): 121.8(2).
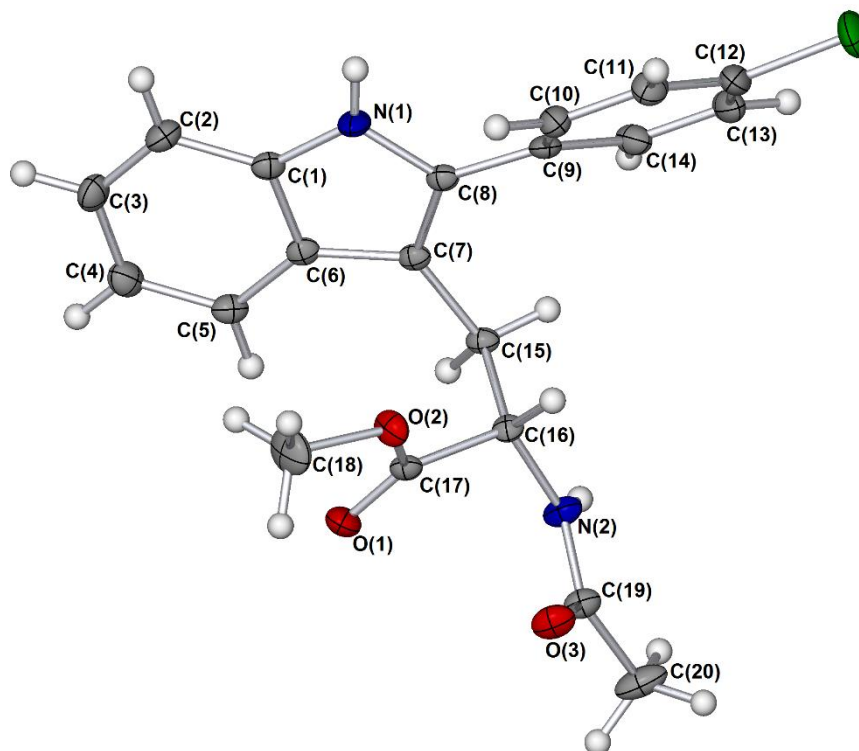
Figure 19 Single crystal X-ray diffraction structure of **210**. Thermal ellipsoids shown with 50% probability and absolute stereochemistry established by anomalous dispersion. Selected bond lengths (Å): C(7)–C(15): 1.500(2), C(7)–C(8): 1.369(3), N(1)–C(8): 1.382(3), C(8)–C(9): 1.475(3), C(12)–Cl(1): 1.743(2). Selected bond angles (°): C(7)–C(8)–C(9): 131.44(17), N(1)–C(8)–C(9): 119.04(16).

2.5 Green Metrics

For the tryptophan analogues where complete substrate conversion was recorded the desired arylation product could be isolated without the need for silica gel flash column chromatography, which provided a distinct practical benefit over the equivalent diaryliodonium salt methodologies, in addition to the selective formation of one arylation product. This advantage is reflected through calculation of some simple green metrics, comparing the two novel protocols detailed in this chapter with the Fairlamb group's previously developed conditions, which were produced using the Chem21 unified metrics toolkit for the simple phenyl derivative **75** (**Table 8**).[135]

Table 8 Comparison of mass-based metrics for several direct arylation conditions.[a]

Entry	1	2	3	4
Additives	PhI(OAc)$_2$ / PhB(OH)$_2$	PhB(OH)$_2$ / Cu(OAc)$_2$	[PhMesI]OTf	[PhN$_2$]BF$_4$
Yield / %	56	93	85	100
Temp. / °C	40	40	25	RT
Solvent	AcOH	AcOH	EtOAc	EtOAc
AE	48	88	46	74
RME	16	62	24	74
OE	33	70	52	100
MI	6902	4139	4504	602

[a] Calculated using the Chem21 unified metrics toolkit.[135] AE = atom economy, RME = reaction mass efficiency, OE = optimum efficiency, MI = (total) mass intensity.

In addition to an increase in yield and decrease in reaction temperature from our initial set of conditions, several key mass-based metrics have been improved upon. Those conditions which utilise hypervalent iodine reagents (**Table 8**, Entries 1 and 3) have noticeably lower values for atom economy (AE), the theoretical maximum efficiency for a transformation. While the Cu^{II} co-catalysed conditions (**Table 8**, Entry 2) do not suffer from this, they do however require the undesirable addition of a second transition metal (in addition to the drawbacks with certain peptides highlighted above). These trends are also observed for the reaction mass efficiency (RME), which incorporates both yield and stoichiometry to the

simpler AE calculation, thus giving a measure of the observed reaction efficiency as compared to the theoretical value provided by AE. This can be rationalised through use of the optimum efficiency metric, which directly correlates these two factors, highlighting the aryldiazonium salt methodology (**Table 8**, Entry 4) as the most atom- and mass-efficient overall.

The most striking improvement can be seen in the mass intensity (MI) value, which is an order of magnitude lower for the aryldiazonium salt conditions (**Table 8**, Entry 4) as compared to the initial conditions (**Table 8**, Entry 1). The primary reason for this dramatic increase is the removal of purification by flash column chromatography, with other secondary effects including the number of equivalents of arylating agent used for each set of conditions. Finally, switching the reaction solvent from neat acetic acid to the more benign ethyl acetate has a demonstrable health impact, as acetic acid has been ranked as a 'problematic' reaction solvent by the recently-published Chem21 solvent selection guide[136] (while ethyl acetate is ranked as 'recommended').

2.6 Conclusion

Several different and complementary protocols for the direct Pd-mediated *C*2-arylation of tryptophan **74** have been developed and shown to proceed under mild conditions. In order to address issues involving undesirable peptidic dihydroxylation in a Pd/Cu co-catalytic system, protocols applying electrophilic diaryliodonium salts have been demonstrated to afford high conversions when applied to both single tryptophan residues and tryptophan-containing peptides. Asymmetric variants of these salts have shown good selectivity, albeit with a small amount of undesirable donation of the dummy aromatic component. To address this issue, aryldiazonium salts have been successfully applied to this transformation to afford several aryltryptophan analogues in excellent yield, in addition to the selective functionalisation of two peptides shown to be incompatible with previous reaction conditions. Calculation of several key green metrics has shown that these latter conditions also offer a significant improvement over previously reported methods in terms of optimum efficiency, mass intensity, synthetic utility and selectivity. Use of a Pd–OTs catalytic system has also been shown to allow for a significant decrease in catalyst loading in some cases.

Part of the work described in this chapter has been included in several recent publications (see Appendix 1).[119,137]

Chapter 3: Direct Arylation Reactions Using Heterogeneous Catalysis

3.1 Background

The importance of Pd-mediated reactions in organic synthesis is without question, as the ability to selectively form carbon–carbon bonds in the presence of other molecular functionality is unparalleled in its utility (see Chapter 1). The issue that remains however is the elemental sustainability of this rare and precious metal, which increasingly leads to prohibitive costs and issues surrounding the criticality of supply chains.[138] One solution to this problem is to research the potential of mediating selective C–C bond formation by using cheaper and more elementally-sustainable first-row transition metals, such as Mn,[139,140] Fe[141,142] or Co.[143-145] An alternative approach is to determine whether current Pd catalysts can be used more effectively, by recycling the precious metal from each reaction and preventing it from entering waste streams.[37-40] Central to this latter approach is to understand that many ubiquitous Pd (pre)catalysts often display heterogeneous-type catalytic behaviour, typically through speciation to form higher-order Pd colloids or nanoparticles under commonly-found experimental conditions. This is evident in both Pd-mediated cross-coupling and more recently in C–H bond functionalisation reactions; the activity of pre-formed PdNP catalysts can therefore be evaluated and compared to their *in situ* counterparts in such reactions.[57] Studies by the Fairlamb group on the direct arylation of benzoxazole **216** and benzothiazole **218** under Pd/Cu-catalysed reaction conditions demonstrated a significant deleterious air effect when Pd(OAc)$_2$ was used as a catalyst (**Scheme 63**).[57]

a)

216

I–⟨⟩ **1**

[Pd] (5 mol%)
CuI, CsF, DMF
120 °C, 24 h

217: Pd(OAc)$_2$, 27%
    Pd(OAc)$_2$, 71% (Schlenk)
    PVP–Pd **13**, 79%

b)

218

218: Pd(OAc)$_2$, 23%
    Pd(OAc)$_2$, 53% (Schlenk)
    PVP–Pd **13**, 59%
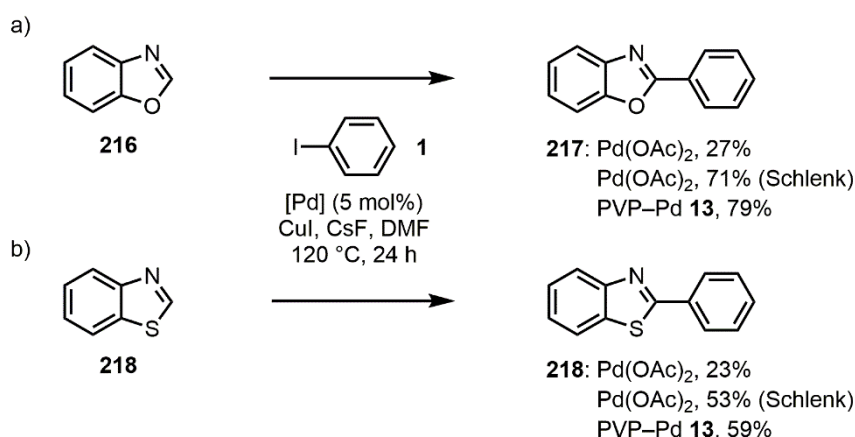
Scheme 63 Direct arylation using Pd(OAc)$_2$ and PVP–Pd of a) benzoxazole **216** and b) benzothiazole **218**.

TEM analysis of the reaction mixtures demonstrated that the nanoparticles generated from Pd(OAc)$_2$ were larger and more varied in size under Schlenk conditions, suggesting that these larger particles were more active under the reaction conditions. If the pre-synthesised nanoparticle catalyst PVP–Pd **13** was applied in place of Pd(OAc)$_2$ however, rigorous exclusion of air (under typical Schlenk conditions) was found to be no longer necessary to achieve equivalent conversion to product. The PdNPs obtained from this catalyst are however much smaller (*ca.* 2 nm) than those formed from Pd(OAc)$_2$ under air-free conditions (*ca.* 6 nm), suggesting that the PVP polymer may have prevented oxidative leaching in this example. A long-term study on the stability of PVP–Pd catalysts by McGlacken *et al.* concludes that low-index particles display preferential susceptibility to oxidation on their high-energy facets, such as the (110) facets found on nanocubes. Correspondingly, octahedral particles display greater stability as they contain mostly lower-energy (111) facets. Conversely particles containing high-index surfaces, such as concave nanocubes, displayer superior stability due to stronger chemisorption to the PVP polymer.[146]

Sanford's reaction conditions for the direct arylation of indoles with Pd(OAc)$_2$, using a mixture of **14** and **22** in acetic acid,[81] were also observed by Fairlamb and co-workers to produce visible PdNPs within seconds of substrate addition. This discernible formation of Pd^0 contrasts with the Pd$^{II/IV}$ catalytic manifold proposed to operate in this system, although such precipitates could simply exist as a catalyst deactivation pathway. If the nominally heterogeneous catalyst PVP–Pd **13** was applied in place of Pd(OAc)$_2$ however, a significant quantity of the desired arylation product **34** was formed (**Scheme 64**), providing evidence for Pd$^{0/II}$ catalysis.[57]
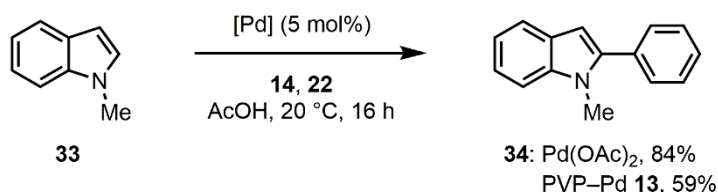
Scheme 64 Direct arylation of N-methylindole using Pd(OAc)$_2$ and PVP–Pd **13**.

When analogous examination was applied to the direct arylation of tryptophan **74** using similar conditions, rapid propagation of PdNPs was again observed to occur within minutes, presumably concomitant with substrate turnover. Importantly, an aliquot taken from this reaction and analysed by TEM demonstrated the presence of PdNPs of *ca.* 2 nm in size. When the nanoparticulate catalyst PVP–Pd **13** was again used in place of Pd(OAc)$_2$ under otherwise identical conditions, an equivalent yield of isolated product **75** was obtained, demonstrating the utility of nominally heterogeneous Pd catalysts in this manifold (**Scheme 65**).
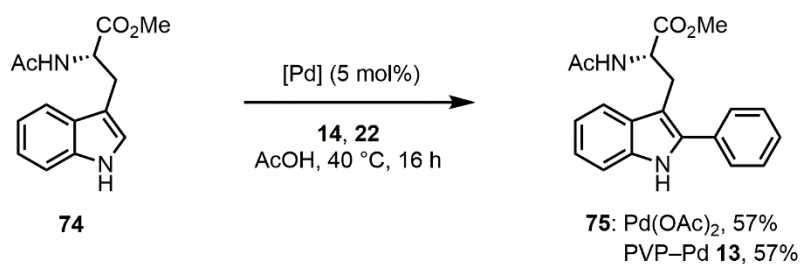
Scheme 65 Direct arylation of tryptophan **74** using Pd(OAc)$_2$-derived and supported PdNPs.

While the PVP–Pd catalyst **13** used in the examples above demonstrates excellent versatility and reproducibility in terms of its nanoparticle size and morphology, it could be argued that bespoke catalysts such as this will always have an intrinsically lower utility than those with widespread commercially availability, particularly within time-critical industries such as drug discovery. This leads to the conclusion that research efforts should be directed towards the re-appropriation of more commonly available heterogeneous Pd catalysts for direct C–H bond functionalisation chemistry. Palladium supported on activated carbon (Pd/C), widely used as a heterogeneous hydrogenation catalyst for many years, has also attention for its utility in the formation of carbon–carbon bonds in cross-coupling catalysis.[37-40] Glorius and co-workers have recently described the use of this catalyst for the direct arylation of benzo[*b*]thiophenes with aryl chlorides, to afford a range of *C*3-arylated products with excellent regioselectivity (**Scheme 66**).[147]
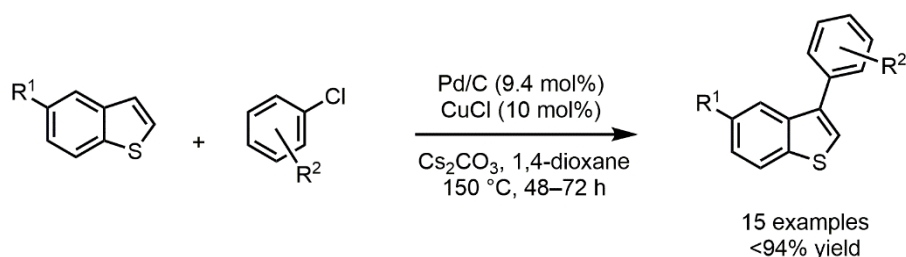
Scheme 66 Direct *C*3-arylation of benzo[*b*]thiophenes with aryl chlorides using Pd/C.

Several tests for heterogeneous catalysis[20] were performed and no active homogeneous Pd species could be detected under the reaction conditions; rapid stirring was also found to be critical to ensure good conversion to product, which is often suggestive of heterogeneous catalysis. Several nominally homogeneous Pd sources such as Pd(OAc)$_2$ proved able to catalyse this reaction, although fascinatingly these demonstrated a complete switch in regioselectivity to form exclusively the *C*2-arylated products. Subsequent development by the same group on the arylation of thiophenes, benzo[*b*]thiophenes and other related heterocycles demonstrated that a switch from aryl chlorides to diaryliodonium salts allowed for much milder conditions to be applied (**Scheme 67**).[148]
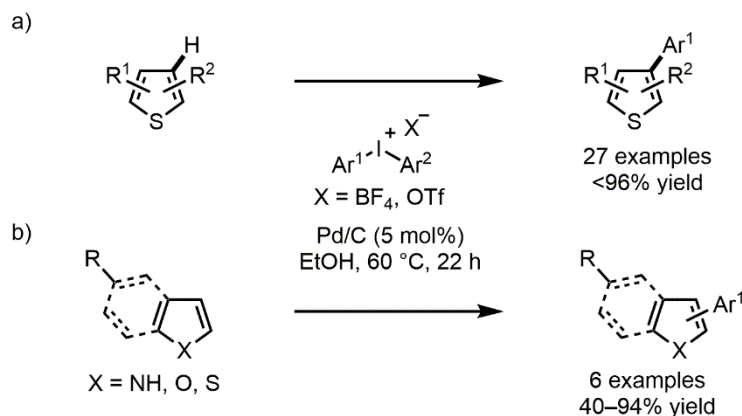
Scheme 67 Direct arylation using Pd/C of a) thiophenes and b) related heterocycles.

The same heterogeneity tests as in their previous work were performed and again these demonstrated evidence of heterogeneous catalysis, although poor catalyst recyclability was also observed which suggested that Pd leaching likely occurred under these oxidising conditions. Pd leaching is also suggested as the source of catalytically active palladium in later work from the same group, which detailed the direct arylation of triphenylene **220**, naphthalene **221** and other polyaromatic hydrocarbons (PAHs) using Pd/C. In many of these examples, functionalisation of the most hindered C–H bond typically occurred, giving generally high α:β selectivity in the products obtained (**Scheme 68**).[149]
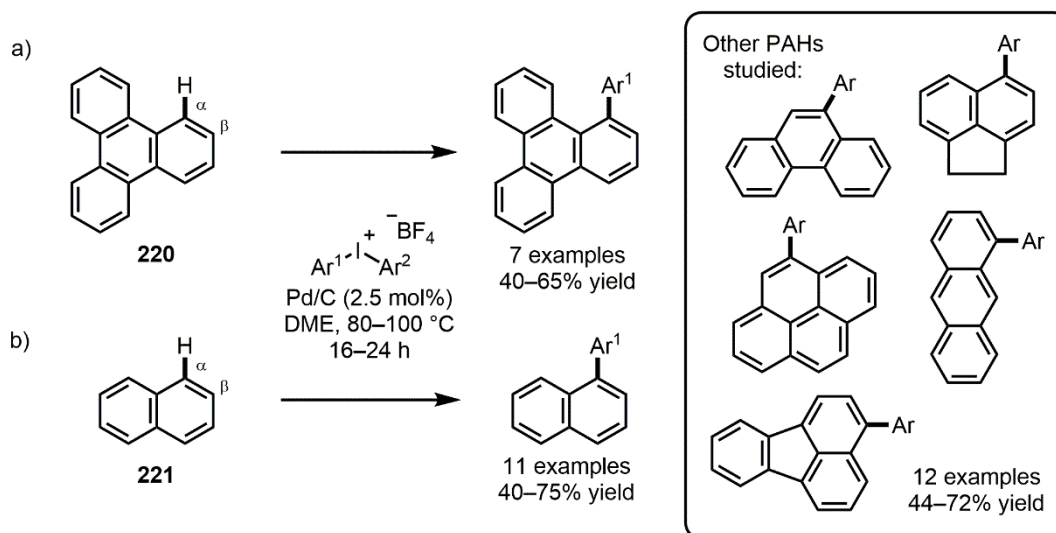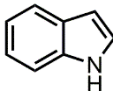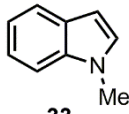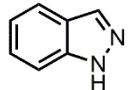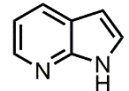
Scheme 68 Direct arylation of PAHs using Pd/C including a) triphenlyene **220** and b) naphthalene **221**.

The relevance of higher-order Pd species in C–H bond functionalisation processes and the activity of pre-synthesised PdNPs encapsulated by a wide variety of supports (including Pd/C) in this chemistry has recently been reviewed in detail (see Appendix 1).[20]

94

3.2 Direct Arylations Using Aryldiazonium Salts

The mild and atom efficient conditions for the direct arylation of tryptophan **74** using aryldiazonium salts previously developed in this project (see Chapter 2) represent a synthetically useful method of performing direct arylation reactions, without the stoichiometric iodoarene waste usually generated from their electrophilic iodine(III) counterparts, diaryliodonium salts. It was hypothesised that combination of these atom efficient coupling partners with recyclable heterogeneous Pd catalysis would represent a significant improvement in the sustainability of direct arylation processes, as well as generating valuable novel methodology. Thus far, the combination of heterogeneous PdNPs with aryldiazonium salts has been limited to applications in the Suzuki–Miyaura,[97] Heck–Matsuda[98,104] and Stille[99] cross-couplings. Initial efforts at developing a general direct arylation methodology focused on the attempted reaction of several simple yet medicinally relevant nitrogen heterocycles.[150] Reaction of indole **45** or *N*-methylindole **33** with phenyldiazonium salt **48** and Pd(OAc)$_2$ at 60 °C afforded a complex mixture of products due to violent reaction with **48**, so were abandoned as substrates (**Table 9**, Entries 1 and 2). Indazole **222** was unreactive under these conditions, purification of this reaction mixture by silica gel column chromatography afforded complete recovery of starting material (**Table 9**, Entry 3). 7-azaindole **223** was unstable under these conditions, so two further reactions were performed at reduced temperatures (40 °C and room temperature), which prevented decomposition but afforded no conversion of starting material (**Table 9**, Entry 4).

Table 9 Nitrogen heterocycle screening for direct arylation with phenyldiazonium salt **48**.[a]

Entry	Substrate	Reaction outcome
1	**45**	Complex mixture obtained
2	**33**	Complex mixture obtained
3	**222**	No reaction
4	**223**	Decomposition of starting material[b]

[a] All reactions conducted with substrate (0.30 mmol, 1 eq.), **48** (58 mg, 0.30 mmol, 1 eq.), Pd(OAc)$_2$ (3.4 mg, 0.015 mmol, 5 mol%) and EtOAc (3 mL) at 60 °C for 22 h. [b] Analogous reactions of this substrate at 40 °C and RT showed no conversion of starting material.

In an attempt to address the lack of reactivity of indazole **222**, the free NH group was protected according to literature conditions[151,152] using methyl iodide and base, providing the desired methyl indazole **224** in good yield (**Scheme 69**).
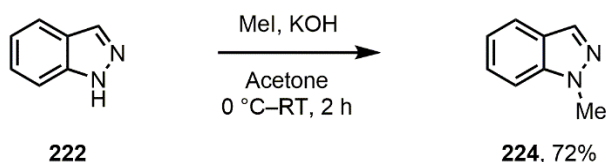
Scheme 69 Methyl protection of indazole **222**.

224 was then subjected to the conditions described in **Table 9**, Entry 3, but no conversion of starting material was observed (**Scheme 70**).
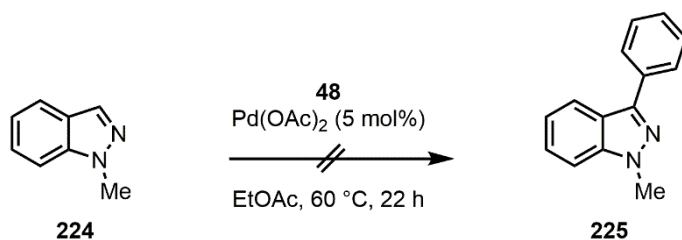
Scheme 70 Attempted direct arylation of **224**.

Carbonyl-containing protecting groups were proposed as an alternative to methyl protection, as these could potentially aid coordination of the Pd catalyst, facilitating C–H bond functionalisation. Reaction of **222** with ethyl trifluoroacetate **165** under basic conditions in either THF or acetonitrile however afforded no conversion to the desired *N*-Tfa protected indazole **226** (**Scheme 71**).
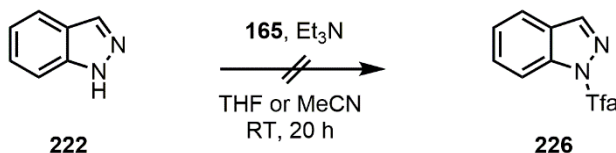
Scheme 71 Attempted Tfa-protection of indazole **222**.

Reaction of **222** with Boc$_2$O under basic conditions[153] however proceeded smoothly to provide a single product by TLC analysis of the reaction mixture. Following purification by silica gel column chromatography a clear oil was obtained in a yield of 98%, ^{1}H NMR spectroscopic analysis of which subsequently revealed an equal mixture of two species (**Scheme 72**).
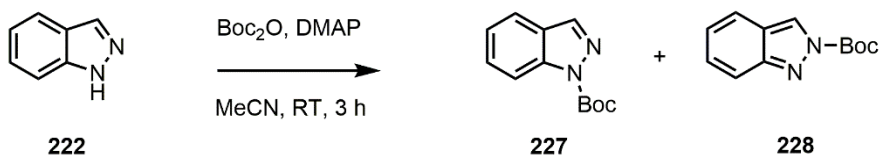
Scheme 72 Boc protection of indazole **222**.

One of these two species was confirmed as the desired *N*-Boc indazole **227** through comparison of the ^{1}H NMR signals with literature values, while the other is putatively assigned as **228**, obtained through isomerisation of the indazole **222** anion following deprotonation (**Scheme 73**).
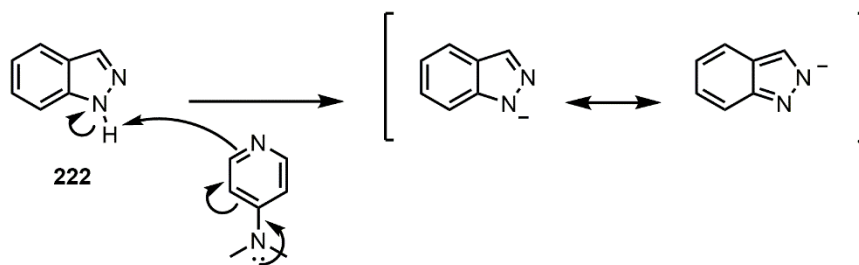
Scheme 73 Proposed isomerisation of indazole **222** following deprotonation.

Reaction of indazole **222** with Ac$_2$O under basic conditions also proceeded smoothly to give a single product by TLC analysis of the reaction mixture. Once again however, following purification a clear oil was obtained (in a yield of 79%) which ^{1}H NMR spectroscopic analysis demonstrated to be a mixture of two products, analogous to those formed in the attempted Boc protection (**Scheme 74**).
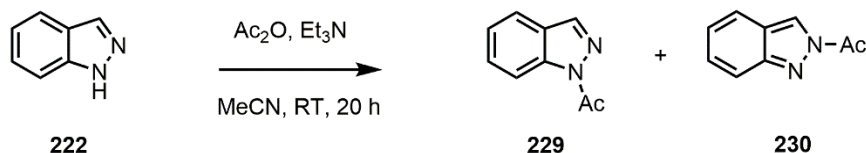
Scheme 74 Acetyl protection of indazole **222**.

Following this lack of success with indazole **222**, efforts were turned to the remaining nitrogen-containing heterocycle, 7-azaindole **223**. Reaction of **223** with methyl iodide[154] afforded the methyl protected azaindole **231** in high yield (**Scheme 75**).
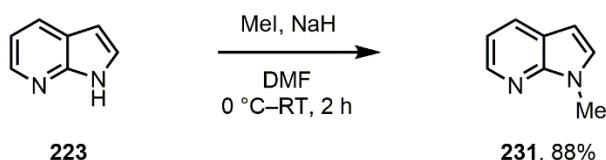
Scheme 75 Methyl protection of 7-azaindole **223**.

The attempted reaction of **231** with phenyldiazonium salt **48** in the presence of Pd(OAc)$_2$ at 40 °C in ethyl acetate afforded no conversion after 24 h. A switch of solvent to ethanol however provided the desired *C*2-arylation product in 39% conversion, as determined by ^{1}H NMR spectroscopic analysis (**Scheme 76**).
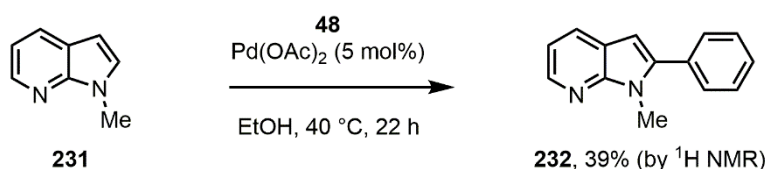
Scheme 76 Direct arylation of protected azaindole **231** with phenyldiazonium salt **48**.

Application of palladium on activated charcoal or PVP–Pd to this reaction afforded no conversion of starting material, even after 40 h at 60 °C (**Scheme 77**).
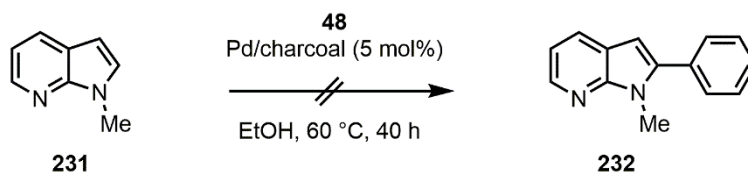
Scheme 77 Attempted direct arylation of **231** using heterogeneous Pd catalysts.

With all attempts at developing a general C–H bond functionalisation methodology to combine aryldiazonium salts with heterogeneous Pd catalysts stymied, the specific reaction between tryptophan **74** and phenyldiazonium salt **48** (Chapter 2) was examined. When palladium supported on activated carbon (Pd/C) was applied in place of the previously used Pd(OAc)$_2$ however, no reaction was seen in either ethyl acetate or ethanol at 60 °C (**Scheme 78**).
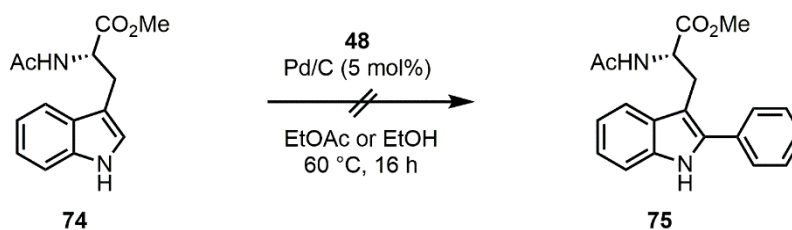
Scheme 78 Attempted functionalisation of tryptophan **74** mediated by Pd/C.

3.3 Direct Arylations Using Diaryliodonium Salts

3.3.1 Simple Nitrogen-Containing Heterocycles
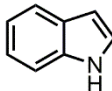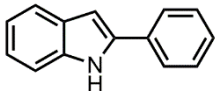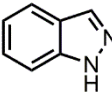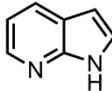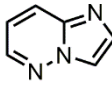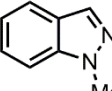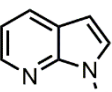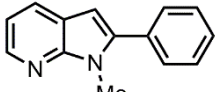
Due to the lack of success in combining heterogeneous Pd catalysis with atom efficient aryldiazonium salt coupling partners, a return to the use of diaryliodonium salts was proposed, as there is a greater body of evidence in the literature to suggest that these species can be mediated by heterogeneous Pd^0 catalysis (*vide supra*). To begin, the symmetric diphenyliodonium tetrafluoroborate salt **233** was synthesised in a one-pot process from iodobenzene **1** using the method of Olofsson and co-workers (**Scheme 79**).[155]
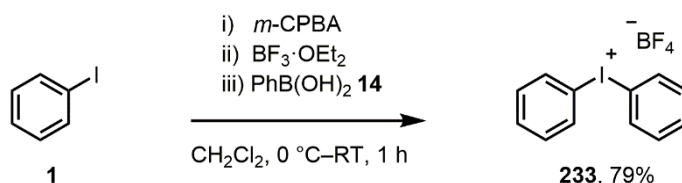
Scheme 79 Synthesis of diphenyliodonium tetrafluoroborate **233**.

The mild conditions published by Glorius *et al*. (**Scheme 67**)[148] utilising this species were then initially applied to a substrate screen of the same medicinally relevant nitrogen heterocycles as used previously,[150] the results of which are summarised in **Table 10**. Note that Pd(OAc)$_2$ was used in place of Pd/C for this initial screening. Under these conditions, indole **45** was successfully reacted to form the *C*2-arylated product **234** in moderate yield (**Table 10**, Entry 1). The heterocycles indazole **222** or 7-azaindole **223** were however unreactive under these conditions (**Table 10**, Entries 2 and 3). Pyridazine **235** and methylindazole **224** were similarly unreactive, an observation also made when these reactions were conducted over 4 days, or in ethyl acetate (**Table 10**, Entries 4 and 5). The methyl-protected azaindole **231** was however cleanly converted to give the *C*2-arylation product **232** in good yield (**Table 10**, Entry 6).

Table 10 Nitrogen heterocycle screening for direct arylation with diaryliodonium salt **233**.[a]
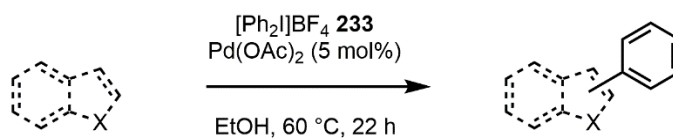
Entry	Substrate	Reaction outcome[b]
1	**45**	**234**, 55%
2	**222**	No reaction
3	**223**	No reaction
4	**235**	No reaction[c]
5	**224**	No reaction[c]
6	**231**	**232**, 79%

[a] All reactions conducted with substrate (0.30 mmol, 1 eq.), **233** (155 mg, 0.42 mmol, 1.4 eq.), Pd(OAc)$_2$ (3.4 mg, 0.015 mmol, 5 mol%) and EtOH (1.5 mL) at 60 °C for 22 h. [b] Where applicable, isolated yield following purification by silica gel flash column chromatography is provided. [c] Extension of the reaction time to 4 days showed no conversion of starting material, while analogous reactions of these substrates in EtOAc also demonstrated no conversion of starting material.

Following successful transformation of azaindole **231** mediated by Pd(OAc)$_2$, this substrate was then screened against a range of heterogeneous palladium sources to test their efficacy in this protocol (**Table 11**).

Table 11 Catalyst screen for direct arylation of azaindole **231**.[a]
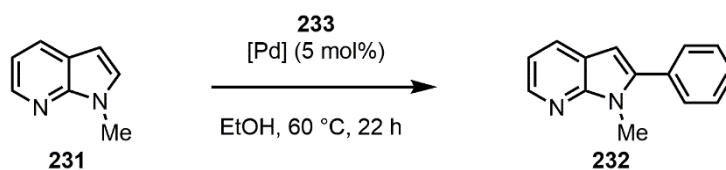
Entry	Pd catalyst	Conv. / %[b]
1	Pd/C (5 wt% Pd)	19
2	Pd/C (10 wt% Pd)	0
3	Pd/charcoal	100
4	Pd 'black'	0
5	Pd/CaCO$_3$/Pb (Lindlar catalyst)	3
6	Pd(OH)$_2$/C (Pearlman's catalyst)	0
7	PdO	0

[a] All reactions conducted with **231** (40 mg, 0.30 mmol, 1 eq.), **233** (155 mg, 0.42 mmol, 1.4 eq.), Pd catalyst (0.015 mmol, 5 mol%) and EtOH (1.5 mL) at 60 °C for 22 h. [b] As determined by ^{1}H NMR spectroscopic analysis of the crude reaction mixture following an aqueous workup.

Two different forms of palladium supported on activated carbon were tested, each containing a different Pd loading. In the first example, a catalyst containing 5% by weight palladium supported on activated carbon (Sigma Aldrich, catalogue number 205680) provided modest conversion to the desired product **232** (**Table 11**, Entry 1). Surprisingly, when the analogous catalyst containing 10% by weight palladium (Sigma Aldrich, catalogue number 205699) was tested, no activity was observed (**Table 11**, Entry 2). Even more surprisingly, when a catalyst containing 5% by weight palladium supported on activated charcoal (Sigma Aldrich, catalogue number 75992) was used, complete conversion to the desired product **232** was noted (**Table 11**, Entry 3). The heterogeneous Pd^0 catalysts Pd 'black' and the Lindlar catalyst provided no activity in this reaction (**Table 11**, Entries 4 and 5), while the heterogeneous Pd^{II} catalysts Pd(OH)$_2$/C and PdO were similarly unreactive (**Table 11**, Entries 6 and 7). These observations agree with those made by Glorius and co-workers, who noted severe incongruities in the activities and yields obtained thereof when utilising Pd/C from different commercial sources in this chemistry.[148] It is clear that differing manufacturing methods and even variances between batches of supposedly identical catalysts have to be

seriously considered in these reactions, as they will undoubtedly significantly impact on the size and morphology of the resultant Pd particles.

3.3.2 Biologically Relevant Heterocycles

With the proof that simple nitrogen heterocycles could be functionalised directly under relatively mild conditions, using a combination of heterogeneous palladium and diaryliodonium salts, the amino acid tryptophan was examined in order to provide an exemplification of this approach for more complex substrates. While commercially available Pd catalysts such as Pd/C present many practical advantages, the lack of control over particle size and morphology adds a significant element of irreproducibility to syntheses employing such catalysts. It was decided therefore that the PdNP catalyst PVP–Pd **13** would be tested alongside Pd/C, as its synthesis provides well-controlled, regular nanoparticles typically between 2–5 nm in diameter (*vide supra*).[32,33] Simple reduction of $PdCl_2$ with aqueous acid in the presence of a (poly)vinylpyrrolidone polymer **12** provides quantitative amounts of a well-dispersed nanoparticle catalyst (**Scheme 80**).
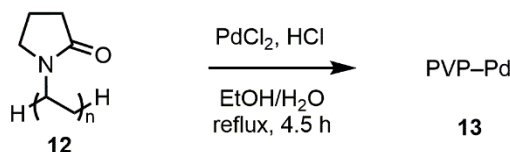
Scheme 80 Synthesis of PVP–Pd **13**.

The nanoparticles are prevented from thermodynamically favourable agglomeration through interaction with the amide functionality in the polymer **12**, creating a stabilising encapsulation effect (**Figure 20**).

Figure 20 Cartoon schematic of PdNP encapsulation in PVP–Pd **13**.

Analysis of these polymer-supported particles (8 wt% Pd) was performed by TEM, with several images recorded in order to ensure that data representative of the population as a whole was used for subsequent analysis. A typical image is shown in **Figure 21**, which indicates that well-defined PdNPs of approximately 3 nm in diameter are encapsulated by the PVP, remaining stable in the solid-state after evaporation of the reaction solvent. The images obtained all correlate well and have over 68% of the particles lying within the normal Gaussian distribution range (mean ± std. dev.).
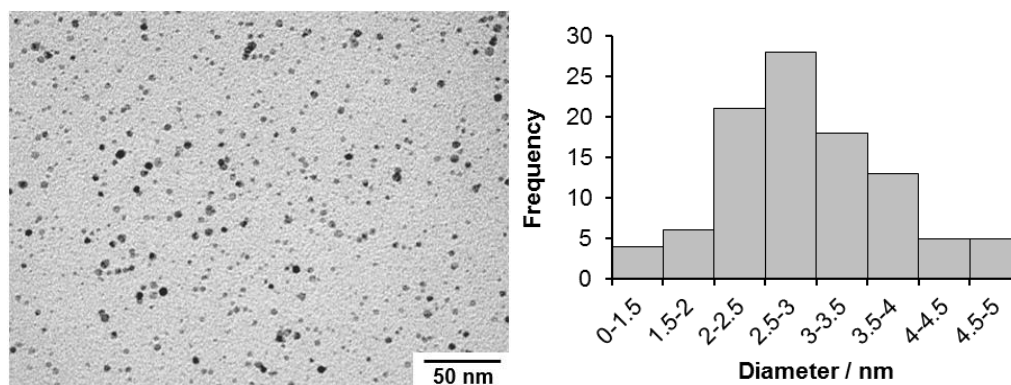
n = 100, mean = 2.98 nm, std. dev. 0.80, median = 3.00, mode = 3.30

Figure 21 TEM image and particle size analysis for PVP–Pd **13**.

Protected tryptophan derivative **74** was subjected to the previously optimised conditions for direct C–H bond functionalisation using the asymmetric diaryliodonium salt [PhMesI]OTf **140** (see Chapter 2), with PVP–Pd **13** used in place of Pd(OAc)$_2$; no conversion of starting material was observed under these conditions however (**Scheme 81**).
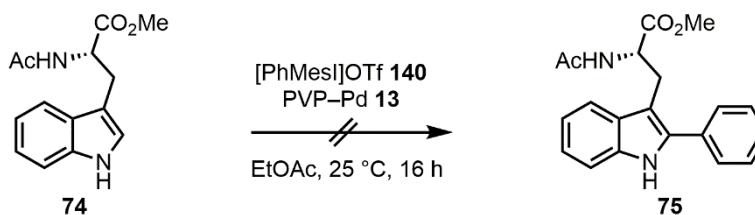
Scheme 81 Attempted functionalisation of tryptophan **74** with PVP–Pd **13**.

When performing this reaction, it was noted that the PVP–Pd **13** catalysed used had changed significantly in both colour and composition since its synthesis, approximately 30 months previously. Freshly synthesised this catalyst is a black crystalline solid; the sample used for the reaction in **Scheme 81** was a greyish powder containing large metallic particles, presumably of agglomerated Pd. This implies that this catalyst slowly decreases in stability over time when stored at ambient temperature under air, losing its coordination from the PVP polymer **12** and forming large unreactive Pd agglomerates, in an oxidative process as

suggested by McGlacken and co-workers.[146] PVP–Pd **13** was thus freshly synthesised and simple visual inspection highlighted the significant changes that had occurred over time (**Figure 22**). This catalyst was used for all of the experiments subsequently detailed in this chapter, except where specifically indicated otherwise.
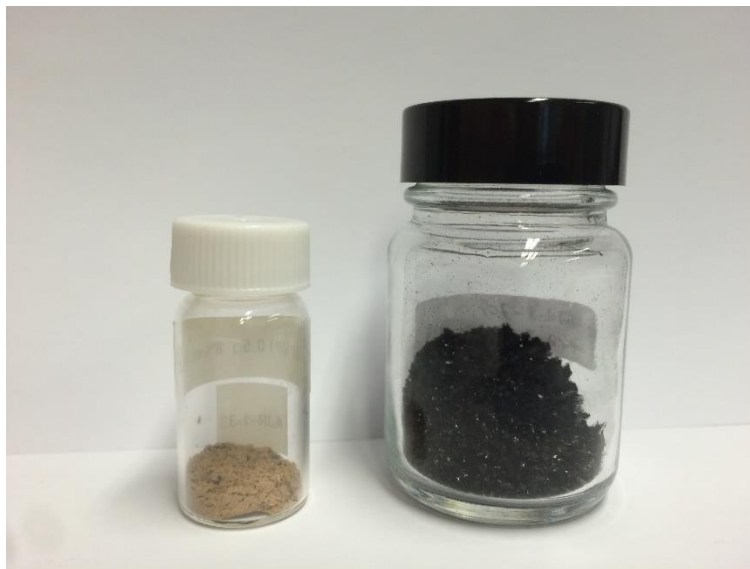
Figure 22 PVP–Pd **13** after approximately 30 months (left) and freshly-synthesised (right).

While these investigations were ongoing, a preparation of surfactant-free, DMF-stabilised PdNPs of approximately 1–1.5 nm in diameter was noted in the literature.[59] Recalling the high activity of DMF–PdNPs formed *in situ* in previous work from the Fairlamb group,[48,49,57] it was decided to investigate the potential of this catalyst. Following several attempted syntheses, it was found that modifications to the original procedure had to be made in order to prepare the DMF–PdNPs **236**. Specifically, the reaction had to be carried out in the presence of air, performing the reaction under an inert atmosphere led only to the formation of visible Pd black; a large reaction headspace was also found to be beneficial, as were low levels of amine impurities in the DMF used. DMF–PdNPs **236** were applied to a low temperature Stille cross-coupling and were demonstrated to have activity equivalent to that of a succinimide-based Pd catalyst in DMF, consistent with the proposal that DMF-stabilised particles were forming *in situ* in this system.[156] The synthetic reliability of this catalyst was a source of concern however, so two reactions were performed side-by-side under identical conditions, using the same glassware and starting materials. These demonstrated substantially different outcomes; one reaction produced the intended clear yellow solution of DMF–PdNPs **236**, while the other resulted in a black particulate suspension (**Figure 23**). These experiments provided a stark indication of the capricious nature of the synthesis of this catalyst, so plans to use it for the direct arylation reactions in this chapter were abandoned.

$$PdCl_2 \xrightarrow[\text{140 °C, 6 h, air}]{\text{DMF/H}_2\text{O}} \text{DMF–PdNPs } \mathbf{236}$$
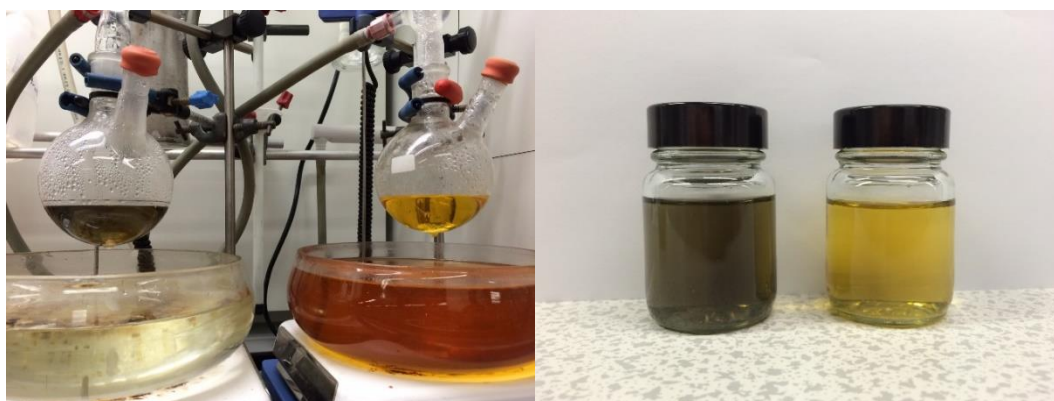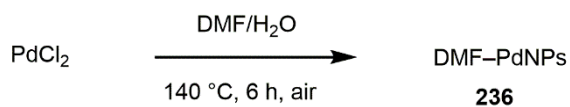
Figure 23 Synthesis of DMF–PdNPs **236**.

Returning to the direct arylation of tryptophan, it was decided to use a symmetric diaryliodonium salt rather than the asymmetric **140**, in order to reduce the number of potential products from this reaction; unselective donation of the mesityl 'dummy' group having been previously noted (see Chapter 2). Diphenyliodonium triflate **38** was therefore synthesised in a high-yielding one-pot process from iodobenzene diacetate **22** and benzene **237** (**Scheme 82**),[124] in addition to the tetrafluoroborate salt **233** already synthesised (**Scheme 79**).
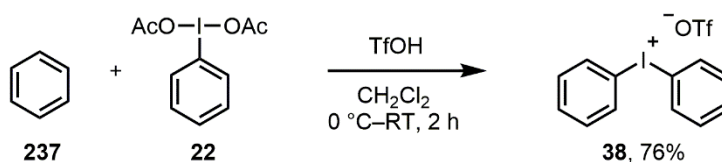
Scheme 82 Synthesis of diphenyliodonium triflate **38**.

A screening of various conditions was then undertaken against tryptophan **74** using heterogeneous Pd sources PVP–Pd **13**, Pd/C (Sigma Aldrich, catalogue number 205680) and Pd/charcoal (Sigma Aldrich, catalogue number 75992), in combination with diaryliodonium salts (**Table 12**).

Table 12 Reaction screening for direct arylation of tryptophan **74** with heterogeneous Pd sources.[a]
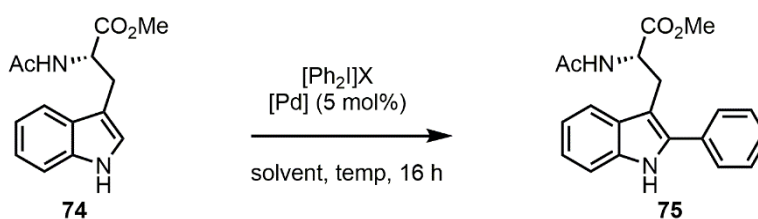
Entry	Solvent	Temp. / °C	Pd. catalyst	X	Conv.[b] (yield)[c] / %
1	EtOAc	37	PVP–Pd **13**	⁻OTf	0
2	EtOAc	60	PVP–Pd **13**	⁻OTf	0
3	EtOAc	60	PVP–Pd **13**	⁻BF$_4$	0
4	AcOH	37	PVP–Pd **13**	⁻OTf	8
5	AcOH	60	PVP–Pd **13**	⁻OTf	80
6	AcOH	60	PVP–Pd **13**	⁻BF$_4$	80
7	AcOH	80	PVP–Pd **13**	⁻OTf	91
8	AcOH	37	Pd/C	⁻BF$_4$	0
9	AcOH	60	Pd/C	⁻BF$_4$	100
10	EtOH	60	Pd/C	⁻BF$_4$	84
11	EtOH	60	Pd/C	⁻BF$_4$	100 (85)[d]
12	EtOH	60	Pd/charcoal	⁻BF$_4$	100 (98)[d]

[a] All reactions conducted with **74** (52 mg, 0.20 mmol, 1 eq.), **38** (172 mg, 0.40 mmol, 2 eq.) or **233** (147 mg, 0.40 mmol, 2 eq.), Pd catalyst (0.01 mmol, 5 mol%) and solvent (2 mL) at 60 °C for 16 h. [b] As determined by ^{1}H NMR spectroscopic analysis of the crude reaction mixture following filtration through a silica gel pad using EtOAc. [c] After purification by silica gel column chromatography. [d] Reaction time extended to 22 h.

This screening demonstrated that this protocol has a strong temperature dependence, with no conversion observed at 37 °C, the temperature at which complete conversion was observed when using Pd(OAc)$_2$ (**Table 12**, Entries 1, 4 and 8). Additionally, no conversion was seen in EtOAc, even at elevated temperatures (**Table 12** Entries 1–3). No counter-ion effect was observed in those examples tested (**Table 12**, Entries 2–3 and 5–6). The sudden change in

reactivity when the protic solvents AcOH or EtOH were applied hints at leaching behaviour to generate the active catalytic species, as evidenced by previous studies within the Fairlamb group[48,49] and others,[25] although evidence to contradict this is presented by Glorius and co-workers.[148] All three catalysts tested displayed good reactivity in this transformation, although PVP–Pd **13** was arguably less active than Pd/C, providing slightly lower conversion after 16 h under otherwise comparable reaction conditions (**Table 12**, Entries 6 and 9). A successful switch from AcOH to the less harmful EtOH was facilitated by an increase in reaction time from 16 h to 22 h (**Table 12**, Entries 9–11). When purification was performed, it was noted that in order to obtain isolated yields comparable to the conversion seen by ^{1}H NMR spectroscopic analysis of the crude reaction mixture (**Table 12**, Entries 11–12), care had to be taken during workup and purification. The ideal method was found to be filtration through a silica gel pad using EtOAc, followed by evaporation of the solvent and direct purification by dry-loaded silica gel column chromatography. This effect is believed to result from the relatively high quantities of activated carbon in these reaction mixtures potentially sequestering some organic reaction products during other workup protocols *e.g.* filtration through Celite™ and/or aqueous washing.

The acidic conditions shown in **Table 12**, Entry 6 were also exemplified on two peptides, previously functionalised using analogous conditions with Pd(OAc)$_2$ (see chapter 2). High conversions to the desired arylation products were seen when using Pd/C, albeit at higher temperatures than when using Pd(OAc)$_2$ (Scheme 83).
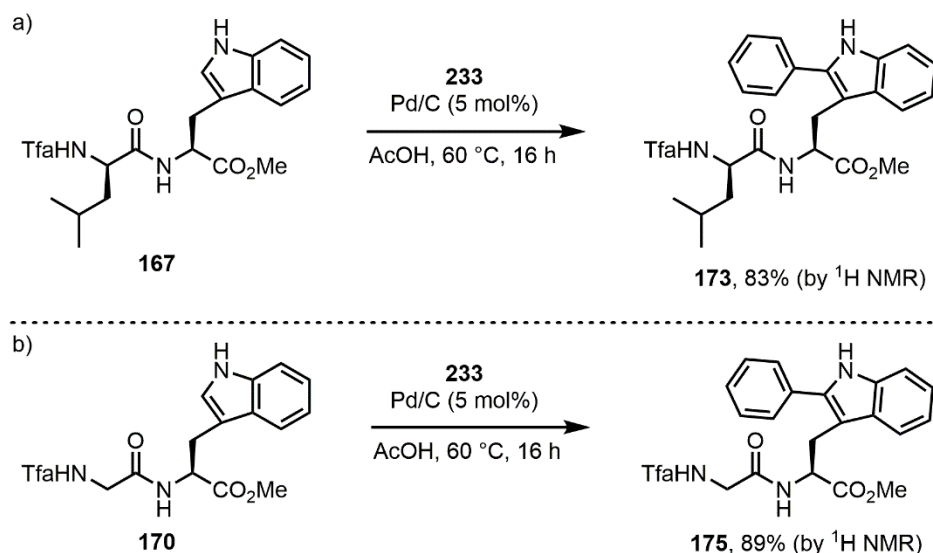
Scheme 83 Direct arylation of peptides using Pd/C.

3.4 Kinetic Studies

It is clear that when evaluating heterogeneous-like behaviour in Pd catalysis, significant differences can be observed not only between different catalysts (*vide supra*) but also between supposedly uniform catalysts, obtained from different suppliers (see work by Glorius *et al*. using Pd/C).[147,148] This difference in activity is usually observed in the literature merely as a function of isolated yield or more commonly, conversion by GC–MS, used primarily as a tool to identify the most effective method of improving conversion under otherwise fixed conditions. This manner of evaluating catalytic behaviour however conceals a multitude of sins, as the most efficient catalysts may not always be identified in this fashion.

For example, imagine a direct arylation reaction conducted using Pd catalysis in DMF at 140 °C. Single variable solvent and temperature screening for this reaction has indicated that when using $Pd(OAc)_2$, these conditions provide the desired product in 20% conversion after 8 hours and 40% conversion after 24 hours. The experimentalists therefore conclude that a reaction time of 24 hours is 'optimal', and begin their heterogeneous catalyst screening. At this point one can propose two potential scenarios for two different Pd catalysts. In the first, catalyst A cleanly converts the substrate of choice in 80% conversion within 1 hour, but is then deactivated by some other process (such as the elevated temperature causing nanoparticle agglomeration and thus loss of activity). No further conversion occurs, so measurement of crude reaction conversion by GC analysis after 24 hours indicates that catalyst A gives a product conversion of 80%. Meanwhile, catalyst B only reaches 10% conversion after 1 hour, but is not deactivated by the reaction conditions so continues to react with the substrate at the same rate. After 24 hours therefore, 100% conversion to product is observed by GC analysis, catalyst B is declared the most active catalyst and all subsequent investigations are performed using this catalyst. From these scenarios, one can infer that catalyst A has superior activity in this reaction (in terms of TOF), yet this would have gone unnoticed by the experimentalists merely examining the outcome of their reactions by crude GC conversion. It may even be the case that catalyst A would have tolerated lower reaction temperatures while maintaining its activity.

Kinetic analysis of novel reactions is therefore of paramount importance in this field,[66] particularly where non-linear kinetic effects often associated with heterogeneous catalysis are likely to occur.[34,35,157-159] These principles were applied to studying the direct arylation of some simple heterocycles using diaryliodonium salts and Pd catalysis using the conditions of Glorius and co-workers (*vide supra*).[148] Four Pd catalyst sources were identified which provide a useful test of two ubiquitous precatalysts, a supported catalyst and well-defined Pd nanoparticulate catalyst, namely: $Pd(OAc)_2$ (>99% purity, Precious Metals Online),

Pd$_2$(dba)$_3$·CHCl$_3$ **238** (91% purity, based on Ananikov's method, see Chapters 4 and 6),[11] Pd/C (5 wt%, Sigma Aldrich, catalogue number 205680, lot number 06230AJ-298) and PVP– Pd **13**. These four catalysts were initially applied to the direct arylation of *N*-methylindole **33** and the reaction followed by *ex situ* GC analysis (details provided in Appendix 5) as shown in **Figure 24**.
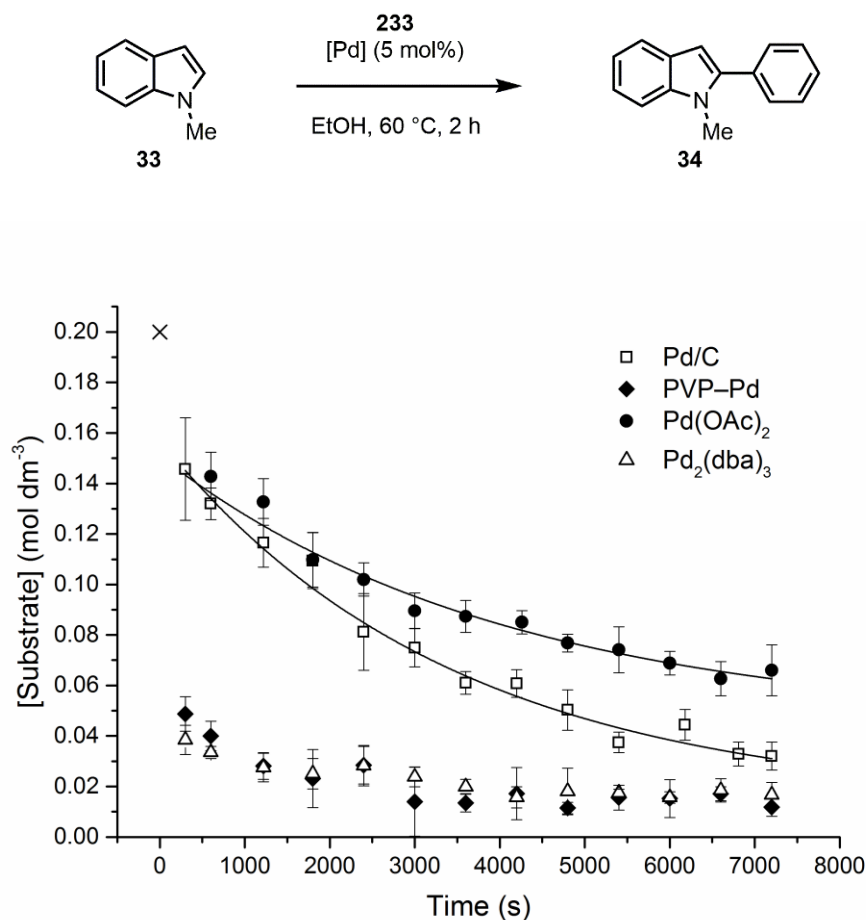
Figure 24 Direct arylation of *N*-methylindole **33** at 60 °C over 2 h. Fitting to an exponential decay equation is shown where appropriate. × = starting concentration of substrate at t = 0. Reactions performed by L. Neumann.

N-methylindole **33** demonstrated high reactivity with all four catalysts tested, especially so when using either **13** or **238** as a catalyst; within 5 minutes 72% and 81% conversion of starting material was observed, respectively. Line fitting to an exponential decay equation for the other catalysts (Pd(OAc)$_2$ and Pd/C) suggests that these reactions are 1st order with respect to substrate, although more detailed studies would be required to validate this approximation (details provided in Appendix 5). The above kinetic studies were repeated at a lower temperature (50°C), in order to provide greater discrimination between the activity of these catalysts (**Figure 25**).
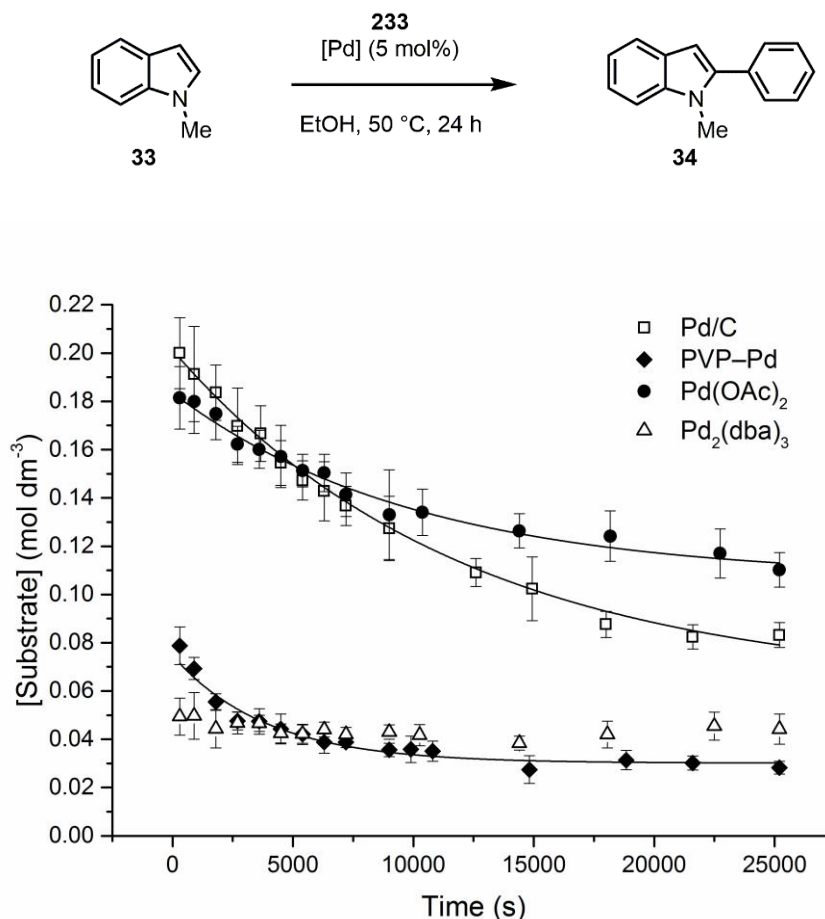
Figure 25 Direct arylation of *N*-methylindole **33** at 50 °C over 24 h. Fitting to an exponential decay equation is shown where appropriate. Detailed analysis over the initial 7 hours shown, final conversions by GC after 24 h; Pd/C: 83%, PVP–Pd **13**: 100%, Pd(OAc)$_2$, 66%, Pd$_2$(dba)$_3$ **238**: 88%. Reactions performed by L. Neumann.

Once again, **13** and **238** proved to be the most active catalysts for this transformation. It is interesting to note that these two catalysts produced similar reaction profiles, which implies similarly between the active catalytic species in these examples (see Chapter 4 for other evidence of PdNP propagation from Pd$_2$(dba)$_3$·CHCl$_3$ **238**). Conversely, Pd/C and Pd(OAc)$_2$ produced wholly different reaction profiles, which were however akin to one another. These results suggest that the nanoparticles produced from Pd(OAc)$_2$ and Pd/C are similar, yet distinct from the nanoparticles produced by **13** and **238**. It may be that PdNPs are not actively catalysing this reaction, the active species instead consisting of leached mononuclear/lower-order Pd species. If this is the case, then perhaps the parallels between catalysts manifests as a result of similar leaching rates. It is also interesting to note that of the catalysts tested, only PVP–Pd **13** led to complete starting material consumption after 24 h. Despite its relatively slow initial rate, Pd/C eventually provides conversion akin to that using **238**, which is much more active in the early stages of the reaction. Pd(OAc)$_2$ however does not however achieve these levels of conversion; the activity of this catalyst eventually drops off, despite matching

that of Pd/C initially. This type of behaviour can be rationalised if the deactivating agglomeration of PdNPs is more facile in the absence of a supporting matrix such as activated carbon, even if the PdNPs originally formed from Pd(OAc)$_2$ and Pd/C are similar. Conversely, little difference is seen in the reaction profiles when using either **13** or **238** as the catalyst.

A quantitative comparison was also made between the old and new batches of **13**, which were qualitatively compared above (**Figure 22**). Monitoring of the activity of these two catalysts for the direct arylation of *N*-methylindole **33** demonstrated significant differences in activity (**Figure 26**). A comparison of freshly synthesised PVP–Pd catalysts with their artificially time- and heat-aged counterparts found that the nanoparticle size in this catalyst had a strong heat dependence, but no discernible time-dependence (when stored at ambient temperature).[160] This investigation was however carried out over a few months, as opposed to the 30-month period of time covered by the PVP–Pd **13** shown in **Figure 22**.
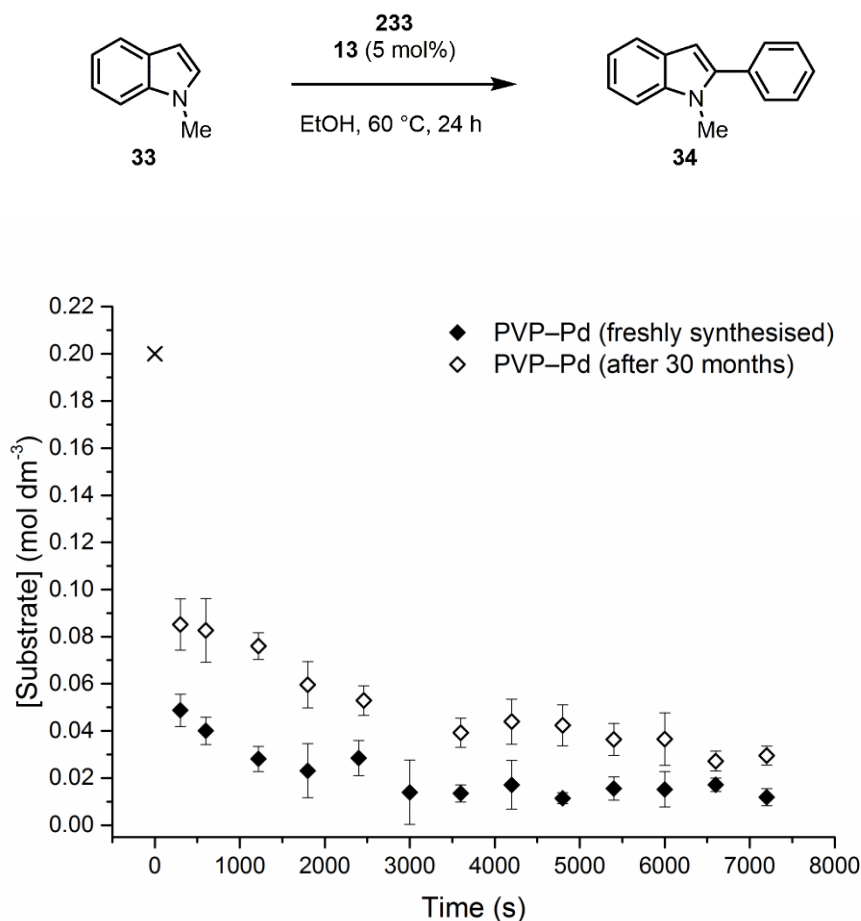
Figure 26 Direct arylation of *N*-methylindole **33** using freshly synthesised and 30-month old PVP–Pd **13**. × = starting concentration of substrate at t = 0. Reactions performed by L. Neumann.

The four catalysts shown above were also studied in the reaction of benzofuran **239** at 60 °C, the kinetic profiles from which are shown in **Figure 27**.
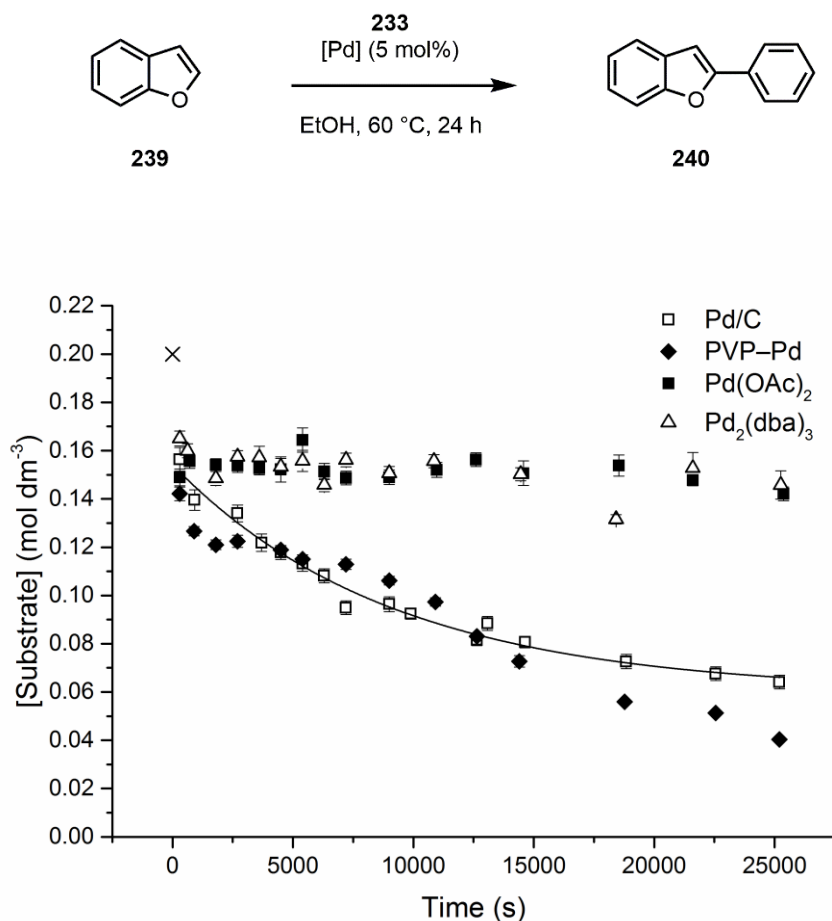
Figure 27 Direct arylation of benzofuran **239** over 24 h. Fitting to an exponential decay equation is shown where appropriate. Detailed analysis over the initial 7 hours shown, final conversions by GC after 24 h; Pd/C: 88%, PVP–Pd **13**: 91%, Pd(OAc)$_2$, 31%, Pd$_2$(dba)$_3$ **238**: 31%. × = starting concentration of substrate at t = 0. Reactions performed by L. Neumann.

Overall, this substrate demonstrated lower activity towards the desired transformation than methylindole **33**. PVP–Pd **13** was again the most active catalyst, providing *ca.* 29% conversion within 5 minutes, and >90% after 24 hours. Interestingly, Pd/C performed very similarly to **13**, in stark contrast to its poor performance when using **33** as a substrate. Pd(OAc)$_2$ and **238** however displayed poor activity for this transformation. These results demonstrated a clear substrate dependence on the catalytic activity for this transformation; whether this is due to variation in PdNP formation or behaviour, or a difference in leaching rates is unclear. The major product was confirmed by ^{1}H NMR spectroscopic analysis as the *C*2-arylated regioisomer, after isolation using silica gel column chromatography in a yield of 31%, from a separate reaction catalysed by Pd(OAc)$_2$. Butylthiophene **241** was also examined under these conditions, the kinetic profiles from which are shown in **Figure 28**.
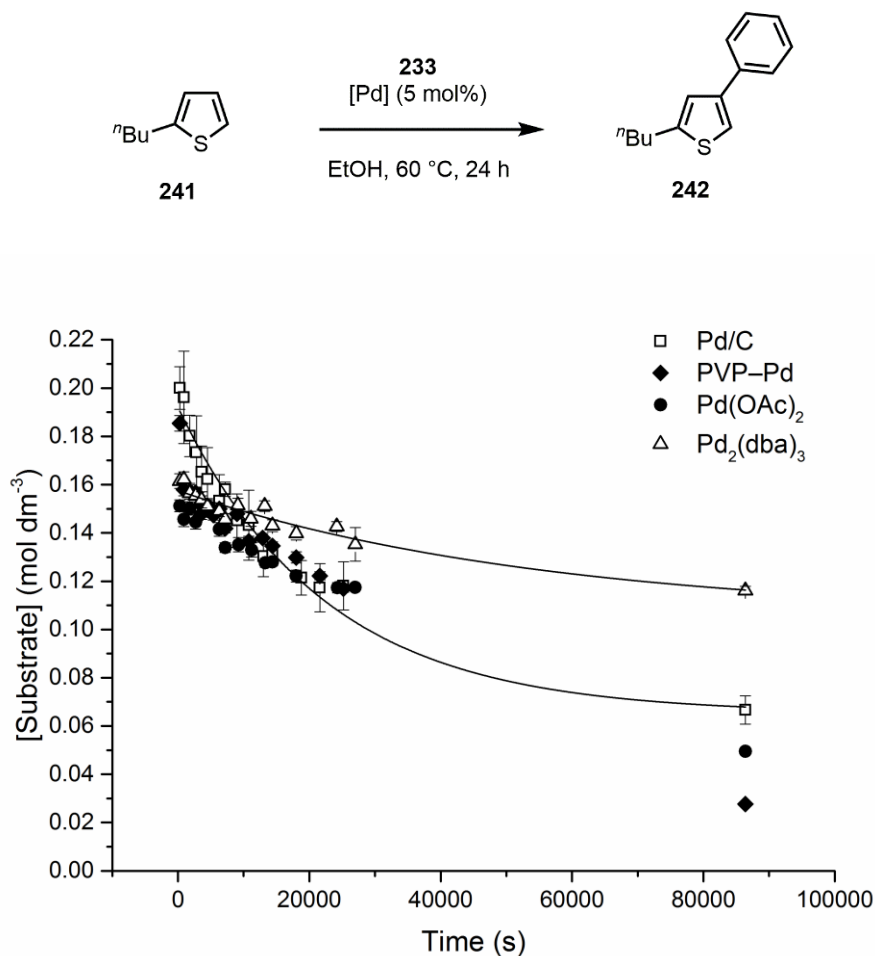
Figure 28 Direct arylation of butylthiophene **241** over 24 h. Fitting to an exponential decay equation is shown where appropriate. Final conversions by GC after 24 h; Pd/C: 66%, PVP–Pd **13**: 86%, Pd(OAc)₂, 75%, Pd₂(dba)₃ **238**: 42%. Reactions performed by L. Neumann.

This substrate demonstrated activity lower than that of either **33** or **239**, as expected, but did reach 86% conversion after 24 hours when using **13** as a catalyst (which was again the most reactive catalysts of those tested). Little difference between catalysts was observed in the initial period of reactivity, which provided such a clear discrimination between catalysts when using either **33** or **239** as substrates. The final conversion obtained however varied between the worst-performing catalyst **238** (42%) and the best-performing catalyst **13** (86%). The major product was confirmed by ^{1}H NMR spectroscopic analysis as the *C*3-arylated regioisomer, after isolation using silica gel column chromatography from two separate reactions catalysed by Pd(OAc)₂ (49%) and PVP–Pd **13** (69%).

The substrates tested thus far were all reported by Glorius *et al*. to be active under their conditions, when using Pd/C as a catalyst.[148] It was hypothesised that 2-*n*-butylfuran **243** should also prove effective in this protocol, but the original publication[148] states that reaction of this substrate with **233** using Pd/C leads to degradation of the starting materials. Conversion to the desired arylated product **245** is however reported when the strongly electron-deficient diaryliodonium salt **244** is used (**Scheme 84**).
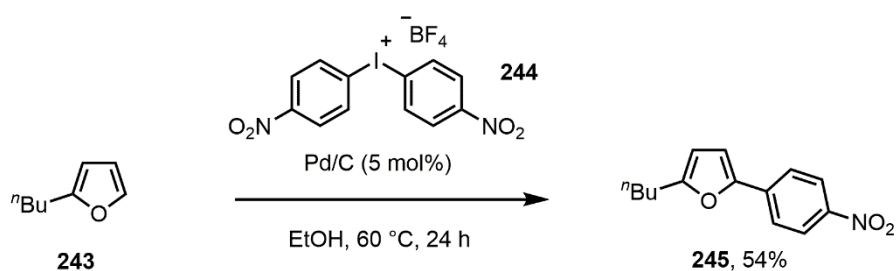
Scheme 84 Direct arylation of butylfuran **243** with electron-deficient diaryliodonium salt **244**.

No other details on this degradation were provided, so some initial studies were performed to evaluate the reaction of this substrate (**Figure 29**). Surprisingly, reaction of **243** under the standard conditions using the same four catalysts as used previously provided good conversion of starting material. Reactivity not dissimilar to that of benzofuran **239** was realised, with **13** and Pd/C proving the most effective catalysts with complete conversion after 24 hours seen. Pd(OAc)$_2$ and **238** were less effective, with *ca*. 70–75% conversion observed after 24 hours. The activity of these four Pd catalysts is similar over the first hour of the reaction, but the distinction between the different catalysts tested becomes apparent after this point.
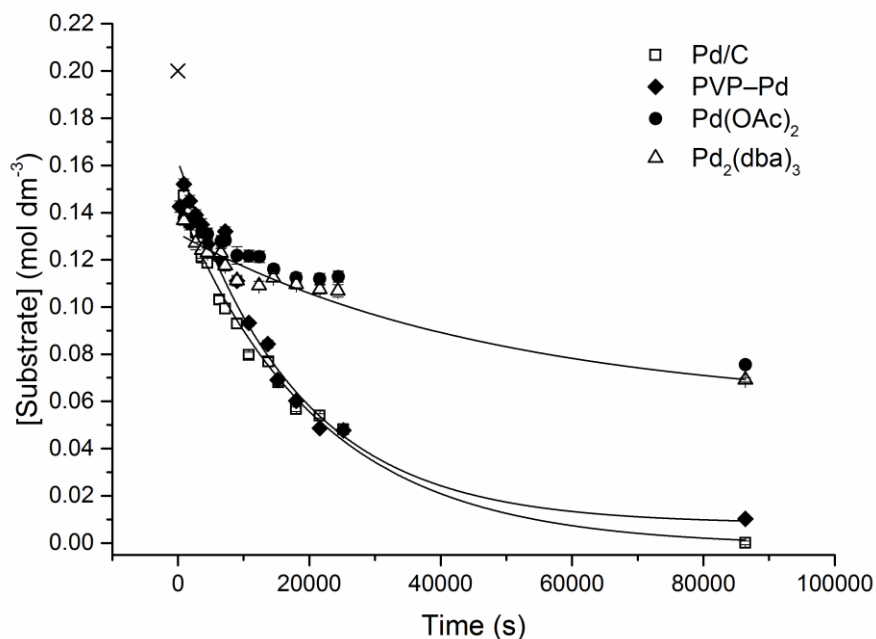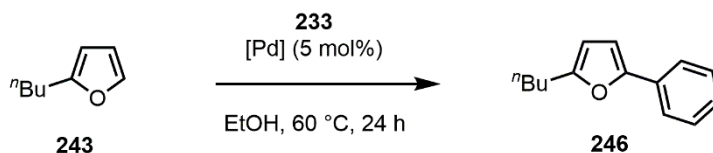
Figure 29 Direct arylation of butylfuran **243** over 24 h. Fitting to an exponential decay equation is shown where appropriate. Final conversions by GC after 24 h; Pd/C: 100%, PVP–Pd **13**: 95%, Pd(OAc)$_2$, 62%, Pd$_2$(dba)$_3$ **238**: 65%. × = starting concentration of substrate at t = 0. Reactions performed by L. Neumann.

In order to gain a complete picture of the reactivity of this substrate under conditions catalysed by Pd/C, this reaction was repeated at a higher temperature (70 °C) and samples taken at regular intervals until reaction completion after *ca.* ten hours. This demonstrated loss of starting material **243** concomitant with product **246** formation, with no evidence of side-products as a result of degradation behaviour observed (**Figure 30**).
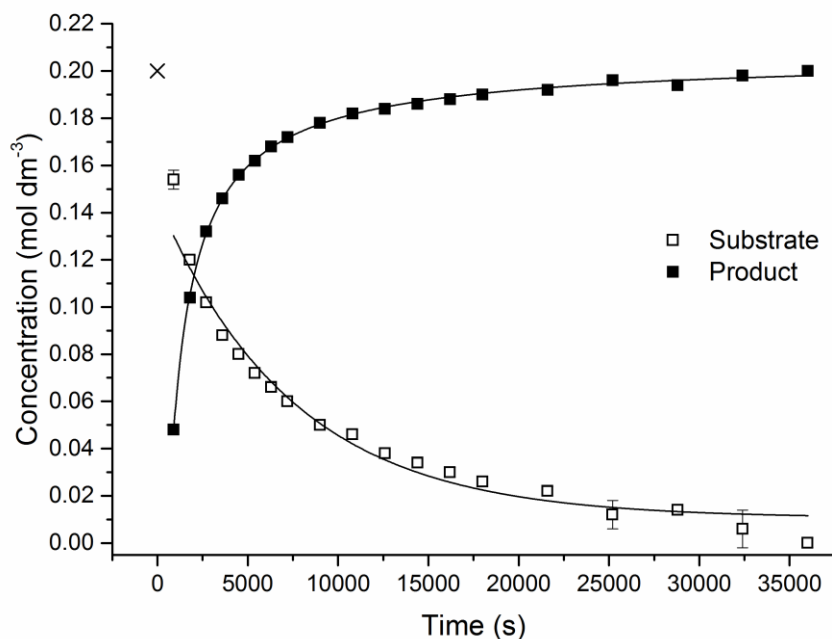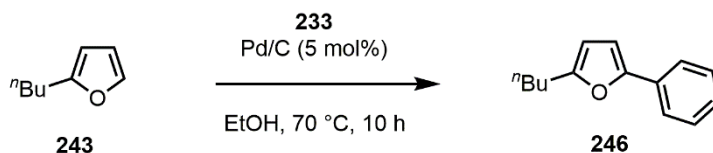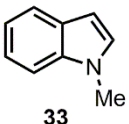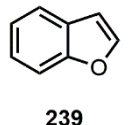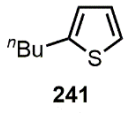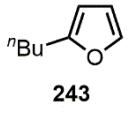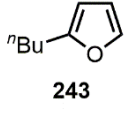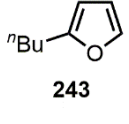
Figure 30 Direct arylation of butylfuran **243** over 10 h at 70 °C. Fitting to an exponential decay (substrate **243**) or logarithmic growth (product **246**) equation is shown where appropriate. × = starting concentration of substrate at t = 0. Reactions performed by L. Neumann.

It is not clear at this point why this substrate provides excellent reactivity in this system, in contrast to that reported. It may be that the different sources of Pd/C used provide fundamentally different forms of catalytically active Pd, alternatively an impurity such as those reported for other commercially available Pd catalysts may be present,[18] which manifests itself when using this substrate. It was noted during these investigations that purification of the 2-arylated product **246** from the Pd/C-catalysed reactions was challenging, as was the case when using tryptophan **74** as a substrate (*vide supra*). Attempted purification of several reactions catalysed by Pd/C afforded inseparable mixtures of the desired product and biphenyl, as confirmed by TLC, EI–GC–MS and ¹H NMR spectroscopic analysis. Iodobenzene is also present as a major byproduct (b.p. 188 °C), which complicates matter further due to the relatively low boiling point of the desired product (95 °C).[161] Purification by silica gel column chromatography of a separate reaction catalysed by PVP–Pd **13** afforded the desired product in a yield of 45%, which was confirmed as the *C*2-arylated regioisomer by ¹H NMR spectroscopic analysis.

Analysis of the initial stages of reaction using these substrates allowed fitting of simple exponential decay equations, as shown in the appropriate figures. Good fits were obtained in the majority of cases; where line fitting could not be performed this is suspected to be the result of rapid initial reactivity followed by loss of catalytic activity, for example the reaction of benzofuran with $Pd(OAc)_2$ as catalyst (**Figure 27**). These analyses allowed for a rough approximation of the initial rate of reaction (k_{obs}) for the majority of substrate and catalyst combinations; these are shown in **Table 13**.

Table 13 Approximate observed rate constants (k_{obs}) for direct arylation reactions.[a]

Entry	Substrate	Pd/C	PVP–Pd 13	$Pd(OAc)_2$	$Pd_2(dba)_3$ 238
1	33	$(9.2 \pm 0.5) \times 10^{-6}$	$(1.3 \pm 0.1) \times 10^{-5}$	$(9.7 \pm 0.4) \times 10^{-6}$	-
2	239	$(6.3 \pm 0.8) \times 10^{-6}$	-	-	-
3	241	$(6.1 \pm 0.6) \times 10^{-6}$	-	-	$(2.6 \pm 0.3) \times 10^{-6}$
4	243	$(7.1 \pm 0.6) \times 10^{-6}$	$(4.8 \pm 0.5) \times 10^{-6}$	$(1.6 \pm 0.1) \times 10^{-6}$	$(3.3 \pm 0.5) \times 10^{-6}$
5	243	$(9.3 \pm 0.9) \times 10^{-6}$	N/A	N/A	N/A
6[b]	243	$(9.4 \pm 1.6) \times 10^{-6}$	N/A	N/A	N/A

[a] Rate constants calculated from initial rates using a fitted exponential decay equation, using at least 5 recorded data points with $\geq 90\%$ correlation. All rates shown in s^{-1}. In many cases, extremely rapid conversion occurs within *ca*. 5 mins (the first recorded data point), which has not been considered in these data. Hyphens indicate those reactions which cannot be fitted to this exponential decay equation.
[b] Rate constant for product **246** formation calculated from initial rates using a fitted logarithmic growth.

It should be noted that these cannot be considered as empirically accurate values due to the rough approximation present in the exponential decay line fitting. They are intended simply as a guide to the approximate activity of each of the catalysts tested. Errors in these values are calculated from the standard deviation of a linear regression of the initial reaction rates, obtained by the 'least squares' method. These rate constants are broadly similar to one another, lying between *ca*. 1×10^{-6} and 1×10^{-5} s^{-1} for all the catalyst/substrate combinations tested. By comparison, a pseudo first-order rate of constant of $3.5(2) \times 10^{-4}$ s^{-1} for the arylation of 2-methylthiophene has been previously reported, although this was measured when using the bespoke dimeric catalyst $[PdAr(\mu\text{-}OAc)(PPh_3)]_2$.[162]

3.5 Conclusion

Several attempts have been made to develop a generic protocol for the arylation of nitrogen-containing heterocycles using aryldiazonium salts, building on the methodology successfully applied to the amino acid tryptophan **74** (see Chapter 2). These have met with limited success; of those examples tested, only 7-azaindole **231** could be functionalised in the desired manner. Attempted application of heterogeneous Pd sources to this class of reactions have been similarly unsuccessful, the scarcity of such examples in the literature perhaps indicates the significant challenge this poses.

The direct arylation of several simple heterocycles, in addition to the amino acid tryptophan **74** and tryptophan-containing peptides, has however been achieved using a combination of diaryliodonium salts and heterogeneous Pd sources. Significant discrepancies in reaction conversions when using several variations of palladium supported on activated carbon have been noted. The pre-synthesised nanoparticle catalyst PVP–Pd **13** has also been demonstrated as an effective catalyst in this chemistry; **13** has however been shown both qualitatively and quantitatively to degrade over many months under air at ambient temperature, with a concomitant loss of activity in the direct arylation of methylindole **33**. Reaction profile analysis has shown a substrate effect on catalyst activity in these transformations, in addition to the observation of similar activity between apparently distinct catalysts (e.g. $Pd(OAc)_2$ and Pd/C), which suggests Pd speciation and higher-order Pd catalyst effects. Butylfuran **243** which was reported to be unstable under these reaction conditions has in fact been shown to react effectively to provide the desired direct arylation product in quantitative conversion.

Chapter 4: Analysis of Pd₂(dba)₃ Complexes

4.1 Introduction

The widely-used Pd^0 precursor complex, $Pd_2(dba)_3$ (dba = *E*, *E'*-dibenzylideneacetone **247**), is ubiquitous in synthetic chemistry.[163] It has been extensively studied within the Fairlamb group, where work has shown that modifying the core structure with a variety of ligands to generate '$L_2Pd^0(\eta^2$-dba)' complexes, can provide profound variations in catalytic behaviour.[164] The reasons for this are simple; the dba ligand plays a non-innocent role in the catalytic activity of 'L_nPd^0' complexes, generated *in situ* prior to oxidative addition reactions with aryl halides. This was first reported by Jutand and co-workers, who studied the equilibrium behaviour of solvated 'L_2Pd^0' and '$L_2Pd^0(\eta^2$-dba)' species, using phosphine ligands.[165] The concentration of the active oxidative addition species 'L_2Pd^0' was found to be dependent on its equilibrium position with unreactive '$L_2Pd^0(\eta^2$-dba)' species; an increase in the number of equivalents of phosphine used therefore shifts the equilibrium towards the active 'L_2Pd^0' species, increasing activity (**Scheme 85**).
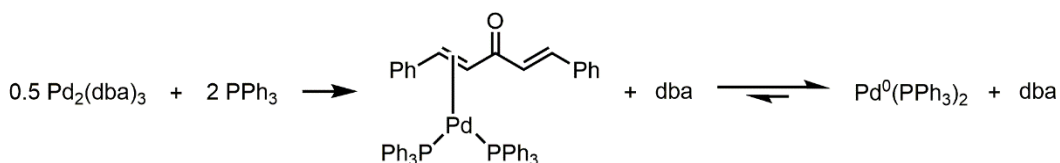
Scheme 85 Equilibrium between $L_2Pd^0(\eta^2$-dba) and L_2Pd^0 species.

This key complex is typically synthesised by reduction of sodium tetrachloropalladate(II) in MeOH in the presence of the free ligand **247** (**Scheme 86**). Initially this complex was incorrectly characterised as $Pd(dba)_2$ based on IR and elemental analysis data;[166] it was later proposed to consist of three dba ligands asymmetrically coordinated around two palladium centres, with a fourth loosely coordinated or 'solvating' dba ligand, giving complex $Pd_2(dba)_3 \cdot$dba **248**.[167-169]
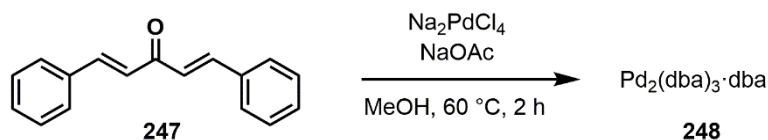
Scheme 86 Synthesis of $Pd_2(dba)_3 \cdot$dba **249**.

More recently, preparation of this complex from the readily available precursor palladium(II) acetate has been published in a procedure purporting to afford both high yields and purities (**Scheme 87**).[170] This is achieved *via* recrystallisation from chloroform, affording the adduct

complex $Pd_2(dba)_3 \cdot CHCl_3$ **238**, while allowing removal of excess free dba ligand **247** and elemental Pd (*i.e.* nanoparticulate Pd^0). It is important to note that $Pd_2(dba)_3$ has been reported to react with $CHCl_3$ under certain conditions to form cluster complexes.[171]
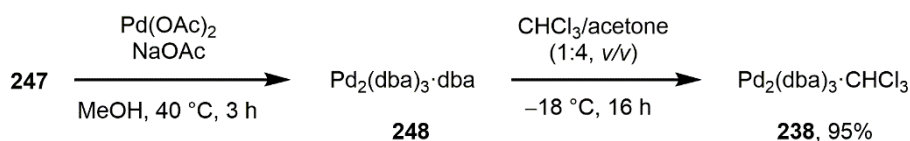
Scheme 87 Synthesis of $Pd_2(dba)_3 \cdot CHCl_3$ **238**.

This synthesis is proposed to avoid the pitfalls resulting from poor characterisation of commercially available '$Pd_2(dba)_3$', as high levels of variation were found, with up to 40% of Pd nanoparticles (PdNPs) present in many samples. These PdNPs were found in a range of sizes, from 10–200 nm, along with free ligand **247** and the desired complex **248**. Recrystallisation such as that in **Scheme 87** allows for the 'purity' of the catalyst to be determined prior to its use, as diffusion-ordered spectroscopy (DOSY) was utilised to delineate the typically complex ^{1}H NMR of complex **238**, allowing for characterisation of the major and minor isomers, in addition to free ligand **247** (**Figure 31**).
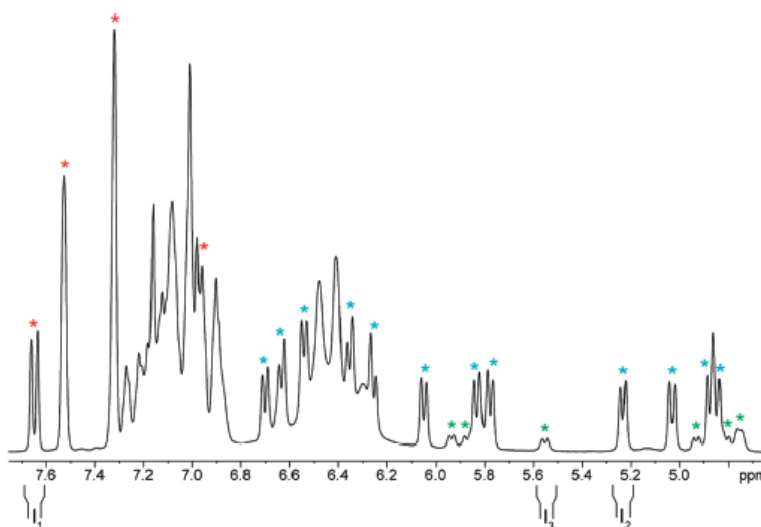
Figure 31 Partial ^{1}H NMR spectrum of $Pd_2(dba)_3 \cdot CHCl_3$ in $CDCl_3$ at 600 MHz: alkene signals corresponding to the major (blue) and minor (green) isomers of complex **238**, along with free ligand **247** (red). Integral regions used for calculation of purity are highlighted as I_1–I_3. Reprinted with permission from *Organometallics* **2012**, *31*, 2302–2309. Copyright 2012 American Chemical Society.

The 'purity' (*i.e.* the amount of complexed ligand **238** versus free ligand **247**) can thus be evaluated simply by comparing the ^{1}H NMR ratios of the appropriate signals (**Equation 1**).

$$\text{Purity} = \frac{[\text{major isomer} + \text{minor isomer}]}{\left[\left(\text{major isomer} + \text{minor isomer} + \left(\frac{\text{free ligand}}{2}\right)\right)\right]} \times 100\%$$

$$= \frac{[I_2 + I_3]}{[I_2 + I_3 + \left(\frac{I_1}{2}\right)} \times 100\%$$

Equation 1 Purity determination of complex **238** from ¹H NMR integrals.

In this work the solution-phase structure of complex **238** was also discussed, with high-field ¹H NMR spectroscopic data being used to assert that the dba ligands were coordinated in a symmetric *s-cis, s-cis* fashion around the palladium centres. This contradicted an earlier study by Kawazura *et al.*, who found that the dba ligands coordinated in an asymmetric *s-cis, s-trans* fashion (**Figure 32**).[172] These latter observations were subsequently supported by detailed ¹H and ¹³C NMR studies, in addition to DFT calculations, performed within the Fairlamb group.[173]

s-cis, s-cis   *s-cis, s-trans*   *s-trans, s-trans*
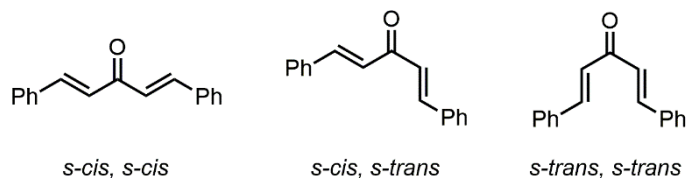
Figure 32 Possible conformational alignment of dba ligand **247**.

The facile propagation of PdNPs from this complex was proposed in the Ananikov study as a potentially useful source of catalytically competent, heterogeneous Pd nanocatalysts. In a subsequent publication from the same group, activated carbon was shown to exhibit an efficient capture mechanism of these particles, obtained by degradation of complex **238** in chloroform at 40 °C. These reactive Pd markers were used to demonstrate >2000 reactive Pd centres per 1 µm^2 of carbon surface area.[174]

The ambiguity surrounding the true coordination environment of this complex in solution and in the solid state, in addition to its ability to form PdNPs under very mild conditions, provided ample opportunity for further study of this important Pd^0 (pre)catalyst.

4.2 Synthesis and Characterisation

To complete characterisation of the complex of interest (**238**), preparation of the chloroform adduct *via* the protocol in **Scheme 87** was performed. Recrystallisation in several solvents was successful and single crystal X-ray structures obtained for three analogues; Pd₂(dba)₃·CHCl₃ **238**, Pd₂(dba)₃·CH₂Cl₂ **249** and Pd₂(dba)₃·C₆H₆ **250**. The high quality structures obtained for the chloroform adduct is shown in **Figure 33** and **Figure 34**, with all structures included in Appendix 2.
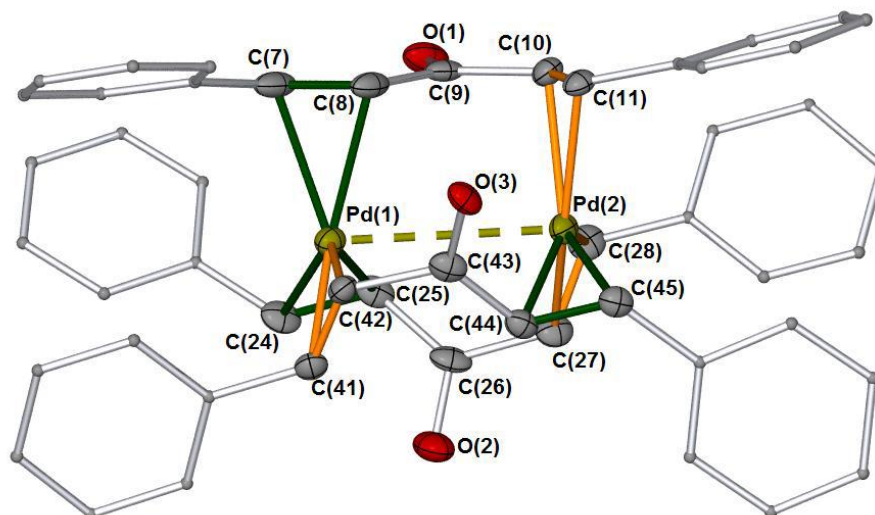
Figure 33 Single crystal X-ray diffraction structure of **238** (major isomer). Thermal ellipsoids shown with 50% probability, hydrogen atoms and solvating chloroform removed for clarity. Selected bond lengths (Å): Pd(1)–C(7): 2.303(3), Pd(1)–C(8): 2.248(3), C(7)–C(8): 1.358(4), Pd(1)–C(24): 2.279(4), Pd(1)–C(25): 2.251(4), C(24)–C(25): 1.364(6), Pd(1)–C(41): 2.202(3), Pd(1)–C(42): 2.220(3), C(41)–C(42): 1.393(5), Pd(2)–C(10): 2.222(3), Pd(2)–C(11): 2.244(3), C(10)–C(11): 1.395(4), Pd(2)–C(27): 2.244(4), Pd(2)–C(28): 2.241(4), C(27)–C(28): 1.392(6), Pd(2)–C(44): 2.244(3), Pd(2)–C(45): 2.280(3), C(44)–C(45): 1.359(5). Pd(1)–Pd(2) bond distance: 3.244 Å.
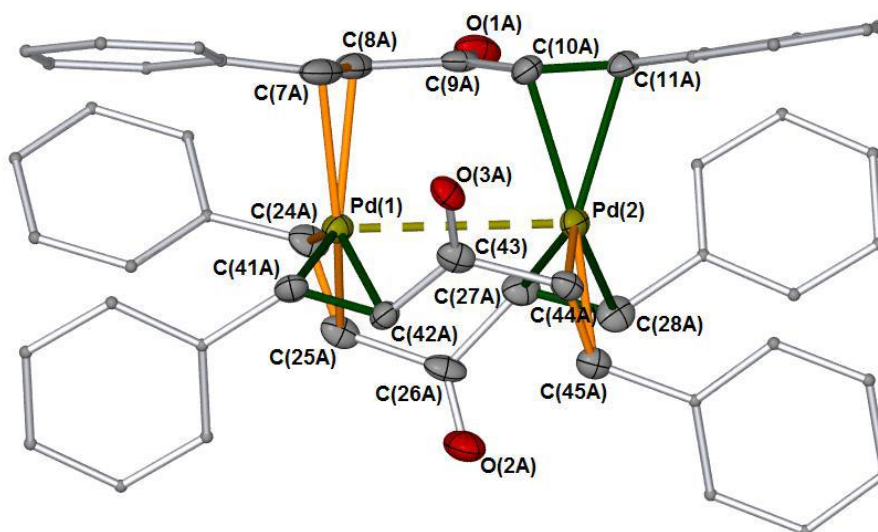
Figure 34 Single crystal X-ray diffraction structure of **238** (minor isomer). Thermal ellipsoids shown with 50% probability, hydrogen atoms and solvating chloroform removed for clarity. Selected bond lengths (Å): Pd(1)–C(7A): 2.275(11), Pd(1)–C(8A): 2.297(11), C(7A)–C(8A): 1.368(19), Pd(1)–C(24A): 2.243(6), Pd(1)–C(25A): 2.254(6), C(24A)–C(25A): 1.390(9), Pd(1)–C(41A): 2.211(7), Pd(1)–C(42A): 2.207(7), C(41A)–C(42A): 1.339(10), Pd(2)–C(10A): 2.192(11), Pd(2)–C(11A): 2.272(10), C(10A)–C(11A): 1.332(9), Pd(2)–C(27A): 2.274(6), Pd(2)–C(28A): 2.242(6), C(27A)–C(28A): 1.352(9), Pd(2)–C(44A): 2.267(7), Pd(2)–C(45A): 2.311(7), C(44A)–C(45A): 1.394(10). Pd(1)–Pd(2) bond distance: 3.244 Å.

In these structures, each of the three dba ligands are disordered over two positions, with the major isomer depicted in **Figure 33** and the minor isomer depicted in **Figure 34** (ratio major:minor is 79:21). These isomers result from the asymmetric environment of the coordinating alkenes, as they can occupy either an s-*cis* (green) or s-*trans* (orange) orientation with respect to the carbonyl group of the ligand. The average C=C bond distances are 1.3603 Å for the s-*cis* alkenes and 1.3930 Å for the s-*trans* alkenes, indicating a weaker s-*trans* alkene bond. Additionally, the C–Pd distances for the s-*cis* alkenes are C_α–Pd = 2.247 Å and C_β–Pd = 2.287 Å, and C_α–Pd = 2.228 Å and C_β–Pd = 2.229 Å for the s-*trans* alkenes, indicating a higher level of asymmetry in the s-*cis* bonds than in the s-*trans* bonds. These two observations taken together appear to demonstrate a higher level of π-backbonding (and thus more sp³, cyclometallopropane-like character) in the s-*trans* alkenes (**Figure 35**).
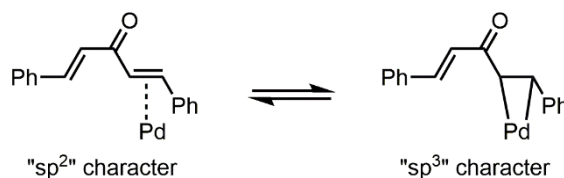
Figure 35 Representative alkene binding from dba ligand **247** to palladium.

When complex **238** was analysed by ¹H NMR spectroscopy and the integrals applied to **Equation 1**, the purity was found to be 91%, contrasting with the reported value of 98% immediately post-synthesis.[170] This value is the maximum obtained during the course of this project, representing *ca.* ten syntheses of complex **238** (and was in fact obtained under rigorously air-free conditions, using dry distilled solvent, which was not specified in the published procedure).[170] Representative purities lie in the region of 80–89%. The exchange rates of the different isomers of complex **238** in solution was proposed as a source of this discrepancy, so a variable temperature NMR (VT–NMR) study was performed to evaluate the effect of temperature on the rate of exchange. The hypothesis in this instance was that cryogenic temperatures could slow down the exchange process sufficiently to allow the delineation of this effect on the NMR timescale. When a ¹H NMR spectrum of complex **238** was recorded at −35 °C (238 K), it became apparent that a small quantity of an as-yet unidentified species overlapped with the signal typically used to calculate the quantity of the major isomer (*ca.* 5.29 ppm, ■). Another suitable region was thus identified (*ca.* 6.12 ppm, ●) and used as a measure of the concentration of the major isomer in solution (**Figure 36**). The signal used to calculate the quantity of minor isomer remained unchanged from that shown in **Figure 31** (*ca.* 5.60 ppm, ○). The integrals recorded (and thus the derived purity) differed slightly as a function of temperature (in this experiment, 89% at 298 K and 83% at 238 K), giving credence to the explanation that complex exchange in solution introduces

variability in the purity measurement. The measurements made by Ananikov *et al*. were recorded on a different spectrometer, at 600 MHz,[170] so these factors alone could easily have introduced the *ca*. 10% error observed in this calculation of purity.
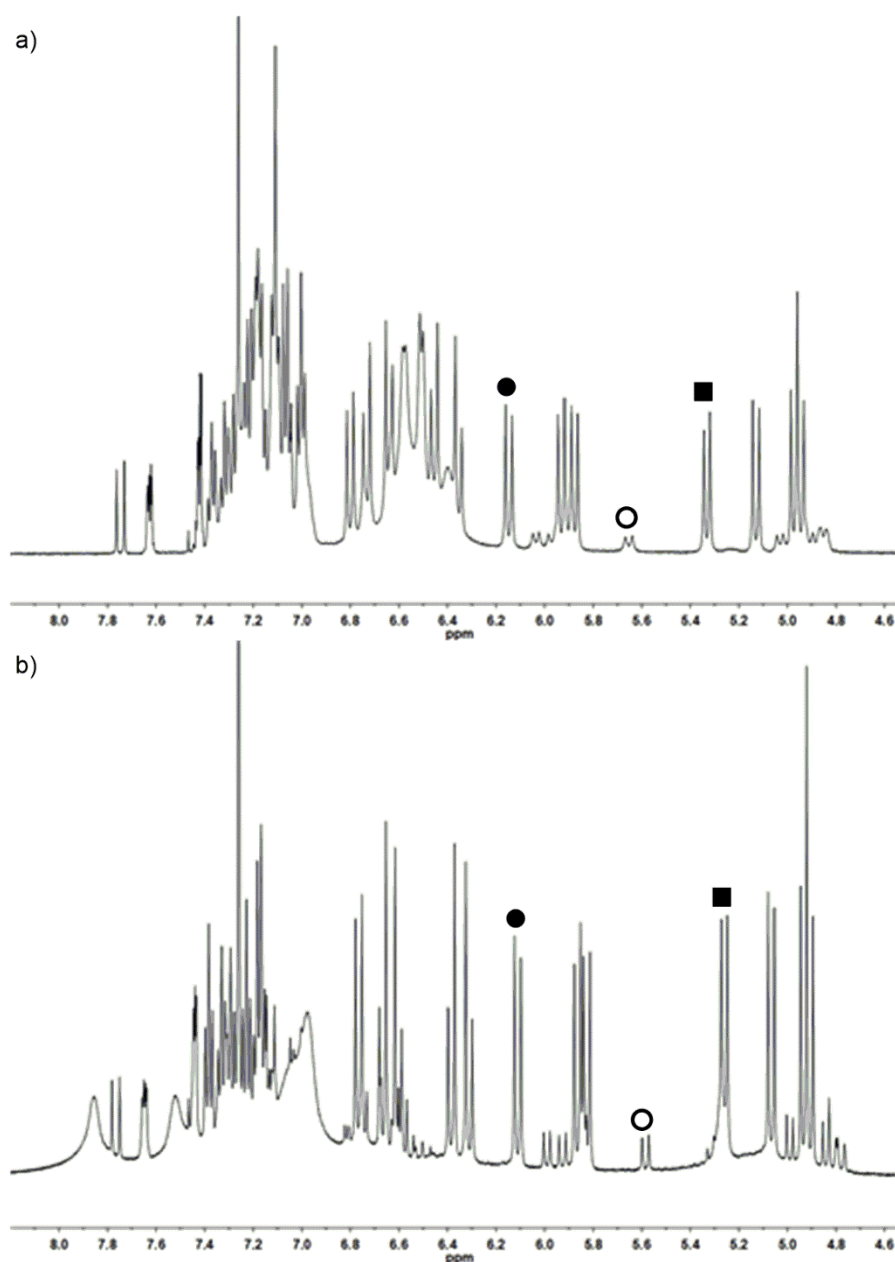
Figure 36 ^{1}H NMR spectra of **238** in CDCl$_3$ at a) 298 K b) 238 K; major isomer signal used by Ananikov *et al*. (■), major isomer signal (●) and minor isomer signal (○) used in this study.

To further evaluate the exchange process of both isomers of complex **238**, as well as the free ligand **247**, ^{1}H NMR spectra of complex **238** (at 500 MHz using 64 scans, in CDCl$_3$) were recorded at several temperatures between 238–298 K. The full-width at half-maximum (FWHM) of each of the key integral signals used in the purity determination (with the exception of the signal at *ca*. 5.29 ppm, *vide supra*) was then measured and compared. This

gave an indication of the relative exchange rates of these species, as signal broadening is an effect typically associated with exchange on the NMR timescale *i.e.* the larger the measured FWHM, the greater the degree of exchange. The results from this experiment are provided in **Figure 37**.
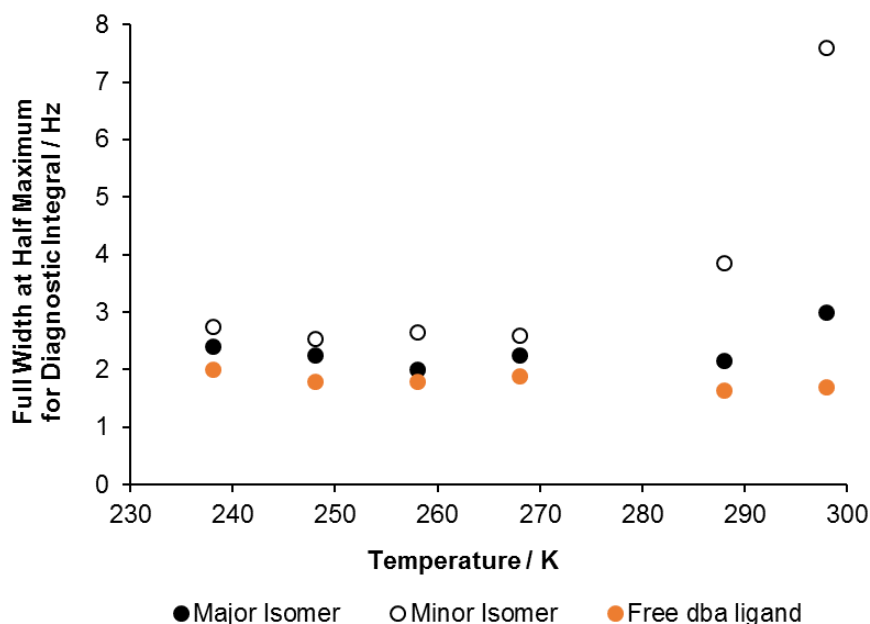
Figure 37 Intensity of key integrals for complex **238** as a function of temperature.

Interestingly, this experiment demonstrated that the exchange rates of the species involved differ significantly at non-cryogenic temperatures. This means that the two isomers of complex **238** display different intra- and intermolecular exchange rates, introducing error into the integral signals used in the purity determination proposed by Ananikov *et al.*, [170] supporting the same conclusion drawn through comparison of the integrals at different temperatures (**Figure 36**).

4.3 Activation/Degradation to Form Pd Clusters

The facile propagation of PdNPs from this complex, as detailed by Ananikov *et al.*,[170] was proposed to occur through initial dissociation of the dba ligand **247** followed by rapid agglomeration of the resulting thermodynamically unstable Pd^0 atoms. A putative model for this process could centre around protonation of the keto moiety of the dba ligand **247**, reducing the electron density of the alkene and resulting in dissociation from the metal centre. If this were the case, degradation of complex **238** should be initiated either by water or acid; indeed, in their work Ananikov and co-workers note that degradation could result "by reaction with acid traces and other impurities in the [NMR] solvent".

To probe the formation of these PdNPs (or Pd clusters) indirectly, the ^{1}H NMR method detailed above (despite its limitations) could therefore be used to monitor the ratio of complexed versus free ligand as a function of time; by definition, as free ligand **247** is released there should also be a concomitant release of elemental Pd^0. Several experiments were therefore performed to evaluate the effect of water and acid independently. For the control study 5 mg of complex **238**, manipulated in a glovebox, was dissolved in 0.5 mL of $CDCl_3$ that had been degassed, dried and de-acidified over CaH_2. ^{1}H NMR spectra were then recorded under air-free conditions in a Young's tap NMR tube after 10 min, then every 30 min for 24 h; the resulting integrals were subsequently used to generate values for the quantity of complex over time. A second analogous experiment was then performed using reagent grade $CDCl_3$, which was measured by ^{1}H NMR to contain 144 ppm water, using 1,3,5-trimethylbenzene **141** as an internal standard. Two further experiments were also performed in dry, degassed and de-acidified $CDCl_3$ that had been doped with the acid $[HNPhMe_2]^+ [BF_4]^-$ **252**, used primarily because of its solubility in chloroform. This acid is readily prepared from commercially available *N*, *N*-dimethylaniline **251** in one step (**Scheme 88**).
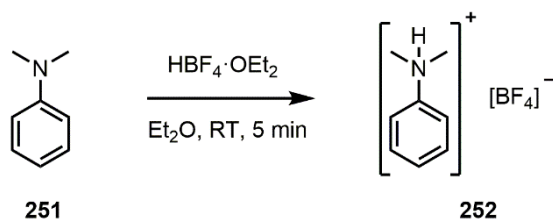
Scheme 88 Synthesis of chloroform-soluble acid **252**.

The amounts used to initiate degradation were one equivalent of acid **252** with respect to complex **238** and three equivalents with respect to complex **238** (1 equivalent per dba ligand **247**). The results from these four experiments are overlaid in **Figure 38**.
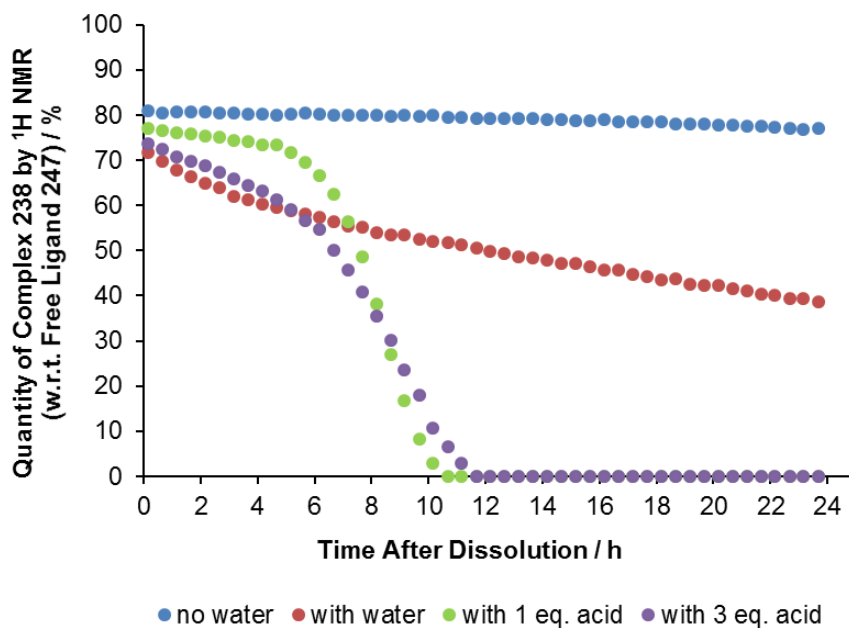
Figure 38 Behaviour of complex **238** in CDCl₃, monitored by ^{1}H NMR spectroscopic analysis.

Figure 38 clearly shows that the relative concentration of complex **238** decreases over time, with respect to free ligand **247** concentration, in the presence of both water and acid. Conversely, it displays relatively higher stability in solution under anhydrous, air-free conditions (eventually reaching complete decomposition after 11 days in solution). When treated with one equivalent of acid **252**, complete degradation of complex **238** occurs in less than 11 hours, with the resultant ^{1}H NMR spectrum matching that of free ligand **247** and visible Pd 'mirroring' on the sides of the NMR tube qualitatively indicating elemental Pd^0 formation. The profile for the acid-catalysed degradation appears to demonstrate two distinct phases; a slow first step occurring between 0–6 hours after dissolution where the relative concentration of complex **238** decreases by 8%, followed by a rapid second step between 6–11 hours after dissolution where the relative concentration decreases by 70%. This behaviour is difficult to rationalise by the simple model proposed above, but could be explained by autocatalytic Pd complex formation; the [BF₄]$^−$ counter-ion of acid **252** is known to stabilise PdNPs in other systems.[175] While not identical, this broad trend is also seen when using three equivalents of acid **252**. Notably, during the initial period degradation of the complex is more rapid, possibly due to an increased rate of initial ligand protonation.

To delineate any potential counter-ion effect, complex **238** was treated with two other organic soluble acids, acetic acid (AcOH) and trifluoroacetic acid (TFA). Treatment with AcOH (10 eq. or 359 eq. w.r.t **238**, 100 μL in 5 mL CDCl₃) had no effect on complex **238**, with no degradation seen by ^{1}H NMR after several days. Ten equivalents of TFA did however initiate degradation, the profile for which is shown in **Figure 39**, with the data from acid **252** overlaid

for comparison. When 298 equivalents of TFA were used (100 μL in 5 mL $CDCl_3$), decomposition to free ligand **247** and elemental Pd occurred within seconds. This also occurred when complex **238** was treated with $HBF_4 \cdot OEt_2$ (1 eq. w.r.t **238**).
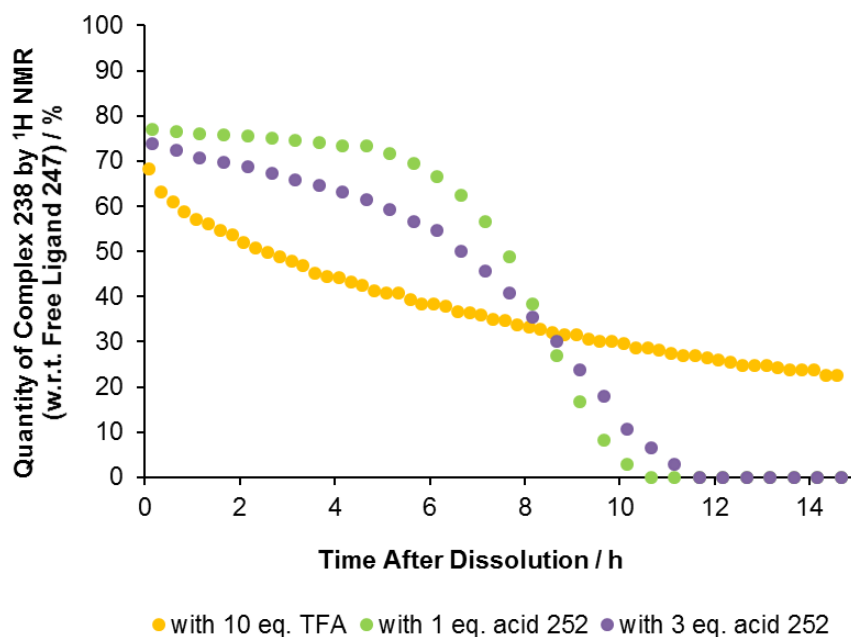
Figure 39 Behaviour of complex **238** in $CDCl_3$ when treated with acid, monitored by ^1H NMR spectroscopic analysis.

Comparison of the experiments shown in **Figure 39** indicates that using TFA to initiate decomposition of complex **238** produces a simpler kinetic profile, which lacks the two-phase behaviour seen when using acid **252**. As highlighted above this may result from the ability of $[BF_4]^-$ to stabilise PdNPs in the latter case, producing unusual degradation profiles due to involvement by higher-order Pd species, such as $[Pd^0_x dba_y]$ clusters. To probe this more directly (as opposed to the indirect observations provided by ^1H NMR signals of ligand **247**), Fourier-transform ion cyclotron resonance mass spectrometry (FT–ICR–MS) was performed on a methanol/DCM solution of complex **238** and demonstrated the presence of Pd clusters containing between three and eight Pd atoms, all with two dba ligands. (**Figure 40**).
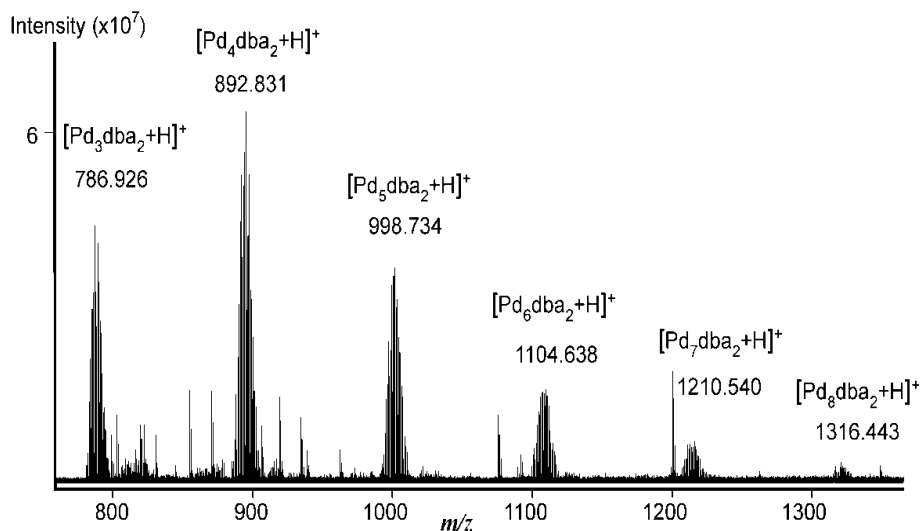
Figure 40 FT–ICR–MS spectrum showing $[Pd_xdba_2H]^+$ cluster species formed from complex **238**.

The most abundant ion detected *via* this method was $[Pd_4(dba)_2H]^+$, so density functional theory (DFT) calculations were performed by a collaborating group in Birmingham[176] to determine the relative energies of several possible conformations for this specific cluster in the gas phase (**Figure 41**). Perhaps surprisingly, the conformation of calculated lowest energy was the linear conformer of four Pd atoms, positioned in-between the two dba ligands (**Figure 41**a).
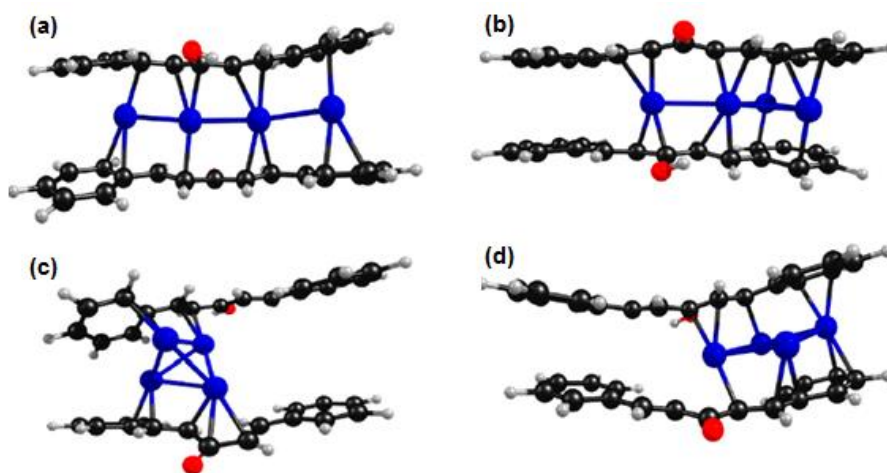
Figure 41 DFT-calculated possible structures for the species $[Pd_4(dba)_2H]^+$ in the gas phase: (a) linear, (b) Y-shaped, (c) rhombic, (d) tetrahedral.

This cluster formation would result in a small increase in the concentration of free dba by ^{1}H NMR initially, as complex **238** degrades to elemental Pd^0 and free dba ligand (**Figure 38** and **Figure 39**). The free dba liberated would then be sequestered by multinuclear elemental Pd^0, forming $[Pd^0_xdba_y]$ clusters. As these clusters grow, eventually they would reach a point where they were no longer soluble and would precipitate out, liberating a large quantity of

130

free dba ligand into solution. This would cause a large increase in the observed concentration of free dba by ^{1}H NMR, leading to the observed rapid decomposition several hours after dissolution of complex **238** (**Figure 38** and **Figure 39**). In an analogous experiment, electrospray ionisation mass spectrometry (ESI–MS) was used to demonstrate that clusters containing varying numbers of both Pd atoms and dba ligands could also be observed (**Figure 42**).
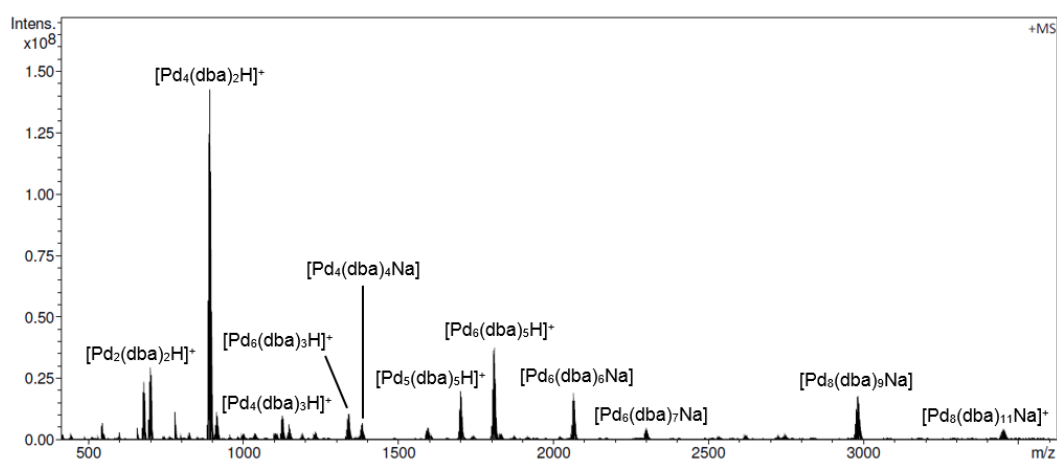
Figure 42 ESI–MS spectrum showing [Pd$_x$dba$_y$H/Na]$^+$ cluster species formed from complex **238**.

Once again, the most abundant ion detected in solution was [Pd$_4$(dba)$_2$H]$^+$, the detected masses for which are shown in **Figure 43**. A full comparison of the observed isotope patterns against their calculated values is provided in Appendix 6.
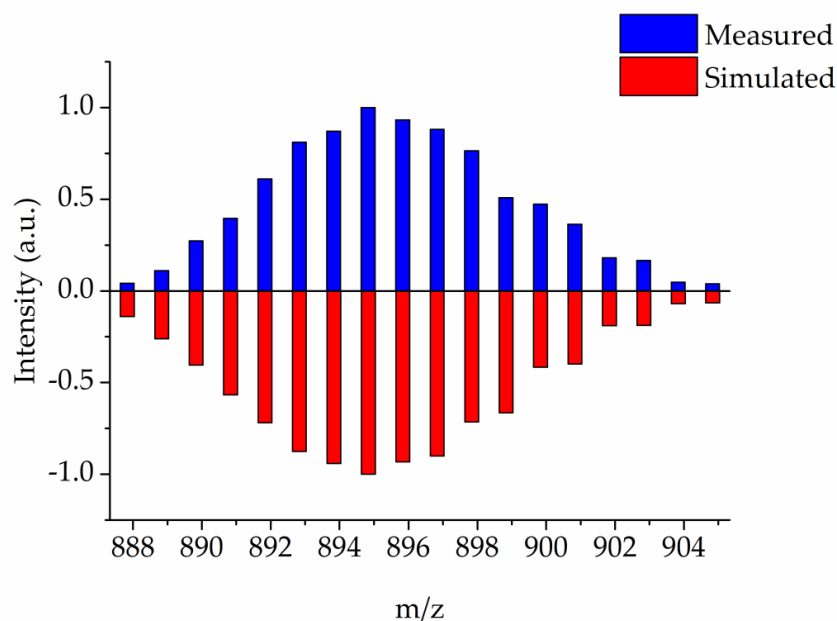
Figure 43 Measured vs. simulated mass values for [Pd$_4$(dba)$_2$H]$^+$ cluster detected by ESI–MS.

During this experiment, the ion corresponding to the [Pd$_4$dba$_5$H]$^+$ cluster was isolated and subjected to secondary ionisation (ESI–MS–MS), producing the smaller clusters [Pd$_4$dba$_3$H]$^+$ and [Pd$_4$dba$_2$H]$^+$. Interestingly, the relative intensity of these ions increased as a function of collision energy (0–65 V); in other words, the greater the secondary collision energy, the greater the relative concentration of clusters with fewer dba ligands (**Figure 44**).
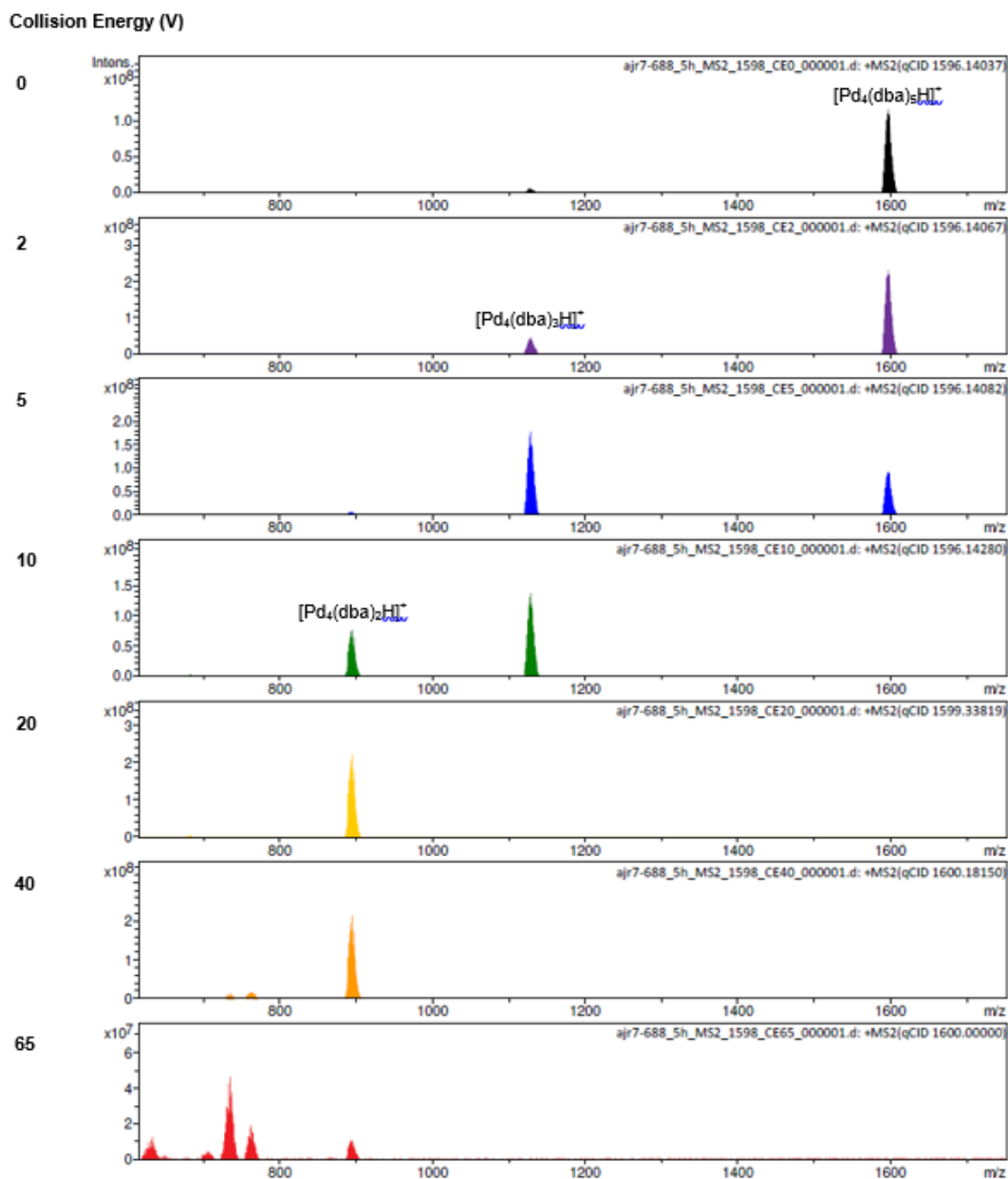
Figure 44 ESI–MS–MS spectra of [Pd$_4$dba$_y$H]$^+$ cluster species.

The evidence from **Figure 44** implies that the larger Pd$^0_4$dba$_y$ species form from the smaller ones *i.e.* there is rapid addition of dba ligands to the initially forming, stable [Pd$_4$dba$_2$H]$^+$ ion. This is highlighted by the fractional bar chart presented in **Figure 45**, which compares the relative abundance of the observed ions as a function of secondary collision energy.
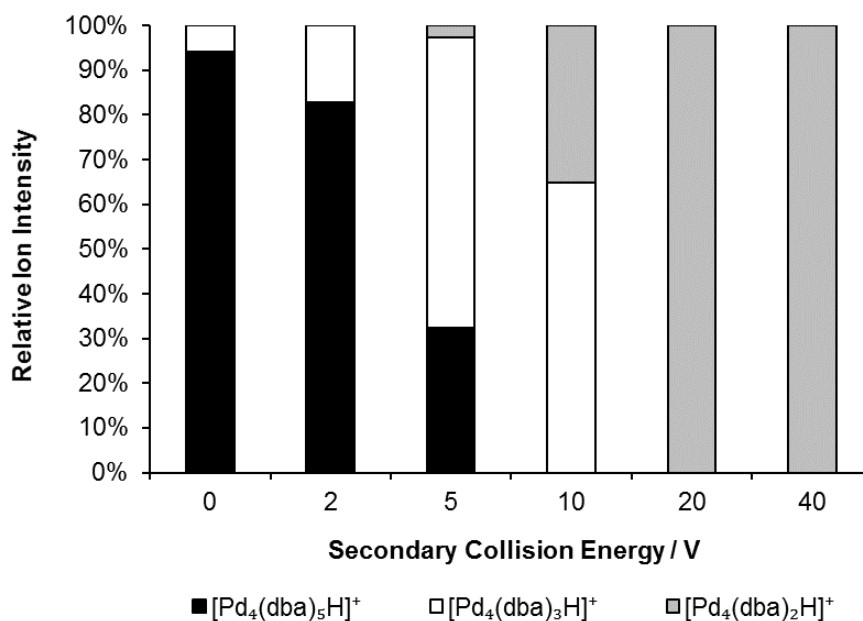
Figure 45 Relative abundance of $[Pd_4dba_yH]^+$ cluster species as a function of secondary collision energy.

As ESI–MS proved a suitable method by which to study the dynamic, cluster-forming behaviour of complex **238** in solution, two similar experiments were devised to attempt to extrapolate structural and kinetic data. These would ideally provide direct evidence of Pd cluster formation from complex **238** as a function of time, complementary to the ^{1}H NMR experiments shown in **Figure 38** and **Figure 39** which provided indirect evidence of this process.

In the first experiment, a solution of acid **252** in anhydrous chloroform was added to a solution of complex **238** in anhydrous chloroform under nitrogen. This mixture was then stirred at room temperature for eight hours, with a sample taken every 30 minutes and analysed by ESI–MS. The $Pd_4(dba)_2$ species was again the major Pd cluster signal seen in all spectra, so the peak height for this cluster (ion $[Pd_2(dba)_4Na]^+$) was normalised to 100% and the peak heights for all other species were monitored relative to this value. While similar ions were observed as in the previous study (Figure 42), no appreciable change in the relative intensities of these ions was observed as a function of time. Specifically, no increase in the relative concentration of larger Pd clusters, as compared to smaller Pd clusters, was observed. An analogous experiment was thus performed, with samples taken every two minutes for a half hour period, which were subsequently analysed by ESI–MS, in order to monitor any rapid changes that might occur in the early stages of the reaction (**Table 14**).

Table 14 Pd$_x$dba$_y$ clusters formed from **238** as a function of time.[a]

Time / min	0	2	4	6	8	10	30
Ion Detected	**Relative Intensity / %[b]**						
[Pd₂(dba)₂H]⁺	0	22.1	21.3	22.6	24.5	20.1	25.1
[Pd₂(dba)₄H]⁺	91.2	0	0	0	0	0	0
[Pd₂(dba)₄Na]⁺	65.1	14.3	15.6	14.3	13	19.2	9.1
[Pd₂(dba)₅Na]⁺	34.3	4.4	4.4	4.1	3.8	5.5	2.8
[Pd₄(dba)₂H]⁺	0	0	0	0	0	0	0
[Pd₄(dba)₂Na]⁺	100	100	100	100	100	100	100
[Pd₄(dba)₃H]⁺	0	0	0	2	2.1	0	2.5
[Pd₄(dba)₄Na]⁺	0	0	0	0	0	0	0
[Pd₄(dba)₅H]⁺	8.4	19.8	18.3	25.9	23.6	24.1	19.9
[Pd₄(dba)₇Na]⁺	15.5	7.6	9	7.7	7.5	10.4	5
[Pd₄(dba)₈Na]⁺	11	4.4	4.5	3.9	3.7	5.3	2.6
[Pd₆(dba)₅Na]⁺	15.9	41.4	40.8	55	58	55.1	44.4
[Pd₆(dba)₈H]⁺	1.4	8.3	6.6	15.8	16.5	10.6	9
[Pd₆(dba)₉Na]⁺	7.5	8.2	8.2	7.7	6.9	8	1.7
[Pd₆(dba)₁₀Na]⁺	0	1.3	0	0	0	0	0

[a] Reaction conducted with **238** (100 mg, 0.09 mmol, 1 eq.) and **252** (18 mg, 0.09 mmol, 1 eq.) in dry CHCl₃ (10 mL) under N₂. [b] Intensities normalised to the [Pd₄(dba)₂H]⁺ ion at 100%.

The only significant change in ion distribution was observed before and after addition of the acid, this distribution did not however change further as a function of time. The intensity of two clusters containing two Pd atoms, $Pd_2(dba)_4$ and $Pd_2(dba)_5$, is markedly reduced after addition of acid. The relative intensity of the $Pd_2(dba)_2$ cluster is increased however, possibly due to greater stability of this species versus those Pd clusters with two Pd atoms and a greater number of dba ligands. Conversely, the quantity of $Pd_4(dba)_5$ and $Pd_6(dba)_5$ clusters significantly increases upon addition of acid **252**, which may indicate a growth of Pd clusters upon addition of acid, as suggested above.

These studies provide some structural information about the degradation observed by ^{1}H NMR (**Figure 38** and **Figure 39**). Direct evidence for the growth of $Pd^0_x(dba)_y$ clusters has been found, with at least two pathways observed. The first appears spontaneous; in solution dissociation of dba ligand **247** releases Pd^0 from complex **238**, which agglomerates to form a relatively stable $Pd^0_4(dba)_2$ cluster. Rapid addition of free ligand **238** in solution then occurs to give secondary $Pd^0_4(dba)_{2+x}$ clusters. Upon addition of acid **252**, a decrease in the concentration of smaller clusters is concurrent with an increase in the concentration of larger clusters, importantly these secondary clusters contain not just additional ligand **247** but consist of greater number of Pd atoms. This behaviour is suggestive of increased concentrations of free ligand **247** and elemental Pd^0 in solution, as a result of acid-promoted ligand dissociation from complex **238**. The expected increase in the concentration of larger Pd clusters as a function of time was not observed, it may be however that the ions observed are on the limit of solubility. Large species are therefore not observable under these conditions due to rapid growth and subsequent insolubility. These observations would agree with the unusual two-phase degradation behaviour seen through observation of the ligand signals by ^{1}H NMR (**Figure 38** and **Figure 39**). Finally, it is important to note that when stored at 5 °C in the dark, complex **238** shows long-term stability in the solid state, ascertained by both ^{1}H NMR spectroscopic analysis and elemental (CHN) analysis. Atmospheric air has no appreciable deleterious effect on the stability of this complex in the solid state.

4.4 Conclusion

The important Pd^0 precursor complex $Pd_2(dba)_3$ has been prepared and recrystallized in several solvents. Several high-quality single-crystal X-ray diffraction structures have been obtained, allowing for the complex asymmetric alkene binding of the dba ligands to be characterised in both the major and minor isomers of the complex. The exchange rates of these two isomers in solution were shown to differ from one another and free ligand **247** through the use of VT–NMR. The stability of the chloroform adduct of this complex (**238**) when exposed to both water and acid has been probed by NMR and MS studies; direct and indirect evidence of $Pd^0_x(dba)_y$ cluster formation under these conditions has been obtained. These observations taken together appear to demonstrate that complex **238** is a viable source of catalytically active PdNPs under commonly found experimental conditions.

Part of the work described in this chapter has been included in a recent publication (see Appendix 1).[173]

Chapter 5: Conclusions and Future Work

5.1 Conclusions

The research presented in this thesis has explored the development and application of Pd-catalysed C–H bond functionalisation methodologies, with a particular focus on direct arylation reactions. Central to this work has been the pursuit of novel methods for the selective functionalisation of the essential amino acid tryptophan **74**, as well as related tryptophan-containing peptides. Arylated tryptophan compounds such as **75**, the key target compound in this project, display greatly enhanced fluorescence compared to their parent structures.[109,112,119] Previous approaches have required either; pre-functionalisation through borylation,[110] bromination[112] and iodination,[117] or high temperatures[114] and stoichiometric additives such as AgBF$_4$ or TFA.[115] A combination of diaryliodonium salts and catalytic palladium has been established to provide access to this important class of compounds, without these disadvantages. Further development has led to the application of aryldiazonium salts as electrophilic coupling partners, allowing access to a wide range of derivatised tryptophan structures in excellent yields. Using these in tandem with a Pd–OTs catalytic system has also allowed the catalyst loading to be significantly reduced. (**Scheme 89**).
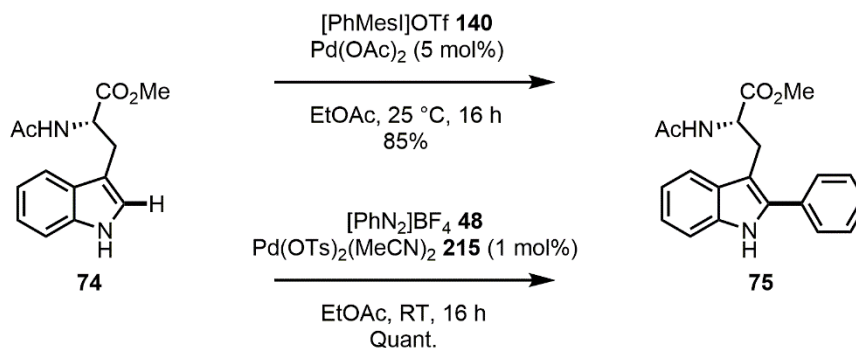
Scheme 89 Reaction conditions for the direct arylation of tryptophan **74** developed in this project.

Calculation of some simple mass-based green metrics for these processes has demonstrated that these latter conditions offer a significant improvement over all previously reported methods in terms of optimum efficiency, mass intensity, synthetic utility and selectivity. These protocols have also been demonstrated to be effective in the modification of several small tryptophan-containing peptides, affording several novel functionalised molecules (**Figure 46**).
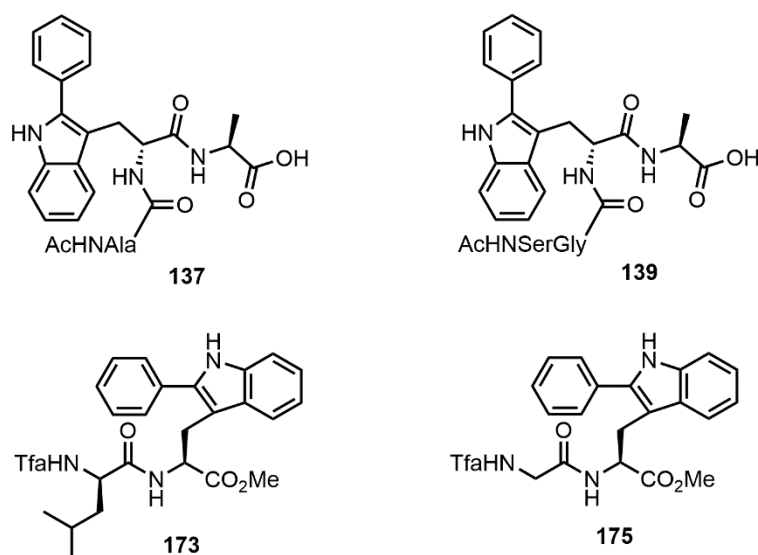
Figure 46 Key molecules obtained through the direct arylation of peptides.

The reaction conditions using aryldiazonium salts shown in **Scheme 89** were subsequently explored as a more general direct arylation methodology, with a view to combining these atom-efficient coupling partners with heterogeneous Pd catalysis. Efforts to apply this chemistry to the functionalisation of several medicinally relevant nitrogen heterocycles met with limited success; of the substrates and conditions screened only 7-azaindole **231** demonstrated any reactivity when using Pd(OAc)$_2$ as a catalyst, and this protocol demonstrated no activity when using heterogeneous Pd catalysts. This observation was also made when returning to tryptophan **74** as a substrate, indicating that direct arylation reactions combining aryldiazonium salts and heterogeneous Pd catalysis is a significant challenge, a deduction supported by the scarcity of examples in the literature.

Following recently published work by Glorius and co-workers,[148] the combination of diaryliodonium salts and heterogeneous Pd catalysts has been shown able to produce high reactivity in several direct arylation reactions. The direct arylation of the amino acid tryptophan **74** and tryptophan-containing peptides **167** and **170** has for example been achieved under these conditions. The pre-synthesised nanoparticle catalyst PVP–Pd **13** was also demonstrated as an effective catalyst in this chemistry; **13** has however been shown both qualitatively and quantitatively to degrade over many months under air at ambient temperature, with a concomitant loss of activity. An interesting dichotomy in activity between several apparently similar forms of Pd supported on activated carbon has been noted in this chemistry, suggestive of distinct sizes and/or morphologies of the Pd particles present in these ubiquitous catalysts. The activity of these catalysts for the direct arylation of 7-azindole **231** is shown as an example (**Scheme 90**).
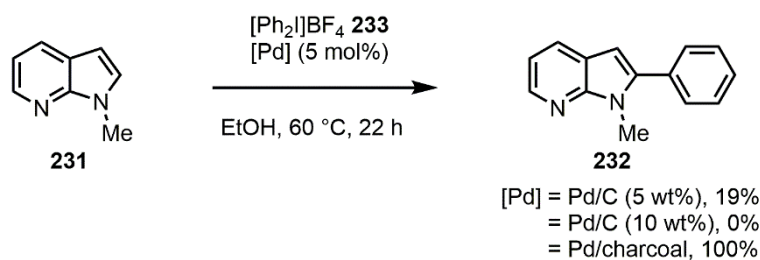
Scheme 90 Direct arylations of **231** highlighting differences in Pd/C catalysts.

Reaction profile analysis using *ex situ* GC sampling has been used to evaluate the activity of four Pd catalysts, Pd(OAc)$_2$, Pd$_2$(dba)$_3$.CHCl$_3$ **238**, Pd/C and PVP–Pd **13**, in the direct arylation of several simple heterocycles. This demonstrated remarkable similarities in catalytic behaviour between apparently distinct catalysts, implying that dissimilar catalysts can function as precatalysts for the formation of a single comparable active catalyst phase; speciation to form PdNPs or clusters is proposed as one possible mechanism in this process. A pronounced substrate effect has also been noted in these studies, which goes some way towards suggesting that reaction conditions including model substrate choice may in some cases be more important than the particular Pd (pre)catalyst used. These studies highlighted the importance of kinetic analysis in reactions mediated by Pd catalysis, as opposed to evaluating catalyst performance merely as a function of yield.

The structure and degradation behaviour of the important Pd^0 pre-catalyst Pd$_2$(dba)$_3$·CHCl$_3$ **238** has also been studied, with a view to its potential as a source of catalytically active PdNPs. Analysis of the X-ray diffraction structures of several solvent adducts of this complex has allowed the asymmetric binding of the dba ligands to the metal centres to be characterised, in both the major and minor isomers of this complex (ratio major:minor is 79:21). Solution-phase analysis of **238** by ^{1}H NMR spectroscopy has also demonstrated that the exchange rates of the two isomers and free dba ligand differ from one another; they also vary significantly as a function of temperature. This means that reported[170] methods of determining the absolute amount of complex as compared to free ligand by ^{1}H NMR cannot be viewed as an empirically accurate measure. Finally, the stability of **238** when exposed to water and acid has been probed by both ^{1}H NMR and MS studies; direct and indirect evidence of speciation to form Pd^0_x(dba)$_y$ clusters has been observed, which are proposed as a precursor to larger PdNPs (**Figure 47**). These observations demonstrate that **238** is a viable source of catalytically active PdNPs under commonly found experimental conditions, such as those observed in the direct arylation methodologies detailed above.
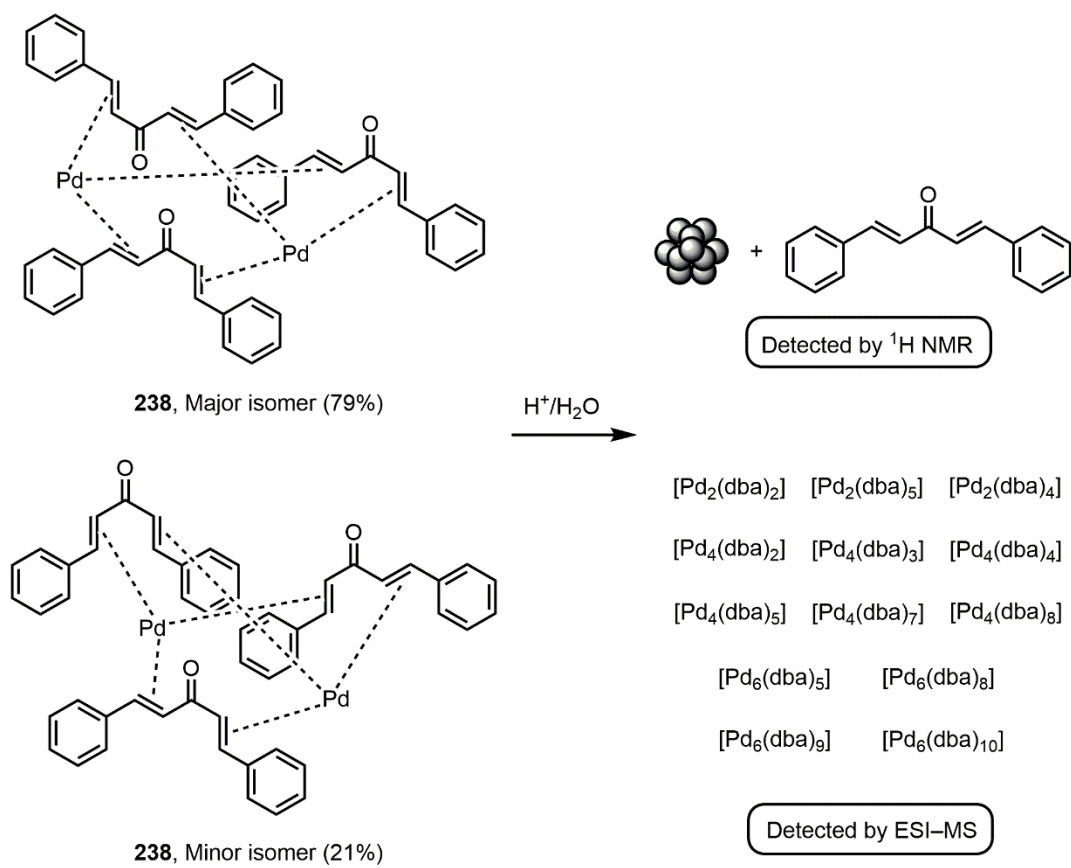
Figure 47 Degradation behaviour of **238** as observed by ^{1}H NMR and ESI–MS analysis.

5.2 Future Work

5.2.1 Mechanism of Tryptophan Functionalisation

The synthetic work performed during this project has produced several protocols for the direct C–H bond functionalisation of tryptophan and tryptophan-containing peptides (**Scheme 89**). The methodology utilising aryldiazonium salts is particularly novel, further investigation into the mechanism of this transformation therefore has significant value. The *C2*-arylated product **75** possesses a Stokes shift of 62 nm relative to starting material **74**, enabling the kinetic profile of the arylation reaction to be examined by UV–visible spectroscopic analysis. Initial studies performed within the Fairlamb group have shown that the product evolution curve from a reaction catalysed by Pd(OAc)$_2$ exhibits an unusual sigmoidal kinetic trace (**Figure 48**),[131] which certainly merits further investigation.
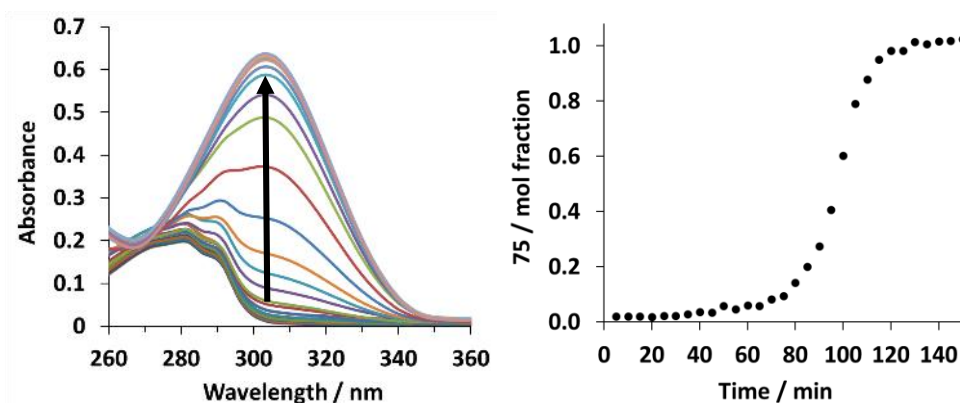
Figure 48 (a) UV–visible spectra showing formation of **75** at 304 nm (5 min intervals) at 37 °C. (b) Plot showing evolution of **75** over time.

As highlighted in Chapter 2, significant rate enhancements were observed with the addition of catalytic TsOH due to removal of the observed induction period;[131,132] this effect was also seen when using pre-catalyst Pd(OTs)$_2$(MeCN)$_2$ **215**, which is known to form the catalytically relevant species **253**.[133,134] It is therefore possible that the arylation proceeds *via* a key tryptophan coordination complex such as **254** (**Scheme 91**).
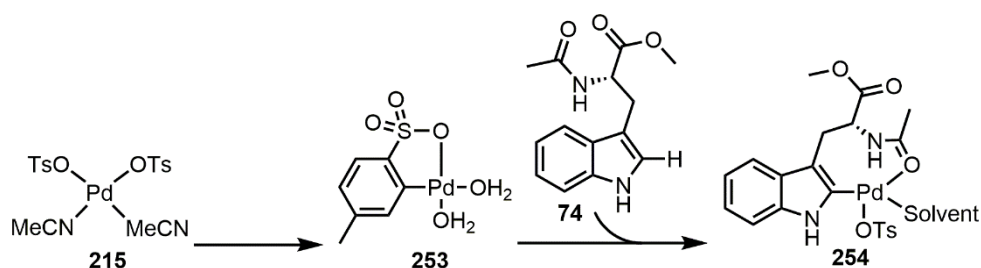
Scheme 91 Pre-catalyst activation and proposed tryptophan intermediate.

If species **254** is indeed a key intermediate, it implies a non-innocent role for the amine protecting group used. Mono-protected amino acids are well established as useful ligands for the acceleration of catalytic processes,[177] tailoring of these protecting groups could therefore provide significant mechanistic information. Investigation of the initial rates of reaction for the cross-section of substrates shown in **Figure 49** would provide a useful platform to probe this hypothesis.
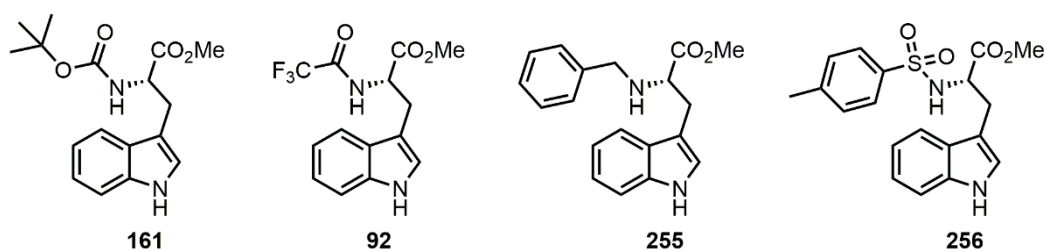
Figure 49 Alternative *N*-terminus protected tryptophan substrates.

5.2.2 Further Tryptophan Derivatives

A recent publication has detailed the selective *C*7-borylation of tryptophans using Ir catalysis,[178] providing a facile method of generating valuable tryptophan structures to test in the novel arylation conditions developed in this project (**Scheme 92**).
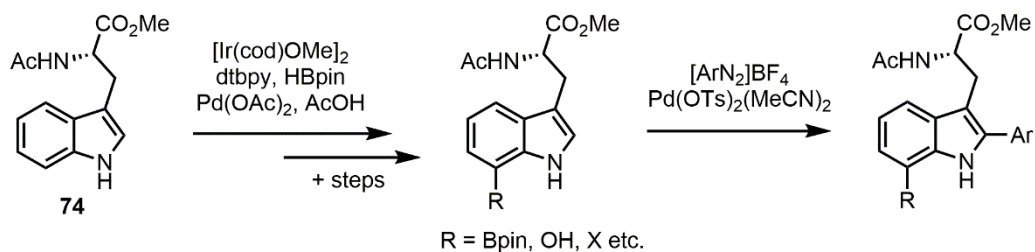
Scheme 92 Orthogonal borylation/arylation conditions for tryptophan **74**.

Along similar lines, those tryptophan derivatives containing *C*2-aryl halide motifs already synthesised (Chapter 2) could be subjected to standard cross coupling conditions in order to generate products with modified fluorescence properties (**Scheme 93**).
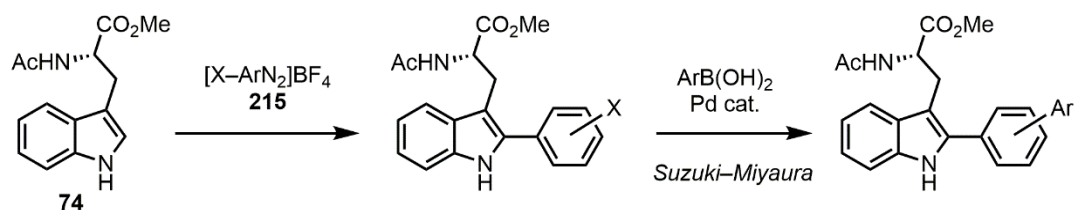
Scheme 93 Sequential arylation/cross-coupling for tryptophan **74.**

5.2.3 Direct Arylations Using Aryldiazonium Salts

Examples of direct arylation reactions using aryldiazonium salts as the arene coupling partner are rare in the literature.[101,102] The work performed on tryptophan **74** within this project provides a stark indication of their potential utility, if suitable reaction conditions can be found. Attempts in this direction have met with limited success in this project; some encouraging signs, such as the successful arylation of 7-azaindole **231**, have however been seen (Chapter 3). While there is great interest in the arylation of indoles both in the literature and in this report, recent developments in medicinal chemistry have highlighted the need for research to focus on more unusual scaffolds, based on both the statistical trends seen in the hit-rate of potential drug candidates and the need for novel structures to ensure intellectual property rights.[179] With this in mind, a focus on the direct arylation of non-typical heterocycles would provide an interesting avenue of research, particularly if this could be coupled with the heterogeneous palladium catalysis detailed above. A recent paper by Groom *et al.* highlights a range of such heterocycles[180] and some potential candidates that might be suitable for direct arylations are shown in **Figure 50**.
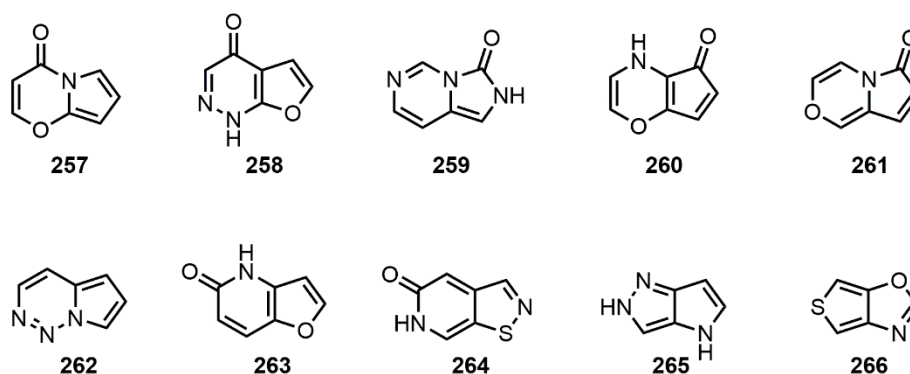
Figure 50 Potential heterocyclic substrates for novel direct arylation methodologies.

To paraphrase a recent review, "a significant increase in the number of new ring systems would not necessarily lead to an associated increase in success rates for drug discovery projects. A suggested alternative strategy is to focus first on the assembly of existing drug ring systems in novel configurations".[150] Development of a versatile direct arylation methodology with good green metrics such as that shown in **Scheme 89** would provide a suitable platform to explore novel drug space in this fashion. Several of the potential substrates shown in **Figure 50** have more than one site which could be functionalised by direct arylation, so there is a possibility that a site-selective arylation methodology could be developed to functionalise at more than one position on the heteroaromatic. Glorius and co-workers have shown that appropriate choice of Pd catalyst can provide such regioselectivity in similar protocols.[147] This is an area where research efforts could be focused in an attempt

to not only produce selective arylation procedures for medicinally-useful compounds, but also to provide a link to the development of a range of rationally-designed palladium catalysts which can be used to perform differing, selective transformations.

5.2.4 Direct C–H Bond Functionalisations Using Pd Nanocatalysts

Despite its widespread use as a heterogeneous hydrogenation catalyst, Pd/C has only recently been explored for other Pd-mediated catalysis in any detail, usually in cross-coupling reactions.[37-40] Glorius and co-workers are particularly notable for their continuing development of C–H bond functionalisation reactions using this catalyst.[147-149] The direct arylation of several common heterocycles such as (benzo)thiophene, indole and (benzo)furan have been demonstrated to be effectively catalysed by this cheap, readily available Pd source. One drawback of these protocols however lies in the poor degree of characterisation of such catalysts; Glorius and co-workers have in fact noted severe incongruities in the activities and yields obtained thereof when utilising Pd/C from different commercial sources. To date, no specific analysis of how the catalyst structure/morphology relates to its activity in these reactions has been performed. In this project (Chapter 3) similarities in catalytic behaviour between apparently distinct Pd catalysts have been demonstrated, suggesting formation of a comparable active catalytic phase, such as PdNPs, in these reactions. It may be that PdNPs are not actively catalysing these reactions, the active species instead consisting of leached mononuclear/lower-order Pd species. If this is the case, then perhaps the parallels between catalyst type manifests as a result of similar leaching rates.

Conversely many well-defined Pd nanocatalysts have been synthesised and their catalytic activities (often in hydrogenation reactions) correlated to specific features of their size and/or shape.[181-183] Effectively controlling the morphology of these nanocatalysts, usually through appropriate choice of stabilising and surface-capping agents along with carefully-tailored reduction rates, is far from a routine operation however. Such specific syntheses are typically capricious, with centrifugation often applied to produce the desired nanocatalysts in very low yields, thus reducing the synthetic appeal of these processes.[184-187] These species can also demonstrate significant deterioration from their original size or shape over time.[146]

In light of this dichotomy, between the development of operational ease in elegant C–H bond functionalisation protocols using Pd nanocatalysts and the judicious structure/activity relationships explored in other heterogeneous catalytic processes, there is significant scope for an exploration of how these two concepts can be effectively combined. Typical conditions for the synthesis Pd nanocatalysts begin with reduction of the Pd precursor Na_2PdCl_4 by ascorbic acid, in the presence of PVP **12** as a stabiliser and KBr as a surface capping agent.

By using varying ratios of these reagents, as well of modification of the temperature and duration of the synthesis, a number of structurally varied catalysts can be prepared (some examples are highlighted in **Table 15**).[188]

Table 15 Nanoparticle shapes obtained through variation of synthetic conditions.

Entry	Reducing agent	Capping agent	Temp. / °C	Particle shape
1	Ascorbic acid	-	100	Truncated octahedron
2	-	-	100	Hexagonal/triangular plate
3	Ascorbic acid	KBr	100	Rod
4	Ascorbic acid	KBr	80	Cube

The nanocatalysts could be supported on activated carbon to generate supported particles,[189] in order to mimic the operational ease found with commercially available Pd/C, as well as preventing distortions of the size or morphology of the desired catalyst. With these well-defined Pd catalysts in hand, a screen of various heterocyclic compounds against the direct arylation protocols developed in this project could be performed. There is also potential for site selectivity to be affected in those heterocycles with multiple activated C–H bonds. It would be remarkable if this site selectivity could be achieved through perceptive choice of nanocatalyst morphology, providing an important link to the development of rationally-designed heterogeneous palladium nanocatalysts which can be used to perform differing, selective transformations.

Finally, the evidence that $Pd_2(dba)_3 \cdot CHCl_3$ **238** serves as a competent source of PdNPs raises the possibility that the activity of these particles can be evaluated (Chapter 4). Aging studies on **238** could be used to provide PdNPs of different sizes and/or morphologies, the activity of which could be tested and compared in a model catalytic reaction, in order to gain important mechanistic insight. Crucially, this would extend the reported equilibrium between 'L_2Pd^0' and '$L_2Pd^0(\eta^2\text{-dba})$' to include multinuclear Pd colloids with varying ratios of dba **247** ligand (**Figure 47**).

Chapter 6: Experimental

6.1 General Experimental Details

Solvents and Reagents

Commercially sourced solvents and reagents were purchased from Acros Organics, Alfa Aesar, Fisher Scientific, Fluorochem, Sigma-Aldrich or VWR and used as received unless otherwise noted. Petrol refers to the fraction of petroleum ether boiling in the range of 40–60 °C. Dry acetonitrile, dichloromethane, THF and toluene were obtained from a Pure Solv MD-7 solvent machine and stored under nitrogen. The acetonitrile, dichloromethane and THF were also degassed by bubbling nitrogen gas through the solvent with sonication. Dry methanol was obtained by storing over activated 3 Å molecular sieves under nitrogen. Dry chloroform was obtained by stirring with K_2CO_3 overnight, then distilling over P_2O_5 under N_2. Dry acetone was obtained by distilling over K_2CO_3 under N_2. Dry Et_3N and DIPEA were obtained by distillation over potassium hydroxide and stored under nitrogen. Dry DMSO was purchased from Acros Organics and used as received. Dry, degassed $CDCl_3$ was obtained by stirring over anhydrous CaH_2 for 24 h then using the freeze-pump-thaw method (3 cycles). This was then distilled at high vacuum (0.03 mm Hg) and stored in a Braun Unilab dry glove box. Dry, degassed DMSO-d_6 was obtained by stirring over activated molecular sieves for 4 days then using the freeze-pump-thaw method (3 cycles). This was then distilled at high vacuum (0.03 mm Hg) under heating and stored in a Braun Unilab dry glove box.

Typical Conditions

Room temperature (RT) refers to reactions where no thermostatic control was applied and was recorded as 16–23 °C. Reactions requiring anhydrous or air-free conditions were performed in dry solvent under an argon or nitrogen atmosphere using oven- or flame-dried glassware. Nitrogen gas was oxygen-free and dried immediately prior to use by passing through a column of potassium hydroxide pellets and silica. Where indicated, a Braun Unilab dry glove box was used (<0.5 ppm O_2).

Flash Chromatography

Thin layer chromatography (TLC) analysis was performed using Merck 5554 aluminium backed silica plates. Spots were visualised by the quenching of ultraviolet light (λ_{max} = 254 nm) then stained and heated with one of *p*-anisaldehyde or potassium permanganate as appropriate. Retention factors (R_f) are quoted to two decimal places and reported along with the solvent system used in parentheses. All flash column chromatography was performed

146

using either Merck 60 or Fluorochem 60 Å silica gel (particle size 40–63 μm) and the solvent system used is reported in parentheses.

Optical Rotations

Optical rotations were recorded using a digital polarimeter at 20 °C (using the sodium D line, 259 nm) with a path length of 100 mm, with the solvent and concentration used indicated in the text. The appropriate solvent was used as a background with ten readings taken for each sample and the average $[\alpha]_D$ values in units of 10^{-1} deg cm^3 g^{-1} quoted to one decimal place.

Melting Points

Melting points were recorded using a Stuart digital SMP3 machine using a temperature ramp of 3 °C min^{-1} and are quoted to the nearest whole number. Where applicable, decomposition (dec.) is noted.

Nuclear Magnetic Resonance Spectroscopy

All NMR spectra were recorded on either a Jeol ECS400, Jeol ECX400 or Bruker AV500 spectrometer at 298 K, unless otherwise specified. Chemical shifts are reported in parts per million (ppm) of tetramethylsilane. Coupling constants (*J*) are reported in Hz and quoted to ±0.5 Hz. Multiplicities are described as singlet (s), doublet (d), triplet (t), quartet (q), quintet (quin), sextet, (sext), heptet (hept), multiplet (m), apparent (app) and broad (br). Spectra were processed using MestReNova. Copies of NMR spectra for all compounds are provided in Appendix 7.

Proton (^{1}H) spectra were typically recorded at 400 MHz. Alternatively and where specified, spectra were recorded on a Bruker AV500 spectrometer at 500 MHz. Chemical shifts are internally referenced to residual undeuterated solvent ($CHCl_3$ δ_H = 7.26 ppm) and given to two decimal places.

Carbon-13 (^{13}C) spectra were recorded at 101 MHz. Chemical shifts are internally referenced to residual solvent ($CDCl_3$ δ_C = 77.16 ppm) and given to one decimal place.

Boron-11 (^{11}B) spectra were recorded at 128 MHz and obtained with ^{1}H decoupling. Chemical shifts are externally referenced to $BF_3 \cdot OEt_2$ and given to one decimal place.

Fluorine-19 (^{19}F) spectra were recorded at 376 MHz and obtained with ^{1}H decoupling. Chemical shifts are externally referenced to $CFCl_3$ and given to one decimal place.

Phosphorus-31 (^{31}P) spectra were recorded at 162 MHz and obtained with ^{1}H decoupling. Chemical shifts are externally referenced to H_3PO_4 and given to one decimal place.

Mass Spectrometry

Electrospray ionisation (ESI) mass spectrometry was performed using a Bruker Daltronics micrOTOF spectrometer. Liquid induction field desorption ionisation (LIFDI) mass spectrometry was performed using a Waters GCT Premier mass spectrometer. Mass to charge ratios (*m/z*) are reported in Daltons with percentage abundance in parentheses along with the corresponding fragment ion, where known. Where complex isotope patterns were observed, the most abundant ion is reported. High resolution mass spectra (HRMS) are reported with less than 5 ppm error.

Infrared Spectroscopy

Infrared spectra were recorded using a Bruker Alpha FT-IR spectrometer and were carried out as ATR. Absorption maxima (v_{max}) are reported in wavenumbers (cm^{-1}) to the nearest whole number and described as weak (w), medium (m), strong (s) or broad (br).

UV-Visible Spectroscopy

UV-visible spectroscopy was performed on a Jasco V-560 spectrometer, with a background taken in the appropriate solvent prior to recording spectra, using a quartz cell with a path length of 1 cm. The wavelength of maximum absorption (λ_{max}) is reported in nm along with the extinction coefficient (ε) in mol dm^{-3} cm^{-1}. Copies of the appropriate absorption spectra and Beer–Lambert plots are given in Appendix 3.

Gas Chromatography

Gas chromatographic analysis was carried out using a Varian GC-430 gas chromatogram. Statistical analyses were performed using Microsoft Excel and Origin. Method details and copies of the appropriate calibration plots are provided in Appendix 5.

Elemental Analysis

Elemental (CHN) analysis was carried out using an Exeter Analytical CE-440 Elemental Analyser. All values are given as percentages to two decimal places.

X-Ray Crystallography

Diffraction data were collected at 110 K on an Agilent SuperNova diffractometer MoKα radiation ($\lambda = 0.71073$ Å). Data collection, unit cell determination and frame integration were carried out with CrysalisPro. Absorption coefficients were applied using face indexing and the ABSPACK absorption correction software within CrysalisPro. Structures were solved and refined using Olex2[190] implementing SHELX algorithms and the Superflip[191-193] structure

solution program. Structures were solved by charge flipping, Patterson or direct methods and refined with the ShelXL[194] package using full-matrix least squares minimisation. All non-hydrogen atoms were refined anisotropically. Where applicable, absolute configurations were established by anomalous dispersion. Resolved structures, crystal data and structural refinement are provided in Appendix 2.

Transmission Electron Microscopy

Transmission electron microscopy was performed at the Department of Biology Technology Facility, University of York, using an FEI Technai 12 G2 BioTWIN microscope operating at 120 kV, and images were captured using an SIS Megaview III camera. Samples were prepared by suspending *ca.* 1 mg of material in reagent grade ethanol with vigorous shaking, applying a small amount to a TEM grid, and allowing the solvent to evaporate. The grids used were 200 mesh copper grids with a Formvar/carbon support film. The resulting images were enlarged and particle sizes measured manually. Statistical analyses were performed and histograms drawn using Microsoft Excel 2010 with the Data Analysis ToolPak.

6.2 General Procedures

General Procedure A: Synthesis of aryldiazonium tetrafluoroborates in water[129]

The appropriate aniline (1 eq.) was dissolved in deionised water and HBF_4 (50 wt% in H_2O, 2 eq.) before being cooled to 0 °C with stirring. A solution of $NaNO_2$ (1 eq.) in deionised water was then added dropwise and the mixture was stirred vigorously for 30 min during which time a precipitate formed. After 30 min this was collected by filtration through a glass sinter and the solid dissolved in a minimum amount of acetone. Et_2O was then added to precipitate the aryldiazonium tetrafluoroborate which was collected by filtration through a glass sinter and washed with further Et_2O until the filtrate ran clear, then dried *in vacuo* to afford the desired compound, which was subsequently stored at −18 °C.

General Procedure B: Synthesis of aryldiazonium tetrafluoroborates in ethanol[130]

The appropriate aniline (1 eq.) was dissolved in ethanol and HBF_4 (50 wt% in H_2O, 2 eq.) before being cooled to 0 °C with stirring. A 90% solution of *tert*-butylnitrite (2 eq.) was then added dropwise and the mixture was allowed to warm to room temperature with stirring for 1 h. After 1 h Et_2O was added to precipitate the aryldiazonium tetrafluoroborate which was collected by filtration through a glass sinter and washed with further Et_2O until the filtrate ran clear, then dried *in vacuo* to afford the desired compound, which was subsequently stored at −18 °C.

General Procedure C: Direct arylation of tryptophan with aryldiazonium salts

To a microwave tube was added tryptophan **74** (50 mg, 0.192 mmol, 1 eq.), the appropriate aryldiazonium salt (0.192 mmol, 1 eq.), Pd(OAc)$_2$ (2.2 mg, 9.6 μmol, 5 mol%) and EtOAc (5 mL). The reaction mixture was stirred at RT for 16 h. After 16 h the resulting brown reaction mixture was filtered through Celite then washed with sat. aq. NaHCO$_3$. The organic layer was collected and dried over MgSO$_4$, filtered and evaporated to give a brown solid. When purification was required, it was performed using dry-loaded flash column chromatography with a SiO$_2$ stationary phase and the solvent system specified for each compound.

General Procedure D: Kinetic study of the direct arylation of heterocycles

To a microwave vial fitted with magnetic stirrer bar was added diaryliodonium salt **233** (309 mg, 0.84 mmol, 1.4 eq.), Pd catalyst (5 mol%) and EtOH (3 mL). To initiate the reaction, substrate (0.6 mmol, 1 eq.) was added, the vial sealed with a septum and the reaction stirred at 60 °C for 24 h in a pre-heated solid heating block. The progress of the reaction was monitored by GC, using an external standard solution of mesitylene (139 μL in 100 mL EtOH, 9.975×10^{-3} mol dm^{-3}). Sampling was performed by taking 80 μL aliquots, adding these to an Eppendorf tube containing Celite and centrifuging for 10 min. After 10 min 30 μL of the supernatant layer was removed and diluted with mesitylene standard (0.6 mL). This sample was then analysed by GC, using an initial temperature of 60 °C (1 min), followed by a ramp of 30 °C min^{-1} to 250 °C, giving a total run time of 9.33 min. Three injections were performed for each data point.

6.3 Synthetic Procedures and Compound Data

Throughout this section, laboratory notebook references are given for the experiment from which the synthetic procedure is quoted. For experiment references for specific data, see the relevant NMR spectra in Appendix 7. Known compounds prepared using literature procedures are indicated with a literature reference next to the compound name. Known compounds prepared using novel procedures are compared to literature analytical data and referenced accordingly.

Methyl (2*S*)-2-amino-3-(1*H*-indol-3-yl)propanoate hydrochloride (135)[121]
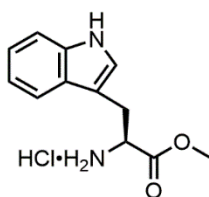
To a round-bottomed flask was added MeOH (50 mL) which was cooled to −15 °C, before addition of thionyl chloride (4.3 mL, 7.02 g, 59 mmol, 2.4 eq.) dropwise at −15 °C. After complete addition, L-Tryptophan **73** (5 g, 24.5 mmol, 1 eq.) was added in three portions, resulting in a white suspension. The mixture was then warmed to RT and stirred for 24 h, during which time a clear orange solution was formed. Deionised water (5 mL) was added to the reaction mixture and the solvent evaporated to afford the *title compound* as an off-white solid (6.24 g, quant.).

M.P. 205–206 °C dec. (lit.[195] 214 °C dec.); ^{1}H NMR (400 MHz, CD$_3$OD, δ): 10.61 (br s, 1H), 7.54 (dt, *J* = 8.0, 1.0 Hz, 1H), 7.40 (dt, *J* = 8.0, 1.0 Hz, 1H), 7.22 (s, 1H), 7.14 (ddd, *J* = 8.0, 7.0, 1.0 Hz, 1H), 7.07 (ddd, *J* = 8.0, 7.0, 1.0 Hz, 1H), 4.33 (dd, *J* = 7.5, 5.5 Hz, 1H), 3.79 (s, 3H), 3.46 (dd, *J* = 15.0, 5.5 Hz, 1H), 3.37 (dd, *J* = 15.0, 7.5 Hz, 1H); ^{13}C NMR (101 MHz, CD$_3$OD, δ): 170.8, 138.3, 128.2, 125.6, 122.9, 120.3, 118.8, 112.7, 107.4, 54.6, 53.6, 27.5; ESI–MS *m/z* (ion, rel. %): 219 ([C$_{12}$H$_{15}$N$_2$O$_2$]$^+$, 100); ESI–HRMS *m/z*: 219.1130 [C$_{12}$H$_{15}$N$_2$O$_2$]$^+$ (C$_{12}$H$_{15}$N$_2$O$_2$ requires 219.1128); IR (solid-state ATR, cm^{-1}): 3259 (w), 2856 (w, br), 1747 (s), 1501 (m), 1436 (m), 1351 (m), 1210 (m), 1108 (m), 730 (s); Elemental anal.: C 56.44, H 5.85, N 10.87 (C$_{12}$H$_{15}$ClN$_2$O$_2$ requires C 56.58, H 5.94, N 11.00).

Lab book reference number: AJR-8-710

Methyl (2*S*)-2-acetamido-3-(1*H*-indol-3-yl)propanoate (74)[121]
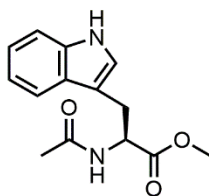
To a two-necked round-bottomed flask fitted with a reflux condenser was added tryptophan **135** (3 g, 13.7 mmol, 1 eq.), Et$_3$N (2 mL, 1.45 g, 14.3 mmol, 1.05 eq.) and THF (150 mL). The mixture was stirred to give a white suspension before being cooled to 0 °C, then acetic anhydride (1.4 mL, 1.5 g, 15.1 mmol, 1.1 eq.) was added in one portion. The reaction was then stirred for 2 h at reflux to give a white suspension. After 2 h this was added to deionised

water (150 mL) and extracted into EtOAc (3 × 150 mL). The organic layers were combined and washed sequentially with 1 M aq. HCl (100 mL), sat. aq. NaHCO$_3$ (100 mL) and brine (100 mL). The organic layer was collected, dried over MgSO$_4$, filtered and evaporated to afford the *title compound* as an off-white solid (2.69 g, 75%).

R_f 0.08 (petrol/EtOAc, 1:1.5, *v/v*); $[\alpha]_D$ = +41.5 (*c* 0.10, CHCl$_3$); M.P. 154–155 °C (lit.[195] 155–156 °C); ^{1}H NMR (400 MHz, CDCl$_3$, δ): 8.27 (s, 1H), 7.53 (dd, *J* = 8.0, 1.0 Hz, 1H), 7.39–7.33 (m, 1H), 7.19 (ddd, 8.0, 7.0, 1.0 Hz, 1H), 7.12 (ddd, *J* = 8.0, 7.0, 1.0 Hz, 1H), 6.97 (d, *J* = 8.0 Hz, 1H), 6.03 (d, *J* = 8.0 Hz, 1H), 4.96 (dt, *J* = 8.0, 5.0 Hz, 1H), 3.70 (s, 3H), 3.35 (dd, *J* = 15.0, 5.0 Hz, 1H), 3.30 (dd, *J* = 15.0, 5.0 Hz, 1H), 1.95 (s, 3H); ^{13}C NMR (101 MHz, CDCl$_3$, δ): 172.6, 169.4, 136.1, 127.1, 123.7, 120.1, 118.4, 118.0, 111.5, 109.6, 53.2, 51.8, 27.1, 22.3; ESI–MS *m/z* (ion, %): 261 ([M+H]$^+$, 5), 283 ([M+Na]$^+$, 100); ESI–HRMS *m/z*: 283.1053 [M+Na]$^+$ (C$_{14}$H$_{16}$N$_2$O$_3$Na requires 283.1053); IR (solid-state, ATR, cm^{-1}): 3405 (w), 3315 (m), 1732 (s), 1661 (s), 1520 (s), 1434 (m), 1220 (s), 1123 (m), 746 (s), 665 (m), 613 (m), 519 (s), 427 (s); Elemental anal.: C 64.34, H 6.23, N 10.47 (C$_{14}$H$_{16}$N$_2$O$_3$ requires C 64.60, H 6.20, N 10.76).

Lab book reference number: AJR-8-711

Methyl (2*S*)-2-acetamido-3-(2-phenyl-1*H*-indol-3-yl)propanoate (75)

Method A: To a microwave tube was added phenylboronic acid **14** (47 mg, 0.384 mmol, 2 eq.), aryliodonium salt **22** (123 mg, 0.384 mmol, 2 eq.), Pd(OAc)$_2$ (2 mg, 9.6 µmol, 5 mol%) and AcOH (5 mL). The reaction mixture was stirred at 40 °C for 10 min. To the resulting orange-brown solution was added tryptophan **74** (50 mg, 0.192 mmol, 1 eq.). The reaction was stirred at 40 °C for 16 h. After 16 h the resulting black reaction mixture was filtered through Celite and evaporated to give a brown solid. This was dissolved in EtOAc (10 mL) then washed with sat. aq. NaHCO$_3$. The organic layer was collected, dried over MgSO$_4$, filtered and evaporated to give a brown solid. Purification by dry-loaded flash column chromatography (SiO$_2$, petrol/EtOAc, 1:1.5, *v/v*) afforded the *title compound* as an off-white solid (36 mg, 56%).

Method B: To a microwave tube was added tryptophan **74** (50 mg, 0.192 mmol, 1 eq.), diaryliodonium salt **140** (181 mg, 0.384 mmol, 2 eq.), Pd(OAc)$_2$ (2 mg, 9.6 µmol, 5 mol%)

and EtOAc (5 mL). The reaction mixture was stirred at 25 °C for 16 h. After 16 h the resulting black reaction mixture was filtered through Celite then washed with sat. aq. NaHCO$_3$. The organic layer was collected and dried over MgSO$_4$, filtered and evaporated to give a brown solid. Purification by dry-loaded flash column chromatography (SiO$_2$, petrol/EtOAc, 1:1.5, *v/v*) afforded the *title compound* as an off-white solid (55 mg, 85%).

Method C: Synthesised using general procedure C with aryldiazonium salt **48** (37 mg, 0.192 mmol, 1 eq.) to afford the *title compound* as an off-white solid (65 mg, quant.).

Method D: Synthesised as in method C using Pd(OTs)$_2$(MeCN)$_2$ **215** (5.1 mg, 9.6 µmol, 5 mol%) in place of Pd(OAc)$_2$ and a reaction time of 6 h to afford the *title compound* as an off-white solid (65 mg, quant.).

Method E: Synthesised as in method D using Pd(OTs)$_2$(MeCN)$_2$ **215** (1 mg, 1.92 µmol, 1 mol%) and a reaction time of 16 h to afford the *title compound* as an off-white solid (65 mg, quant.).

Method F: To a microwave tube was added tryptophan **74** (52 mg, 0.20 mmol, 1 eq.), diaryliodonium salt **233** (147 mg, 0.40 mmol, 2 eq.), Pd/C (5 wt%, 21 mg, 10 µmol, 5 mol%) and EtOH (2 mL). The reaction mixture was stirred at 60 °C for 22 h. After 22 h the reaction mixture was allowed to cool to RT, then filtered through a silica pad with EtOAc. The solvent was evaporated and the crude mixture purified by dry-loaded flash column chromatography (SiO$_2$, petrol/EtOAc, 1:1.5, *v/v*) afforded the *title compound* as an off-white solid (57 mg, 85%).

Method G: Synthesised as in method F using Pd/charcoal (5 wt%, 21 mg, 10 µmol, 5 mol%) in place of Pd/C. Purification by dry-loaded flash column chromatography afforded the *title compound* as an off-white solid (66 mg, 98%).

R_f 0.27 (petrol/EtOAc, 1:1.5, *v/v*); [α]$_D$ = +47.3 (*c* 0.10, CHCl$_3$); M.P. 83–84 °C (lit.[196] 85–86 °C); ^{1}H NMR (400 MHz, CDCl$_3$, δ): 8.20 (s, 1H), 7.60–7.54 (m, 3H), 7.51–7.45 (m, 2H), 7.42–7.34 (m, 2H), 7.21 (ddd, *J* = 8.0, 7.0, 1.0 Hz, 1H), 7.14 (ddd, *J* = 8.0, 7.0, 1.0 Hz, 1H), 5.79 (d, *J* = 8.0 Hz, 1H), 4.84 (dt, *J* = 8.0, 5.0 Hz, 1H), 3.55 (dd, *J* = 15.0, 5.0 Hz, 1H), 3.52 (dd, *J* = 15.0, 5.0 Hz, 1H), 3.29 (s, 3H), 1.66 (s, 3H); ^{13}C NMR (101 MHz, (CDCl$_3$, δ): 172.3, 169.8, 136.1, 135.8, 133.3, 129.6, 129.3, 128.9, 128.4, 128.2, 127.4, 122.7, 120.2, 119.0, 111.1, 106.9, 52.9, 52.2, 26.7, 23.0; ESI–MS *m/z* (ion, %): 337 ([M+H]$^+$, 40), 359 ([M+Na]$^+$, 100); ESI–HRMS *m/z*: 337.1546 [M+H]$^+$ (C$_{20}$H$_{21}$N$_2$O$_3$ requires 337.1547); IR (solid-state ATR, cm^{-1}): 3272 (w, br), 1735 (m), 1651 (m), 1519 (m), 1436 (m), 1373 (m), 1215 (m), 739 (s), 696 (s), 496 (m); UV–vis (EtOAc, nm): λ$_{max}$ 304 (ε = 17626 mol dm^{-3} cm^{-1}).

Crystals suitable for X-ray diffraction were grown by slow diffusion from a solution of hexane/Et$_2$O (1:3, *v/v*).

The analytical data obtained was in accordance with the literature.[196]

Lab book reference number (method A): AJR-1-82

Lab book reference number (method B): AJR-3-252

Lab book reference number (method C): AJR-4-365

Lab book reference number (method D): AJR-6-596

Lab book reference number (method E): AJR-7-605

Lab book reference number (method F): AJR-8-741

Lab book reference number (method E): AJR-8-759

Deuterium-labelling experiment in the direct arylation of tryptophan (75/*d$_5$*-75)
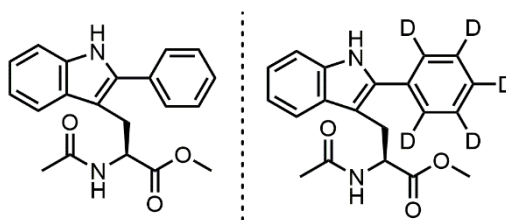
To a microwave tube was added *d$_5$*-phenylboronic acid *d$_5$*-**14** (49 mg, 0.384 mmol, 2 eq.), aryliodonium salt **22** (123 mg, 0.384 mmol, 2 eq.), Pd(OAc)$_2$ (2 mg, 9.6 μmol, 5 mol%) and AcOH (5 mL). The reaction mixture was stirred at 40 °C for 10 min. To the resulting orange-brown solution was added tryptophan **74** (50 mg, 0.192 mmol, 1 eq.). The reaction was stirred at 40 °C for 16 h. After 16 h the resulting black reaction mixture was filtered through Celite and evaporated to give a brown solid. This was dissolved in EtOAc (10 mL) then washed with sat. aq. NaHCO$_3$. The organic layer was collected, dried over MgSO$_4$, filtered and evaporated to give a brown solid. Purification by dry-loaded flash column chromatography (SiO$_2$, petrol/EtOAc, 1:1.5, *v/v*) afforded the two *title compounds* as inseparable off-white solids (24 mg, 37%).

R$_f$ 0.27 (petrol/EtOAc, 1:1.5, *v/v*); ESI–MS *m/z* (ion, %): 337 ([M+H]$^+$, 8), 342 ([*d$_5$*-M+H]$^+$, 10), 359 ([M+Na]$^+$, 90), 364 ([*d$_5$*-M+Na]$^+$, 100); ESI–HRMS *m/z*: 359.1369 [M+Na]$^+$ (C$_{20}$H$_{20}$N$_2$NaO$_3$ requires 359.1366), 364.1681 [*d$_5$*-M+Na]$^+$ (C$_{20}$H$_{15}$D$_5$N$_2$NaO$_3$ requires 364.1680).

Lab book reference number: AJR-2-93

(2*S*)-2-[(2*R*)-2-[(2*S*)-2-acetamidopropanamido]-3-(2-phenyl-1*H*-indol-3-yl) propanamido]propanoic acid (137)
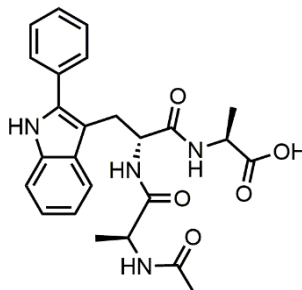
Method A: To a microwave tube was added peptide **136** (10 mg, 0.026 mmol, 1 eq.), phenylboronic acid **14** (16 mg, 0.13 mmol, 5 eq.), Cu(OAc)$_2$ (2.8 mg, 0.0156 mmol, 60 mol%), Pd(OAc)$_2$ (1.8 mg, 7.8 µmol, 30 mol%) and AcOH (1 mL). The reaction mixture was stirred at 40 °C for 16 h. The solvent was removed under reduced pressure to give a brown residue, which was analysed by HPLC–ESI–MS.

Method B: To a microwave tube was added peptide **136** (10 mg, 0.026 mmol, 1 eq.), diaryliodonium salt **140** (25 mg, 0.052 mmol, 2 eq.), Pd(OAc)$_2$ (0.6 mg, 2.6 µmol, 10 mol%) and ^{i}PrOH (1 mL). The reaction mixture was stirred at 25 °C for 16 h. The resulting brown reaction mixture was filtered through Celite with MeOH (5 mL) and the solvent removed under reduced pressure to give a brown residue, which was analysed by HPLC–ESI–MS.

Method C: To a microwave tube was added peptide **136** (10 mg, 0.026 mmol, 1 eq.), aryldiazonium salt **48** (10 mg, 0.052 mmol, 2 eq.), Pd(OAc)$_2$ (1.2 mg, 5.2 µmol, 20 mol%) and ^{i}PrOH (1 mL). The reaction mixture was stirred at RT for 16 h. The resulting brown reaction mixture was filtered through Celite with MeOH (5 mL) and the solvent removed under reduced pressure to give a brown residue, which was analysed by HPLC–ESI–MS.

ESI–MS m/z (ion, %): 465 ([M+H]$^+$, 100).

Lab book reference number (method A): TJW/7/53/597 (*reaction conducted by T. Williams*)

Lab book reference number (method B): AJR-6-543

Lab book reference number (method C): AJR-6-539

(2*S*)-2-[(2*R*)-2-{2-[(2*R*)-2-acetamido-3-hydroxypropanamido]acetamido}-3-(2-phenyl-1*H*-indol-3-yl)propanamido]propanoic acid (139)
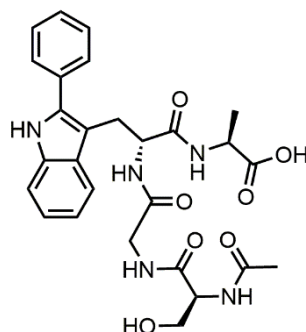
Method A: To a microwave tube was added peptide **138** (10 mg, 0.022 mmol, 1 eq.), phenylboronic acid **14** (13 mg, 0.11 mmol, 5 eq.), Cu(OAc)$_2$ (2.4 mg, 0.0132 mmol, 60 mol%), Pd(OAc)$_2$ (1.5 mg, 0.0066 mmol, 30 mol%) and AcOH (1 mL). The reaction mixture was stirred at 40 °C for 16 h. The solvent was removed under reduced pressure to give a brown residue, which was analysed by HPLC–ESI–MS.

Method B: To a microwave tube was added peptide **138** (10 mg, 0.022 mmol, 1 eq.), diaryliodonium salt **140** (21 mg, 0.044 mmol, 2 eq.), Pd(OAc)$_2$ (0.5 mg, 0.0022 mmol, 10 mol%) and ^{i}PrOH (1 mL). The reaction mixture was stirred at 25 °C for 16 h. The resulting brown reaction mixture was filtered through Celite with MeOH (5 mL) and the solvent removed under reduced pressure to give a brown residue, which was analysed by HPLC–ESI–MS.

Method C: To a microwave tube was added peptide **138** (10 mg, 0.022 mmol, 1 eq.), aryldiazonium salt **48** (8.4 mg, 0.044 mmol, 2 eq.), Pd(OAc)$_2$ (1.0 mg, 4.4 μmol, 20 mol%) and ^{i}PrOH (1 mL). The reaction mixture was stirred at RT for 16 h. The resulting brown reaction mixture was filtered through Celite with MeOH (5 mL) and the solvent removed under reduced pressure to give a brown residue, which was analysed by HPLC–ESI–MS.

ESI–MS m/z (ion, %): 538 ([M+H]$^+$, 100).

Lab book reference number (method A): TJW/7/55/598 (*reaction conducted by T. Williams*)

Lab book reference number (method B): AJR-6-544

Lab book reference number (method C): AJR-6-540

Phenyl(2,4,6-trimethylphenyl)iodonium trifluoromethanesulfonate (140)[124]
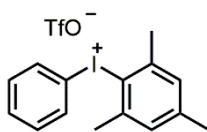
Aryliodonium salt **22** (3.22 g, 10 mmol, 1 eq.) and 1,3,5-trimethylbenzene **141** (1.54 mL, 1.32 g, 11 mmol, 1.1 eq.) were added to a round-bottomed flask and dissolved in CH_2Cl_2 (20 mL) with stirring. The mixture was cooled to 0 °C then trifluoromethanesulfonic acid (0.96 mL, 1.65 g, 11 mmol, 1.1 eq.) was added dropwise with stirring. After complete addition the reaction was stirred for 2 h over which time it was allowed to warm to RT. After 2 h the mixture was evaporated to give an orange-white residue to which Et_2O was added to precipitate a white solid. This was filtered through a glass sinter and washed on the filter with further Et_2O until the filtrate ran clear. This was then dried *in vacuo* at 100 °C to afford the *title compound* as a white solid (4.49 g, 95%).

M.P. 149–150 °C (lit.[197] 147–148 °C); ^{1}H NMR (400 MHz, CDCl$_3$, δ): 7.69 (d, *J* = 7.5 Hz, 2H), 7.51 (t, *J* = 7.5 Hz, 1H), 7.39 (t, *J* = 7.5 Hz, 2H), 7.09 (s, 2H), 2.61 (s, 6H), 2.34 (s, 3H); ^{13}C NMR (101 MHz, CDCl$_3$, δ): 144.5, 142.6, 133.1, 132.4, 131.9, 130.5, 120.5, 111.8, 27.2, 21.2; ^{19}F NMR (376 MHz, CDCl$_3$, δ): −78.2; ESI–MS *m/z* (ion, %): 323 ([M−OTf]$^+$, 100); ESI–HRMS *m/z*: 323.0303 [M−OTf]$^+$ ($C_{15}H_{16}I$ requires 323.0291); IR (solid-state, ATR, cm^{-1}): 3060 (w), 2919 (w), 1445 (m), 1247 (s), 1222 (s), 1158 (s), 1025 (s), 985 (m), 945 (w), 857 (m), 741 (s), 683 (m), 632 (s), 574 (m), 515 (s), 454 (m); Elemental anal.: C 40.43, H 3.24 ($C_{16}H_{16}F_3IO_3S$ requires C 40.69, H 3.41).

Lab book reference number: AJR-4-318

Optimisation of the direct arylation of tryptophan
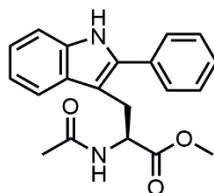
To a microwave tube was added tryptophan **74** (50 mg, 0.192 mmol, 1 eq.), diaryliodonium salt **140** (181 mg, 0.384 mmol, 2 eq.), Pd(OAc)$_2$ (2 mg, 9.6 μmol, 5 mol%) and solvent (5 mL). The reaction mixture was stirred at 25 °C for 16 h. After 16 h the resulting reaction mixture was filtered through Celite then washed with sat. aq. NaHCO$_3$. The organic layer was collected and dried over MgSO$_4$, filtered and evaporated to give a brown solid, which was subsequently analysed by ^{1}H NMR spectroscopy.

Lab book reference number (AcOH): AJR-3-212 (conducted at 40 °C)

Lab book reference number (MeCN): AJR-3-247

Lab book reference number (Acetone): AJR-3-249

Lab book reference number (DCM): AJR-3-248

Lab book reference number (DMF): AJR-4-285

Lab book reference number (DMSO): AJR-3-251

Lab book reference number (1,4-dioxane): AJR-3-260

Lab book reference number (H$_2$O): AJR-3-258

Lab book reference number (MeOH): AJR-3-255

Lab book reference number (EtOH): AJR-3-256

Lab book reference number (^{i}PrOH): AJR-3-261

Methyl (2*S*)-2-acetamido-3-[2-(2,4,6-trimethylphenyl)-1*H*-indol-3-yl]propanoate (142)
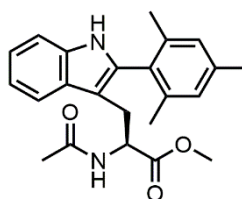
Method A: *Title compound* was isolated as an off-white solid side product from the synthesis of **75** by method B (2 mg, 3%).

Method B: Synthesised using general procedure C (with a reaction time of 24 h) with aryldiazonium salt **48** (45 mg, 0.192 mmol, 1 eq.). Purification by dry-loaded flash column chromatography (SiO$_2$, petrol/EtOAc, 1:1, *v/v*) afforded the *title compound* as an off-white solid (60 mg, 83%).

Method C: Synthesised as in method B using Pd(OTs)$_2$(MeCN)$_2$ **215** (5.1 mg, 9.6 µmol, 5 mol%) in place of Pd(OAc)$_2$. Purification by dry-loaded flash column chromatography (SiO$_2$, petrol/EtOAc, 1:1, *v/v*) afforded the *title compound* as an off-white solid (55 mg, 75%).

Method D: Reaction conducted as in method C using Pd(OTs)$_2$(MeCN)$_2$ **215** (2.5 mg, 4.8 µmol, 2.5 mol%) to afford a crude brown solid. ^{1}H NMR spectroscopic analysis indicated 72% conversion to the *title compound*, which was not purified.

Method E: Reaction conducted as in method C using Pd(OTs)$_2$(MeCN)$_2$ **215** (1 mg, 1.92 μmol, 1 mol%) to afford a crude brown solid. ^{1}H NMR spectroscopic analysis indicated 45% conversion to the *title compound*, which was not purified.

R_f 0.31 (petrol/EtOAc, 1:1, *v/v*); [α]$_D$ = +35.2 (*c* 0.10, CHCl$_3$); M.P. 158–159 °C; ^{1}H NMR (400 MHz, CDCl$_3$, δ): 7.89 (br s, 1H), 7.61 (m, 1H), 7.37–7.33 (m, 1H), 7.20 (ddd, *J* = 8.0, 7.0, 1.5 Hz, 1H), 7.14 (ddd, *J* = 8.0, 7.0, 1.5 Hz, 1H), 6.99 (s, 1H), 6.97 (s, 1H), 5.64 (d, *J* = 7.5 Hz, 1H), 4.72 (dt, *J* = 7.5, 5.0 Hz, 1H), 3.47 (s, 3H), 3.17 (dd, *J* = 15.0, 5.0 Hz, 1H), 3.02 (dd, *J* = 15.0, 5.0 Hz, 1H), 2.35 (s, 3H), 2.11 (s, 3H), 2.10 (s, 3H), 1.75 (s, 3H); ^{13}C NMR (101 MHz, (CDCl$_3$, δ): 172.5, 169.9, 138.9, 138.3, 138.2, 135.9, 134.7, 128.8, 122.1, 119.9, 118.8, 110.9, 108.0, 100.1, 53.1, 52.3, 27.2, 23.1, 21.3, 20.4, 20.3; ESI–MS *m/z* (ion, %): 379 ([M+H]$^+$, 40), 401 ([M+Na]$^+$, 100); ESI–HRMS *m/z*: 379.2015 [M+H]$^+$ (C$_{23}$H$_{27}$N$_2$O$_3$ requires 379.2016); IR (solid-state, ATR, cm^{-1}): 3402 (w), 3289 (w, br), 2953 (w), 2919 (w), 2852 (w), 1741 (s), 1646 (s), 1515 (m), 1458 (m), 1435 (s), 1373 (m), 1304 (w), 1293 (w), 1260 (w), 1239 (w), 1218 (s), 1129 (m), 1031 (m), 1012 (m), 987 (w), 854 (m), 798 (m), 744 (s), 591 (m), 505 (s), 445 (m); UV–vis (DMSO, nm): λ$_{max}$ 288 (ε = 15092 mol dm^{-3} cm^{-1}).

Crystals suitable for X-ray diffraction were grown by overnight diffusion from a solution of CH$_2$Cl$_2$.

Lab book reference number (method A): AJR-3-252

Lab book reference number (method B): AJR-5-402

Lab book reference number (method C): AJR-7-654

Lab book reference number (method D): AJR-7-647

Lab book reference number (method E): AJR-7-631

Phenyl(2,4,6-tri-*iso*-propylphenyl)iodonium trifluoromethanesulfonate (143)[124]
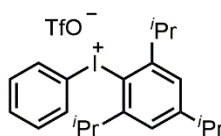
Aryliodonium salt **22** (805 mg, 2.5 mmol, 1 eq.) and 1,3,5-tri-*iso*-propylbenzene (665 μL, 562 mg, 2.75 mmol, 1.1 eq.) were added to a round-bottomed flask and dissolved in CH$_2$Cl$_2$ (5 mL) with stirring. The mixture was cooled to 0 °C then trifluoromethanesulfonic acid (241 μL, 413 mg, 2.75 mmol, 1.1 eq.) was added dropwise with stirring. After complete addition the reaction was stirred for 2 h over which time it was allowed to warm to RT. After 2 h the

mixture was evaporated to give an orange-white residue to which Et$_2$O was added to precipitate a white solid. This was filtered through a glass sinter and washed on the filter with further Et$_2$O until the filtrate ran clear. This was then dried *in vacuo* at 100 °C to afford the *title compound* as a white solid (1.19 g, 86%).

M.P. 177–179 °C (lit.[124] 169–179 °C); ^{1}H NMR (400 MHz, CDCl$_3$, δ): 7.70–7.65 (m, 2H), 7.58–7.52 (m, 1H), 7.47–7.40 (m, 2H), 7.19 (s, 2H), 3.25 (quin, J = 6.5 Hz, 2H), 2.96 (hept, J = 7.0 Hz, 1H), 1.26 (dd, J = 15.0, 7.0 Hz, 18H); ^{13}C NMR (101 MHz, CDCl$_3$, δ): 155.9, 152.6, 132.7, 132.1, 125.5, 120.4, 113.0, 39.7, 34.4, 24.4, 23.8; ESI–MS *m/z* (ion, %): 407 ([M−OTf]$^+$, 100); ESI–HRMS *m/z*: 407.1247 [M−OTf]$^+$ (C$_{21}$H$_{28}$I requires 407.1230); Elemental anal.: C 47.26, H 4.93 (C$_{22}$H$_{28}$F$_3$IO$_3$S requires C 47.49, H 5.07).

Lab book reference number: AJR-2-165

Phenyl(2,4,6-trimethylphenyl)iodonium tetrafluoroborate (144)[124]
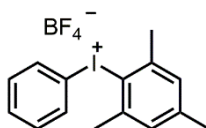
Phenylboronic acid **14** (305 mg, 2.5 mmol, 1 eq.) was added to a round-bottomed flask, dissolved in CH$_2$Cl$_2$ (50 mL) and cooled to 0 °C. BF$_3$·OEt$_2$ (0.3 mL, 390 mg, 2.75 mmol, 1.1 eq.) was added dropwise and the solution stirred for 10 min before addition of a solution of aryliodonium salt **23** (910 mg, 2.5 mmol, 1 eq.) in CH$_2$Cl$_2$ (10 mL) dropwise over 10 min. After complete addition the reaction was stirred for 2 h over which time it was allowed to warm to RT. After 2 h a sat. aq. sodium tetrafluoroborate solution (50 mL) was added and the solution stirred vigorously for 30 min. After this time the phases were separated and the aqueous layer extracted twice with CH$_2$Cl$_2$ (2 × 50 mL). The organic layers were combined, dried over MgSO$_4$, filtered and evaporated to give an off-white solid. The product was precipitated from a hot CH$_2$Cl$_2$ solution of the crude residue by addition of cold Et$_2$O. This solid was filtered through a glass sinter and washed with Et$_2$O before being dried *in vacuo* to afford the *title compound* as a white solid (728 mg, 71%).

^{1}H NMR (400 MHz, CDCl$_3$, δ): 7.75–7.65 (m, 2H), 7.62–7.52 (m, 1H), 7.44 (ddt, J = 8.5, 8.0 Hz, 2H), 7.13 (dd, J = 1.5, 1.0 Hz, 2H), 2.63 (s, 6H), 2.37 (s, 3H); ^{13}C NMR (101 MHz, CDCl$_3$, δ): 145.1, 143.1, 133.0, 132.8, 132.2, 130.8, 118.9, 110.7, 101.0, 27.4, 21.3; ^{11}B NMR (128 MHz, CDCl$_3$, δ): −2.0; ^{19}F NMR (376 MHz, CDCl$_3$, δ): −147.3 (m, ^{1}J$_{F\_10_B}$, 4F), −147.3 (m, ^{1}J$_{F\_11_B}$, 4F); ESI–MS *m/z* (ion, %): 323 ([M−BF$_4$]$^+$, 100); ESI–HRMS *m/z*: 323.0306

$[M-BF_4]^+$ ($C_{15}H_{16}I$ requires 323.0291); Elemental anal.: C 44.04, H 3.83 ($C_{15}H_{16}BF_4I$ requires C 43.94, H 3.93).

Lab book reference number: AJR-2-158

Phenyl(2,4,6-trimethylphenyl)iodonium hexafluorophosphate (145)[124]
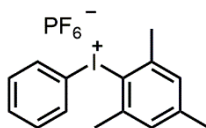
Phenylboronic acid **14** (305 mg, 2.5 mmol, 1 eq.) was added to a round-bottomed flask, dissolved in CH_2Cl_2 (50 mL) and cooled to 0 °C. $BF_3 \cdot OEt_2$ (0.3 mL, 390 mg, 2.75 mmol, 1.1 eq.) was added dropwise and the solution stirred for 10 min before addition of a solution of aryliodonium salt **23** (910 mg, 2.5 mmol, 1 eq.) in CH_2Cl_2 (10 mL) dropwise over 10 min. After complete addition the reaction was stirred for 2 h over which time it was allowed to warm to RT. After 2 h a sat. aq. sodium hexafluorophosphate solution (50 mL) was added and the solution stirred vigorously for 30 min. After this time the phases were separated and the aqueous layer extracted twice with CH_2Cl_2 (2 × 50 mL). The organic layers were combined, dried over $MgSO_4$, filtered and evaporated to give an off-white solid. The product was precipitated from a hot CH_2Cl_2 solution of the crude residue by addition of cold Et_2O. This solid was filtered through a glass sinter and washed with Et_2O before being dried *in vacuo* to afford the *title compound* as a white solid (443 mg, 38%).

M.P. 182–183 °C ; ^{1}H NMR (400 MHz, $(CD_3)_2SO$, δ): 8.03–7.92 (m, 2H), 7.68–7.58 (m, 1H), 7.55–7.45 (m, 2H), 7.22 (s, 2H), 2.60 (s, 6H), 2.29 (s, 3H); ^{13}C NMR (101 MHz, $(CD_3)_2SO$, δ): 143.1, 141.6, 134.5, 131.9, 129.8, 122.6, 114.5, 26.3, 20.5; ^{19}F (376 MHz, $(CD_3)_2SO$, δ): −70.0 (d, $^1J_{F-P}$ = 711.5 Hz); ^{31}P NMR (162 MHz, $(CD_3)_2SO$, δ): −143.6 (hept, $^1J_{P-F}$ = 711.5 Hz); ESI–MS *m/z* (ion, %): 323 ($[M-PF_6]^+$, 100); ESI–HRMS *m/z*: 323.0303 $[M-PF_6]^+$ ($C_{15}H_{16}I$ requires 323.0291); IR (solid-state, ATR, cm^{-1}): 1584 (w), 1564 (w), 1470 (w), 1444 (w), 1383 (w), 1302 (w), 982 (w), 825 (s), 732 (m), 677 (w), 648 (w), 556 (s), 448 (w); Elemental anal.: C 38.70, H 3.28 ($C_{15}H_{16}F_6IP$ requires C 38.48, H 3.44).

Lab book reference number: AJR-2-163

Phenyl(2,4,6-trimethylphenyl)iodonium hexafluorostibate (146)[198]
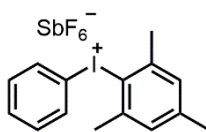
Diaryliodonium trifluoromethanesulfonate salt **140** (945 mg, 2.0 mmol, 1 eq.) was added to a round-bottomed flask equipped with a magnetic stirrer, dissolved in MeCN (3 mL) and stirred at RT for 5 min. To this was added a solution of $NaSbF_6$ (1.55 g, 6.0 mmol, 3 eq.) in deionised water (20 mL) and the resultant mixture stirred vigorously for 30 min at RT. After 30 min CH_2Cl_2 was added and the phases separated. The aqueous layer was then extracted three times with CH_2Cl_2 (3 × 50 mL). The organic layers were combined, dried over $MgSO_4$, filtered and Et_2O added to precipitate a white solid. This solid was filtered through a glass sinter and washed with Et_2O before being dried *in vacuo* to afford the *title compound* as a white solid (1.05 g, 94%).

M.P. 172–173 °C; ^{1}H NMR (400 MHz, $(CD_3)_2SO$, δ): 8.02–7.94 (m, 2H), 7.67–7.59 (m, 1H), 7.50 (ddd, J = 8.5, 7.5, 1.5 Hz, 2H), 7.26–7.18 (m, 2H), 2.60 (s, 6H), 2.29 (s, 3H); ^{13}C NMR (101 MHz, $(CD_3)_2SO$, δ): 143.2, 141.6, 134.5, 131.9, 129.8, 122.6, 114.5, 26.3, 20.5; ^{19}F (376 MHz, $(CD_3)_2SO$, δ): −77.7; ESI–MS *m/z* (ion, %): 323 ([M−SbF_6]^+, 100); ESI–HRMS *m/z*: 323.0294 [M−SbF_6]^+ ($C_{15}H_{16}I$ requires 323.0291).

Lab book reference number: AJR-4-338

Counter-ion screen for the direct arylation of tryptophan
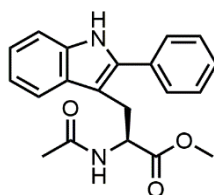
To a microwave tube was added tryptophan **74** (50 mg, 0.192 mmol, 1 eq.), the appropriate diaryliodonium salt (0.384 mmol, 2 eq.), $Pd(OAc)_2$ (2 mg, 9.6 μmol, 5 mol%) and EtOAc (5 mL). The reaction mixture was stirred at 25 °C for 16 h. After 16 h the resulting reaction mixture was filtered through Celite then washed with sat. aq. $NaHCO_3$. The organic layer was collected and dried over $MgSO_4$, filtered and evaporated to give a brown solid, which was subsequently analysed by ^{1}H NMR spectroscopy.

Lab book reference number (¯OTf): AJR-3-252

Lab book reference number (¯BF_4): AJR-3-263

Lab book reference number (⁻PF₆): AJR-3-264

Lab book reference number (⁻SbF₆): AJR-4-340

Diphenyliodonium tosylate (132)[199]
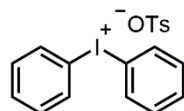
Diphenyliodonium tetrafluoroborate **233** (2.02 g, 5.49 mmol, 1 eq.) was added to a round-bottomed flask equipped with a magnetic stirrer and dissolved in CH_2Cl_2 (25 mL). To this was added a solution of NaOTs (10.7 g, 55 mmol, 10 eq.) in deionised water (50 mL) and the resultant mixture stirred vigorously for 30 min at RT. After 30 min the phases were separated and the aqueous layer extracted three times with CH_2Cl_2. The organic layers were combined and evaporated, before being redissolved in CH_2Cl_2 (25 mL). To this was added a solution of NaOTs (10.7 g, 55 mmol, 10 eq.) in deionised water (50 mL) and the resultant mixture stirred vigorously for 30 min at RT. After 30 min the phases were separated and the aqueous layer extracted three times with CH_2Cl_2. The organic layers were combined and evaporated, then Et_2O was added and the mixture kept at −18 °C overnight. The resultant precipitate was filtered through a glass sinter and washed with Et_2O before being dried *in vacuo* to afford the *title compound* as an off-white solid (1.26 g, 51%).

M.P. 152–155 °C (lit.[200] 160–161 °C); ^{1}H NMR (400 MHz, $(CD_3)_2SO$, δ): 7.93 (d, J = 8.0 Hz, 4H), 7.46 (t, J = 7.5 Hz, 2H), 7.41 (d, J = 8.0 Hz, 2H), 7.30 (t, J = 7.5 Hz, 4H), 6.97 (d, J = 8.0 Hz, 2H), 2.27 (s, 3H); ^{13}C NMR (101 MHz, $(CD_3)_2SO$, δ): 142.7, 139.4, 135.4, 131.6, 131.6, 128.6, 126.0, 115.7, 21.4; ESI–MS *m/z* (ion, %): 281 ([M−OTs]$^+$, 100); ESI–HRMS *m/z*: 280.9827 [M−OTs]$^+$ ($C_{12}H_{10}I$ requires 280.9822).

Lab book reference number: AJR-5-433

Evaluation of Ackermann conditions in the direct arylation of tryptophan
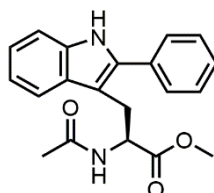
To an oven-dried Schlenk tube equipped with a magnetic stirrer bar was added tryptophan **74** (65 mg, 0.25 mmol, 1 eq.) and diphenyliodonium salt **132** (170 mg, 0.375 mmol, 1.5 eq.). For entries 3 and 4, Pd(OAc)$_2$ (2.8 mg, 12.5 µmol, 5 mol%) was also added at this stage. The

Schlenk tube was then evacuated and backfilled with N_2 (3 cycles) for entries 1 and 3; for entries 2 and 4 it was left open to air. Dry DMF (2 mL) was added and the reaction stirred at 100 °C for 17 h. After 17 h the reaction was allowed to cool to RT, then those reactions containing $Pd(OAc)_2$ (entries 3 and 4) were filtered through Celite with EtOAc. Deionised water (5 mL) was added and extracted into EtOAc (2×20 mL). The organic layers were then combined and dried over $MgSO_4$, filtered and evaporated to give a brown solid, which was subsequently analysed by ^1H NMR spectroscopy.

Lab book reference number (entry 1): AJR-5-436

Lab book reference number (entry 2): AJR-5-438

Lab book reference number (entry 3): AJR-5-437

Lab book reference number (entry 4): AJR-5-439

Methyl (2*S*)-2-[(2*S*)-2-{[(*tert*-butoxy)carbonyl]amino}-4-methylpentanamido]-3-(1*H*-indol-3-yl)propanoate (149)[126]
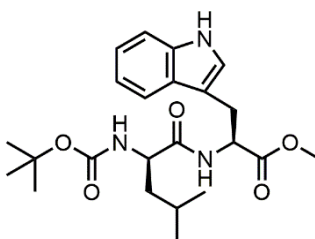
Acid **148** (463 mg, 2 mmol, 1 eq.), amine **135** (560 mg, 2.2 mmol, 1.1 eq.) and DEPBT (718 mg, 2.4 mmol, 1.2 eq.) were added to a round-bottomed flask which was fitted with a septum and flushed with argon from a balloon for 20 min. After 20 min dry, distilled DIPEA (1.4 mL, 1.03 g, 8 mmol, 4 eq.) and dry CH_2Cl_2 (20 mL) were added *via* syringe to give a yellow solution and the reaction stirred at RT for 2 h. After 2 h the reaction mixture was washed with sat. aq. NH_4Cl and extracted three times with CH_2Cl_2. The organic layers were combined, dried over $MgSO_4$, filtered and evaporated to give a crude yellow residue. Purification by dry-loaded flash column chromatography (SiO_2, petrol/EtOAc, 1:1, *v/v*) afforded the *title compound* as an off-white solid (473 mg, 55%).

R_f 0.42 (petrol/EtOAc, 1:1, *v/v*); ^1H NMR (400 MHz, $CDCl_3$, δ): 8.26 (br s, 1H), 7.52 (d, *J* = 8.0 Hz, 1H), 7.33 (d, *J* = 8.0 Hz, 1H), 7.17 (td, *J* = 8.0, 7.5, 1.0 Hz, 1H), 7.10 (td, *J* = 7.5, 7.1, 1.0 Hz, 1H), 7.05–6.98 (m, 1H), 6.59 (d, *J* = 8.0 Hz, 1H), 4.95–4.79 (m, 2H), 4.11 (br s, 1H), 3.65 (s, 3H), 3.31 (d, *J* = 5.0 Hz, 2H), 1.68–1.53 (m, 2H), 1.41 (s, 9H), 0.94–0.80 (m, 5H); ^{13}C NMR (101 MHz, $CDCl_3$, δ): 172.4, 172.2, 155.7, 136.2, 127.7, 123.2, 122.3, 119.7,

118.7, 111.4, 109.9, 80.1, 53.3, 53.0, 52.5, 41.5, 28.4, 27.7, 24.8, 23.0, 22.0; ESI–MS *m/z* (ion, %): 432 ([M+H]$^+$, 100), 454 ([M+Na]$^+$, 100); ESI–HRMS *m/z*: 432.2494 [M+H]$^+$ (C$_{23}$H$_{34}$N$_3$O$_5$ requires 432.2493).

Lab book reference number: AJR-4-312

Methyl (2*S*)-2-[(2*R*)-2-amino-4-methylpentanamido]-3-(1*H*-indol-3-yl)propanoate (150)[126]
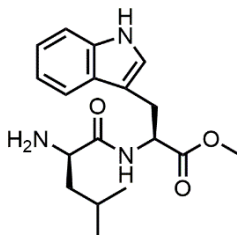
To a round-bottomed flask equipped with a magnetic stirrer bar was added *N*-Boc dipeptide **149** (440 mg, 1.02 mmol, 1 eq.), which was then dissolved in a mixture of CH$_2$Cl$_2$ (8 mL) and trifluoroacetic acid (2 mL). Anisole (220 μL, 221 mg, 2.04 mmol, 2 eq.) was then added and the reaction stirred at RT for 2 h, during which time the solution turned dark red. After 2 h the solvent was evaporated to afford a brown solid (338 mg, quant.) which was used in the next step without further purification or characterisation.

Lab book reference number: AJR-4-316

Methyl (2*S*)-2-[(2*R*)-2-[(2*S*)-2-amino-3-methylbutanamido]-4-methylpentanamido]-3-(1*H*-indol-3-yl)propanoate (152)[126]
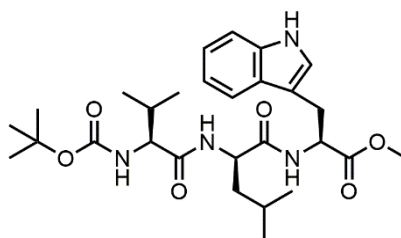
Acid **151** (202 mg, 0.93 mmol, 1 eq.), amine **150** (338 mg, 1.02 mmol, 1.1 eq.) and DEPBT (335 mg, 1.12 mmol, 1.2 eq.) were added to a round-bottomed flask which was fitted with a septum and flushed with argon from a balloon for 20 min. After 20 min dry, distilled DIPEA (0.65 mL, 481 mg, 3.72 mmol, 4 eq.) and dry CH$_2$Cl$_2$ (9.3 mL) were added *via* syringe to give a yellow solution and the reaction stirred at RT for 2 h. After 2 h the reaction mixture was washed with sat. aq. NH$_4$Cl and extracted three times with CH$_2$Cl$_2$. The organic layers were combined, dried over MgSO$_4$, filtered and evaporated to give a crude yellow residue.

Purification by dry-loaded flash column chromatography (SiO$_2$, petrol/EtOAc, 1:1, *v/v*) afforded the *title compound* as an off-white solid (266 mg, 54%).

R_f 0.22 (petrol/EtOAc, 1:1, *v/v*); ^{1}H NMR (400 MHz, CDCl$_3$, δ): 8.44 (br s, 1H), 7.49 (dd, *J* = 8.0, 1.0 Hz, 1H), 7.33 (dt, *J* = 8.0, 1.0 Hz, 1H), 7.16 (ddd, *J* = 8.0, 7.0, 1.0 Hz, 1H), 7.09 (ddd, *J* = 8.0, 7.0, 1.0 Hz, 1H), 7.01–6.95 (m, 1H), 6.64 (d, *J* = 8.0 Hz, 1H), 6.34 (d, *J* = 8.5 Hz, 1H), 4.98 (d, *J* = 9.0 Hz, 1H), 4.86 (dt, *J* = 8.0, 5.5 Hz 1H), 4.46 (td, *J* = 9.0, 5.5 Hz, 1H), 3.90 (t, *J* = 7.5 Hz, 1H), 3.65 (s, 3H), 3.29 (dd, *J* = 5.5, 3.0 Hz, 2H), 2.14–2.01 (m, 1H), 1.69–1.53 (m, 2H), 1.44 (s, 9H), 0.94–0.76 (m, 11H); ^{13}C NMR (101 MHz, CDCl$_3$, δ): 172.1, 171.8, 171.3, 136.2, 127.6, 123.4, 122.2, 119.7, 118.6, 111.5, 109.6, 80.5, 60.2, 52.8, 52.5, 51.6, 40.8, 30.6, 28.4, 27.6, 24.7, 23.0, 22.0, 19.3, 17.5; ESI–MS *m/z* (ion, %): 531 ([M+H]$^+$, 60), 553 ([M+Na]$^+$, 100); ESI–HRMS *m/z*: 553.3010 [M+Na]$^+$ (C$_{28}$H$_{42}$N$_4$NaO$_6$ requires 553.2997).

Lab book reference number: AJR-4-317

Methyl (2*S*)-2-[(2*R*)-2-[(2*S*)-2-amino-3-methylbutanamido]-4-methylpentanamido]-3-(1*H*-indol-3-yl)propanoate (153)[126]
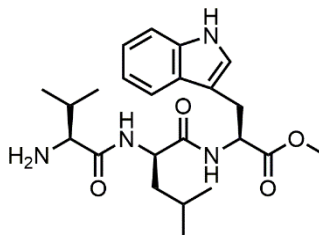
To a round-bottomed flask equipped with a magnetic stirrer bar was added *N*-Boc tripeptide **152** (240 mg, 0.45 mmol, 1 eq.), which was then dissolved in a mixture of CH$_2$Cl$_2$ (3.6 mL) and trifluoroacetic acid (0.9 mL). Anisole (100 µL, 97 mg, 0.90 mmol, 2 eq.) was then added and the reaction stirred at RT for 1 h. After 1 h the solvent was evaporated to afford a red solid (194 mg, quant.) which was used in the next step without further purification or characterisation.

Lab book reference number: AJR-4-321

Methyl (2*R*)-2-amino-4-methylpentanoate hydrochloride (155)
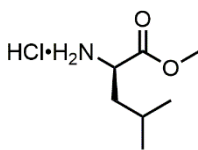
Thionyl chloride (3.04 mL, 4.98 g, 41.9 mmol, 1.1 eq.) was added dropwise at 0 °C to a round-bottomed flask containing MeOH (30 mL). L-Leucine **154** (5 g, 38.1 mmol, 1 eq.) was then added in three portions, resulting in a white suspension. The reaction mixture was warmed to 40 °C and stirred for 16 h. During this time a clear solution was formed. Water (5 mL) was added to the reaction mixture and the solvent removed under reduced pressure to afford the *title compound* as an off-white solid (6.72 g, 97%).

^{1}H NMR (400 MHz, CD$_3$OD, δ): 4.04 (t, *J* = 6.5 Hz, 1H), 3.84 (s, 3H), 1.87–1.65 (m, 3H), 0.99 (dd, *J* = 6.0, 4.0 Hz, 6H); ^{13}C NMR (101 MHz, CD$_3$OD, δ): 171.5, 53.8, 52.5, 40.6, 25.5, 22.5, 22.4; ESI–MS *m/z* (ion, %): 146 ([C$_7$H$_{16}$NO$_2$]$^+$, 100); ESI–HRMS *m/z*: 146.1176 [C$_7$H$_{16}$NO$_2$]$^+$ (C$_7$H$_{16}$NO$_2$ requires 146.1176).

The analytical data obtained was in accordance with the literature.[201]

Lab book reference number: AJR-4-320

Methyl (2*R*)-2-[(2*S*)-2-{[(*tert*-butoxy)carbonyl]amino}-4-methylpentanamido]-4-methylpentanoate (156)[126]
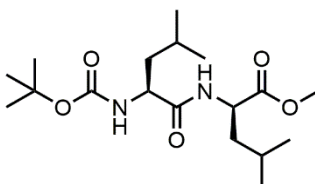
Acid **148** (1 g, 4.32 mmol, 1 eq.), amine **155** (863 mg, 4.75 mmol, 1.1 eq.) and TBTU (1.66 g, 5.18 mmol, 1.2 eq.) were added to a round-bottomed flask which was fitted with a septum and flushed with argon from a balloon for 20 min. After 20 min dry, distilled DIPEA (3 mL, 2.2 g, 17.28 mmol, 4 eq.) and dry CH$_3$CN (43 mL) were added *via* syringe to give a yellow solution and the reaction stirred at RT for 2 h. After 2 h the reaction mixture was washed with sat. aq. NH$_4$Cl and extracted three times with CH$_2$Cl$_2$. The organic layers were combined, dried over MgSO$_4$, filtered and evaporated to give a crude yellow residue. Purification by dry-loaded flash column chromatography (SiO$_2$, petrol/EtOAc, 1:1, *v/v*) afforded the *title compound* as a white solid (1.37 g, 88%).

167

R_f 0.58 (petrol/EtOAc, 1:1, *v/v*); ^{1}H NMR (400 MHz, CDCl$_3$, δ): 6.43 (d, *J* = 8.5 Hz, 1H), 4.93–4.79 (m, 1H), 4.61 (td, *J* = 8.5, 4.5 Hz, 1H), 4.16–4.02 (m, 1H), 3.72 (s, 3H), 1.73–1.60 (m, 6H), 1.44 (s, 9H), 0.98–0.87 (m, 12H); ^{13}C NMR (101 MHz, CDCl$_3$, δ): 173.3, 173.3, 172.3, 100.1, 52.4, 50.7, 28.4, 24.9, 24.8, 23.0, 21.9; ESI–MS *m/z* (ion, %): 359 ([M+H]$^+$, 50), 381 ([M+Na]$^+$, 100); ESI–HRMS *m/z*: 359.2539 [M+H]$^+$ (C$_{18}$H$_{35}$N$_2$O$_5$ requires 359.2540).

Lab book reference number: AJR-4-322

(2*R*)-2-[(2*S*)-2-[(methoxycarbonyl)amino]-4-methylpentanamido]-4-methylpentanoic acid (157)[126]
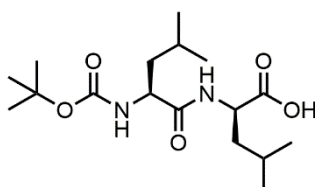
To a round-bottomed flask equipped with a magnetic stirrer bar was added *O*-Me dipeptide **156** (800 mg, 2.23 mmol, 1 eq.) and LiOH·H$_2$O (374 mg, 8.92 mmol, 4 eq.). MeOH (22 mL) was then added and the solution stirred at RT for 16 h. After 16 h the solution was acidified to pH 1 using 1M HCl, then extracted into CH$_2$Cl$_2$ three times. The organic layers were combined, dried over MgSO$_4$, filtered and evaporated to afford a white solid (744 mg, 97%), which was used in the next step without further purification or characterisation.

Lab book reference number: AJR-4-325

Methyl (2*S*)-2-[(2*R*)-2-[(2*S*)-2-[(2*R*)-2-[(2*S*)-2-{[(*tert*-butoxy)carbonyl]amino}-4-methylpentanamido]-4-methylpentanamido]-3-methylbutanamido]-4-methylpentanamido]-3-(1*H*-indol-3-yl)propanoate (158)[126]
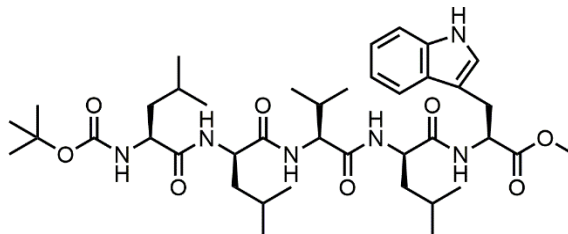
Acid **157** (141 mg, 0.41 mmol, 1 eq.), amine **153** (194 mg, 0.45 mmol, 1.1 eq.) and DEPBT (147 mg, 0.49 mmol, 1.2 eq.) were added to a round-bottomed flask which was fitted with a septum and flushed with argon from a balloon for 20 min. After 20 min dry, distilled DIPEA (0.29 mL, 212 mg, 1.64 mmol, 4 eq.) and dry CH$_3$CN (4.1 mL) were added *via* syringe to

give a yellow solution and the reaction stirred at RT for 2 h. After 2 h the reaction mixture was washed with sat. aq. NH$_4$Cl and extracted three times with CH$_2$Cl$_2$. The organic layers were combined, dried over MgSO$_4$, filtered and evaporated to give a crude yellow residue. Purification by dry-loaded flash column chromatography (SiO$_2$, petrol/EtOAc, 1:3, *v/v*) afforded the *title compound* as a brown solid (209 mg, 67%).

R_f 0.50 (petrol/EtOAc, 1:3, *v/v*); ^{1}H NMR (400 MHz, CD$_3$OD, δ): 7.50 (dt, *J* = 8.0, 1.0 Hz, 1H), 7.32 (dt, *J* = 8.0, 1.0 Hz, 1H), 7.11–7.05 (m, 2H), 7.00 (ddd, *J* = 8.0, 7.0, 1.0 Hz, 1H), 4.70 (dd, *J* = 7.5, 6.0 Hz, 1H), 4.45 (ddt, *J* = 9.0, 6.0, 2.5 Hz, 2H), 4.13–4.04 (m, 2H), 3.63 (s, 2H), 3.28–3.17 (m, 2H), 2.04–1.93 (m, 1H), 1.70–1.50 (m, 9H), 1.46–1.41 (m, 9H), 0.98–0.79 (m, 24H); ^{13}C NMR (101 MHz, CD$_3$OD, δ): 175.6, 174.5, 174.4, 173.7, 173.3, 157.8, 138.0, 128.7, 124.5, 122.4, 119.8, 119.1, 112.3, 110.4, 80.5, 60.1, 54.8, 54.7, 54.5, 53.2, 52.9, 52.6, 52.6, 42.1, 42.0, 32.1, 30.1, 28.7, 28.5, 25.9, 25.8, 25.7, 23.5, 23.5, 23.4, 22.3, 22.1, 19.8, 19.7, 18.9; ESI–MS *m/z* (ion, %): 757 ([M+H]$^+$, 7), 775 ([M+NH$_4$]$^+$, 60), 779 ([M+Na]$^+$, 100); ESI–HRMS *m/z*: 779.4692 [M+Na]$^+$ (C$_{40}$H$_{64}$N$_6$NaO$_8$ requires 779.4678).

Lab book reference number: AJR-4-326

Methyl (2*S*)-2-[(2*R*)-2-[(2*S*)-2-[(2*R*)-2-[(2*S*)-2-{[(*tert*-butoxy)carbonyl]amino}-4-methylpentanamido]-4-methylpentanamido]-3-methylbutanamido]-4-methylpentanamido]-3-(2-phenyl-1*H*-indol-3-yl)propanoate (159)
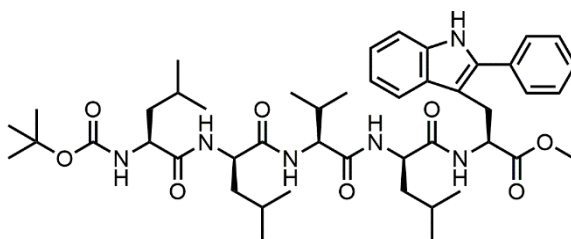
To a microwave tube was added peptide **158** (145 mg, 0.192 mmol, 1 eq.), aryliodonium salt **140** (181 mg, 0.384 mmol, 2 eq.), Pd(OAc)$_2$ (13 mg, 0.058 mmol, 30 mol%) and EtOAc (5 mL). The reaction mixture was stirred at 25 °C for 16 h. After 16 h the resulting black reaction mixture was filtered through Celite then washed with sat. aq. NaHCO$_3$. The organic layer was collected and dried over MgSO$_4$, filtered and evaporated to give a brown solid.

The *title compound* could not be isolated from starting material **158**.

ESI–MS *m/z* (ion, %): 855 ([M+Na]$^+$, 20); ESI–HRMS *m/z*: 855.4980 [M+Na]$^+$ (C$_{46}$H$_{68}$N$_6$NaO$_8$ requires 855.4996).

Lab book reference number: AJR-4-341

Methyl (2*S*)-2-[(2*R*)-2-{[(*tert*-butoxy)carbonyl]amino}-4-methylpentanamido]-3-(2-phenyl-1*H*-indol-3-yl)propanoate (160)

To a microwave tube was added dipeptide **149** (83 mg, 0.192 mmol, 1 eq.), phenylboronic acid **14** (47 mg, 0.384 mmol, 2 eq.), Cu(OAc)$_2$ (3.5 mg, 0.0192 mmol, 10 mol%), Pd(OAc)$_2$ (2 mg, 9.6 μmol, 5 mol%) and AcOH (5 mL). The reaction mixture was stirred at 40 °C for 16 h. After 16 h the resulting black reaction mixture was filtered through Celite and the solvent removed under reduced pressure to give a brown solid. This was dissolved in EtOAc (10 mL) then washed with sat. aq. NaHCO$_3$. The organic layer was collected, dried over MgSO$_4$, filtered and evaporated to give a brown solid. Purification by dry-loaded flash column chromatography (SiO$_2$, petrol/EtOAc, 1.5:1, *v/v*) afforded the *title compound* as an off-white solid (30 mg, 31%).

R_f 0.37 (petrol/EtOAc, 1.5:1, *v/v*); M.P. 55–58 °C; ¹H NMR (400 MHz, CDCl$_3$, δ): 8.24 (br s, 1H), 7.63–7.54 (m, 3H), 7.51–7.45 (m, 2H), 7.41–7.33 (m, 2H), 7.20 (ddd, *J* = 8.0, 7.0, 1.0 Hz, 1H), 7.15 (ddd, *J* = 8.0, 7.0, 1.0 Hz, 1H), 6.35 (d, *J* = 7.5 Hz, 1H), 4.81 (d, *J* = 7.5 Hz, 1H), 4.56–4.43 (m, 1H), 3.92 (s, 1H), 3.50 (d, *J* = 6.0 Hz, 2H), 3.30 (s, 3H), 1.57–1.47 (m, 3H), 1.41 (s, 9H), 0.84 (dd, *J* = 6.5, 2.5 Hz, 6H); ¹³C NMR (101 MHz, CDCl$_3$, δ): 172.2, 172.0, 136.0, 135.8, 133.2, 129.7, 129.5, 129.3, 128.4, 128.3, 122.8, 120.2, 119.2, 115.5, 111.1, 52.2, 41.6, 28.4, 27.2, 24.7, 23.2; ESI–MS *m/z* (ion, %): 508 ([M+H]$^+$, 30), 530 ([M+Na]$^+$, 100); ESI–HRMS *m/z*: 508.2814 [M+H]$^+$ (C$_{29}$H$_{38}$N$_3$O$_5$ requires 508.2806); IR (solid-state, ATR, cm^{-1}): 3395 (m, br), 3312 (m, br), 2956 (m), 2929 (m), 2870 (m), 2028 (w), 1885 (w), 1696 (s), 1659 (s), 1604 (w), 1594 (w), 1501 (s), 1455 (s), 1367 (s), 1248 (m), 1217 (m), 1164 (s), 1047 (w), 1021 (w), 910 (w), 741 (s), 698 (m); UV–vis (DMSO, nm): λ$_{max}$ 308 (ε = 12870 mol dm^{-3} cm^{-1}).

Lab book reference number: AJR-4-308

Methyl (2S)-2-{[(*tert*-butoxy)carbonyl]amino}-3-(1H-indol-3-yl)propanoate (161)[202]
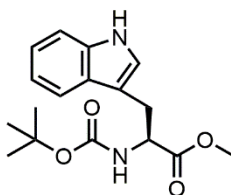
To a round-bottomed flask containing a solution of tryptophan **135** (1 g, 3.9 mmol, 1 eq.) and K_2CO_3 (539 mg, 3.9 mmol, 1 eq.) in deionised water (10 mL) was added a solution of di-*tert*-butyl dicarbonate (851 mg, 3.9 mmol, 1 eq.) in acetone (10 mL) at 0 °C with stirring. The solution was stirred for 2 h during which time it was allowed to warm to RT. After 2 h the acetone was removed under reduced pressure and deionised water added. This was extracted into EtOAc three times, dried over $MgSO_4$, filtered and evaporated to afford the *title compound* as an off-white solid (1.06 g, 85%).

$[\alpha]_D$ = +43.1 (*c* 0.10, $CHCl_3$); Mp 146–148 °C (lit.[203] 145–146 °C); ^1H NMR (400 MHz, $CDCl_3$, δ): 8.20 (br s, 1H), 7.55 (d, *J* = 8.0 Hz, 1H), 7.35 (dt, *J* = 8.0, 1.0 Hz, 1H), 7.19 (ddd, *J* = 8.0, 7.0, 1.0 Hz, 1H), 7.12 (ddd, *J* = 8.0, 7.0, 1.0 Hz, 1H), 6.99 (d, *J* = 8.0 Hz, 1H), 5.09 (d, *J* = 8.0 Hz, 1H), 4.64 (dt, *J* = 8.0, 5.0 Hz, 1H), 3.68 (s, 3H), 3.31 (dd, *J* = 15.0, 5.0 Hz, 1H), 3.29 (dd, *J* = 15.0, 5.0 Hz, 1H), 1.43 (s, 9H); ^{13}C NMR (101 MHz, $CDCl_3$, δ): 172.9, 155.4, 136.3, 127.6, 123.0, 122.1, 119.5, 118.6, 111.4, 109.8, 80.0, 54.3, 52.3, 28.4, 28.0; ESI–MS *m/z* (ion, %): 319 ([M+H]$^+$, 14), 341 ([M+Na]$^+$, 100); ESI–HRMS *m/z*: 341.1465 [M+Na]$^+$ ($C_{17}H_{22}N_2NaO_4$ requires 341.1472).

Lab book reference number: AJR-4-337

Methyl (2*S*)-2-{[(*tert*-butoxy)carbonyl]amino}-3-(2-phenyl-1*H*-indol-3-yl)propanoate (162)
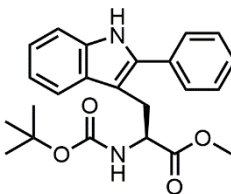
To a microwave tube was added tryptophan **161** (61 mg, 0.192 mmol, 1 eq.), diaryliodonium salt **140** (181 mg, 0.384 mmol, 2 eq.), $Pd(OAc)_2$ (2 mg, 9.6 μmol, 5 mol%) and EtOAc (5 mL). The reaction mixture was stirred at 25 °C for 16 h. After 16 h the resulting reaction mixture was filtered through Celite then washed with sat. aq. $NaHCO_3$. The organic layer was collected and dried over $MgSO_4$, filtered and evaporated to give a brown solid.

Attempted purification by dry-loaded flash column chromatography (SiO₂, petrol/EtOAc, 1:1, *v/v*) could not afford the *title compound*.

Lab book reference number: AJR-4-315

(2*S*)-2-Acetamido-4-methylpentanoic acid (163)[204]
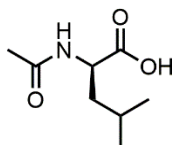
To a round-bottomed flask containing L-Leucine **154** (1 g, 7.6 mmol, 1 eq.) was added a mixture of 1,4-dioxane and deionised water (26 mL, 1:1, *v/v*) to form a white suspension, then NaHCO₃ (1.28 g, 15.2 mmol, 2 eq.) was added with stirring. Acetic anhydride (0.72 mL, 776 mg, 7.6 mmol, 1 eq.) was added dropwise over 10 min then the reaction was heated to 60 °C to form a clear solution. The solution was stirred at 60 °C for 16 h then evaporated. The resulting residue was redissolved in deionised water and acidified to pH 1.5 with 1M HCl. This was extracted into EtOAc three times, dried over MgSO₄, filtered and evaporated to afford the *title compound* as a white solid (1.11 g, 84%).

¹H NMR (400 MHz, CD₃OD, δ): 4.48–4.34 (m, 1H), 1.98 (s, 3H), 1.78–1.64 (m, 1H), 1.64–1.54 (m, 2H), 0.97 (d, *J* = 6.5 Hz, 3H), 0.93 (d, *J* = 6.5 Hz, 3H); ¹³C NMR (101 MHz, CD₃OD, δ): 176.1, 173.4, 52.1, 41.6, 26.1, 23.4, 22.3, 21.8; ESI–MS *m/z* (ion, %): 174 ([M+H]⁺, 10), 196 ([M+Na]⁺, 100); ESI–HRMS *m/z*: 174.1124 [M+H]⁺ (C₈H₁₆NO₃ requires 174.1125); Elemental anal.: C 55.69, H 8.72, N 8.05 (C₈H₁₅NO₃ requires C 55.47, H 8.73, N 8.09).

Lab book reference number: AJR-4-309

Methyl (2*S*)-2-[(2*R*)-2-acetamido-4-methylpentanamido]-3-(1*H*-indol-3-yl)propanoate (164)
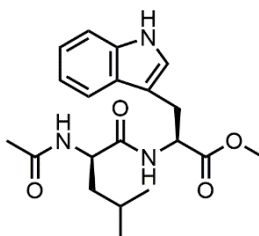
Acid **163** (200 mg, 1.15 mmol, 1 eq.), amine **135** (323 mg, 1.27 mmol, 1.1 eq.) and DEPBT (413 mg, 1.38 mmol, 1.2 eq.) were added to a round-bottomed flask which was fitted with a septum and flushed with argon from a balloon for 20 min. After 20 min dry, distilled DIPEA

(802 μL, 595 mg, 4.60 mmol, 4 eq.) and dry CH_2Cl_2 (12 mL) were added *via* syringe to give a yellow solution and the reaction stirred at RT for 2 h. After 2 h the reaction mixture was washed with sat. aq. NH_4Cl and extracted three times with CH_2Cl_2. The organic layers were combined, dried over $MgSO_4$, filtered and evaporated to give a crude yellow residue. Attempted purification by dry-loaded flash column chromatography (SiO_2, EtOAc/MeOH, 98:2, *v/v*) could not afford the *title compound*.

Lab book reference number: AJR-4-311

Methyl (2*S*)-3-(1*H*-indol-3-yl)-2-(trifluoroacetamido)propanoate (92)
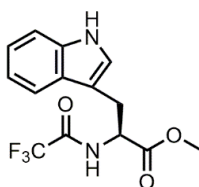
To a round-bottomed flask containing tryptophan **135** (1.27 g, 5 mmol, 1 eq.) was added triethylamine (0.75 mL, 0.54 g, 5 mmol, 1 eq.) and MeOH (2.5 mL) and the resulting suspension stirred for 5 min. After 5 min ethyl trifluoroacetate **165** (0.85 mL, 1.01 g, 6.35 mmol, 1.27 eq.) was added and the mixture stirred at RT for 16 h, during which time a clear solution formed. After 16 h the solvent was evaporated and the resulting residue acidified with 2M HCl, before being extracted into EtOAc three times. The organic layers were combined then washed with brine, dried over $MgSO_4$, filtered and evaporated to afford the *title compound* as an off-white solid (1.35 g, 90%).

R_f 0.16 (petrol/EtOAc, 3:1, *v/v*); $[\alpha]_D$ = +50.7 (*c* 0.10, $CHCl_3$); M.P. 108–109 °C (lit.[205] 107–109 °C); ^1H NMR (400 MHz, $CDCl_3$, δ): 8.25 (br s, 1H), 7.54–7.47 (m, 1H), 7.36 (dt, *J* = 8.0, 1.0 Hz, 1H), 7.22 (ddd, *J* = 8.0, 7.0, 1.0 Hz, 1H), 7.15 (ddd, *J* = 8.0, 7.0, 1.0 Hz, 1H), 6.96 (d, *J* = 8.0 Hz, 1H), 6.95 (s, 1H), 4.94 (dt, *J* = 8.0, 5.0 Hz, 1H), 3.73 (s, 3H), 3.42 (m, 2H); ^{13}C NMR (101 MHz, $CDCl_3$, δ): 170.8, 156.9 (q, $^2J_{C–F}$ = 37.5), 136.2, 127.4, 123.1, 122.6, 120.0, 118.3, 116.3 (q, $^1J_{C–F}$ = 287.0), 111.6, 108.8, 53.5, 53.0, 27.2; ^{19}F NMR (376 MHz, $CDCl_3$, δ): −75.8; ESI–MS *m/z* (ion, %): 315 ($[M+H]^+$, 50), 332 ($[M+NH_4]^+$, 40), 337 ($[M+Na]^+$, 100), 353 ($[M+K]^+$, 10); ESI–HRMS *m/z*: 315.0950 $[M+H]^+$ ($C_{14}H_{14}F_3N_2O_3$ requires 315.0951).

The analytical data obtained was in accordance with the literature.[206]

Lab book reference number: AJR-4-343

(2*R*)-4-Methyl-2-(trifluoroacetamido)pentanoic acid (166)
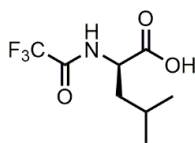
To a round-bottomed flask containing L-Leucine **154** (1 g, 7.6 mmol, 1 eq.) was added triethylamine (1.06 mL, 769 mg, 7.6 mmol, 1 eq.) and MeOH (7.6 mL) and the resulting suspension stirred for 5 min. After 5 min ethyl trifluoroacetate **165** (1.13 mL, 1.35 g, 9.5 mmol, 1.25 eq.) was added and the mixture stirred at RT for 16 h, during which time a clear solution formed. After 16 h the solvent was evaporated and the resulting residue acidified with 2M HCl, before being extracted into EtOAc three times. The organic layers were combined then washed with brine, dried over MgSO$_4$, filtered and evaporated to afford the *title compound* as an off-white solid (1.67 g, 97%).

$[\alpha]_D$ = +31.6 (*c* 0.10, CHCl$_3$); M.P. 75–77 °C (lit.[207] 76–77 °C dec.); ^{1}H NMR (400 MHz, CD$_3$OD, δ): 4.48 (dd, *J* = 10.0, 5.0 Hz, 1H), 1.81–1.60 (m, 3H), 0.97 (d, *J* = 6.0 Hz, 3H), 0.94 (d, *J* = 6.0 Hz, 3H); ^{13}C NMR (101 MHz, CD$_3$OD, δ):174.4, 158.9 (q, $^2J_{C–F}$ = 38.0 Hz), 117.5 (q, $^1J_{C–F}$ = 287.0 Hz), 52.4, 40.7, 26.1, 23.3, 21.5; ^{19}F NMR (376 MHz, CD$_3$OD, δ): −77.0; ESI–MS *m/z* (ion, %): 250 ([M+Na]$^+$, 100); ESI–HRMS *m/z*: 250.0665 [M+Na]$^+$ (C$_8$H$_{12}$F$_3$NNaO$_3$ requires 250.0661).

The analytical data obtained was in accordance with the literature.[208]

Lab book reference number: AJR-4-334

Methyl (2*S*)-3-(1*H*-indol-3-yl)-2-[(2*R*)-4-methyl-2-trifluoroacetamido)pentanamido] propanoate (167)
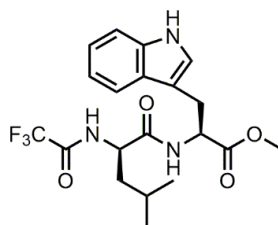

Acid **166** (500 mg, 2.2 mmol, 1 eq.), amine **135** (616 mg, 2.42 mmol, 1.1 eq.) and DEPBT (790 mg, 2.64 mmol, 1.2 eq.) were added to a round-bottomed flask which was fitted with a septum and flushed with argon from a balloon for 20 min. After 20 min dry, distilled DIPEA (1.5 mL, 1.14 g, 8.8 mmol, 4 eq.) and dry CH$_2$Cl$_2$ (22 mL) were added *via* syringe to give a yellow solution and the reaction stirred at RT for 2 h. After 2 h the reaction mixture was

washed with sat. aq. NH$_4$Cl and extracted three times with CH$_2$Cl$_2$. The organic layers were combined, dried over MgSO$_4$, filtered and evaporated to give a crude yellow residue. Purification by dry-loaded flash column chromatography (SiO$_2$, petrol/EtOAc, 1:1, *v/v*) afforded the *title compound* as an off-white solid (568 mg, 60%).

R_f 0.48 (petrol/EtOAc, 1:1, *v/v*); $[\alpha]_D$ = +33.9 (*c* 0.10, CHCl$_3$); M.P. 129–131 °C; ^{1}H NMR (400 MHz, CDCl$_3$, δ): 8.19 (br s, 1H), 7.48 (d, *J* = 8.0 Hz, 1H), 7.36–7.33 (m, 1H), 7.23–7.08 (m, 2H), 6.98 (d, *J* = 2.0 Hz, 1H), 6.45 (d, *J* = 8.0 Hz, 1H), 4.97–4.84 (m, 1H), 4.51–4.36 (m, 1H), 3.70 (s, 3H), 3.38–3.25 (m, 2H), 1.68 (s, 1H), 1.62–1.41 (m, 3H), 1.29–1.18 (m, 3H), 0.89–0.75 (m, 6H); ^{19}F NMR (376 MHz, CDCl$_3$, δ): −75.6; ^{13}C NMR (101 MHz, CDCl$_3$, δ): 172.0, 170.4, 157.1 (q, $^2J_{C-F}$ = 37.5 Hz), 136.2, 127.5, 123.3, 122.5, 120.0, 118.4, 116.6 (q, $^1J_{C-F}$ = 288.0 Hz), 111.5, 109.3, 53.2, 52.7, 52.2, 41.5, 27.6, 24.7, 22.7, 22.1; ESI–MS *m/z* (ion, %): 428 ([M+H]$^+$, 75), 450 ([M+Na]$^+$, 100); ESI–HRMS *m/z*: 450.1612 [M+Na]$^+$ (C$_{20}$H$_{24}$F$_3$N$_3$NaO$_4$ requires 450.1611); IR (solid-state, ATR, cm^{-1}): 3277 (w, br), 3084 (w), 2959 (w), 2933 (w), 2873 (w), 1714 (s), 1652 (s), 1551 (m), 1439 (m), 1341 (m), 1209 (s), 1184 (s), 1156 (s), 1094 (w), 1010 (w), 988 (w), 742 (s), 719 (m), 652 (m), 632 (m), 521 (m); UV–vis (DMSO, nm): λ_{max} 282 (ε = 5734 mol dm^{-3} cm^{-1}).

Lab book reference number: AJR-4-344

2-(Trifluoroacetamido)acetic acid (169)
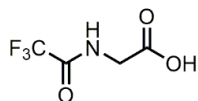
To a round-bottomed flask containing glycine **168** (826 mg, 11 mmol, 1 eq.) was added triethylamine (1.5 mL, 1.11 g, 11 mmol, 1 eq.) and MeOH (5.5 mL) and the resulting suspension stirred for 5 min. After 5 min ethyl trifluoroacetate **165** (1.7 mL, 1.99 g, 14 mmol, 1.27 eq.) was added and the mixture stirred at RT for 16 h, during which time a clear solution formed. After 16 h the solvent was evaporated and the resulting residue acidified with 2M HCl, before being extracted into EtOAc three times. The organic layers were combined then washed with brine, dried over MgSO$_4$, filtered and evaporated to afford the *title compound* as a white solid (1.68 g, 89%).

M.P. 119–121 °C (lit.[209] 118–119 °C dec.); ^{1}H NMR (400 MHz, CD$_3$OD, δ): 4.00 (s, 2H); ^{13}C NMR (101 MHz, CD$_3$OD, δ): 171.5, 159.4 (q, $^2J_{C-F}$ = 37.5 Hz), 117.4 (q, $^1J_{C-F}$ = 286.0 Hz), 41.7; ^{19}F NMR (376 MHz, CD$_3$OD, δ): −77.3; ESI–MS *m/z* (ion, %): 194 ([M+Na]$^+$, 100); ESI–HRMS *m/z*: 194.0033 [M+Na]$^+$ (C$_4$H$_4$F$_3$NNaO$_3$ requires 194.0035).

The analytical data obtained was in accordance with the literature.[210]

Lab book reference number: AJR-4-342

**Methyl (2*S*)-3-(1*H*-indol-3-yl)-2-[2-(trifluoroacetamido)acetamido]propanoate (170)**
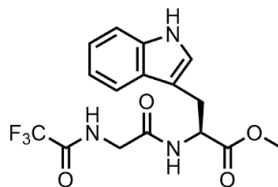
Acid **169** (100 mg, 0.58 mmol, 1 eq.), amine **135** (163 mg, 0.64 mmol, 1.1 eq.) and TBTU (225 mg, 0.70 mmol, 1.2 eq.) were added to a round-bottomed flask which was fitted with a septum and flushed with argon from a balloon for 20 min. After 20 min dry, distilled DIPEA (0.4 mL, 300 mg, 2.32 mmol, 4 eq.) and dry CH_3CN (5.8 mL) were added *via* syringe to give a yellow solution and the reaction stirred at RT for 2 h. After 2 h the reaction mixture was washed with sat. aq. NH_4Cl and extracted three times with CH_2Cl_2. The organic layers were combined, dried over $MgSO_4$, filtered and evaporated to give a crude yellow residue. Purification by dry-loaded flash column chromatography (SiO_2, petrol/EtOAc, 1:3, *v/v*) afforded the *title compound* as an off-white solid (201 mg, 93%).

R_f 0.52 (petrol/EtOAc, 1:3, *v/v*); $[\alpha]_D$ = +40.7 (*c* 0.10, CHCl$_3$); M.P. 53–55 °C; ^{1}H NMR (400 MHz, CDCl$_3$, δ): 8.28–8.18 (br s, 1H), 7.50–7.44 (m, 1H), 7.38 (t, *J* = 5.0 Hz, 1H), 7.30 (dt, *J* = 8.0, 1.0 Hz, 1H), 7.18 (ddd, *J* = 8.0, 7.0, 1.2 Hz, 1H), 7.11 (ddd, *J* = 8.0, 7.0, 1.0 Hz, 1H), 6.94 (d, *J* = 2.5 Hz, 1H), 6.57 (d, *J* = 8.0 Hz, 1H), 4.93 (dt, *J* = 8.0, 5.5 Hz, 1H), 3.85–3.74 (m, 2H), 3.73 (s, 3H), 3.37–3.24 (m, 2H); ^{13}C NMR (101 MHz, CDCl$_3$, δ): 172.3, 166.8, 157.3 (q, $^2J_{C-F}$ = 38.0 Hz), 136.2, 127.4, 123.2, 122.5, 120.0, 118.3, 116.6 (q, $^1J_{C-F}$ = 287.0 Hz), 111.6, 109.4, 53.2, 52.8, 42.5, 27.5; ^{19}F NMR (376 MHz, CDCl$_3$, δ): −75.6; ESI–MS *m/z* (ion, %): 372 ([M+H]$^+$, 10), 394 ([M+Na]$^+$, 100); ESI–HRMS *m/z*: 394.0988 [M+Na]$^+$ ($C_{16}H_{16}F_3N_3NaO_4$ requires 394.0985); IR (solid-state, ATR, cm^{-1}): 3391 (m), 3341 (m), 1729 (m), 1704 (s), 1654 (m), 1560 (m), 1532 (m), 1445 (m), 1351 (m), 1215 (s), 1184 (s), 1150 (s), 1005 (m), 968 (m), 742 (s), 608 (s), 536 (s), 428 (s); UV–vis (DMSO, nm): λ_{max} 284 (ε = 10138 mol dm^{-3} cm^{-1}).

Lab book reference number: AJR-4-345

Methyl (2*S*)-3-(2-phenyl-1*H*-indol-3-yl)-2-(trifluoroacetamido)propanoate (171)
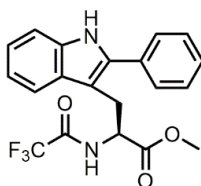
To a microwave tube was added tryptophan **92** (58 mg, 0.192 mmol, 1 eq.), aryliodonium salt **140** (181 mg, 0.384 mmol, 2 eq.), Pd(OAc)$_2$ (2 mg, 9.6 µmol, 5 mol%) and EtOAc (5 mL). The reaction mixture was stirred at 25 °C for 16 h. After 16 h the resulting black reaction mixture was filtered through Celite then washed with sat. aq. NaHCO$_3$. The organic layer was collected and dried over MgSO$_4$, filtered and evaporated to give a brown solid. Purification by dry-loaded flash column chromatography (SiO$_2$, petrol/EtOAc, 3:1, *v/v*) afforded the *title compound* as an off-white solid (59 mg, 82%).

R$_f$ 0.32 (petrol/EtOAc, 3:1, *v/v*); [α]$_D$ = +42.4 (*c* 0.10, CHCl$_3$); M.P. 155–156 °C; ^{1}H NMR (400 MHz, CDCl$_3$, δ): 8.15 (br s, 1H), 7.58–7.52 (m, 3H), 7.50 (dd, *J* = 8.0, 7.0 Hz, 2H), 7.44–7.36 (m, 2H), 7.23 (ddd, *J* = 8.0, 7.0, 1.0 Hz, 1H), 7.19–7.14 (m, 1H), 6.64 (d, *J* = 8.0 Hz, 1H), 4.83 (dt, *J* = 8.0, 5.5 Hz, 1H), 3.61 (dd, *J* = 5.5, 1.0 Hz, 2H), 3.35 (s, 3H); ^{13}C NMR (101 MHz, CDCl$_3$, δ): 170.7, 156.7 (q, $^2J_{C-F}$ = 37.5), 136.5, 135.8, 132.6, 129.3, 129.1, 128.5, 128.4, 122.9, 120.4, 118.7, 114.9 (q, $^1J_{C-F}$ = 288.0 Hz), 111.2, 105.6, 53.4, 52.6, 26.5; ^{19}F NMR (376 MHz, CDCl$_3$, δ): −75.9; ESI–MS *m/z* (ion, %): 391 ([M+H]$^+$, 10), 408 ([M+NH$_4$]$^+$, 35), 413 ([M+Na]$^+$, 100), 429 ([M+K]$^+$, 10); ESI–HRMS *m/z*: 413.1074 [M+Na]$^+$ (C$_{20}$H$_{17}$F$_3$N$_2$NaO$_3$ requires 413.1083).

The analytical data obtained was in accordance with the literature.[211]

Lab book reference number: AJR-4-346

Methyl (2*S*)-2-(trifluoroacetamido)-3-[2-(2,4,6-trimethylphenyl)-1*H*-indol-3-yl] propanoate (172)
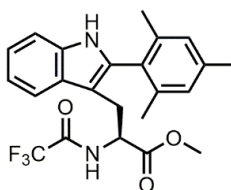
Method A: *Title compound* was isolated as an off-white solid side product from the synthesis of **171** (14 mg, 17%).

Method B: To a microwave tube was added tryptophan **92** (60 mg, 0.192 mmol, 1 eq.), aryldiazonium salt **196** (45 mg, 0.192 mmol, 1 eq.), Pd(OAc)$_2$ (2 mg, 9.6 µmol, 5 mol%) and EtOAc (5 mL). The reaction mixture was stirred at RT for 16 h. After 16 h the resulting brown reaction mixture was filtered through Celite then washed with sat. aq. NaHCO$_3$. The organic layer was collected and dried over MgSO$_4$, filtered and evaporated to give a brown solid. Purification by dry-loaded flash column chromatography (SiO$_2$, petrol/EtOAc, 3:1, *v/v*) afforded the *title compound* as an off-white solid (54 mg, 65%).

R_f 0.42 (petrol/EtOAc, 3:1, *v/v*); $[\alpha]_D$ = +34.4 (*c* 0.10, CHCl$_3$); M.P. 58–60 °C; ^{1}H NMR (400 MHz, CDCl$_3$, δ): 8.00 (br s, 1H), 7.59 (dd, *J* = 8.0, 1.0 Hz, 1H), 7.39–7.34 (m, 1H), 7.22 (ddd, *J* = 8.0, 7.0, 1.0 Hz, 1H), 7.17 (ddd, *J* = 8.0, 7.0, 1.0 Hz, 1H), 6.99 (d, *J* = 2.5 Hz, 2H), 6.58 (d, *J* = 7.5 Hz, 1H), 4.76 (td, *J* = 7.0, 5.5 Hz, 1H), 3.50 (s, 3H), 3.26 (dd, *J* = 15.0, 5.5 Hz, 1H), 3.13 (dd, *J* = 15.0, 7.0 Hz, 1H), 2.36 (s, 3H), 2.10 (s, 3H), 2.09 (s, 3H); ^{13}C NMR (101 MHz, CDCl$_3$, δ): 170.8, 157.0 (q, $^2J_{C-F}$ = 38.0 Hz), 139.0, 138.1, 135.9, 135.2, 128.7, 128.3, 128.0, 122.2, 120.0, 118.4 (q, $^1J_{C-F}$ = 288.0 Hz), 111.1, 106.7, 53.5, 52.7, 27.0, 21.2, 20.1; ^{19}F NMR (376 MHz, CDCl$_3$, δ): −75.7; ESI–MS *m/z* (ion, %): 433 ([M+H]$^+$, 5), 450 ([M+NH$_4$]$^+$, 40), 455 ([M+Na]$^+$, 100), 471 ([M+K]$^+$, 5); ESI–HRMS *m/z*: 455.1547 [M+Na]$^+$ (C$_{23}$H$_{23}$F$_3$N$_2$NaO$_3$ requires 455.1553); IR (solid-state, ATR, cm^{-1}): 3391 (w, br), 2955 (w), 2919 (w), 2851 (w), 1712 (s), 1614 (w), 1543 (w), 1458 (m), 1439 (m), 1378 (w), 1344 (w), 1292 (m), 1206 (s), 1163 (s), 1011 (w), 909 (m), 853 (w), 731 (s), 510 (m); UV–vis (DMSO, nm): λ_{max} 288 (ε = 9725 mol dm^{-3} cm^{-1}).

Lab book reference number (method A): AJR-4-346

Lab book reference number (method B): AJR-5-427

Methyl (2*S*)-2-[(2*R*)-4-methyl-2-(trifluoroacetamido)pentanamido]-3-(2-phenyl-1*H*-indol-3-yl)propanoate (173)

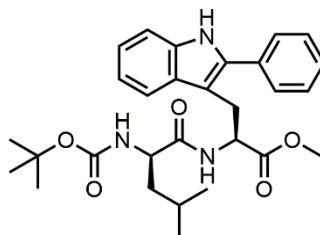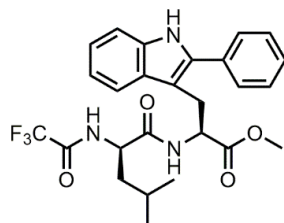*Method A*: To a microwave tube was added dipeptide **167** (82 mg, 0.192 mmol, 1 eq.), diaryliodonium salt **140** (181 mg, 0.384 mmol, 2 eq.), Pd(OAc)$_2$ (2 mg, 9.6 µmol, 5 mol%) and EtOAc (5 mL). The reaction mixture was stirred at 25 °C for 16 h. After 16 h the resulting black reaction mixture was filtered through Celite then washed with sat. aq. NaHCO$_3$. The organic layer was collected and dried over MgSO$_4$, filtered and evaporated to give a brown

solid. Purification by dry-loaded flash column chromatography (SiO$_2$, petrol/EtOAc, 3:1, *v/v*) afforded the *title compound* as a yellow solid (63 mg, 65%).

Method B: To a microwave tube equipped with magnetic stirrer bar was added dipeptide **167** (43 mg, 0.10 mmol, 1 eq.), diaryliodonium salt **233** (74 mg, 0.20 mmol, 2 eq.), Pd/C (5 wt%, 11 mg, 5 mol%) and AcOH (1 mL). The vial was sealed with a septum and the reaction stirred at 60 °C for 16 h. After 16 h the reaction mixture was allowed to cool to RT, filtered through a silica pad with EtOAc and evaporated to give a brown residue, which was subsequently analysed by ^{1}H NMR spectroscopy.

R_f 0.19 (petrol/EtOAc, 3:1, *v/v*); [α]$_D$ = +43.8 (*c* 0.10, CHCl$_3$); M.P. 83–85 °C dec; ^{1}H NMR (400 MHz, CDCl$_3$, δ): 8.18 (br s, 1H), 7.57–7.53 (m, 3H), 7.49 (ddt, *J* = 8.0, 6.5, 1.0 Hz, 2H), 7.42–7.35 (m, 2H), 7.25–7.19 (m, 1H), 7.15 (ddd, *J* = 8.0, 7.0, 1.0 Hz, 1H), 6.91–6.84 (m, 1H), 5.93–5.83 (m, 1H), 4.79 (dq, *J* = 7.5, 5.5, 5.0 Hz, 1H), 3.96 (td, *J* = 8.0, 5.0 Hz, 1H), 3.65–3.48 (m, 2H), 3.38 (s, 3H), 1.54–1.34 (m, 3H), 0.82–0.75 (m, 6H); ^{13}C NMR (101 MHz, CDCl$_3$, δ): 171.7, 170.1, 156.6 (q, $^2J_{C–F}$ = 37.5 Hz), 136.2, 135.8, 132.9, 129.3, 129.2, 129.1, 128.4, 128.3, 128.2, 122.8, 120.2, 118.6 (q, $^1J_{C–F}$ = 287.5 Hz), 111.2, 106.2, 53.3, 52.3, 51.8, 42.0, 26.6, 24.6, 22.7, 22.1; ^{19}F NMR (376 MHz, CDCl$_3$, δ): −72.4; ESI–MS *m/z* (ion, %): 504 ([M+H]$^+$, 5), 521 ([M+NH$_4$]$^+$, 15), 526 ([M+Na]$^+$, 100), 542 ([M+K]$^+$, 5); ESI–HRMS *m/z*: 526.1925 [M+Na]$^+$ (C$_{26}$H$_{28}$F$_3$N$_3$NaO$_4$ requires 526.1924); IR (solid-state, ATR, cm^{-1}): 3337 (w, br), 3061 (w), 2958 (w), 2930 (w), 2873 (w), 1715 (m), 1658 (s), 1530 (m), 1448 (m), 1209 (s), 1155 (s), 742 (s), 698 (s); UV–vis (DMSO, nm): λ$_{max}$ 308 (ε = 20467 mol dm^{-3} cm^{-1}).

Lab book reference number (method A): AJR-4-348

Lab book reference number (method b): AJR-8-737

Methyl (2*S*)-2-[(2*R*)-4-methyl-2-(trifluoroacetamido)pentanamido]-3-[2-(2,4,6-trimethylphenyl)-1*H*-indol-3-yl]propanoate (174)
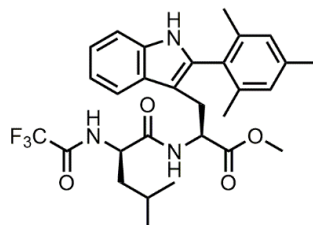
Title compound was isolated as a yellow solid side product from the synthesis of **173** (13 mg, 12%).

179

R_f 0.29 (petrol/EtOAc, 3:1, *v/v*); $[\alpha]_D$ = +31.1 (*c* 0.10, CHCl$_3$); ^{1}H NMR (400 MHz, CDCl$_3$, δ): 7.87 (br s, 1H), 7.61–7.56 (m, 1H), 7.39–7.34 (m, 1H), 7.22 (td, *J* = 8.0, 7.5, 1.0 Hz, 1H), 7.17 (td, *J* = 7.5, 1.0 Hz, 1H), 7.03 (d, *J* = 3.5 Hz, 2H), 6.91–6.85 (m, 1H), 5.67 (d, *J* = 7.0 Hz, 1H), 4.69 (td, *J* = 7.5, 4.5 Hz, 1H), 4.19–4.08 (m, 1H), 3.54 (s, 3H), 3.23 (dd, *J* = 15.0, 5.0 Hz, 1H), 3.01 (dd, *J* = 15.0, 7.5 Hz, 1H), 2.35 (s, 3H), 2.12 (s, 3H), 2.08 (s, 3H), 1.54–1.41 (m, 3H), 0.96–0.64 (m, 6H); ^{13}C NMR (101 MHz, CDCl$_3$, δ): 171.8, 170.3, 156.7 (q, $^2J_{C-F}$ = 37.5 Hz), 139.4, 138.3, 137.9, 135.8, 134.7, 129.00, 128.9, 128.4, 128.0, 122.4, 120.1, 118.4, 116.5 (q, $^1J_{C-F}$ = 288.0 Hz), 111.1, 107.6, 53.5, 52.5, 51.8, 42.6, 29.6, 27.1, 24.6, 22.8, 22.3, 21.2, 20.3; ^{19}F NMR (376 MHz, CDCl$_3$, δ): −75.8; ESI–MS *m/z* (ion, %): 546 ([M+H]$^+$, 2), 563 ([M+NH$_4$]$^+$, 15), 568 ([M+Na]$^+$, 100), 584 ([M+K]$^+$, 2); ESI–HRMS *m/z*: 568.2384 [M+Na]$^+$ (C$_{29}$H$_{34}$F$_3$N$_3$NaO$_4$ requires 568.2394); IR (solid-state, ATR, cm^{-1}): 3391 (w), 3341 (w, br), 2957 (w), 2927 (w), 1710 (m), 1661 (s), 1529 (m), 1458 (m), 1439 (m), 1353 (w), 1210 (s), 1155 (s), 1008 (s), 909 (w), 853 (w), 731 (s); UV–vis (DMSO, nm): λ$_{max}$ 290 (ε = 8712 mol dm^{-3} cm^{-1}).

Lab book reference number: AJR-4-348

Methyl (2*S*)-3-(2-phenyl-1*H*-indol-3-yl)-2-[2-(trifluoroacetamido)acetamido] propanoate (175)
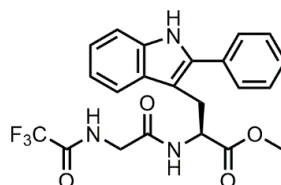
Method A: To a microwave tube was added dipeptide **170** (71 mg, 0.192 mmol, 1 eq.), diaryliodonium salt **140** (181 mg, 0.384 mmol, 2 eq.), Pd(OAc)$_2$ (2 mg, 9.6 µmol, 5 mol%) and EtOAc (5 mL). The reaction mixture was stirred at 25 °C for 16 h. After 16 h the resulting black reaction mixture was filtered through Celite then washed with sat. aq. NaHCO$_3$. The organic layer was collected and dried over MgSO$_4$, filtered and evaporated to give a brown solid. Purification by dry-loaded flash column chromatography (SiO$_2$, petrol/EtOAc, 1.5:1, *v/v*) afforded the *title compound* as an off-white solid (41 mg, 48%).

Method B: To a microwave tube equipped with magnetic stirrer bar was added dipeptide **170** (74 mg, 0.20 mmol, 1 eq.), diaryliodonium salt **233** (147 mg, 0.40 mmol, 2 eq.), Pd/C (5 wt%, 21 mg, 5 mol%) and AcOH (2 mL). The vial was sealed with a septum and the reaction stirred at 60 °C for 16 h. After 16 h the reaction mixture was allowed to cool to RT, filtered through a silica pad with EtOAc and evaporated to give a brown residue, which was subsequently analysed by ^{1}H NMR spectroscopy.

R_f 0.28 (petrol/EtOAc, 1.5:1, *v/v*); $[\alpha]_D$ = +51.0 (*c* 0.10, CHCl$_3$); M.P. 82–84 °C; ^{1}H NMR (400 MHz, CDCl$_3$, δ): 8.22 (br s, 1H), 7.55–7.49 (m, 3H), 7.46 (dd, *J* = 8.0, 7.0 Hz, 2H), 7.40–7.33 (m, 2H), 7.22 (ddd, *J* = 8.0, 7.0, 1.0 Hz, 1H), 7.12 (ddd, *J* = 8.0, 7.0, 1.0 Hz, 1H), 6.93 (br s, 1H), 6.00 (d, *J* = 7.5 Hz, 1H), 4.83 (dt, *J* = 7.5, 5.0, 1H), 3.70–3.60 (m, 2H), 3.42 (s, 3H), 3.30–3.20 (m, 2H); ^{13}C NMR (101 MHz, CDCl$_3$, δ): 171.6, 166.1, 156.7 (q, $^2J_{C-F}$ = 37.5 Hz), 141.9, 136.3, 135.8, 133.2, 129.4, 129.2, 128.3, 128.3, 128.1, 122.9, 120.3, 118.7, 114.9 (q, $^1J_{C-F}$ = 287.0 Hz), 111.2, 106.2, 53.3, 52.6, 42.0, 26.3; ^{19}F NMR (376 MHz, CDCl$_3$, δ): −75.7; ESI–MS *m/z* (ion, %): 470 ([M+Na]$^+$, 100); ESI–HRMS *m/z*: 470.1292 [M+Na]$^+$ (C$_{22}$H$_{20}$F$_3$N$_3$NaO$_4$ requires 470.1298); IR (solid-state, ATR, cm^{-1}): 3340 (w, br), 3061 (w), 2954 (w), 2930 (w), 1722 (m), 1666 (m), 1528 (m), 1441 (m), 1351 (m), 1211 (s), 1153 (s), 1074 (w), 1004 (m), 908 (m), 730 (m), 698 (s), 515 (s); UV–vis (DMSO, nm): λ$_{max}$ 308 (ε = 20684 mol dm^{-3} cm^{-1}).

Lab book reference number (method A): AJR-4-349

Lab book reference number (method B): AJR-8-736

Methyl (2*S*)-2-[2-(trifluoroacetamido)acetamido]-3-[2-(2,4,6-trimethylphenyl)-1*H*-indol-3-yl]propanoate (176)
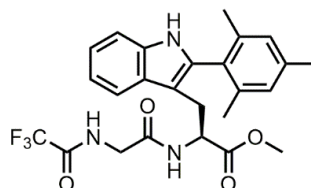
Method A: *Title compound* was isolated as an off-white solid side product from the synthesis of **175** (4 mg, 4%).

Method B: To a microwave tube was added dipeptide **170** (71 mg, 0.192 mmol, 1 eq.), aryldiazonium salt **196** (45 mg, 0.192 mmol, 1 eq.), Pd(OAc)$_2$ (2 mg, 9.6 µmol, 5 mol%) and EtOAc (5 mL). The reaction mixture was stirred at RT for 24 h. After 24 h the resulting brown reaction mixture was filtered through Celite then washed with sat. aq. NaHCO$_3$. The organic layer was collected and dried over MgSO$_4$, filtered and evaporated to give a brown solid. Purification by dry-loaded flash column chromatography (SiO$_2$, petrol/EtOAc, 1:1, *v/v*) afforded the *title compound* as an off-white solid (43 mg, 46%).

R_f 0.57 (petrol/EtOAc, 1:1, *v/v*); $[\alpha]_D$ = +33.3 (*c* 0.10, CHCl$_3$); M.P. 90–92 °C; ^{1}H NMR (400 MHz, CDCl$_3$, δ): 7.87 (br s, 1H), 7.56 (dd, *J* = 8.0, 1.0 Hz, 1H), 7.36 (dt, *J* = 8.0, 1.0 Hz, 1H), 7.22 (ddd, *J* = 8.0, 7.0, 1.0 Hz, 1H), 7.16 (ddd, *J* = 8.0, 7.0, 1.0 Hz, 1H), 7.05–7.00 (m, 2H), 6.89 (d, *J* = 1.0 Hz, 1H), 5.74 (d, *J* = 7.5 Hz, 1H), 4.76 (dt, *J* = 7.5, 5.5 Hz, 1H), 3.74 (dd, *J*

= 17.0, 4.5 Hz, 1H), 3.57 (dd, *J* = 17.0, 4.5 Hz, 1H), 3.50 (s, 3H), 3.18 (d, *J* = 5.5 Hz, 2H), 2.36 (s, 3H), 2.14 (s, 3H), 2.10 (s, 3H); ^{13}C NMR (101 MHz, CDCl$_3$, δ): 171.7, 166.2, 156.0 (q, $^2J_{C-F}$ = 37.5 Hz), 139.3, 138.2, 138.1, 135.8, 134.7, 128.9, 128.8, 128.6, 128.6, 122.3, 120.0, 118.4, 115.7 (q, $^1J_{C-F}$ = 287.0 Hz), 111.1, 107.4, 53.5, 52.5, 42.1, 27.0, 21.2, 20.3, 20.2; ^{19}F NMR (376 MHz, CDCl$_3$, δ): −75.7; ESI–MS *m/z* (ion, %): 512 ([M+Na]$^+$, 100); ESI–HRMS *m/z*: 512.1773 [M+Na]$^+$ (C$_{25}$H$_{26}$F$_3$N$_3$NaO$_4$ requires 512.1768); IR (solid-state, ATR, cm^{-1}): 3339 (w, br), 2959 (w), 2919 (w), 2850 (w), 1718 (m), 1670 (m), 1523 (m), 1458 (m), 1437 (m), 1260 (s), 1157 (s), 1006 (m), 853 (m), 800 (m), 744 (s), 517 (m); UV–vis (DMSO, nm): λ$_{max}$ 288 (ε = 12188 mol dm^{-3} cm^{-1}).

Lab book reference number (method A): AJR-4-349

Lab book reference number (method B): AJR-5-429

Benzenediazonium tetrafluoroborate (48)
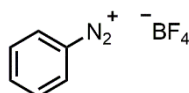
Method A: Synthesised using general procedure A from phenylamine **177** (0.91 mL, 931 mg, 10 mmol, 1 eq.) in deionised water (5.5 mL) to afford the *title compound* as a white solid (1.25 g, 65%).

Method B: Synthesised using general procedure B from phenylamine **177** (0.91 mL, 931 mg, 10 mmol, 1 eq.) in EtOH (3 mL) to afford the *title compound* as a white solid (1.92 g, quant.).

M.P. 103–105 °C (lit.[212] 101 °C dec.); ^{1}H NMR (400 MHz, (CD$_3$)$_2$SO, δ): 8.67 (dd, *J* = 8.5, 1.0 Hz, 2H), 8.26 (tt, *J* = 7.5, 1.0 Hz, 1H), 7.98 (ddt, *J* = 8.5, 7.5, 1.0 Hz, 2H); ^{13}C NMR (101 MHz, (CD$_3$)$_2$SO, δ): 140.8, 132.7, 131.2, 116.1; ^{11}B NMR (128 MHz, (CD$_3$)$_2$SO, δ): −2.3; ^{19}F NMR (376 MHz, (CD$_3$)$_2$SO, δ): −148.1 (m, $^1J_{F\_^{10}B}$, 4F), −148.1 (m, $^1J_{F\_^{11}B}$, 4F); ESI–MS *m/z* (ion, %): 105 ([M−BF$_4$]$^+$, 100); ESI–HRMS *m/z*: 105.0480 [M−BF$_4$]$^+$ (C$_6$H$_5$N$_2$ requires 105.0447).

The analytical data obtained was in accordance with the literature.[212]

Lab book reference number (Method A): AJR-4-360

Lab book reference number (Method B): LAH-1-78 (*reaction conducted by A. Hammarback*)

4-Methylbenzene-1-diazonium tetrafluoroborate (192)
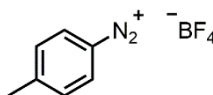
Synthesised using general procedure B from 4-amino-1-methylbenzene **178** (1.07 g, 10 mmol, 1 eq.) in EtOH (3 mL) to afford the *title compound* as a white solid (1.78 g, 86%).

M.P. 106–107 °C (lit.[213] 101–102 °C); ^{1}H NMR (400 MHz, (CD$_3$)$_2$SO, δ): 8.58–8.51 (m, 2H), 7.83–7.75 (m, 2H), 2.57 (s, 3H); ^{13}C NMR (101 MHz, (CD$_3$)$_2$SO, δ): 153.94, 132.7, 131.8, 112.0, 22.4; ^{11}B NMR (128 MHz, (CD$_3$)$_2$SO, δ): −2.3; ^{19}F NMR (376 MHz, (CD$_3$)$_2$SO, δ): −148.0 (m, $^1J_{F-^{10}B}$, 4F), −148.1 (m, $^1J_{F-^{11}B}$, 4F); ESI–MS *m/z* (ion, %): 119 ([M−BF$_4$]$^+$, 100); ESI–HRMS *m/z*: 119.0603 [M−BF$_4$]$^+$ (C$_7$H$_7$N$_2$ requires 119.0604).

The analytical data obtained was in accordance with the literature.[213]

Lab book reference number: THS-1-3 (*reaction conducted by T. Sheridan*)

4-*tert*-butylbenzene-1-diazonium tetrafluoroborate (193)
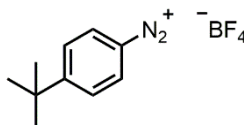
Synthesised using general procedure B from 4-*tert*-butylaniline **179** (0.8 mL, 746 mg, 5 mmol, 1 eq.) in EtOH (1.5 mL) to afford the *title compound* as a white solid (963 mg, 78%).

M.P. 93–94 °C (lit.[214] 91 °C); ^{1}H NMR (400 MHz, (CD$_3$)$_2$SO, δ): 8.62–8.56 (m, 2H), 8.06–8.00 (m, 2H), 1.35 (s, 9H); ^{13}C NMR (101 MHz, (CD$_3$)$_2$SO, δ): 165.5, 132.8, 128.5, 112.2, 36.5, 30.2; ^{11}B NMR (128 MHz, (CD$_3$)$_2$SO, δ): −2.3; ^{19}F NMR (376 MHz, (CD$_3$)$_2$SO, δ): −148.1 (m, $^1J_{F-^{10}B}$, 4F), −148.1 (m, $^1J_{F-^{11}B}$, 4F); ESI–MS *m/z* (ion, %): 161 ([M−BF$_4$]$^+$, 100); ESI–HRMS *m/z*: 161.1070 [M−BF$_4$]$^+$ (C$_{10}$H$_{13}$N$_2$ requires 161.1073).

The analytical data obtained was in accordance with the literature.[214]

Lab book reference number: AJR-8-716

1-Naphthalene-1-diazonium tetrafluoroborate (194)
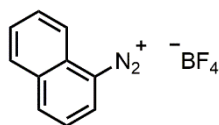
Synthesised using general procedure B from 1-naphthylamine **180** (0.48 g, 3.33 mmol, 1 eq.) in EtOH (1.7 mL) to afford the *title compound* as a brown solid (0.75 g, 93%).

M.P. 104–106 °C (lit.[215] 105–107 °C); ^{1}H NMR (400 MHz, (CD$_3$)$_2$SO, δ): 9.20 (dd, J = 8.0, 1.0 Hz, 1H), 8.94 (dt, J = 8.5, 1.0 Hz, 1H), 8.51 (dq, J = 8.5, 1.0 Hz, 1H), 8.43 (ddd, J = 8.0, 1.0, 0.5 Hz, 1H), 8.12 (ddd, J = 8.5, 7.0, 1.5 Hz, 1H), 8.06 (t, J = 8.0 Hz, 1H), 7.97 (ddd, J = 8.0, 7.0, 1.0 Hz, 1H); ^{13}C NMR (101 MHz, (CD$_3$)$_2$SO, δ): 142.6, 137.2, 132.6, 132.2, 130.3, 129.9, 127.1, 126.4, 122.4, 111.1; ^{11}B NMR (128 MHz, (CD$_3$)$_2$SO, δ): −2.3; ^{19}F NMR (376 MHz, (CD$_3$)$_2$SO, δ): −148.1 (m, $^1J_{F-^{10}B}$, 4F), −148.1 (m, $^1J_{F-^{11}B}$, 4F); ESI–MS *m/z* (ion, %): 155 ([M−BF$_4$]$^+$, 100); ESI–HRMS *m/z*: 155.0607 [M−BF$_4$]$^+$ (C$_{10}$H$_7$N$_2$ requires 155.0604).

The analytical data obtained was in accordance with the literature.[216]

Lab book reference number: LAH-1-39 (*reaction conducted by A. Hammarback*)

4-Phenylbenzene-1-diazonium tetrafluoroborate (195)
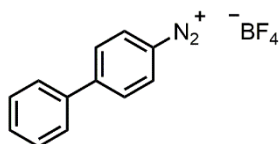
Synthesised using general procedure B from 4-phenylaniline **181** (846 mg, 5 mmol, 1 eq.) in EtOH (1.5 mL) to afford the *title compound* as a brown solid (870 mg, 65%).

M.P. 118–119 °C (lit.[217] 111–112 °C); ^{1}H NMR (400 MHz, (CD$_3$)$_2$SO, δ): 8.76–8.70 (m, 2H), 8.36–8.29 (m, 2H), 7.95–7.88 (m, 2H), 7.65–7.56 (m, 3H); ^{13}C NMR (101 MHz, (CD$_3$)$_2$SO, δ): 151.5, 136.4, 133.5, 130.8, 129.6, 129.0, 128.0, 113.3; ^{11}B NMR (128 MHz, (CD$_3$)$_2$SO, δ): −2.3; ^{19}F NMR (376 MHz, (CD$_3$)$_2$SO, δ): −148.1 (m, $^1J_{F-^{10}B}$, 4F), −148.1 (m, $^1J_{F-^{11}B}$, 4F); EI–MS *m/z* (ion, %): 154 ([M−BF$_4$−N$_2$]$^+$, 100); EI–HRMS *m/z*: 154.0782 [M−BF$_4$−N$_2$]$^+$ (C$_{12}$H$_{10}$ requires 154.0783).

The analytical data obtained was in accordance with the literature.[218]

Lab book reference number: AJR-8-717

2,4,6-Trimethylbenzene-1-diazonium tetrafluoroborate (196)
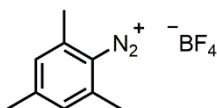
Method A: Synthesised using general procedure A from 2,4,6-trimethylphenylamine **182** (1.4 mL, 1.35 g, 10 mmol, 1 eq.) in deionised water (5.5 mL) to afford the *title compound* as a white solid (1.09 g, 47%).

Method B: Synthesised using general procedure B from 2,4,6-trimethylphenylamine **182** (1.4 mL, 1.35 g, 10 mmol, 1 eq.) in EtOH (3 mL) to afford the *title compound* as a white solid (2.34 g, quant.).

M.P. 84–85 °C; ^{1}H NMR (400 MHz, (CD$_3$)$_2$SO, δ): 7.40 (s, 2H), 2.57 (s, 6H), 2.39 (s, 3H); ^{13}C NMR (101 MHz, (CD$_3$)$_2$SO, δ): 153.4, 143.7, 130.7, 112.0, 22.1, 18.1; ^{11}B NMR (128 MHz, (CD$_3$)$_2$SO, δ): −2.3; ^{19}F NMR (376 MHz, (CD$_3$)$_2$SO, δ): −148.1 (m, $^1J_{F\_^{10}B}$, 4F), −148.2 (m, $^1J_{F\_^{11}B}$, 4F); ESI–MS *m/z* (ion, %): 147 ([M−BF$_4$]$^+$, 100); ESI–HRMS *m/z*: 147.0916 [M−BF$_4$]$^+$ (C$_9$H$_{11}$N$_2$ requires 147.0917).

The analytical data obtained was in accordance with the literature.[219]

Lab book reference number (Method A): AJR-5-376

Lab book reference number (Method B): LAH-1-38 (*reaction conducted by A. Hammarback*)

4-Methoxybenzene-1-diazonium tetrafluoroborate (197)
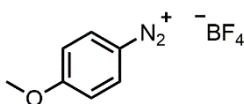
Method A: Synthesised using general procedure A from 4-methoxyaniline **183** (1.23 g, 10 mmol, 1 eq.) in deionised water (5.5mL) to afford the *title compound* as a white solid (182 mg, 8%).

Method B: Synthesised using general procedure B from 4-methoxyaniline **183** (1.23 g, 10 mmol, 1 eq.) in EtOH (3 mL) to afford the *title compound* as a white solid (2.16 g, 98%).

M.P. 145–147 °C (lit.[220] 143 °C); ^{1}H NMR (400 MHz, (CD$_3$)$_2$SO, δ): 8.64–8.58 (m, 2H), 7.51–7.45 (m, 2H), 4.04 (s, 3H); ^{13}C NMR (101 MHz, (CD$_3$)$_2$SO, δ): 168.8, 136.2, 117.3, 103.4, 57.5; ^{11}B NMR (128 MHz, (CD$_3$)$_2$SO, δ): −2.3; ^{19}F NMR (376 MHz, (CD$_3$)$_2$SO, δ):

−148.1 (m, $^1J_{F\_^{10}B}$, 4F), −148.1 (m, $^1J_{F\_^{11}B}$, 4F); ESI–MS *m/z* (ion, %): 135 ([M−BF$_4$]$^+$, 100); ESI–HRMS *m/z*: 135.0548 [M−BF$_4$]$^+$ (C$_7$H$_7$N$_2$O requires 135.0553).

The analytical data obtained was in accordance with the literature.[212]

Lab book reference number (Method A): AJR-5-406

Lab book reference number (Method B): LAH-1-34 (*reaction conducted by A. Hammarback*)

4-Phenoxybenzene-1-diazonium tetrafluoroborate (198)
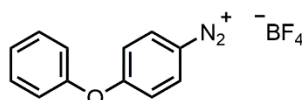
Synthesised using general procedure B from 4-phenoxyaniline **184** (1.85 g, 10 mmol, 1 eq.) in EtOH (3 mL) to afford the *title compound* as an off-white solid (2.71 g, 95%).

M.P. 167–170 °C (lit.[213] 177–178 °C); ^{1}H NMR (400 MHz, (CD$_3$)$_2$SO, δ): 8.67–8.60 (m, 2H), 7.61–7.54 (m, 2H), 7.45–7.37 (m, 3H), 7.33–7.27 (m, 2H); ^{13}C NMR (101 MHz, (CD$_3$)$_2$SO, δ): 167.1, 152.7, 136.6, 131.0, 126.9, 121.0, 118.7, 106.0; ^{11}B NMR (128 MHz, (CD$_3$)$_2$SO, δ): −2.3; ^{19}F NMR (376 MHz, (CD$_3$)$_2$SO, δ): −148.1 (m, $^1J_{F\_^{10}B}$, 4F), −148.1 (m, $^1J_{F\_^{11}B}$, 4F); ESI–MS *m/z* (ion, %): 197 ([M−BF$_4$]$^+$, 100); ESI–HRMS *m/z*: 197.0706 [M−BF$_4$]$^+$ (C$_{12}$H$_9$N$_2$O requires 197.0709).

The analytical data obtained was in accordance with the literature.[213]

Lab book reference number: AJR-8-722

4-Fluorobenzene-1-diazonium tetrafluoroborate (199)
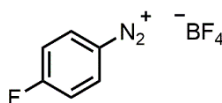
Method A: Synthesised using general procedure A from 4-aminofluorobenzene **185** (0.95 mL, 1.11 g, 10 mmol, 1 eq.) in deionised water (5.5 mL) to afford the *title compound* as a white solid (1.10 g, 52%).

Method B: Synthesised using general procedure B from 4-aminofluorobenzene **185** (0.95 mL, 1.11 g, 10 mmol, 1 eq.) to afford the *title compound* as a white solid (2.05 g, 98%).

M.P. 164–165 °C (lit.[212] 161–162 °C); ^{1}H NMR (400 MHz, (CD$_3$)$_2$SO, δ): 8.83–8.77 (m, 2H), 7.93–7.85 (m, 2H); ^{13}C NMR (101 MHz, (CD$_3$)$_2$SO, δ): 168.4 (d, *J* = 267.0 Hz), 137.0 (d, *J*

= 12.0 Hz), 119.4 (d, J = 25 .0 Hz), 111.9 (d, J = 3.0 Hz); ^{11}B NMR (128 MHz, (CD$_3$)$_2$SO, δ): −2.3; ^{19}F NMR (376 MHz, (CD$_3$)$_2$SO, δ): −87.1, −148.0 (m, $^1J_{F\_^{10}B}$, 4F), −148.1 (m, $^1J_{F\_^{11}B}$, 4F); ESI–MS *m/z* (ion, %): 123 ([M−BF$_4$]$^+$, 100); ESI–HRMS *m/z*: 123.0353 [M−BF$_4$]$^+$ (C$_6$H$_4$FN$_2$ requires 123.0353).

The analytical data obtained was in accordance with the literature.[212]

Lab book reference number (Method A): AJR-5-415

Lab book reference number (Method B): LAH-1-25 (*reaction conducted by A. Hammarback*)

4-Bromobenzene-1-diazonium tetrafluoroborate (200)
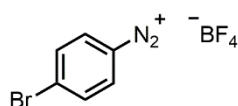
Method A: Synthesised using general procedure A from 4-aminobromobenzene **186** (1.72 g, 10 mmol, 1 eq.) in deionised water (5.5 mL) to afford the *title compound* as a white solid (887 mg, 33%).

Method B: Synthesised using general procedure B from 4-aminobromobenzene **186** (1.72 g, 10 mmol, 1 eq.) in EtOH (3 mL) to afford the *title compound* as a white solid (2.52 g, 93%).

M.P. 138–140 °C (lit.[213] 138 °C dec.); ^{1}H NMR (400 MHz, (CD$_3$)$_2$SO, δ): 8.60–8.55 (m, 2H), 8.29–8.24 (m, 2H); ^{13}C NMR (101 MHz, (CD$_3$)$_2$SO, δ): 136.6, 134.5, 134.0, 115.2; ^{11}B NMR (128 MHz, (CD$_3$)$_2$SO, δ): −2.3; ^{19}F NMR (376 MHz, (CD$_3$)$_2$SO, δ): −148.1 (m, $^1J_{F\_^{10}B}$, 4F), −148.2 (m, $^1J_{F\_^{11}B}$, 4F); ESI–MS *m/z* (ion, %): 183 ([M−BF$_4$]$^+$, 100); ESI–HRMS *m/z*: 182.9556 [M−BF$_4$]$^+$ (C$_6$H$_4$BrN$_2$ requires 182.9552).

The analytical data obtained was in accordance with the literature.[212]

Lab book reference number (Method A): AJR-5-373

Lab book reference number (Method B): LAH-1-23 (*reaction conducted by A. Hammarback*)

3-Bromobenzene-1-diazonium tetrafluoroborate (201)
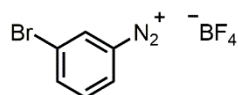
Method A: Synthesised using general procedure A from 3-aminobromobenzene **187** (1.09 mL, 1.72 g, 10 mmol, 1 eq.) in deionised water (5.5 mL) to afford the *title compound* as a white solid (1.18 g, 44%).

Method B: Synthesised using general procedure B from 3-aminobromobenzene **187** (1.09 mL, 1.72 g, 10 mmol, 1 eq.) in EtOH (3 mL) to afford the *title compound* as a white solid (2.71 g, quant.).

M.P. 140–142 °C (lit.[213] 145 °C); ^{1}H NMR (400 MHz, (CD$_3$)$_2$SO, δ): 8.96 (dd, J = 2.0, 2.0 Hz, 1H), 8.69 (ddd, J = 8.5, 2.0, 1.0 Hz, 1H), 8.49 (ddd, J = 8.5, 2.0, 1.0 Hz, 1H), 7.92 (dd, J = 8.5, 8.5 Hz, 1H); ^{13}C NMR (101 MHz, (CD$_3$)$_2$SO, δ): 143.8, 134.3, 132.8, 131.9, 122.3, 117.8; ^{11}B NMR (128 MHz, (CD$_3$)$_2$SO, δ): −2.3; ^{19}F NMR (376 MHz, (CD$_3$)$_2$SO, δ): −148.0 (m, $^1J_{F-^{10}B}$, 4F), −148.0 (m, $^1J_{F-^{11}B}$, 4F); ESI–MS m/z (ion, %): 183 ([M−BF$_4$]$^+$, 100); ESI–HRMS m/z: 182.9548 [M−BF$_4$]$^+$ (C$_6$H$_4$BrN$_2$ requires 182.9552).

The analytical data obtained was in accordance with the literature.[213]

Lab book reference number (Method A): AJR-5-390

Lab book reference number (Method B): LAH-1-31 (*reaction conducted by A. Hammarback*)

4-Chlorobenzene-1-diazonium tetrafluoroborate (202)
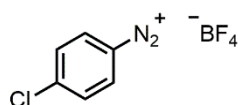
Method A: Synthesised using general procedure A from 4-aminochlorobenzene **188** (1.28 g, 10 mmol, 1 eq.) in deionised water (5.5 mL) to afford the *title compound* as a white solid (556 mg, 25%).

Method B: Synthesised using general procedure B from 4-aminochlorobenzene **188** (1.28 g, 10 mmol, 1 eq.) in EtOH (3 mL) to afford the *title compound* as a white solid (2.15 g, 95%).

M.P. 138–139 °C (lit.[212] 134 °C dec.); ^{1}H NMR (400 MHz, (CD$_3$)$_2$SO, δ): 8.73–8.64 (m, 2H), 8.15–8.07 (m, 2H); ^{13}C NMR (101 MHz, (CD$_3$)$_2$SO, δ): 146.5, 134.4, 131.6, 114.8; ^{11}B NMR (128 MHz, (CD$_3$)$_2$SO, δ): −2.3; ^{19}F NMR (376 MHz, (CD$_3$)$_2$SO, δ): −148.0 (m, $^1J_{F-^{10}B}$, 4F),

−148.0 (m, $^1J_{\text{F−11B}}$, 4F); ESI–MS *m/z* (ion, %): 139 ([M−BF$_4$]$^+$, 100); ESI–HRMS *m/z*: 139.0054 [M−BF$_4$]$^+$ (C$_6$H$_4$ClN$_2$ requires 139.0058).

The analytical data obtained was in accordance with the literature.[212]

Lab book reference number (Method A): AJR-5-375

Lab book reference number (Method B): LAH-1-24 (*reaction conducted by A. Hammarback*)

3-Chlorobenzene-1-diazonium tetrafluoroborate (203)
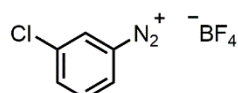
Method A: Synthesised using general procedure A from 3-aminochlorobenzene **189** (1.10 mL, 1.28 g, 10 mmol, 1 eq.) in deionised water (5.5 mL) to afford the *title compound* as a white solid (1.06 g, 47%).

Method B: Synthesised using general procedure B from 3-aminochlorobenzene **189** (1.10 mL, 1.28 g, 10 mmol, 1 eq.) in EtOH (3 mL) to afford the *title compound* as a white solid (2.26 g, quant.).

M.P. 147–148 °C (lit.[219] 148 °C dec.); ^{1}H NMR (400 MHz, (CD$_3$)$_2$SO, δ): 8.85 (dd, *J* = 2.0, 2.0 Hz, 1H), 8.67 (ddd, *J* = 8.5, 2.0, 1.0 Hz, 1H), 8.37 (ddd, *J* = 8.5, 2.0, 1.0 Hz, 1H), 8.01 (dd, *J* = 8.5, 8.5 Hz, 1H); ^{13}C NMR (101 MHz, (CD$_3$)$_2$SO, δ): 141.1, 134.6, 132.9, 131.7, 131.6, 117.8; ^{11}B NMR (128 MHz, (CD$_3$)$_2$SO, δ): −2.2; ^{19}F NMR (376 MHz, (CD$_3$)$_2$SO, δ): −148.0 (m, $^1J_{\text{F−10B}}$, 4F), −148.0 (m, $^1J_{\text{F−11B}}$, 4F); ESI–MS *m/z* (ion, %): 139 ([M−BF$_4$]$^+$, 100); ESI–HRMS *m/z*: 139.0055 [M−BF$_4$]$^+$ (C$_6$H$_4$ClN$_2$ requires 139.0058).

The analytical data obtained was in accordance with the literature.[216]

Lab book reference number (Method A): AJR-5-382

Lab book reference number (Method B): LAH-1-32 (*reaction conducted by A. Hammarback*)

4-(Trifluoromethyl)benzene-1-diazonium tetrafluoroborate (54)
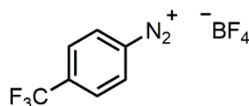
Method A: Synthesised using general procedure A from 4-aminobenzotrifluoride **190** (0.63 mL, 805 mg, 5 mmol, 1 eq.) in deionised water (2.75 mL) to afford the *title compound* as a white solid (416 mg, 32%).

Method B: Synthesised using general procedure A from 4-aminobenzotrifluoride **190** (1.26 mL, 1.61 mg, 10 mmol, 1 eq.) in EtOH (3 mL) to afford the *title compound* as a white solid (2.38 g, 92%).

M.P. 118–119 °C (lit.[221] 105–106 °C); ^{1}H NMR (400 MHz, (CD$_3$)$_2$SO, δ): 8.91 (d, J = 8.5 Hz, 2H), 8.42 (d, J = 8.5 Hz, 2H); ^{13}C NMR (101 MHz, (CD$_3$)$_2$SO, δ): 113.8, 128.3, 122.3 (q, J = 274.0 Hz), 121.3, 110.5; ^{11}B NMR (128 MHz, (CD$_3$)$_2$SO, δ): −2.3; ^{19}F NMR (376 MHz, (CD$_3$)$_2$SO, δ): −62.5, −148.0 (m, $^1J_{F\_^{10}B}$, 4F), −148.1 (m, $^1J_{F\_^{11}B}$, 4F); ESI–MS m/z (ion, %): 173 ([M−BF$_4$]$^+$, 100); ESI–HRMS m/z: 173.0325 [M−BF$_4$]$^+$ (C$_7$H$_4$F$_3$N$_2$ requires 173.0321).

The analytical data obtained was in accordance with the literature.[221]

Lab book reference number (Method A): AJR-4-368

Lab book reference number (Method B): LAH-1-44 (*reaction conducted by A. Hammarback*)

4-Nitrobenzene-1-diazonium tetrafluoroborate (204)
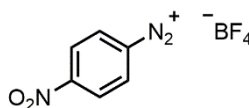
Synthesised using general procedure A from 4-nitroaniline **191** (1.38 g, 10 mmol, 1 eq.) in EtOH (3 mL) to afford the *title compound* as a white solid (2.24 g, 95%).

M.P. 148–151 °C (lit.[212] 155 °C dec.); ^{1}H NMR (400 MHz, (CD$_3$)$_2$SO, δ): 8.95–8.90 (m, 2H), 8.75–8.69 (m, 2H); ^{13}C NMR (101 MHz, (CD$_3$)$_2$SO, δ): 153.3, 134.6, 126.1, 121.9; ^{11}B NMR (128 MHz, (CD$_3$)$_2$SO, δ): −2.3; ^{19}F NMR (376 MHz, (CD$_3$)$_2$SO, δ): −148.1 (m, $^1J_{F\_^{10}B}$, 4F), −148.1 (m, $^1J_{F\_^{11}B}$, 4F); ESI–MS m/z (ion, %): 150 ([M−BF$_4$]$^+$, 100); ESI–HRMS m/z: 150.0304 [M−BF$_4$]$^+$ (C$_6$H$_4$N$_3$O$_2$ requires 150.0298).

The analytical data obtained was in accordance with the literature.[212]

Lab book reference number: LAH-1-41 (*reaction conducted by A. Hammarback*)

Methyl (2*S*)-3-[2-(4-methylphenyl)-1*H*-indol-3-yl]-2-acetamidopropanoate (76)
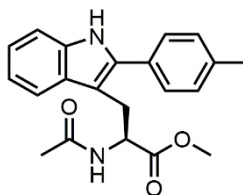
Method A: Synthesised using general procedure C with aryldiazonium salt **192** (40 mg, 0.192 mmol, 1 eq.) to afford the *title compound* as a brown solid (67 mg, quant.).

Method B: Synthesised as in method A using Pd(OTs)$_2$(MeCN)$_2$ **215** (5.1 mg, 9.6 µmol, 5 mol%) in place of Pd(OAc)$_2$ to afford the *title compound* as a brown solid (67 mg, quant.).

R_f 0.32 (petrol/EtOAc, 1:1, *v/v*); [α]$_D$ = +51.9 (*c* 0.10, CHCl$_3$); M.P. 97–99 °C; ^{1}H NMR (400 MHz, CDCl$_3$, δ): 8.14 (br s, 1H), 7.56 (d, *J* = 8.0 Hz, 1H), 7.49–7.43 (m, 2H), 7.38–7.33 (m, 1H), 7.31–7.27 (m, 2H), 7.20 (ddd, *J* = 8.0, 7.0, 1.0 Hz, 1H), 7.13 (ddd, *J* = 8.0, 7.0, 1.0 Hz, 1H), 5.77 (d, *J* = 8.0 Hz, 1H), 4.82 (dt, *J* = 8.0, 5.5 Hz, 1H), 3.54 (dd, *J* = 15.0, 5.5 Hz, 1H), 3.52 (dd, *J* = 15.0, 5.5 Hz, 1H), 3.33 (s, 3H), 2.41 (s, 3H), 1.66 (s, 3H); ^{13}C NMR (101 MHz, (CDCl$_3$, δ): 172.4, 169.7, 138.2, 136.2, 135.7, 130.3, 130.0, 129.6, 128.3, 122.5, 120.1, 118.9, 111.0, 106.6, 52.9, 52.2, 26.8, 23.0, 21.4; ESI–MS *m/z* (ion, %): 351 ([M+H]$^+$, 10), 373 ([M+Na]$^+$, 100); ESI–HRMS *m/z*: 373.1524 [M+Na]$^+$ (C$_{21}$H$_{22}$N$_2$NaO$_3$ requires 373.1523).

The analytical data obtained was in accordance with the literature.[114]

Lab book reference number (method A): AJR-8-715

*Lab book reference number (method B)*: THS-1-64 (*reaction conducted by T. Sheridan*)

Methyl (2*S*)-3-[2-(4-*tert*-butylphenyl)-1*H*-indol-3-yl]-2-acetamidopropanoate (205)
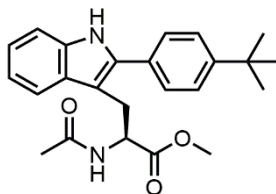
Method A: Synthesised using general procedure C with aryldiazonium salt **193** (48 mg, 0.192 mmol, 1 eq.) to afford the *title compound* as a brown solid (75 mg, quant.).

Method B: Synthesised as in method A using Pd(OTs)$_2$(MeCN)$_2$ **215** (5.1 mg, 9.6 µmol, 5 mol%) in place of Pd(OAc)$_2$ to afford the *title compound* as a brown solid (75 mg, quant.).

R_f 0.30 (petrol/EtOAc, 1:1.5, *v/v*); $[\alpha]_D$ = +68.6 (*c* 0.10, CHCl$_3$); M.P. 153–155 °C; ^{1}H NMR (400 MHz, CDCl$_3$, δ): 8.14 (br s, 1H), 7.56 (d, *J* = 8.0 Hz, 1H), 7.50 (s, 4H), 7.36 (d, *J* = 8.0 Hz, 1H), 7.19 (ddd, *J* = 8.0, 7.0, 1.0 Hz, 1H), 7.13 (ddd, *J* = 8.0, 7.0, 1.0 Hz, 1H), 5.77 (d, *J* = 8.0 Hz, 1H), 4.84 (dt, *J* = 8.0, 5.5 Hz, 1H), 3.56 (app d, *J* = 5.5 Hz, 2H), 3.28 (s, 3H), 1.64 (s, 3H), 1.36 (s, 9H); ^{13}C NMR (101 MHz, (CDCl$_3$, δ): 172.3, 169.7, 151.3, 136.1, 135.7, 130.4, 129.6, 128.1, 126.2, 122.5, 120.1, 118.9, 111.0, 106.5, 52.9, 52.1, 34.9, 31.4, 26.6, 23.0; ESI–MS *m/z* (ion, %): 393 ([M+H]$^+$, 10), 415 ([M+Na]$^+$, 100); ESI–HRMS *m/z*: 393.2169 [M+Na]$^+$ (C$_{24}$H$_{29}$N$_2$O$_3$ requires 393.2173); IR (solid-state ATR, cm^{-1}): 3282 (w, br), 2960 (m), 1738 (m), 1660 (m), 1518 (m), 1436 (m), 1372 (m), 1260 (m), 1214 (m), 1013 (m), 837 (m), 799 (m), 741 (s), 588 (m).

Lab book reference number (method A): AJR-8-718

Lab book reference number (method B): THS-1-65 (*reaction conducted by T. Sheridan*)

Methyl (2*S*)-2-acetamido-3-[2-(1-naphthylphenyl)-1*H*-indol-3-yl]propanoate (206)
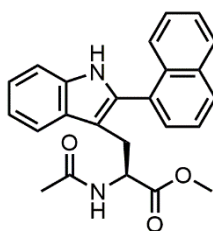
Method A: Synthesised using general procedure C with aryldiazonium salt **194** (50 mg, 0.192 mmol, 1 eq.) to afford the *title compound* as a brown solid (74 mg, quant.).

Method B: Synthesised as in method A using Pd(OTs)$_2$(MeCN)$_2$ **215** (5.1 mg, 9.6 µmol, 5 mol%) in place of Pd(OAc)$_2$ to afford the *title compound* as a brown solid (74 mg, quant.).

R_f 0.15 (petrol/EtOAc, 1:1, *v/v*); M.P. 78–79 °C dec.; ^{1}H NMR (400 MHz, CDCl$_3$, δ): 8.45 (br s, 1H), 7.94 (d, *J* = 8.0 Hz, 2H), 7.80 (d, *J* = 8.0 Hz, 1H), 7.64 (d, *J* = 8.0 Hz, 1H), 7.58–7.45 (m, 4H), 7.37 (d, *J* = 8.0 Hz, 1H), 7.24 (ddd, *J* = 7.5, 1.0 Hz, 1H), 7.19 (ddd, *J* = 7.5, 1.0 Hz, 1H), 5.58 (d, *J* = 8.0 Hz, 1H), 4.68 (dt, *J* = 8.0, 5.0 Hz, 1H), 3.50–2.98 (m, 5H), 1.26 (br s, 3H); ^{13}C NMR (101 MHz, (CDCl$_3$, δ): 172.2, 169.6, 136.0, 134.8, 134.0, 132.4, 130.3, 129.2, 128.8, 128.7, 128.7, 127.2, 126.5, 125.7, 125.6, 122.6, 120.1, 119.0, 111.1, 108.8, 52.9, 52.0, 26.8, 22.6; ESI–MS *m/z* (ion, %): 387 ([M+H]$^+$, 20), 409 ([M+Na]$^+$, 100); ESI–HRMS *m/z*: 387.1695 [M+H]$^+$ (C$_{24}$H$_{23}$N$_2$O$_3$ requires 387.1703); IR (solid-state, ATR, cm^{-1}): 3254 (w, br), 1734 (m), 1653 (s), 1506 (m), 1435 (m), 1371 (s), 1214 (s), 1011 (s), 908 (m), 804 (m), 779 (m), 727 (m), 494 (w).

Lab book reference number (method A): LAH-2-110 (*reaction conducted by A. Hammarback*)

Lab book reference number (method B): AJR-7-679

Methyl (2*S*)-2-acetamido-3-[2-(4-phenylphenyl)-1*H*-indol-3-yl]propanoate (207)
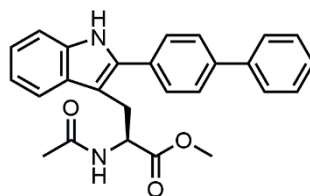
Method A: Synthesised using general procedure C with aryldiazonium salt **195** (52 mg, 0.192 mmol, 1 eq.) to afford the *title compound* as a brown solid (79 mg, quant.).

Method B: Synthesised as in method A using Pd(OTs)$_2$(MeCN)$_2$ **215** (5.1 mg, 9.6 μmol, 5 mol%) in place of Pd(OAc)$_2$ to afford the *title compound* as a brown solid (79 mg, quant.).

R_f 0.27 (petrol/EtOAc, 1:1.5, *v/v*); [α]$_D$ = +94.8 (*c* 0.10, CHCl$_3$); M.P. 205–206 °C; ^{1}H NMR (400 MHz, CDCl$_3$, δ): 8.32 (br s, 1H), 7.74–7.67 (m, 2H), 7.66–7.61 (m, 4H), 7.60–7.56 (m, 1H), 7.52–7.44 (m, 2H), 7.43–7.35 (m, 2H), 7.21 (ddd, *J* = 8.0, 7.0, 1.0 Hz, 1H), 7.15 (ddd, *J* = 8.0, 7.0, 1.0 Hz, 1H), 5.84 (d, *J* = 8.0 Hz, 1H), 4.87 (dt, *J* = 8.0, 5.5 Hz, 1H), 3.62 (dd, *J* = 15.0, 5.5 Hz, 1H), 3.59 (dd, *J* = 15.0, 5.5 Hz, 1H), 3.32 (s, 3H), 1.66 (s, 3H); ^{13}C NMR (101 MHz, (CDCl$_3$, δ): 172.3, 169.7, 140.9, 140.3, 135.9, 135.7, 132.2, 129.7, 129.1, 128.7, 127.9, 127.1, 122.8, 120.2, 119.0, 111.1, 107.2, 100.1, 53.0, 52.2, 26.8, 23.0; ESI–MS *m/z* (ion, %): 413 ([M+H]$^+$, 10), 435 ([M+Na]$^+$, 100); ESI–HRMS *m/z*: 413.1871 [M+H]$^+$ (C$_{26}$H$_{25}$N$_2$O$_3$ requires 413.1860); IR (solid-state, ATR, cm^{-1}): 3406 (w), 3378 (w), 1746 (m), 1655 (s), 1460 (m), 1449 (m), 1374 (m), 1314 (m), 1184 (m), 1008 (w), 982 (w), 842 (w), 767 (m), 743 (s), 734 (m), 697 (m), 535 (s), 512 (m).

Lab book reference number (method A): AJR-8-719

Lab book reference number (method B): THS-1-66 (*reaction conducted by T. Sheridan*)

Methyl (2*S*)-2-acetamido-3-[2-(4-methoxyphenyl)-1*H*-indol-3-yl]propanoate (77)
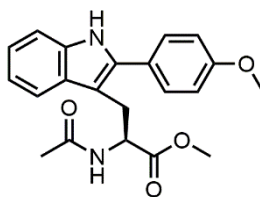
Method A: Synthesised using general procedure C (with a reaction time of 24 h) with aryldiazonium salt **197** (43 mg, 0.192 mmol, 1 eq.) to afford the *title compound* as a brown solid (70 mg, quant.).

Method B: Synthesised as in method A using Pd(OTs)$_2$(MeCN)$_2$ **215** (5.1 mg, 9.6 μmol, 5 mol%) in place of Pd(OAc)$_2$ to afford the *title compound* as a brown solid (70 mg, quant.).

Method C: Reaction conducted as in method B using Pd(OTs)$_2$(MeCN)$_2$ **215** (2.5 mg, 4.8 μmol, 2.5 mol%) to afford a crude brown solid. ^{1}H NMR spectroscopic analysis indicated 49% conversion to the *title compound*, which was not purified.

Method D: Reaction conducted as in method B using Pd(OTs)$_2$(MeCN)$_2$ **215** (1 mg, 1.92 μmol, 1 mol%) to afford a crude brown solid. ^{1}H NMR spectroscopic analysis indicated 40% conversion to the *title compound*, which was not purified.

R$_f$ 0.15 (petrol/EtOAc, 1:1, *v/v*); [α]$_D$ = +34.9 (*c* 0.10, CHCl$_3$); M.P. 202–205 °C; ^{1}H NMR (400 MHz, CDCl$_3$, δ): 8.56 (br s, 1H), 7.54 (d, *J* = 8.0 Hz, 1H), 7.49–7.44 (m, 2H), 7.33 (d, *J* = 8.0 Hz, 1H), 7.17 (ddd, *J* = 8.0, 7.0, 1.5 Hz, 1H), 7.12 (ddd, *J* = 8.0, 7.0, 1.5 Hz, 1H), 6.95–6.90 (m, 2H), 5.85 (d, *J* = 8.0 Hz, 1H), 4.81 (dt, *J* = 8.0, 5.5 Hz, 1H), 3.81 (s, 3H), 3.52 (dd, *J* = 15.0, 5.5 Hz, 1H), 3.48 (dd, *J* = 15.0, 5.5 Hz, 1H), 3.34 (s, 3H), 1.66 (s, 3H); ^{13}C NMR (101 MHz, (CDCl$_3$, δ): 172.4, 169.8, 159.5, 136.1, 135.7, 129.6, 129.5, 125.6, 122.2, 119.9, 118.6, 114.6, 111.1, 105.9, 55.5, 53.0, 52.2, 26.7, 23.0; ESI–MS *m/z* (ion, %): 367 ([M+H]$^+$, 50), 389 ([M+Na]$^+$, 100); ESI–HRMS *m/z*: 389.1458 [M+Na]$^+$ (C$_{21}$H$_{22}$N$_2$NaO$_4$ requires 389.1472).

The analytical data obtained was in accordance with the literature.[114]

Lab book reference number (method A): AJR-5-410

Lab book reference number (method B): AJR-7-653

Lab book reference number (method C): AJR-7-638

Lab book reference number (method D): AJR-7-627

Methyl (2*S*)-2-acetamido-3-[2-(4-phenoxyphenyl)-1*H*-indol-3-yl]propanoate (208)
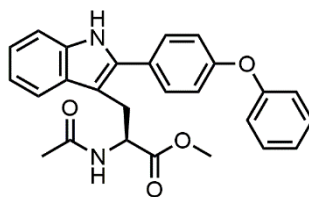
Method A: Synthesised using general procedure C with aryldiazonium salt **198** (55 mg, 0.192 mmol, 1 eq.) to afford the *title compound* as a brown solid (82 mg, quant.).

Method B: Synthesised as in method A using Pd(OTs)$_2$(MeCN)$_2$ **215** (5.1 mg, 9.6 µmol, 5 mol%) in place of Pd(OAc)$_2$ to afford the *title compound* as a brown solid (82 mg, quant.).

R_f 0.29 (petrol/EtOAc, 1:1.5, *v/v*); [α]$_D$ = +85.3 (*c* 0.10, CHCl$_3$); M.P. 72–74 °C; ^{1}H NMR (400 MHz, CDCl$_3$, δ): 8.32 (br s, 1H), 7.56 (d, *J* = 8.0 Hz, 1H), 7.52–7.47 (m, 2H), 7.42–7.36 (m, 2H), 7.35–7.32 (m, 1H), 7.22–7.16 (m, 2H), 7.15–7.11 (m, 1H), 7.10–7.04 (m, 4H), 5.85 (d, *J* = 8.0 Hz, 1H), 4.84 (dt, *J* = 8.0, 5.5 Hz, 1H), 3.52 (dd, *J* = 15.0, 5.5 Hz, 1H), 3.49 (dd, *J* = 15.0, 5.5 Hz, 1H), 3.38 (s, 3H), 1.72 (s, 3H); ^{13}C NMR (101 MHz, (CDCl$_3$, δ): 172.4, 169.7, 157.6, 156.5, 135.8, 135.7, 130.1, 129.8, 129.5, 127.9, 124.1, 122.6, 120.1, 119.6, 119.0, 118.9, 111.1, 106.6, 53.0, 52.2, 26.8, 23.1; ESI–MS *m/z* (ion, %): 429 ([M+H]$^+$, 20), 451 ([M+Na]$^+$, 100); ESI–HRMS *m/z*: 451.1622 [M+Na]$^+$ (C$_{26}$H$_{24}$N$_2$NaO$_4$ requires 451.1628); IR (solid-state, ATR, cm^{-1}): 3266 (w, br), 2961 (w), 1736 (m), 1654 (m), 1588 (w), 1487 (s), 1458 (m), 1436 (m), 1372 (w), 1229 (s), 1012 (m), 869 (m), 840 (m), 795 (m), 743 (s), 692 (m), 486 (w).

Lab book reference number: AJR-8-723

Lab book reference number (method B): THS-1-67 (*reaction conducted by T. Sheridan*)

Methyl (2*S*)-3-[2-(4-fluorophenyl)-1*H*-indol-3-yl]-2-acetamidopropanoate (120)
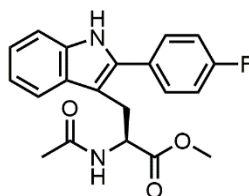
Method A: Synthesised using general procedure C with aryldiazonium salt **199** (40 mg, 0.192 mmol, 1 eq.) to afford the *title compound* as a brown solid (68 mg, quant.).

Method B: Synthesised as in method A using Pd(OTs)$_2$(MeCN)$_2$ **215** (5.1 mg, 9.6 µmol, 5 mol%) in place of Pd(OAc)$_2$ to afford the *title compound* as a brown solid (68 mg, quant.).

R_f 0.23 (petrol/EtOAc, 1:1, *v/v*); $[\alpha]_D$ = +54.4 (*c* 0.10, CHCl₃); M.P. 213–216 °C dec.; ¹H NMR (400 MHz, CDCl₃, δ): 8.18 (br s, 1H), 7.56 (ddt, *J* = 8.0, 1.5, 1.0 Hz, 1H), 7.54–7.48 (m, 2H), 7.34 (dt, *J* = 8.0, 1.0 Hz, 1H), 7.20 (ddd, *J* = 8.0, 7.0, 1.0 Hz, 1H), 7.17–7.12 (m, 3H), 5.84 (d, *J* = 8.0 Hz, 1H), 4.83 (dt, *J* = 8.0, 5.5 Hz, 1H), 3.51 (dd, *J* = 15.0, 5.5 Hz, 1H), 3.46 (dd, *J* = 15.0, 5.5 Hz, 1H), 3.33 (s, 3H), 1.70 (s, 3H); ¹³C NMR (101 MHz, (CDCl₃, δ): 172.3, 169.7, 162.9 (q, $^1J_{C-F}$ = 249.0 Hz), 135.8, 135.1, 130.3 (d, $^3J_{C-F}$ = 8.0 Hz), 129.5, 129.4 (d, $^4J_{C-F}$ = 3.5 Hz), 122.8, 120.3, 119.0, 116.3 (d, $^2J_{C-F}$ = 21.5 Hz), 111.1, 107.0, 52.9, 52.2, 26.8, 23.1; ¹⁹F NMR (376 MHz, CDCl₃, δ): −112.8–−112.9 (m); ESI–MS *m/z* (ion, %): 355 ([M+H]⁺, 60), 377 ([M+Na]⁺, 100); ESI–HRMS *m/z*: 355.1442 [M+H]⁺ (C₂₀H₂₀FN₂O₃ requires 355.1452).

The analytical data obtained was in accordance with the literature.[211]

Lab book reference number (method A): AJR-5-417

Lab book reference number (method B): AJR-7-655

Methyl (2*S*)-3-[2-(4-bromophenyl)-1*H*-indol-3-yl]-2-acetamidopropanoate (79)
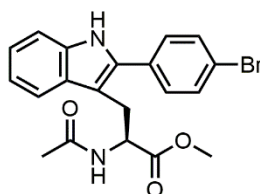
Method A: Synthesised using general procedure C with aryldiazonium salt **200** (52 mg, 0.192 mmol, 1 eq.) to afford the *title compound* as a brown solid (80 mg, quant.).

Method B: Synthesised as in method A using Pd(OTs)₂(MeCN)₂ **215** (5.1 mg, 9.6 µmol, 5 mol%) in place of Pd(OAc)₂ to afford the *title compound* as a brown solid (80 mg, quant.).

R_f 0.31 (petrol/EtOAc, 1:1, *v/v*); $[\alpha]_D$ = +44.0 (*c* 0.10, CHCl₃); M.P. 74–75 °C dec.; ¹H NMR (400 MHz, CDCl₃, δ): 8.36 (br s, 1H), 7.60–7.54 (m, 3H), 7.44–7.39 (m, 2H), 7.34 (dt, *J* = 8.0, 1.0 Hz, 1H), 7.21 (ddd, *J* = 8.0, 7.0, 1.0 Hz, 1H), 7.14 (ddd, *J* = 8.0, 7.0, 1.0 Hz, 1H), 5.85 (d, *J* = 8.0 Hz, 1H), 4.83 (dt, *J* = 8.0, 5.5 Hz, 1H), 3.52 (dd, *J* = 15.0, 5.5 Hz, 1H), 3.47 (dd, *J* = 15.0, 5.5 Hz, 1H), 3.33 (s, 3H), 1.70 (s, 3H); ¹³C NMR (101 MHz, (CDCl₃, δ): 172.3, 169.8, 135.9, 134.8, 132.4, 132.2, 129.9, 129.5, 123.0, 122.2, 120.3, 119.1, 111.2, 107.4, 53.0, 52.2, 26.9, 23.1; ESI–MS *m/z* (ion, %): 415 ([M+H]⁺, 30), 437 ([M+Na]⁺, 100); ESI–HRMS *m/z*: 437.0474 [M+Na]⁺ (C₂₀H₁₉BrN₂NaO₃ requires 437.0471).

The analytical data obtained was in accordance with the literature.[114]

Lab book reference number (method A): AJR-5-401

Lab book reference number (method B): AJR-7-656

Methyl (2*S*)-3-[2-(3-bromophenyl)-1*H*-indol-3-yl]-2-acetamidopropanoate (209)
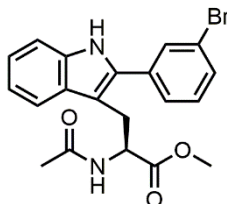
Method A: Synthesised using general procedure C with aryldiazonium salt **201** (43 mg, 0.192 mmol, 1 eq.) to afford the *title compound* as a brown solid (80 mg, quant.).

Method B: Synthesised as in method A using Pd(OTs)$_2$(MeCN)$_2$ **215** (5.1 mg, 9.6 μmol, 5 mol%) in place of Pd(OAc)$_2$. Purification by dry-loaded flash column chromatography (SiO$_2$, petrol/EtOAc, 1:1, *v/v*) afforded the *title compound* as a brown solid (55 mg, 69%).

R_f 0.28 (petrol/EtOAc, 1:1, *v/v*); [α]$_D$ = +50.5 (*c* 0.10, CHCl$_3$); M.P. 82–84 °C dec.; ^{1}H NMR (400 MHz, CDCl$_3$, δ): 8.27 (br s, 1H), 7.71 (t, *J* = 1.5 Hz, 1H), 7.58 (ddt, *J* = 8.0, 1.5, 1.0 Hz, 1H), 7.53–7.48 (m, 2H), 7.38–7.32 (m, 2H), 7.22 (ddd, *J* = 8.0, 7.0, 1.0 Hz, 1H), 7.15 (ddd, *J* = 8.0, 7.0, 1.0 Hz, 1H), 5.84 (d, *J* = 8.0 Hz, 1H), 4.85 (dt, *J* = 8.0, 5.5 Hz, 1H), 3.53 (dd, *J* = 15.0, 5.5 Hz, 1H), 3.48 (dd, *J* = 15.0, 5.5 Hz, 1H), 3.34 (s, 3H), 1.72 (s, 3H); ^{13}C NMR (101 MHz, CDCl$_3$, δ): 172.3, 169.7, 135.9, 135.3, 134.4, 131.2, 131.1, 130.8, 129.4, 127.1, 123.2, 123.1, 120.4, 119.2, 111.2, 107.9, 52.9, 52.2, 26.8, 23.1; ESI–MS *m/z* (ion, %): 415 ([M+H]$^+$, 50), 437 ([M+Na]$^+$, 100); ESI–HRMS *m/z*: 415.0658 [M+H]$^+$ (C$_{20}$H$_{20}$BrN$_2$O$_3$ requires 415.0652); IR (solid-state, ATR, cm^{-1}): 3264 (w, br), 3057 (w), 2951 (w), 2924 (w), 2850 (w), 1732 (m), 1651 (s), 1596 (m), 1518 (m), 1435 (s), 1372 (m), 1261 (m), 1214 (s), 1010 (m), 787 (m), 741 (s), 687 (s), 594 (m), 507 (m), 437 (m); UV–vis (DMSO, nm): λ$_{max}$ 312 (ε = 19398 mol dm^{-3} cm^{-1}).

Lab book reference number (method A): AJR-5-407

Lab book reference number (method B): AJR-7-666

Methyl (2*S*)-3-[2-(4-chlorophenyl)-1*H*-indol-3-yl]-2-acetamidopropanoate (210)
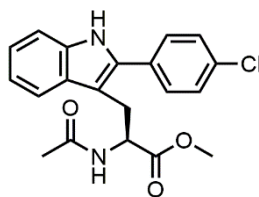
Method A: Synthesised using general procedure C with aryldiazonium salt **202** (43 mg, 0.192 mmol, 1 eq.). Purification by dry-loaded flash column chromatography (SiO$_2$, petrol/EtOAc, 1:1, *v/v*) afforded the *title compound* as a brown solid (52 mg, 73%).

Method B: Synthesised as in method A using Pd(OTs)$_2$(MeCN)$_2$ **215** (5.1 mg, 9.6 µmol, 5 mol%) in place of Pd(OAc)$_2$. Purification by dry-loaded flash column chromatography (SiO$_2$, petrol/EtOAc, 1:1, *v/v*) afforded the *title compound* as a brown solid (57 mg, 80%).

R_f 0.39 (petrol/EtOAc, 1:1, *v/v*); [α]$_D$ = +45.6 (*c* 0.10, CHCl$_3$); M.P. 202 °C dec.; ^{1}H NMR (400 MHz, CDCl$_3$, δ): 8.19 (br s, 1H), 7.57 (dt, *J* = 8.0, 1.0, 1.0 Hz, 1H), 7.53–7.48 (m, 2H), 7.47–7.43 (m, 2H), 7.38–7.33 (m, 1H), 7.22 (ddd, *J* = 8.0, 7.0, 1.0 Hz, 1H), 7.15 (ddd, *J* = 8.0, 7.0, 1.0 Hz, 1H), 5.82 (d, *J* = 8.0 Hz, 1H), 4.84 (dt, *J* = 8.0, 5.5 Hz, 1H), 3.51 (dd, *J* = 15.0, 5.5 Hz, 1H), 3.46 (dd, *J* = 15.0, 5.5 Hz, 1H), 3.33 (s, 3H), 1.71 (s, 3H); ^{13}C NMR (101 MHz, (CDCl$_3$, δ): 172.3, 169.7, 135.9, 134.8, 134.2, 131.7, 129.6, 129.5, 129.5, 123.0, 120.4, 119.1, 111.2, 107.5, 53.0, 52.2, 26.9, 23.1; ESI–MS *m/z* (ion, %): 371 ([M+H]$^+$, 30), 393 ([M+Na]$^+$, 100); ESI–HRMS *m/z*: 371.1166 [M+H]$^+$ (C$_{20}$H$_{20}$ClN$_2$O$_3$ requires 371.1157).

Crystals suitable for X-ray diffraction were grown by slow diffusion from a solution of CH$_2$Cl$_2$.

The analytical data obtained was in accordance with the literature.[211]

Lab book reference number (method A): AJR-5-405

Lab book reference number (method B): AJR-7-667

Methyl (2*S*)-3-[2-(3-chlorophenyl)-1*H*-indol-3-yl]-2-acetamidopropanoate (211)
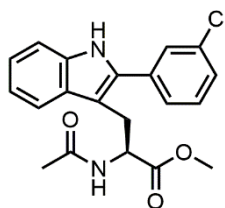
Method A: Synthesised using general procedure C with aryldiazonium salt **203** (43 mg, 0.192 mmol, 1 eq.). Purification by dry-loaded flash column chromatography (SiO$_2$, petrol/EtOAc, 1:1, *v/v*) afforded the *title compound* as a brown solid (45 mg, 63%).

Method B: Synthesised as in method A using Pd(OTs)$_2$(MeCN)$_2$ **215** (5.1 mg, 9.6 µmol, 5 mol%) in place of Pd(OAc)$_2$. Purification by dry-loaded flash column chromatography (SiO$_2$, petrol/EtOAc, 1:1, *v/v*) afforded the *title compound* as a brown solid (57 mg, 80%).

R_f 0.26 (petrol/EtOAc, 1:1, *v/v*); $[\alpha]_\text{D}$ = +54.4 (*c* 0.10, CHCl$_3$); M.P. 78–79 °C dec.; ^{1}H NMR (400 MHz, CDCl$_3$, δ): 8.19 (br s, 1H), 7.61–7.54 (m, 2H), 7.47 (dt, *J* = 7.5, 1.5 Hz, 1H), 7.45–7.39 (m, 1H), 7.36 (ddd, *J* = 7.5, 2.5, 1.5 Hz, 2H), 7.22 (ddd, *J* = 8.0, 7.0, 1.0 Hz, 1H), 7.15 (ddd, *J* = 8.0, 7.0, 1.0 Hz, 1H), 5.83 (d, *J* = 8.0 Hz, 1H), 4.85 (dt, *J* = 8.0, 5.5 Hz, 1H), 3.54 (dd, *J* = 15.0, 5.5 Hz, 1H), 3.51 (dd, *J* = 15.0, 5.5 Hz, 1H), 3.34 (s, 3H), 1.72 (s, 3H); ^{13}C NMR (101 MHz, (CDCl$_3$, δ): 172.3, 169.7, 135.9, 135.2, 135.1, 134.5, 130.6, 129.5, 128.3, 128.2, 126.6, 123.2, 120.4, 119.3, 111.2, 107.9, 52.9, 52.2, 26.9, 23.1; ESI–MS *m/z* (ion, %): 371 ([M+H]$^+$, 90), 393 ([M+Na]$^+$, 100); ESI–HRMS *m/z*: 393.0963 [M+Na]$^+$ (C$_{20}$H$_{19}$ClN$_2$NaO$_3$ requires 393.0976); IR (solid-state, ATR, cm^{-1}): 3271 (w, br), 3059 (w), 2952 (w), 2852 (w), 1733 (m), 1651 (s), 1597 (m), 1520 (m), 1436 (m), 1372 (s), 1214 (s), 788 (s), 737 (s), 688 (m); UV–Vis (DMSO, nm): λ_max 312 (ε = 15639 mol dm^{-3} cm^{-1}).

Lab book reference number (method A): AJR-5-408

Lab book reference number (method B): AJR-7-667

Bis(acetonitrile)palladium ditosylate (215)[222]
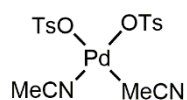
Pd(OAc)$_2$ (500 mg, 2.23 mmol, 1 eq.) was added to a Schlenk tube equipped with a magnetic stirrer which was then sealed, evacuated and purged with N$_2$ three times. Dry MeCN (45 mL) was added with stirring to give an orange–brown solution. To this was added a solution of *para*-toluenesulfonic acid (2.07 g, 12.04 mmol, 5.4 eq.) in dry MeCN (30 mL) *via* cannula,

which resulted in a yellow solution. Dry Et$_2$O (50 mL) was then added to precipitate a yellow solid and the mixture left to stand for 20 min with no stirring. After 20 min the excess Et$_2$O was removed by filter cannula and the resulting solid washed with dry Et$_2$O (20 mL), which was then removed by filter cannula. The resulting solid was dried briefly under vacuum to afford the *title compound* as a cream solid (944 mg, 80%).

Note: Dissociation of MeCN ligands is facile in solution, the ratio of complexed *p*-TsOH:complexed MeCN:free MeCN by ^{1}H NMR was measured as 1:0.6:1.3.

Mp 130–135 °C dec; ^{1}H NMR (400 MHz, CD$_3$OD, δ): 7.72 (d, *J* = 8.0 Hz, 4H), 7.25 (d, *J* = 8.0 Hz, 4H), 2.56 (s, complexed MeCN, 2H), 2.38 (s, 6H), 2.03 (s, free MeCN, 4H); ^{13}C NMR (125 MHz, CD$_3$OD, δ): 142.6, 137.6, 130.0, 127.0, 21.3; IR (solid-state, ATR, cm^{-1}): 3007, 2992, 2929, 2337, 1595, 1491, 1398, 1348, 1283, 1177, 1142, 1097, 1028, 1015, 947, 814, 712, 675, 642, 629, 554, 507, 438.

Lab book reference number (method A): AJR-6-532

Effect of MeCN on direct arylation of tryptophan
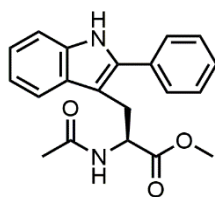
To a microwave tube was added tryptophan **74** (50 mg, 0.192 mmol, 1 eq.), aryldiazonium salt **48** (37 mg, 0.192 mmol, 1 eq.), Pd(OAc)$_2$ (2 mg, 9.6 μmol, 5 mol%), MeCN (1 μL, 789 μg, 19.2 μmol, 10 mol%) and EtOAc (5 mL). The reaction mixture was stirred at RT for 16 h. After 16 h the resulting brown reaction mixture was filtered through Celite then washed with sat. aq. NaHCO$_3$. The organic layer was collected and dried over MgSO$_4$, filtered and evaporated to afford the *title compound* as an off-white solid (64 mg, quant.).

Lab book reference number: AJR-7-681

Attempted direct arylation of indole
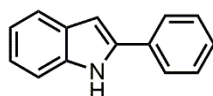
To a microwave tube was added phenyldiazonium salt **48** (58 mg, 0.30 mmol, 1 eq.) and Pd(OAc)$_2$ (3.4 mg, 15 μmol, 5 mol%). Indole **45** (35 mg, 0.30 mmol, 1 eq.) was then added. Upon addition phenyldiazonium salt **48** visibly darkened to red, followed by black. This

heated up rapidly and began visibly smoking, which subsided after 2 min. EtOAc (3 mL) was added to give a dark red solution which was stirred at 60 °C for 16 h. After 16 h TLC analysis of the reaction mixture indicated a large number of species, so the reaction was abandoned.

Lab book reference number: AJR-5-453

Attempted direct arylation of methylindole
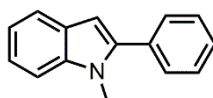
To a microwave tube was added 1-methylindole **33** (37 μL, 39 mg, 0.30 mmol, 1 eq.), phenyldiazonium salt **48** (58 mg, 0.30 mmol, 1 eq.), Pd(OAc)$_2$ (3.4 mg, 15 μmol, 5 mol%) and EtOAc (3 mL). The mixture was then stirred at 60 °C for 16 h. After 16 h TLC (SiO$_2$, petrol/EtOAc, 4:1, *v/v*) analysis of the reaction mixture indicated a large number of species. The resulting dark red reaction mixture was filtered through Celite then washed with sat. aq. NaHCO$_3$. The organic layer was collected and dried over MgSO$_4$, filtered and evaporated to give a brown residue. Analysis by ^{1}H NMR spectroscopic analysis indicated a large number of species, so the reaction was abandoned.

Lab book reference number: AJR-5-454

Attempted direct arylation of indazole
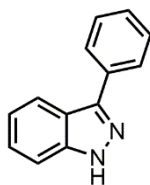
To a microwave tube was added indazole **222** (35 mg, 0.30 mmol, 1 eq.), phenyldiazonium salt **48** (58 mg, 0.30 mmol, 1 eq.), Pd(OAc)$_2$ (3.4 mg, 15 μmol, 5 mol%) and EtOAc (3 mL). The mixture was then stirred at 60 °C for 16 h. After 16 h the reaction mixture was filtered through Celite then washed with sat. aq. NaHCO$_3$. The organic layer was collected and dried over MgSO$_4$, filtered and evaporated to give a brown residue. Analysis by ^{1}H NMR spectroscopic analysis indicated only starting material. Purification by dry-loaded flash column chromatography (SiO$_2$, petrol/EtOAc, 1:1, *v/v*) afforded the *starting material* as an off-white solid (35 mg, quant.).

Lab book reference number: AJR-6-468

Attempted direct arylation of 7-azaindole at 60 °C
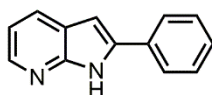
To a microwave tube was added 7-azaindole **223** (35 mg, 0.30 mmol, 1 eq.), phenyldiazonium salt **48** (58 mg, 0.30 mmol, 1 eq.), Pd(OAc)$_2$ (3.4 mg, 15 μmol, 5 mol%) and EtOAc (3 mL). The mixture was then stirred at 60 °C for 16 h. After 16 h TLC (SiO$_2$, petrol/EtOAc, 1:1, *v/v*) analysis of the reaction mixture indicated a large number of species. The reaction mixture was filtered through Celite then washed with sat. aq. NaHCO$_3$. The organic layer was collected and dried over MgSO$_4$, filtered and evaporated to give a brown residue. Analysis by ^{1}H NMR spectroscopic analysis indicated a large number of species, so the reaction was abandoned.

Lab book reference number: AJR-6-469

Attempted direct arylation of 7-azaindole at 40 °C
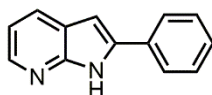
To a microwave tube was added 7-azaindole **223** (35 mg, 0.30 mmol, 1 eq.), phenyldiazonium salt **48** (58 mg, 0.30 mmol, 1 eq.), Pd(OAc)$_2$ (3.4 mg, 15 μmol, 5 mol%) and EtOAc (3 mL). The mixture was then stirred at 40 °C for 16 h. After 16 h TLC (SiO$_2$, petrol/EtOAc, 1:1, *v/v*) analysis of the reaction mixture indicated no conversion of starting material, so the reaction was abandoned.

Lab book reference number: AJR-6-477

Attempted direct arylation of 7-azaindole at RT
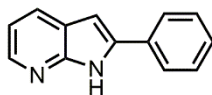
To a microwave tube was added 7-azaindole **223** (35 mg, 0.30 mmol, 1 eq.), phenyldiazonium salt **48** (58 mg, 0.30 mmol, 1 eq.), Pd(OAc)$_2$ (3.4 mg, 15 μmol, 5 mol%) and EtOAc (3 mL). The mixture was then stirred at RT for 16 h. After 16 h TLC (SiO$_2$, petrol/EtOAc, 1:1, *v/v*) analysis of the reaction mixture indicated no conversion of starting material, so the reaction was abandoned.

Lab book reference number: AJR-6-473

1-Methylindazole (224)[152]
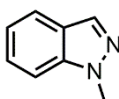
To a round-bottomed flask equipped with a magnetic stirrer bar was added indazole **222** (1 g, 8.46 mmol, 1 eq.). This was dissolved in acetone (10 mL) with stirring, before being cooled to 0 °C. KOH (1.42 g, 25.4 mmol, 3 eq.) was then added, the flask was sealed with a septum and flushed with N_2 from a balloon. The reaction mixture was then stirred at 0 °C for 1 h, then MeI (0.8 mL, 1.8 g, 12.7 mmol, 1.5 eq.) was added dropwise at 0 °C. After complete addition the reaction was allowed to warm to RT with stirring for 1 h. After 1 h the KOH was filtered off using a glass sinter and the solvent evaporated. Purification by wet-loaded flash column chromatography (SiO$_2$, petrol/EtOAc, 4:1, *v/v*) afforded the *title compound* as a white solid (810 mg, 72%).

R_f 0.55 (petrol/EtOAc, 4:1, *v/v*); M.P. 60–61 °C (lit.[152] 58–59 °C); ^{1}H NMR (400 MHz, CDCl$_3$, δ): 7.99 (s, 1H), 7.73 (dt, *J* = 8.0, 1.0 Hz, 1H), 7.41–7.38 (m, 2H), 7.18–7.12 (m, 1H), 4.08 (s, 3H); ^{13}C NMR (101 MHz, CDCl$_3$, δ): 140.0, 132.8, 126.3, 124.1, 121.2, 120.5, 109.0, 35.6; EI–GC–MS *m/z* (ion): 132 [C$_8$H$_8$N$_2$]$^+$; EI–HRMS *m/z*: 132.0688 [C$_8$H$_8$N$_2$]$^+$ (C$_8$H$_8$N$_2$ requires 132.0687).

Lab book reference number: AJR-6-498

Attempted direct arylation of 1-methylindazole (225)
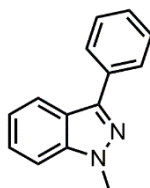
To a microwave tube was added 1-methylindazole **224** (40 mg, 0.30 mmol, 1 eq.), phenyldiazonium salt **48** (58 mg, 0.30 mmol, 1 eq.), Pd(OAc)$_2$ (3.4 mg, 15 μmol, 5 mol%) and EtOAc (3 mL). The mixture was then stirred at 60 °C for 16 h. After 16 h TLC (SiO$_2$, petrol/EtOAc, 1:1, *v/v*) analysis of the reaction mixture indicated no conversion of starting material, so the reaction was abandoned.

Lab book reference number: AJR-8-758

Attempted Tfa-protection of 1-methylindazole (226)
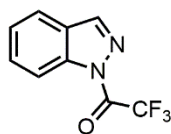
To a round-bottomed flask equipped with magnetic stirrer bar was added indazole **222** (100 mg, 0.85 mmol, 1 eq.). The flask was sealed with a septum and flushed with nitrogen from a balloon for 10 mins, then Et₃N (131 μL, 95 mg, 0.94 mmol, 1.1 eq.) and solvent (0.85 mL) were added *via* syringe. The mixture was cooled to 0 °C, then ethyl trifluoroacetate **165** (112 μL, 134 mg, 0.94 mmol, 1.1 eq.) was added dropwise. After complete addition the reaction was allowed to warm to RT and stirred for 20 h. No conversion of starting material was observed.

Lab book reference number (MeCN): AJR-6-495

Lab book reference number (THF): AJR-6-501

Boc-protection of 1-methylindazole (227)[153]
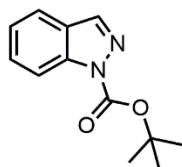
To a round-bottomed flask equipped with magnetic stirrer bar was added indazole **222** (591 mg, 5 mmol, 1 eq.) and DMAP (12 mg, 0.1 mmol, 2 mol%). The flask was sealed with a septum and flushed with nitrogen from a balloon for 10 mins, then dry MeCN (7 mL) was added *via* syringe. To this mixture was added a solution of Boc₂O (1.31 g, 6 mmol, 1.2 eq.) in dry MeCN (3 mL) to give a clear solution. This was stirred at RT for 3 h. After 3 h the solvent was evaporated and the residue redissolved in Et₂O. Deionised water was added and the mixture extracted into Et₂O three times. The organic layers were collected and dried over MgSO₄, filtered and evaporated to give an orange oil. Purification by wet-loaded flash column chromatography (SiO₂, petrol/Et₂O, 2:1, *v/v*) afforded an inseparable mixture of the *title compound* and **228** as a clear oil (1.0 g, 98%).

Lab book reference number: AJR-6-487

Attempted Ac-protection of 1-methylindazole (229)
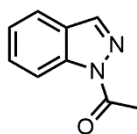
To a round-bottomed flask equipped with magnetic stirrer bar was added indazole **222** (100 mg, 0.85 mmol, 1 eq.). The flask was sealed with a septum and flushed with nitrogen from a balloon for 10 mins, then Et$_3$N (131 μL, 95 mg, 0.94 mmol, 1.1eq.) and MeCN (0.85 mL) were added *via* syringe. The mixture was cooled to 0 °C, then Ac$_2$O (89 μL, 96 mg, 0.94 mmol, 1.1 eq.) was added dropwise. After complete addition the reaction was allowed to warm to RT and stirred for 20 h. After 3 h deionised water was added and the mixture extracted into EtOAc three times. The organic layers were collected and washed with 1M HCl and brine, then dried over MgSO$_4$, filtered and evaporated to give a clear oil. Purification by wet-loaded flash column chromatography (SiO$_2$, petrol/EtOAc, 4:1, *v/v*) afforded an inseparable mixture of the *title compound* and **230** as a white solid (107 mg, 79%).

Lab book reference number: AJR-6-494

1-Methyl-7-azaindole (231)[154]
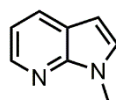
To a round-bottomed flask equipped with a magnetic stirrer bar was added 7-azaindole **223** (1 g, 8.46 mmol, 1 eq.). This was dissolved in DMF (5 mL) with stirring, before being cooled to 0 °C. The flask was sealed with a septum and flushed with N$_2$ from a balloon for 10 mins, then NaH (244 mg, 10.15 mmol, 1.2 eq.) was added and the reaction stirred at 0 °C for 1 h. After 1 h MeI (0.58 mL, 1.32 g, 9.31 mmol, 1.1 eq.) was added dropwise at 0 °C. After complete addition the reaction was allowed to warm to RT with stirring for 1 h. After 1 h ice-cold deionised water was added to quench the reaction, which was then extracted into EtOAc three times. The organic layers were combined and washed five times with deionised water, then washed with brine, dried over MgSO$_4$, filtered and evaporated to give an orange oil. This was purified directly by filtration through a silica plug (SiO$_2$, EtOAc) to afford the *title compound* as a yellow oil (0.98 g, 88%).

^{1}H NMR (400 MHz, CDCl$_3$, δ): 8.34 (dd, *J* = 5.0, 1.0 Hz, 1H), 7.91 (dt, *J* = 8.0, 1.0 Hz, 1H), 7.18 (d, *J* = 3.5 Hz, 1H), 7.05 (ddd, *J* = 8.0, 5.0, 1.0 Hz, 1H), 6.45 (dd, *J* = 3.5, 1.0 Hz, 1H), 3.90 (d, *J* = 1.0 Hz, 3H); ^{13}C NMR (101 MHz, CDCl$_3$, δ): 147.9, 142.9, 129.2, 128.9, 120.7,

115.6, 99.4, 31.4; ESI–MS *m/z* (ion, %): 133 ([M+H]$^+$, 100); ESI–HRMS *m/z*: 133.0763 [M+H]$^+$ (C$_8$H$_9$N$_2$ requires 133.0760).

Lab book reference number: AJR-6-480

1-methyl-2-phenyl-7-azaindole (232)
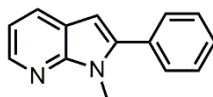
Method A: To a microwave tube equipped with magnetic stirrer bar was added 1-methyl-7-azaindole **231** (40 mg, 0.30 mmol, 1 eq.), aryldiazonium salt **48** (58 mg, 0.30 mmol, 1 eq.), Pd(OAc)$_2$ (3.4 mg, 15 µmol, 5 mol%) and EtOH (3 mL). The reaction mixture was stirred at 40 °C for 22 h. After 22 h the reaction mixture was filtered through Celite with EtOAc then washed with sat. aq. NaHCO$_3$. The organic layer was collected and dried over MgSO$_4$, filtered and evaporated to give a brown solid, which was subsequently analysed by ^{1}H NMR spectroscopy.

Method B: To a microwave tube equipped with magnetic stirrer bar was added 1-methyl-7-azaindole **231** (100 mg, 0.76 mmol, 1 eq.), diaryliodonium salt **233** (390 mg, 1.06 mmol, 1.4 eq.), Pd(OAc)$_2$ (8.4 mg, 37.5 µmol, 5 mol%) and EtOH (3.8 mL). The vial was sealed with a septum and the reaction stirred at 60 °C for 22 h. After 22 h the reaction mixture was allowed to cool to RT, then filtered through Celite with EtOAc, washed with sat. aq. NaHCO$_3$, dried over MgSO$_4$, filtered and evaporated to give a brown residue. Purification by dry-loaded flash column chromatography (SiO$_2$, petrol/Et$_2$O, 1:1, *v/v*) to afford the *title compound* as a yellow oil (125 mg, 79%).

R_f 0.26 (petrol/Et$_2$O, 1:1, *v/v*); ^{1}H NMR (400 MHz, CDCl$_3$, δ): 8.36 (dd, *J* = 5.0, 1.5 Hz, 1H), 7.91 (dd, *J* = 8.0, 1.5 Hz, 1H), 7.58–7.54 (m, 2H), 7.52–7.47 (m, 2H), 7.46–7.41 (m, 1H), 7.09 (dd, *J* = 8.0, 5.0 Hz, 1H), 6.52 (s, 1H), 3.89 (s, 3H); ^{13}C NMR (101 MHz, CDCl$_3$, δ): 149.4, 142.8, 142.0, 132.5, 129.3, 128.8, 128.4, 128.3, 120.8, 116.2, 99.5, 30.0; ESI–MS *m/z* (ion, %): 209 ([M+H]$^+$, 100); ESI–HRMS *m/z*: 209.1074 [M+H]$^+$ (C$_{14}$H$_{13}$N$_2$ requires 209.1073).

Lab book reference number (method A): AJR-6-520

Lab book reference number (method B): AJR-6-489

Diphenyliodonium tetrafluoroborate (233)[155]
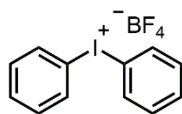
To a round-bottomed flask equipped with a magnetic stirrer bar was added *m*CPBA (≤77%, 7.39 g, 33 mmol, 1.1 eq.), which was then dissolved in CH_2Cl_2 (100 mL). Iodobenzene **1** (3.4 mL, 6.12 g, 30 mmol, 1 eq.) was added to this solution, then $BF_3 \cdot OEt_2$ (9.2 mL, 10.6 g, 75 mmol, 2.5 eq.) was added dropwise. The resultant solution was stirred at RT for 30 min, then cooled to 0 °C. $PhB(OH)_2$ **14** (4.02 g, 33 mmol, 1.1 eq.) was then added at 0 °C. After complete addition, the reaction was allowed to warm to RT with stirring over 15 min. After 15 min the crude reaction mixture was filtered through a silica pad, first eluting with CH_2Cl_2, then CH_2Cl_2/MeOH (20:1, *v/v*). The second fraction was collected and concentrated *in vacuo*. Et_2O was added to precipitate an off-white solid, which was filtered through a glass sinter and washed with further Et_2O, before being dried *in vacuo* to afford the *title compound* as an off-white solid (7.82 g, 71%).

M.P. 136–138 °C (lit.[223] 136–138 °C); ^{1}H NMR (400 MHz, $(CD_3)_2SO$, δ): 8.25 (dd, *J* = 8.0, 1.0 Hz, 4H), 7.73–7.62 (m, 2H), 7.57–7.51 (m, 4H); ^{13}C NMR (101 MHz, $(CD_3)_2SO$, δ): 135.2, 132.1, 131.8, 116.5; ESI-MS *m/z* (ion, rel. %): 281 ($[C_{12}H_{10}I]^+$, 100); ESI-HRMS *m/z*: 280.9824 $[C_{12}H_{10}I]^+$ ($C_{12}H_{10}I$ requires 280.9822).

Lab book reference number: AJR-8-727

2-Phenylindole (234)
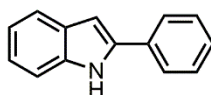
To a microwave tube equipped with magnetic stirrer bar was added indole **45** (35 mg, 0.30 mmol, 1 eq.), diaryliodonium salt **233** (155 mg, 0.42 mmol, 1.4 eq.), $Pd(OAc)_2$ (3.4 mg, 15 µmol, 5 mol%) and EtOH (1.5 mL). The vial was sealed with a septum and the reaction stirred at 60 °C for 22 h. After 22 h the reaction mixture was allowed to cool to RT and purified directly by wet-loaded flash column chromatography (SiO_2, pentane/EtOAc, 9:1, *v/v*) to afford the *title compound* as a white solid (32 mg, 55%).

R_f 0.46 (pentane/EtOAc, 9:1, *v/v*); ^{1}H NMR (400 MHz, $CDCl_3$, δ): 8.33 (br s, 1H), 7.70–7.64 (m, 3H), 7.49–7.40 (m, 3H), 7.38–7.31 (m, 1H), 7.22 (m, 1H), 7.15 (m, 1H), 6.85 (s, 1H); ^{13}C NMR (101 MHz, $CDCl_3$, δ): 138.0, 136.9, 132.5, 129.4, 129.2, 127.9, 125.3, 122.5, 120.8,

120.4, 111.0, 100.1; ESI–MS *m/z* (ion, %): 194 ([M+H]$^+$, 100); ESI–HRMS *m/z*: 194.0968 [M+H]$^+$ (C$_{14}$H$_{12}$N requires 194.0964).

Lab book reference number: AJR-7-641

Attempted direct arylation of indazole

To a microwave tube equipped with magnetic stirrer bar was added indazole **222** (35 mg, 0.30 mmol, 1 eq.), diaryliodonium salt **233** (155 mg, 0.42 mmol, 1.4 eq.), Pd(OAc)$_2$ (3.4 mg, 15 μmol, 5 mol%) and EtOH (1.5 mL). The vial was sealed with a septum and the reaction stirred at 60 °C for 22 h. After 22 h analysis of the crude reaction mixture by TLC (SiO$_2$, petrol/EtOAc, 1:1:, *v/v*) indicated no conversion of starting material, so the reaction was abandoned.

Lab book reference number: AJR-6-470

Attempted direct arylation of 7-azaindole
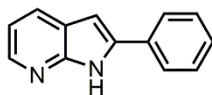
To a microwave tube equipped with magnetic stirrer bar was added 7-azaindole **223** (35 mg, 0.30 mmol, 1 eq.), diaryliodonium salt **233** (155 mg, 0.42 mmol, 1.4 eq.), Pd(OAc)$_2$ (3.4 mg, 15 μmol, 5 mol%) and EtOH (1.5 mL). The vial was sealed with a septum and the reaction stirred at 60 °C for 22 h. After 22 h analysis of the crude reaction mixture by TLC (SiO$_2$, petrol/EtOAc, 1:1, *v/v*) indicated no conversion of starting material, so the reaction was abandoned.

Lab book reference number: AJR-6-471

Attempted direct arylation of pyridazine
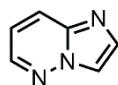
To a microwave tube equipped with magnetic stirrer bar was added pyridazine **235** (36 mg, 0.30 mmol, 1 eq.), diaryliodonium salt **233** (155 mg, 0.42 mmol, 1.4 eq.), Pd(OAc)$_2$ (3.4 mg,

15 µmol, 5 mol%) and EtOH (1.5 mL). The vial was sealed with a septum and the reaction stirred at 60 °C for 4 days. After 4 days analysis of the crude reaction mixture by TLC (SiO₂, petrol/EtOAc, 4:1, *v/v*) indicated no conversion of starting material, so the reaction was abandoned.

Lab book reference number: AJR-6-479

Attempted direct arylation of 1-methylindazole (225)

To a microwave tube equipped with magnetic stirrer bar was added 1-methylindazole **224** (40 mg, 0.30 mmol, 1 eq.), diaryliodonium salt **233** (155 mg, 0.42 mmol, 1.4 eq.), Pd(OAc)₂ (3.4 mg, 15 µmol, 5 mol%) and EtOH (1.5 mL). The vial was sealed with a septum and the reaction stirred at 60 °C for 4 days. After 4 days analysis of the crude reaction mixture by TLC (SiO₂, petrol/EtOAc, 4:1, *v/v*) indicated no conversion of starting material, so the reaction was abandoned.

Lab book reference number: AJR-6-478

Catalyst screening for 1-methyl-2-phenyl-7-azaindole (232)
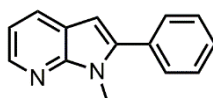
To a microwave tube equipped with magnetic stirrer bar was added 1-methyl-7-azaindole **231** (40 mg, 0.30 mmol, 1 eq.), diaryliodonium salt **233** (155 mg, 0.42 mmol, 1.4 eq.), Pd catalyst (5 mol%) and EtOH (1.5 mL). The vial was sealed with a septum and the reaction stirred at 60 °C for 22 h. After 22 h the reaction mixture was allowed to cool to RT, then filtered through Celite with EtOAc, washed with sat. aq. NaHCO₃, dried over MgSO₄, filtered and evaporated to give a brown residue, which was subsequently analysed by ¹H NMR spectroscopy.

Lab book reference number (Pd/C, 5 wt%): AJR-6-511

Lab book reference number (Pd/C, 10 wt%): AJR-6-517

Lab book reference number (Pd/charcoal): AJR-6-512

Lab book reference number (Pd black): AJR-6-516

Lab book reference number (Lindlar): AJR-6-515

Lab book reference number (Pearlman's): AJR-6-513

Lab book reference number (PdO): AJR-6-514

PVP–Pd (13)

To a three-necked round-bottomed flask fitted with a mechanical stirrer and reflux condenser was added PdCl$_2$ (255 mg, 1.44 mmol, 1 eq.), HCl (0.2 M, 14.4 mL) and deionised water (706 mL). The reaction mixture was stirred for 1 h to give an orange solution. PVP **12** (3.2 g, 28.3 mmol, 14 eq.), deionised water (672 mL) and EtOH (1000 mL) were added and the reaction heated to reflux with stirring for 4.5 h. The mixture was cooled to ambient temperature and the solvent removed under reduced pressure to give a brittle, glassy black solid. This was crushed with a pestle and mortar then dried *in vacuo* to give the product as a black crystalline solid (3.40 g).

IR (solid-state ATR, cm^{-1}): 2953 (w, br), 1640 (s), 1421 (s), 1288 (s).

Lab book reference number: AJR-1-33, AJR-8-709

DMF-stabilised PdNPs (236)

To a 250 mL two-necked round-bottomed flask equipped with a magnetic stirrer bar and reflux condenser was added DMF (15 ml). This was heated to 140 °C before a suspension of PdCl$_2$ (2.6 mg, 15 µmol) in deionised water (150 µL) was added. The resulting solution was heated at 140 °C for 6 h to yield the product as a clear yellow solution. Often the product could not be obtained, and a black particulate solution was seen instead.

Lab book reference number: AJR-5-463, AJR-5-464

Diphenyliodonium trifluoromethanesulfonate (38)[124]
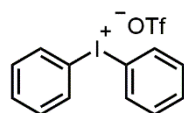
Aryliodonium salt **22** (1 g, 3.1 mmol, 1 eq.) and benzene **237** (303 µL, 266 mg, 3.41 mmol, 1.1 eq.) were added to a round-bottomed flask and dissolved in CH$_2$Cl$_2$ (6 mL) with stirring. The mixture was cooled to 0 °C then trifluoromethanesulfonic acid (301 µL, 512 mg, 3.41 mmol, 1.1 eq.) was added dropwise with stirring. After complete addition the reaction was

stirred for 2 h over which time it was allowed to warm to RT. After 2 h the mixture was evaporated to give an orange-white residue to which Et$_2$O was added to precipitate a white solid. This was filtered through a glass sinter and washed on the filter with further Et$_2$O until the filtrate ran clear. This was then dried *in vacuo* at 100 °C to afford the *title compound* as an off-white solid (1.02 g, 76%).

M.P. 174–176 °C (lit.[224] 175–177 °C); ^{1}H NMR (400 MHz, (CD$_3$)$_2$SO, δ):8.28–8.22 (m, 4H), 7.70–7.64 (m, 2H), 7.57–7.50 (m, 4H); ^{13}C NMR (101 MHz, (CD$_3$)$_2$SO, δ): 135.2, 132.1, 131.8, 116.5; ^{19}F NMR (376 MHz, CDCl$_3$, δ): −77.7; ESI–MS *m/z* (ion, %): 280 ([M−OTf]$^+$, 100); ESI–HRMS *m/z*: 280.9830 [M−OTf]$^+$ (C$_{12}$H$_{10}$I requires 280.9822).

Lab book reference number: AJR-8-726

Screening for the direct arylation of tryptophan (75)
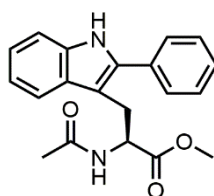
To a microwave tube equipped with magnetic stirrer bar was added tryptophan **74** (52 mg, 0.20 mmol, 1 eq.), diaryliodonium triflate salt **38** (172 mg, 0.40 mmol, 2 eq.) or diaryliodonium tetrafluoroborate salt **233** (147 mg, 0.40 mmol, 2 eq.), Pd catalyst (5 mol%) and solvent (2 mL). The vial was sealed with a septum and the reaction stirred at 60 °C for 16 h. After 16 h the reaction mixture was allowed to cool to RT, filtered through a silica pad with EtOAc and evaporated to give a brown residue, which was subsequently analysed by ^{1}H NMR spectroscopy.

Lab book reference number (entry 1): AJR-8-712

Lab book reference number (entry 2): AJR-8-729

Lab book reference number (entry 3): AJR-8-730

Lab book reference number (entry 4): AJR-8-720

Lab book reference number (entry 5): AJR-8-714

Lab book reference number (entry 6): AJR-8-728

Lab book reference number (entry 7): AJR-8-725

Lab book reference number (entry 8): AJR-8-735

Lab book reference number (entry 9): AJR-8-733

Lab book reference number (entry 10): AJR-8-734

1-Methyl-2-phenylindole (34)
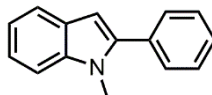
Method A: The initial kinetics for formation of the *title compound* were recorded using general procedure D (temperature decreased to 50 °C) with Pd/C (64 mg), PVP–Pd **13** (40 mg), Pd(OAc)$_2$ (6.7 mg) or Pd$_2$(dba)$_3$ **238** (15.5 mg).

Method B: The initial kinetics for formation of the *title compound* were recorded using general procedure D with Pd/C (64 mg), PVP–Pd **13** (40 mg), Pd(OAc)$_2$ (6.7 mg) or Pd$_2$(dba)$_3$ **238** (15.5 mg).

^{1}H NMR (400 MHz, CDCl$_3$, δ): 7.64 (d, *J* = 8.0 Hz, 1H), 7.56–7.46 (m, 4H), 7.45–7.36 (m, 2H), 7.28–7.23 (m, 1H), 7.18–7.12 (m, 1H), 6.57 (s, 1H), 3.76 (s, 3H); ^{13}C NMR (101 MHz, CDCl$_3$, δ): 141.7, 138.5, 133.0, 129.5, 128.6, 128.1, 128.0, 121.8, 120.6, 120.0, 109.7, 101.8, 31.3.

Lab book reference number (method A, Pd/C): ln_1a_07 (*reaction conducted by L. Neumann*)

Lab book reference number (method A, PVP–Pd): ln_1c_04 (*reaction conducted by L. Neumann*)

Lab book reference number (method A, Pd(OAc)$_2$): ln_1f_05 (*reaction conducted by L. Neumann*)

Lab book reference number (method A, Pd$_2$(dba)$_3$): ln_1g_05 (*reaction conducted by L. Neumann*)

Lab book reference number (method B, Pd/C): ln_1a_06 (*reaction conducted by L. Neumann*)

Lab book reference number (method B, PVP–Pd): ln_1c_02_new (*reaction conducted by L. Neumann*)

Lab book reference number (method B, Pd(OAc)$_2$): ln_1f_03 (*reaction conducted by L. Neumann*)

Lab book reference number (method B, Pd₂(dba)₃): ln_1g_02 (*reaction conducted by L. Neumann*)

Comparison of PVP–Pd batches using 1-Methyl-2-phenylindole

The initial kinetics for formation of the *title compound* were recorded using general procedure D with PVP–Pd **13** (40 mg).

Lab book reference number: ln_1c_02_old (*reaction conducted by L. Neumann*)

Lab book reference number: ln_1c_02_new (*reaction conducted by L. Neumann*)

2-phenylbenzofuran (240)
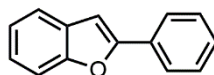
The initial kinetics for formation of the *title compound* were recorded using general procedure D with Pd/C (64 mg), PVP–Pd **13** (40 mg), Pd(OAc)$_2$ (6.7 mg) or Pd$_2$(dba)$_3$ **238** (15.5 mg).

To a microwave tube equipped with magnetic stirrer bar was added benzofuran **239** (33 μL, 35 mg, 0.30 mmol, 1 eq.), diaryliodonium salt **233** (155 mg, 0.42 mmol, 1.4 eq.), Pd(OAc)$_2$ (3.4 mg, 0.015 mmol, 5 mol%) and EtOH (1.5 mL). The vial was sealed with a septum and the reaction stirred at 60 °C for 22 h. After 22 h the reaction mixture was allowed to cool to RT, filtered through a silica pad with EtOAc and evaporated to give a brown residue, which was purified directly by wet-loaded flash column chromatography (SiO$_2$, petrol) to afford the *title compound* as a white solid (18 mg, 31%).

^{1}H NMR (400 MHz, CDCl$_3$, δ): 7.92–7.87 (m, 2H), 7.63–7.59 (m, 1H), 7.57–7.53 (m, 1H), 7.50–7.44 (m, 2H), 7.40–7.35 (m, 1H), 7.31 (ddd, J = 8.0, 7.0, 1.5 Hz, 1H), 7.26 (ddd, J = 8.0, 7.0, 1.5 Hz, 1H), 7.05 (d, J = 1.0 Hz, 1H); ^{13}C NMR (101 MHz, CDCl$_3$, δ): 156.0, 155.0, 130.6, 129.3, 128.9, 128.7, 125.1, 124.4, 123.1, 121.0, 111.3, 101.4; EI–GC–MS *m/z* (ion): 194 [C$_{14}$H$_{10}$O]$^+$; EI–HRMS *m/z*: 194.0720 [C$_{14}$H$_{10}$O]$^+$ (C$_{14}$H$_{10}$O requires 194.0732).

Lab book reference number (Pd/C): ln_3a (*reaction conducted by L. Neumann*)

Lab book reference number (PVP–Pd): ln_3c (*reaction conducted by L. Neumann*)

Lab book reference number (Pd(OAc)₂): ln_3f (*reaction conducted by L. Neumann*)

Lab book reference number (Pd₂(dba)₃): ln_3g (*reaction conducted by L. Neumann*)

Lab book reference number: AJR-7-642

4-*n*-butyl-2-phenylthiophene (242)
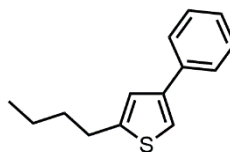
The initial kinetics for formation of the *title compound* were recorded using general procedure D with Pd/C (64 mg), PVP–Pd **13** (40 mg), Pd(OAc)$_2$ (6.7 mg) or Pd$_2$(dba)$_3$ **238** (15.5 mg).
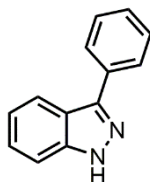
Method A: To a microwave tube equipped with magnetic stirrer bar was added 2-*n*-butylthiophene **241** (42 mg, 0.30 mmol, 1 eq.), diaryliodonium salt **233** (155 mg, 0.42 mmol, 1.4 eq.), Pd(OAc)$_2$ (3.4 mg, 0.015 mmol, 5 mol%) and EtOH (1.5 mL). The vial was sealed with a septum and the reaction stirred at 60 °C for 22 h. After 22 h the reaction mixture was allowed to cool to RT, filtered through a silica pad with EtOAc and evaporated to give a brown residue, which was purified directly by wet-loaded flash column chromatography (SiO$_2$, petrol) to afford the *title compound* as a clear oil (32 mg, 49%).

Method B: Synthesised as in method A using PVP–Pd **13** (20 mg, 0.015 mmol, 5 mol%) in place of Pd(OAc)$_2$. Purification by wet-loaded flash column chromatography (SiO$_2$, petrol) afforded the *title compound* as a clear oil (45 mg, 69%).

^{1}H NMR (400 MHz, CDCl$_3$, δ): 7.61–7.56 (m, 2H), 7.42–7.36 (m, 2H), 7.31–7.25 (m, 1H), 7.24 (d, *J* = 1.5 Hz, 1H), 7.09 (dt, *J* = 1.5, 1.0 Hz, 1H), 2.87 (t, *J* = 7.5 Hz, 2H), 1.77–1.67 (m, 2H), 1.50–1.38 (m, 2H), 0.97 (t, *J* = 7.5 Hz, 3H); ^{13}C NMR (101 MHz, CDCl$_3$, δ): 146.8, 141.9, 136.4, 128.8, 127.0, 126.4, 123.5, 117.9, 33.9, 30.0, 22.4, 14.0; ESI–MS *m/z* (ion): 217 [C$_{14}$H$_{17}$S]$^+$; ESI–HRMS *m/z*: 217.1024 [C$_{14}$H$_{17}$S]$^+$ (C$_{14}$H$_{17}$S requires 217.1045).

Lab book reference number (Pd/C): ln_5a (*reaction conducted by L. Neumann*)

Lab book reference number (PVP–Pd): ln_5c (*reaction conducted by L. Neumann*)

Lab book reference number (Pd(OAc)$_2$): ln_5f (*reaction conducted by L. Neumann*)

Lab book reference number (Pd$_2$(dba)$_3$): ln_5g (*reaction conducted by L. Neumann*)

Lab book reference number (method A): AJR-7-643

Lab book reference number (method B): AJR-7-731

5-*n*-butyl-2-phenylfuran (246)
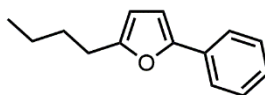
The initial kinetics for formation of the *title compound* were recorded using general procedure D with Pd/C (64 mg), PVP–Pd **13** (40 mg), Pd(OAc)$_2$ (6.7 mg) or Pd$_2$(dba)$_3$ **238** (15.5 mg).

The initial kinetics were also studied using procedure D, with the temperature increased to 70 °C over 10 h, using Pd/C (64 mg).

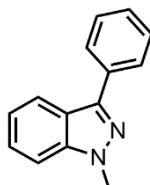*Method A*: To a microwave tube equipped with magnetic stirrer bar was added 2-*n*-butylfuran **243** (42 μL, 37 mg, 0.30 mmol, 1 eq.), diaryliodonium salt **233** (155 mg, 0.42 mmol, 1.4 eq.), PVP–Pd **13** (20 mg, 0.015 mmol, 5 mol%) and EtOH (1.5 mL). The vial was sealed with a septum and the reaction stirred at 60 °C for 22 h. After 22 h the reaction mixture was allowed to cool to RT, filtered through a silica pad with EtOAc and evaporated to give a brown residue, which was purified directly by dry-loaded flash column chromatography (SiO$_2$, petrol) to afford the *title compound* as a clear oil (27 mg, 45%).

Method B: Synthesised as in method B using Pd/C (32 mg, 0.015 mmol, 5 mol%) in place of PVP–Pd **13**. Purification by dry-loaded flash column chromatography (SiO$_2$, petrol) to afford an inseparable mixture of the *title compound* and biphenyl as a clear oil (45 mg).

^{1}H NMR (400 MHz, CDCl$_3$, δ): 7.68–7.63 (m, 2H), 7.40–7.34 (m, 2H), 7.23 (tt, *J* = 7.5, 1.0 Hz, 1H), 6.56 (d, *J* = 3.0 Hz, 1H), 6.08 (dt, *J* = 3.0, 1.0 Hz, 1H), 2.70 (app t, *J* = 7.5 Hz, 2H), 1.70 (tt, *J* = 7.5, 6.5 Hz, 2H), 1.44 (app sext, *J* = 7.5 Hz, 2H), 0.97 (t, *J* = 7.5 Hz, 3H); ^{13}C NMR (101 MHz, CDCl$_3$, δ): 156.6, 152.2, 131.4, 128.7, 126.8, 123.4, 107.0, 105.8, 30.4, 28.0, 22.4, 14.0; EI–GC–MS *m/z* (ion): 200 [C$_{14}$H$_{16}$O]$^+$; EI–HRMS *m/z*: 200.1202 [C$_{14}$H$_{16}$O]$^+$ (C$_{14}$H$_{16}$O requires 200.1201).

Lab book reference number (Pd/C): ln_6a (*reaction conducted by L. Neumann*)

Lab book reference number (PVP–Pd): ln_6c (*reaction conducted by L. Neumann*)

Lab book reference number (Pd(OAc)$_2$): ln_6f (*reaction conducted by L. Neumann*)

Lab book reference number (Pd$_2$(dba)$_3$): ln_6g (*reaction conducted by L. Neumann*)

Lab book reference number: AJR-8-743

Lab book reference number (method A): AJR-8-732

Lab book reference number (method B): AJR-8-739, AJR-8-740, AJR-8-742

(1*E*,4*E*)-1,5-diphenylpenta-1,4-dien-3-one (247)
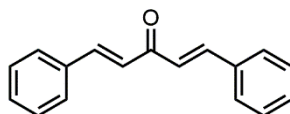
To a round-bottomed flask equipped with a magnetic stirrer was added NaOH (4.7 g, 117 mmol, 2.5 eq.), deionised water (91 mL) and EtOH (66 mL), before being cooled to 0 °C. Acetone (3.45 mL, 2.73 g, 47 mmol, 1 eq.) and benzaldehyde (9.60 mL, 9.98 g, 94 mmol, 1 eq.) were then added dropwise with stirring over 15 min. After complete addition the reaction was allowed to warm to RT over 40 min with stirring, during which time a yellow precipitate formed. After 40 min this was filtered through a glass sinter and washed with deionised water (3 × 25 mL). The resultant solid was dissolved in a minimum amount of hot (70 °C) ethyl acetate and then rapidly cooled to 0 °C using an ice bath to produce yellow crystals. These were dried *in vacuo* to afford the *title compound* as a yellow crystalline solid (6.86 g, 62%).

M.P. 111–112 °C (lit.[225] 110–112 °C); ^{1}H NMR (400 MHz, CDCl$_3$, δ): 7.75 (d, *J* = 16.0 Hz, 2H), 7.65–7.58 (m, 4H), 7.45–7.38 (m, 6H), 7.09 (d, *J* = 16.0 Hz, 2H); ^{13}C NMR (101 MHz, CDCl$_3$, δ): 189.3, 143.7, 135.2, 130.9, 129.4, 128.8, 125.8; ESI–MS *m/z* (ion, %): 235 ([M+H]$^+$, 100), 257 ([M+Na]$^+$, 40); ESI–HRMS *m/z*: 235.1110 [M+H]$^+$ (C$_{17}$H$_{15}$O requires 235.1117); IR (solid-state ATR, cm^{-1}): 1649 (m), 1588 (m), 1446 (m), 979 (s), 753 (s), 691 (s); Elemental anal.: C 87.20, H 6.04 (C$_{17}$H$_{14}$O requires C 87.15, H 6.02).

Lab book reference number: AJR-1-3

Tris((1*E*,4*E*)-1,5-diphenylpenta-1,4-dien-3-one)dipalladium(0)·CHCl$_3$ (238)[170]

Major isomer   Minor isomer
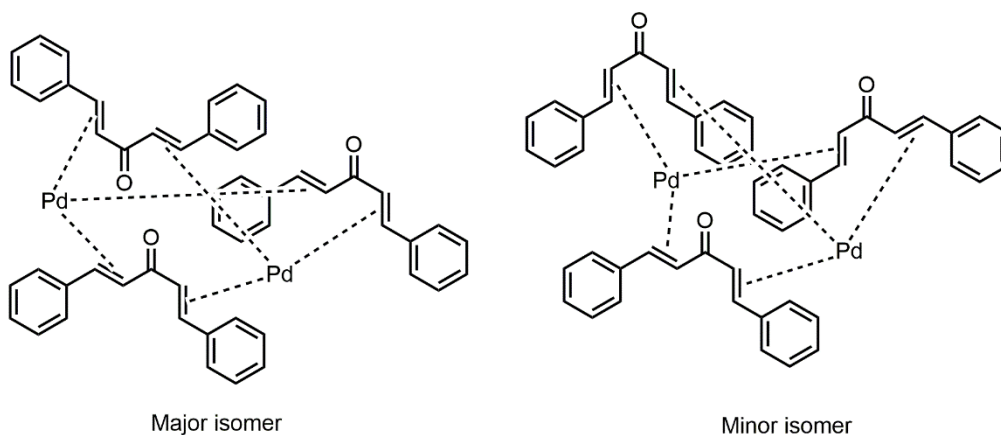
Method A: To a round-bottomed flask equipped with a magnetic stirrer was added Pd(OAc)$_2$ (100 mg, 0.45 mol, 1 eq.), dba **247** (209 mg, 0.89 mmol, 2 eq.), NaOAc (365 mg, 4.45 mol,

10 eq.) and MeOH (10 mL). The reaction was stirred at 40 °C for 3 h. After 3 h the resultant dark precipitate was filtered through a glass sinter and washed with MeOH (2 × 5 mL), deionised water (3 × 5 mL) then MeOH (2 × 5 mL). The dark purple residue was rinsed through the sinter with dry, freshly distilled CHCl$_3$ (30 mL) and the solvent removed to yield a purple residue. This was redissolved in a minimum amount of dry, freshly distilled CHCl$_3$ (7 mL), then dry, freshly distilled acetone (20 mL) was added and the solution kept at −18 °C for 18 h. After 18 h the dark purple precipitate formed was filtered through a glass sinter and washed with cold (5 °C) dry, freshly distilled acetone (2 × 5 mL) then dried *in vacuo* at 40 °C for 30 min to afford the *title compound* as a purple crystalline solid (188 mg, 82%). The purity was subsequently measured by ^{1}H NMR spectroscopic analysis as 84%.

Method B: To a Schlenk tube equipped with a magnetic stirrer bar was added Pd(OAc)$_2$ (100 mg, 0.45 mol, 1 eq.), dba **247** (209 mg, 0.89 mmol, 2 eq.) and NaOAc (365 mg, 4.45 mol, 10 eq.). The Schlenk tube was placed under vacuum and refilled with nitrogen three times, then dry MeOH (10 mL) was added and the mixture stirred at 40 °C for 3 h. After 3 h the solvent was removed by filter cannula and the residue washed with dry MeOH (2 × 5 mL). The resulting residue was then redissolved in dry CHCl$_3$ (20 mL) and the solution transferred to a clean Schlenk tube under N$_2$ *via* filter cannula. The reaction Schlenk tube was then rinsed with dry CHCl$_3$ (10 mL) and this was transferred under N$_2$ *via* filter cannula to the CHCl$_3$ solution. This solvent was then removed to give a dark purple residue, which was redissolved in dry CHCl$_3$ (20 mL). Dry acetone (80 mL) was then added and the solution kept at −18 °C for 16 h. After 16 h the solvent was removed *via* filter cannula and the dark purple precipitate washed with cold (5 °C) dry acetone (2 × 5 mL) then dried *in vacuo* to afford the *title compound* as a purple crystalline solid (128 mg, 55%). The purity was subsequently measured by ^{1}H NMR spectroscopic analysis as 91%.

Note: the integrals for multiplets in the ^{1}H NMR data have not been reported due to the coincidence of multiple environments from both isomers and dissociated free ligand rendering such assignment extraneous. Signals corresponding to the minor isomer have been denoted with an asterisk.

M.P. 120–122 °C dec. (lit.[168] 120–122 °C dec.); ^{1}H NMR (500 MHz, CDCl$_3$, δ): 7.75 (d, *J* = 16.0 Hz, 1H,), 7.65–7.60* (m), 7.45–6.92* (m), 6.83–6.31* (m), 6.15 (d, *J* = 13.0 Hz, 1H), 6.03* (d, *J* = 12.5 Hz, 1H), 6.00–5.90* (m, 3H), 5.87 (d, *J* = 12.5 Hz, 1H), 5.65* (d, *J* = 14.0 Hz, 1H), 5.33 (d, *J* = 12.5 Hz, 1H), 5.13 (d, *J* = 13.0 Hz, 1H), 5.03* (d, *J* = 13.0 Hz, 1H), 4.96 (app t, *J* = 13.0 Hz, 2 H), 4.90–4.80* (m, 3 H); LIFDI–MS *m/z* (ion, %): 235 ([C$_{17}$H$_{15}$O]$^+$, 100), 915 ([M+H]$^+$, 10); IR (solid-state ATR, cm^{-1}): 1609 (m), 1574 (m), 1539 (m), 1484

(m), 1442 (m), 1332 (m), 1184 (m), 974 (w), 757 (s), 696 (s), 557 (m); Elemental anal.: C 60.25, H 4.30 ($Pd_2C_{52}H_{43}O_3Cl_3$ requires C 60.34, H 4.19).

Crystals suitable for X-ray diffraction were grown by layering of a saturated $CHCl_3$ solution with *n*-hexane to afford the $Pd_2(dba)_3 \cdot CHCl_3$ adduct **238**. Crystals of the $Pd_2(dba)_3 \cdot CH_2Cl_2$ **249** and $Pd_2(dba)_3 \cdot C_6H_6$ **250** adducts were grown by slow evaporation from saturated solutions of CH_2Cl_2 and benzene, respectively.

Lab book reference number (Method A): AJR-8, pp. 91–92

Lab book reference number (Method B): AJR-4-335

N, *N*-dimethylanilinium tetrafluoroborate (252)
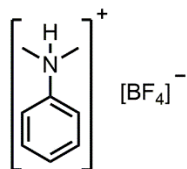
To Schlenk tube fitted with a magnetic stirrer was added aniline **251** (1 mL, 1 g, 8.25 mmol, 1 eq.). The Schlenk tube was then evacuated and backfilled with N_2 three times, before dry Et_2O (5 mL) was added with stirring. $HBF_4 \cdot OEt_2$ (1.2 mL, 1.42 g, 9.08 mmol, 1.1 eq.) was then added dropwise and after complete addition a biphasic mixture was formed, consisting of a cloudy upper Et_2O layer and a lower brown oil layer. The Et_2O layer was removed *via* cannula and the brown oil evaporated to form an off-white solid. This was redissolved in dry CH_2Cl_2 (5 mL), then dry Et_2O (5 mL) was added with stirring which formed the same brown oil as before. The Et_2O layer was removed *via* cannula and the brown oil evaporated to form an off-white solid. This was redissolved in dry CH_2Cl_2 (5 mL), then dry Et_2O (5 mL) was added with stirring, which caused an off-white solid to precipitate. The Et_2O was removed *via* cannula, then the solid with washed with fresh dry Et_2O (5 mL). This was removed *via* cannula then the solid was dried *in vacuo* to afford the *title compound* as an off-white solid (1.54 g, 89%).

M.P. 48–51 °C; ^{1}H NMR (400 MHz, CD_2Cl_2, δ): 9.51 (br s, 1H), 7.65–7.50 (m, 5H), 3.33 (d, *J* = 5.0 Hz, 6H); ^{13}C NMR (101 MHz, (CD_2Cl_2, δ): 142.3, 131.5, 120.6, 85.3, 48.6; ^{11}B NMR (128 MHz, CD_2Cl_2, δ): −1.9; ^{19}F NMR (376 MHz, CD_2Cl_2, δ): −151.1 (m, $^1J_{F-^{10}B}$, 4F), −151.1 (m, $^1J_{F-^{11}B}$, 4F); ESI–MS *m/z* (ion, %): 122 ([M−BF_4]$^+$, 100); ESI–HRMS *m/z*: 122.0965 [M−BF_4]$^+$ ($C_8H_{12}N$ requires 122.0964).

Lab book reference number: AJR-7-680

Behaviour of 238 in dry, degassed CDCl₃ under anhydrous conditions

To a Young's NMR tube handled in a dry glove box was added complex **238** (5 mg, 4.4 µmol, 1 eq.) dissolved in dry, degassed $CDCl_3$ (0.5 mL). ^{1}H NMR spectra were then recorded at 500 MHz 10 min after dissolution, then every 30 min for 24 h.

Lab book reference number: AJR-2-132

Behaviour of 238 in reagent grade CDCl₃

To an NMR tube was added complex **238** (5 mg, 4.4 µmol, 1 eq.) dissolved in $CDCl_3$ (0.5 mL). ^{1}H NMR spectra were then recorded at 500 MHz 10 min after dissolution, then every 30 min for 24 h.

Lab book reference number: AJR-2-128

Behaviour of 238 under anhydrous conditions with 1 eq. acid 252

In a dry glove box, acid **252** (0.92 mg, 4.4 µmol, 1 eq.) was dissolved in dry, degassed $CDCl_3$ (0.5 mL). This solution was then added to complex **238** (5 mg, 4.4 µmol, 1 eq.) and the resultant solution transferred to a Young's NMR tube. ^{1}H NMR spectra were then recorded at 500 MHz 10 min after dissolution, then every 30 min for 24 h.

Lab book reference number: AJR-2-138

Behaviour of 238 under anhydrous conditions with 3 eq. acid 252

In a dry glove box, acid **252** (2.8 mg, 13.2 µmol, 1 eq.) was dissolved in dry, degassed $CDCl_3$ (0.5 mL). This solution was then added to complex **238** (5 mg, 4.4 µmol, 1 eq.) and the resultant solution transferred to a Young's NMR tube. ^{1}H NMR spectra were then recorded at 500 MHz 10 min after dissolution, then every 30 min for 24 h.

Lab book reference number: AJR-2-141

Behaviour of 238 under anhydrous conditions with 10 eq. AcOH

To a Young's NMR tube handled in a dry glove box was added complex **238** (5 mg, 4.4 µmol, 1 eq.) dissolved in dry, degassed $CDCl_3$ (0.5 mL). This was removed from the glove box and AcOH (2.5 µL, 2.6 mg, 44 µmol, 10 eq.) was added under a flow of nitrogen. ^{1}H NMR spectra were then recorded at 500 MHz 10 min after dissolution, then every 30 min for 16 h. No degradation of the complex was observed during this period.

Lab book reference number: AJR-7-639

Behaviour of 238 under anhydrous conditions with 359 eq. AcOH

To a Young's NMR tube handled in a dry glove box was added complex **238** (5 mg, 4.4 µmol, 1 eq.) dissolved in dry, degassed $CDCl_3$ (0.5 mL). This was removed from the glove box and AcOH (100 µL, 95 mg, 1.58 mmol, 359 eq.) was added under a flow of nitrogen. ^{1}H NMR spectra were then recorded at 500 MHz 10 min after dissolution, then every 30 min for 16 h. No degradation of the complex was observed during this period.

Lab book reference number: AJR-7-677

Behaviour of 238 under anhydrous conditions with 10 eq. TFA

To a Young's NMR tube handled in a dry glove box was added complex **238** (5 mg, 4.4 µmol, 1 eq.) dissolved in dry, degassed $CDCl_3$ (0.5 mL). This was removed from the glove box and TFA (3.4 µL, 5 mg, 44 µmol, 10 eq.) was added under a flow of nitrogen. ^{1}H NMR spectra were then recorded at 500 MHz 10 min after dissolution, then every 30 min for 16 h.

Lab book reference number: AJR-7-670

Behaviour of 238 under anhydrous conditions with 298 eq. TFA

To a Young's NMR tube handled in a dry glove box was added complex **238** (5 mg, 4.4 µmol, 1 eq.) dissolved in dry, degassed $CDCl_3$ (0.5 mL). This was removed from the glove box and TFA (100 µL, 149 mg, 1.31 mmol, 298 eq.) was added under a flow of nitrogen. Visible decomposition to Pd black was observed within seconds. A ^{1}H NMR spectra was recorded at 500 MHz 10 min after dissolution, which matched that of the free ligand **247**.

Lab book reference number: AJR-7-675

Behaviour of 238 under anhydrous conditions with HBF₄·OEt₂

To a Young's NMR tube handled in a dry glove box was added complex **238** (5 mg, 4.4 µmol, 1 eq.) dissolved in dry, degassed $CDCl_3$ (0.5 mL). This was removed from the glovebox and HBF₄·OEt₂ (0.6 µL, 0.7 mg, 4.4 µmol, 1 eq.) was added under a flow of nitrogen. Visible decomposition to Pd black was observed within seconds. A ^{1}H NMR spectra was recorded at 500 MHz 10 min after dissolution, which matched that of the free ligand **247**.

Lab book reference number: AJR-7-637

ESI–MS study of complex 238

To a microwave tube equipped with a magnetic stirrer was added complex **238** (10 mg, 8.8 µmol, 1 eq.) and $CHCl_3$ (0.5 mL). In a separate microwave vial, acid **252** (1.8 mg, 8.8 µmol, 1 eq.) was dissolved in $CHCl_3$ (0.5 mL). The latter solution was then added to the solution containing complex **238**, the microwave vial was sealed and the reaction stirred at RT for 5 h. After 5 h an aliquot (4 µL) was removed and diluted 100-fold with a solution of CH_2Cl_2:MeOH (400 µL, 2:1, *v/v*). This was then analysed by ESI–MS with a carrier gas flow rate of 1200 µL h^{-1}.

Lab book reference number: AJR-7-688

ESI–MS study of complex 238 over eight hours

In a glove (dry) box, complex **238** (100 mg, 0.09 mmol, 1 eq.) was dissolved in dry, degassed $CHCl_3$ (5 mL) in a microwave vial equipped with magnetic stirrer. In a separate microwave vial, acid **252** (18 mg, 0.09 mmol, 1 eq.) was dissolved in dry, degassed $CHCl_3$ (5 mL). The latter solution was then added to the solution containing complex **238**, the microwave vial was sealed and the reaction stirred at RT for 5 min. After 5 min an aliquot (10 µL) was removed, then 4 µL of this solution was diluted 100-fold with a solution of CH_2Cl_2:MeOH (400 µL, 2:1, *v/v*). This was then analysed by ESI–MS with a carrier gas flow rate of 1200 µL h^{-1}. This sampling process was repeated every 30 min for 8 h.

Lab book reference number: AJR-8-705

ESI–MS study of complex 238 over 30 minutes

In a glove (dry) box, complex **238** (100 mg, 0.09 mmol, 1 eq.) was dissolved in dry, degassed $CHCl_3$ (5 mL) in a microwave vial equipped with magnetic stirrer. After complete dissolution, an aliquot (10 µL) was removed, then 4 µL of this solution was diluted 100-fold with a solution of CH_2Cl_2:MeOH (400 µL, 2:1, *v/v*). This was then analysed by ESI–MS with a carrier gas flow rate of 1200 µL h^{-1}. In a separate microwave vial, acid **252** (18 mg, 0.09 mmol, 1 eq.) was dissolved in dry, degassed $CHCl_3$ (5 mL). This solution was then added to the solution containing complex **238**, the microwave vial was sealed and the reaction stirred at RT for 2 min. After 2 min an aliquot (10 µL) was removed, then 4 µL of this solution was diluted 100-fold with a solution of CH_2Cl_2:MeOH (400 µL, 2:1, *v/v*). This was then analysed by ESI–MS with a carrier gas flow rate of 1200 µL h^{-1}. This sampling process was repeated every 2 min for 30 min.

Lab book reference number: AJR-8-707

Appendix 1: Published Papers

The following section contains, in chronological order, reproductions of papers which have been published with the contributions of the author in connection with the work described in this thesis.

1. Kapdi, A. R.; Whitwood, A. C.; Williamson, D. C.; Lynam, J. M.; Burns, M. J.; Williams, T. J.; Reay, A. J.; Holmes, J.; Fairlamb, I. J. S.; The elusive structure of $Pd_2(dba)_3$. Examination by isotopic labeling, NMR spectroscopy, and X-ray diffraction analysis: synthesis and characterization of $Pd_2(dba\text{-}Z)_3$ complexes, *J. Am. Chem. Soc.* **2013**, *135*, 8388–8399.

2. Williams, T. J.; Reay, A. J.; Whitwood, A. C.; Fairlamb, I. J. S.; A mild and selective Pd-mediated methodology for the synthesis of highly fluorescent 2-arylated tryptophans and tryptophan-containing peptides: a catalytic role for Pd^0 nanoparticles?, *Chem. Commun.* **2014**, *50*, 3052–3054.

3. Reay, A. J.; Williams, T. J.; Fairlamb, I. J. S.; Unified mild reaction conditions for C2-selective Pd-catalysed tryptophan arylation, including tryptophan-containing peptides, *Org. Biomol. Chem.* **2015**, *13*, 8298–8309.

4. Reay, A. J.; Fairlamb, I. J. S.; Catalytic C–H bond functionalisation chemistry: the case for quasi-heterogeneous catalysis, *Chem. Commun.*, **2015**, *51*, 16289–16307.

The Elusive Structure of Pd$_2$(dba)$_3$. Examination by Isotopic Labeling, NMR Spectroscopy, and X-ray Diffraction Analysis: Synthesis and Characterization of Pd$_2$(dba-Z)$_3$ Complexes

Anant R. Kapdi,[†] Adrian C. Whitwood, David C. Williamson, Jason M. Lynam, Michael J. Burns, Thomas J. Williams, Alan J. Reay, Jordan Holmes, and Ian J. S. Fairlamb*

Department of Chemistry, University of York, Heslington, York, North Yorkshire, YO10 5DD, United Kingdom

S *Supporting Information*

ABSTRACT: Pd^0$_2$(dba)$_3$ (dba = *E,E*-dibenzylidene acetone) is the most widely used Pd^0 source in Pd-mediated transformations. Pd^0$_2$(dba-Z)$_3$ (Z = dba aryl substituents) complexes exhibit remarkable and differential catalytic performance in an eclectic array of cross-coupling reactions. The precise structure of these types of complexes has been confounding, since early studies in 1970s to the present day. In this study the solution and solid-state structures of Pd^0$_2$(dba)$_3$ and Pd^0$_2$(dba-Z)$_3$ have been determined. Isotopic labeling (^{2}H and ^{13}C) has allowed the solution structures of the freely exchanging major and minor isomers of Pd^0$_2$(dba)$_3$ to be determined at high field (700 MHz). DFT calculations support the experimentally determined major and minor isomeric structures, which show that the major isomer of Pd^0$_2$(dba)$_3$ possesses bridging dba ligands found exclusively in a *s-cis,s-trans* conformation. For the minor isomer one of the dba ligands is found exclusively in a *s-trans,s-trans* conformation. Single crystal X-ray diffraction analysis of Pd^0$_2$(dba)$_3$·CHCl$_3$ (high-quality data) shows that all three dba ligands are found over two positions. NMR spectroscopic analysis of Pd^0$_2$(dba-Z)$_3$ reveals that the aryl substituent has a profound effect on the rate of Pd-olefin exchange and the global stability of the complexes in solution. Complexes containing the aryl substituents, 4-CF$_3$, 4-F, 4-t-Bu, 4-hexoxy, 4-OMe, exhibit well-resolved ^{1}H NMR spectra at 298 K, whereas those containing 3,5-OMe and 3,4,5-OMe exhibit broad spectra. The solid-state structures of three Pd^0$_2$(dba-Z)$_3$ complexes (4-F, 4-OMe, 3,5-OMe) have been determined by single crystal X-ray diffraction methods, which have been compared with Goodson's X-ray structure of Pd^0$_2$(dba-4-OH)$_3$.
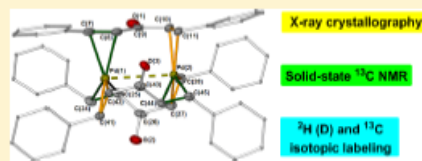
■ INTRODUCTION

Pd^0$_2$(dba)$_3$ is the most widely used Pd^0 precursor complex in synthesis and catalysis.[1] Since early studies in the 1970s, determination of the precise structure of Pd^0$_2$(dba)$_3$ has proven confounding *vide infra*. Dba acts as an olefin,[2] enone,[2] or 1,4-dien-3-one ligand and is often noninnocent[3] (i.e., involved in key steps) in catalytic processes.[4] [Pd^0(η^2-dba)L$_n$] (L = phosphine or N-heterocyclic carbene) complexes are formed in catalytic processes, generated by addition of ligand to Pd^0$_2$(dba)$_3$;[5] dba-ligation affects the concentration of Pd^{0}L$_n$ species available for oxidative addition with organohalides, the first committed step in cross-coupling processes, and can act positively in regulating the concentration of Pd^{0}L$_n$ when reactive organohalides are used (e.g., ArI) and reduce Pd agglomeration which can form large inactive Pd^0 clusters.[6] Recent selected examples where Pd^0$_2$(dba)$_3$ has been employed as a powerful catalyst system are given in Scheme 1, which range from a remarkable macrocyclization,[7] N^1-selective arylation of unsymmetrical imidazoles,[8] and a highly selective polycondensation process.[9]

By electronically tuning the aryl groups of dba (e.g., dba-Z,[10] where Z = OMe, *t*-Bu, H, F, CF$_3$), the noninnocent behavior has been exploited experimentally in several cross-coupling

processes,[11] and their effects supported by theoretical studies.[12] The dba-Z ligands also influence transmetalation and reductive elimination steps[13] and reduce the rate of β-hydrogen elimination in "Pd^{II}-σ-alkyl" complexes.[14] This latter finding facilitates intramolecular Heck reactions of alkenyl tethered alkyl bromides to give *exo*-cyclopentene products (providing dba-4-OMe is used). Furthermore, dba-4-Z (Z = CF$_3$ or OMe) ligands influence regiochemical effects in the cross-coupling of aryl halides with allylic siliolate salts.[15] The design of dba-structures incorporating thienyl (th) rings affords Pd^0$_2$(th-dba)$_3$ complexes, allowing oxidative addition rates to be controlled.[16] Pd$_2$(dba-4-OH)$_3$ and Pd$_2$(dba-4-OAc)$_3$ complexes have been adapted for use in aqueous Suzuki polycondensation reactions.[17]

In this paper we detail the synthesis and characterization of several Pd^0 complexes containing symmetrical aryl-substituted 'dba-Z' ligands. In order to achieve this task it has been necessary to study the solution and solid-state structures of the parent complex, Pd^0$_2$(dba)$_3$, and unambiguously determine its structure by use of isotopic labeling (^{2}H and ^{13}C). The solid-

Scheme 1. Powerful Pd₂(dba)₃-Mediated Coupling Processes

Figure 1. Three conformations for dba (I–III) and the solution structure(s) of $Pd^0{}_2(dba)_3$. Bold lines denote strong olefin bonding interactions (f > e > d), and dashed lines denote weak olefin bonding interactions (c > b > a). (A) and (B) are the isomers proposed as most likely in the Kawazura study.
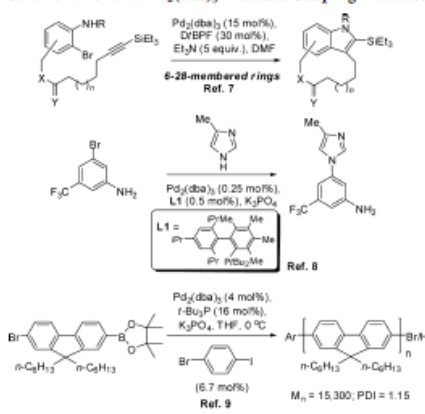
state characterization of a series of Pd₂(dba-Z)₃·CH₂Cl₂ complexes (Z = 3,5-OMe, 4-OMe, and 4-F) has been conducted by X-ray diffraction. The study is placed into context with that reported for Pd₂(dba-4-OH)₃,[17] specifically the importance associated with intermolecular H-bonding stabilizing one isomeric form (with no apparent conformational disorder) of the dba-backbone in the dinuclear Pd[0] complexes. For several $Pd_n(dba-Z)_{n+1}$ complexes it has been possible to probe their solution behavior and stability, by ^{1}H NMR spectroscopy, which is comparable to the spectroscopic data for Pd₂(dba)₃.

■ **RESULTS AND DISCUSSION**

Structure of Pd⁰₂(dba)₃ in CDCl₃ and Additional Context. In 1978 the solution behavior of Pd⁰₂(dba)₃·CHCl₃ [hereafter 'Pd⁰₂(dba)₃' unless reference is made to an alternative solvate] was valiantly investigated by Kawazura and co-workers[18] by a combination of ^{1}H NMR spectroscopy (at 100 MHz), ^{2}H labeling, and computational simulation. This work showed that each olefin in Pd⁰₂(dba)₃ can be found in a distinct chemical environment. That is six olefins coordinate to two chemically unique Pd[0] atoms, with each dba acting as a "η²-olefin,η²-olefin" bridging ligand. To explain why six olefins are observed spectroscopically one needs to consider that: (i) dba can exist in one of three 1,4-dien-3-one conformations (I–III, Figure 1); (ii) the preferred conformation for dba in binding Pd[0] in the dinuclear complex, Pd₂(dba)₃, being s-cis,s-trans (II); and (iii) the strength of the η²-olefin-metal bonding interactions, via coordination through s-cis and s-trans olefins, is different; the proposed solution-state structure of 'Pd₂(dba)₃' (one of two possible isomers) is shown in Figure 1.

The Kawazura study[18] relied on two pieces of information: (i) NOE proton contacts between neighboring olefins within two of the three coordinating dba ligands; and (ii) the chemical shift difference between α- and β-protons within individual olefins ($\Delta\alpha\beta = \delta\beta - \alpha$). This latter information can provide an indication of the enone conformation in dba.[19] For example in the noncoordinated dba the s-cis form has a minimum $\Delta\alpha\beta$
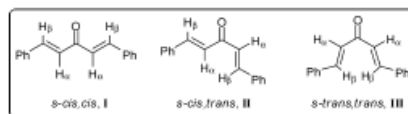
value of 0.5 ppm and in the s-trans form a maximum value of 1.5 ppm.

Deformation toward the s-skew form causes $\Delta\alpha\beta$ to increase for the s-cis conformer, whereas it decreases for the s-trans conformer. By extrapolation coordinated olefins with a small $\Delta\alpha\beta$ value (δ 0.069–0.186 ppm) were proposed to be in the s-cis form, whereas those with a large value (δ 0.631–0.965 ppm) were in a s-trans form. However, our recent work[20] on 'dba-coordinated' metal complexes (Rh, Pd, Pt, and Cu)[21] show that these ranges are underestimated, leaving the structural connectivity reliant on NOE contacts and a low-resolution ^{1}H NMR spectrum. It is clear that there are few structures containing palladium that are more spectroscopically confounding than 'Pd₂(dba)₃'.

In a study reported in 2012, Zalesskiy and Ananikov reported[22] high-field (600 MHz) NMR spectroscopic data for 'Pd₂(dba)₃' as a mixture of two isomers—the first time a second 'minor' isomer was reported in solution.[23] Through a combination of COSY, LR-COSY, HSQC, HMBC, and NOESY measurements, the authors proposed that the dba ligands in Pd₂(dba)₃ were in fact found in a s-cis,s-cis conformation, standing in stark contrast with the Kawazura study. [1]H DOSY measurements confirmed that the major and minor isomeric species had identical diffusion coefficients, i.e., two forms of Pd⁰₂(dba)₃. Following on from work on Pd⁰₂(dba-Z)₃ complexes, we were aware of their intricate solution NMR spectra (see later), due to their inherent low symmetry, dba-Z lability, and inter- and intramolecular exchange. On symmetry reasons alone it seemed unlikely that a s-cis,s-cis conformation would be preferred, i.e., on the NMR time scale all three ligands and associated olefins (six) would be expected to bind Pd[0] to the same extent, e.g., as averaged signals with only two α- and β-proton environments, which is not the case (free exchange occurs at ca. 298 K). The s-cis,s-cis conformations were discounted for these reasons in the Kawazura study.[18] Given these details, an independent high-field NMR spectroscopic study on the structure of Pd⁰₂(dba)₃ in solution (CDCl₃) was conducted. We selected Pd⁰₂(dba)₃·dba as from experience some free dba ligand is observed spectroscopically in solutions

224

Journal of the American Chemical Society

of $Pd^0_2(dba)_3$·solvent (solvent = $CHCl_3$, CH_2Cl_2, or benzene). At this point it is worth noting that $Pd^0_2(dba)_3$ is potentially sensitive in solution to photooxidation [λ_{max} = 520 nm (MLCT) in $CHCl_3$],[24] in addition to thermal degradation. A ^1H NMR spectrum (700 MHz) of $Pd^0_2(dba)_3$·dba [hereafter $Pd^0_2(dba)_3$] in alumina-filtered $CDCl_3$ reveals the Pd^0-olefin bonding interactions (Figure 2).
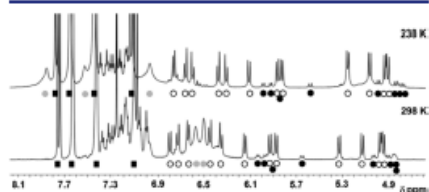
Figure 2. 700 MHz ^1H NMR spectra of $Pd^0_2(dba)_3$·dba at 298 K (bottom) and 238 K (top) (in $CDCl_3$, referenced to residual $CHCl_3$ at δ 7.26). Key: closed black square, free dba; closed gray circle, ortho-aryl protons; open circles, olefin protons in major species; closed black circles, olefin protons in minor species.

Free dba ligand is observed in the ^1H NMR spectrum (highlighted by black squares). Proton integration reveals the stoichiometry as $Pd^0_2(dba)_3$·dba (in agreement with the C,H composition indicated by elemental analysis). Two broad signals, indicative of an exchange process, are observed at ca. δ 6.35–6.65 ppm which are the shielded ortho-protons of the aromatic groups (ca. 12 H) connecting the 1,4-dienone moieties of three dba ligands in $Pd^0_2(dba)_3$ (indicated by gray circles). These broad signals overlap with resolved olefin protons in the same chemical shift region (at 298 K). Cooling

this solution to 238 K, where negligible inter- or intramolecular exchange occurs (established by EXSY experiments), resulted in the broad aromatic protons shifting to higher chemical shift (three broad signals at ca. δ 7.0, 7.55 and 7.85), leaving 12 resolved Pd^0-olefin protons signals.

The three dba ligands thus bridge two Pd^0 atoms in an unsymmetrical manner, e.g., "η^2-olefin,η^2-olefin", involving the coordination of six independent alkenes, i.e., three distinct dba ligands. Shown by open circles are the olefin protons attributed to six unique olefins in $Pd^0_2(dba)_3$. In both spectra run at 298 and 238 K, a minor species was also observed, akin to that reported by Zalesskiy and Ananikov.[22] Highlighted by black circles are eight olefin protons (Figure 2), which belong to the minor species (ratio of major/minor isomeric species 1:0.23 at 298 K).

The connectivity of each alkene in both major and minor isomers needed to be confirmed by a combination of NMR experiments and isotopic labeling (deuterium and ^{13}C; Figures 3 and 4). The latter was necessary to ascertain the position of
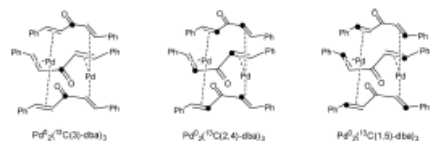
Figure 4. ^{13}C Isotopically labeled $Pd^0_2(dba)_3$ complexes synthesized for this study (black circle indicates the position of ^{13}C).

the α- and β-protons, which could allow each olefin to be located accurately. The isotopically labeled dba ligands and Pd^0 complexes were prepared in an identical manner to $Pd^0_2(dba)_3$
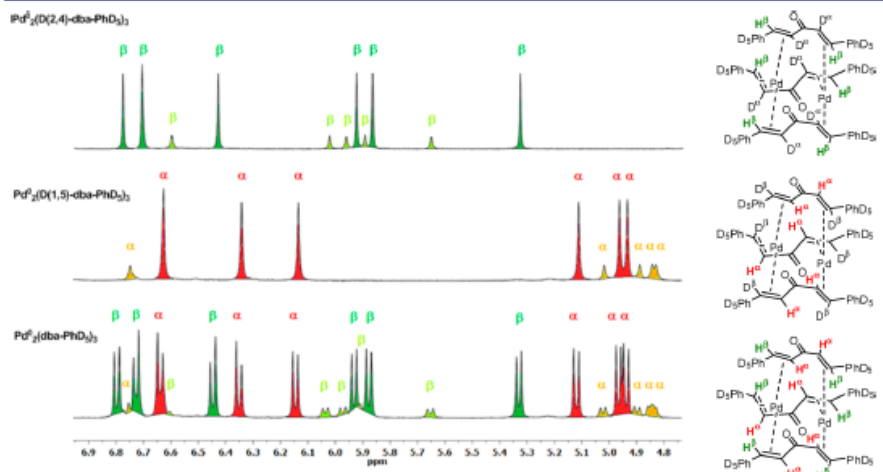
Figure 3. 700 MHz ^1H NMR spectra (at 298 K) of $Pd^0_2(D(2,4)$-dba-$PhD_5)_3$, $Pd^0_2(D(1,5)$-dba-$PhD_5)_3$, and $Pd^0_2(dba$-$PhD_5)_3$ (red and green colors used to depict the α- and β-protons in the major isomer). Note that ^1H–^2H spin–spin couplings are not observed in these spectra.

225

on small scale (typically 100 mg) (Figure 4). The ^{1}H NMR spectra of the deuterium-labeled Pd^0 complexes are shown in Figure 3.

Considering the major isomer then, the ^{1}H NMR spectrum for Pd$^0_2$(dba-PhD$_5$)$_3$ shows the α-protons (red) and β-protons (green), which were located by comparison with the spectra of Pd$^0_2$(D(1,5)-dba-PhD$_5$)$_3$ and Pd$^0_2$(D(2,4)-dba-PhD$_5$)$_3$. The protons do not exhibit spin–spin coupling to deuterium due to exchange at 298 K (in combination with small quadrupolar effects). The spectra for Pd$^0_2$(D(2,4)-dba-PhD$_5$)$_3$ and Pd$^0_2$(D-(1,5)-dba-PhD$_5$)$_3$ also reveal additional minor isomeric proton signals, shown in light green for the former complex and orange for the latter complex. These isomers were overlapping with the major species in the spectrum of Pd$^0_2$(dba-PhD$_5$)$_3$ [and unlabeled Pd$^0_2$(dba)$_3$].

As the ^{2}H labeling had been successful in locating the α- and β-protons in the major isomer of Pd$^0_2$(dba)$_3$ (and most of them in the minor isomer), we anticipated that ^{13}C labeling would provide valuable ^{13}C NMR spectroscopic data; due to the limited solubility of Pd$^0_2$(dba)$_3$ in CDCl$_3$ (ca. 5 mg/mL) it was deemed necessary to synthesize ^{13}C labeled analogues. The ^{13}C{^{1}H} NMR spectra of Pd$^0_2$(^{13}C(3)-dba)$_3$, Pd$^0_2$(^{13}C(2,4)-dba)$_3$, and Pd$^0_2$(^{13}C(1,5)-dba)$_3$ are shown in Figure 5, and the spectroscopic data is collated in Table 1. ^{13}C labeling shows the positions of all the ^{13}C nuclei within the 1,4-dien-3-one backbone of the three dba ligands, in both major and minor
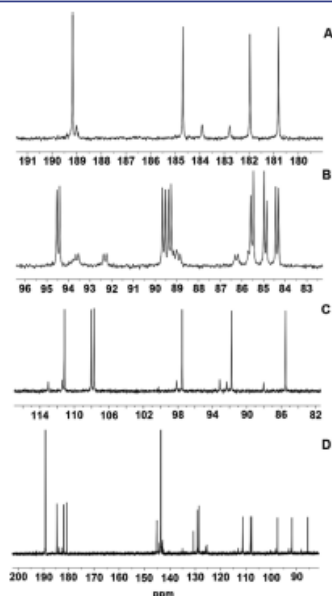
Figure 5. ^{13}C{^{1}H} NMR spectra (at 300 K, 125 MHz) of: (A) Pd$^0_2$(^{13}C(3)-dba)$_3$; (B) Pd$^0_2$(^{13}C(2,4)-dba)$_3$; (C) Pd$^0_2$(^{13}C(1,5)-dba)$_3$; (D) ^{13}C{^{1}H} NMR spectrum following addition of 1 equiv of ^{13}C(1,5)-dba to a CDCl$_3$ solution of Pd$^0_2$(^{13}C(3)-dba)$_3$.

isomers, and also reveals valuable ^{13}C–^{13}C spin–spin coupling information, e.g., in Pd$^0_2$(^{13}C(2,4)-dba)$_3$.

For the major and minor species of Pd$^0_2$(dba)$_3$ there are six independent olefins, confirming their isomeric relationship. In the major isomer the carbonyl moieties [located from Pd$^0_2$(^{13}C(3)-dba)$_3$] are all found in different chemical environments and shifted between δ 4.5–8.4 from the free dba ligand (δ 189.2). The minor isomer exhibits a similar coordination shift for two of the three dba ligands (δ 5.3 and 6.4). However, the remaining C=O signal exhibits a shift of only δ 0.2, which is very close to the free ligand. This latter signal could belong to a dba contaminant, rather than the minor isomer, leaving the remaining dba C=O overlapping with the major isomer of the Pd$^0_2$(^{13}C(3)-dba)$_3$.

The α-carbons (six) in the major isomer are in different chemical environments shifted to δ 84.4–94.5, and $^2J_{CC}$ coupling is observed between olefins within the same dba ligand. Three α-carbons can be grouped δ 84.4–85.5 and the remaining α-carbons δ 89.3–94.5. The magnitude of the coupling across the six α-carbons is 15.8–16.2 Hz ($\pm$0.1 Hz). Similar carbon signals are seen for the minor isomer; indeed the average coordination shifts from the free ligand are similar in both major and minor isomers (37.6 and 36.4 ppm, respectively). The coordination shift difference between the lowest and highest chemical shift signals was 10.1 and 8.0, for the major and minor isomers, respectively.

The β-carbons (six) in the major isomer are also in different chemical environments shifted to δ 85.5–111.2. Three β-carbons can be grouped δ 85.5–97.5 and the remaining β-carbons δ 107.7–111.2. Four β-carbon signals for the minor isomer can be grouped δ 88.0–98.1, with the remaining β-carbons δ 111.4–113.0. The average coordination shifts from the free ligand are similar in both major and minor isomers (43.3 and 44.3 ppm, respectively). The coordination shift difference between the lowest and highest chemical shift signals was 25.7 and 25.0 ppm for the major and minor isomers, respectively. Interestingly, four of the β-carbon signals in the minor isomer have a coordination shift >45 ppm, whereas only three of the β-carbon signals are >45 ppm in the major isomer. It is clear from these ^{13}C NMR spectra that the β-carbons are more responsive to coordination to Pd^0 than the α-carbons. EXSY experiments on this isotopically labeled derivative show that the exchange mechanism is complex (see SI for spectra). Spectrum D (Figure 5) shows the rapid exchange of added ^{13}C(1,5)-dba to Pd$^0_2$(^{13}C(3)-dba)$_3$ (in CDCl$_3$).

In keeping with the Kawazura study three of the olefins (H1 through to H6) are involved in strong binding to Pd^0 (denoted by 'S' in Table 1), and three olefins (H7–H12) are involved in weak binding (denoted by 'W' in Table 1). This was originally proposed by considering the average olefin chemical shifts.[18] It is noticeable that all the S olefins are found in a s-trans conformation with respect to the carbonyl group, whereas W olefins are found in a s-cis conformation. Thus, the 'S' olefins have average chemical shifts of δ 5.18 (olefin f), 5.45 (olefin e), and δ 5.56 (olefin d) and 'W' olefins δ 6.43 (olefin c), δ 6.51 (olefin b), and δ 6.72 (olefin a). A ^{13}C–COSY experiment confirmed the connection of α-carbons ($^2J_{CC}$ coupled), which along with ^{1}H–^{13}C HSQC experiments (see SI) allowed all the α- and β-carbons to be connected to their respective protons.

$^1J_{CH}$ couplings (ca. 157–160 Hz) are observed in ^{1}H NMR spectra of both Pd$^0_2$(^{13}C(2,4)-dba)$_3$ and Pd$^0_2$(^{13}C(1,5)-dba)$_3$, although no change in the magnitude of coupling as a function of chemical environment was recorded.

226

Article

Table 1. Combined ^{1}H and ^{13}C NMR Spectroscopic Data for the Major Isomer of Pd$^0_2$(dba)$_3$ in CDCl$_3$

olefin[a]	δ_α/ppm[b]	δ_β/ppm[b]	$\delta_{\beta-\alpha}$/ppm[c]	$\delta_{ave\,\alpha\beta}$[d]	J/Hz[e]	NOE[f]	olefin binding strength[g]	HMQC[h]	conformer/olefin (a–f)/dba (I–III)[i]
H1–H5	4.9 (H1)	5.9 (H5)	1.0	5.45	12.7 $^3J_{5H-4H5}$	H5β-H8α	S	C5–H5--H1	s-trans, e, I
C1–C5	84.9 (C1)	97.5 (C5)	12.6	91.0	15.8 $^2J_{C1-C2}$				
H2–H4	5.0 (H2)	5.36 (H4)	0.36	5.18	12.4 $^3J_{5H-5H}$	H4β-H10α	S	C4–H4--H2	s-trans, f, II
C2–C4	84.4 (C2)	85.5 (C4)	1.2	84.7	162 $^1J_{C3-C10}$				
H3–H6	5.16 (H3)	5.96 (H6)	0.8	5.56	13.0 $^3J_{5H-5H6}$	H6β-H7α	S	C6–H6--H3	s-trans, d, III
C3–C6	94.5 (C3)	91.8 (C6)	-2.7	92.9	15.8 $^2J_{C5-C7}$				
H7–H12	6.18 (H7)	6.83 (H12)	0.65	6.51	13.2 $^3J_{5H-5H12}$	H7α-H6β	W	C12–H12--H7	s-cis, b, III
C7–C12	89.6 (C7)	108.1 (C12)	18.5	98.7	15.8 $^2J_{C5-C3}$				
H8–H9	6.38 (H8)	6.48 (H9)	0.1	6.43	13.2 $^3J_{5H-5H9}$	H8α-H5β	W	C9–H9--H8	s-cis, c, I
C8–C9	85.5 (C8)	107.7 (C9)	22.2	96.4	15.8 $^2J_{C5-C1}$				
H10–H11	6.67 (H10)	6.76 (H11)	0.09	6.72	13.4 $^3J_{5H10-5H11}$	H10α-H4β	W	C11–H11--H10	s-cis, a, II
C10–C11	89.3 (C10)	111.2 (C11)	21.8	100	162 $^1J_{C10-C2}$				

[a]Protons numbered from the lowest chemical shift (H1) to highest chemical shift (H12). [b]Position of α- and β-protons was located from the ^{1}H and ^{13}C NMR spectra of the ^{2}H and ^{13}C labeled Pd$^0_2$(dba)$_3$ complexes. [c]Chemical shift difference between α- and β-protons. [d]Average chemical shift between α- and β-protons. [e]Spin–spin coupling constants determined from 1D ^{1}H and ^{13}C NMR spectra [with assistance from ^{1}H–COSY and ^{13}C-HMQC spectra (at 298 K), see SI]. [f]Determined by NOE measurements (quantitative; magnitude of NOE, ca. 10%). [g]Strength of olefin binding: for the strongest binding average ^{1}H and ^{13}C chemical shifts of α- and β-protons δ_{1H} 5.18–5.56 (δ_C 84.7–92.9) and weakest binding δ_{1H} 6.43–6.72 (δ_C 96.4–100). [h]The ^{1}H–^{13}C correlations were determined by an HMQC experiment with Pd$^0_2$(^{13}C(1,5)-dba), described as $^1J_{CxH}$ and $^2J_{CxH}$ e.g., $^1J_{C-5H5}$ and $^1J_{C-5H}$. [i]Conformation of alkene connected to the C=O group (determined by NOE), specific olefin (from ^{1}H–COSY) lettered according to average ^{1}H and ^{13}C chemical shifts of α- and β-protons (the olefin with the weakest binding to Pd^0 is denoted 'a' and that with the strongest binding 'f'. ^{13}C–^{13}C COSY (125 MHz) correlated signals for Pd$^0_2$(^{13}C(2,4)-dba), are 94.5 (C3) and 89.6 (C7) (conformer III); 89.3 (C10) and 84.4 (C2) (conformer II); 85.5 (C8) and 84.9 (C1) (conformer I).

With the data above in hand one can employ HSQC/HMQC and NOESY experiments to fully connect the protons and carbon environments in the individual dba ligands. The full structural connectivity of the major isomer of Pd$^0_2$(dba)$_3$ could be essentially deduced from the ^{1}H–COSY and NOESY data of the unlabeled Pd$^0_2$(dba)$_3$ (at 238 K, where there is negligible inter- or intramolecular exchange) (Figure 6 and Table 1). The NOE interactions (cross-peaks) provide unequivocal proof that each ligand in the major isomer is s-cis,s-trans. Specifically, H5β-H8α, H4β-H10α, and H6β-H7α (summarized in Figure 7).

The spectroscopic data for the minor isomer of Pd$^0_2$(dba)$_3$ are collated in the SI (summarized in Figure 8). Four of the olefins (H1′ through to H8′) are involved in strong binding to Pd^0 ($\delta_{ave\,\alpha\beta}$ < 5.5 ppm), and two olefins (H9′-H12′) are involved in weak binding (detected by ^{13}C–^{1}H correlations, HMQC, having very small αβ chemical shift separations).

The NOE data for the unlabeled complex allowed two of the olefins in one dba ligand to be paired, that is the β-protons H5′β and H7′β, which is therefore s-trans,s-trans. 2D NOESY on the Pd$^0_2$(D(2,4)-dba-PhD$_5$)$_3$ compound showed the same NOE cross-peak between the β-protons H5′ and H7′. A weak correlation is seen for H8′β with a proton at d 6.76. Due to resolution issues we could not fully deduce the proton–carbon connectivity for the minor isomer from HMQC or HSQC experiments (see SI). The ^{13}C–^{13}C COSY (125 MHz) spectrum of Pd$^0_2$(^{13}C(2,4)-dba)$_3$ in CDCl$_3$ showed well-resolved correlated signals; 93.6 and 89.1; 92.3 and 85.6; 88.9 and 86.2.

DFT Calculations. We estimate that there are 64 potential isomers of Pd$^0_2$(dba)$_3$. Considering the substantial computational effort needed to determine accurate structures for all of these isomers, DFT calculations were conducted on the four most likely isomers of Pd$^0_2$(dba)$_3$ (Table 2). The starting point used for the calculations was Goodson's X-ray structure of Pd$^0_2$(dba-4,4′-OH)$_3$,[17] which shows only one isomer in the

solid state (denoted isomer M in Table 2). Isomer M has the lowest relative energy (set to 0) of the four isomeric structures. Altering the conformation of one dba ligand in isomer M, i.e., the conformation of one enone (s-cis ↔ s-trans) gives isomers N and O. The isomer containing a s-trans,s-trans ligand is lower in relative energy than the isomer containing a s-cis,s-cis ligand. The structure containing all s-trans enones at Pd1 and all s-cis enones at Pd2 has the highest relative energy of the series. The order of relative energy (stability) is M < N < O ≪ P. Therefore, the most likely isomers, in comparison with the NMR spectroscopic data presented above, are M and N, i.e., major and minor isomers of Pd$^0_2$(dba)$_3$, respectively (Figure 9). It is interesting to note that the olefins occupying a s-trans conformation in isomers M and N are more strongly bound to Pd^0 in both isomeric structures, which is in keeping with the synergic (back-bonding) arguments that the s-trans olefin protons are more shielded than the s-cis olefins.

Single Crystal X-ray Structure of Pd$^0_2$(dba)$_3$·CHCl$_3$. There have been several X-ray crystal structure determinations of Pd$^0_2$(dba)$_3$·solvent (solvent = CH$_2$Cl$_2$[25] and CHCl$_3$;[34] for the former two ligands were found to be s-cis,s-trans and one ligand s-cis,s-cis, whereas the latter showed all ligands to be s-cis,s-trans).[26] The 'best structure' was reported by Pregosin and co-workers[27] in the late 1990s, which indicated that two of the dba ligands were disordered over two positions (around the 1,4-dien-3-one moieties),[28] that is complicated by conformational changes in the dba ligand (vis-à-vis s-cis and s-trans geometrical issues). Following many attempts over the last 10 years we are pleased to have accomplished a high-quality X-ray structure determination of Pd$^0_2$(dba)$_3$·CHCl$_3$ (the crystallized Pd$^0_2$(dba)$_3$·CHCl$_3$ was dissolved in fresh CHCl$_3$ and layered with hexane affording small purple crystals), giving final R indexes $[I \geq 2\sigma (I)]$ $R_1 = 0.0333$, w$R_2 = 0.0720$ (monoclinic, $P2_1/n$ space group, $Z = 4$). The data show that all three ligands are disordered over two positions each, with a ratio of 79:21

Journal of the American Chemical Society   Article
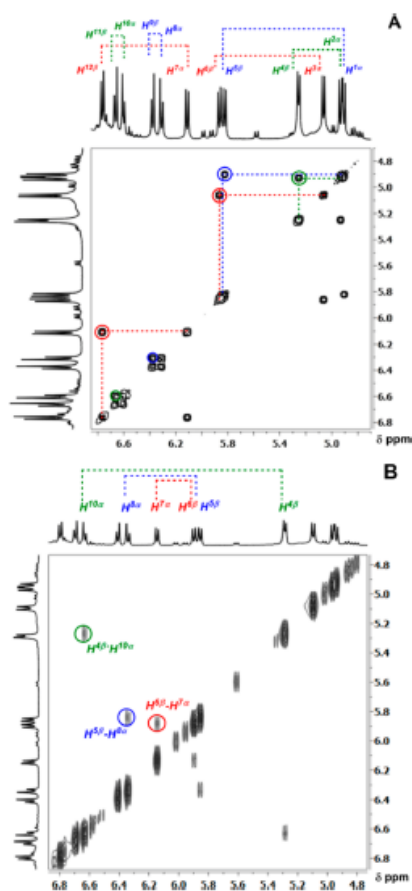
Figure 6. 700 MHz spectra of Pd⁰₂(dba)₃ (CDCl₃, 238 K). (A) ¹H–COSY; (B) ¹H NOESY spectrum (correlations for major isomer).

Figure 7. Proton connectivity in the major isomer of Pd⁰₂(dba)₃ established by COSY and NOESY experiments.
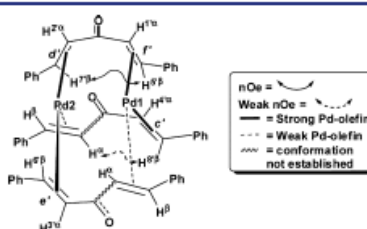
Figure 8. Proton connectivity in the minor isomer of Pd⁰₂(dba)₃ established by COSY and NOESY experiments. Note that it was not possible to accurately assign the positions of 4 protons, which have not been numbered, but they are weakly coordinated.

Table 2. Relative Energies for Pd⁰₂(dba)₃ Isomers by DFT

isomer	ΔE/kJmol⁻¹	$\Delta G_{298.15}$/kJmol⁻¹
Pd2(s-Z_β-Z_δ-E), Pd1 (s-E_β-E_δ-s-Z), M	0	0
Pd2(s-E_β-E_δ-Z), Pd1(s-E_β-E_δ-Z), N	3	5
Pd2(s-Z_β-E_δ-Z), Pd1(s-Z_β-Z_δ-E), O	16	16
Pd2(s-Z_β-Z_δ-Z), Pd1(s-E_β-E_δ-E), P	26	23

(Figure 10; note the *s-cis* olefins are shown bonded in green and *s-trans* olefins shown bonded in orange). Both isomeric forms are shown for clarity (A and B). The Pd(1)–Pd(2) bond distance is 3.244 Å. The average *s-cis* C=C bond distances in isomer 1 is 1.3603 Å. For the *s-trans* C=C bonds the average distance is 1.393 Å. It is noticeable from the C–Pd bond distances that the *s-cis* C=C bonds are coordinating in an asymmetric fashion (average Cα–Pd = 2.247 Å, Cβ–Pd = 2.287 Å), whereas the *s-trans* C=C bonds are more symmetric (average Cα–Pd = 2.228 Å, Cβ–Pd = 2.229 Å), indicating that there is more back-bonding in the *s-trans* C=C bonds.[25]

Synthesis and Characterization of Pd⁰₂(dba-Z)₃ Complexes. The Pd₂(dba-Z)₃·L complexes containing different

dba-Z ligands with varying aryl substituents were prepared by the method described by Ishii in 1970 (procedure A, Figure 11).[30] A large stock solution of Na₂PdCl₄ in MeOH was used for the synthesis of several Pd₂(dba-Z)ₙ₊₁ complexes. The required dba-Z ligand (3 equiv) was added to a MeOH solution of Na₂PdCl₄ and heated to 60 °C until complete dissolution. The exact composition of this mixture remains unknown. A Pdᴵᴵ complex, e.g., Na₂PdClₙ₊₂(dba-Z)₂, is a likely structure for the intermediate species, which is subsequently reduced. Six equiv of NaOAc were added to this solution, assisting the reduction process in alcoholic solvent (Pdᴵᴵ → Pd⁰). On cooling solutions to ambient temperature the complexes precipitate as brown-maroon or purple solids (note: Pd black is formed in all cases—usually deposited on the glassware surface). Following precipitation from solution, which usually occurs at 60 °C, the complexes are filtered (at ambient temperature), washed with MeOH and water, and then dried *in vacuo* (on a glass frit); small quantities of acetone or acetone/water (1:2, v/v) can be used to improve the purity of the complexes (note: for the majority of the complexes some product dissolution was observed using acetone alone, which lowers the overall yields). A series of Pd₂(dba-Z)₃·L complexes were prepared in this

228
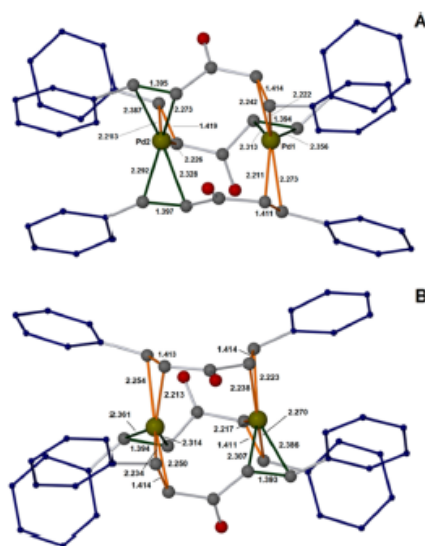
Figure 9. DFT calculated structures of (A) the major isomer of $Pd^0_2(dba)_3$ (M) and (B) the minor isomer of $Pd^0_2(dba)_3$ (N) (most likely isomers in solution). The bonds shown in green highlight the *s-cis* olefins and those shown in orange the *s-trans* olefins.

Figure 10. X-ray structure of $Pd^0_2(dba)_3 \cdot CHCl_3$: (A) isomer 1; (B) isomer 2. Thermal ellipsoids set to 50% (not shown for the phenyl groups for reasons of clarity; H-atoms not shown). The fragmented bond denotes the Pd(1)···Pd(2) bond. The bonds shown in green highlight the *s-cis* olefins and those shown in orange the *s-trans* olefins (arbitrary atom numbering used).

manner in acceptable yields (Table 3). The purity of the complexes was ascertained principally by element analysis (based on carbon and hydrogen percentage compositions). While one can ascertain the Pd:dba ratio for $Pd_2dba_3 \cdot dba$ in $CDCl_3$ by ^{1}H NMR spectroscopy, we believe it is not suitable for assaying the purity of $Pd_2(dba-Z)_3 \cdot L$ complexes, as they degrade to give Pd nanoparticles/particles in $CDCl_3$ (i.e., the outcome is dependent on the time between dissolution and spectroscopic analysis). This degradation process is well-known for $Pd^0_2(dba)_3$ in certain solvents[31] or reducing conditions, being a valuable precursor to Pd nanoparticles.[32]

For reactions where the dba-Z ligand was not fully dissolved, Pd^0 particle formation occurred quite readily (inferred by elemental analysis and low carbon and hydrogen composition and the appearance of fine particulate Pd black).[33]

It is pertinent to mention that several of these $Pd_2(dba-Z)_3 \cdot L$ complexes react cleanly with PPh_3 (in DMF) to afford $Pd^0(\eta^2\text{-}dba\text{-}Z)(PPh_3)_2$ complexes, which have been characterized by NMR spectroscopic analysis and cyclic voltammetric methods.[11b]

We have also tested the synthesis of the $Pd_2(dba-Z)_3 \cdot L$ complexes by the method described by Ishii in 1974 (procedure B),[34-35] from $PdCl_2$ [dba-Z ligand (3.3 equiv) and NaOAc (ca. 8 equiv) in MeOH, heated for 5 min at 50 °C, then $PdCl_2$ (1 equiv) added with heating for 4 h]. The $Pd_2(dba-4,4'-OHexyl)_3 \cdot dba-4,4'-OHexyl$ complex was prepared by this procedure. Dissolution in $CHCl_3$ showed that '$Pd_2(dba-4,4'-OHexyl)_3$' was as stable as the parent complex (TEM analysis showed negligible Pd nanoparticle formation). $Pd_2(dba-4-t-$

$Bu)_3 \cdot dba-4-t-Bu$ was also synthesized via procedure B in a similar yield (78%).

^{1}H NMR Spectroscopic Analysis of $Pd_2(dba-Z)_3$ Complexes. ^{1}H NMR spectra of the $Pd_2(dba-Z)_3$ complexes in $CDCl_3$ (ca. 5 mg in 0.7 mL) were obtained (Figure 12). Complexes where Z = OMe possess limited solubility in $CDCl_3$ (especially 3,4,5-OMe and 3,5-OMe derivatives, spectra A and B, Figure 12). Moreover, within hours these complexes degrade in $CDCl_3$ (liberating free dba-Z ligand). Nevertheless a ^{1}H NMR spectral overlay shows that all the complexes exhibit diagnostic Pd^0-olefin interactions (ca. 5–7 ppm), akin to

Figure 11. Synthesis of symmetrical $Pd_2(dba-Z)_3 \cdot L$ complexes.

Table 3. Yields of $Pd_2(dba-Z)_3 \cdot L$ Complexes

$Pd_2(dba-Z)_3 \cdot L$ (L = dba-Z or H_2O)	yield/%
$Pd_2(dba-3,4,5-OMe)_3$	59
$Pd_2(dba-3,5-OMe)_3 \cdot dba-3,5-OMe$	53
$Pd_2(dba-4-OMe)_3$	72
$Pd_2(dba-4-OHexyl)_3 \cdot dba-4-OHexyl$	70
$Pd_2(dba-4-t-Bu)_3$	75
$Pd_2(dba-4-F)_3 \cdot H_2O$	80
$Pd_2(dba-4-CF_3)_3 \cdot dba-4-CF_3$	69

8394

dx.doi.org/10.1021/ja403259c | J. Am. Chem. Soc. 2013, 135, 8388–8399

229
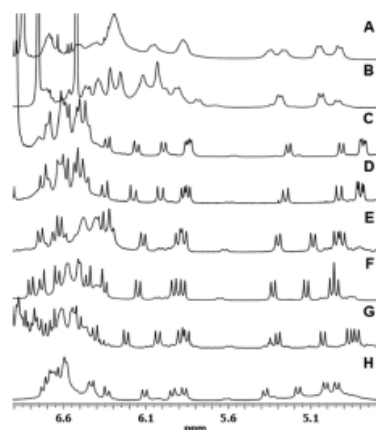
Figure 12. ^1H NMR spectra of $Pd^0_2(dba\text{-}Z)_3$ in $CDCl_3$ at 300 K (500 MHz, unless otherwise specified): (A) $Pd^0_2(dba\text{-}3,4,5\text{-}OMe)_3$; (B) $Pd^0_2(dba\text{-}3,5\text{-}OMe)_3$; (C) $Pd^0_2(dba\text{-}4\text{-}OMe)_3$; (D) $Pd^0_2(dba\text{-}4\text{-}OHexyl)_3$ (note 400 MHz spectrum); (E) $Pd^0_2(dba\text{-}4\text{-}t\text{-}Bu)_3$; (F) $Pd^0_2(dba)_3$; (G) $Pd^0_2(dba\text{-}4\text{-}F)_3$; (H) $Pd^0_2(dba\text{-}4\text{-}CF_3)_3$.

Figure 13. Selected ^{13}C-MAS spectra [100.56 MHz (recycle delays ca. 2–5 s, spin rate ca. 10 kHz)] of the $Pd_2(dba\text{-}Z)_3$ complexes: (A) $Pd^0_2(dba\text{-}3,4,5\text{-}OMe)_3$; (B) $Pd^0_2(dba\text{-}4\text{-}OMe)_3$; (C) $Pd^0_2(dba\text{-}4\text{-}t\text{-}Bu)_3$; (D) $Pd^0_2(dba)_3$; (E) $Pd^0_2(dba\text{-}4\text{-}F)_3$; (F) $Pd^0_2(dba\text{-}4\text{-}CF_3)_3$. Peaks colored orange are attributed as Pd-olefin carbon signals and red are attributed carbonyl signals.

$Pd_2(dba)_3$. That is in most cases there are 12 olefinic protons as expected in these dinuclear Pd complexes. ^1H COSY spectra of several complexes exhibit proton–proton correlations that are similar to $Pd_2(dba)_3$. We did not observe spectral broadening for $Pd_2(dba\text{-}4\text{-}OMe)_3$ and $Pd_2(dba\text{-}4\text{-}OHexyl)_3$.

Some broadening is observed for $Pd_2(dba\text{-}4\text{-}CF_3)_3$, although the signals for the major isomer are relatively sharp. Minor isomers for several of these complexes (uncharacterized) are evidenced by the small peaks in the ^1H NMR spectra, akin to $Pd_2(dba)_3$.

It is interesting to note that the position (chemical shift) of the olefin protons is affected to a certain degree by the remote aryl substituents, indicative of electronic communication in the complexes and in keeping with the electronic differences observed at the olefins in dba-Z derivatives.[12,36] Particularly noticeable is the shift of the most shielded olefin protons, H1 and H2, in spectra C and D in Figure 12.

The limited solubility of the $Pd^0_2(dba\text{-}Z)_3$ complexes prevented their solution ^{13}C NMR spectra from being obtained. However, the solid-state ^{13}C MAS spectra of a number of complexes gave some useful information (Figure 13). The parent complex, $Pd^0_2(dba)_3$, exhibits ^{13}C signals for Pd-olefins (ca. δ 80–105 ppm) and carbonyl moieties (ca. δ 180 ppm). Spinning side-bands are observed on the outer edges of the spectrum. For $Pd^0_2(dba\text{-}4\text{-}F)_3$ the intrinsic line width is quite high (spectral resolution is relatively limited), which could be a result of fluorine being in the system. For all other complexes there is a hint that the intrinsic line widths are relatively low, i.e., there are a high number of overlapping lines with similar shifts that limits the resolution, evidence for ligand inequivalence in each complex and multiple structures (i.e., conformers) in the asymmetric unit. It is important to emphasize that the solid-state structures of the $Pd^0_2(dba\text{-}Z)_3$ complexes mirror that of $Pd^0_2(dba)_3$ by ^{13}C MAS NMR.

X-ray Structures of Selected $Pd_2(dba\text{-}Z)_3$·L Complexes. Three $Pd_2(dba\text{-}Z)_3$ complexes (Z = 3,5-OMe, 4-OMe, and 4-F) could be crystallized from a CH_2Cl_2 solution layered with diethyl ether at room temperature. As with $Pd_2(dba)_3$·$CHCl_3$ we were able to obtain X-ray diffraction data for which structural refinement was possible. For example $Pd_2(dba\text{-}3,5\text{-}OMe)_3$·$CH_2Cl_2$ crystallized in the $P2_1/c$ space group (monoclinic, Z = 4) (Figure 14). The two alkenes in each ligand coordinating both Pd^0 centers are essentially eclipsed. Interestingly, the complex contains one dba-3,5-OMe ligand that can be found over two positions (occupancy = 0.682(3):0.318(3) or ca. 2.1:1). Similar disorder was noted for $Pd_2(dba\text{-}H)_3$·CH_2Cl_2 *vide supra*. The phenyl moieties and positions of the carbonyl groups in both conformers were resolved in the case of $Pd_2(dba\text{-}3,5\text{-}OMe)_3$·$CH_2Cl_2$. In essence, for each conformer there is a strict requirement for these moieties to exhibit different orientations. The Pd···Pd distance is 3.2314(5) Å, which compares with 3.244 Å in our X-ray structure of $Pd_2(dba\text{-}H)_3$·$CHCl_3$ and is indicative of a nonbonding interaction; the electron count on each Pd^0 center is 16. The tightly packed structure of $Pd_2(dba\text{-}3,5\text{-}OMe)_3$·$CH_2Cl_2$ is also illustrated in Figure 14, which shows that each Pd^0 atom is effectively shielded from solvent (or other ligands) in the solid state. There is also significant steric congestion between the 3,5-methoxy substituents in neighboring dba-3,5-OMe ligands.

Considering the major isomer of $[Pd_2(dba\text{-}3,5\text{-}OMe)_3$·$CH_2Cl_2]$, it is instructive to compare the C=C bond lengths of the coordinated ligand to each Pd center (Figure 15). For Pd1 the C=C bond, C(52A)–C(53A), orientated *s-trans* to the C=O group is significantly longer than the other two C=C bonds, one orientated *s-cis*, C(10)–C(11), and the other

each palladium center there is a *s-trans* C═C bond that is substantially longer than the other C═C bonds, indicative of back-bonding. The free ligand dba-3,5-OMe (see SI for X-ray structure) was found to (fortuitously) adopt a *s-cis,s-trans* conformation in a single crystal, with both C═C bonds showing the same distance (within error). The longest C═C bond, C(52A)—C(53A) in the complex is ca. 0.09 Å longer than the same bond in the free ligand.

The X-ray diffraction data for Pd₂(dba-4-OMe)₃·CH₂Cl₂ (monoclinic, $P2_1/n$ space group, $Z = 4$) and Pd₂(dba-4-F)₃·CH₂Cl₂ (triclinic, $P\bar{1}$, $Z = 2$) show that dba-Z ligand disorder is seen about the 1,4-dien-3-one moieties. In the case of Pd₂(dba-4-F)₃·CH₂Cl₂ each dba-4-F ligand is disordered over two positions; all could be satisfactorily modeled in a similar manner to Pd⁰₂(dba)₃·CHCl₃ (*vide supra*). The solvate molecules of crystallization appear to be crucial. In this context the X-ray structure[37] of Pd⁰₂(dba-4′—OH)₃ requires further examination. In this structure extensive H-bonding interactions between neighboring hydroxyls and carbonyl groups lock and stabilize the structure (Figure 16), which leads to only one isomeric form being observed in the solid-state. This is a unique case and stands in contrast to the other related structures detailed in this paper.

Figure 14. Top: X-ray structure of Pd₂(dba-3,5-OMe)₃·CH₂Cl₂. Hydrogens and 1 CH₂Cl₂ molecule omitted for clarity; one dba-3,5-OMe ligand is found over 2 positions [i.e., C(49A)-C(50A) and C(52A)-C(53A)] (only one ligand position shown). The bonds shown in green highlight the *s-cis* olefins and those shown in orange the *s-trans* olefins (arbitrary atom numbering used). Bottom: Space-filling models (each ligand has been colored red, blue and green to allow differentiation), left - side-on perspective and right - end-on perspective.
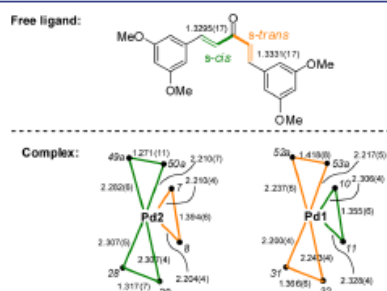
Figure 15. Selected bond lengths (X-ray diffraction data) of the olefins in the free ligand, dba-3,5-OMe, and Pd₂(dba-3,5-OMe)₃·CH₂Cl₂. We note that C49a—C50a is a particularly short C═C bond (larger estimated standard deviations are observed within the disordered ligand). The bonds shown in green highlight the *s-cis* olefins and those shown in orange the *s-trans* olefins.

s-trans, C(31)—C(32). The latter *s-cis* and *s-trans* C═C bonds are identical (within the error limits).

For Pd2 it is apparent that the C═C bond orientated *s-trans* to the C═O group, C(7)—C(8), is significantly longer than the two C═C bonds orientated *s-cis*, C(28)—C(29) and C(49A)—C(50A) (for the latter, foreshortening of this C═C bond can be explained in part by excessive thermal motion). Thus, for

Figure 16. H-bonding network seen for Pd⁰₂(dba-4,4′-OH)₃. Key H-bonding interactions (shown as blue fragmented bonds): O(2)···H-(7A)—O(7) = 1.689 Å, O(5)···H(4A)—O(4) = 1.819 Å, O(7)···H-(9A)—O(9) = 1.910 Å, O(8)···H(6A)—O(6) = 1.806 Å. The bonds shown in green highlight the *s-cis* olefins and those shown in orange the *s-trans* olefins.

■ CONCLUSION

The solution and solid-state structures of Pd⁰₂(dba)₃ and Pd⁰₂(dba-Z)₃-type complexes have been comprehensively determined. In the case of the former parent complex isotopic labeling (²H and ¹³C) was necessary to determine the solution structures of the freely exchanging major and minor isomers of Pd⁰₂(dba)₃; in the case of the major isomer of Pd⁰₂(dba)₃ this is unambiguous. It consists of three *s-cis,s-trans* ligands, where the *s-cis* olefins are weakly bound to Pd⁰ and the *s-trans* olefins strongly bound. Asymmetric dba coordination results, with one Pd⁰ atom coordinated to two *s-trans* olefins and one *s-cis* olefin, and the second Pd⁰ atom coordinated to two *s-cis* olefins and

one *s-trans* olefin. The minor isomer of $Pd^0_2(dba)_3$ possesses a *s-trans,s-trans* ligand and the chemical shifts of the β-protons indicate that four of the six olefins are *s-trans* and strongly bound to both Pd^0 centers, with the other two olefins being *s-cis*. This study brings about a resolution to the confounding molecular structure[18,22] of this ubiquitous complex in solution.

Theoretical calculations (DFT) support the feasibility of the experimentally determined major and minor isomeric structures in solution. The major isomer of $Pd^0_2(dba)_3$ contained three bridging dba ligands found exclusively in a *s-cis,s-trans* conformation. The minor isomer of $Pd^0_2(dba)_3$ reveals that one dba ligand is found exclusively in a *s-trans,s-trans* conformation. A high-resolution X-ray structure determination of $Pd^0_2(dba)_3$·$CHCl_3$ shows that all three dba ligands are disordered over two positions, which is an issue associated with the conformational flexibility around the 1,4-dien-3-one moiety in the solid-state.

NMR spectroscopic analysis of $Pd^0_2(dba-Z)_3$ reveals that the aryl substituent has a profound effect on the rate of Pd-olefin exchange (evidenced by the relative sharpness of their ^1H NMR spectra), in addition to their stability in solution (e.g., in $CDCl_3$). The solid-state structures of three $Pd^0_2(dba-Z)_3$·solvent complexes (4-F, 4-OMe, 3,5-OMe) have been determined by single crystal X-ray diffraction methods. As with $Pd^0_2(dba)_3$·$CHCl_3$, varying degrees of dba-Z disorder were observed, where the Z-substituent affects the distribution of isomers produced, an observation especially noticeable in the solid-state.

■ EXPERIMENTAL SECTION

General details for this section (NMR, MS, IR, UV—vis, X-ray, elemental analysis, TEM) are detailed in the SI. Important synthetic procedures and characterization data are presented below. Deuterium-labeled $Pd^0_2(D(2,4)-dba-PhD_5)_3$·$D(2,4)-dba-PhD_5$, $Pd^0_2(D(1,5)-dba-PhD_5)_3$·$D(1,5)-dba-PhD_5$, and $Pd^0_2(dba-PhD_5)_3$·dba-PhD_5 complexes have been previously reported.[18] Details of the ^{13}C-labeled dba compounds, and all other dba-Z ligands, are given in the SI (including representative NMR spectra).

General Synthesis of $Pd_2(dba)_3$·L and $Pd_2(dba-Z)_3$·L (L = dba/ dba-Z or solvate). Procedure A: NaCl (3.28 g, 56 mmol) was added to a solution of $PdCl_2$ (4.97 g, 28 mmol) in methanol (140 mL) and stirred at ambient temperature under an inert atmosphere for 24 h. The dark-brown solution was then filtered through a plug of cotton wool and concentrated *in vacuo* to approximately one-half of its original volume. The solution was warmed to 60 °C, and then dba (88 mmol, 3.1 equiv) was added (or dba-Z). The resulting mixture was stirred at 60 °C for 15 min, and then sodium acetate (13.78 g, 0.168 mol, 6 equiv) was added. The mixture was allowed to cool to ambient temperature (with no external cooling) and stirred for 2 h until a dark-red/purple precipitate was observed, which was filtered and washed with methanol (2 × 100 mL), water (2 × 50 mL), and finally acetone (2 × 5 mL). The product was partially dried under suction. The solid was transferred to a Schlenk flask and slowly dried by passage of nitrogen gas (with stirring) overnight. This gave the desired complexes as maroon/purple microcrystalline solids. These reactions work on a scale as low as ca. 0.1 g $PdCl_2$, in addition to using aliquots from stock solutions of Na_2PdCl_4 in methanol.

Procedure B: This procedure is similar to that reported by Ishii and co-workers[34] ($PdCl_2$, dba or dba-Z, NaOAc in MeOH at 40—50 °C) and by our group[16] for $Pd^0_2(th_n$-dba)_3·th_n-dba derivatives.

Characterization data for $Pd_2(dba)_3$·$CHCl_3$: Anal. calcd for $C_{52}H_{43}O_3Pd_2Cl_3$ (1135.09), C 60.34, H 4.19; Found, C 60.25, H 4.3. Single crystals of this pure material were grown from a saturated $CHCl_3$ solution layered with hexane, which gave purple rod-like crystals, from which one single crystal was selected for X-ray diffraction. Also noted were the formation of hexagon crystals,

however the X-ray diffraction data quality was poor, and a reasonable structure could not be determined.

Characterization Data for $Pd_2(dba-Z)_3$·dba-Z. In all cases the minor isomer could not be fully assigned, therefore the proton signals given are for the major isomer. The aromatic regions are broad in all cases; overlapping signals are observed for both major and minor isomeric forms for each complex. In all cases where resolved olefin proton signals are observed, we propose that the ligands adopt a *s-cis,s-trans* conformation, i.e., having a similar structure to the major isomer of $Pd^0_2(dba)_3$. The reactions were typically run using 0.1—0.25 g of $PdCl_2$.

[$Pd^0_2(dba-4-F)_3$·H_2O]. Yield = 80%; Mp 134—136 °C; UV (THF, nm) 518 (d—d); ^1H NMR 4.82 (1H, d, $^3J_{HH}$ = 12.5 Hz, H1), 4.87 (1H, d, $^3J_{HH}$ = 12.5 Hz, H2), 5.03 (1H, d, $^3J_{HH}$ = 13 Hz, H3), 5.30 (1H, d, $^3J_{HH}$ = 12.5 Hz, H4), 5.85 (1H, d, $^3J_{HH}$ = 13.5 Hz, H5), 5.89 (1H, d, $^3J_{HH}$ = 13 Hz, H6), 6.03 (1H, d, $^3J_{HH}$ = 13.5 Hz, H7), 6.22 (1H, d, $^3J_{HH}$ = 13 Hz, H8), 6.41 (1H, d, $^3J_{HH}$ = 13.5 Hz, H9), 6.44—7.03 (ca. 27 H, ArH, 3 olefin protons H10—H12); Anal. calcd for $C_{51}H_{38}F_6O_4Pd_2$ (1041.68), C 58.80, H 3.68; Found, C 58.95, H 4.10. Crystals suitable for X-ray analysis were grown from a CH_2Cl_2 solution of the complex (ca. 20 mg) layered with diethyl ether.

[$Pd^0_2(dba-4-t-Bu)_3$]. Yield = 75%; Mp 139—140 °C; UV (THF, nm) 533 (d—d); ^1H NMR 4.91 (1H, d, $^3J_{HH}$ = 13 Hz, H1), 4.95 (1H, d, $^3J_{HH}$ = 12.5 Hz, H2), 5.09 (1H, d, $^3J_{HH}$ = 13 Hz, H3), 5.30 (1H, d, $^3J_{HH}$ = 12 Hz, H4), 5.87 (1H, d, $^3J_{HH}$ = 13.5 Hz, H5), 5.91 (1H, d, $^3J_{HH}$ = 13 Hz, H6), 6.12 (1H, d, $^3J_{HH}$ = 13 Hz, H7), 6.31 (1H, d, $^3J_{HH}$ = 13.5 Hz, H8), 6.37 (1H, d, $^3J_{HH}$ = 13.5 Hz, H9), 6.60 (1H, d, $^3J_{HH}$ = 13.5 Hz, H10), 6.65 (1H, d, $^3J_{HH}$ = 13.5 Hz, H11), 6.74 (1H, d, $^3J_{HH}$ = 13.5 Hz, H12), 6.39—6.54 (ca. 6H, br m, overlapping with olefin protons H9—H10), 6.93—7.21 (ca. 12H, br m). Note: *t*-Bu protons overlapping with free ligand at δ 1.34; ESI-MS: *m/z* 821.1 [Pd(dba-4-*t*-Bu)_2 + Na]$^+$ (6), 929.1 [Pd_2(dba-4-*t*-Bu)_2Na]$^+$ (58); Anal. calcd for $C_{75}H_{90}O_3Pd_2$ (1252.36), C 71.93, H 7.24; Found, C 72.31, H 6.77. Crystals were grown from a CH_2Cl_2 solution of the complex (ca. 20 mg) layered with diethyl ether, however these gave poor quality X-ray diffraction data (a cif file is available from the authors).

[$Pd^0_2(dba-4-OMe)_3$]. Yield = 72%; Mp 141—143 °C; UV (THF, nm) 533 (d—d); ^1H NMR 4.78 (1H, d, $^3J_{HH}$ = 12.5 Hz, H1), 4.79 (1H, d, $^3J_{HH}$ = 12 Hz, H2), 4.91 (1H, d, $^3J_{HH}$ = 13 Hz, H3), 5.24 (1H, d, $^3J_{HH}$ = 12 Hz, H4), 5.84 (1H, d, $^3J_{HH}$ = 12.5 Hz, H5), 5.85 (1H, d, $^3J_{HH}$ = 12.5 Hz, H6), 5.99 (1H, d, $^3J_{HH}$ = 13 Hz, H7), 6.16 (1H, d, $^3J_{HH}$ = 13 Hz, H8), 6.33 (1H, d, $^3J_{HH}$ = 13 Hz, H9), ca. 6.1—7.5 (ca. 27H, br m, overlapping with olefin protons H10—H12). Note: Overlapping methoxy signals at δ 3.79, 3.80, and 3.82 (broad signals); ESI-MS: *m/z* (%) = 716.9 [Pd(dba-4-OMe)_2 + Na]$^+$ (6), 824.9 [Pd_2(dba-4-OMe)_2Na]$^+$ (66), 929.9 [Pd_2(dba-4-OMe)_2Na]$^+$ (61), 1035.8 [Pd_4(dba-4-OMe)_2Na]$^+$ (84); Anal. calcd for $C_{57}H_{54}O_9Pd_2$ (1095.87), C 62.47, H 4.97; Found, C 62.03, H 4.95. Crystals suitable for X-ray analysis were grown from a CH_2Cl_2 solution of the complex (ca. 20 mg) layered with diethyl ether.

[$Pd^0_2(dba-4-OHexyl)_3$·dba-4-OHexyl]. Yield = 70%; Mp 104—107 °C; UV ($CDCl_3$, nm) 540 (d—d); ^1H NMR 4.79 (1H, d, $^3J_{HH}$ = 12.5 Hz, H1), 4.80 (1H, d, $^3J_{HH}$ = 12 Hz, H2), 4.93 (1H, d, $^3J_{HH}$ = 13 Hz, H3), 5.25 (1H, d, $^3J_{HH}$ = 12 Hz, H4), 5.85 (1H, d, $^3J_{HH}$ = 12.5 Hz, H5), 5.87 (1H, d, $^3J_{HH}$ = 13 Hz, H6), 6.01 (1H, d, $^3J_{HH}$ = 13 Hz, H7), 6.18 (1H, d, $^3J_{HH}$ = 13.5 Hz, H8), 6.35 (1H, d, $^3J_{HH}$ = 13.5 Hz, H9), 6.41—6.80 (ca. 27H, br m, overlapping with olefin protons H10—H12). Note: Overlapping alkyl protons with free ligand at 0.92, 1.35, 1.48, 1.80, and 3.98 (broad signals). LIFDI-MS: *m/z* (%) = 1516.9 [Pd_2(dba-4-OHexyl)_3]$^{•+}$ (100); 1516.66 (calcd); Anal. calcd for $C_{116}H_{152}O_{12}Pd_2$ (1515.66), C 71.4, H 7.85; Found, C 71.61, H 7.76.

[$Pd^0_2(dba-4-CF_3)_3$·dba-4-CF_3·H_2O]. Yield = 69%; Mp 151—152 °C; UV (THF, nm) 534 (d—d); ^1H NMR 4.95 (1H, d, $^3J_{HH}$ = 13 Hz, H1), 5.02 (1H, d, $^3J_{HH}$ = 12.5 Hz, H2), 5.19 (1H, d, $^3J_{HH}$ = 13 Hz, H3), 5.39 (1H, d, $^3J_{HH}$ = 12.5 Hz, H4), 5.88 (1H, d, $^3J_{HH}$ = 13 Hz, H5), 5.95 (1H, d, $^3J_{HH}$ = 13 Hz, H6), 6.12 (1H, d, $^3J_{HH}$ = 13 Hz, H7), 6.35 (1H, d, $^3J_{HH}$ = 13.5 Hz, H8), 6.45 (1H, d, $^3J_{HH}$ = 13.5 Hz, H9), 6.41—6.80 (ca. 15H, br m, overlapping with olefin protons H10—H12), 7.27—7.58 (ca. 12H, br m); ESI-MS: *m/z* (%) = 846 [Pd_2(dba-4-

CF$_3$)$_2$]$^+$ (10), 975 [Pd$_2$(dba-4-CF$_3$)$_2$Na]$^+$ (15); Anal. calcd for C$_{56}$H$_{26}$F$_{12}$O$_2$Pd (865.01), C 52.76, H 3.03; Found, C 52.72, H 2.98.

[Pd^0$_2$(dba-3,5-OMe)$_3$·dba-3,5-OMe]. Due to the broadness of the proton signals the proton integrals are not reliable; selected data is therefore quoted (i.e., the peaks observed). The observed spin–spin coupling constants are averaged because of the exchange on the NMR time scale (due to intra- and intermolecular exchange). Yield = 53%; Mp 134–135 °C; UV (THF, nm) 530 (d–d); ^{1}H NMR 4.94 (1H, d, 12 Hz, H1), 5.04 (2H, d, 12 Hz, H2/H3), 5.29 (2H, d, 12 Hz, H4/H5), 5.78 (1H, d, 12 Hz, H6), ca. 6.2–7.5 (ca. 24 H, overlapping with olefin protons H7–H12). Note: Overlapping methoxy signals at δ 3.57–3.77 (broad signals). The free ligand exhibits a methoxy signal at 3.84; ESI-MS: m/z (%) = 838.9 [Pd$_1$(dba-3,5-OMe)$_2$ + Na]$^+$ (14), 944.9 [Pd$_2$(dba-3,5-OMe)$_2$Na]$^+$ (100); Anal. calcd for C$_{42}$H$_{44}$O$_{10}$Pd (815.21), C 61.88, H 5.44; Found, C 62.55, H 5.19. Crystals suitable for X-ray analysis were grown from a CH$_2$Cl$_2$ solution of the complex (ca. 20 mg) layered with diethyl ether.

[Pd^0$_2$(dba-3,4,5-OMe)$_3$]. Due to the broadness of the proton signals, the proton integrals are not reliable; selected data is therefore quoted (i.e., the peaks observed). Yield = 59%; Mp 194–197 °C; UV (THF, nm) 529 (d–d); ^{1}H NMR 4.92 (2H, d, 11 Hz, H1/H2), 5.05 (2H, d, 11 Hz, H3/H4), 5.21–5.31 (broad signal), 5.30–5.42 (broad signal), 5.82–5.93 (broad signal), 6.02–6.10 (broad signal), 6.17–6.55 (broad signal), 6.65–6.76 (broad signal). Note: Overlapping methoxy signals at 3.62, 3.68, 3.80, and 3.83 (broad signals). The liberated ligand exhibits methoxy signals at 3.90 and 3.92; Anal. calcd for C$_{69}$H$_{78}$O$_{21}$Pd$_2$ (1456.19), C 56.91, H 5.40; Found, C 57.31, H 5.46.

Details of DFT Calculations. All calculations were performed using the TURBOMOLE V5.10 package using the resolution of identity (RI) approximation.[38] Initial optimizations were performed at the (RI-)BP86/SV(P) level, followed by frequency calculations at the same level. All minima were confirmed as such by the absence of imaginary frequencies. Energies, geometries, and vibrational frequencies are presented in the SI. Single-point calculations on the (RI-)BP86/SV(P) optimized geometries were performed using the hybrid PBE0 functional and the flexible def2-TZVPP basis set. The (RI-)PBE0/def2-TZVPP SCF energies were corrected for their zero point energies (ΔE), thermal energies, and entropies (obtained from the (RI-)BP86/SV(P)-level frequency calculations at 298.15 K, Δ$G_{298.15}$). In all calculations, a 28 electron quasi-relativistic ECP replaced the core electrons of Pd. No symmetry constraints were applied during optimizations.

■ ASSOCIATED CONTENT

⑤ Supporting Information

All other synthetic procedures, characterization data (representative spectra), details, and X-ray diffraction details. This material is available free of charge via the Internet at http://pubs.acs.org.

■ AUTHOR INFORMATION

Corresponding Author
ian.fairlamb@york.ac.uk

Present Address
†Department of Chemistry, Institute of Chemical Technology, Matunga, Mumbai-400019, India

Notes
The authors declare no competing financial interest.

■ ACKNOWLEDGMENTS

■ REFERENCES

(1) (a) Littke, A. F.; Fu, G. C. Angew. Chem., Int. Ed. 2002, 41, 4176–4211. (b) Nolan, S. P. In N-Heterocyclic Carbenes in Synthesis; Wiley-VCH: Weinheim, 2006, pp 1–304. (c) Glorius, F. N.Topics in Organometallic Chemistry. In Heterocyclic Carbenes in Transition Metal Catalysis; Springer-Verlag: Berlin, 2006, Vol. 21, pp 1–218. (d) de Meijere, A.; Diederich, F. In Metal Catalyzed Cross-Coupling Reactions; Wiley-VCH: Weinheim, 2004, Vol. II.

(2) Moulton, B. E.; Duhme-Klair, A. K.; Fairlamb, I. J. S.; Lynam, J. M.; Whitwood, A. C. Organometallics 2007, 26, 6354–6365.

(3) (a) Amatore, C.; Jutand, A. Coord. Chem. Rev. 1998, 178–180, 511–528. (b) Amatore, C.; Jutand, A.; Meyer, G. Inorg. Chim. Acta 1998, 273, 76–84. (c) Jarvis, A. G.; Fairlamb, I. J. S. Curr. Org. Chem. 2011, 22, 3175–3196.

(4) Fairlamb, I. J. S. In Encyclopedia of Reagents for Organic Synthesis, John Wiley & Sons, Ltd: Hoboken, NJ, 2008; DOI: 10.1002/047084289X.rt400.pub2.

(5) (a) Amatore, C.; Jutand, A.; Khalil, F.; M'Barki, M. A.; Mottier, L. Organometallics 1993, 12, 3168–3178. (b) Fairlamb, I. J. S. Org. Biomol. Chem. 2008, 6, 3645–3656.

(6) The π-acidic alkene can increase catalyst stability, see: (a) Scrivanti, A.; Beghetto, V.; Matteoli, U.; Antonaroli, S.; Marini, A.; Mandoj, F.; Paolesse, R.; Crociani, B. Tetrahedron Lett. 2004, 45, 5861–5864. (b) Scrivanti, A.; Beghetto, V.; Matteoli, U.; Antonaroli, S.; Marini, A.; Crociani, B. Tetrahedron 2005, 61, 9752–9758. Fluorous dba-type ligands stabilize Pd nanoparticles, see: (c) Moreno-Mañas, M.; Pleixats, R.; Villarroya, S. Organometallics 2001, 20, 4524–4528. (d) Moreno-Mañas, M.; Pleixats, R.; Villarroya, S. Chem. Commun. 2002, 60–61. (e) Tristany, M.; Courmarcel, J.; Dieudonné, P.; Moreno-Mañas, M.; Pleixats, R.; Rimola, A.; Sodupe, M.; Villarroya, S. Chem. Mater. 2006, 18, 716–722.

(7) Brezzano, S. P.; Poudel, Y. B.; Boger, D. L. J. Am. Chem. Soc. 2013, 135, 1600–1606.

(8) Ueda, S.; Su, M.; Buchwald, S. L. J. Am. Chem. Soc. 2012, 134, 700–706.

(9) Zhang, H.-H.; Xing, C.-H.; Hu, Q.-S. J. Am. Chem. Soc. 2012, 134, 13156–13159.

(10) In our previous papers, see refs 5b and 11, we have referred to the aryl substituted dibenzylidene acetones as dba-n,n'-Z, which in this paper is simplified to dba-Z for symmetrical compounds.

(11) (a) Fairlamb, I. J. S.; Kapdi, A. R.; Lee, A. F. Org. Lett. 2004, 6, 4435–4438. (b) Macé, Y.; Kapdi, A. R.; Fairlamb, I. J. S.; Jutand, A. Organometallics 2006, 25, 1795–1800. (c) Fairlamb, I. J. S.; Kapdi, A. R.; Lee, A. F.; McGlacken, G. P.; Weissburger, F.; de Vries, A. H. M.; Schmieder-van de Vondervoort, L. Chem—Eur. J. 2006, 12, 8750–8761. For related work with ionic chalcones, see: (d) Bauerlein, P. S.; Fairlamb, I. J. S.; Jarvis, A. G.; Lee, A. F.; Müller, C.; Slattery, J. M.; Thatcher, R. J.; Vogt, D.; Whitwood, A. C. Chem. Commun. 2009, 5734–5736.

8398

dx.doi.org/10.1021/ja403259c | J. Am. Chem. Soc. 2013, 135, 8381–8399

(12) Fairlamb, I. J. S.; Lee, A. F. *Organometallics* **2007**, *26*, 4087–4089.

(13) (a) Zhao, Y.; Wang, H.; Hou, X.; Hu, Y.; Lei, A.; Zhang, H.; Zhu, L. *J. Am. Chem. Soc.* **2006**, *128*, 15048–15049.   For related ligand effects, see: (b) Liu, Q.; Duan, H.; Luo, X.; Tang, Y.; Li, G.; Huang, R.; Lei, A. *Adv. Synth. Catal.* **2008**, *350*, 1349–1354. (c) Luo, X.; Zhang, H.; Duan, H.; Liu, Q.; Zhu, L.; Zhang, T.; Lei, A. *Org. Lett.* **2007**, *9*, 4571–4574. (d) Shi, W.; Luo, Y.; Luo, X.; Chao, L.; Zhang, H.; Wang, J.; Lei, A. *J. Am. Chem. Soc.* **2008**, *130*, 14713–14720.

(14) Firmansjah, L.; Fu, G. C. *J. Am. Chem. Soc.* **2007**, *129*, 11340–11341.

(15) (a) Denmark, S. E.; Werner, N. S. *J. Am. Chem. Soc.* **2008**, *130*, 16382–16393. (b) Denmark, S. E.; Werner, N. S. *J. Am. Chem. Soc.* **2010**, *132*, 3612–3620.

(16) Sehnal, P.; Taghzouti, H.; Fairlamb, I. J. S.; Jutand, A.; Lee, A. F.; Whitwood, A. C. *Organometallics* **2009**, *28*, 824–829.

(17) Eddy, J. W.; Davey, E. A.; Malsom, R. D.; Ehle, A. R.; Kassel, S.; Goodson, F. E. *Macromolecules* **2009**, *42*, 8611–8614.

(18) Kawazura, H.; Tanaka, H.; Yamada, K.-i.; Takahashi, T.; Ishii, Y. *Bull. Chem. Soc. Jpn.* **1978**, *51*, 3466–3470.

(19) Tanaka, H.; Yamada, K.-i.; Kawazura, H. *J. Chem. Soc., Perkin Trans. II* **1978**, 231–235.

(20) Jarvis, A. G. PhD thesis, University of York, U.K., 2010.

(21) (a) Jarvis, A. G.; Whitwood, A. C.; Fairlamb, I. J. S. *Dalton Trans.* **2011**, *40*, 3695–3702. (b) Jarvis, A. G.; Sehnal, P. E.; Bajwa, S. E.; Whitwood, A. C.; Zhang, X.; Cheung, M. S.; Lin, Z.; Fairlamb, I. J. S. *Chem. Eur. J.* **2013**, *19*, 6034–6043.

(22) Zalesskiy, S. S.; Ananikov, V. P. *Organometallics* **2012**, *31*, 2302–2309.

(23) Preliminary data from our isotopic labeling study, highlighted herein, which showed the major and minor isomers of $Pd^0_2(dba)_3$ were reported (presented by Fairlamb, I. J. S.) at two separate international conferences: (a) ICOMC conference in Zaragoza, Spain in July 2006. (b) Canadian Chemical Society conference, Winnipeg, Canada in May 2007.

(24) Flash photolysis experiments on $Pd^0_2(dba)_3$, resulting in complex deactivation, have been reported, see: Hubig, M. S.; Drouin, M. A.; Michel, A.; Harvey, P. D. *Inorg. Chem.* **1992**, *31*, 5375–5380.

(25) (a) Pierpont, C. G.; Mazza, M. C. *Inorg. Chem.* **1974**, *13*, 1891–1895. (b) Mazza, M. C.; Pierpont, C. G. *J. Chem. Soc., Chem. Commun.* **1973**, 207–208.

(26) The X-ray structure of $Pd(dba)_3$·benzene has been determined: Mazza, M. C.; Pierpont, C. G. *Inorg. Chem.* **1973**, *12*, 2955–2959.

(27) Selvakumar, K.; Valentini, M.; Wörle, M.; Pregosin, P. S.; Albinati, A. *Organometallics* **1999**, *18*, 1207–1215.

(28) In Pregosin's structure of $Pd_2(dba)_3$·CH_2Cl_2 (ref 27) the phenyl groups in the different dba conformers were not differentiated, although excessive thermal disorder was seen.

(29) Zhao, H.; Ariafard, A.; Lin, Z. *Inorg. Chim. Acta* **2006**, *359*, 3527–3534.

(30) Takahashi, Y.; Ito, T.; Sakai, S.; Ishii, Y. *J. Chem. Soc., Dalton Trans.* **1970**, 1065–1066.

(31) Franzen, S. *J. Chem. Educ.* **2011**, *88*, 619–623   and references cited therein.

(32) (a) Franzen, S.; Cerruti, M.; Leonard, D. N.; Duscher, G. *J. Am. Chem. Soc.* **2007**, *129*, 15340–15346. (b) Leonard, D. N.; Cerruti, M.; Duscher, G.; Franzen, S. *Langmuir* **2008**, *24*, 7803–7809. (c) Leonard, D. N.; Franzen, S. *J. Phys. Chem. C* **2009**, *113*, 12706–12714.

(33) We did not characterize the Pd particles formed in the majority of these reactions, as one can observe them by the naked eye, indicating that they are large (>10 μm).

(34) Ukai, T.; Kawazura, H.; Ishii, Y.; Bonnet, J. J.; Ibers, J. A. *J. Organomet. Chem.* **1974**, *65*, 253–266.

(35) See ref 16 – from this previous work we used *procedure B* to access palladium complexes containing thienyl analogues of dibenzylideneacetone (dba), without issue.

(36) (a) Harvey, P. D.; Adar, F.; Gray, H. B. *J. Am. Chem. Soc.* **1989**, *111*, 1312–1315. (b) Hubig, S. M.; Drouin, M.; Michel, A.; Harvey, P. D. *Inorg. Chem.* **1992**, *31*, 5375–5380.

(37) SQUEEZE was used to correct for disordered solvent, as there appears to be a large void/channel in the center of the unit cell which may be a place for solvent to aggregate. While this is not an issue for the actual structure determination, it could affect the values of R and $wR2$.

(38) (a) Csaszar, P.; Pulay, P. *J. Mol. Struct.* **1984**, *114*, 31–34. (b) Ahlrichs, R.; Bar, M.; Haser, M.; Horn, H.; Kolmel, C. *Chem. Phys. Lett.* **1989**, *162*, 165–169. (c) Eichkorn, K.; Treutler, O.; Ohm, H.; Haser, M.; Ahlrichs, R. *Chem. Phys. Lett.* **1995**, *240*, 283–289. (d) Treutler, O.; Ahlrichs, R. *J. Chem. Phys.* **1995**, *102*, 346–354. (e) Eichkorn, K.; Weigend, F.; Treutler, O.; Ahlrichs, R. *Theo.Chem. Acc.* **1997**, *97*, 119–124. (f) Arnim, M. v.; Ahlrichs, R. *J. Chem. Phys.* **1999**, *111*, 9183–9190. (g) Deglmann, P.; Furche, F. *J. Chem. Phys.* **2002**, *117*, 9535–9538. (h) Deglmann, P.; Furche, F.; Ahlrichs, R. *Chem. Phys. Lett.* **2002**, *362*, 511–518. (i) Deglmann, P.; May, K.; Furche, F.; Ahlrichs, R. *Chem. Phys. Lett.* **2004**, *384*, 103–107.

8399

dx.doi.org/10.1021/ja403259c | *J. Am. Chem. Soc.* 2013, 135, 8388–8399

ChemComm

COMMUNICATION

A mild and selective Pd-mediated methodology for the synthesis of highly fluorescent 2-arylated tryptophans and tryptophan-containing peptides: a catalytic role for Pd⁰ nanoparticles?†

Thomas J. Williams, Alan J. Reay, Adrian C. Whitwood and Ian J. S. Fairlamb*

A Pd-mediated direct C–H bond functionalisation of tryptophan has been developed, both as a single amino acid residue and within peptides. Important mechanistic insight into this process has been gained by characterising a Pd catalytically competent nanoparticle phase which evolves during the early stages of reaction.

The functionalisation and modification of complex biomolecules by the formation of C–C bonds has benefited significantly from the development of mild conditions for Pd-mediated cross-coupling reactions.[1] Pioneering work by Davis and co-workers has, for example, demonstrated that it is possible to perform Suzuki–Miyaura reactions on proteins containing genetically incorporated aryl iodides.[2] Metal-mediated direct functionalisation of C–H bonds in complex molecule synthesis is a rapidly expanding field, including in the total synthesis of natural compounds.[3] We have reported the mild and selective direct C–H functionalisation of highly sensitive purine nucleosides, *e.g.* adenosine and 2′-deoxyadenosine.[4] As part of these studies we have been able to gain valuable mechanistic insight, most notably characterizing the formation of Pd/Cu-containing nanoparticles during substrate turnover. In this study, we have turned our attention to the mild[5] C–H bond functionalisation of amino acids,[6] specifically tryptophan, a hydrophobic indole-containing amino acid which alters the structure and function of proteins, and is a fluorescent marker.[7]

The C–H bond functionalisation of indoles mediated by Pd is well established.[8] We recognised that Sanford's methodology[8d] could be applied to selectively functionalise tryptophan, which employs PhB(OH)₂ and PhI(OAc)₂ as reagents, forming diaryliodonium salts *in situ*,[9] and catalytic Pd(OAc)₂. These reactions could proceed *via* a Pd[II/IV] catalytic manifold.[10] In this paper we detail the selective arylation of tryptophan and tryptophan-containing peptides under mild catalytic conditions.

Department of Chemistry, University of York, York, UK YO10 5DD.
E-mail: ian.fairlamb@york.ac.uk

† Electronic supplementary information (ESI) available: Experimental details and crystallographic data. CCDC 968490 and 968491. For ESI and crystallographic data in CIF or other electronic format see DOI: 10.1039/c3cc48481e
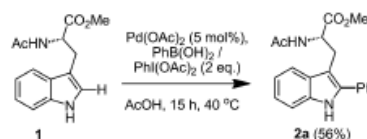
Fig. 1 Direct arylation of tryptophan under mild conditions.

Sanford's reaction conditions were initially applied to *N*-acetyl, *O*-methyl protected-tryptophan **1** to afford, after column chromatography, 2-phenyltryptophan **2** in 56% yield (Fig. 1). Changes to the catalytic conditions included modifying the Pd catalyst and loading, solvent, inert atmosphere and reaction temperature, but no increase in yield was recorded. Optimal turnover numbers and yields were seen between 2.5–5 mol% Pd.

Intriguingly, reaction of **1** with PhB(OH)₂ and PhI(OAc)₂ led to the rapid formation of Pd⁰ nanoparticles (PdNPs) during the first few minutes of the reaction. This finding is in keeping with another Pd-mediated C–H bond functionalisation of benzoxazoles using PhI(OAc)₂, which we recently reported upon.[11] The *in situ* generated PdNPs from reaction **1** → **2a** were encapsulated by addition of exogenous polymer stabiliser (*i.e.* polyvinylpyrrolidinone, PVP), which was added to an aliquot of the reaction mixture after 1 h (2.5 mL, containing ∼4.8 μmol Pd; 10 equiv. PVP added and AcOH removed at 40 °C and *ca.* 0.750 mmHg). This allows reliable analysis of the size and distribution of the PdNPs without concern that solvent removal leads to metal aggregation. Transmission electron microscopy (TEM) confirmed the presence of the encapsulated PdNPs (*n* = 100; average PdNP size is 2.52 nm, represented in Fig. 2).[12]

Pre-synthesised PVP-PdNPs[13] (average size ∼1.8 nm, Pd⁰, 5 mol%) were also found to be a viable catalytic species for the tryptophan arylation, affording **2a** in 57% yield (Fig. 3). This result shows that PdNPs are catalytically competent under the reaction conditions. In the example given in Fig. 1, we propose that the PdNPs are acting as a reservoir for Pd⁰, akin to related Heck arylation chemistry.[14] Glorius and co-workers have nicely

This journal is © The Royal Society of Chemistry 2014

235

Communication
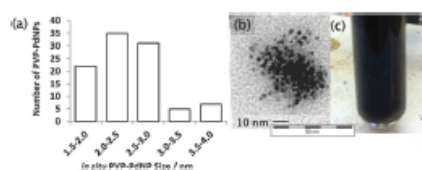
Fig. 2 (a) Histogram of particle size (diameter, nm) for a sample of PdNPs (encapsulated by PVP); (b) TEM image of PVP-encapsulated PdNPs after 1 h heating; (c) appearance of PdNPs in reaction.
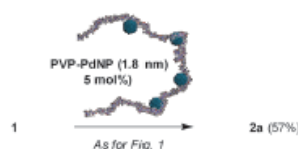
Fig. 3 Pre-synthesised PVP-PdNPs are catalytically competent species in the arylation of **1** to afford **2a**.
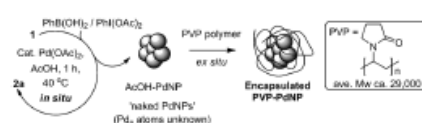
Scheme 1 PVP-encapsulation of *in situ* generated PdNPs from the reaction detailed in Fig. 1 (TEM characterisation in Fig. 2).
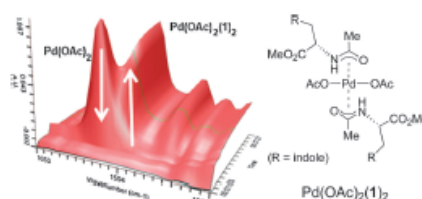
Fig. 4 Changes in the IR spectra observed on the reaction of Pd(OAc)$_2$ (1616 cm^{-1}) with **1**, affording Pd(OAc)$_2$(**1**)$_2$ (1606 cm^{-1}).

shown that heterogeneous C–H bond activation is viable in benzo[*b*]thiophene arylation (Scheme 1).[15]

The reaction of tryptophan **1** with Pd(OAc)$_2$ (1:1) in THF at ambient temperature (0.5 h) was monitored by *in situ* infrared spectroscopy (Fig. 4). The carbonyl stretching band at 1616 cm^{-1} is Pd(OAc)$_2$, which disappears on addition of **1**, with the appearance of a new band at 1606 cm^{-1}, proposed to be Pd(OAc)$_2$(**1**)$_2$. Only small changes were noted by ^{1}H NMR spectroscopic analysis, which is in keeping with the tryptophan ligand being weakly coordinated to Pd^{II}. Crucially, Pd(OAc)$_2$(**1**)$_2$ rapidly reduces to form Pd^0 and is the seed that leads to the generation of PdNPs under the catalytic conditions – amine ligands lower the Pd^{II} reduction potential to give Pd^0 ions.[4b]
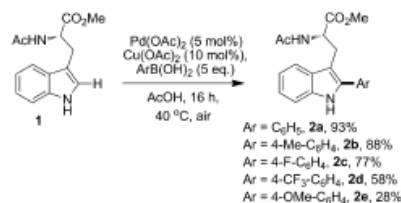
Fig. 5 Arylation of tryptophan using Cu(OAc)$_2$ as a co-catalyst.

Following this study, some limitations were revealed in terms of the substrate scope using Pd(OAc)$_2$ as the precatalyst.‡ For example, a simple switch from PhB(OH)$_2$ to 4-MeC$_6$H$_4$B(OH)$_2$ led to the biaryl compound derived from the latter only {PhI(OAc)$_2$ could be aiding oxidative homocoupling of the aryl boronic acid}.[16] Simply switching the oxidant to Cu(OAc)$_2$ afforded **2a** in 93% yield (under the conditions described in Fig. 5). Here, Cu(OAc)$_2$ is assisting the reoxidation of Pd^0 (with O$_2$ from air). This was confirmed by conducting the same reaction under an Ar atmosphere, which showed ∼11% conversion to **2a**, *i.e.* a single turn-over of the Cu^{II} co-catalyst. A series of analogues (**2b**–**2d**) were formed in good yields using this procedure. The electron-rich *p*-anisoyl boronic acid was susceptible to oxidative homocoupling, leading to **2e** being formed in modest yield, expected under oxidative conditions.

The specific optical rotations of the products, and analysis by chiral HPLC, indicated that the arylated tryptophan products maintained their stereochemical purity (see ESI†).

Single crystal X-ray diffraction structures for analogues **2c** and **2d** (Fig. 6), confirm absolutely their structural connectivity. The data shows in the solid-state that the aryl and indole groups deviate from planarity, which is likely a crystal packing effect. The conformational preference of the ester, amino and aryl moieties could affect the intrinsic fluorescence properties and provide a useful starting point for future TDDFT calculations.

UV-vis and fluorescence measurements reveal the effect of the different aryl groups within the tryptophan framework (Fig. 7). The most electronically distinct analogues, **2d** (4-CF$_3$) and **2e** (4-OMe), exhibit the highest absorption shifts, generating a characteristic V-shape. Such a correlation has been reported by Marder and co-workers in 1,4-bis(*p-R*-phenylethynyl)benzenes
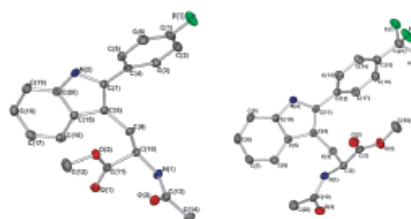
Fig. 6 Single crystal X-ray structures for **2c** (left) and **2d** (right); ellipsoids shown at 50%, H-atoms omitted.

236

ChemComm
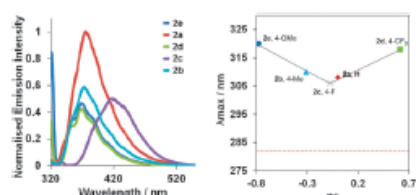
Fig. 7 Fluorescence spectra for 2-aryl-tryptophan **2a–e** (the red dotted line denotes the cut-off from amino acid residues in proteins).

Table 1 UV-vis data and Stokes shifts for 2-aryl-tryptophans **2a–e**[a]

Compound	Abs. λ_{max} (nm)	Em. (nm)	Stokes shift	ε/cm^{-1} mol^{-1} dm^{-3}
2a	308	370	62	9120
2b	310	375	65	8893
2c	306	416	110	14 684
2d	318	368	50	10 297
2e	320	368	48	11 644

[a] Solutions of **2a–e** in CH$_2$Cl$_2$.

Scheme 2 Direct C–H functionalisation of two selected peptides.

and 2,5-bis(phenylethynyl) thiophenes, and could be an indication of a push–pull type system within the series **2a–e**.[17] The largest fluorescence intensity is seen for **2a** – the other compounds **2b–e** exhibit lower fluorescen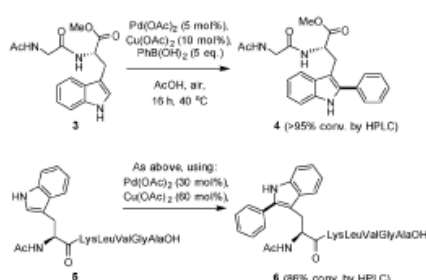ce intensity. Within the series of **2a–e**, **2c** (4-F) exhibits the largest Stokes shift. Moreover, the emission wavelength is red-shifted relative to free tryptophan (*ca.* 360 nm) (Table 1).

Selective arylation of peptides. We have successfully applied our best reaction conditions (given in Fig. 5) to the arylation of dipeptide **3** (Scheme 2), which gave **4** in >95% conversion (by HPLC analysis). When applied to a more complicated system – the six residue peptide AcTrpLysLeuValGlyAlaOH **5** – in a reaction with PhB(OH)$_2$ to give **6** – it was necessary to increase catalyst loading to 30 mol% and 60 mol% for Pd and Cu respectively. This reaction proceeded in good conversion (86%).

In summary, we have reported a mild and selective direct C–H functionalisation reaction for the amino acid tryptophan, both as a single residue and as a residue in short and longer-chained peptides. It is tempting to suggest that the amino acid may play some role in interacting with and stabilising the PdNPs, particularly for the

longer peptides, especially as it is known that certain peptides template (by reduction) the formation of specifically-sized and shaped PdNPs.[18] These aspects pertaining to C–H bond functionalisation are currently being investigated within our laboratories.

Notes and references

‡ As PdNPs are formed rapidly in this chemistry, we define Pd(OAc)$_2$ as a precatalyst.

1 S. De Ornellas, T. J. Williams, C. G. Baumann and I. J. S. Fairlamb, in *Catalytic C-H/C-X Bond Activation*, ed. X. Ribas, RSC Publishing, Cambridge, 2013.
2 (a) J. M. Chalker, C. S. C. Wood and B. G. Davis, *J. Am. Chem. Soc.*, 2009, **131**, 16346; (b) C. D. Spicer and B. G. Davis, *Chem. Commun.*, 2011, **47**, 1698; (c) C. D. Spicer, T. Triemer and B. G. Davis, *J. Am. Chem. Soc.*, 2012, **134**, 800.
3 (a) L. Ackermann, R. Vicente and A. R. Kapdi, *Angew. Chem., Int. Ed.*, 2009, **48**, 9792. For a beautiful example, see: (b) M. E. Kieffer, K. V. Chuang and S. E. Reisman, *J. Am. Chem. Soc.*, 2013, **135**, 5557.
4 (a) T. E. Storr, A. G. Firth, K. Wilson, K. Darley, C. G. Baumann and I. J. S. Fairlamb, *Tetrahedron*, 2008, **64**, 6125; (b) T. E. Storr, C. G. Baumann, R. J. Thatcher, S. De Ornellas, A. C. Whitwood and I. J. S. Fairlamb, *J. Org. Chem.*, 2009, **74**, 5810; (c) T. E. Storr, J. A. Strohmeier, C. G. Baumann and I. J. S. Fairlamb, *Chem. Commun.*, 2010, **46**, 6470. For the characterisation of Pd nanoparticles in Sonogashira reactions of bromo-purines, see: (d) A. G. Firth, K. Wilson, C. G. Baumann and I. J. S. Fairlamb, *Nucleosides, Nucleotides Nucleic Acids*, 2011, **30**, 168.
5 J. Wencel-Delord, T. Dröge, F. Liu and F. Glorius, *Chem. Soc. Rev.*, 2011, **40**, 4740.
6 2-Arylated tryptophans can be accessed by C–H bond activation using cationic Pd, microwave heating and reaction temperatures ranging from 80–150 °C, typically 90 °C, see: (a) S. Preciado, L. Mendive-Tapia, F. Albericio and R. Lavilla, *J. Org. Chem.*, 2013, **78**, 8129; (b) J. Ruiz-Rodriguez, F. Albericio and R. Lavilla, *Chem.–Eur. J.*, 2010, **16**, 1124. The selective C-2 alkylation of tryptophan by Pd^{II}/norbornene-promoted C–H activation has been reported, see: (c) H. K. Potukuchi and T. Bach, *J. Org. Chem.*, 2013, **78**, 12263.
7 J. T. Vivian and P. R. Callis, *Biophys. J.*, 2001, **80**, 2093.
8 (a) N. Lebrasseur and I. Larrosa, *J. Am. Chem. Soc.*, 2008, **130**, 2926; (b) S.-D. Yang, C.-L. Sun, Z. Fang, B.-H. Li, Y.-Z. Li and Z.-J. Shi, *Angew. Chem., Int. Ed.*, 2008, **47**, 1473; (c) J. Zhao, Y. Zhang and K. Cheng, *J. Org. Chem.*, 2008, **73**, 7428; (d) N. R. Deprez, D. Kalyani, A. Krause and M. S. Sanford, *J. Am. Chem. Soc.*, 2006, **128**, 4972.
9 We have established that the reaction of **1** with d_5-PhB(OH)$_2$ and PhI(OAc)$_2$ affords a mixture of deuterated and non-deuterated 2-phenyl-tryptophan **2a** in a *ca.* 1 : 1.5 ratio (by MS studies).
10 P. Sehnal, R. J. K. Taylor and I. J. S. Fairlamb, *Chem. Rev.*, 2010, **110**, 824.
11 T. J. Williams and I. J. S. Fairlamb, *Tetrahedron Lett.*, 2013, **54**, 2906.
12 Unsupported PdNPs were characterised at a similar size (±0.3 nm) – see ESI† for TEM images.
13 (a) A. F. Lee, P. J. Ellis, I. J. S. Fairlamb and K. Wilson, *Dalton Trans.*, 2010, **39**, 10473; (b) P. J. Ellis, I. J. S. Fairlamb, S. F. J. Hackett, K. Wilson and A. F. Lee, *Angew. Chem., Int. Ed.*, 2010, **49**, 1820.
14 (a) J. G. de Vries, *Dalton Trans.*, 2006, 421; (b) M. Reetz and J. G. de Vries, *Chem. Commun.*, 2004, 1559.
15 D.-T. D. Tang, K. Collins and F. Glorius, *J. Am. Chem. Soc.*, 2013, **135**, 7450.
16 J. M. Davidson and C. Triggs, *J. Chem. Soc. A*, 1968, 1324.
17 (a) P. Nguyen, Y. A. Zheng, L. Agocs, G. Lesley and T. B. Marder, *Inorg. Chim. Acta*, 1994, **220**, 289; (b) J. S. Siddle, R. M. Ward, J. C. Collings, S. R. Rutter, L. Porres, L. Applegarth, A. Beeby, A. S. Batsanov, A. L. Thompson, J. A. K. Howard, A. Boucekkine, K. Costuas, J. F. Halet and T. B. Marder, *New J. Chem.*, 2007, **31**, 841.
18 C.-Y. Chiu, Y. Li and Y. Huang, *Nanoscale*, 2010, **2**, 927; J. Cookson, *Platinum Met. Rev.*, 2012, **56**, 83.

237

Organic & Biomolecular Chemistry

PAPER

Unified mild reaction conditions for C2-selective Pd-catalysed tryptophan arylation, including tryptophan-containing peptides†

Alan J. Reay, Thomas J. Williams and Ian J. S. Fairlamb*

Pd-mediated C–H bond functionalisation protocols have been designed and developed on tryptophan derivatives and tryptophan-containing peptides. The examination of different arylation reactions (three sets of different conditions A–C), all of which are notable for their low temperatures ($\leq$40 °C), allowed identification of unified and complementary synthetic approaches toward a series of functionalised tryptophan-containing products. Tryptophan-containing peptides demonstrated to be susceptible to aromatic oxidation were successfully and selectively modified through the application of diaryliodonium salts in good yields.

Introduction

Pd-mediated cross-couplings for the formation of C–C bonds are well established and effective methods for selective functionalisation and modification of simple molecular systems.[1] Metal-mediated direct C–H bond functionalisation has emerged as a viable alternative[2] to classical cross-coupling methodologies as they eliminate, either in part or in full, the need for substrate pre-functionalisation, which potentially presents improved utility in the synthesis of natural products[3] and biomolecules.[4] For example, we have reported the mild[5] and selective direct C–H bond functionalisation of sensitive purine nucleosides, adenosine and 2'-deoxyadenosine.[6] In this paper we have focused on the development of unified synthetic protocols facilitating the mild and efficient arylation of tryptophan derivatives and tryptophan-containing peptides.
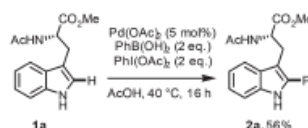
Tryptophan is a hydrophobic, indole-containing amino acid which alters the structure of proteins and is a natural fluorescent marker.[7] Extension of the π-system within tryptophans, through conjugation with an aromatic group, significantly improves the intrinsic photophysical properties of the indole motif, which has been evidenced in 2-aryl-,[8] 5-aryl- and 7-aryl-tryptophans.[9c] The 2-aryl-tryptophans can be accessed via classical Pd-mediated cross-couplings,[9] or frontier-leading C–H bond functionalisations.[10] Ackermann et al. have reported the selective metal-free arylation of engineered indole derivatives

on non-natural peptidic scaffolds.[11a] The conditions facilitated selective C2-arylation of the synthetic indole, in the presence of a tryptophan.[11b]

Recently, we communicated a convenient method for the C2-selective Pd-mediated direct arylation of a tryptophan derivative 1a and tryptophan-containing peptides.[8] The initial work for our Pd-mediated C–H bond functionalisation processes utilised conditions reported by Sanford et al. using PhB(OH)$_2$ and PhI(OAc)$_2$.[12] This allowed access to the desired C2-arylation product 2a in moderate yield ("Conditions A", Scheme 1). The notable advantage of this protocol is the mild temperature and use of readily available reagents to effect the desired transformation.

It was found subsequently that eliminating PhI(OAc)$_2$ and adding Cu(OAc)$_2$ as a co-catalyst for re-oxidation of the Pd^0 (atmospheric air being the terminal oxidant) afforded 2a in an improved yield of 93%. This methodology was then demonstrated on a series of arylboronic acids under the conditions described in Scheme 2 ("Conditions B").

"Conditions B" were successfully applied to the arylations of two selected tryptophan-containing peptides 3 and 5

Department of Chemistry, University of York, Heslington, York, YO10 5DD, UK.
E-mail: ian.fairlamb@york.ac.uk; Tel: +44 (0)1904 324091
†Electronic supplementary information (ESI) available: HPLC-ESI-MS data for peptide arylations, UV-Vis spectra for novel compounds and NMR spectra for all compounds. See DOI: 10.1039/c5ob01174d

Scheme 1 Direct arylation of tryptophan with PhI(OAc)$_2$ using "Conditions A".

Organic & Biomolecular Chemistry

Ar = C_6H_5, **2a**, 93%
Ar = 4-Me-C_6H_4, **2b**, 88%
Ar = 4-OMeC_6H_4, **2c**, 28%
Ar = 4-F-C_6H_4, **2d**, 77%
Ar = 4-CF_3-C_6H_4, **2e**, 58%
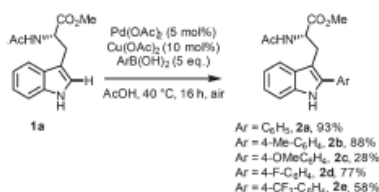
Scheme 2 Direct arylation of **1a** with Cu(OAc)₂ as a co-catalyst using "Conditions B".
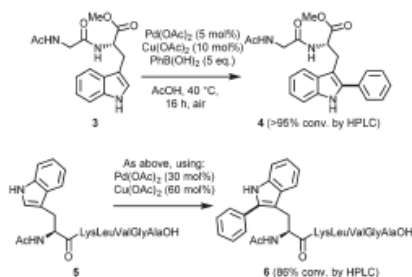
Scheme 3 Direct arylation of two selected peptides using "Conditions B".

(Scheme 3), both of which afforded high conversion to the desired arylation products **4** and **6**, respectively.

Results and discussion

With the primary goal of identifying unified synthetic protocols facilitating the mild and efficient arylation of tryptophan derivatives and tryptophan-containing peptides, a focus was placed on understanding the role of the proposed oxidant in the reaction described in Scheme 1, namely PhI(OAc)₂.

An analogous experiment was conducted using d_5-PhB-(OH)₂ (Scheme 4), which allows the delineation of the structure

Ar = C_6H_5, **2a**
Ar = C_6D_5, **2a-d_5** } 56%, 1:1
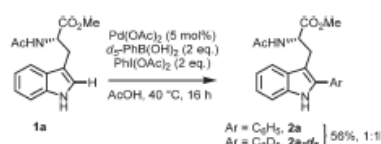
Scheme 4 Direct arylation of tryptophan with d_5-PhB(OH)₂ using "Conditions A". Ratio of isotopologues **2a** and **2a-d_5** determined by ESI-HRMS.

of the arylating reagent formed *in situ*, *i.e.* whether the arylating reagent was derived from PhB(OH)₂, PhI(OAc)₂ or both.

ESI-HRMS (+ve mode) analysis of the product isotopologues from this reaction indicated that an approximately 1 : 1 mixture of H- and D-labelled products were formed under the reaction conditions. The outcome suggests that PhI(OAc)₂ is not simply acting as an oxidant. Indeed, it has been proposed previously that a mixture of an organoboronic acid and PhI(OAc)₂ can form an I[III]-based arylating agent *in situ* under similar reaction conditions. Our observation makes a more convincing case for a role of an *in situ* generated symmetrical Ph₂I^{+} species, which adequately accounts for our observation.[13]

The non-selective aryl donation from the diaryliodonium(III) species presented a potential synthetic problem, as it required that the aryl group of the organoboronic acid matched that of the I[III] reagent, an issue which would become significant for the introduction of substituted aromatic groups. The higher-yielding "Conditions B" appeared an ideal way of circumventing this dilemma.

In other work on the peptide arylation reactions mediated by Pd and Cu, in the presence of PhB(OH)₂ alone, it was found that two specific tryptophan-containing peptides were susceptible to aromatic oxidation, namely Ac-AlaTrpAla-OH and Ac-SerGlyTrpAla-OH **9** (Scheme 5). From the reaction of AlaTrpAla-OH **7**, arylation was noted along with complete loss of starting material; HPLC-MS analysis also revealed the for-
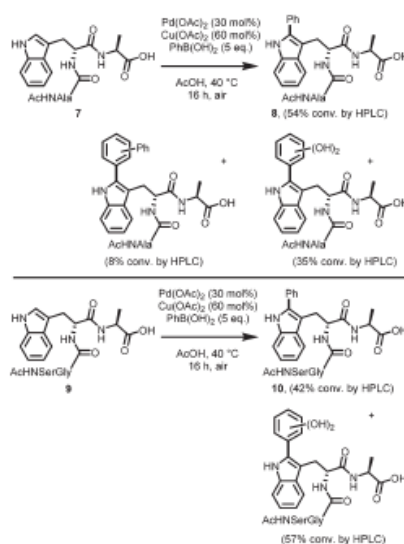
Scheme 5 Direct arylation of two peptides containing a C-terminal alanine residue using "Conditions B".

This journal is © The Royal Society of Chemistry 2015

Org. Biomol. Chem., 2015, **13**, 8298–8309 | **8299**

mation of dihydroxylated byproducts as well as diarylated byproducts (selectivity ratio 1 : 0.6 : 0.1). The reaction of Ac-Ser-GlyTrpAla-OH **9** afforded the desired arylation product and similar dihydroxylation byproducts (selectivity ratio 1 : 1.4). The involvement of Cu^{II} in the oxidation process (*i.e.* oxidative C–H bond activation)[14] appears to be critical, as does the presence of a terminal alanine neighbouring tryptophan. Free C-terminus alanines are known to form stable complexes with Cu^{II},[15] therefore it is proposed that such species are responsible for the observed hydroxylation of the arylated peptide products.

Given these limitations we chose to avoid the use of Cu^{II} as a co-catalyst, thus circumventing the over-oxidation issues. It was hypothesised that utilising a single arylating reagent would be more appealing, also avoiding O_2 as the terminal oxidant required in the Pd/Cu chemistry. Upon recalling our observations regarding the formation of Ph_2I^+ species *in situ*, we examined the reactivity of pre-synthesised highly electrophilic diaryliodine(III) salts, which have garnered a great deal of interest for use in C–H bond functionalisations in recent years.[16] These species can be furnished with a sterically-hindered aryl group which does not transfer in the catalytic process to Pd (and the organic substrate), in tandem with a second aryl group that can incorporate a range of chemical substituents.

Reaction of two equivalents of the [MesPhI]OTf salt **11a** (readily synthesised in a high-yielding one-pot procedure)[17] with **1a** is shown under the conditions described in Table 1. Pleasingly, in acetic acid this gave the desired arylation product **2a** in a yield of 65% (entry 1), indicating that a Cu^{II} co-

catalyst is not necessary for the reaction. Variation of the solvent showed that MeCN, acetone or DMF were not viable (entries 2–4). Increasing yields, in a range of alcohols, were recorded, in the order MeOH < EtOH < ^{i}PrOH (entries 5–7). The best solvent however, was found to be EtOAc, which showed full conversion to **2a** (entry 8, "Conditions C").
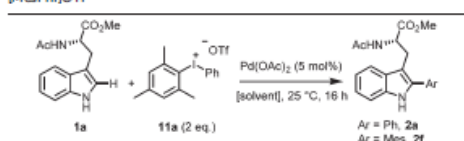
In addition to the desired phenylated product **2a**, a small amount of the mesitylated product **2f** was also isolated, formed by donation of the sterically hindered mesityl group, giving a product ratio of **2a** : **2f** of ca. 10 : 1 prior to purification. In an attempt to prevent this non-selective arylation, the optimised conditions found in the solvent screen (Table 1, entry 8) were used with another sterically-hindered 2,4,6-tri-isopropylphenyl group on the iodonium salt (**11b**). This however did not have the desired effect, as it appeared to lower the reactivity of the system and reduce product selectivity, with the ratio of **2a** to tri-isopropylphenyl side product **2g** being 5 : 1 (Table 1, entry 9).

Application of "Conditions C" to small tryptophan-containing peptides was next examined to assess the methodology against more structurally complex systems. A protection/deprotection strategy was chosen to prepare small tryptophan-containing dipeptides, but the *N*-Ac protecting group previously used for compound **1a** proved synthetically challenging when utilised in these dipeptides. A switch to an *N*-Boc protecting group was therefore explored. During these efforts it was discovered that when the optimised arylation conditions shown in Table 1, entry 8 ("Conditions C") were applied to *N*-Boc, *O*-Me protected tryptophan **1b**, only a trace of the desired arylation product was observed. Unreacted starting material **1a** was recovered along with the expected side products from the diaryliodonium salts used (*i.e.* iodobenzene/iodomesitylene). A switch to the *N*-Tfa protecting group circumvented this problem and when "Conditions C" were applied to the *N*-Tfa, *O*-Me protected tryptophan **1c** the desired arylation product **12a** was obtained in 82% isolated yield (with 17% of the undesired mesityl product **12b**) (Scheme 6).

"Conditions C" were demonstrated on the dipeptides Tfa-GlyTrp-OMe **13** and Tfa-LeuTrp-OMe **15** (Scheme 7), affording the desired arylation products **14a** and **16a** in moderate to good yields, thus highlighting the utility of this protocol when applied to small tryptophan-containing peptides.

"Conditions C" were also applied to peptides **7** and **9**, which had proved problematic with the Cu-containing "Conditions B" (Scheme 5), affording the desired arylation products

Table 1 Solvent screening in the direct arylation of **1a** using [MesPhI]OTf[a]

Entry	Solvent	$2a^{a,b}$, % (yield, %)[c]	$2f^{a,b}$, % (yield, %)[c]
1	AcOH (at 40 °C)	70 (65)	0
2	MeCN	0	0
3	Acetone	0	0
4	DMF	0	0
5	MeOH	12	0
6	EtOH	15	0
7	^{i}PrOH	47	3
8	EtOAc[d]	91 (85)	9 (3)
9	EtOAc[e,f]	50	10

[a] All reactions conducted with **1a** (0.192 mmol), **11a** (0.384 mmol), Pd(OAc)$_2$ (5 mol%) and solvent (5 mL) at 25 °C, unless otherwise stated. [b] Conversion determined by ^{1}H NMR spectroscopic analysis. [c] Following flash column chromatography. [d] Referred to throughout as "Conditions C". [e] Using iodonium triflate salt **11b** (0.384 mmol), containing a 2,4,6-tri-isopropylphenyl group, instead of **11a**. [f] 50% **2a**, 10% **2g** rather than **2f**, 40% starting material (**1a**).
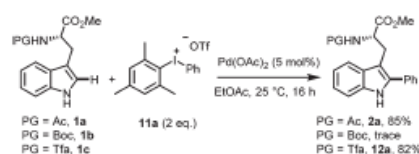
Scheme 6 Effect of *N*-protecting group on the direct arylation of tryptophans using "Conditions C".

240

Organic & Biomolecular Chemistry
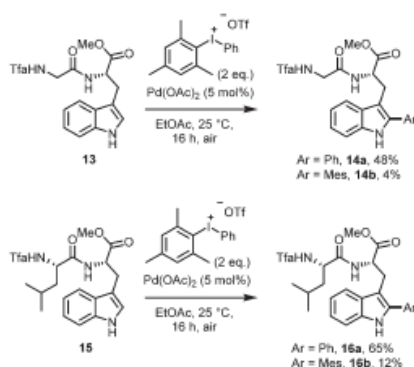
Scheme 7 Direct arylation of two selected peptides using a diaryliodonium salt ("Conditions C").

Scheme 8 Direct arylation of peptides susceptible to dihydroxylation using a diaryliodonium salt.
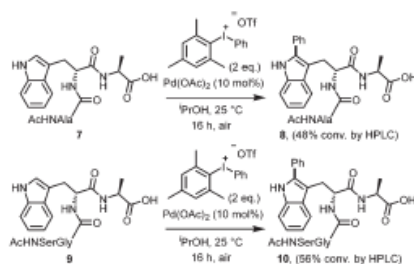
8 and **10** (Scheme 8); for these polar molecules, isopropanol was used in place of ethyl acetate as the reaction solvent. None of the mesityl byproduct was detected in these reactions, possibly because of greater steric encumbrance from the peptides as compared to a single tryptophan residue. Importantly "Conditions C" provide complete selectivity for the desired arylation products, addressing the drawbacks of "Conditions B" highlighted, pleasingly this is also achieved at significantly lower catalyst loadings.

Conclusion

The global aim of this study was to develop synthetic protocols that facilitate the mild and efficient arylation of tryptophan derivatives and tryptophan-containing peptides. This has been broadly achieved, with the different reaction conditions (A–C) being particularly attractive and highly complementary.

Our previous work demonstrated the use of both an aryl boronic acid/iodobenzene diacetate system ("Conditions A") as well as conditions utilising Cu(II) as a co-catalyst ("Conditions B").[8] These conditions allowed several C2-aryl tryptophan analogues to be accessed in high yields. The use of a Cu[II] salt was shown to be incompatible with certain peptidic motifs; in the examples tested a free C-terminal alanine neighbouring tryptophan proved problematic, leading to aromatic oxidation (major competing side reactions) and also diarylation (minor competing side reaction), demonstrating poor product selectivity (1 : 0.6 : 0.1 and 1 : 1.4).

Our methodology was therefore extended to the use of pre-synthesised asymmetric diaryliodonium salts ("Conditions C"), the arylation conditions for which have been developed and optimised to proceed effectively at 25 °C in ethyl acetate under air (which is not necessary as an oxidant, but allows reactions to be run conveniently without the need for inert conditions). Other advantages of "Conditions C" include the avoidance of strong oxidants and metal co-catalysts (*e.g.* Cu[II]). These conditions have been successfully applied to small tryptophan-containing peptides and the desired arylation products obtained with complete selectively and in synthetically useful yields, without the undesirable aromatic oxidation previously observed.

Our current work is involved with extending these methodologies to more complex systems, as well as examining the underlying mechanisms involved with the arylation of **1a** and derivatives under the different reaction conditions described within this paper.

Experimental

General experimental details

Commercially available reagents were purchased from Sigma Aldrich, Fluorochem, Fisher Scientific, Alfa Aesar or Acros Organics and used as received unless otherwise noted. Room temperature (rt) refers to reactions where no thermostatic control was applied and was recorded as 16–22 °C. Petrol refers to the fraction of petroleum ether boiling in the range of 40–60 °C. Dry THF was first obtained from a Pure Solv MD-7 solvent machine and stored under nitrogen, then dried further and any hydroperoxide species removed by refluxing over sodium for 3 days and distilling under argon. Dry methanol was obtained by drying over activated 3 Å molecular sieves and storing under nitrogen. Triethylamine (Et₃N) and diisopropyl-ethylamine (DIPEA) were distilled from potassium hydroxide and stored under nitrogen. Air sensitive procedures were performed using standard Schlenk techniques and carried out in oven- or flame-dried glassware. Nitrogen gas was oxygen free and dried immediately prior to use by passing through a column of potassium hydroxide pellets and silica. Thin layer chromatography (TLC) analysis was performed using Merck 5554 aluminium backed silica plates and visualised using UV light (λ_{max} = 254 nm). All flash column chromatography was performed using Merck silica gel 60 (particle size 40–63 μm)

Paper

and a solvent system as stated in the text. Retardation factors are quoted to two decimal places. Optical rotations were recorded using a JASCO DIP-370 digital polarimeter at 20 °C (using the sodium D line, 259 nm) using a path length of 100 mm and at a concentration indicated in the text. The appropriate solvent was used as a background with ten readings taken for each sample and the average $[\alpha]_D$ values in units of 10^{-1} deg cm^3 g^{-1} are quoted to one decimal place. Melting points were recorded using a Stuart digital SMP3 machine and are quoted to the nearest whole number. Where applicable, decomposition (dec) is noted. NMR spectra were recorded on either a Jeol ECS400 or Jeol ECX400 spectrometer and processed using MestReNova. Spectra were typically recorded at 298 K, unless otherwise specified. Chemical shifts are reported in parts per million (ppm). Coupling constants are reported in Hz and quoted to ±0.5 Hz. Multiplicities are described as singlet (s), doublet (d), triplet (t), quartet (q), quintet (quin), sextet, (sext), heptet (hept), multiplet (m), apparent (app) and broad (br). ^{1}H NMR spectra were typically recorded at 400 MHz. Chemical shifts are internally referenced to residual undeuterated solvent and given to two decimal places. ^{13}C NMR spectra were recorded at 101 MHz. Chemical shifts are internally referenced to residual undeuterated solvent and given to one decimal place. ^{11}B NMR spectra were recorded at 128 MHz and obtained with ^{1}H decoupling. Chemical shifts are externally referenced to BF$_3$·OEt$_2$ and given to one decimal place. ^{19}F NMR spectra were recorded at 376 MHz and obtained with ^{1}H decoupling. Chemical shifts are externally referenced to CFCl$_3$ and given to one decimal place. ^{31}P NMR spectra were recorded at 162 MHz and obtained with ^{1}H decoupling. Chemical shifts are externally referenced to H$_3$PO$_4$ and given to one decimal place. Mass spectrometry was performed using a Bruker Daltronics micrOTOF spectrometer using electrospray ionization (ESI). Mass to charge ratios (m/z) are reported in Daltons with percentage abundance in parentheses along with the corresponding fragment ion, where known. Where complex isotope patterns were observed, the most abundant ion is reported. High resolution mass spectra are reported with <5 ppm error. IR spectrometry was performed using a Bruker Alpha FT-IR spectrometer and signals are reported in wavenumbers (cm^{-1}) to the nearest whole number. UV-visible spectroscopy was performed using a Jasco V-560 spectrometer. A baseline in the appropriate solvent was obtained prior to recording spectra. Elemental (CHN) analysis was carried out using an Exeter Analytical CE-440 Elemental Analyser. All values are given as percentages to two decimal places. "Conditions A" and "Conditions B" are also reported in our preliminary communication on this work.[ii]

General procedure 1: direct arylation using arylboronic acids ("Conditions B")[ii]

To a microwave tube was added substrate (1 eq.), the desired boronic acid (2 eq.), Cu(OAc)$_2$ (10 mol%), Pd(OAc)$_2$ (5 mol%) and AcOH. The reaction mixture was stirred at 40 °C for 16 h. The resulting brown reaction mixture was filtered through Celite then washed with sat. aq. NaHCO$_3$. The organic layer

was collected and dried over MgSO$_4$, filtered and the solvent removed under reduced pressure to give the crude residue. The residue was dry-loaded onto silica gel and purified by flash column chromatography to give the title compound.

General procedure 2: preparation of diaryl iodonium salts[17]

Bis(acetyloxy)phenyl-λ^3-iodane (1 eq.) and the desired aryl substrate (1.1 eq.) were added to a round-bottomed flask and dissolved in CH$_2$Cl$_2$. The mixture was cooled to 0 °C then trifluoromethanesulfonic acid (1.1 eq.) was added dropwise with stirring. After complete addition the reaction was stirred for 2 h over which time it was allowed to warm to rt. After 2 h the solvent was removed under reduced pressure to give an orange-white residue to which Et$_2$O was added to precipitate a white solid. This was filtered through a glass sinter and washed on the filter with more Et$_2$O until the filtrate ran clear of coloured components. The solid was then dried *in vacuo* at 100 °C to give the title compound.

General procedure 3: direct arylation using diaryl iodonium salts ("Conditions C")

To a microwave tube was added substrate (1 eq.), the desired diaryl iodonium salt (2 eq.), Pd(OAc)$_2$ (5 mol%) and EtOAc. The reaction mixture was stirred at 25 °C for 16 h. The resulting black reaction mixture was filtered through Celite then washed with sat. aq. NaHCO$_3$. The organic layer was collected and dried over MgSO$_4$, filtered and the solvent removed under reduced pressure to give the crude residue. This was dry-loaded onto silica gel and purified by flash column chromatography to give the title compound.

Methyl (2S)-2-amino-3-(1H-indol-3-yl)propanoate hydrochloride.[18] To a Schlenk tube under N$_2$ was added dry MeOH (50 mL). Thionyl chloride (4.3 mL, 7.02 g, 59 mmol, 2.4 eq.) was added dropwise at −15 °C. L-Tryptophan 20 (5 g, 24.5 mmol, 1 eq.) was then added in three portions, resulting in a white suspension. The reaction mixture was warmed to ambient temperature and stirred for 24 h. During this time a clear orange solution was formed. Water (5 mL) was added to the reaction mixture and the solvent removed under reduced pressure to give product as an off-white solid (6.18 g, 99%). Mp 205–206 °C dec (lit.[19] 214 °C dec); ^{1}H NMR (400 MHz, CD$_3$OD, δ): 10.61 (br s, 1H), 7.54 (dt, J = 8.0, 1.0 Hz, 1H), 7.40 (dt, J = 8.0, 1.0 Hz, 1H), 7.22 (s, 1H), 7.14 (ddd, J = 8.0, 7.0, 1.0 Hz, 1H), 7.07 (ddd, J = 8.0, 7.0, 1.0 Hz, 1H), 4.33 (dd, J = 7.5, 5.5 Hz, 1H), 3.79 (s, 3H), 3.46 (dd, J = 15.0, 5.5 Hz, 1H), 3.37 (dd, J = 15.0, 7.5 Hz, 1H); ^{13}C NMR (101 MHz, CD$_3$OD, δ): 170.8, 138.3, 128.2, 125.6, 122.9, 120.3, 118.8, 112.7, 107.4, 54.6, 53.6, 27.5; ESI-MS m/z (ion, %): 219 ([M − Cl]$^+$, 100); ESI-HRMS m/z: 219.1130 [M − Cl]$^+$ (calc. for C$_{12}$H$_{15}$N$_2$O$_2$ 219.1128); IR (solid state ATR, cm^{-1}): 3259, 2856, 1747, 1501, 1436, 1351, 1210, 1108, 730; anal. calc. for C$_{12}$H$_{15}$ClN$_2$O$_2$: C 56.58, H 5.94, N 11.00 found: C 56.44, H 5.85, N 10.87.

Methyl (2S)-2-acetamido-3-(1H-indol-3-yl)propanoate, 1a.[18] To a three-necked round-bottomed flask fitted with a reflux condenser and purged with N$_2$ was added methyl

(2*S*)-2-amino-3-(1*H*-indol-3-yl)propanoate hydrochloride (3 g, 13.7 mmol, 1 eq.), dry THF (150 mL) and dry triethylamine (2 mL). The mixture was stirred to give a white suspension before being cooled to 0 °C, then acetic anhydride (1.4 mL, 1.5 g, 15.1 mmol, 1.1 eq.) was added in one portion. The reaction was then stirred for 2 h at 80 °C to give a white suspension. This was added to deionised water (150 mL) and extracted into EtOAc (3 × 150 mL). The organic layers were combined and washed sequentially with 1 M aq. HCl (100 mL), sat. aq. NaHCO$_3$ (100 mL) and brine (100 mL). The organic layer was collected and dried over MgSO$_4$, filtered and the solvent removed under reduced pressure to give a colourless oil. Trituration with Et$_2$O resulted in the product as an off-white solid (2.93 g, 82%). $[\alpha]_D$ = +41.5 (*c* 0.10, CHCl$_3$); Mp 154–155 °C (lit.[19] 155–156 °C); ^{1}H NMR (400 MHz, CDCl$_3$, δ): 8.27 (s, 1H), 7.53 (dd, *J* = 8.0, 1.0 Hz, 1H), 7.39–7.33 (m, 1H), 7.19 (ddd, 8.0, 7.0, 1.0 Hz, 1H), 7.12 (ddd, *J* = 8.0, 7.0, 1.0 Hz, 1H), 6.97 (d, *J* = 2.5 Hz, 1H), 6.03 (d, *J* = 8.0 Hz, 1H), 4.96 (dt, *J* = 8.0, 5.0 Hz, 1H), 3.70 (s, 3H), 3.35 (dd, *J* = 15.0, 5.0 Hz, 1H), 3.29 (dd, *J* = 15.0, 5.0 Hz, 3H); ^{13}C NMR (101 MHz, CDCl$_3$, δ): 172.6, 169.4, 136.1, 127.1, 123.7, 120.1, 118.4, 118.0, 111.5, 109.6, 53.2, 51.8, 27.1, 22.3; ESI-MS *m/z* (ion, %): 261 ([M + H]$^+$, 5), 283 ([M + Na]$^+$, 100); ESI-HRMS *m/z*: 283.1053 [M + Na]$^+$ (calc. for C$_{14}$H$_{16}$N$_2$O$_3$Na 283.1053); IR (solid state, ATR, cm^{-1}): 3405, 3315, 1732, 1661, 1520, 1434, 1220, 1123, 746, 665, 613, 519, 427; anal. calc. for C$_{14}$H$_{16}$N$_2$O$_3$: C 64.60, H 6.20, N 10.76 found C 64.34, H 6.23, N 10.47.

Methyl (2*S*)-2-{[(*tert*-butoxy)carbonyl]amino}-3-(1*H*-indol-3-yl)propanoate, 1b.[20] To a round-bottomed flask containing a solution of methyl (2*S*)-2-amino-3-(1*H*-indol-3-yl)propanoate hydrochloride (100 mg, 0.39 mmol, 1 eq.) and K$_2$CO$_3$ (54 mg, 0.39, 1 eq.) in deionised water (1 mL) was added a solution of di-*tert*-butyl dicarbonate (85 mg, 0.39 mmol, 1 eq.) in acetone (1 mL) at 0 °C with stirring. The solution was stirred for 2 h during which time it was allowed to warm to rt. After 2 h the acetone was removed under reduced pressure and deionised water added. This was extracted into EtOAc three times, dried over MgSO$_4$, filtered and the solvent removed under reduced pressure to give the product as an off-white solid (117 mg, 94%). $[\alpha]_D$ = +43.1 (*c* 0.10, CHCl$_3$); Mp 146–148 °C (lit.[21] 145–146 °C); ^{1}H NMR (400 MHz, CDCl$_3$, δ): 8.20 (br s, 1H), 7.58–7.53 (m, 1H), 7.35 (dt, *J* = 8.0, 1.0 Hz, 1H), 7.19 (ddd, *J* = 8.0, 7.0, 1.0 Hz, 1H), 7.12 (ddd, *J* = 8.0, 7.0, 1.0 Hz, 1H), 6.99 (s, 1H), 5.09 (d, *J* = 8.0 Hz, 1H), 4.71–4.59 (m, 1H), 3.68 (s, 3H), 3.29 (dd, *J* = 5.5, 3.0 Hz, 2H), 1.43 (s, 9H); ^{13}C NMR (101 MHz, CDCl$_3$, δ): 172.9, 155.4, 136.3, 127.6, 123.0, 122.1, 119.5, 118.6, 111.4, 109.8, 80.0, 54.3, 52.3, 28.4, 28.0; ESI-MS *m/z* (ion, %): 319 ([M + H]$^+$, 14), 341 ([M + Na]$^+$, 100); ESI-HRMS *m/z*: 341.1465 [M + Na]$^+$ (calc. for C$_{17}$H$_{22}$N$_2$NaO$_4$ 341.1472).

Methyl (2*S*)-3-(1*H*-indol-3-yl)-2-(trifluoroacetamido)propanoate, 1c.[22] To a round-bottomed flask containing methyl (2*S*)-2-amino-3-(1*H*-indol-3-yl)propanoate hydrochloride (1.27 g, 5 mmol, 1 eq.) was added Et$_3$N (0.75 mL, 0.54 g, 5 mmol, 1 eq.) and MeOH (2.5 mL) and the resulting suspension stirred for 5 min. After 5 min ethyl trifluoroacetate (0.85 mL, 1.01 g, 6.35 mmol, 1.27 eq.) was added and the mixture stirred at rt

for 16 h, during which time a clear solution formed. After 16 h the solvent was removed under reduced pressure and the resulting residue acidified with 2 M HCl, before being extracted into EtOAc three times. The organic layers were combined then washed with brine, dried over MgSO$_4$, filtered and the solvent removed under reduced pressure to give the product as an off-white solid (1.35 g, 90%). R_f 0.16 (3 : 1 petrol/ EtOAc v/v); $[\alpha]_D$ = +50.7 (*c* 0.10, CHCl$_3$); Mp 108–109 °C (lit.[23] 107–109 °C); ^{1}H NMR (400 MHz, CDCl$_3$, δ): 8.30–8.18 (br s, 1H), 7.54–7.47 (m, 1H), 7.36 (dt, *J* = 8.0, 1.0 Hz, 1H), 7.22 (ddd, *J* = 8.0, 7.0, 1.0 Hz, 1H), 7.15 (ddd, *J* = 8.0, 7.0, 1.0 Hz, 1H), 6.96 (d, *J* = 2.5 Hz, 1H), 6.95 (s, 1H), 4.94 (dt, *J* = 8.0, 5.0 Hz, 1H), 3.73 (s, 3H), 3.42 (dd, *J* = 5.0, 1.0 Hz, 2H); ^{13}C NMR (101 MHz, CDCl$_3$, δ): 170.8, 156.9 (q, $^2J_{CF}$ = 37.5), 136.2, 127.4, 123.1, 122.6, 120.0, 118.3, 116.3 (q, $^1J_{CF}$ = 287.0), 111.6, 108.8, 53.5, 53.0, 27.2; ^{19}F NMR (376 MHz, CDCl$_3$, δ): −75.8; ESI-MS *m/z* (ion, %): 315 ([M + H]$^+$, 50), 332 ([M + NH$_4$]$^+$, 40), 337 [M + Na]$^+$, 100), 353 ([M + K]$^+$, 10); ESI-HRMS *m/z*: 315.0950 [M + H]$^+$ (calc. for C$_{14}$H$_{14}$F$_3$N$_2$O$_3$ 315.0951).

Methyl (2*S*)-2-acetamido-3-(2-phenyl-1*H*-indol-3-yl)propanoate, 2a. Method A ("Conditions A"): To a microwave tube was added phenylboronic acid (47 mg, 0.384 mmol, 2 eq.), bis(acetyloxy)phenyl-λ^3-iodane (123 mg, 0.384 mmol, 2 eq.), Pd(OAc)$_2$ (2 mg, 9.6 µmol, 5 mol%) and AcOH (5 mL). The reaction mixture was stirred at 40 °C for 10 min. To the resulting orange-brown solution was added methyl (2*S*)-2-acetamido-3-(1*H*-indol-3-yl)propanoate (50 mg, 0.192 mmol, 1 eq.) **1a**. The reaction was stirred at 40 °C for 16 h. The resulting black reaction mixture was filtered through Celite, and the solvent removed under reduced pressure to give a brown solid. This was dissolved in EtOAc (10 mL) then washed with sat. aq. NaHCO$_3$. The organic layer was collected and dried over MgSO$_4$, filtered and the solvent removed under reduced pressure to give a brown solid. This was dry-loaded onto silica gel and purified by flash column chromatography (40% petrol/ EtOAc, v/v) to give product as an off-white solid (36 mg, 56%). **Method B:** Synthesised using General Procedure 1 from methyl (2*S*)-2-acetamido-3-(1*H*-indol-3-yl)propanoate **1a** (50 mg, 0.192 mmol, 1 eq.), phenylboronic acid (47 mg, 0.384 mmol, 2 eq.), Cu(OAc)$_2$ (3.5 mg, 19.2 µmol, 10 mol%) and Pd(OAc)$_2$ (2 mg, 9.6 µmol, 5 mol%) in AcOH (5 mL). Flash column chromatography (40% petrol/EtOAc, v/v) gave the product as an off-white solid (60 mg, 93%). **Method C:** Synthesised using General Procedure 3 from methyl (2*S*)-2-acetamido-3-(1*H*-indol-3-yl)propanoate **1a** (50 mg, 0.192 mmol, 1 eq.), phenyl (2,4,6-trimethylphenyl)iodonium trifluoromethanesulfonate **11a** (181 mg, 0.384 mmol, 2 eq.) and Pd(OAc)$_2$ (2 mg, 9.6 µmol, 5 mol%) in EtOAc (5 mL). Flash column chromatography (40% petrol/EtOAc, v/v) gave the product as an off-white solid (55 mg, 85%). R_f 0.27 (40% petrol/EtOAc v/v); $[\alpha]_D$ = +47.3 (*c* 0.10, CHCl$_3$); Mp 83–84 °C (lit.[24] 85–86 °C); ^{1}H NMR (400 MHz, CDCl$_3$, δ): 8.20 (s, 1H), 7.60–7.54 (m, 3H), 7.51–7.45 (m, 1H), 7.42–7.34 (m, 2H), 7.21 (ddd, *J* = 8.0, 7.0, 1.0 Hz, 1H), 7.14 (ddd, *J* = 8.0, 7.0, 1.0 Hz, 1H), 5.79 (d, *J* = 8.0 Hz, 1H), 4.84 (dt, *J* = 8.0, 5.5 Hz, 1H), 3.55 (dd, *J* = 5.5, 1.0 Hz, 2H), 3.29 (s, 3H), 1.66 (s, 3H); ^{13}C NMR (101 MHz, (CDCl$_3$, δ): 172.3,

243

169.9, 136.1, 135.9, 133.3, 129.4, 129.1, 128.4, 128.0, 122.5, 120.0, 118.8, 111.2, 106.5, 52.9, 52.1, 26.6, 22.9; ESI-MS m/z (ion, %): 337 $[M + H]^+$, 40), 359 $[M + Na]^+$, 100); ESI-HRMS m/z: 337.1546 $[M + H]^+$ (calc. for $C_{20}H_{20}N_2O_3$ 337.1547); IR (solid state ATR, cm^{-1}): 3272, 1735, 1651, 1519, 1436, 1373, 1215, 739, 696, 496.

Methyl (2S)-2-acetamido-3-[2-(4-methylphenyl)-1H-indol-3-yl]propanoate, 2b. Synthesised using General Procedure 1 from methyl (2S)-2-acetamido-3-(1H-indol-3-yl)propanoate 1a (50 mg, 0.192 mmol, 1 eq.), 4-methylphenylboronic acid (52 mg, 0.384 mmol, 2 eq.), Cu(OAc)$_2$ (3.5 mg, 19.2 μmol, 10 mol%) and Pd(OAc)$_2$ (2 mg, 9.6 μmol, 5 mol%) in AcOH (5 mL). Flash column chromatography (1 : 1 petrol/EtOAc, v/v) gave the product as an off-white solid (59 mg, 88%). R_f 0.32 (1 : 1 EtOAc/petrol); $[\alpha]_D$ = +51.9 (c 0.11, CHCl$_3$); Mp 97–99 °C; ^{1}H NMR (400 MHz, CDCl$_3$, δ): 8.09 (s, 1H), 7.56 (d, J = 8.0 Hz, 1H), 7.48–7.44 (m, 2H), 7.36 (d, J = 8.0 Hz, 1H), 7.30 (d, J = 8.0 Hz, 2H), 7.19 (ddd, J = 8.0, 7.0, 1.0 Hz, 1H), 7.13 (ddd, J = 8.0, 7.0, 1.0 Hz, 1H), 5.77 (d, J = 8.0 Hz, 1H), 4.82 (dt, J = 8.0, 5.5 Hz, 1H), 3.53 (d, J = 5.5 Hz, 1H), 3.52 (d, J = 5.5 Hz, 1H), 3.33 (s, 3H), 2.41 (s, 3H), 1.66 (s, 3H); ^{13}C NMR (126 MHz, CDCl3, δ): 172.3, 169.8, 138.0, 136.2, 135.7, 130.3, 128.2, 122.4, 120.0, 118.8, 111.1, 106.4, 60.5, 53.0, 52.1, 26.7, 22.9, 21.3, 14.3; ESI-MS m/z (ion, %): 391 $[M + H]^+$), 100); ESI-HRMS m/z: 350.1628 $[M + H]^+$ (calc. for $C_{21}H_{22}N_2O_3$ 350.1630); IR (solid state ATR, cm^{-1}) 3331, 2951, 1731, 1657, 1506, 1372, 1305, 1215, 1010, 822, 742; UV-Vis (DMSO, nm) λ_{max} 310 (ε = 8893 mol dm^{-3} cm^{-1}).

Methyl (2S)-2-acetamido-3-[2-(4-methoxyphenyl)-1H-indol-3-yl]propanoate, 2c. Synthesised using General Procedure 1 from methyl (2S)-2-acetamido-3-(1H-indol-3-yl)propanoate 1a (50 mg, 0.192 mmol, 1 eq.), 4-methoxyphenylboronic acid (58 mg, 0.384 mmol, 2 eq.), Cu(OAc)$_2$ (3.5 mg, 19.2 μmol, 10 mol%) and Pd(OAc)$_2$ (2 mg, 9.6 μmol, 5 mol%) in AcOH (5 mL). Flash column chromatography (1 : 1 petrol/EtOAc, v/v) gave the product as a brown solid (20 mg, 28%). R_f 0.15 (1 : 1 EtOAc/petrol v/v); $[\alpha]_D$ = +34.9 (c 0.10, CHCl$_3$); Mp 202–205 °C; ^{1}H NMR (400 MHz, CDCl$_3$, δ): 8.56 (br s, 1H), 7.57–7.51 (m, 1H), 7.46–7.39 (m, 2H), 7.34–7.28 (m, 1H), 7.17 (dd, J = 7.0, 1.5 Hz, 1H), 7.12 (dd, J = 7.0, 1.5 Hz, 1H), 6.95–6.90 (m, 2H), 5.85 (d, J = 8.0 Hz, 1H), 4.81 (dt, J = 8.0, 5.5 Hz, 1H), 3.81 (s, 3H), 3.48 (d, J = 5.5 Hz, 2H), 3.34 (s, 3H), 1.66 (s, 3H); ^{13}C NMR (101 MHz, CDCl$_3$, δ): 172.4, 169.8, 159.5, 136.1, 135.7, 129.6, 129.5, 125.6, 122.2, 119.9, 118.6, 114.6, 111.1, 105.9, 55.5, 53.0, 52.2, 26.7, 23.0; ESI-MS m/z (ion, %): 367 $[M + H]^+$, 50), 389 $[M + Na]^+$, 100); ESI-HRMS m/z: 389.1458 $[M + Na]^+$ (calc. for $C_{21}H_{24}N_2NaO_4$ 389.1472).

Methyl (2S)-2-acetamido-3-[2-(4-fluorophenyl)-1H-indol-3-yl]propanoate, 2d. Synthesised using General Procedure 1 from methyl (2S)-2-acetamido-3-(1H-indol-3-yl)propanoate 1a (50 mg, 0.192 mmol, 1 eq.), 4-fluorophenylboronic acid (54 mg, 0.384 mmol, 2 eq.), Cu(OAc)$_2$ (3.5 mg, 19.2 μmol, 10 mol%) and Pd(OAc)$_2$ (2 mg, 9.6 μmol, 5 mol%) in AcOH (5 mL). Flash column chromatography (1 : 1 petrol/EtOAc, v/v) gave the product as a brown solid (52 mg, 77%). R_f 0.23 (1 : 1 EtOAc/petrol v/v); $[\alpha]_D$ = +54.4 (c 0.10, CHCl$_3$); Mp 213–216 °C

dec; ^{1}H NMR (400 MHz, CDCl$_3$, δ): 8.18 (br s, 1H), 7.56 (ddt, J = 8.0, 1.5, 1.0 Hz, 1H), 7.54–7.48 (m, 2H), 7.34 (dt, J = 8.0, 1.0 Hz, 1H), 7.20 (ddd, J = 8.0, 7.0, 1.0 Hz, 1H), 7.17–7.12 (m, 3H), 5.84 (d, J = 8.0 Hz, 1H), 4.83 (dt, J = 8.0, 5.5 Hz, 1H), 3.56–3.40 (m, 2H), 3.33 (s, 3H), 1.70 (s, 3H); ^{13}C NMR (101 MHz, (CDCl$_3$, δ): 172.3, 169.7, 162.9 (d, $^1J_{CF}$ = 249.0 Hz), 135.8, 135.1, 130.3 (d, $^3J_{CF}$ = 8.0 Hz), 129.5, 129.4 (d, $^4J_{CF}$ = 3.5 Hz), 122.8, 120.3, 119.0, 116.3 (d, $^2J_{CF}$ = 21.5 Hz), 111.1, 107.0, 52.9, 52.2, 26.8, 23.1; ^{19}F NMR (376 MHz, CDCl$_3$, δ): −112.8–−112.9 (m); ESI-MS m/z (ion, %): 355 $[M + H]^+$, 60), 377 $[M + Na]^+$, 100); ESI-HRMS m/z: 355.1442 $[M + H]^+$ (calc. for $C_{20}H_{20}FN_2O_3$ 355.1452).

Methyl (2S)-2-acetamido-3-[2-[4-(trifluoromethyl)phenyl]-1H-indol-3-yl}propanoate, 2e. Synthesised using General Procedure 1 from methyl (2S)-2-acetamido-3-(1H-indol-3-yl) propanoate 1a (50 mg, 0.192 mmol, 1 eq.), 4-(trifluoromethyl)-phenylboronic acid (36 mg, 0.384 mmol, 2 eq.), Cu(OAc)$_2$ (3.5 mg, 19.2 μmol, 10 mol%) and Pd(OAc)$_2$ (2 mg, 9.6 μmol, 5 mol%) in AcOH (5 mL). Flash column chromatography (1 : 1 petrol/EtOAc, v/v) gave the product as a brown solid (45 mg, 58%). R_f 0.34 (1 : 1 EtOAc/petrol); $[\alpha]_D$ = +62.0 (c 0.13, CHCl$_3$); Mp 202–206 °C; ^{1}H NMR (400 MHz, CDCl$_3$, δ): 8.41 (s, 1H), 7.72–7.63 (m, 4H), 7.58 (d, J = 8.0 Hz, 1H), 7.35 (d, J = 8.0 Hz, 1H), 7.22 (ddd, J = 8.2, 7.0, 1.2 Hz, 1H), 7.15 (ddd, J = 8.2, 7.0, 1.2 Hz, 1H), 5.87 (d, J = 8.0 Hz, 1H), 4.84 (dt, J = 8.0, 5.2 Hz, 1H), 3.59–3.48 (m, 2H), 3.29 (s, 3H), 1.67 (s, 3H); ^{13}C NMR (101 MHz, CDCl3, δ): 172.2, 169.9, 136.9, 136.1, 134.3, 129.9 (q, $^2J_{CF}$ = 32.0 Hz), 129.5, 128.5, 126.1 (q, $^3J_{CF}$ = 4.0 Hz), 124.1 (q, $^1J_{CF}$ = 247.0 Hz), 123.3, 120.4, 119.2, 111.4, 108.2, 53.0, 52.2, 27.0, 23.0; ESI-MS m/z (ion, %): 405 $[M + H]^+$, 30), 427 $[M + Na]^+$, 100); ESI-HRMS m/z: 405.1410 $[M + H]^+$ (calc. for $C_{21}H_{20}F_3N_2O_3$ 405.1421); IR (solid state ATR, cm^{-1}) 3288, 2925, 2860, 1730, 1651, 1505, 1438, 1285, 1245, 1215, 1027, 835, 743; UV-Vis (DMSO, nm) λ_{max} 318 (ε = 10297 mol dm^{-3} cm^{-1}).

Methyl (2S)-2-acetamido-3-[2-(2,4,6-trimethylphenyl)-1H-indol-3-yl]propanoate, 2f. Synthesised using General Procedure 3 from methyl (2S)-2-acetamido-3-(1H-indol-3-yl)-propanoate 1a (50 mg, 0.192 mmol, 1 eq.), phenyl (2,4,6-trimethylphenyl)iodonium trifluoromethanesulfonate 11a (181 mg, 0.384 mmol, 2 eq.) and Pd(OAc)$_2$ (2 mg, 9.6 μmol, 5 mol%) in EtOAc (5 mL). Flash column chromatography (40% petrol/EtOAc, v/v) gave the product as an off-white solid (2 mg, 3%). R_f 0.31 (1 : 1 EtOAc/petrol v/v); $[\alpha]_D$ = +35.2 (c 0.10, CHCl$_3$); Mp 158–159 °C; ^{1}H NMR (400 MHz, CDCl$_3$, δ): 7.89 (br s, 1H), 7.61 (ddt, J = 7.5, 1.5, 1.0 Hz, 1H), 7.37–7.33 (m, 1H), 7.20 (dd, J = 8.0, 1.5 Hz, 1H), 7.16 (d, J = 7.5 Hz, 1H), 6.99 (ddt, J = 4.0, 1.5, 1.0 Hz, 2H), 5.64 (d, J = 7.5 Hz, 1H), 4.72 (ddd, J = 7.5, 7.0, 5.0 Hz, 1H), 3.47 (s, 3H), 3.17 (dd, J = 15.0, 5.0 Hz, 1H), 3.02 (dd, J = 15.0, 7.0 Hz, 1H), 2.35 (s, 3H), 2.11 (d, J = 1.0 Hz, 6H), 1.75 (s, 3H); ^{13}C NMR (101 MHz, (CDCl$_3$, δ): 172.5, 169.9, 138.9, 138.3, 138.2, 135.9, 134.7, 128.8, 128.7, 128.7, 128.6, 122.1, 119.9, 118.8, 110.9, 108.0, 100.1, 53.1, 52.3, 27.2, 23.1, 21.3, 20.4, 20.3; ESI-MS m/z (ion, %): 379 $[M + H]^+$, 40), 401 $[M + Na]^+$, 100); ESI-HRMS m/z: 379.2015 $[M + H]^+$ (calc. for $C_{23}H_{27}N_2O_3$ 379.2016); IR (solid state, ATR, cm^{-1}): 3402, 3289, 2953, 2919, 2852, 1741, 1646, 1515, 1458, 1435, 1373,

1304, 1293, 1260, 1239, 1218, 1129, 1031, 1012, 987, 854, 798, 744, 591, 505, 445; UV-Vis (DMSO, nm): λ_{max} 288 (ε = 15 092 mol dm^{-3} cm^{-1}).

2-Acetamidoacetic acid. To a round-bottomed flask was added glycine (5 g, 66.6 mmol, 1 eq.) and water (150 mL). To this, acetic anhydride (18.9 mL, 20.4 g, 200 mmol, 3 eq.) was added dropwise and the reaction mixture was stirred at rt for 1 h. The mixture was then cooled to 4 °C for 16 h, and the resulting precipitate collected by filtration through a sintered funnel to give product as a white solid (4.46 g, 57%). Mp 207–208 °C (lit.[25] 206–208 °C dec); ^{1}H NMR (400 MHz, (CD$_6$)$_2$SO) δ 12.51 (s, 1H), 8.18 (s, 1H), 3.71 (d, J = 6.0 Hz, 2H), 1.84 (s, 3H); ^{13}C NMR (101 MHz, (CD$_3$)$_2$SO) δ 171.5, 169.6, 40.6, 22.3; ESI-MS m/z (ion, %): 118 ([M + H]$^+$, 40), 140 ([M + Na]$^+$, 100); ESI-HRMS m/z: 118.0501 [M + H]$^+$ (calc. for C$_4$H$_8$NO$_3$ 118.0499); IR (solid state ATR, cm^{-1}) 3350, 1944, 1897, 1717, 1580, 1547, 1439, 1379, 1351, 1276, 1227, 1137, 993, 902. 682.

Methyl (2S)-2-(2-acetamidoacetamido)-3-(1H-indol-3-yl)-propanoate, 3. To a Schlenk tube was added methyl (2S)-2-amino-3-(1H-indol-3-yl)propanoate hydrochloride (190 mg, 0.872 mmol, 1 eq.), 2-Acetamidoacetic acid (102 mg, 0.872 mmol, 1 eq.) and N-(3-Dimethylaminopropyl)-N′-ethyl-carbodiimide hydrochloride (EDC·HCl) (167 mg, 0.872 mmol, 1 eq.). The reaction mixture was placed under vacuum and refilled with N$_2$, and this process repeated twice. Dry CH$_2$Cl$_2$ (5 mL) was added, and the mixture stirred for 16 h at ambient temperature. The solvent was removed under reduced pressure. The resulting residue was dissolved in EtOAc (15 mL) and washed with 1 M aq. HCl (20 mL), sat. aq. NaHCO$_3$ (40 mL) and brine (40 mL). The organic layer was collected and dried over MgSO$_4$, filtered and the solvent removed under reduced pressure to give product as a white solid (96 mg, 35%). $[\alpha]_D$ = +36.5 (c 0.10, CHCl$_3$). Mp 98–102 °C (lit.[26] 178 °C); ^{1}H NMR (400 MHz, CD$_3$OD) δ 7.48 (dt, J = 8.0, 1.0 Hz, 1H), 7.31 (dt, J = 8.0, 1.0 Hz, 1H), 7.10–7.04 (m, 3H), 7.00 (ddd, J = 8.0, 7.0, 1.0 Hz, 1H), 4.73 (dd, J = 7.0, 6.0 Hz, 1H), 3.83 (d, J = 16.5, 1H), 3.78 (d, J = 16.5 Hz, 1H), 3.64 (s, 3H), 3.27 (ddd, J = 14.5, 7.0, 0.5 Hz, 1H), 3.19 (ddd, J = 14.5, 7.0, 0.5 Hz, 1H), 1.92 (s, 3H); ^{13}C NMR (101 MHz, CD$_3$OD) δ 173.9, 173.7, 171.4, 138.0, 128.7, 124.6, 122.5, 119.9, 119.1, 112.3, 110.3, 54.8, 52.7, 49.0, 43.4, 28.4; ESI-MS m/z (ion, %): 318 ([M + H]$^+$, 20), 340 ([M + Na]$^+$, 100); ESI-HRMS m/z: 318.1433 [M + H]$^+$ (calc. for C$_{16}$H$_{20}$N$_3$O$_4$ 318.1448); IR (solid state ATR, cm^{-1}) 3286, 2947, 1737, 1655, 1610, 1508, 1460, 1439, 1372, 1285, 1248, 1215, 1177, 1030.

Methyl (2S)-2-(2-acetamidoacetamido)-3-(2-phenyl-1H-indol-3-yl)propanoate, 4. Synthesised using General Procedure 1 from methyl (2S)-2-(2-acetamidoacetamido)-3-(1H-indol-3-yl)-propanoate 3 (10 mg, 0.032 mmol, 1 eq.), phenylboronic acid (20 mg, 0.16 mmol, 5 eq.), Cu(OAc)$_2$ (0.6 mg, 3.2 μmol, 10 mol %) and Pd(OAc)$_2$ (0.36 mg, 1.6 μmol, 5 mol%) in AcOH (0.5 mL). Flash column chromatography (2% MeOH/EtOAc, v/v) gave the product as an off-white solid (42 mg, 68%). R_f 0.24 (2% MeOH/EtOAc, v/v); $[\alpha]_D$ = +32.1 (c 0.10, CHCl$_3$); Mp 199 °C dec; ^{1}H NMR (400 MHz, CDCl$_3$) δ 8.50 (s, 1H),

7.61–7.50 (m, 3H), 7.50–7.41 (m, 2H), 7.39–7.33 (m, 2H), 7.19 (ddd, J = 8.0, 7.0, 1.5 Hz, 1H), 7.15 (s, ddd, J = 8.0, 7.0, 1.5, 1H), 6.18 (br d, J = 8.0 Hz, 1H), 5.95 (br t, J = 5.0 Hz, 1H), 4.80 (dt, J = 8.0, 5.5 Hz, 1H), 3.66–3.38 (m, 4H), 3.34 (s, 3H), 1.87 (s, 3H); ^{13}C NMR (101 MHz, CDCl$_3$) δ 171.8, 170.3, 168.3, 136.2, 135.9, 133.2, 129.4, 129.3, 128.4, 128.2, 122.8, 120.2, 118.8, 111.3, 106.5, 77.4, 53.1, 52.3, 42.7, 26.6, 23.0; ESI-MS m/z (ion, %): 394 ([M + H]$^+$, 10), 416 ([M + Na]$^+$, 100); ESI-HRMS m/z: 394.1763 [M + H]$^+$ (calc. for C$_{22}$H$_{24}$N$_3$O$_4$ 394.1761).

Arylated product of Ac-TrpLysLeuValGlyAla-OH 5, 6. To a microwave tube was added peptide 5 (10 mg, 0.014 mmol, 1 eq.), phenylboronic acid (8.5 mg, 0.07 mmol, 5 eq.), Cu(OAc)$_2$ (1.5 mg, 0.0084 mmol, 60 mol%), Pd(OAc)$_2$ (0.9 mg, 0.0042 mmol, 30 mol%) and AcOH (1 mL). The reaction mixture was stirred at 40 °C for 16 h. The solvent was removed under reduced pressure to give a brown residue, which was analysed by HPLC-ESI-MS. ESI-MS m/z (ion, %): 791 (M$^+$, 86).

Arylated product of Ac-AlaTrpAla-OH 7, 8. Method A: To a microwave tube was added peptide 7 (10 mg, 0.026 mmol, 1 eq.), phenylboronic acid (16 mg, 0.13 mmol, 5 eq.), Cu(OAc)$_2$ (2.8 mg, 0.0156 mmol, 60 mol%), Pd(OAc)$_2$ (1.8 mg, 0.0078 mmol, 30 mol%) and AcOH (1 mL). The reaction mixture was stirred at 40 °C for 16 h. The solvent was removed under reduced pressure to give a brown residue, which was analysed by HPLC-ESI-MS. **Method B:** To a microwave tube was added peptide 7 (10 mg, 0.026 mmol, 1 eq.), phenyl(2,4,6-trimethylphenyl)iodonium trifluoromethanesulfonate, **11a** (25 mg, 0.052 mmol, 2 eq.), Pd(OAc)$_2$ (0.6 mg, 0.0026 mmol, 10 mol%) and ^{i}PrOH (1 mL). The reaction mixture was stirred at 25 °C for 16 h. The resulting brown reaction mixture was filtered through Celite with MeOH (5 mL) and the solvent removed under reduced pressure to give a brown residue, which was analysed by HPLC-ESI-MS. ESI-MS m/z (ion, %): 465 ([M + H]$^+$, 100).

Arylated product of Ac-SerGlyTrpAla-OH 9, 10. Method A: To a microwave tube was added peptide 9 (10 mg, 0.022 mmol, 1 eq.), phenylboronic acid (13 mg, 0.11 mmol, 5 eq.), Cu(OAc)$_2$ (2.4 mg, 0.0132 mmol, 60 mol%), Pd(OAc)$_2$ (1.5 mg, 0.0066 mmol, 30 mol%) and AcOH (1 mL). The reaction mixture was stirred at 40 °C for 16 h. The solvent was removed under reduced pressure to give a brown residue, which was analysed by HPLC-ESI-MS. **Method B:** To a microwave tube was added peptide 9 (10 mg, 0.022 mmol, 1 eq.), phenyl(2,4,6-trimethylphenyl)iodonium trifluoromethanesulfonate, **11a** (21 mg, 0.044 mmol, 2 eq.), Pd(OAc)$_2$ (0.5 mg, 0.0022 mmol, 10 mol%) and ^{i}PrOH (1 mL). The reaction mixture was stirred at 25 °C for 16 h. The resulting brown reaction mixture was filtered through Celite with MeOH (5 mL) and the solvent removed under reduced pressure to give a brown residue, which was analysed by HPLC-ESI-MS. ESI-MS m/z (ion, %): 538 ([M + H]$^+$, 100).

Phenyl(2,4,6-trimethylphenyl)iodonium trifluoromethane-sulfonate, 11a. Synthesised using General Procedure 2 from bis(acetyloxy)phenyl-λ^3-iodane (3.22 g, 10 mmol, 1 eq.), 1,3,5-trimethylbenzene (1.54 mL, 1.32 g, 11 mmol, 1.1 eq.) and trifluoromethanesulfonic acid (0.96 mL, 1.65 g, 11 mmol,

Paper

1.1 eq.) in CH$_2$Cl$_2$ (20 mL) to give the product as a white solid (4.49 g, 95%). Mp 149–150 °C (lit.[27] 147–148 °C); ^{1}H NMR (400 MHz, CDCl$_3$, δ): 7.69 (d, *J* = 7.5 Hz, 2H), 7.51 (t, *J* = 7.5 Hz, 1H), 7.39 (t, *J* = 7.5 Hz, 2H), 7.09 (s, 2H), 2.61 (s, 6H), 2.34 (s, 3H); ^{13}C NMR (101 MHz, CDCl$_3$, δ): 144.5, 142.6, 133.1, 132.4, 131.9, 130.5, 120.5, 111.8, 27.2, 21.2; ^{19}F NMR (376 MHz, CDCl$_3$, δ): −78.2 (s, 3F); ESI-MS *m/z* (ion, %): 323 ([M − OTf]$^+$, 100); ESI-HRMS *m/z*: 323.0303 [M − OTf]$^+$ (calc. for C$_{15}$H$_{16}$I 323.0291); IR (solid state, ATR, cm^{-1}): 3060, 2919, 1445, 1247, 1222, 1158, 1025, 985, 945, 857, 741, 683, 632, 574, 515, 454; anal. calc. for C$_{16}$H$_{16}$F$_3$IO$_3$S: C 40.69, H 3.41 found: C 40.43, H 3.24.

Phenyl(2,4,6-triisopropylphenyl)iodonium trifluoromethanesulfonate, 11b. Synthesised using General Procedure 2 from bis(acetyloxy)phenyl-λ^3-iodane (805 mg, 2.5 mmol, 1 eq.), 1,3,5-triisopropylbenzene (665 µl, 562 mg, 2.75 mmol, 1.1 eq.) and trifluoromethanesulfonic acid (241 µL, 413 mg, 2.75 mmol, 1.1 eq.) in CH$_2$Cl$_2$ (5 mL) to give the product as a white solid (1.19 g, 86%). Mp 177–179 °C (lit.[17] 169–179 °C); ^{1}H NMR (400 MHz, CDCl$_3$, δ): 7.70–7.65 (m, 2H), 7.58–7.52 (m, 1H), 7.47–7.40 (m, 2H), 7.19 (s, 2H), 3.25 (quin, *J* = 6.5 Hz, 2H), 2.96 (hept, *J* = 7.0 Hz, 1H), 1.26 (dd, *J* = 15.0, 7.0 Hz, 18H); ^{13}C NMR (101 MHz, CDCl$_3$, δ): 193.8, 155.9, 152.6, 132.7, 132.1, 125.5, 120.4, 113.0, 100.1, 39.7, 34.4, 24.4, 23.8; ESI-MS *m/z* (ion, %): 407 ([M − OTf]$^+$, 100); ESI-HRMS *m/z*: 407.1247 [M − OTf]$^+$ (calc. for C$_{21}$H$_{28}$I 407.1230); anal. calc. for C$_{22}$H$_{28}$F$_3$IO$_3$S: C 47.49, H 5.07 found: C 47.26, H 4.93.

Methyl (2S)-3-(2-phenyl-1H-indol-3-yl)-2-(trifluoroacetamido)-propanoate, 12a. Synthesised using General Procedure 3 from methyl (2S)-3-(1H-indol-3-yl)-2-(trifluoroacetamido)propanoate **1c** (58 mg, 0.192 mmol, 1 eq.), phenyl (2,4,6-trimethylphenyl)-iodonium trifluoromethanesulfonate **11a** (181 mg, 0.384 mmol, 2 eq.) and Pd(OAc)$_2$ (2 mg, 9.6 µmol, 5 mol%) in EtOAc (5 mL). Flash column chromatography (3 : 1 petrol/EtOAc, v/v) gave the product as an off-white solid (59 mg, 82%). *R$_f$* 0.32 (3 : 1 petrol/EtOAc, v/v); [*α*]$_D$ = +42.4 (*c* 0.10, CHCl$_3$); Mp 155–156 °C; ^{1}H NMR (400 MHz, CDCl$_3$, δ): 8.15 (br s, 1H), 7.58–7.52 (m, 3H), 7.50 (dd, *J* = 8.0, 7.0 Hz, 2H), 7.44–7.36 (m, 2H), 7.23 (ddd, *J* = 8.0, 7.0, 1.0 Hz, 1H), 7.19–7.14 (m, 1H), 6.64 (d, *J* = 8.0 Hz, 1H), 4.83 (dt, *J* = 8.0, 5.5 Hz, 1H), 3.61 (dd, *J* = 5.5, 1.0 Hz, 2H), 3.35 (s, 3H); ^{13}C NMR (101 MHz, CDCl$_3$, δ): 170.7, 156.7 (q, *J* = 37.5), 136.5, 135.8, 132.6, 129.3, 129.1, 128.5, 128.4, 122.9, 120.4, 118.7, 114.9 (q, *J* = 288.0 Hz), 111.2, 105.6, 53.4, 52.6, 26.5; ^{19}F NMR (376 MHz, CDCl$_3$, δ): −75.9; ESI-MS *m/z* (ion, %): 391 ([M + H]$^+$, 10), 408 ([M + NH$_4$]$^+$, 35), 413 ([M + Na]$^+$, 100), 429 ([M + K]$^+$, 10); ESI-HRMS *m/z*: 413.1074 [M + Na]$^+$ (calc. for C$_{20}$H$_{17}$F$_3$N$_2$NaO$_3$ 413.1083).

Methyl (2S)-3-(2-phenyl-1H-indol-3-yl)-2-(trifluoroacetamido)-propanoate, 12b. Synthesised using General Procedure 3 from methyl (2S)-3-(1H-indol-3-yl)-2-(trifluoroacetamido)propanoate **1c** (58 mg, 0.192 mmol, 1 eq.), phenyl (2,4,6-trimethylphenyl)-iodonium trifluoromethanesulfonate **11a** (181 mg, 0.384 mmol, 2 eq.) and Pd(OAc)$_2$ (2 mg, 9.6 µmol, 5 mol%) in EtOAc (5 mL). Flash column chromatography (3 : 1 petrol/EtOAc, v/v) gave the product as an off-white solid (14 mg, 17%). *R$_f$* 0.42 (3 : 1 petrol/EtOAc v/v); [*α*]$_D$ = +34.4 (*c* 0.10, CHCl$_3$); Mp 58–60 °C; ^{1}H NMR (400 MHz, CDCl$_3$, δ): 8.00 (br s, 1H), 7.59 (dd, *J* = 8.0, 1.0 Hz, 1H), 7.39–7.34 (m, 1H), 7.22 (ddd, *J* = 8.0, 7.0, 1.0 Hz, 1H), 7.17 (ddd, *J* = 8.0, 7.0, 1.0 Hz, 1H), 6.99 (d, *J* = 2.5 Hz, 2H), 6.58 (d, *J* = 7.5 Hz, 1H), 4.76 (td, *J* = 7.0, 5.5 Hz, 1H), 3.50 (s, 3H), 3.26 (dd, *J* = 15.0, 5.5 Hz, 1H), 3.13 (dd, *J* = 15.0, 7.0 Hz, 1H), 2.36 (s, 3H), 2.10 (s, 3H), 2.09 (s, 3H); ^{13}C NMR (101 MHz, CDCl$_3$, δ): 170.8, 157.0 (q, $^2J_{CF}$ = 38.0 Hz), 139.0, 138.1, 135.9, 135.2, 128.7, 128.3, 128.0, 122.2, 120.0, 118.4 (q, $^1J_{CF}$ = 288.0 Hz), 111.1, 106.7, 53.5, 52.7, 27.0, 21.2, 20.1; ^{19}F NMR (376 MHz, CDCl$_3$, δ): −75.7; ESI-MS *m/z* (ion, %): 433 ([M + H]$^+$, 5), 450 ([M + NH$_4$]$^+$, 40), 455 ([M + Na]$^+$, 100), 471 ([M + K]$^+$, 5); ESI-HRMS *m/z*: 455.1547 [M + Na]$^+$ (calc. for C$_{23}$H$_{23}$F$_3$N$_2$NaO$_3$ 455.1553); IR (solid state, ATR, cm^{-1}): 3391, 2955, 2919, 2851, 1712, 1614, 1543, 1458, 1439, 1378, 1344, 1292, 1206, 1163, 1011, 909, 853, 731, 510; UV-Vis (DMSO, nm): λ$_{max}$ 288 (ε = 9725 mol dm^{-3} cm^{-1}).

2-(Trifluoroacetamido)acetic acid.[22] To a round-bottomed flask containing glycine (826 mg, 11 mmol, 1 eq.) was added Et$_3$N (1.5 mL, 1.11 g, 11 mmol, 1 eq.) and MeOH (5.5 mL) and the resulting suspension stirred for 5 min. After 5 min ethyl trifluoroacetate (1.7 mL, 1.99 g, 14 mmol, 1.27 eq.) was added and the mixture stirred at rt for 16 h, during which time a clear solution formed. After 16 h the solvent was removed under reduced pressure and the resulting residue acidified with 2 M HCl, before being extracted into EtOAc three times. The organic layers were combined then washed with brine, dried over MgSO$_4$, filtered and the solvent removed under reduced pressure to give the product as a white solid (1.68 g, 89%). Mp 119–121 °C (lit.[28] 118–119 °C dec); ^{1}H NMR (400 MHz, CD$_3$OD, δ): 4.00 (s, 2H); ^{13}C NMR (101 MHz, CD$_3$OD, δ): 171.5, 159.4 (q, $^2J_{CF}$ = 37.5 Hz), 117.4 (q, $^1J_{CF}$ = 286.0 Hz), 41.7; ^{19}F NMR (376 MHz, CD$_3$OD, δ): −77.3; ESI-MS *m/z* (ion, %): 194 ([M + Na]$^+$, 100); ESI-HRMS *m/z*: 194.0033 [M + Na]$^+$ (calc. for C$_4$H$_4$F$_3$NNaO$_3$ 194.0035).

Methyl (2S)-3-(1H-indol-3-yl)-2-[2-(trifluoroacetamido) acetamido]propanoate, 13. 2-(Trifluoroacetamido)acetic acid (100 mg, 0.58 mmol, 1 eq.), methyl (2S)-2-amino-3-(1H-indol-3-yl)propanoate (163 mg, 0.64 mmol, 1.1 eq.) and *O*-(benzo-triazol-1-yl)-*N,N,N',N'*-tetramethyluronium tetrafluoroborate (TBTU) (225 mg, 0.70 mmol, 1.2 eq.) were added to a round-bottomed flask which was fitted with a septum and flushed with argon from a balloon for 20 min. After 20 min dry, distilled DIPEA (0.4 mL, 300 mg, 2.32 mmol, 4 eq.) and dry CH$_3$CN (5.8 mL) were added *via* syringe to give a clear solution and the reaction was stirred at rt for 2 h. After 2 h CH$_2$Cl$_2$ was added, then the reaction mixture was washed with sat. aq. NH$_4$Cl and extracted three times with CH$_2$Cl$_2$. The organic layers were combined, dried over MgSO$_4$, filtered and the solvent removed under reduced pressure to give a crude residue. This was dry-loaded onto silica gel and purified by flash column chromatography (3 : 1 EtOAc/petrol, v/v) to give the product as an off-white solid (201 mg, 93%). *R$_f$* 0.52 (3 : 1 EtOAc/petrol v/v); [*α*]$_D$ = +40.7 (*c* 0.10, CHCl$_3$); Mp 53–55 °C; ^{1}H NMR (400 MHz, CDCl$_3$, δ): 8.28–8.18 (br s, 1H), 7.50–7.44 (m, 1H), 7.38 (t, *J* = 5.0 Hz, 1H), 7.30 (dt, *J* = 8.0, 1.0 Hz, 1H), 7.18 (ddd, *J* = 8.0, 7.0, 1.2 Hz, 1H), 7.11 (ddd, *J* =

8306 | *Org. Biomol. Chem.*, 2015, **13**, 8298–8309

This journal is © The Royal Society of Chemistry 2015

246

Organic & Biomolecular Chemistry

8.0, 7.0, 1.0 Hz, 1H), 6.94 (d, J = 2.5 Hz, 1H), 6.57 (d, J = 8.0 Hz, 1H), 4.93 (dt, J = 8.0, 5.5 Hz, 1H), 3.85–3.74 (m, 2H), 3.73 (s, 3H), 3.37–3.24 (m, 2H); ^{13}C NMR (101 MHz, CDCl$_3$, δ): 172.3, 166.8, 157.3 (q, $^2J_{CF}$ = 38.0 Hz), 136.2, 127.4, 123.2, 122.5, 120.0, 118.3, 116.6 (q, $^1J_{CF}$ = 287.0 Hz), 111.6, 109.4, 53.2, 52.8, 42.5, 27.5; ^{19}F NMR (376 MHz, CDCl$_3$, δ): −75.6; ESI-MS m/z (ion, %): 372 ([M + H]$^+$, 10), 394 ([M + Na]$^+$, 100); ESI-HRMS m/z: 394.0988 [M + Na]$^+$ (calc. for C$_{16}$H$_{16}$F$_3$N$_3$NaO$_4$ 394.0985); IR (solid state, ATR, cm^{-1}): 3391, 3341, 1729, 1704, 1654, 1560, 1532, 1445, 1351, 1215, 1184, 1150, 1005, 968, 742, 608, 536, 428; UV-Vis (DMSO, nm): λ_{max} 284 (ε = 10 138 mol dm^{-3} cm^{-1}).

Methyl (2S)-3-(2-phenyl-1H-indol-3-yl)-2-[2-(trifluoroaceta-mido)acetamido]propanoate, 14a. Synthesised using General Procedure 3 from methyl (2S)-3-(1H-indol-3-yl)-2-[2-(trifluoro-acetamido)acetamido]propanoate 9 (71 mg, 0.192 mmol, 1 eq.), phenyl (2,4,6-trimethylphenyl)iodonium trifluoromethane-sulfonate 11a (181 mg, 0.384 mmol, 2 eq.) and Pd(OAc)$_2$ (2 mg, 9.6 μmol, 5 mol%) in EtOAc (5 mL). Flash column chromato-graphy (40% EtOAc/petrol, v/v) gave the product as an off-white solid (41 mg, 48%). R_f 0.28 (40% EtOAc/petrol, v/v); $[\alpha]_D$ +51.0 (c 0.10, CHCl$_3$); Mp 82–84 °C; ^{1}H NMR (400 MHz, CDCl$_3$, δ): 8.22 (br s, 1H), 7.55–7.49 (m, 3H), 7.46 (dd, J = 8.0, 7.0 Hz, 2H), 7.40–7.33 (m, 2H), 7.22 (ddd, J = 8.0, 7.0, 1.0 Hz, 1H), 7.12 (ddd, J = 8.0, 7.0, 1.0 Hz, 1H), 6.93 (br s, 1H), 6.00 (d, J = 7.5 Hz, 1H), 4.83 (dt, J = 7.5, 5.0, 1H), 3.70–3.60 (m, 2H), 3.42 (s, 3H), 3.30–3.20 (m, 2H); ^{13}C NMR (101 MHz, CDCl$_3$, δ): 171.6, 166.1, 156.7 (q, $^2J_{CF}$ = 37.5 Hz), 141.9, 136.3, 135.8, 133.2, 129.4, 129.2, 128.3, 128.3, 128.1, 122.9, 120.3, 118.7, 114.9 (q, $^1J_{CF}$ = 287.0 Hz), 111.2, 106.2, 53.3, 52.6, 42.0, 26.3; ^{19}F NMR (376 MHz, CDCl$_3$, δ): −75.7; ESI-MS m/z (ion, %): 470 ([M + Na]$^+$, 100); ESI-HRMS m/z: 470.1292 [M + Na]$^+$ (calc. for C$_{22}$H$_{20}$F$_3$N$_3$NaO$_4$ 470.1298); IR (solid state, ATR, cm^{-1}): 3340, 3061, 2954, 2930, 1722, 1666, 1528, 1441, 1351, 1211, 1153, 1074, 1004, 908, 730, 698, 515; UV-Vis (DMSO, nm): λ_{max} 308 (ε = 20 684 mol dm^{-3} cm^{-1}).

Methyl (2S)-2-[2-(trifluoroacetamido)acetamido]-3-[2-(2,4,6-trimethylphenyl)-1H-indol-3-yl]propanoate, 14b. Synthesised using General Procedure 3 from methyl (2S)-3-(1H-indol-3-yl)-2-[2-(trifluoroacetamido)acetamido]propanoate 13 (71 mg, 0.192 mmol, 1 eq.), phenyl (2,4,6-trimethylphenyl)iodonium trifluoromethanesulfonate 11a (181 mg, 0.384 mmol, 2 eq.) and Pd(OAc)$_2$ (2 mg, 9.6 μmol, 5 mol%) in EtOAc (5 mL). Flash column chromatography (40% EtOAc/petrol, v/v) gave the product as an off-white solid (4 mg, 4%). R_f 0.38 (40% EtOAc/petrol, v/v); $[\alpha]_D$ +33.3 (c 0.10, CHCl$_3$); Mp 90–92 °C; ^{1}H NMR (400 MHz, CDCl$_3$, δ): 7.87 (br s, 1H), 7.56 (dd, J = 8.0, 1.0 Hz, 1H), 7.36 (dt, J = 8.0, 1.0 Hz, 1H), 7.22 (ddd, J = 8.0, 7.0, 1.0 Hz, 1H), 7.16 (ddd, J = 8.0, 7.0, 1.0 Hz, 1H), 7.05–7.00 (m, 2H), 6.89 (d, J = 1.0 Hz, 1H), 5.74 (d, J = 7.5 Hz, 1H), 4.76 (dt, J = 7.5, 5.5 Hz, 1H), 3.74 (dd, J = 17.0, 4.5 Hz, 1H), 3.57 (dd, J = 17.0, 4.5 Hz, 1H), 3.50 (s, 3H), 3.18 (d, J = 5.5 Hz, 2H), 2.36 (s, 3H), 2.14 (s, 3H), 2.10 (s, 3H); ^{13}C NMR (101 MHz, CDCl$_3$, δ): 171.7, 166.2, 156.0 (q, $^2J_{CF}$ = 37.5 Hz), 139.3, 138.2, 138.1, 135.8, 134.7, 128.9, 128.8, 128.6, 128.6, 122.3, 120.0, 118.4, 115.7 (q, $^1J_{CF}$ = 287.0 Hz), 111.1, 107.4, 53.5, 52.5, 42.1, 27.0, 21.2,

20.3, 20.2; ^{19}F NMR (376 MHz, CDCl$_3$, δ): −75.7; ESI-MS m/z (ion, %): 512 ([M + Na]$^+$, 100); ESI-HRMS m/z: 512.1773 [M + Na]$^+$ (calc. for C$_{25}$H$_{26}$F$_3$N$_3$NaO$_4$ 512.1768); IR (solid state, ATR, cm^{-1}): 3339, 2959, 2919, 2850, 1718, 1670, 1523, 1458, 1437, 1260, 1157, 1006, 853, 800, 744, 517; UV-Vis (DMSO, nm): λ_{max} 288 (ε = 12 188 mol dm^{-3} cm^{-1}).

(2R)-4-Methyl-2-(trifluoroacetamido)pentanoic acid.[22] To a round-bottomed flask containing L-leucine (1 g, 7.6 mmol, 1 eq.) was added Et$_3$N (1.06 mL, 769 mg, 7.6 mmol, 1 eq.) and MeOH (7.6 mL) and the resulting suspension stirred for 5 min. After 5 min ethyl trifluoroacetate (1.13 mL, 1.35 g, 9.5 mmol, 1.25 eq.) was added and the mixture stirred at rt for 16 h, during which time a clear solution formed. After 16 h the solvent was removed under reduced pressure and the resulting residue acidified with 2 M HCl, before being extracted into EtOAc three times. The organic layers were combined then washed with brine, dried over MgSO$_4$, filtered and the solvent removed under reduced pressure to give the product as a white solid (1.67 g, 97%). $[\alpha]_D$ = +31.6 (c 0.10, CHCl$_3$); Mp 75–77 °C (lit.[29] 76–77 °C dec); ^{1}H NMR (400 MHz, CD$_3$OD, δ): 4.48 (dd, J = 10.0, 5.0 Hz, 1H), 1.81–1.60 (m, 3H), 0.97 (d, J = 6.0 Hz, 3H), 0.94 (d, J = 6.0 Hz, 3H); ^{13}C NMR (101 MHz, CD$_3$OD, δ): 174.4, 158.9 (q, $^2J_{CF}$ = 38.0 Hz), 117.5 (q, $^1J_{CF}$ = 287.0 Hz), 52.4, 40.7, 26.1, 23.3, 21.5; ^{19}F NMR (376 MHz, CD$_3$OD, δ): −77.0; ESI-MS m/z (ion, %): 250 ([M + Na]$^+$, 100); ESI-HRMS m/z: 250.0665 [M + Na]$^+$ (calc. for C$_8$H$_{12}$F$_3$NNaO$_3$ 250.0661).

Methyl (2S)-3-(1H-indol-3-yl)-2-[(2R)-4-methyl-2-tri-fluoro-acetamido)pentanamido] propanoate, 15. (2R)-4-Methyl-2-(trifluoroacetamido)pentanoic acid (500 mg, 2.2 mmol, 1 eq.), methyl (2S)-2-amino-3-(1H-indol-3-yl)propanoate (616 mg, 2.42 mmol, 1.1 eq.) and 3-(Diethoxyphosphoryloxy)-1,2,3-benzotriazin-4(3-H)-one (DEPBT) (790 mg, 2.64 mmol, 1.2 eq.) were added to a round-bottomed flask which was fitted with a septum and flushed with argon from a balloon for 20 min. After 20 min dry, distilled DIPEA (1.5 mL, 1.14 g, 8.8 mmol, 4 eq.) and dry CH$_2$Cl$_2$ (22 mL) were added via syringe to give a yellow solution and the reaction was stirred at rt for 2 h. After 2 h the reaction mixture was washed with sat. aq. NH$_4$Cl and extracted three times with CH$_2$Cl$_2$. The organic layers were combined, dried over MgSO$_4$, filtered and the solvent removed under reduced pressure to give a crude yellow residue. This was dry-loaded onto silica gel and purified by flash column chromatography (1:1 EtOAc/petrol, v/v) to give the product as an off-white solid (568 mg, 60%). R_f 0.48 (1:1 EtOAc/pxetrol v/v); $[\alpha]_D$ = +33.9 (c 0.10, CHCl$_3$); Mp 129–131 °C; ^{1}H NMR (400 MHz, CDCl$_3$, δ): 8.19 (br s, 1H), 7.48 (d, J = 8.0 Hz, 1H), 7.36–7.33 (m, 1H), 7.23–7.08 (m, 2H), 6.98 (d, J = 2.0 Hz, 1H), 6.45 (d, J = 8.0 Hz, 1H), 4.97–4.84 (m, 1H), 4.51–4.36 (m, 1H), 3.70 (s, 3H), 3.38–3.25 (m, 2H), 1.68 (s, 1H), 1.62–1.41 (m, 3H), 1.29–1.18 (m, 3H), 0.89–0.75 (m, 6H); ^{13}C NMR (101 MHz, CDCl$_3$, δ): 172.0, 170.4, 157.1 (q, $^2J_{CF}$ = 37.5 Hz), 136.2, 127.5, 123.3, 122.5, 120.0, 118.4, 116.6 (q, $^1J_{CF}$ = 288.0 Hz), 111.5, 109.3, 53.2, 52.7, 52.2, 41.5, 27.6, 24.7, 22.7, 22.1; ^{19}F NMR (376 MHz, CDCl$_3$, δ): −75.6; ESI-MS m/z (ion, %): 428 ([M + H]$^+$, 75), 450 ([M + Na]$^+$, 100); ESI-HRMS m/z: 450.1612 [M + Na]$^+$ (calc. for C$_{20}$H$_{24}$F$_3$N$_3$NaO$_4$ 450.1611);

247

Paper

IR (solid state, ATR, cm^{-1}): 3277, 3084, 2959, 2933, 2873, 1714, 1652, 1551, 1439, 1341, 1209, 1184, 1156, 1094, 1010, 988, 742, 719, 652, 632, 521; UV-Vis (DMSO, nm): λ_{max} 282 (ε = 5734 mol dm^{-3} cm^{-1}).

Methyl (2S)-2-[(2R)-4-methyl-2-(trifluoroacetam-ido)pentan-amido]-3-(2-phenyl-1H-indol-3-yl)propanoate, 16a. Synthesised using General Procedure 3 from methyl (2S)-3-(1H-indol-3-yl)-2-[(2R)-4-methyl-2-(trifluoroacetamido)pentanamido]propanoate 15 (82 mg, 0.192 mmol, 1 eq.), phenyl (2,4,6-trimethylphenyl)-iodonium trifluoromethanesulfonate 11a (181 mg, 0.384 mmol, 2 eq.) and Pd(OAc)$_2$ (2 mg, 9.6 µmol, 5 mol%) in EtOAc (5 mL). Flash column chromatography (3 : 1 petrol/EtOAc, v/v) gave the product as a yellow solid (63 mg, 65%). R_f 0.19 (3 : 1 petrol/EtOAc, v/v); $[\alpha]_D$ = +43.8 (c 0.10, CHCl$_3$); Mp 83–85 °C dec; ^{1}H NMR (400 MHz, CDCl$_3$, δ): 8.18 (br s, 1H), 7.57–7.53 (m, 3H), 7.49 (ddt, J = 8.0, 6.5, 1.0 Hz, 2H), 7.42–7.35 (m, 2H), 7.25–7.19 (m, 1H), 7.15 (ddd, J = 8.0, 7.0, 1.0 Hz, 1H), 6.91–6.84 (m, 1H), 5.93–5.83 (m, 1H), 4.79 (dq, J = 7.5, 5.5, 5.0 Hz, 1H), 3.96 (td, J = 8.0, 5.0 Hz, 1H), 3.65–3.48 (m, 2H), 3.38 (s, 3H), 1.54–1.34 (m, 3H), 0.82–0.75 (m, 6H); ^{13}C NMR (101 MHz, CDCl$_3$, δ): 171.7, 170.1, 156.6 (q, $^2J_{CF}$ = 37.5 Hz), 136.2, 135.8, 132.9, 129.3, 129.2, 129.1, 128.4, 128.3, 128.2, 122.8, 120.2, 118.6 (q, $^1J_{CF}$ = 287.5 Hz), 111.2, 106.2, 53.3, 52.3, 51.8, 42.0, 26.6, 24.6, 22.7, 22.1; ^{19}F NMR (376 MHz, CDCl$_3$, δ): −72.4; ESI-MS m/z (ion, %): 504 ([M + H]$^+$, 5), 521 ([M + NH$_4$]$^+$, 15), 526 ([M + Na]$^+$, 100), 542 ([M + K]$^+$, 5); ESI-HRMS m/z: 526.1925 [M + Na]$^+$ (calc. for C$_{26}$H$_{28}$F$_3$N$_3$NaO$_4$ 526.1924); IR (solid state, ATR, cm^{-1}): 3337, 3061, 2958, 2930, 2873, 1715, 1658, 1530, 1448, 1209, 1155, 742, 698; UV-Vis (DMSO, nm): λ_{max} 308 (ε = 20 467 mol dm^{-3} cm^{-1}).

Methyl (2S)-2-[(2R)-4-methyl-2-(trifluoroacetamido) pentan-amido]-3-[2-(2,4,6-trimethylphenyl)-1H-indol-3-yl]propanoate, 16b. Synthesised using General Procedure 3 from methyl (2S)-3-(1H-indol-3-yl)-2-[(2R)-4-methyl-2-(trifluoroacetamido)pentan-amido]propanoate 15 (82 mg, 0.192 mmol, 1 eq.), phenyl (2,4,6-trimethylphenyl)iodonium trifluoromethanesulfonate 11a (181 mg, 0.384 mmol, 2 eq.) and Pd(OAc)$_2$ (2 mg, 9.6 µmol, 5 mol%) in EtOAc (5 mL). Flash column chromatography (3 : 1 petrol/EtOAc, v/v) gave the product as a yellow solid (13 mg, 12%). R_f 0.29 (3 : 1 petrol/EtOAc, v/v); $[\alpha]_D$ = +31.1 (c 0.10, CHCl$_3$); ^{1}H NMR (400 MHz, CDCl$_3$, δ): 7.87 (br s, 1H), 7.61–7.56 (m, 1H), 7.39–7.34 (m, 1H), 7.22 (td, J = 8.0, 7.5, 1.0 Hz, 1H), 7.17 (td, J = 7.5, 1.0 Hz, 1H), 7.03 (d, J = 3.5 Hz, 2H), 6.91–6.85 (m, 1H), 5.67 (d, J = 7.0 Hz, 1H), 4.69 (td, J = 7.5, 4.5 Hz, 1H), 4.19–4.08 (m, 1H), 3.54 (s, 3H), 3.23 (dd, J = 15.0, 5.0 Hz, 1H), 3.01 (dd, J = 15.0, 7.5 Hz, 1H), 2.35 (s, 3H), 2.12 (s, 3H), 2.08 (s, 3H), 1.54–1.41 (m, 3H), 0.96–0.64 (m, 6H); ^{13}C NMR (101 MHz, CDCl$_3$, δ): 171.8, 170.3, 156.7 (q, $^2J_{CF}$ = 37.5 Hz), 139.4, 138.3, 137.9, 135.8, 134.7, 129.00, 128.9, 128.4, 128.0, 122.4, 120.1, 118.4, 116.5 (q, $^1J_{CF}$ = 288.0 Hz), 111.1, 107.6, 53.5, 52.5, 51.8, 42.6, 29.6, 27.1, 24.6, 22.8, 22.3, 21.2, 20.3; ^{19}F NMR (376 MHz, CDCl$_3$, δ): −75.8; ESI-MS m/z (ion, %): 546 ([M + H]$^+$, 2), 563 ([M + NH$_4$]$^+$, 15), 568 ([M + Na]$^+$, 100), 584 [M + K]$^+$, 2); ESI-HRMS m/z: 568.2384 [M + Na]$^+$ (calc. for C$_{29}$H$_{34}$F$_3$N$_3$NaO$_4$ 568.2394); IR (solid state, ATR, cm^{-1}): 3391, 3341, 2957, 2927, 1710, 1661, 1529, 1458, 1439,

1353, 1210, 1155, 1008, 909, 853, 731; UV-Vis (DMSO, nm): λ_{max} 290 (ε = 8712 mol dm^{-3} cm^{-1}).

Acknowledgements

Notes and references

1 (a) S. De Ornellas, T. J. Williams, C. G. Baumann and I. J. S. Fairlamb, in *Catalytic C–H/C–X Bond Activation*, ed. X. Ribas, RSC Publishing, Cambridge, 2013; (b) T. O. Ronson, R. J. K. Taylor and I. J. S. Fairlamb, *Tetrahedron*, 2014, 71, 989; (c) K. C. Nicolaou, P. G. Bulger and D. Sarlah, *Angew. Chem., Int. Ed.*, 2005, 44, 4442. An elegant example of the Suzuki–Miyaura reaction performed on proteins containing genetically incorporated aryl iodides can be found in. (d) C. D. Spicer, T. Triemer and B. G. Davis, *J. Am. Chem. Soc.*, 2012, 134, 800.

2 L. Ackermann, R. Vicente and A. R. Kapdi, *Angew. Chem., Int. Ed.*, 2009, 48, 9792.

3 (a) J. Yamaguchi, A. D. Yamaguchi and K. Itami, *Angew. Chem., Int. Ed.*, 2012, 51, 8960. For a beautiful example, see: (b) M. E. Kieffer, K. V. Chuang and S. E. Reisman, *J. Am. Chem. Soc.*, 2013, 135, 5557.

4 A. F. M. Noisier and M. A. Brimble, *Chem. Rev.*, 2014, 114, 8775.

5 J. Wencel-Delord, T. Dröge, F. Liu and F. Glorius, *Chem. Soc. Rev.*, 2011, 40, 4740.

6 (a) T. E. Storr, A. G. Firth, K. Wilson, K. Darley, C. G. Baumann and I. J. S. Fairlamb, *Tetrahedron*, 2008, 64, 6125; (b) T. E. Storr, C. G. Baumann, R. J. Thatcher, S. De Ornellas, A. C. Whitwood and I. J. S. Fairlamb, *J. Org. Chem.*, 2009, 74, 5810; (c) T. E. Storr, J. A. Strohmeier, C. G. Baumann and I. J. S. Fairlamb, *Chem. Commun.*, 2010, 46, 6470.

7 J. T. Vivian and P. R. Callis, *Biophys. J.*, 2001, 80, 2093.

8 T. J. Williams, A. J. Reay, A. C. Whitwood and I. J. S. Fairlamb, *Chem. Commun.*, 2014, 50, 3052.

9 For C2-arylated tryptophan using the Suzuki–Miyaura reaction, see: (a) F. Kolundzic, M. N. Noshi, M. Tjandra, M. Movassaghi and S. J. Miller, *J. Am. Chem. Soc.*, 2011, 133, 9104. An example of the S–M reaction performed on the tryptophan-containing natural product apicidin can be found in: (b) S. L. Colletti, C. Li, M. H. Fisher, M. J. Wyvratt and P. T. Meinke, *Tetrahedron Lett.*, 2000, 7825. The S–M reaction can also be used to access 5- and 7-arylated tryptophans: (c) A. D. Roy, R. J. M. Goss, G. K. Wagner and M. Winn, *Chem. Commun.*, 2008, 4831.

248

10 (a) J. Ruiz-Rodríguez, F. Albericio and R. Lavilla, *Chem. – Eur. J.*, 2010, **16**, 1124; (b) S. Preciado, L. Mendive-Tapia, F. Albericio and R. Lavilla, *J. Org. Chem.*, 2013, **78**, 8129. For the post-synthetic direct *C2*-arylation of a tryptophan-containing natural product, see: (c) S. Preciado, L. Mendive-Tapia, C. Torres-García, R. Zamudio-Vázquez, V. Soto-Cerrato, R. Pérez-Tomás, F. Albericio, E. Nicolás and R. Lavilla, *Med. Chem. Commun.*, 2013, **4**, 1171. For a sophisticated Pd-mediated peptidic macrocyclisation *via* the intramolecular *C2*-arylation of a tryptophan residue, see: (d) H. Dong, C. Limberakis, S. Liras, D. Price and K. James, *Chem. Commun.*, 2012, **48**, 11644. For the direct *C2*-arylation of a protected tryptophan derivative using Ru, see: (e) L. Ackermann and A. V. Lygin, *Org. Lett.*, 2011, **13**, 3332.

11 (a) Y. Zhu, M. Bauer, J. Ploog and L. Ackermann, *Chem. – Eur. J.*, 2014, **20**, 13099; (b) We have established that when the Ackermann conditions ([Ph₂I]OTs, DMF, 100 °C, 17 h) are applied to the protected tryptophan **1a**, no *C2*-arylation is observed. Addition of Pd(OAc)₂ (5 mol%) afforded 93% conversion to the desired arylation product **2a**. Air has no appreciable effect.

12 N. R. Deprez, D. Kalyani, A. Krause and M. S. Sanford, *J. Am. Chem. Soc.*, 2006, **128**, 4972.

13 We have also established that the reaction of **1a** with either 4-Me-C₆H₄B(OH)₂ or 4-OMe-C₆H₄B(OH)₂ and PhI(OAc)₂ affords a similar mixture of 2-arylated tryptophan products in a *ca*. 1 : 1 ratio by ESI-HRMS.

14 For selected papers on hydroxylation of organic compounds by C–H bond activation with Cuᴵᴵ/O₂ systems, see: (a) G. Izzet, J. Zeitouny, H. Akdas-Killig, Y. Frapart, S. Me'nage, B. Douziech, I. Jabin, Y. Le Mest and O. Reinaud, *J. Am. Chem. Soc.*, 2008, **130**, 9514; (b) A. Kunishita, M. Kubo, H. Sugimoto, T. Ogura, K. Sato, T. Takui and S. Itoh, *J. Am. Chem. Soc.*, 2009, **131**, 2788; (c) R. L. Peterson, R. A. Himes, H. Kotani, T. Suenobu, L. Tian, M. A. Siegler, E. I. Solomon, S. Fukuzumi and K. D. Karlin, *J. Am. Chem. Soc.*, 2011, **133**, 1702; (d) J. Gallardo-Donaire and R. Martin, *J. Am. Chem. Soc.*, 2013, **135**, 9350.

15 For cupric complexes of alanine, see: (a) H. Borsook and K. V. Thimann, *J. Biol. Chem.*, 1932, **98**, 671. The X-ray single crystal structure of L-(tryptophyl-glycinato)copper(II) shows how a free carboxylate amino acid neighbouring a tryptophan can coordinate Cuᴵᴵ, see: (b) O. R. Nascimento, A. J. Costa-Filho, D. I. De Morais, J. Ellena and L. F. Delboni, *Inorg. Chim. Acta*, 2001, **312**, 133.

16 For reviews, see: (a) N. R. Deprez and M. S. Sanford, *Inorg. Chem.*, 2007, **46**, 1924; (b) E. A. Merritt and B. Olofsson, *Angew. Chem., Int. Ed.*, 2009, **48**, 9052. Selected examples: (c) L. L. Suarez and M. F. Greaney, *Chem. Commun.*, 2011, **47**, 7992; (d) T. E. Storr and M. F. Greaney, *Org. Lett.*, 2013, **15**, 1410; (e) J. Malmgren, A. Nagendiran, C.-W. Tai, J.-E. Bäckvall and B. Olofsson, *Chem. – Eur. J.*, 2014, **20**, 13531.

17 R. J. Phipps, N. P. Grimster and M. J. Gaunt, *J. Am. Chem. Soc.*, 2008, **130**, 8172.

18 E. F. Evans, N. J. Lewis, I. Kapfer, G. Macdonald and R. J. K. Taylor, *Synth. Commun.*, 1997, **27**, 1819.

19 D. R. Appleton, R. C. Babcock and B. R. Copp, *Tetrahedron*, 2001, **57**, 10181.

20 G. Cardillo, L. Gentilucci, C. Tomasini and L. Tomasoni, *Tetrahedron: Asymmetry*, 1995, **6**, 1947.

21 K. Sato and A. P. Kozikowski, *Tetrahedron Lett.*, 1989, **30**, 4073.

22 G. T. Notte and T. Sammakia, *J. Am. Chem. Soc.*, 2006, **128**, 4230.

23 P. A. Stadler, *Helv. Chim. Acta*, 1978, **61**, 1675.

24 E. Angelini, C. Balsamini, F. Bartoccini, S. Lucarini and G. Piersanti, *J. Org. Chem.*, 2008, **73**, 5654.

25 B. S. Holla, K. V. Malini, B. K. Sarojini and B. Poojary, *Synth. Commun.*, 2005, **35**, 333.

26 K. Hasizume and Y. Shimonishi, *Bull. Chem. Soc. Jpn.*, 1981, **54**, 3806.

27 T. Kitamura, J.-I. Matsuyuki and H. Taniguchi, *Synthesis*, 1994, 147.

28 W. Steglich and S. Hinze, *Synthesis*, 1976, 399.

29 T. T. Otani and M. R. Briley, *J. Pharm. Sci.*, 1979, **68**, 496.

This journal is © The Royal Society of Chemistry 2015

Org. Biomol. Chem., 2015, **13**, 8298–8309 | **8309**

249

ChemComm

FEATURE ARTICLE

Catalytic C–H bond functionalisation chemistry: the case for quasi-heterogeneous catalysis

Alan J. Reay and Ian J. S. Fairlamb*

This feature article examines the potential of heterogeneous Pd species to mediate catalytic C–H bond functionalisation processes employing suitable substrates (*e.g.* aromatic/heteroaromatic compounds). A focus is placed on the reactivity of supported and non-supported Pd nanoparticle (PdNPs) catalysts, in addition to the re-appropriation of well-established heterogeneous Pd catalysts such as Pd/C. Where possible, reasonable comparisons are made between PdNPs and traditional 'homogeneous' Pd precatalyst sources (which form PdNPs). The involvement of higher order Pd species in traditional cross-coupling processes, such as Mizoroki–Heck, Sonogashira and Suzuki–Miyaura reactions, allows the exemplification of potential future topics for study in the area of catalytic C–H bond functionalisation processes.

Introduction

Great effort has been directed towards the selective and catalytic functionalisation of C–H bonds.[1,2] These processes are usually mediated by a transition metal for which the reaction mechanisms are often intriguing and where the products formed are useful in many areas of scientific research and endeavour.

Removing substrate pre-functionalisation usually minimises downstream chemical waste, while eliminating the need for prior mandatory reaction steps for the installation of chemical functionality which is ultimately lost in the final and desired chemical transformation. One can compare three complementary reactions (Scheme 1): (a) a traditional cross-coupling reaction of an organohalide with an organometallic reagent; (b) the direct reaction of an organohalide or organometallic with a substrate containing a reactive C–H bond (note: a base is needed for the former and an oxidant for the latter); (c) the selective reaction of two substrates containing C–H bonds (by an oxidative dehydrogenative process). There is thus a strong case for developing synthetic methods that facilitate the selective C–H bond functionalisation of any desired molecule. Couplings at C–H bonds can be made involving sp, sp^2 and sp^3 centres, although the latter might be viewed as challenging.

In terms of elemental sustainability it is important that effort is directed towards unlocking the potential of cheaper, less toxic and more abundant metals as catalysts. In doing so it is essential to examine the overall waste associated with a given chemical transformation. It is also imperative that current elemental usage levels, as well as issues regarding the criticality of supply chains, are examined before making the assertion

that a cheaper and more abundant element today will be more readily available than a precious element in, for example, 60 years.[3]

Given the breakthroughs made in the field of catalytic Pd-catalysed cross-coupling chemistry, it is not unreasonable to ask whether research should shift focus to other, more elementally sustainable first-row transition metals such as Mn,[4,5] Fe[6,7] or Co.[8–10] While that is of global importance, it is of equal value to determine whether Pd catalysts can be better utilised and recycled,[11–14] so that future generations can exploit and benefit from the remarkable reactivity of this precious metal. Furthermore, one can question whether the reaction mechanisms involving Pd are fully understood, especially those reactions involving the catalytic functionalisation of C–H bonds. To date the mechanistic picture is dominated by homogeneous catalytic cycles involving one or two Pd atoms, involving Pd[0], Pd[II], Pd[III] and Pd[IV] oxidation states.[15–31] Moreover, researchers are often quick to rule out or entirely ignore a role for heterogeneous species in catalysis, either directly (*i.e.* by substrate activation) or indirectly (*i.e.* acting as a catalyst reservoir, regulating the catalyst concentration).

Central to the topic of this paper is to recognise that precious metal catalysts such as Pd can play a critical role in

Scheme 1 A generic scheme to represent traditional cross-coupling and C–H bond functionalisation processes (in this example, R^1 and R^2 are carbon-centred, M = metal and X = halide or pseudohalide, *i.e.* leaving group).

Department of Chemistry, University of York, Heslington, York, YO10 5DD, UK.
E-mail: ian.fairlamb@york.ac.uk; Tel: +0044 (0)1904 324091

250

Feature Article

the C–H bond functionalisation of organic molecules, where current and new methodologies can be exploited for years to come. A focus is placed on understanding that common Pd precursor catalysts (precatalysts) are able to aggregate to form higher order Pd species (*i.e.* usually nanoparticles), which can become catalytically relevant under an eclectic array of reaction conditions. Established processes and findings from the field of traditional cross-coupling chemistry are described to provide prior context, particularly: (1) the use of well-defined and supported Pd nanoparticles (PdNPs) as catalysts; (2) the evolution, propagation and catalytic role of PdNPs formed *in situ* from common Pd precatalysts. Examples from C–H bond functionalisation reactions studied in our laboratories are showcased, while recent developments in the use of heterogeneous Pd catalysts from a number of sources, including well-defined PdNPs in catalytic C–H bond functionalisation reactions, are discussed in detail. A perspective on the future of this topical area of research is offered at the end of this article.

A brief overview of the role played by Pd nanoparticles in Mizoroki–Heck, Sonogashira and Suzuki–Miyaura cross-coupling reactions

Background

Historically, concerning the nature of the active Pd catalyst species in Mizoroki–Heck cross-coupling reactions, there has been significant debate about the involvement of homogeneous and heterogeneous Pd species. There is unequivocal evidence showing that homogeneous Pd precatalyst sources (*e.g.* Pd(OAc)$_2$) can aggregate to form higher order species such as PdNPs; spherical PdNPs are typically 2–4 nm in size, with substantially different surface areas. The key question for cross-coupling chemistry concerns the catalytic role of PdNPs. Are the aggregated Pd species simply a dead-end for catalysis, *i.e.* an inactive form, or can they act as a Pd reservoir, controlling the active Pd within the catalytic cycle, or are they directly participating in surface catalysis? It is possible to represent this phenomenon as shown in Scheme 2.
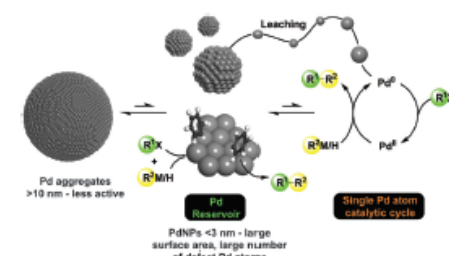
Scheme 2 A schematic representation showing a role for aggregated spherical Pd (Pd reservoir) with leached single Pd atoms.

Fig. 1 Top: A normal roundabout exemplifying a single catalytic cycle; bottom: the reality of Pd-catalyzed cross-coupling chemistry (in the absence of strongly coordinated and well-defined ligands) and their multiple catalytic cycles, here exemplified by the 'magic roundabout' in Swindon, UK (signs sourced from Google images, under creative commons UK search).

It is important to recognise that most studies point to single Pd atoms leaching from the surface of PdNPs. By way of an example, a 2 nm PdNP consists of about 250 Pd atoms, thus if the PdNPs are spherical *i.e.* truncated icosahedra with (111) planes, then about one fifth of these Pd atoms are available for a reaction on the surface. The equilibrium position between Pd reservoir and leached Pd is therefore critical to catalytic activity and efficacy.[32] Many articles and key reviews have grappled with this subject over the years.[33–36] It is not the intention of this article to more broadly discuss these issues, but simply to provide a context to better understand the potential role that higher order Pd species can play in catalytic C–H bond functionalisation chemistry. It is however clear that a multi-ensemble of higher order Pd species plays a key role in traditional catalytic cross-coupling processes, meaning that several catalytic cycles can be operative in solution. The mechanistic picture is nicely illustrated by comparing a simple road roundabout, *i.e.* a catalytic cycle involving a single species, with the multiple 'magic roundabout' found in Swindon in the United Kingdom, the analogy being that several catalytic species operate in similar cycles which contribute to an overall catalytic process (Fig. 1).

The evidence from Mizoroki–Heck and Sonogashira cross-coupling reactions

Central to the topic of this article is recognition of the existence of a Pd reservoir in catalytic cross-coupling processes. Workers at DSM pharma chemicals discovered that the Mizoroki–Heck cross-coupling of bromobenzene with *n*-butyl acrylate mediated by Pd(OAc)$_2$ exhibited an inverse relationship (negative order in Pd) of catalyst activity with catalyst concentration (Fig. 2).[37]

The Pd catalyst loading which gave the highest yield was found to be 0.08 mol% (39 ppm; calculated from the experimental data reported in the original paper). Moving to either lower or higher Pd catalyst loadings resulted in a loss of catalyst
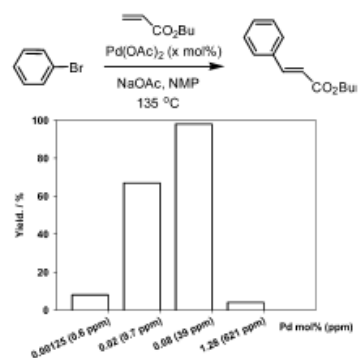
Fig. 2 Inverse relationship between catalytic activity and concentration in a Mizoroki–Heck cross-coupling (de Vries et al., 2003).[37] Adapted with permission from *Org. Lett.*, 2003, **5**, 3285.

Fig. 3 Effect of Pd catalyst loading in the Sonogashira cross-coupling of an activated aryl halide with a terminal alkyne (Fairlamb et al., 2004).[38]

activity. This observation can be attributed to the aggregation of Pd at higher Pd concentrations, which can be associated with the precipitation of Pd black (often seen at the end of cross-coupling reactions when the substrate is exhausted). At this concentration of Pd it is not entirely obvious what the structure of the Pd catalyst is. ESI-MS studies (−ve mode) provided some insight, showing the presence of $PdBr_3^-$ under working reaction conditions. This phenomenon was also noted in the Sonogashira cross-coupling of 4-bromoacetophenone with phenylacetylene using palladacyclic precatalysts in work conducted by our group (Fig. 3).[38] In this case, optimal turnover frequencies (TOFs) were recorded at 0.01 mol% Pd (92 ppm Pd). It is notable that in mechanistically distinct cross-coupling reactions with differing reaction conditions (*i.e.* catalyst structure, solvent type and additives), these reactions are most active when the concentration of Pd is below 100 ppm. We can confidently predict that this is the case for the majority of cross-coupling processes utilising activated organohalide substrates, where transmetallation and reductive elimination are not seen as problematic, *e.g.* side reactions such as homocoupling and hydrodehalogenation/protodemetallation are not seen.

It is worthy of note that Leadbeater and co-workers determined that Pd concentrations as low as *ca.* 20–50 ppb were able to effect certain cross-coupling reactions under microwave conditions in water.[39] Again, these types of reaction typically employ activated substrates (aryl halides), for example reaction of 4-bromoacetophenone with phenylboronic acid in the presence of $Pd(OAc)_2$ (100 ppb) using K_2CO_3 afforded the cross-coupled product in good yield. These research findings serve to show that: (1) low Pd concentrations can be used for certain cross-coupling processes involving activated substrates (thus are also a poor test for catalyst screening); (2) that aggregated Pd species can ultimately cause a drop-off in catalyst efficacy at higher concentrations, leading to non-linear rate relationships with respect to Pd concentration.[40]
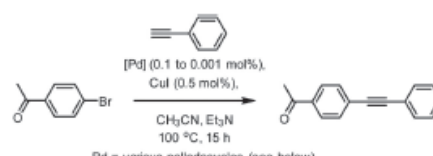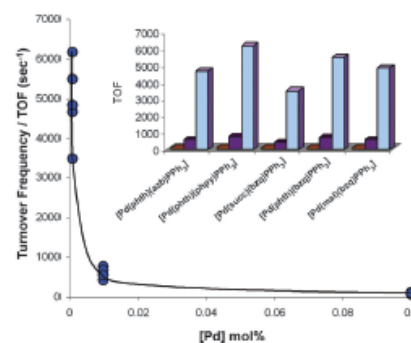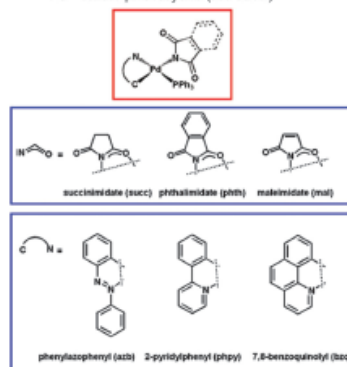
For Mizoroki–Heck cross-couplings the role of the Pd reservoir has been investigated by several research groups, in order to determine whether this reservoir simply releases single atoms into a homogeneous catalytic cycle, or whether the activation of aryl halides occurs directly at Pd surfaces. Evidence for the leaching of catalytically active Pd has been reported from supported Pd catalysts (*e.g.* Pd/C, Pd/SiO_2, $Pd/\gamma-Al_2O_3$).[41,42] The release of Pd is concomitant with recapture of Pd at the surface. The mechanism of leaching has been studied by Dupont and co-workers, who showed that oxidised Pd^{II} species were released into solution from higher order aggregated Pd species stabilised by quaternary ammonium salts.[43]

252

Feature Article

Further support for the leaching of Pd from larger PdNPs ($\sim$15 nm) has been observed in work by Rothenberg and co-workers.[44] Using a reactor containing a membrane which was able to select for particles <5 nm it was demonstrated that sintering of the PdNPs occurred under Mizoroki–Heck cross-coupling conditions (note: PdNPs of less than 5 nm can in theory contain several thousand Pd atoms). In keeping with the work described above, Rothenberg also characterised 'Pd^{II}(X)Ar(L)n' species under working reaction conditions. The same group also followed the formation and subsequent growth of Pd clusters from several Pd^{II} precursors using UV–visible spectroscopy, allowing for modelling of the reduction, cluster growth and aggregation of such species.[45]

X-ray absorption spectroscopic (XAS) analysis by Baiker and co-workers led them to conclude that Pd atom leaching occurs under working reaction conditions. Quick scanning extended X-ray absorption fine structure (QEXAFS) measurements allowed the characterization of PdNPs leached from a solid Pd catalyst (Pd on an Al$_2$O$_3$ support) to be monitored in real time on a sub-second timescale.[46] This technique, requiring synchrotron radiation, allows the local structure of ordered materials such as PdNPs to be characterised, in addition to molecular species like PdBr$_4$$^{2-}$ and Pd$_2$Br$_6$$^{2-}$ anions. The Mizoroki–Heck reaction of bromobenzene and styrene mediated by Pd/Al$_2$O$_3$ only leached Pd at reaction temperatures of 150 °C. Crucially, the species released at this temperature were found to be PdNPs *ca.* 2 nm (*i.e.* during substrate turnover). Interestingly, when the reaction rate started to decrease, pronounced changes in the EXAFS spectra were noted, leading to the characterisation of evolving PdBr$_4$$^{2-}$ and Pd$_2$Br$_6$$^{2-}$ anions. Such species appear to be present towards the latter stages of reaction when the concentration of bromobenzene is low and the concentration of Br$^-$ high. The authors concluded that the leached PdNPs can act beyond a simple Pd reservoir and are themselves catalytically active species, in addition to providing single-atom Pd species which are capable of entering into a traditional homogenous catalytic cycle.

Studies on Suzuki–Miyaura cross-coupling reactions

Working in collaboration with Lee, our group was able to test the catalytic competence of well-defined, polymer-supported PdNPs in a Suzuki–Miyaura cross-coupling reaction of phenyl-boronic acid and iodoanisole in methanol.[47,48] The (poly)vinyl-pyrrolidone (PVP) polymer used is known to support and stabilise PdNPs, preventing agglomeration.[49,50] A colloidal seeding method could therefore be employed to allow preparation of four different sizes of PVP–PdNPs, with mean diameters between 1.8 and 4.0 nm, which could be stored and manipulated easily under air. Upon comparison of the activity of these catalysts as a function of TOF against the total number of surface Pd atoms, a clear trend was observed, with smaller particles displaying greater activity. If however the TOF was normalised against only those Pd atoms contained within defect sites on the truncated cuboctahedral particles, no difference between particle sizes was observed (Fig. 4). This observation makes clear that it is the abundance of surface defect sites which determines the reactivity of such particles in this reaction;
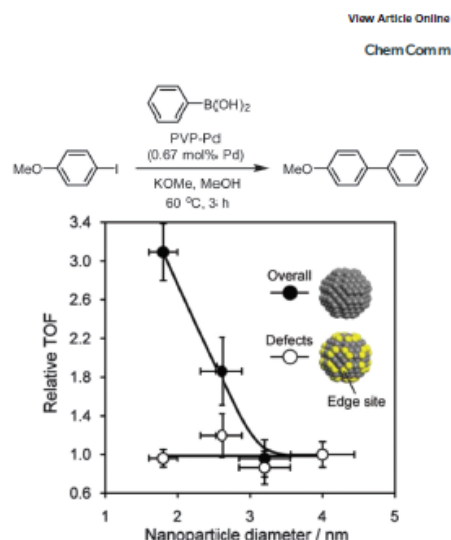
Fig. 4 Relationship between TOF and particle size normalised to either total surface Pd atoms (●) or defect surface Pd atoms (○) in a Suzuki–Miyaura coupling of phenylboronic acid and iodoanisole (Fairlamb *et al.*, 2010).[47,48] Reproduced from ref. 48 with permission from The Royal Society of Chemistry.

simply put, the more defect sites per particle, the more active the catalyst.

It is possible however that this trend was observed due to a preferential solubility of low-coordinate Pd species, leading to a more homogeneous catalytic manifold. To probe this effect further in operando X-ray absorption spectroscopy (XAS) was used to effectively monitor the coordination environment of the PdNPs, allowing for detailed analysis of the heterogeneity of the reaction under normal working conditions. These measurements indicated no sintering or leaching of the catalytically relevant particles during the reaction under the conditions used (Fig. 5), a result confirmed by EXAFS, X-ray photoelectron spectroscopy (XPS) and transmission electron microscopy (TEM) studies. Importantly no induction period was seen, which is consistent with the observation that nanoparticulate Pd is not simply acting as a pre-catalyst or Pd reservoir (*vide supra*); [Pd] responded in a first manner (in contrast to Pd(OAc)$_2$) which exhibits a negative order under the same reaction conditions). Finally, poisoning tests using elemental mercury (detailed below) performed during active substrate turnover caused immediate cessation of catalytic activity; the resultant Pd core/Hg shell particles were successfully characterised by XPS and a 1:1 correlation between the surface Pd and Hg atoms was observed.

Subsequent work by McGlacken and co-workers probed the shape sensitivity of a Suzuki–Miyaura coupling of phenylboronic acid and bromoanisole, catalysed by palladium nanocubes (PdNCs), octahedra (PdOCTs) and cuboctahedra (PdCUOCs).[51]

253

ChemComm
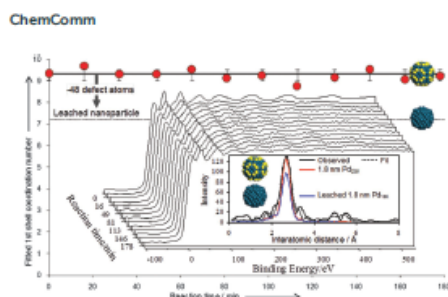
Fig. 5 XAS spectra of a Suzuki–Miyaura cross-coupling indicating no change in PdNP coordination environment during active substrate turnover (Fairlamb et al., 2010).[47,48] Reproduced with permission from *Angew. Chem., Int. Ed.*, 2010, **49**, 1820. Copyright 2010 Wiley-VCH Verlag GmbH & Co.

Intriguingly the authors found that nanocatalysts containing the smallest number of edge and corner atoms (PdNCs) proved the most active in this reaction (Fig. 6a), suggesting a link between activity and the presence of Pd (100) surface facets, rather than the defect sites highlighted *vide supra*. This was further investigated through use of both 10 nm and 20 nm PdNCs (Fig. 6b), the larger particles possessing a much smaller percentage of edge and corner atoms (0.16% for a 20 nm cube compared to 0.4% for a 10 nm cube). Almost identical reaction profiles for the different PdNCs were obtained, with the Pd concentration adjusted to allow for the same number of surface Pd atoms.

This difference in reactivity was ascribed to preferential leaching from the (100) facets of PdNCs, promoted by oxidative etching from O_2. TEM analysis of the nanocatalysts used appeared

Fig. 6 Shape sensitivity in a Suzuki–Miyaura coupling catalysed by Pd nanocatalysts with defined surface facets (McGlacken et al., 2014).[51] Reproduced with permission from *Angew. Chem., Int. Ed.*, 2014, **53**, 4142. Copyright 2014 Wiley-VCH Verlag GmbH & Co.

to show shape distortions resulting from the reaction conditions, while inductively coupled plasma mass spectrometry (ICP-MS) showed the presence of leached Pd in the post-reaction mixtures of all the nanocatalysts used. Greater quantities of leached Pd were found in those reactions which contained PdNCs. Critically this study indicates that the proposed oxidative etching is shape sensitive in nature and that the reaction likely proceeds *via* a (quasi)homogeneous catalytic cycle. It is interesting to note the perceived difference between a heterogeneous and homogeneous manifold in two very similar reactions (Fig. 4 and 6); possibly this results from the different quantities of O_2 present in these reactions, however it is likely that stabilisation of the PdNPs by PVP in the former example plays a key role.

A study on the stability of PVP–Pd catalysts shows that for those particles with low-index surfaces, high energy facets such as the (110) present in PdNCs are the least stable due to their preferential susceptibility to oxidation, while octahedral particles containing mostly (111) facets display correspondingly greater stability. Conversely those particles with high-index surfaces, such as concave nanocubes (PdCNCs), display superior stability due to stronger chemisorption to the PVP polymer.[52] Notably the particles used in the study by Fairlamb *et al.* consist of PVP-capped truncated cuboctahedra, which presents an interesting explanation for the mechanistic dichotomy observed. Work by McGlacken and co-workers extended this concept when examining the use of high-index PdCNCs in a similar Suzuki–Miyaura couplings. In the absence of a stabilising agent such as PVP, the (730) facets present in PdCNCs resulted in greater leaching and thus higher activity when compared to the low-index (100) facets present in PdNCs.[53]

The relevance of Pd nanoparticles as active catalysts in C–H bond functionalisations

Degradation (activation) of $Pd(OAc)_2$

As with the traditional cross-coupling reactions detailed above, it is important to recognise that common Pd (pre)catalysts can often act as Pd reservoirs for the subsequent generation of Pd^0 particles, or indeed as PdNP sources in their own right. During our group's development of conditions for the direct C8-arylation of the purine nucleoside adenosine (Scheme 3),[54] it was observed that agglomerates of insoluble Pd black were formed rapidly from $Pd(OAc)_2$ (note that this precursor complex usually derives from $Pd_3(OAc)_6$ under the reaction conditions employed. In these studies, the formation of Pd/Cu-containing nanoparticles was also observed during substrate turnover. TEM analysis of the reaction mixture demonstrated the formation of 3 nm PdNPs during the latter stages of the reaction. This analysis was conducted using a method developed to trap PdNPs that are generated *in situ*, through addition of 10 monomer equivalents of exogenous PVP polymer to an aliquot of the reaction mixture. This polymer acts as a stabiliser for the particles,[49,50] ensuring that they are not modified by solvent removal or other techniques employed in the preparation of the sample for TEM, thus
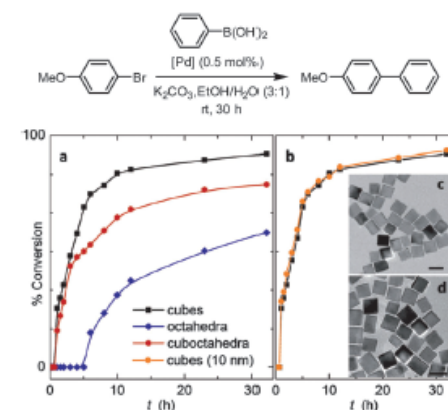
254

Feature Article

ChemComm
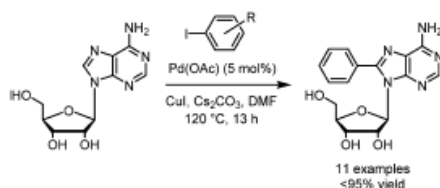
Scheme 3 Direct C8-arylation of adenosine using Pd(OAc)$_2$ (Fairlamb et al., 2008).[54]

enabling more accurate characterisation of the reactive particles. Subsequent investigation of several soluble Pd sources produced the same observation, while maintaining equivalent levels of substrate conversion. Correspondingly insoluble Pd sources such as Pd(OH)$_2$/C and PVP–Pd also functioned as an effective catalyst for this reaction, although the use of high temperatures and DMF (a highly palladophilic solvent) appeared to result in extensive leaching from these nominally heterogeneous Pd sources, producing a quasi-homogeneous catalytic manifold.[54]

During subsequent studies on the direct C8-arylation of the more sensitive 2′-deoxyadenosine substrate (Scheme 4),[55] the previously observed Pd/Cu nanoparticles were shown to be critical to precatalyst activation. Trace levels of dimethylamine impurities in the DMF used for this reaction were found necessary for effective substrate turnover. Screening of several amine additives in this reaction revealed that piperidine was able to produce a similar effect; preparation of the corresponding *trans*-Pd(OAc)$_2$(piperidine)$_2$ catalyst allowed for a more detailed investigation of this phenomenon. This catalyst was observed to rapidly degrade to form well-defined 1.7 nm DMF–PdNPs under the reaction conditions (80 °C), *via* a proposed Pd(piperidine)$_2$(DMF)$_2$ complex. More recently, Obora and co-workers have prepared stabilised forms of both DMF–PdNPs and DMF–Cu/PdNPs.[56-58] Alami et al. have also performed the direct C8-arylation of adenines mediated by Pearlman's catalyst (Pd(OH)$_2$/C) at elevated temperatures in polar aprotic solvents such as DMF and NMP.[59,60] No specific mention of Pd speciation is made, however this likely occurs under these conditions (see example by Fagnou et al., Scheme 11).[61]
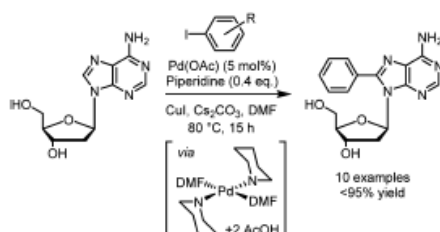
The importance of polar solvents for PdNP proliferation

Such evidence of DMF-stabilised PdNPs makes it clear that solvent effects can prove non-innocent with regards to the nature of the active catalyst formed in many reactions. The solvent must therefore be considered as an intrinsic mechanistic factor. Work by Hii and co-workers[62] on the speciation of Pd(OAc)$_2$ in a Suzuki–Miyaura reaction allowed the potential factors affecting the catalyst activation process to be investigated. It was found that water specifically effects a rapid hydrolytic dissociation of the Pd$_3$(OAc)$_6$ trimer cluster to create an intermediate species, which is subsequently reduced to Pd^0 (in this case by arylboronic acids). The quantity of water present thus specifically controls the amount of catalytically relevant Pd^0 available in the reaction mixture. Furthermore, the nuclearity of Pd(OAc)$_2$ appeared to be directly correlated to the dipole moment of the solvent of choice and more independent of the dielectric constant. Polar aprotic solvents with large dipole moments such as DMF will therefore result in a greater degree of dissociation of Pd(OAc)$_2$ (as was indirectly observed in our work detailed above) than those with small dipole moments, such as toluene.

A method of probing the heterogeneity of Mizoroki–Heck reactions performed in polar aprotic solvents at elevated temperatures has been developed by Djakovitch and co-workers.[63] They found that product selectivity when using cyclic alkenes is strongly dependent on the nature of the catalytic Pd species involved (Scheme 5). Specifically, in their Mizoroki–Heck coupling the most active Pd species are solubilised molecular Pd, while reaction on the surface of metallic Pd promotes dehalogenation. They concluded that concurrent homogeneous and heterogeneous manifolds are therefore in operation. Choi et al. have also documented a HPLC-MS technique to allow detection of ultra-small DMF–PdNPs, which might have passed unobserved by other analytical methods such as TEM.[64]

The degradation of Pd(OAc)$_2$ and Pd$_2$(dba)$_3$ has been utilised by Gómez et al. to produce PdNPs of ca. 2 nm, stabilised by imidazolium-containing ionic liquids[65] (drawing comparison with the earlier work by Dupont and co-workers),[43] while propagation

Scheme 4 Direct C8-arylation of 2′-deoxyadenosine *via* a Pd^0–piperidine complex forming DMF–PdNPs *in situ* (Fairlamb et al., 2009).[55]
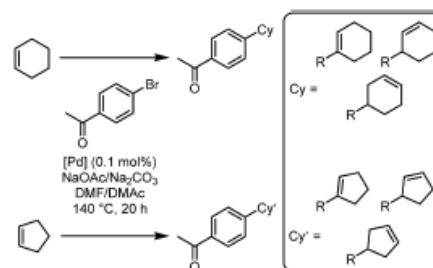
Scheme 5 Mizoroki–Heck reaction using cyclic alkenes as a probe for detection of homogeneous vs. heterogeneous Pd species (Djakovitch et al., 2004).[63]

255

ChemComm
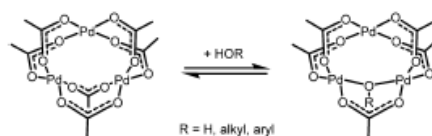
Scheme 6 Equilibrium between Pd$_3$(OAc)$_6$ trimer and μ^2-hydroxide or alkoxide species (Bedford et al., 2015).[72]

Scheme 7 Direct C2-arylation of benzoxazole and benzothiazole using Pd(OAc)$_2$-derived *in situ* and supported PdNPs (Fairlamb et al., 2014).[73]

of PdNPs from Pd(OAc)$_2$ in DMF has also been observed by Ranu *et al.* in the direct acylation of aryl halides[66] and the direct arylation of benzothiazole.[67] This effect was also noted by Langer and co-workers in the direct arylation of pyrroles performed in ionic liquids at elevated temperatures. This protocol was shown to be effective when catalysed by preformed PVP-supported PdNPs of around 1–2 nm.[68] Felpin and co-workers added charcoal as a stabiliser for PdNPs formed *in situ* from Pd(OAc)$_2$ in their direct intramolecular formation of phenanthrenes from stilbenes, with ICP-MS of the post-reaction mixtures used to highlight the affinity of charcoal for these catalytic Pd species.[69] Ananikov and co-workers have also gained detailed insight into the degradation behaviour of Pd$_2$(dba)$_3$ in chloroform,[70] demonstrating an efficient capture mechanism of the resultant PdNPs by activated carbon at 40 °C. By using these reactive Pd markers, they were able to demonstrate >2000 reactive centres per 1 μm^2 of carbon surface area.[71]

More recently, Bedford and co-workers have demonstrated the facile hydrolysis and alcoholysis of Pd(OAc)$_2$ (from its native trimeric form, Pd$_3$(OAc)$_6$).[72] Their work makes clear that in any catalytic process utilising Pd(OAc)$_2$, intermediates such as those shown in Scheme 6 should be considered as relevant species. Furthermore, Pd(OAc)$_2$ must be viewed as a highly labile (pre)-catalyst in solution.

Propagation of PdNPs in C–H bond functionalisations

Our group has established that considerations regarding the activation of Pd(OAc)$_2$ and other related precursors to form well-defined PdNPs can also be extended to several C–H bond functionalisation protocols, allowing for the activity of pre-synthesised PdNP catalysts to be independently tested and compared in these reactions.[73] For example under the conditions detailed in Scheme 4, use of a stabilised PVP-PdNP catalyst allowed for the reaction temperature to be lowered to 60 °C, with no appreciable decrease in conversion.

During studies on the direct C2-arylation of benzoxazole and benzothiazole under the Pd/Cu-catalysed conditions shown in Scheme 7, a significant deleterious air effect was noted on the reaction when using Pd(OAc)$_2$ as the catalyst. If however pre-synthesised PVP-PdNPs were used, rigorous exclusion of air was not required to obtain similar yields of the desired 2-aryl products.

TEM analysis of the reaction mixture using our previously developed sampling technique[54] revealed that the PdNPs generated from Pd(OAc)$_2$ under Schlenk conditions were larger and more varied in size than those generated when air was not
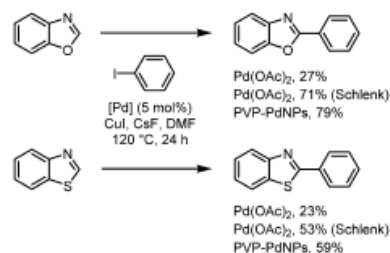
rigorously excluded. This led to the conclusion that these larger particles formed in the absence of air, and were also more active under the reaction conditions. Interestingly however, the pre-synthesised PVP–PdNPs which evidenced equivalent activity, without rigorous exclusion of air, were smaller than those generated from Pd(OAc)$_2$. The PVP polymer may therefore be preventing oxidative Pd leaching in this example (see study on PVP–PdNP stability by McGlacken *et al.*[51] above). Other conditions for the selective C2-arylation of benzoxazole were also investigated to determine the potential involvement of PdNPs in a reported Pd$^{II/IV}$ catalytic manifold (Scheme 8).

The literature conditions for this process necessitated the use of a hypervalent iodine reagent, PhI(OAc)$_2$, as the aryl coupling partner. The similarity to our conditions using iodo-benzene and DMF however prompted us to further examine the behaviour of the Pd catalyst. Upon addition of DMSO to the reaction mixture, a clear colour change to the dark brown of colloidal PdNPs was observed. TEM analysis of this reaction mixture demonstrated PdNPs that were uniformly <5 nm in size, which suggested that Pd^0 species were catalytically relevant under these conditions (Fig. 7). Subsequently, it was found that PhI(OAc)$_2$ rapidly degrades to PhI within 10 min at 150 °C in DMSO; correspondingly, use of PhI as the aryl coupling partner in place of the oxidising PhI(OAc)$_2$ had no effect on the yield of the reaction. In light of these findings it was proposed that this reaction does in fact proceed through a Pd$^{0/II}$ manifold, where PdNPs propagated from the degradation of Pd(OAc)$_2$ are key catalytic species.[74]

More recently, Sanford's conditions for the direct C2-arylation of *N*-methylindole with phenylboronic acid and iodobenzene in acetic acid were explored.[75] It was noted that PdNPs were visibly formed within seconds of substrate addition, so PVP–Pd was
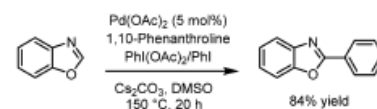
Scheme 8 Direct C2-arylation of benzoxazole with PhI(OAc)$_2$ or PhI (Fairlamb et al., 2013).[74]

256

Feature Article
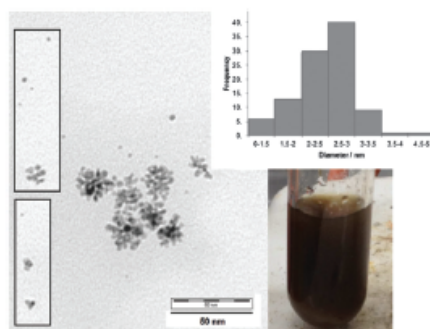
Fig. 7 PdNPs formed *in situ* from the reduction of Pd(OAc)$_2$ in DMSO for the direct C2-arylation of benzoxazole (Fairlamb *et al.*, 2013).[74] Reprinted from *Tetrahedron*, 2014, **70**, 6174. Copyright 2014, with permission from Elsevier.

utilised as a catalyst for this reaction and provided the desired aryl product in 59% yield (Scheme 9).

This methodology was subsequently applied to the direct C2-arylation of a protected tryptophan derivative,[76,77] whereupon the rapid propagation of PdNPs was observed within minutes. TEM analysis of the reaction mixture highlighted the presence of AcOH- and PVP-stabilised nanoparticles; as with the direct arylation of benzoxazole, these particles were uniformly <5 nm in size. Once again, a PVP–Pd catalyst demonstrated equivalent activity in this transformation (Scheme 10).

The examples highlighted above establish that in many reactions, propagation of PdNPs from common Pd precursors to form catalytically competent Pd^0 species is a crucial factor. Moreover, pre-supported PdNP catalysts such as PVP–Pd are a demonstrably viable catalyst for many C–H bond functionalisation protocols.
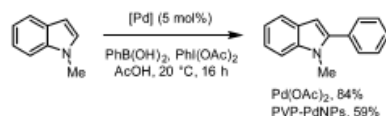
Scheme 9 Direct C2-arylation of *N*-methylindole using Pd(OAc)$_2$ (Sanford *et al.*, 2006)[75] and PVP–PdNPs (Fairlamb *et al.*, 2014).[73]
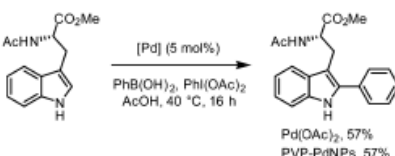
Scheme 10 Direct C2-arylation of a tryptophan derivative using Pd(OAc)$_2$-derived *in situ* and supported PdNPs (Fairlamb *et al.*, 2014).[76]

The use of such catalysts allows for a greater degree of control over potentially complex catalytic manifolds, where a multi-ensemble of higher order Pd species often play a key role.

Activity of supported Pd nanoparticles in C–H bond functionalisation chemistry

Background

To date there are only a handful of supported Pd nanoparticulate catalysts that have been described in the literature for use in C–H bond functionalisation chemistry,[78,79] in contrast to more traditional Pd-catalysed cross-coupling reactions.[11–14] Despite their limited number these catalysts are highly varied and correspondingly they display diverse reactivities. Interestingly both Pd^0 and Pd^{II} supported species are reported, although proposed mechanisms understandably centre on Pd^0/Pd^{II} manifolds; external oxidants are often employed however, allowing for higher oxidation state manifolds to be potentially accessed. A common feature of these catalytic systems is their low Pd loadings, typically resulting from a heterogeneous system where extensive Pd leaching is not observed. This naturally allows for a more effective use of this precious metal catalyst, with some exceptions (*vide infra*). A wide range of organic and inorganic supports have been utilised for the preparation of these species, which have been broadly grouped together into similar classes for the purposes of this article.

Commonly employed heterogeneity tests

The work highlighted in this article and others[33–36,80–82] makes it clear that determining the extent of homogeneous *vs.* heterogeneous catalysis in a given system is often a difficult task, made more so by the lack of any single absolute empirical test for the confirmation of the true nature of the catalytically competent metal species. In many of the examples discussed below, a plethora of tests to indicate proposed heterogeneous behaviour are utilised; for ease these are summarised here and referred to in brief for each example highlighted.

The 'Hg drop test' involves the addition of a large excess (*ca.* 200–500 eq.) of elemental Hg to a reaction mixture, both from the start of a reaction and more commonly, during active turnover of the catalyst under normal working conditions. Hg has been shown to inhibit surface reactions through poisoning of the catalyst; this is believed to occur as a result of surface amalgamation of the mercury with any heterogeneous particles present in the reaction mixture. Addition of mercury to a catalytically relevant metal nanoparticle will therefore retard the ability of such particles to effectively catalyse reactions.[83] A positive result indicates that after addition of Hg, substrate turnover ceases. It is important to note however that due to the high density of elemental Hg, stirring efficiency can have a pronounced effect on the dispersion of the metal throughout the reaction, thus affecting the reliability of this test.

The hot filtration test is applied by filtering the entire reaction mixture through a pre-heated Celite (or other diatomaceous metal scavenger) pad during catalyst turnover. Any nanoparticulate

257

metal species would in theory be filtered out of the mixture by this process, whereas soluble mononuclear species would pass through. Any heterogeneous bases or reagents (*e.g.* K_2CO_3) are recharged and the reaction is continued under normal conditions. A positive result indicates that after filtration, substrate turnover ceases. This test cannot however isolate very small and/or solubilised nanoparticles.

The three-phase test comprises a solid-supported substrate (immobilised on a non-reactive polymer *e.g.* Wang resin) used in place of the normal substrate, with analysis of both reaction mixture and solid support at the end of the reaction to test for leaching. Active homogeneous catalyst species should be able to access the supported substrate and produce solid-supported product under the normal reaction conditions. If the active catalyst is heterogeneous however, it should be unable to interact sufficiently with the encapsulated substrate and provide little or no observable product. It is of course possible that inactive homogeneous particles could be formed *via* leaching, analytical measurements such as ICP-MS can be used to test for this scenario. In order to maintain appropriate scientific rigour, several variants of this basic test are normally performed as control experiments. Typically, the following scenarios are required: (1) normal reaction conditions with solid support added to test for reaction inhibition by the polymer, (2) reaction using both supported and unsupported substrate to observe whether product is formed in solution or on the polymer (or both), (3) reaction using only solid-supported substrate to observe whether product is formed in solution or on the polymer. A positive result for heterogeneous catalytic behaviour would indicate: (1) normal conversion, (2) product seen only in solution, (3) no product observed either on the support or in solution (which would indicate leaching).

The use of resins to distinguish between homogeneous and heterogeneous manifolds is not without its complications however. Fagnou and co-workers utilised this approach when investigating intra- and intermolecular direct arylation reactions mediated by Pd(OH)$_2$/C (Scheme 11).[61] In their case, anchoring of an aryl halide to Wang resin afforded complete conversion to the desired cyclic product, potentially indicating a homogeneous process as a result of Pd leaching.

This experiment does not however confirm whether the active catalytic species are mononuclear Pd or small Pd clusters, as the pore size of Wang resin is sufficiently large as to allow

Scheme 11 Direct intra- and intermolecular arylation reactions using Pd(OH)$_2$/C (Fagnou et al., 2005).[61]
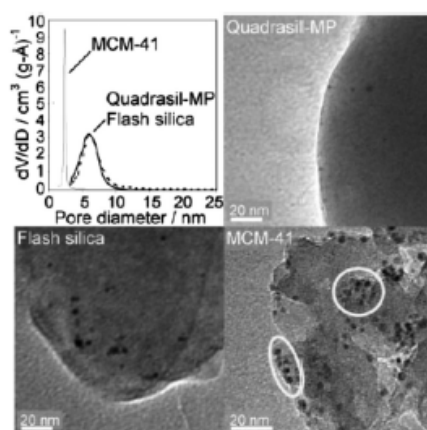
Fig. 8 TEM images evidencing encapsulation of PdNPs within mesoporous silicas and their associated pore-size distributions (Fairlamb et al., 2010).[48] Reproduced from ref. 48 with permission from The Royal Society of Chemistry.

seeding and encapsulation of multinuclear clusters. It has for example been shown that thiolated resins such as Quadrasil-MP, in addition to unfunctionalised mesoporous silicas, are capable of sequestering PdNPs (Fig. 8);[48] such supports therefore cannot be considered selective for soluble Pd. Hazrati and co-workers have also used Pd(OH)$_2$/C to effect the direct C2-arylation of pyrroles at elevated temperatures in triethanolamine, conditions which likely produce similar Pd speciation.[84] Other tests for heterogeneity often used in addition to the methods detailed above are: (a) characterisation of the prepared catalysts before and after use; (b) analysis of the metal content of the post-reaction mixture, and (c) catalyst recyclability studies.

Metal–metal frameworks

One of the largest classes of supported Pd nanocatalysts are metal–metal frameworks incorporating the catalytic Pd source with at least one other metal. An early demonstration of this approach by Djakovitch and co-workers reported the construction of C2-functionalised indoles (Scheme 12a) and their subsequent C3-arylation (Scheme 12b).[85]

This was achieved using both a microporous Pd nano-composite [Pd(NH$_3$)$_4$]/NaY, prepared by ion exchange from a NaY zeolite and a mesoporous silica-based catalyst Pd/SBA-15, prepared by grafting of a Pd–alkoxide catalyst into the pores of a calcined silica (SBA-15). While both catalysts performed equally well in the construction of C2-indoles (Scheme 12a), the mesoporous Pd/SBA-15 proved much more effective in the subsequent C3-arylation (Scheme 12b). Recyclability and leaching experiments for the reaction shown in Scheme 12a indicated that for the microporous [Pd(NH$_3$)$_4$]/NaY catalyst, leaching was extensive and led to a rapid drop-off in conversion upon catalyst reuse.

Feature Article

(a)

R^1 = H, Ts
R^2 = Ph, ^{n}Bu, C(CH$_3$)$_2$OH, (CH$_2$)$_3$CO$_2$CH$_3$
[Pd] = [Pd(NH$_3$)$_4$]/NaY, Pd/SBA-15

16 examples
(8 substrates)
<95% yield

(b)

R = F, NO$_2$
[Pd] = [Pd(NH$_3$)$_4$]/NaY, Pd/SBA-15

4 examples
(2 substrates)
<36% yield
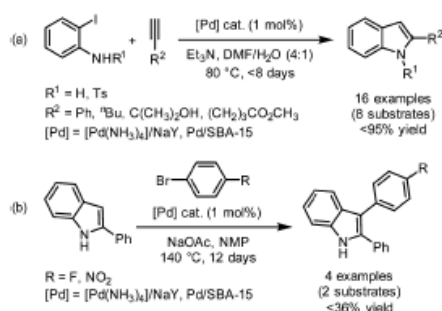
Scheme 12 Construction of C2-functionalised indoles and their subsequent C3-arylation using microporous and mesoporous Pd catalysts (Djakovitch *et al.*, 2006).[85]

This is to be expected under such forcing conditions (high temperatures, excessive reaction times) in palladophilic solvents such as DMF. Interestingly, this was not observed for the mesoporous Pd/SBA-15 catalyst, which demonstrated very little leaching of Pd into solution, possibly indicating a more heterogeneous catalytic manifold.

Subsequent work from the same group established the first completely selective heterogeneously catalysed C3-arylation of C2-substituted, free N–H indoles (Scheme 13) using the Pd nanocomposite, [Pd(NH$_3$)$_4$]/NaY.[86] The authors demonstrated that 1 mol% of this heterogeneous catalyst affords the desired products in similar conversions to those when using 5 mol% of Pd(OAc)$_2$, an observation accounted for by the formation of catalytically inactive Pd black in the latter case. Iodobenzene substrates were incompatible with this system; surprisingly this was not due to homocoupling to produce biphenyl derivatives, as anticipated, but rather because dehalogenation to produce the corresponding benzene derivatives was observed in significant yields (>20%). This may hint at the halide-capturing ability of the nanocomposite, drawing interesting comparisons to commonly utilised Ag salts, often proposed to act as halide scavengers in other C–H bond functionalisation protocols.[87]

Surprisingly, this catalyst also appeared to be highly selective for the C3 position of indole, as no migration to the C2 position to produce 2-phenylindole was observed (as would often be the case with homogeneous Pd manifolds). In general, electron-rich aryl
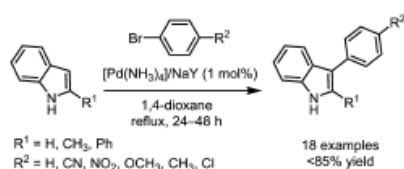
bromides gave higher yields of the desired products than electron-deficient examples.

Ying and co-workers have investigated the use of Pd–polyoxometalate (POM) nanomaterials supported on carbon with the general formula Pd–PV$_x$Mo$_y$/C (x = 0–3, y = 12–9), where the composite material can act as an electron-transfer mediator for re-oxidation of the heterogeneous Pd source (O$_2$ is used as a terminal oxidant).[88] These materials were prepared by reduction of a Pd(NO$_3$)$_2$ salt with NaBH$_4$ in the presence of a carbon support and the appropriate POM, which also provides a suitable capping agent during the synthesis of the PdNPs, ensuring that they are uniform and well-dispersed with diameters of 2–3 nm (in contrast to particles formed in the absence of POM). These catalysts were subsequently evaluated in the C–C bond-forming reaction between acetanilide and n-butyl acrylate in which the Pd–PV$_3$Mo$_9$/C catalyst was found to give the highest yield by a small margin (Table 1, entry 4).

While not commented on by the authors, it appears that there was a slight negative correlation between the Pd loading of the POM catalysts and the yield observed in this reaction (*i.e.* lower Pd loadings by weight in the POM gave a higher yield, all reactions contained 5 mol% Pd). Increasing the temperature to 80 °C allowed the desired product to be obtained in an isolated yield of 76%. The recyclability of the Pd–PV$_3$Mo$_9$/C catalyst was also investigated, whereupon it was discovered that significant POM losses (54%) occurred under the reaction conditions; recovery of the catalyst by centrifugation and reuse resulted in a large drop in product yield (by 23%). If however the catalyst was recovered and reloaded with POM prior to reuse the catalyst retained 97% activity after one use, and 79% after three uses.

Exploration of other methods for the recovery of these precious metal catalysts has demonstrated that magnetism can provide an operationally simple process for catalyst recycling. Lee *et al.* have reported the direct C3-arylation of imidazo[1,2-a]pyridine with aryl bromides, mediated by a magnetically recoverable Pd–Fe$_3$O$_4$ nanoparticle catalyst (Scheme 14).[89]

Following the direct arylation protocol, isolation of the catalyst using a neodymium magnet followed by washing allowed for up to 98% of the catalyst to be recovered. Impressively, the recovered catalyst demonstrated identical catalytic activity under the conditions shown in Scheme 14 even after ten recovery/reuse cycles.

R^1 = H, CH$_3$, Ph
R^2 = H, CN, NO$_2$, OCH$_3$, CH$_3$, Cl

18 examples
<85% yield

Scheme 13 Selective C3-arylation of C2-substituted indoles using a Pd/NaY catalyst (Djakovitch *et al.*, 2008).[86]

Table 1 Catalytic activity of Pd–POM nanomaterials in the oxidative reaction between acetanilide and n-butylacrylate (Ying *et al.*, 2011)[88]

Entry	Catalyst	Pd (wt%)	POM (wt%)	Yield (%)
1	Pd–PMo$_{12}$/C	8.1	15.2	44
2	Pd–PV$_1$Mo$_{11}$/C	12.5	15.1	39
3	Pd–PV$_2$Mo$_{10}$/C	10.4	14.8	41
4	Pd–PV$_3$Mo$_9$/C	7.9	15.2	54
5	Pd/C	17.0	0.0	0
6	Pd/C + PV$_3$Mo$_9$	17.0	0.0	9

259

ChemComm
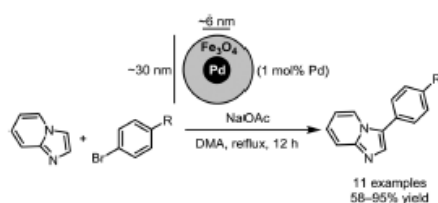
Scheme 14 Direct C3-arylation of imidazo[1,2-a]pyridine using a magnetically recoverable Pd–Fe$_3$O$_4$ nanocatalyst (Lee *et al.*, 2013).[89]

Along similar lines, Wang and co-workers have utilised silica-coated Fe$_3$O$_4$ nanoparticles (SiO$_2$@Fe$_3$O$_4$) to generate immobilised, magnetically recoverable Pd^{II} nanoparticulate catalysts *via* an azide-promoted "click" reaction to give the key 1,4-substituted 1,2,3-trizole linker which acts as a monodentate ligand for Pd^{II} (obtained from Pd(OAc)$_2$).[90] These SiO$_2$@Fe$_3$O$_4$–triazole–Pd particles had good size uniformity, with an average diameter of 140 nm. The prepared catalysts demonstrated good activity in the direct C2-arylation of a range of indoles with aryl boronic acids, although requiring the use of an acidic additive (H$_2$SO$_4$) and molecular oxidant (K$_2$S$_2$O$_8$) (Scheme 15).

N-Methyl protected indoles proved the most effective in this protocol, electron-deficient indoles gave lower yields but a variety of aryl boronic acids (electron-rich, electron-poor and sterically hindered) were well tolerated. As with the previous example, after magnetic recovery and washing these catalysts demonstrated excellent recyclability, with a decrease in yield of only 5% after eight uses. ICP analysis also demonstrated that catalyst leaching was not an issue for this system, as the post-reaction mixture contained less than 0.20 ppm Pd.

Arisawa and co-workers have developed a sulfur-modified Au-supported Pd catalyst, SAuPd, prepared by heating of the SAu material in the presence of Pd(OAc)$_2$ to afford surface-bound PdNPs of *ca.* 5 nm.[91] This was demonstrated to effectively catalyse the alkynylation of a range of aliphatic amides all containing an 8-aminoquinoline directing group with a TIPS-protected bromoalkyne (Scheme 16).

This reaction required extensive optimisation; LiCl was found to inhibit formation of the dialkynylated product (albeit with reduced yield of the desired monoalkynylated product), AgOAc was effective as a oxidant but caused uncontrolled leaching of Pd into the reaction mixture, hence the reaction was

Scheme 16 Alkynylation of an aliphatic amide using a sulfur-modified Au-supported Pd catalyst (Arisawa *et al.*, 2014).[91]

divided into two steps with the SAuPd removed prior to addition of the AgOAc and LiCl. The catalytically active species under these conditions appears to be Pd^{II}; this species has difficulty returning to the SAu surface following leaching, controlling the rate of leaching was therefore critical for catalyst recyclability.

ICP-MS analysis of the reaction mixture and the SAuPd catalyst before and after each reaction was used to determine the extent of leaching and it was found that the catalyst could be recycled and reused up to ten times, although by the tenth reuse the yield had significantly dropped (to 14% from 53%); a more realistic recycle rate would be five times as the yield had decreased by only 7% at this point (Table 2). Inductively coupled plasma mass spectrometry (ICP-MS) performed on the post-reaction mixture show that this corresponds to decreasing amounts of Pd available for the reaction with each reuse (*i.e.* lower catalyst loadings). This catalytic system is therefore interesting because it does not preclude leaching, rather it has been tailored to make effective use of a system where leaching cannot be controlled (if the desired product is to be formed).

A subsequent publication from the same group utilised the SAuPd catalyst for the synthesis of *N*-substituted benzotriazoles

Scheme 15 Direct C2-arylation of indoles with aryl boronic acids using a magnetically recoverable, silica coated Pd^{II} nanocatalyst (Wang *et al.*, 2014).[90]

Table 2 Quantity of Pd found in post-reaction mixture after ten cycles of the directed alkynylation of an amide using SAuPd (Arisawa *et al.*, 2014).[91]

Entry/reaction cycle	Leached Pd^a (ppm, mmol%)	Yield (%)
1	1710 ± 327 (10, 8)	53
2	1203 ± 510 (7, 5)	51
3	906 ± 622 (5, 4)	50
4	570 ± 217 (3, 3)	49
5	743 ± 448 (4, 3)	46
6	570 ± 216 (3, 3)	40
7	303 ± 118 (2, 2)	36
8	480 ± 108 (3, 3)	31
9	323 ± 115 (2, 2)	23
10	233 ± 110 (1, 1)	14

^{a} Leached Pd in ng.

260

Feature Article
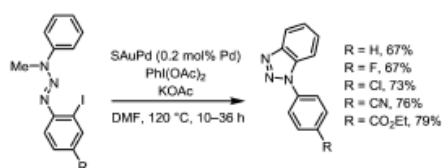
Scheme 17 Synthesis of *N*-substituted benzotriazoles using a sulfur-modified Au-supported Pd catalyst (Arisawa et al., 2014).[92]

Scheme 19 Synthesis of *N*-(2-pyridyl)indoles from *N*-aryl-2-aminopyridines and substituted alkynes using NAP–Mg–Pd[0] (Kantam et al., 2015).[94]

via a succinct Pd-mediated 1,7-migration/cyclization/dealkylation sequence (Scheme 17).[92] It should be noted that a molecular oxidant was again required for this transformation, hinting at the involvement of a catalytically relevant Pd[II] species.

Glorius and co-workers have demonstrated the efficacy of alumina-supported Pd (Pd/Al$_2$O$_3$) in the direct thiolation and selenation of electron-rich heteroarenes (Scheme 18).[93] The heterogeneous catalysts Pd/C, Pd/SiO$_2$ and Pd(OH)$_2$/C also demonstrated some activity for this transformation. High selectivity was observed for reaction at the C5 position (C3 for 6,5-ring systems) over the C3 position (C2 for 6,5-ring systems). A broad range of thiophenes containing electron-donating and electron-withdrawing groups were tolerated, although increased yields were observed for those electron-donating examples. Correspondingly, electron-rich disulfides exhibited higher reactivities than electron-poor examples.

Several synthetic protocols were employed to test the heterogeneity of this reaction. The concentration of Cu and Pd in solution after 16 h under the reaction conditions was measured by total reflection X-ray fluorescence (TXRF); in toluene <80 ppm Cu and <5000 ppm Pd were found, in DCE 440 ppm of Cu and 234 000 ppm Pd were found, after centrifugation values of <80 ppm Cu and <5000 ppm Pd were obtained. Despite these seemingly large values for leached Pd, the hot filtration test showed no further conversion to product after filtration and the three-phase test demonstrated that no active homogeneous palladium species were formed under the reaction conditions. The authors also note that the reaction was dependent on rapid stirring rates, again suggesting heterogeneous catalytic behaviour. Perhaps because of extensive leaching, the Pd/Al$_2$O$_3$ catalyst demonstrated poor recyclability in this system, with yields of 63% and 42% being obtained for the second and third catalyst cycles, respectively (*cf.* 75% for the first cycle).
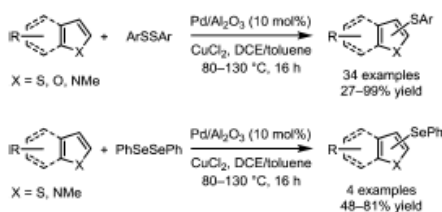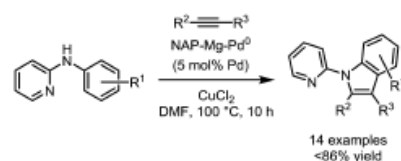
More recently, Kantam and co-workers have used a nano-crystalline magnesium oxide-stabilised Pd[0]NP catalyst (NAP-Mg-Pd[0]) for the synthesis of *N*-(2-pyridyl)indoles *via* a concise oxidative C–H bond functionalisation of *N*-aryl-2-amino-pyridines with substituted alkynes (Scheme 19).[94] This catalyst was prepared by first calcining the magnesium oxide at 450 °C before treatment with Na$_2$PdCl$_4$ to afford a NAP-Mg-PdCl$_4$ catalyst. This was then reduced with NaBH$_4$ to afford the supported Pd[0] catalyst, containing around 0.8 wt% Pd. It would appear that in this reaction the *N*-pyridyl motif is required as a directing group for the Pd catalyst to ensure high regioselec-tivity. During screening it was found that of several oxidants tested, only CuCl$_2$ proved efficacious, while other supported Pd[0] catalysts such as Pd/C provided no conversion.

This protocol was applied to a small range of aryl-amino-pyridines and alkynes, demonstrating good tolerance for electron-donating and electron-withdrawing aryl substituents, while the least hindered C–H bond was selectively functional-ised in all examples tested. Slight differences in conversion were observed with 3-substituted aromatics over the equivalent 4-substituted aromatics. The recyclability of this catalyst was investigated *via* recovery with centrifugation and found to be excellent, with consistent activity found after four cycles. Correspondingly, atomic absorption spectroscopy (AAS) demonstrated no leached Pd in the catalyst after being subjected to the reaction conditions, while TEM indicated no change in size or morphology.

A Pd[II]/Mg–La mixed oxide catalyst prepared by Kantam and co-workers has been demonstrated to effectively catalyse the cyanation of a range of arylpyridines, using a mixture of NH$_4$HCO$_3$ and DMSO as the '⁻CN' source (Scheme 20).[95] This catalyst was prepared by formation of the Mg–La oxide from Mg(NO$_3$)$_2$ and La(NO$_3$)$_3$, followed by impregnation with Pd(NO$_3$)$_2$. This process produced a material with Pd particle sizes of *ca.* 25 nm, containing 9.8 wt% Pd as measured by AAS. Relatively forcing conditions such as elevated temperatures and an external

Scheme 18 Direct thiolation and selenation of electron-rich heterocycles using Pd/Al$_2$O$_3$ (Glorius et al., 2015).[93]

Scheme 20 Cyanation of arylpyridines using a mixed Mg–La supported Pd[II] oxide catalyst (Kantam et al., 2015).[95]

261

ChemComm

Cu oxidant were required however, in addition to the directing pyridyl motif, although the desired products were obtained in good to excellent yields, across a range of election-donating and -withdrawing arylpyridines. It is also interesting to consider whether the nitrate anions are redox active in this chemistry.

The preparation of the catalyst from metal nitrates presents an interesting observation, as Pd nitrates (or systems containing both Pd species and nitrate sources) are known to act as strong oxidants in their own right, particularly when used with directing substrates such as arylpyridines, piperidines or quinolines.[95–98] Additionally, Pd(NO$_3$)$_2$ is known to undergo facile hydrolysis to Pd(OH)$_2$, which can adversely affect the templating process used to synthesise other Pd-metal nanocatalysts.[99] AAS measurements of the post-reaction mixture indicated around 10% Pd leaching from the catalyst after each reaction cycle, although recyclability of the catalyst over four cycles shown no appreciable decrease in conversion. It was therefore proposed by the authors that leached Pd species are the relevant catalytic species in this reaction; removal of the catalyst from the reaction mixture after 3 h did not affect conversion, hinting at the involvement of such leached Pd species.

Metal–organic frameworks

In addition to those metal–metal catalysts detailed above, supported Pd nanoparticulate catalysts incorporating the catalytic Pd source within metal–organic frameworks (MOFs) have also been reported.[100,101] Cao and co-workers described the direct C2-arylation of indoles with aryl halides using the Cr-containing MOF MIL-101 impregnated with PdNPs (Scheme 21).[102] The resulting Pd/MIL-101 material demonstrated two different cavity sizes within its mesoporous structure, 2.9 nm and 3.4 nm, which contained PdNPs with an average diameter of 2.6 ± 0.5 nm. These PdNPs were confirmed as Pd^0 by XPS and were present at an approximately 0.5 wt% loading.

Good to excellent yields were observed for a range of electron-donating and electron-withdrawing aryl iodides in the *meta-* and *para-* positions; aryl bromides and chlorides proved much less effective however, requiring increased temperatures and reaction times. The *N*-substituent on the indole proved critical; electron-donating N–Me and N–*n*Bu indoles generally gave high yields while free N–H or electron-withdrawing N–Ac indoles resulted in severely decreased yields. Finally, a small electronic effect was seen for substituents on the indole ring, with electron-rich indoles providing higher yields, mirroring the effect of the N protecting group.

Post-workup analysis using inductively coupled plasma atomic emission spectroscopy (ICP-AES) showed the presence of only
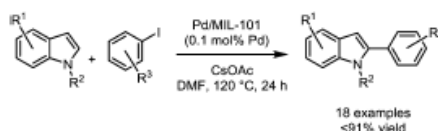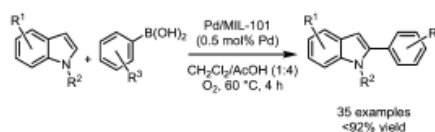
Scheme 22 Direct C2-arylation of indoles with aryl boronic acids using a Cr MOF-supported PdNP catalyst (Cao et al., 2013).[103]

0.4 ppm Pd, indicating little Pd leaching under the reaction conditions, while no leached Cr was observed. Correspondingly this catalyst demonstrated excellent recyclability, with a decrease in yield of only 4% after five uses; TEM analysis after each use indicated little or no PdNP growth or distortion. The hot filtration test also showed no further conversion to product after filtration of the catalyst.

To address the high temperatures and long reaction times needed for this transformation, aryl boronic acids were used in place of aryl halides for the direct C2-arylation of indoles catalysed by Pd/MIL-101 in later work from the same group (Scheme 22).[103]

To facilitate high conversion, it was found that acidic conditions and an oxidising atmosphere were required in this instance, allowing for significant reductions in both reaction time and temperature. Interestingly, greater quantities of the C3-arylated and C2,3-diarylated byproducts were observed in this system when compared to the aryl halide protocol. A broad range of aryl boronic acids were tolerated under these conditions, as were N–Me and free N–H indoles. N–Ac and N–Boc indoles were also effective in several cases, but proved problematic when coupled with electron-deficient indole rings. Addition of the radical initiator TEMPO along with KF circumvented this limitation and allowed access to the desired products in high yields.

As with the previous methodology, application of the hot filtration test indicated that the catalytically competent species was likely heterogeneous in nature, while ICP-AES analysis demonstrated only 0.9 ppm Pd in the post-reaction mixture. Catalyst recyclability was also very good, with a decrease in yield of only 3% after five catalysts uses; powder X-ray diffraction (XRD) indicated that the catalyst had retained its crystallinity even after several recovery/reuse cycles.

Silicon-based frameworks

Another reasonably well-explored method of supporting PdNPs is through the use of modified silicas. One such early example by Cai and co-workers utilised fluorous silica gel to support PdNPs which had been tagged with a perfluoroalkane; this enabled stabilisation by exploiting fluorous–fluorous interactions between the tagged PdNPs and the silica gel support.[104] By this method, PdNPs of around 2 nm were obtained. This catalyst (here defined as Pd/FSG) was evaluated in the direct C2-arylation of a range of indoles with aryl halides (Scheme 23).

As with previous examples highlighted above, N–Me indoles proved the most effective, with free N–H indoles giving reduced yields and N–Ac indoles giving none of the desired product;

Scheme 21 Direct C2-arylation of indoles with aryl iodides using a Cr MOF-supported PdNP catalyst (Cao et al., 2011).[102]
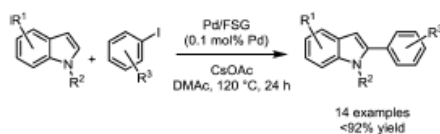
Scheme 23 Direct C2-arylation of indoles with aryl iodides using a fluorous silica gel-supported PdNP catalyst (Cai *et al.*, 2011).[104]

Scheme 25 Direct *ortho*-arylation of benzamides with aryl iodides using a mesoporous silica PdNP catalyst (Srinivasu *et al.*, 2014).[106]

Scheme 26 Formation of a phthalimide–thiophene-based semiconductor via a silica-supported Pd-catalysed direct coupling (Welch *et al.*, 2015).[107]

electron-deficient indole rings also resulted in lower yields. Aryl iodides were found to give higher yields of the desired products than aryl bromides, although a range of aryl iodides containing electron-withdrawing or electron-donating groups were tolerated and as expected, *ortho*-substituted aryl iodides reacted more slowly than *para*-substituted examples. A simple recycling experiment demonstrated excellent catalyst recyclability after five runs (a decrease in yield of 6% was seen), while the hot filtration test and ICP analysis indicated that a heterogeneous catalytic manifold was likely in operation.

Uozumi and co-workers have developed a silicon nanowire hybrid Pd catalyst, SiNA–Pd, obtained by reduction of K_2PdCl_4 onto a prepared Si nanowire surface.[105] This produced PdNPs of *ca.* 5–10 nm diameter, which demonstrated high activity in the direct arylation of a small number of thiophenes and indoles (Scheme 24). No investigation of catalyst recycling or mechanistic determination on this system was performed, although good recyclability was observed when using this catalyst for a series of Mizoroki–Heck couplings of aryl halides with terminal alkenes. The typical hot filtration and ICP-AES tests indicated a probable heterogeneous manifold.

A calcined mesoporous silica has been used by Srinivasu and co-workers to support highly dispersed PdNPs, obtained through loading with $Pd(OAc)_2$.[106] The PS-3 catalyst contains particles of approximately 7–8 nm which display well resolved (111), (200) and (220) planes, indicating face-centered cubic structures. This demonstrated good activity in the *ortho*-arylation of benzamides with aryl iodides (Scheme 25). A broad range of aryl iodides were tolerated, although electron-deficient substrates gave noticeably lower yields. Similarly, amides

containing electron-donating aromatic groups provided higher yields than electron-withdrawing examples.

Catalyst recycling in this system was very good, with equivalent activity and selectivity obtained after five re-uses. Additionally, no leached Pd was detected in the post-reaction mixture by ICP whilst wide-angle XRD performed on the recovered catalyst demonstrated metallic Pd at similar binding energies to the fresh PS-3 catalyst.

Welch and co-workers have explored the activity of a commercially available SiliaCat® Pd-containing catalyst, DPP–Pd, in a direct sp^2–sp^2 coupling reaction to form a phthalimide–thiophene-based semiconductor (Scheme 26).[107] In this example, the Pd catalyst is tethered to a silica support *via* an alkyl phosphine ligand.

Carbon-based frameworks

Several examples of Pd nanocatalysts supported on organic frameworks, in various forms, have been demonstrated to be effective in C–H bond functionalisation processes. Hierso and co-workers have prepared a palladium–polypyrrole catalyst, Pd@PPy, which contains nanoparticulate Pd of approximately 2 nm stabilised within spherical polypyrrole structures.[108] These were easily prepared by the reduction of $[Pd(NH_3)_4Cl_2]$ in the presence of polypyrrole, affording a material notable for its unusually high nanoparticulate Pd loading (35 wt%). Other key features of these nanocatalysts are their highly colloidal nature, as indicated by SEM and TEM images, as well as their high ratio of surface-bound to bulk Pd, as indicated by XPS analysis. This catalyst was shown to be effective in the direct C2-arylation of furans and thiophenes with bromoarenes (Scheme 27).

Scheme 24 Direct arylation of thiophenes and indoles with iodobenzene using a silicon nanowire-supported PdNP catalyst (Uozumi *et al.*, 2014).[105]

263

ChemComm

E = O, S   X = CH, N

9 examples
58–99% yield

Scheme 27 Direct C2-arylation of furans and thiophenes with bromo-arenes using a Pd-polypyrrole nanocatalysts (Hierso et al., 2011).[108]

17 examples
<91% yield

Scheme 29 Direct C2-arylation of indoles with aryliodonium salts using an amino-functionalised mesocellular foam (Olofsson et al., 2014).[111]

Electron-rich and electron-poor aryl bromides were well tolerated under these conditions and 2 examples using bromo-quinolines provided the desired products in high conversion without catalyst poisoning. Steric effects were however shown to be critical, with no conversion seen when using the hindered 2,4,6-trimethylbromobenzene. Catalyst recyclability was investigated and found to give inconsistent results; coupling of 2-n-butylfuran with 4-bromobenzonitrile could be repeated at similar conversions using the recycled catalyst whilst the equivalent coupling with 4-bromoacetophenone failed upon catalyst reuse. Subsequent investigation using TEM established a growth of the PdNP particle sizes from 4 to 7 nm under the reaction conditions, which is likely the cause of the loss of catalytic activity, smaller particles in general providing greater activity due to their higher proportion of surface defect sites (vide supra). Interestingly SEM images indicated no distortion of the spherical polypyrrole support, implying that the majority of the PdNPS dispersed throughout the structure are catalytically relevant (and correspondingly their growth occurs concomitantly).

Ethylenediamine functionalised cellulose (EDAC) has been used to support Cu^I and 5–10 nm PdNPs by Shaabani and co-workers, with the resulting Cu^I/PdNPs@EDAC catalyst demonstrating activity in a 1,3-dipolar cycloaddition/direct arylation sequence (Scheme 28).[109] This procedure tolerated a range of aryl halides containing electron-donating and electron-withdrawing functionality, with the catalyst demonstrating excellent recyclability over four recovery/reuse cycles.

A catalyst comprising PdNPs supported on an amino-functionalised mesocellular foam (Pd^0-AmP-MCF) prepared by the Bäckvall group[110] has been utilised by Olofsson and co-workers in the direct C2-arylation of indoles with aryliodonium salts (Scheme 29).[111] This support contains many mesoporous cavities enabling the stabilisation of well-dispersed 2–3 nm
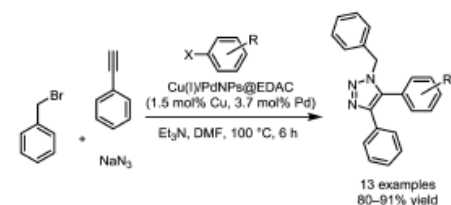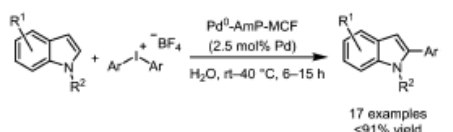
PdNPs; XPS analysis revealed the presence of both Pd^0 and Pd^{II} particles in an approximately 3:1 ratio. The analogous non-reduced Pd^{II}-AmP-MCF did however display decreased reactivity, implying that the Pd^0 species are more competent catalysts in this system.

A series of electron-donating, electron-withdrawing and sterically hindered aryliodonium salts were demonstrated to be effective under the reaction conditions. Some modification of the electronic nature of the indole ring also allowed good conversion to the desired products, notably free N–H indoles were tolerated in some cases. Unfortunately however the use of differentially substituted diaryliodonium salts containing the non-transferable 2,4,6-trimethylphenyl (mesityl) or 2,4,6-triisopropylphenyl (TRIP) dummy groups were less active in this system, limiting their use for the installation of more complex functionality. The recyclability of this catalyst was also investigated, albeit with significantly reduced yields, with losses of 33% conversion observed in the third cycle. ICP-OES analysis however indicated very little leached Pd in the post-reaction mixture (0.6 ppm), hence dispersion of Pd within the mesoporous foam away from the active nanoclusters, into less active aminopropyl groups was suggested as an explanation for the loss of activity. This also may provide an explanation as to why the Pd^{II}-AmP-MCF demonstrated lower activity under these reaction conditions.

A family of macrocyclic cucurbituril frameworks have been used to support PdNPs by Cao and co-workers, the resulting catalysts being demonstrated to effectively catalyse the direct arylation of a range of fluoroarenes with aryl halides.[112] Of the four ring sizes tested (5–8), CB[6]-PdNPs (ca. 3.8 nm) afforded the highest conversion to the desired products (Scheme 30). This is rationalised on the basis of the distinct structures obtained, with TEM indicating that while the PdNPs are uniformly distributed throughout each catalyst, the specific morphology of each differs according to the specific macrocycle used. The shape of the CB[6]-PdNPs appear to be more regular, with less particle clustering than in the CB[5], CB[7] or CB[8]

13 examples
80–91% yield

Scheme 28 Synthesis of trisubstituted triazoles using a cellulose-supported Cu^I/PdNP catalyst (Shaabani et al., 2014).[109]

X = Br, I

15 examples
30–93% yield
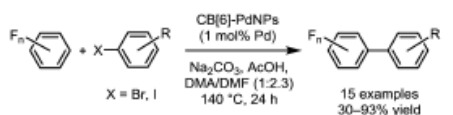
Scheme 30 Direct arylation of fluoroarenes with aryl halides using a cucurbit[6]uril PdNP catalyst (Cao et al., 2015).[112]

264

examples, resulting in greater exposed surface areas for the CB[6]-PdNPs. Additionally, ^{1}H NMR spectroscopic studies indicated stronger interactions between the substrates and CB[5], CB[7] and CB[8], while CB[6] appears to act purely as a PdNP stabilising agent with no substrate/CB[6] interaction observed.

This protocol demonstrated good tolerance for electron-donating and electron-withdrawing aryl halides, providing moderate to high conversions for a range of challenging tri-, tetra- and penta-fluorinated aromatics, albeit with high temperatures and long reaction times. The standard Hg drop and hot filtration tests inhibited the reaction, providing good indications of heterogeneity in this system. This was further supported by high catalyst recyclability, with around 90% of reactivity retained in the fifth cycle; HR-TEM indicated that while the particle size increased during the reaction (to around 10 nm), critically the defect sites on the surface of the PdNPs were well-maintained.

Ellis and co-workers have probed the reaction of Pd[II]NPs supported on multiwalled carbon nanotubes (Pd[II]/MWCNT) in several chelation-assisted direct sp[2] C–H bond functionalisation reactions (Scheme 31).[113] Intriguingly, in many of these examples reactivity distinct from that seen when using the more commonly employed Pd(OAc)$_2$ was realised; increased activity but reduced substrate tolerance was seen in some acetoxylation reactions (Scheme 31a), reduced yields obtained in some alkoxylations (Scheme 31b) and significantly increased rates observed in halogenations using N-bromo- or N-chlorosuccinimide (Scheme 31c).

a) C–H to C–O

Pd[II]/MWCNT
(5 mol% Pd)

PhI(OAc)$_2$
AcOH/MeOH
100–120 °C
0.2–5 h

R = OAc, OMe
4 examples
>99% yield

b) C–H to C–OR

Pd[II]/MWCNT
(5 mol% Pd)

PhI(OAc)$_2$, ROH
100 °C, 3 h

R = MeO, 90%
R = EtO, 73%
R = [i]PrO, 33%
R = [t]Bu, 0%

c) C–H to C–X

Pd[II]/MWCNT
(5 mol% Pd)

NBS/NCS
MeCN/AcOH
100–120 °C
0.2–6 h

R = Cl, Br
8 examples
>92% yield
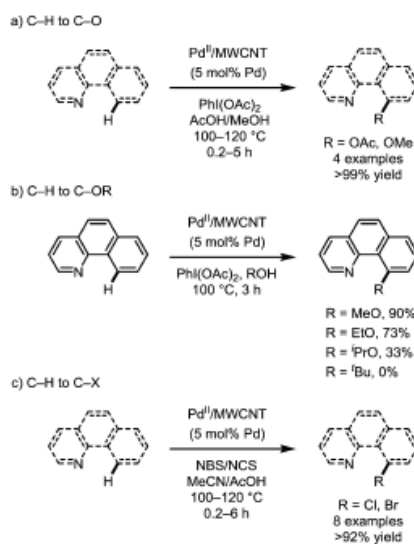
Scheme 31 Direct C–H bond functionalisation of N-chelating substrates under oxidising conditions using a carbon nanotube supported Pd[II]NP catalyst (Ellis et al., 2015).[113]
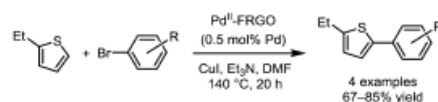
Scheme 32 Direct arylation of 2-ethylthiophene with aryl bromides using a functionalised graphene oxide Pd nanocatalyst (Xi et al., 2015).[114]

Specifically, catalyst recycling in the methoxylation of 8-methyl-quinolone was superb with minimal loss of activity after 16 recovery/reuse cycles (8% decrease); ICP-MS analysis of the post-reaction mixture correspondingly demonstrated almost no leaching with <250 ppb Pd found, while the hot filtration test was seen to prevent further conversion.

Xi and co-workers have prepared a Pd nanocatalyst supported on functional graphene oxide (Pd[II]-FRGO), obtained by doping of a pre-prepared graphene oxide with PdCl$_2$ in DMF at room temperature, producing particles of *ca.* 6 nm with the bulk solid containing approximately 4.8 wt% Pd. This catalyst was shown to be effective in Pd-catalysed cross-coupling processes such as the Suzuki–Miyaura and Mizoroki–Heck reactions, in addition to the direct arylation of 2-ethylthiophene (Scheme 32).[114]

Pd/C for direct C–H bond functionalisation

Despite its widespread use as a heterogeneous hydrogenation catalyst, Pd/C has only recently been examined for other Pd-mediated catalysis, usually in cross-coupling reactions.[11–14] Glorius and co-workers are particularly notable for their continuing development of C–H bond functionalisation reactions using this catalyst. The first such example described the direct arylation of benzo[*b*]thiophenes with aryl chlorides, affording C3-arylated products with extremely high selectivity (Scheme 33).[115] Despite the excellent C3-selectivity, high temperatures and long reaction times were required to provide synthetically useful yields, although the use of typically less activated aryl chlorides over aryl iodides or bromides is of significant benefit. A broad range of aryl chlorides were tolerated, including those with *ortho*-substituents while CuCl was found to be necessary to ensure higher yields, with Lewis acid activation of the benzo[*b*]thiophene its proposed role.

As with more recent work from this group, the hot filtration test showed no further conversion to product after filtration, the three-phase test demonstrated that no active homogeneous palladium species were formed under the reaction conditions and the reaction was seen to be dependent on rapid stirring rates. TXRF spectroscopy demonstrated <4 ppm Pd in the

Pd/C (9.4 mol%)
CuCl (10 mol%)

Cs$_2$CO$_3$, 1,4-dioxane
150 °C, 48–72 h

15 examples
<94% yield
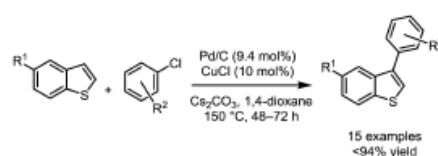
Scheme 33 Direct C3-arylation of benzo[*b*]thiophenes with aryl chlorides using Pd/C (Glorius et al., 2013).[115]

265

ChemComm

post-reaction mixture. Interestingly the source of Pd/C used for this reaction had a pronounced effect on yield, with variation of up to 59% between suppliers observed. This would suggest that the nature of the support or Pd morphology (*vide supra*) is critical to reactivity; correspondingly for other catalytic systems material from different suppliers may prove more efficacious. Some nominally homogeneous Pd catalysts proved able to catalyse this reaction, although fascinatingly these gave a complete switch in selectivity, with exclusively C2-arylated products being obtained.

Subsequent development in the arylation of thiophenes, benzo[*b*]thiophenes and other related heterocycles replaced the aryl chlorides with aryliodonium salts, which allowed for much milder conditions to be used (Scheme 34).[116] This new protocol also demonstrated wide-ranging applicability with regard to substituents on both the thiophene and arylating agent, with differentially substituted aryliodonium salts containing the TRIP dummy group utilised to vary the installed arene. A brief substrate screen also indicated that indoles, furans and benzofurans were reactive under these conditions.

The same heterogeneity tests as before were performed, again indicating a heterogeneous catalytic manifold despite the strongly oxidising conditions. Catalyst recycling was however poor, with a significant decrease (41%) in yield observed after three cycles. Pd(OAc)$_2$ was also shown to catalyse this reaction, albeit with lower efficiency than Pd/C. Intriguingly when the conditions employing Pd(OAc)$_2$ were subjected to the three-phase test, they indicated possible heterogeneous behaviour, leading the authors to suggest that Pd(OAc)$_2$ could be acting as a reservoir for heterogeneous Pd species *i.e.* PdNPs (as highlighted *vide supra*).

More recently, a modification of this protocol was applied to the direct arylation of triphenylene, naphthalene and other related polyaromatic hydrocarbons (PAHs) (Scheme 35).[117] Surprisingly, arylation typically occurred at the most hindered position in these systems, with high $\alpha : \beta$ selectivity observed in many cases.

A series of electron-donating and electron-withdrawing substituents were also demonstrated to give good yields for triphenylene and naphthalene. Attempts to functionalise substituted naphthalenes however met with limited or no success. In all cases side-products were found which resulted from
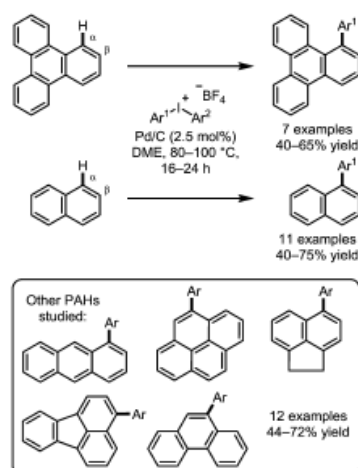
Scheme 35 Direct arylation of triphenylene, naphthalene and related PAHs with aryliodonium salts using Pd/C (Glorius *et al.*, 2015).[117]

polyarylation of the PAH; suppressing this is, to quote the authors, "an unmet challenge". Interestingly, Pd/Al$_2$O$_3$ also proved an effective catalyst, although it gave reduced yields when compared to Pd/C.

Tests for heterogeneity all indicated the same results as with previous methods using Pd/C (*vide supra*), although the authors note that the high temperatures and oxidative conditions used mean it is probable that Pd leaching does occur in this case. The tests performed would seem to indicate that homogeneous Pd was not active in this system, but that does not preclude the possibility of heterogeneous leached Pd (*i.e.* PdNPs) being the active catalyst. The reaction was found to be first-order for Pd, with decreasing induction periods at higher Pd loadings, which is indicative of formation of the active catalyst being the rate-determining step. The reaction was also found to be zeroth-order for naphthalene, with an unusual inverse kinetic isotope effect (KIE) of 0.54, while reactivity was inhibited by addition of TEMPO, BHT and BQ. These mechanistic studies led the authors to conclude that insoluble PdNPs leached into solution from the Pd/C support are the catalytically relevant species in a Pd^0/Pd^{II} manifold, involving a key carbon-centred radical intermediate formed by single electron reduction of the aryliodonium salt.

Conclusions

The case for the involvement of mononuclear (quasi)homogeneous and multinuclear (quasi)heterogeneous catalysis has been made in this article. Examination of the discoveries made in the field of traditional Pd-catalysed cross-coupling with regard to ultra-low
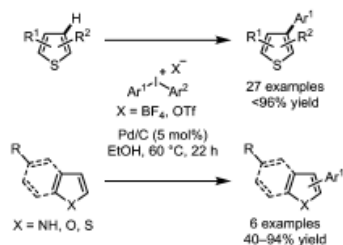
Scheme 34 Direct arylation of thiophenes and related heterocycles with aryliodonium salts using Pd/C (Glorius *et al.*, 2014).[116]

266

Feature Article

ChemComm

catalyst loadings (ppm to ppb), inverse rate correlations and the ability of common Pd precursors to act as catalyst reservoirs, creates a solid foundation upon which to study C–H bond functionalisation processes. An understanding of these complex effects will allow future research to make more effective use of precious Pd, both through reductions in catalyst loading and the recyclability that heterogeneous catalysis can offer.

Discoveries in this area thus far fall into two classifications; groups who wish to develop heterogeneous Pd catalysts then design a system which is exemplified on typically simple substrates, or researchers in the process of creating a desired structural motif encounter heterogeneous behaviour in one of their catalytic transformations and perform tests to evaluate this phenomenon. Combining intelligent heterogeneous catalyst design with the ability to access desirable chemical structures is of paramount importance in the development of this field. The advantages of this approach would be exemplified further if such catalysts could be demonstrated to effect transformations impossible or at least highly challenging for more common homogenous Pd precursors. Pleasingly, some promising progress has been made, with several heterogeneous catalysts demonstrating markedly different reactivity to common Pd precursors, such as increased activity or even differing regioselective outcomes.

Finally, it is highly likely that examples of heterogeneous behaviour have gone unnoticed due to the inherent difficulties in probing it, *i.e.* the tools needed to study processes are not yet universally adopted by synthetic chemists (*e.g.* TEM, XAS, XPS analysis). It is however apparent that new advanced techniques and methods are needed for the characterisation of (quasi)-heterogeneous catalysts generated from homogenous precursor catalysts. This insight has the potential to inform the design of future catalytic processes.†

Acknowledgements

References

1 L. Ackermann, R. Vicente and A. R. Kapdi, *Angew. Chem., Int. Ed.*, 2009, **48**, 9792.
2 J. Yamaguchi, A. D. Yamaguchi and K. Itami, *Angew. Chem., Int. Ed.*, 2012, **51**, 8960.
3 A. J. Hunt, T. J. Farmer and J. H. Clark, in *Element Recovery and Sustainability*, ed. A. J. Hunt, RSC Publishing, Cambridge, UK, 2013, ch. 1, p. 1.
4 G. Cahiez, C. Duplais and J. Buendia, *Chem. Rev.*, 2009, **109**, 1434.

5 R. I. Khusnutdinov, A. R. Bayguzina and U. M. Dzhemilev, *Russ. J. Org. Chem.*, 2012, **48**, 309.
6 A. Correa, O. Garcia Mancheno and C. Bolm, *Chem. Soc. Rev.*, 2008, **37**, 1108.
7 I. Bauer and H.-J. Knölker, *Chem. Rev.*, 2015, **115**, 3170.
8 G. Cahiez and A. Moyeux, *Chem. Rev.*, 2010, **110**, 1435.
9 K. Gao and N. Yoshikai, *Acc. Chem. Res.*, 2014, **47**, 1208.
10 L. Ackermann, *J. Org. Chem.*, 2014, **79**, 8948.
11 Á. Molnár, *Chem. Rev.*, 2011, **111**, 2251.
12 A. Balanta, C. Godard and C. Claver, *Chem. Soc. Rev.*, 2011, **40**, 4973.
13 H.-U. Blaser, A. Indolese, A. Schnyder, H. Steiner and M. Studer, *J. Mol. Catal. A: Chem.*, 2001, **173**, 3.
14 Lunxiang and J. Liebscher, *Chem. Rev.*, 2007, **107**, 133.
15 D. L. Davies, S. M. A. Donald and S. A. Macgregor, *J. Am. Chem. Soc.*, 2005, **127**, 13754.
16 M. Lafrance, C. N. Rowley, T. K. Woo and K. Fagnou, *J. Am. Chem. Soc.*, 2006, **128**, 8754.
17 Y. Boutadla, D. L. Davies, S. A. Macgregor and A. I. Poblador-Bahamonde, *Dalton Trans.*, 2009, 5820.
18 X. Chen, K. M. Engle, D.-H. Wang and J.-Q. Yu, *Angew. Chem., Int. Ed.*, 2009, **48**, 5094.
19 O. Daugulis, H.-Q. Do and D. Shabashov, *Acc. Chem. Res.*, 2009, **42**, 1074.
20 J. M. Racowski, A. R. Dick and M. S. Sanford, *J. Am. Chem. Soc.*, 2009, **131**, 10974.
21 D. C. Powers, M. A. L. Geibel, J. E. M. N. Klein and T. Ritter, *J. Am. Chem. Soc.*, 2009, **131**, 17050.
22 D. C. Powers and T. Ritter, *Nat. Chem.*, 2009, **1**, 302.
23 P. Sehnal, R. J. K. Taylor and I. J. S. Fairlamb, *Chem. Rev.*, 2010, **110**, 824.
24 T. W. Lyons and M. S. Sanford, *Chem. Rev.*, 2010, **110**, 1147.
25 L. Ackermann, *Chem. Rev.*, 2011, **111**, 1315.
26 D. C. Powers, E. Lee, A. Ariafard, M. S. Sanford, B. F. Yates, A. J. Canty and T. Ritter, *J. Am. Chem. Soc.*, 2012, **134**, 12002.
27 K. M. Engle, T.-S. Mei, M. Wasa and J.-Q. Yu, *Acc. Chem. Res.*, 2012, **45**, 788.
28 P. Ricci, K. Krämer, X. C. Cambeiro and I. Larrosa, *J. Am. Chem. Soc.*, 2013, **135**, 13258.
29 A. N. Vedernikov, in *C–H and C–X Bond Functionalization: Transition Metal Mediation*, ed. X. Ribas, RSC Publishing, Cambridge, UK, 2013, ch. 4, p. 108.
30 J. R. Khusnutdinova and L. M. Mirica, in *C–H and C–X Bond Functionalization: Transition Metal Mediation*, ed. X. Ribas, RSC Publishing, Cambridge, UK, 2013, ch. 5, p. 122.
31 J. J. Topczewski and M. S. Sanford, *Chem. Sci.*, 2015, **6**, 70.
32 H. Ramezani-Dakhel, P. A. Mirau, R. R. Naik, M. R. Knecht and H. Heinz, *Phys. Chem. Chem. Phys.*, 2013, **15**, 5488.
33 J. A. Widegren and R. G. Finke, *J. Mol. Catal. A: Chem.*, 2003, **198**, 317.
34 R. H. Crabtree, *Chem. Rev.*, 2012, **112**, 1536.
35 I. J. S. Fairlamb and A. F. Lee, in *C–H and C–X Bond Functionalization: Transition Metal Mediation*, ed. X. Ribas, RSC Publishing, Cambridge, UK, 2013, ch. 3, p. 72.
36 R. H. Crabtree, *Chem. Rev.*, 2015, **115**, 127.
37 A. H. M. de Vries, J. M. C. A. Mulders, J. H. M. Mommers, H. J. W. Henderickx and J. G. de Vries, *Org. Lett.*, 2003, **5**, 3285.
38 I. J. S. Fairlamb, A. R. Kapdi, A. F. Lee, G. Sanchez, G. Lopez, J. L. Serrano, L. Garcia, J. Perez and E. Perez, *Dalton Trans.*, 2004, 3970.
39 N. E. Leadbeater and M. Marco, *Org. Lett.*, 2002, **4**, 2973.
40 C. Deraedt and D. Astruc, *Acc. Chem. Res.*, 2014, **47**, 494.
41 (*a*) F. Zhao, B. M. Bhanage, M. Shirai and M. Arai, *Chem. – Eur. J.*, 2000, **6**, 843. A very recent paper reports the use of a LAPONITE® clay in Mizoroki–Heck type reactions, see: (*b*) J. I. García, F. Invernizzi, A. Leal, A. Martinez and J. A. Mayoral, *RSC Adv.*, 2015, **5**, 59983.
42 J. B. Brazier, B. N. Nguyen, L. A. Adrio, E. M. Barreiro, W. P. Leong, M. A. Newton, S. J. A. Figueroa, K. Hellgardt and K. K. M. Hii, *Catal. Today*, 2014, **229**, 95.
43 C. C. Cassol, A. P. Umpierre, G. Machado, S. I. Wolke and J. Dupont, *J. Am. Chem. Soc.*, 2005, **127**, 3298.
44 M. B. Thathagar, J. E. ten Elshof and G. Rothenberg, *Angew. Chem., Int. Ed.*, 2006, **45**, 2886.

† During the final stages of the preparation of our feature article we noticed the publication of a complementary review article on this topic by McGlacken.[74]

ChemComm

45 A. V. Gaikwad and G. Rothenberg, *Phys. Chem. Chem. Phys.*, 2006, 8, 3669.
46 S. Reimann, J. Stoetzel, R. Frahm, W. Kleist, J.-D. Grunwaldt and A. Baiker, *J. Am. Chem. Soc.*, 2011, 133, 3921.
47 P. J. Ellis, I. J. S. Fairlamb, S. F. J. Hackett, K. Wilson and A. F. Lee, *Angew. Chem., Int. Ed.*, 2010, 49, 1820.
48 A. F. Lee, P. J. Ellis, I. J. S. Fairlamb and K. Wilson, *Dalton Trans.*, 2010, 39, 10473.
49 T. Teranishi and M. Miyake, *Chem. Mater.*, 1998, 10, 594.
50 J. Le Bars, U. Specht, J. S. Bradley and D. G. Blackmond, *Langmuir*, 1999, 15, 7621.
51 G. Collins, M. Schmidt, C. O'Dwyer, J. D. Holmes and G. P. McGlacken, *Angew. Chem., Int. Ed.*, 2014, 53, 4142.
52 G. Collins, M. Schmidt, G. P. McGlacken, C. O'Dwyer and J. D. Holmes, *J. Phys. Chem. C*, 2014, 118, 6522.
53 G. Collins, M. Schmidt, C. O'Dwyer, G. McGlacken and J. D. Holmes, *ACS Catal.*, 2014, 4, 3105.
54 T. E. Storr, A. G. Firth, K. Wilson, K. Darley, C. G. Baumann and I. J. S. Fairlamb, *Tetrahedron*, 2008, 64, 6125.
55 T. E. Storr, C. G. Baumann, R. J. Thatcher, S. De Ornellas, A. C. Whitwood and I. J. S. Fairlamb, *J. Org. Chem.*, 2009, 74, 5810.
56 M. Hyotanishi, Y. Isomura, H. Yamamoto, H. Kawasaki and Y. Obora, *Chem. Commun.*, 2011, 47, 5750.
57 H. Yano, Y. Nakajima and Y. Obora, *J. Organomet. Chem.*, 2013, 745–746, 258.
58 M. Chiba, M. N. Thanh, Y. Hasegawa, Y. Obora, H. Kawasaki and T. Yonezawa, *J. Mater. Chem. C*, 2015, 3, 514.
59 S. Sahnoun, S. Messaoudi, J.-F. Peyrat, J.-D. Brion and M. Alami, *Tetrahedron Lett.*, 2008, 49, 7279.
60 S. Sahnoun, S. Messaoudi, J.-D. Brion and M. Alami, *Org. Biomol. Chem.*, 2009, 7, 4271.
61 M. Parisien, D. Valette and K. Fagnou, *J. Org. Chem.*, 2005, 70, 7578.
62 L. A. Adrio, B. N. Nguyen, G. Guilera, A. G. Livingston and K. K. Hii, *Catal. Sci. Technol.*, 2012, 2, 316.
63 L. Djakovitch, M. Wagner, C. G. Hartung, M. Beller and K. Koehler, *J. Mol. Catal. A: Chem.*, 2004, 219, 121.
64 L. Zhang, Z. Li, Y. Zhang, M. Chin Paau, Q. Hu, X. Gong, S. Shuang, C. Dong, X. Peng and M. M. F. Choi, *Talanta*, 2015, 131, 632.
65 E. Raluy, I. Favier, A. M. Lopez-Vinasco, C. Pradel, E. Martin, D. Madec, E. Teuma and M. Gómez, *Phys. Chem. Chem. Phys.*, 2011, 13, 13579.
66 L. Adak, S. Bhadra and B. C. Ranu, *Tetrahedron Lett.*, 2010, 51, 3811.
67 D. Saha, L. Adak and B. C. Ranu, *Tetrahedron Lett.*, 2010, 51, 5624.
68 P. Ehlers, A. Petrosyan, J. Baumgard, S. Jopp, N. Steinfeld, T. V. Ghochikyan, A. S. Saghyan, C. Fischer and P. Langer, *ChemCatChem*, 2013, 5, 2504.
69 L. Nassar-Hardy, C. Deraedt, E. Fouquet and F.-X. Felpin, *Eur. J. Org. Chem.*, 2011, 4616.
70 S. S. Zalesskiy and V. P. Ananikov, *Organometallics*, 2012, 31, 2302.
71 E. O. Pentsak, A. S. Kashin, M. V. Polynski, K. O. Kvashnina, P. Glatzel and V. P. Ananikov, *Chem. Sci.*, 2015, 6, 3302.
72 R. B. Bedford, J. G. Bowen, R. B. Davidson, M. F. Haddow, A. E. Seymour-Julen, H. A. Sparkes and R. L. Webster, *Angew. Chem., Int. Ed.*, 2015, 54, 6591.
73 C. G. Baumann, S. De Ornellas, J. P. Reeds, T. E. Storr, T. J. Williams and I. J. S. Fairlamb, *Tetrahedron*, 2014, 70, 6174.
74 T. J. Williams and I. J. S. Fairlamb, *Tetrahedron Lett.*, 2013, 54, 2906.
75 N. R. Deprez, D. Kalyani, A. Krause and M. S. Sanford, *J. Am. Chem. Soc.*, 2006, 128, 4972.
76 T. J. Williams, A. J. Reay, A. C. Whitwood and I. J. S. Fairlamb, *Chem. Commun.*, 2014, 50, 3052.
77 A. J. Reay, T. J. Williams and I. J. S. Fairlamb, *Org. Biomol. Chem.*, 2015, 13, 8298.
78 R. Cano, A. F. Schmidt and G. P. McGlacken, *Chem. Sci.*, 2015, 6, 5338.
79 L. Djakovitch and F.-X. Felpin, *ChemCatChem*, 2014, 6, 2175.
80 W. M. Alley, I. K. Hamdemir, K. A. Johnson and R. G. Finke, *J. Mol. Catal. A: Chem.*, 2010, 315, 1.
81 E. Bayram, J. C. Linehan, J. L. Fulton, J. A. S. Roberts, N. K. Szymczak, T. D. Smurthwaite, S. Özkar, M. Balasubramanian and R. G. Finke, *J. Am. Chem. Soc.*, 2011, 133, 18889.
82 M. Pagliaro, V. Pandarus, R. Ciriminna, F. Béland and P. Demma Carà, *ChemCatChem*, 2012, 4, 432.
83 J. A. Widegren, M. A. Bennett and R. G. Finke, *J. Am. Chem. Soc.*, 2003, 125, 10301.
84 F. Jafarpour, S. Rahiminejadan and H. Hazrati, *J. Org. Chem.*, 2010, 75, 3109.
85 L. Djakovitch, V. Dufaud and R. Zaidi, *Adv. Synth. Catal.*, 2006, 348, 715.
86 G. Cusati and L. Djakovitch, *Tetrahedron Lett.*, 2008, 49, 2499.
87 N. Lebrasseur and I. Larrosa, *J. Am. Chem. Soc.*, 2008, 130, 2926.
88 L. L. Chng, J. Zhang, J. Yang, M. Amoura and J. Y. Ying, *Adv. Synth. Catal.*, 2011, 353, 2988.
89 J. Lee, J. Chung, S. M. Byun, B. M. Kim and C. Lee, *Tetrahedron*, 2013, 69, 5660.
90 L. Zhang, P. Li, C. Liu, J. Yang, M. Wang and L. Wang, *Catal. Sci. Technol.*, 2014, 4, 1979.
91 M. Al-Amin, M. Arisawa, S. Shuto, Y. Ano, M. Tobisu and N. Chatani, *Adv. Synth. Catal.*, 2014, 356, 1631.
92 K. Takagi, M. Al-Amin, N. Hoshiya, J. Wouters, H. Sugimoto, Y. Shiro, H. Fukuda, S. Shuto and M. Arisawa, *J. Org. Chem.*, 2014, 79, 6366.
93 S. Vásquez-Céspedes, A. Ferry, L. Candish and F. Glorius, *Angew. Chem., Int. Ed.*, 2015, 54, 5772.
94 P. V. Reddy, M. Annapurna, P. Srinivas, P. R. Likhar and M. Lakshmi Kantam, *New J. Chem.*, 2015, 39, 3399.
95 R. Kishore, J. Yadav, B. Venu, A. Venugopal and M. Lakshmi Kantam, *New J. Chem.*, 2015, 39, 5259.
96 S. E. Bajwa, T. E. Storr, L. E. Hatcher, T. J. Williams, C. G. Baumann, A. C. Whitwood, D. R. Allan, S. J. Teat, P. R. Raithby and I. J. S. Fairlamb, *Chem. Sci.*, 2012, 3, 1656.
97 K. J. Stowers, A. Kubota and M. S. Sanford, *Chem. Sci.*, 2012, 3, 3192.
98 I. J. S. Fairlamb, *Angew. Chem., Int. Ed.*, 2015, 54, 10415.
99 Y. Sun, B. Mayers and Y. Xia, *Adv. Mater.*, 2003, 15, 641.
100 A. Dhakshinamoorthy, A. M. Asiri and H. Garcia, *Chem. Soc. Rev.*, 2015, 44, 1922.
101 A. Dhakshinamoorthy and H. Garcia, *Chem. Soc. Rev.*, 2012, 41, 5262.
102 Y. Huang, Z. Lin and R. Cao, *Chem. – Eur. J.*, 2011, 17, 12706.
103 Y. Huang, T. Ma, P. Huang, D. Wu, Z. Lin and R. Cao, *ChemCatChem*, 2013, 5, 1877.
104 L. Wang, W.-B. Yi and C. Cai, *Chem. Commun.*, 2011, 47, 806.
105 Y. M. A. Yamada, Y. Yuyama, T. Sato, S. Fujikawa and Y. Uozumi, *Angew. Chem., Int. Ed.*, 2014, 53, 127.
106 T. Parsharamulu, D. Venkanna, M. Lakshmi Kantam, S. K. Bhargava and P. Srinivasu, *Ind. Eng. Chem. Res.*, 2014, 53, 20075.
107 S. M. McAfee, J. S. J. McCahill, C. M. Macaulay, A. D. Hendsbee and G. C. Welch, *RSC Adv.*, 2015, 5, 26097.
108 V. A. Zinovyeva, M. A. Vorotyntsev, I. Bezverkhyy, D. Chaumont and J.-C. Hierso, *Adv. Funct. Mater.*, 2011, 21, 1064.
109 S. Keshipour and A. Shaabani, *Appl. Organomet. Chem.*, 2014, 28, 116.
110 M. Shakeri, C.-W. Tai, E. Göthelid, S. Oscarsson and J.-E. Bäckvall, *Chem. – Eur. J.*, 2011, 17, 13269.
111 J. Malmgren, A. Nagendiran, C.-W. Tai, J.-E. Bäckvall and B. Olofsson, *Chem. – Eur. J.*, 2014, 20, 13531.
112 M. Cao, D. Wu, W. Su and R. Cao, *J. Catal.*, 2015, 321, 62.
113 S. Korwar, K. Brinkley, A. R. Siamaki, B. F. Gupton and K. C. Ellis, *Org. Lett.*, 2015, 17, 1782.
114 S. Wang, D. Hu, W. Hua, J. Gu, Q. Zhang, X. Jia and K. Xi, *RSC Adv.*, 2015, 5, 53935.
115 D.-T. D. Tang, K. D. Collins and F. Glorius, *J. Am. Chem. Soc.*, 2013, 135, 7450.
116 D.-T. D. Tang, K. D. Collins, J. B. Ernst and F. Glorius, *Angew. Chem., Int. Ed.*, 2014, 53, 1809.
117 K. D. Collins, R. Honeker, S. Vasquez-Cespedes, D.-T. D. Tang and F. Glorius, *Chem. Sci.*, 2015, 6, 1816.

268

Appendix 2: X-Ray Diffraction Data

Crystallographic data for compound 75
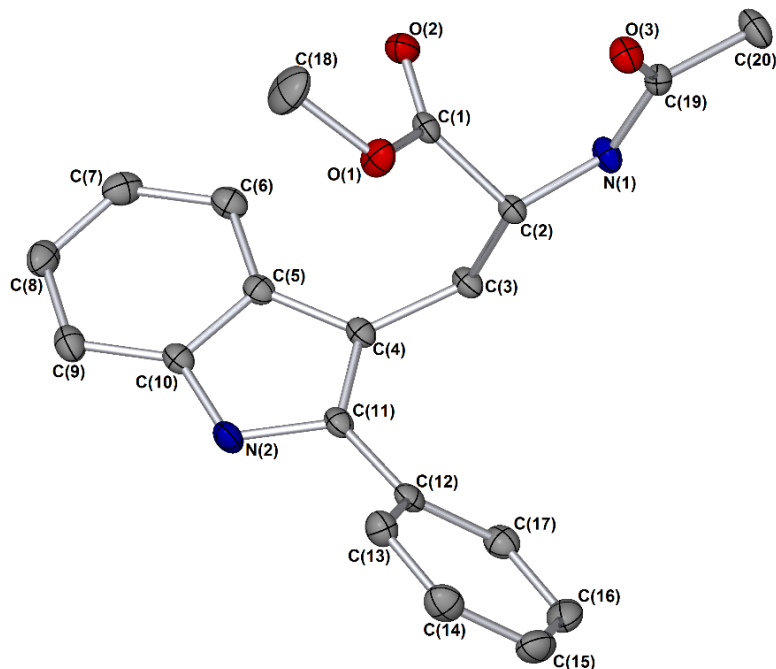
Figure 51 Single crystal X-ray diffraction structure of **75**. Thermal ellipsoids shown with 50% probability and hydrogen atoms removed for clarity. Selected bond lengths (Å): C(3)–C(4): 1.500(3), C(4)–C(11): 1.375(3), N(2)–C(11): 1.388(2), C(11)–C(12): 1.475(3). Selected bond angles (°): C(4)–C(11)–C(12): 131.75(18), N(2)–C(11)–C(12): 118.71(17).

Table 16 Crystal data and structure refinement for ijsf1413 (compound **75**).

Identification code	ijsf1413
Empirical formula	$C_{20}H_{20}N_2O_3$
Formula weight	336.38
Temperature / K	110.05(10)
Crystal system	trigonal
Space group	R3
a / Å	21.2602(5)
b / Å	21.2602(5)
c / Å	10.1814(3)
α / Å	90
β / Å	90
γ / Å	120
Volume / Å^3	3985.4(2)
No. of formula units per unit cell, Z	9
ρ_{calc} mg / mm^3	1.261
m / mm^{-1}	0.086
F(000)	1602.0
Crystal size / mm^3	$0.2757 \times 0.1814 \times 0.1572$
Radiation	MoKα ($\lambda = 0.71073$)
2Θ range for data collection / °	5.966 to 64.01
Index ranges	$-23 \leq h \leq 31$, $-26 \leq k \leq 25$, $-15 \leq l \leq 13$
Reflections collected	6369
Independent reflections	4199 [$R_{int} = 0.0191$]
Data/restraints/parameters	4199/1/236
Goodness-of-fit on F^2	1.049
Final R indexes [I>=2σ (I)]	$R_1 = 0.0363$, $wR_2 = 0.0863$
Final R indexes [all data]	$R_1 = 0.0404$, $wR_2 = 0.0901$
Largest diff. peak/hole / e Å^{-3}	0.28/-0.22

Crystallographic data for compound 142
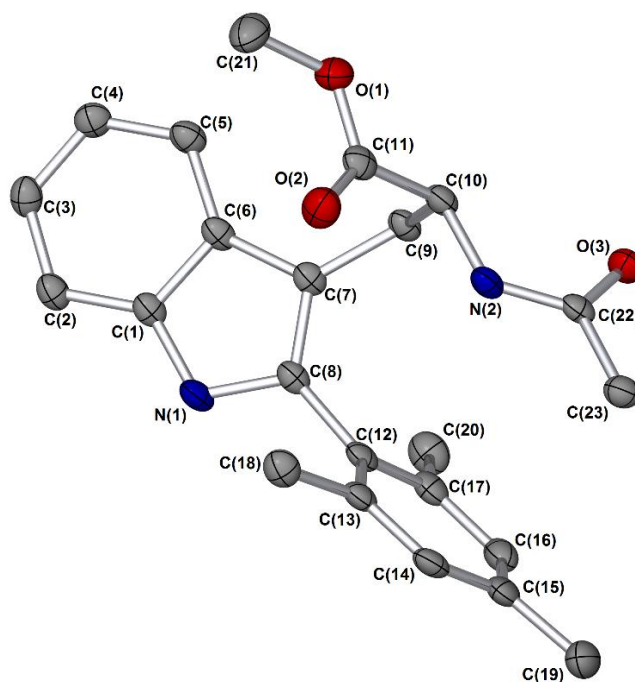
Figure 52 Single crystal X-ray diffraction structure of **142**. Thermal ellipsoids shown with 50% probability and hydrogen atoms removed for clarity. Selected bond lengths (Å): C(7)–C(9): 1.506(3), C(7)–C(8): 1.378(3), N(1)–C(8): 1.378(3), C(8)–C(12): 1.484(3). Selected bond angles (°): C(7)– C(8)–C(12): 128.9(2), N(1)–C(8)–C(12): 121.8(2).

Table 17 Crystal data and structure refinement for ijsf1488 (compound **142**).

Identification code	ijsf1488
Empirical formula	$C_{23}H_{26}N_2O_3$
Formula weight	378.46
Temperature / K	110.05(10)
Crystal system	monoclinic
Space group	$P2_1$
a / Å	8.7152(3)
b / Å	13.5902(4)
c / Å	8.7625(3)
α / Å	90
β / Å	100.507(3)
γ / Å	90
Volume / Å^3	1020.44(6)
No. of formula units per unit cell, Z	2
ρ_{calc} mg / mm^3	1.232
μ / mm^{-1}	0.655
F(000)	404.0
Crystal size / mm^3	$0.2485 \times 0.1431 \times 0.0656$
Radiation	CuKα (λ = 1.54184)
2Θ range for data collection / °	10.268 to 134.116
Index ranges	$-9 \leq h \leq 10, -16 \leq k \leq 16, -10 \leq l \leq 10$
Reflections collected	6691
Independent reflections	3634 [R_{int} = 0.0256, R_{sigma} = 0.0341]
Data/restraints/parameters	3634/1/357
Goodness-of-fit on F^2	1.029
Final R indexes [I>=2σ (I)]	R_1 = 0.0334, wR_2 = 0.0865
Final R indexes [all data]	R_1 = 0.0350, wR_2 = 0.0882
Largest diff. peak/hole / e Å^{-3}	0.21/−0.18

Crystallographic data for compound 210
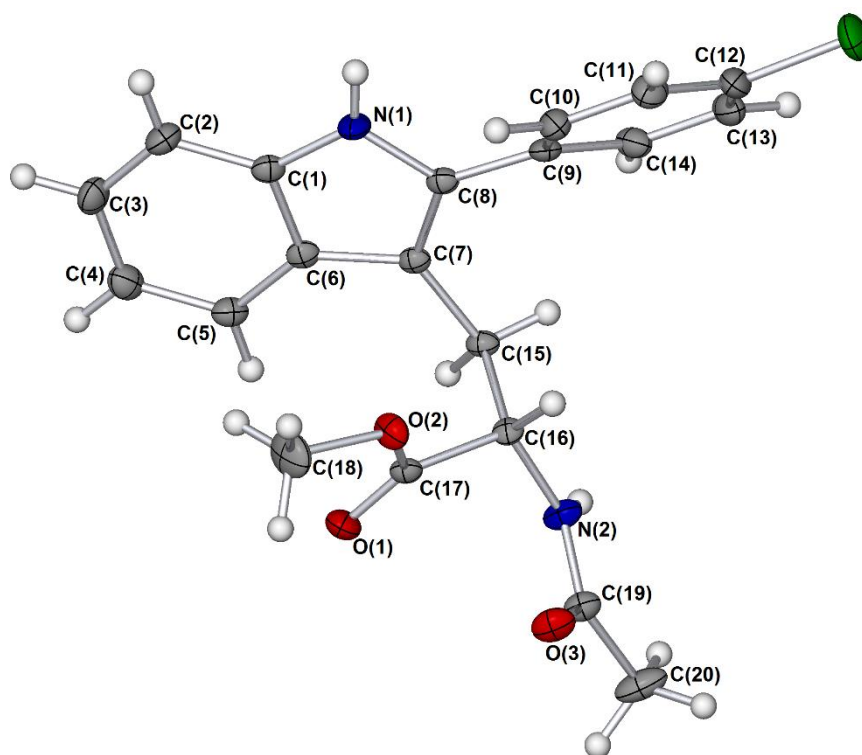
Figure 53 Single crystal X-ray diffraction structure of **210**. Thermal ellipsoids shown with 50% probability and absolute stereochemistry established by anomalous dispersion. Selected bond lengths (Å): C(7)–C(15): 1.500(2), C(7)–C(8): 1.369(3), N(1)–C(8): 1.382(3), C(8)–C(9): 1.475(3), C(12)–Cl(1): 1.743(2). Selected bond angles (°): C(7)–C(8)–C(9): 131.44(17), N(1)–C(8)–C(9): 119.04(16).

Table 18 Crystal data and structure refinement for ijsf1487 (compound **210**).

Identification code	ijsf1487
Empirical formula	$C_{20}H_{19}ClN_2O_3$
Formula weight	370.82
Temperature / K	110.05(10)
Crystal system	trigonal
Space group	R3
a / Å	20.7806(2)
b / Å	20.7806(2)
c / Å	11.18107(13)
α / Å	90
β / Å	90
γ / Å	120
Volume / Å^3	4181.48(10)
No. of formula units per unit cell, Z	9
ρ_{calc} mg / mm^3	1.325
μ / mm^{-1}	2.004
F(000)	1746.0
Crystal size / mm^3	$0.183 \times 0.1321 \times 0.0705$
Radiation	CuKα (λ = 1.54184)
2Θ range for data collection / °	8.51 to 134.026
Index ranges	$-24 \leq h \leq 24$, $-24 \leq k \leq 24$, $-13 \leq l \leq 13$
Reflections collected	19066
Independent reflections	3300 [$R_{int} = 0.0214$, $R_{sigma} = 0.0128$]
Data/restraints/parameters	3300/1/245
Goodness-of-fit on F^2	1.051
Final R indexes [I>=2σ (I)]	$R_1 = 0.0217$, $wR_2 = 0.0550$
Final R indexes [all data]	$R_1 = 0.0219$, $wR_2 = 0.0552$
Largest diff. peak/hole / e Å^{-3}	0.16/−0.23

Crystallographic data for compound 238
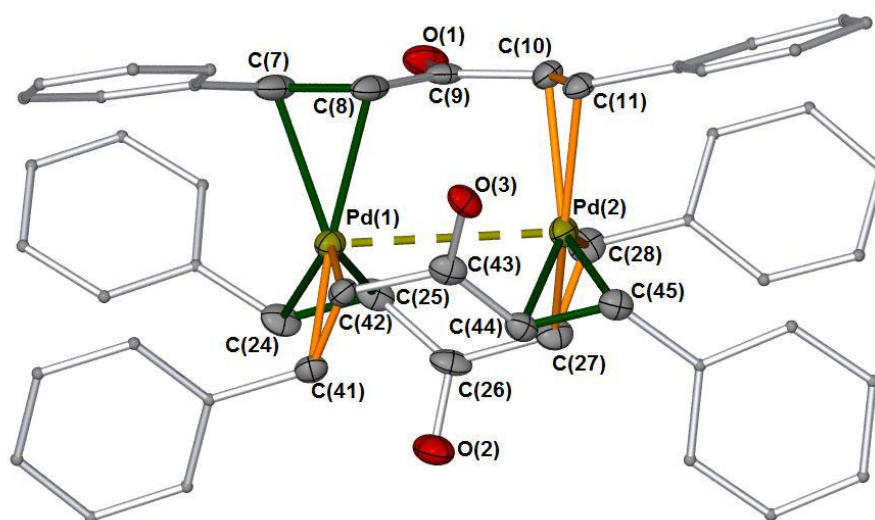
Figure 54 Single crystal X-ray diffraction structure of complex **238** (major isomer). Thermal ellipsoids shown with 50% probability, hydrogen atoms and solvating chloroform removed for clarity. Selected bond lengths (Å): Pd(1)–C(7): 2.303(3), Pd(1)–C(8): 2.248(3), C(7)–C(8): 1.358(4), Pd(1)–C(24): 2.279(4), Pd(1)–C(25): 2.251(4), C(24)–C(25): 1.364(6), Pd(1)–C(41): 2.202(3), Pd(1)–C(42): 2.220(3), C(41)–C(42): 1.393(5), Pd(2)–C(10): 2.222(3), Pd(2)–C(11): 2.244(3), C(10)–C(11): 1.395(4), Pd(2)–C(27): 2.244(4), Pd(2)–C(28): 2.241(4), C(27)–C(28): 1.392(6), Pd(2)–C(44): 2.244(3), Pd(2)–C(45): 2.280(3), C(44)–C(45): 1.359(5). Pd(1)–Pd(2) bond distance: 3.244 Å.
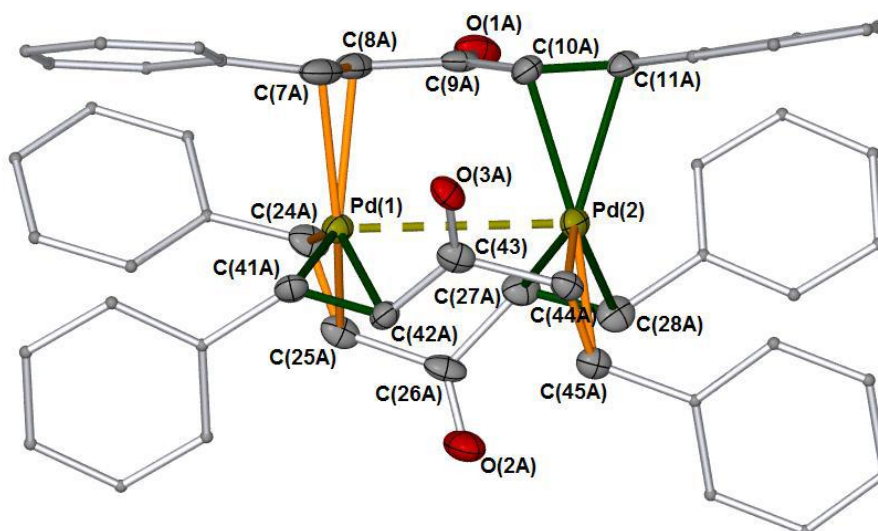
Figure 55 Single crystal X-ray diffraction structure of complex **238** (minor isomer). Thermal ellipsoids shown with 50% probability, hydrogen atoms and solvating chloroform removed for clarity. Selected bond lengths (Å): Pd(1)–C(7A): 2.275(11), Pd(1)–C(8A): 2.297(11), C(7A)–C(8A): 1.368(19), Pd(1)–C(24A): 2.243(6), Pd(1)–C(25A): 2.254(6), C(24A)–C(25A): 1.390(9), Pd(1)–C(41A): 2.211(7), Pd(1)–C(42A): 2.207(7), C(41A)–C(42A): 1.339(10), Pd(2)–C(10A): 2.192(11), Pd(2)–C(11A): 2.272(10), C(10A)–C(11A): 1.332(9), Pd(2)–C(27A): 2.274(6), Pd(2)–C(28A): 2.242(6), C(27A)–C(28A): 1.352(9), Pd(2)–C(44A): 2.267(7), Pd(2)–C(45A): 2.311(7), C(44A)–C(45A): 1.394(10). Pd(1)–Pd(2) bond distance: 3.244 Å.

Table 19 Crystal data and structure refinement for ijsf1227 (compound **238**).

Identification code	ijsf1227
Empirical formula	$C_{52}H_{43}Cl_3O_3Pd_2$
Formula weight	1035.01
Temperature / K	110.00(10)
Crystal system	monoclinic
Space group	$P2_1/n$
a / Å	13.3506(2)
b / Å	13.27319(12)
c / Å	24.3667(3)
α / Å	90
β / Å	101.3288(14)
γ / Å	90
Volume / Å³	4233.77(9)
No. of formula units per unit cell, Z	4
ρ_{calc} mg / mm³	1.624
m / mm^{-1}	1.084
F(000)	2088.0
Crystal size / mm³	$0.1342 \times 0.1177 \times 0.1018$
2Θ range for data collection / °	5.9 to 60.16
Index ranges	$-9 \le h \le 18, -16 \le k \le 18, -34 \le l \le 28$
Reflections collected	25517
Independent reflections	12430 [$R_{int} = 0.0250$]
Data/restraints/parameters	12430/26/631
Goodness-of-fit on F^2	1.073
Final R indexes [I>=2σ (I)]	$R_1 = 0.0333$, $wR_2 = 0.0720$
Final R indexes [all data]	$R_1 = 0.0464$, $wR_2 = 0.0796$
Largest diff. peak/hole / e Å^{-3}	0.84/−0.61

Crystallographic data for compound 249
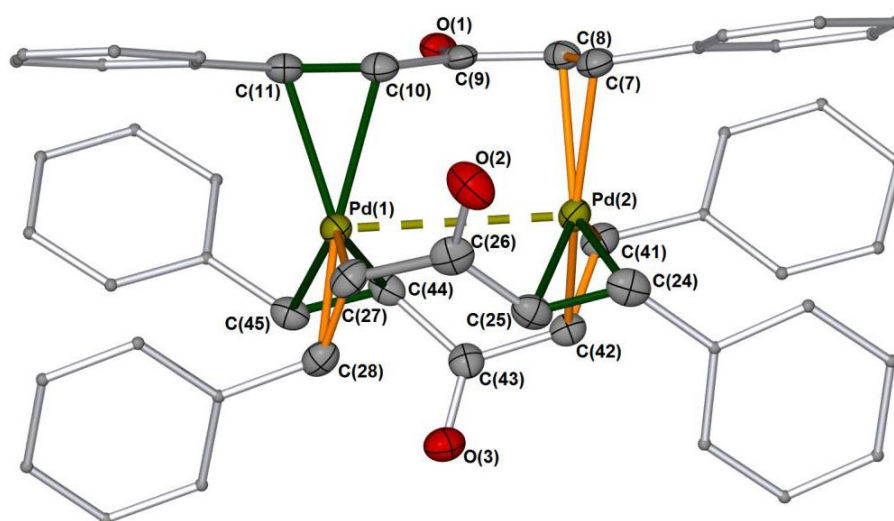
Figure 56 Single crystal X-ray diffraction structure of complex **249** (major isomer). Thermal ellipsoids shown with 50% probability, hydrogen atoms and solvating methylene chloride removed for clarity.

277

Table 20 Crystal data and structure refinement for ijsf1232 (compound **249**).

Identification code	ijsf1232
Empirical formula	$C_{52}H_{44}Cl_2O_3Pd_2$
Formula weight	1000.57
Temperature / K	110.00(10)
Crystal system	triclinic
Space group	P-1
a / Å	12.2214(4)
b / Å	12.8052(3)
c / Å	15.0153(3)
α / Å	114.651(2)
β / Å	96.795(2)
γ / Å	95.356(2)
Volume / Å^3	2094.03(9)
No. of formula units per unit cell, Z	2
ρ_{calc} mg / mm^3	1.587
m / mm^{-1}	1.031
F(000)	1012.0
Crystal size / mm^3	$0.3172 \times 0.1571 \times 0.0798$
2Θ range for data collection / °	5.94 to 64.28
Index ranges	$-17 \leq h \leq 18$, $-18 \leq k \leq 18$, $-21 \leq l \leq 22$
Reflections collected	37706
Independent reflections	13493 [$R_{int} = 0.0487$]
Data/restraints/parameters	13493/21/635
Goodness-of-fit on F^2	1.086
Final R indexes [I>=2σ (I)]	$R_1 = 0.0395$, $wR_2 = 0.0907$
Final R indexes [all data]	$R_1 = 0.0531$, $wR_2 = 0.1009$
Largest diff. peak/hole / e Å^{-3}	1.06/−1.34

Crystallographic data for compound 250
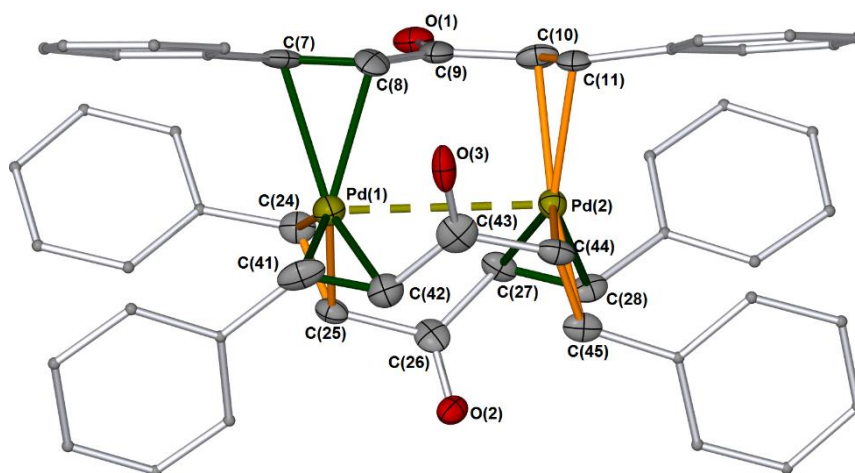
Figure 57 Single crystal X-ray diffraction structure of complex **250** (major isomer). Thermal ellipsoids shown with 50% probability, hydrogen atoms and solvating benzene removed for clarity.

Table 21 Crystal data and structure refinement for ijsf1302 (compound **250**).

Identification code	ijsf1302
Empirical formula	$C_{57}H_{48}O_3Pd_2$
Formula weight	993.75
Temperature / K	109.95(10)
Crystal system	monoclinic
Space group	$P2_1/c$
a / Å	13.6130(3)
b / Å	23.3621(5)
c / Å	15.2236(4)
α / Å	90
β / Å	114.397(3)
γ / Å	90
Volume / Å^3	4409.22(17)
No. of formula units per unit cell, Z	4
ρ_{calc} mg / mm^3	1.497
m / mm^{-1}	0.862
F(000)	2024.0
Crystal size / mm^3	$0.0881 \times 0.0626 \times 0.0492$
2Θ range for data collection / °	5.7 to 50.7
Index ranges	$-15 \leq h \leq 16, -24 \leq k \leq 28, -18 \leq l \leq 12$
Reflections collected	17380
Independent reflections	8075 [R_{int} = 0.0377]
Data/restraints/parameters	8075/15/662
Goodness-of-fit on F^2	1.062
Final R indexes [I>=2σ (I)]	R_1 = 0.0440, wR_2 = 0.0953
Final R indexes [all data]	R_1 = 0.0613, wR_2 = 0.1038
Largest diff. peak/hole / e Å^{-3}	0.71/−0.87

Appendix 3: UV–Visible Spectroscopic Data
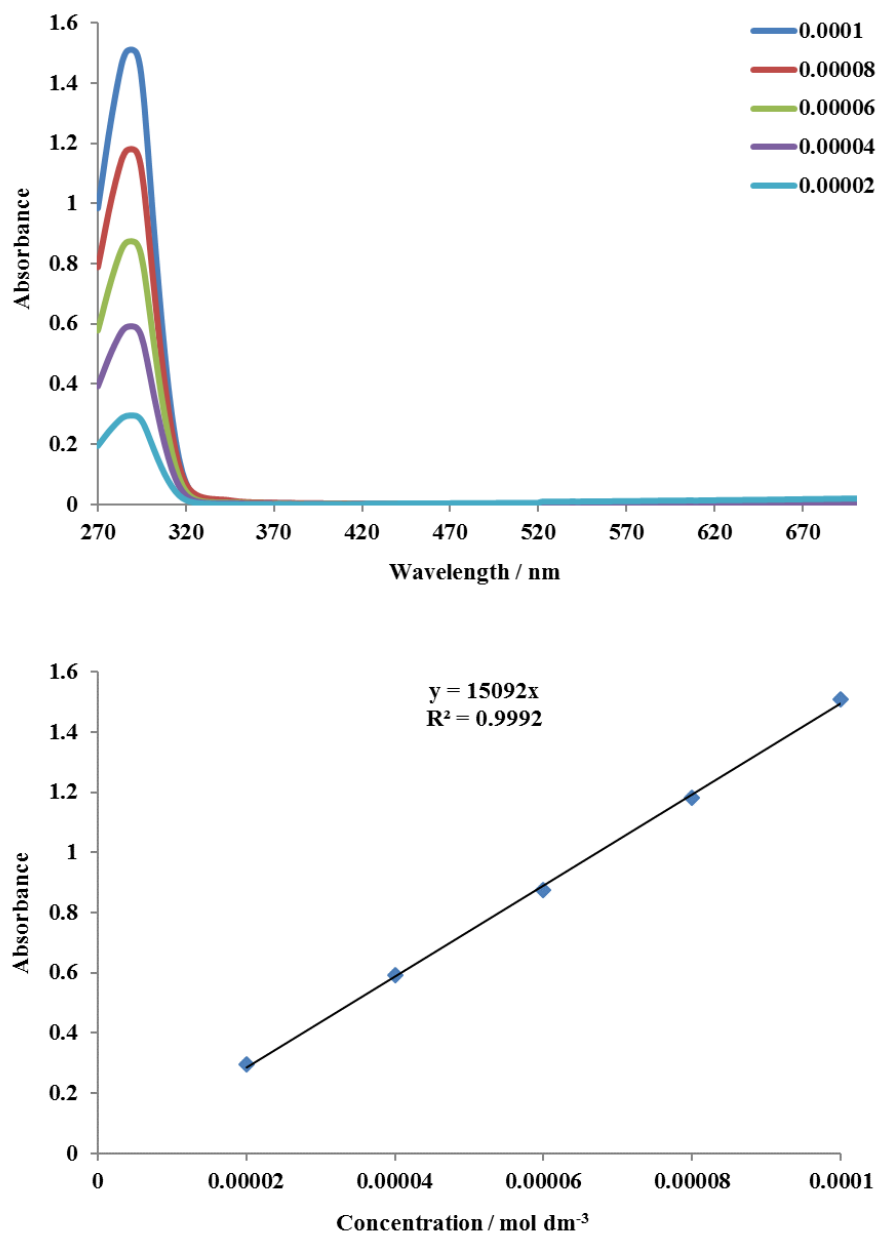
Figure 58 UV–visible spectroscopic analysis for compound **142**.

$$y = 12870x$$
$$R^2 = 1$$
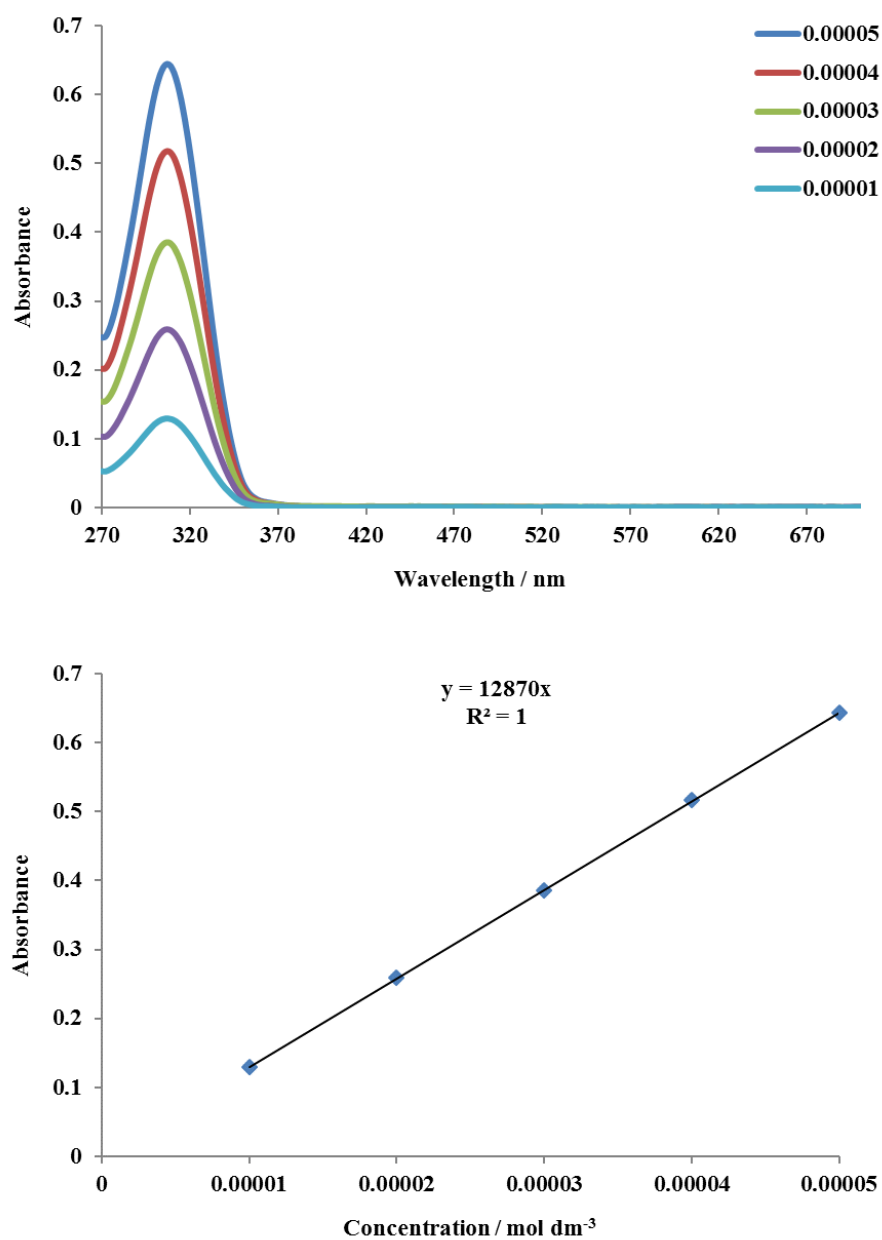
Figure 59 UV–visible spectroscopic analysis for compound **160**.
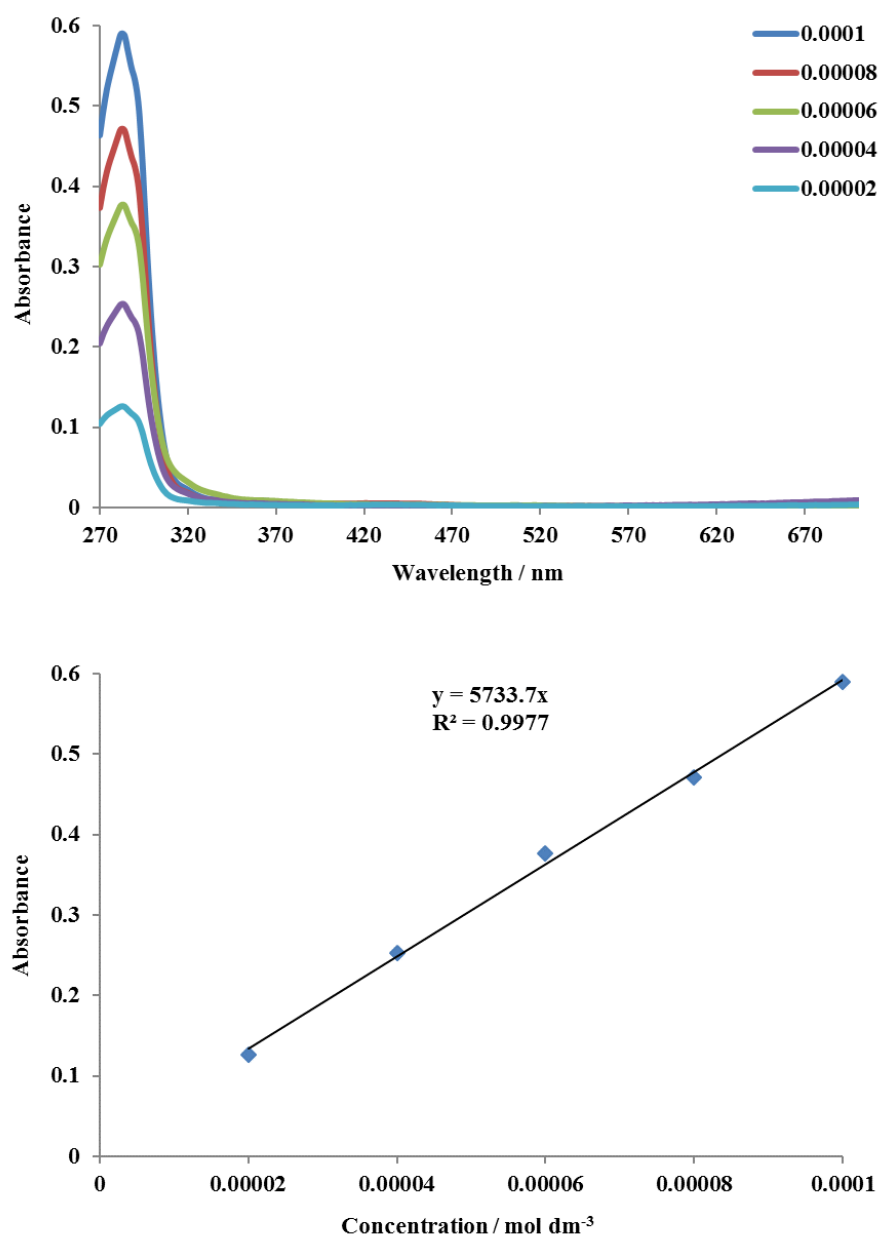
Figure 60 UV–visible spectroscopic analysis for compound **167**.
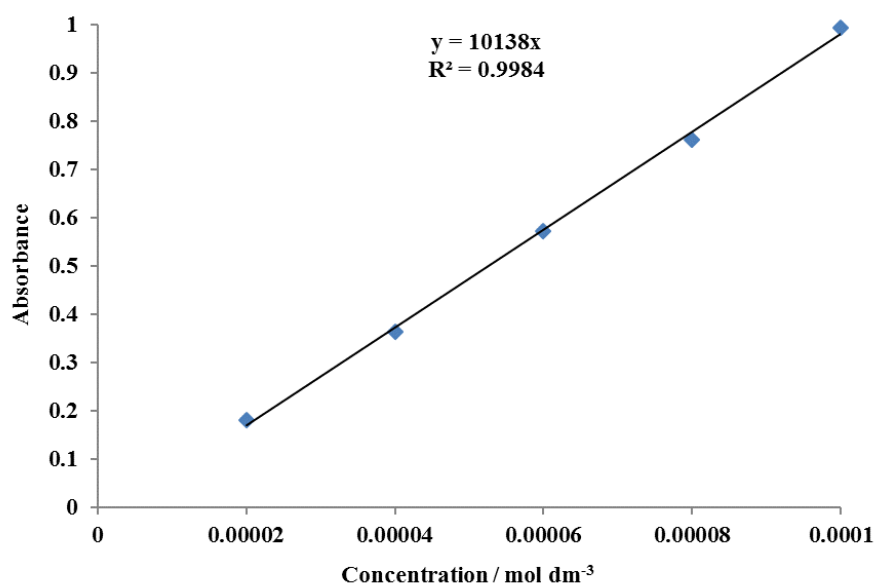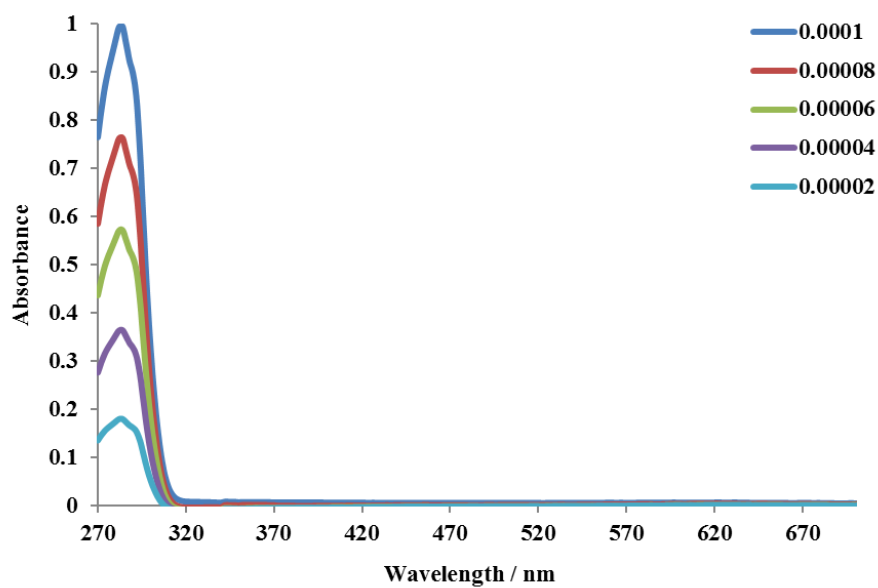
Figure 61 UV–visible spectroscopic analysis for compound **170**.

y = 9725.4x
R² = 1
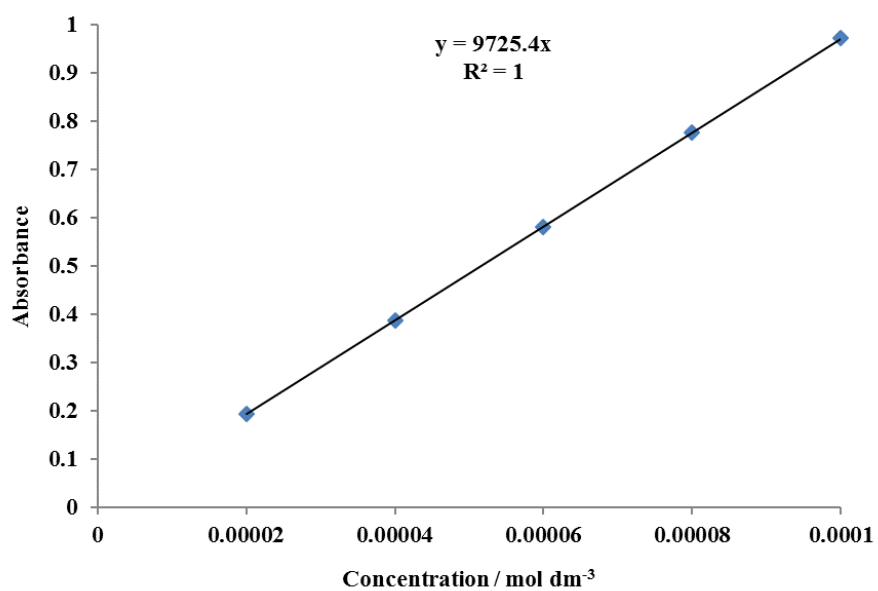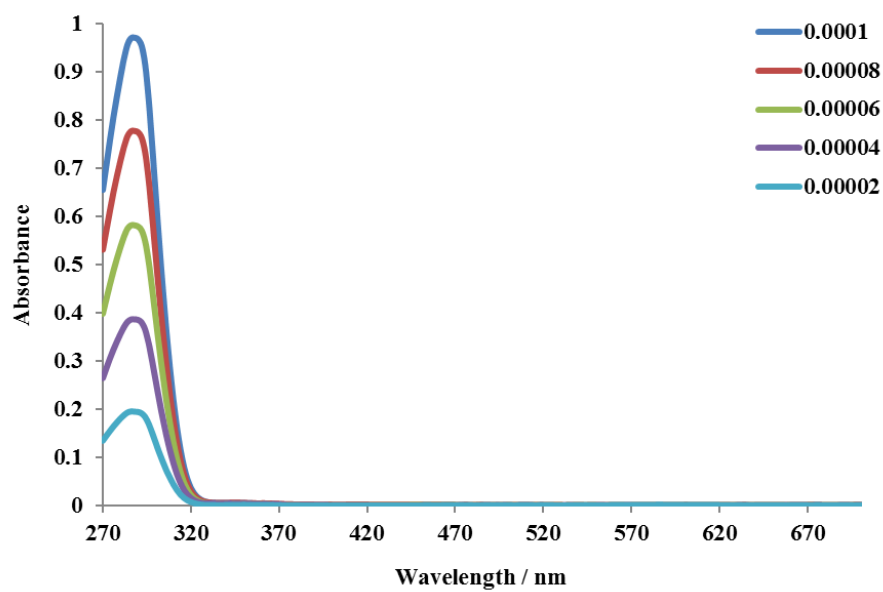
Figure 62 UV–visible spectroscopic analysis for compound **172**.

285

$$y = 20467x$$
$$R^2 = 0.9998$$
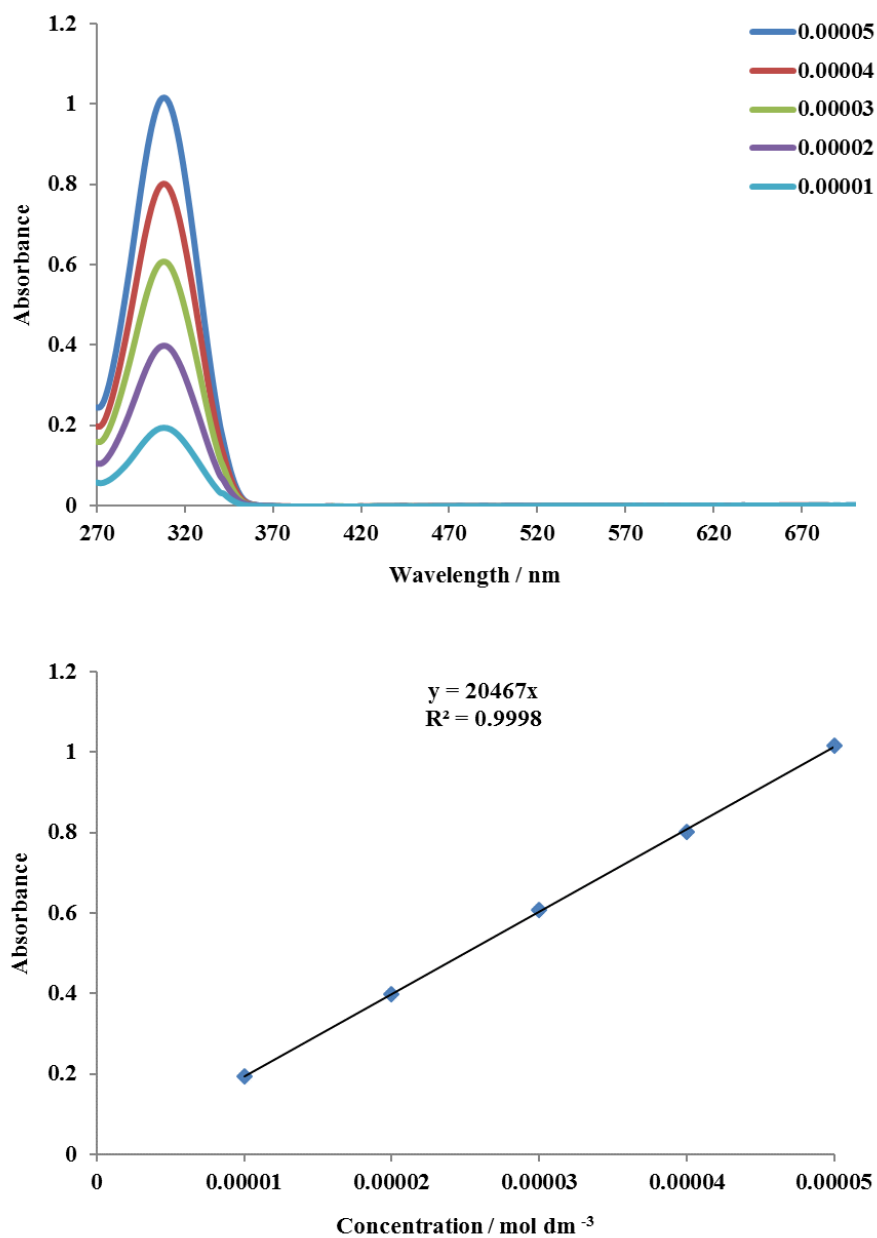
Figure 63 UV–visible spectroscopic analysis for compound **173**.

286
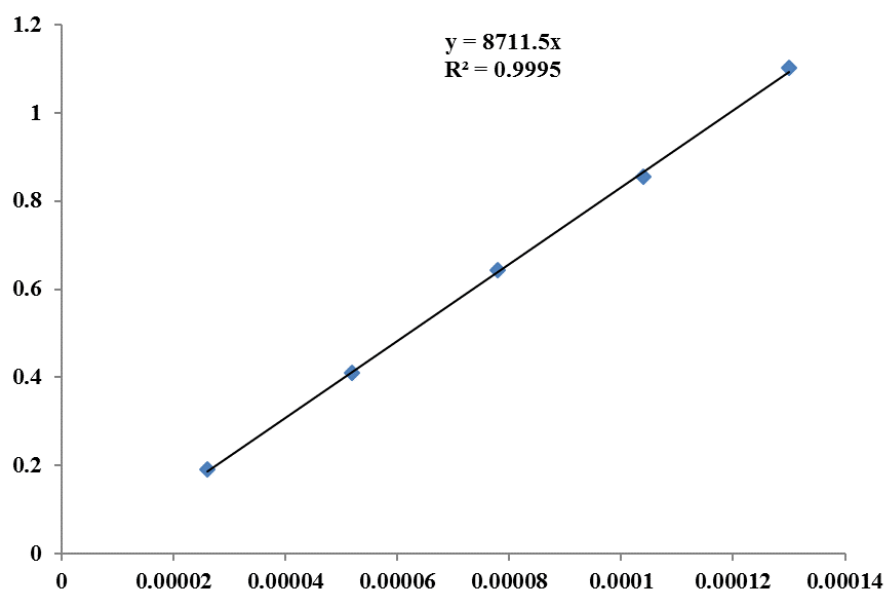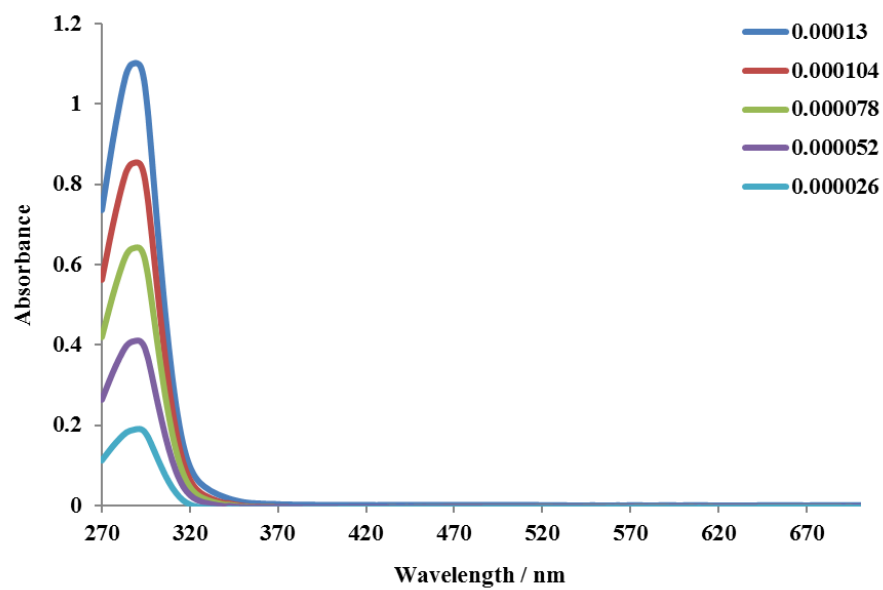
Figure 64 UV–visible spectroscopic analysis for compound **174**.

$y = 20684x$
$R^2 = 0.9994$
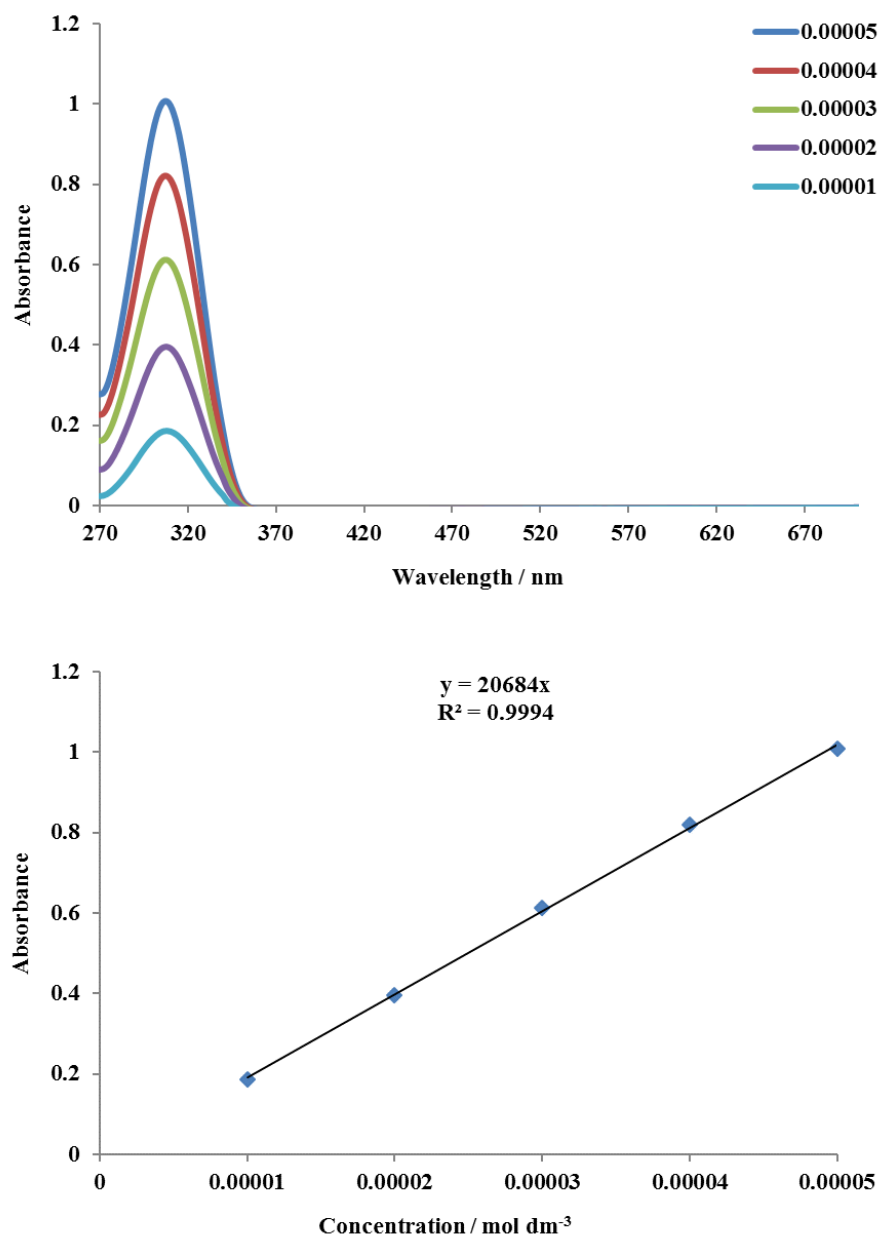
Figure 65 UV–visible spectroscopic analysis for compound **175**.

$$y = 12188x$$
$$R^2 = 0.9996$$
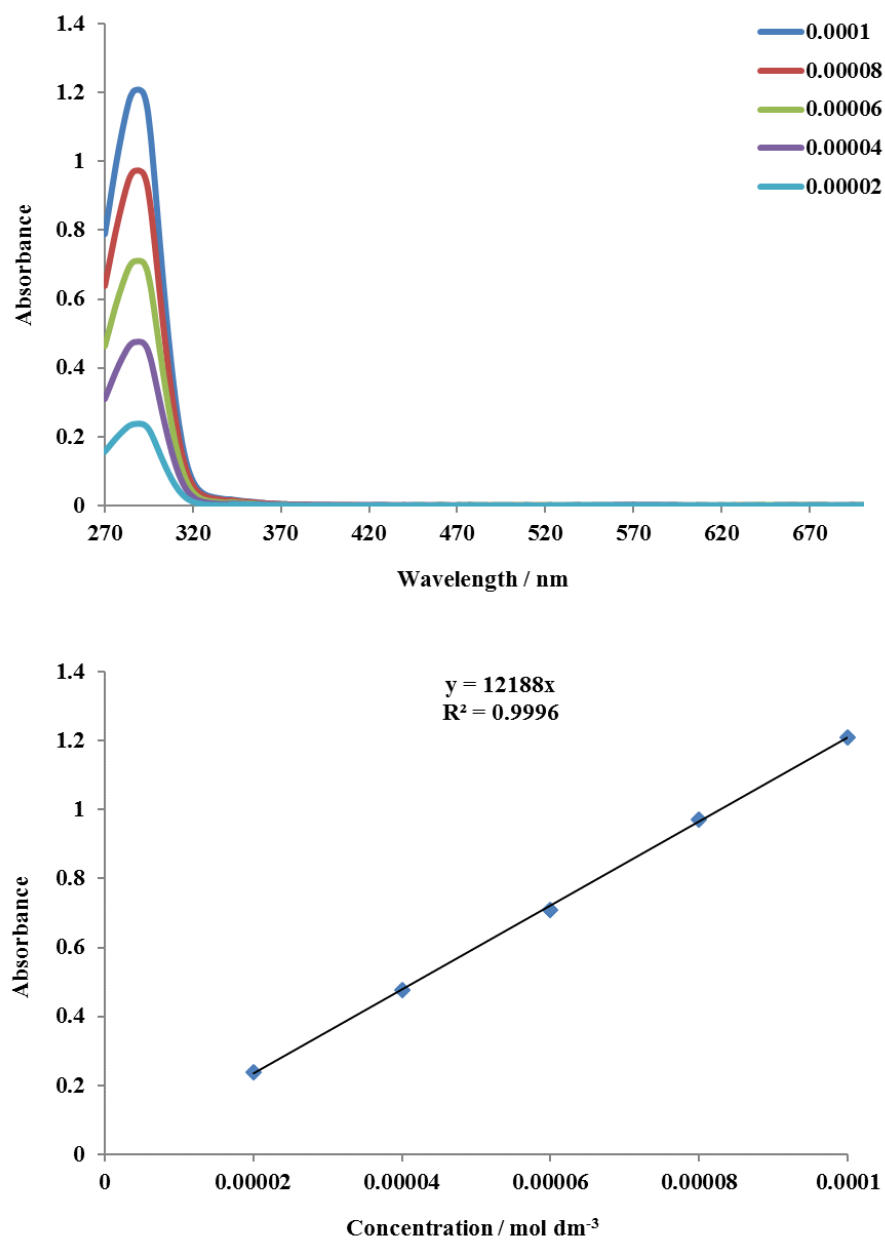
Figure 66 UV–visible spectroscopic analysis for compound **176**.

289

$$y = 19398x$$
$$R^2 = 1$$
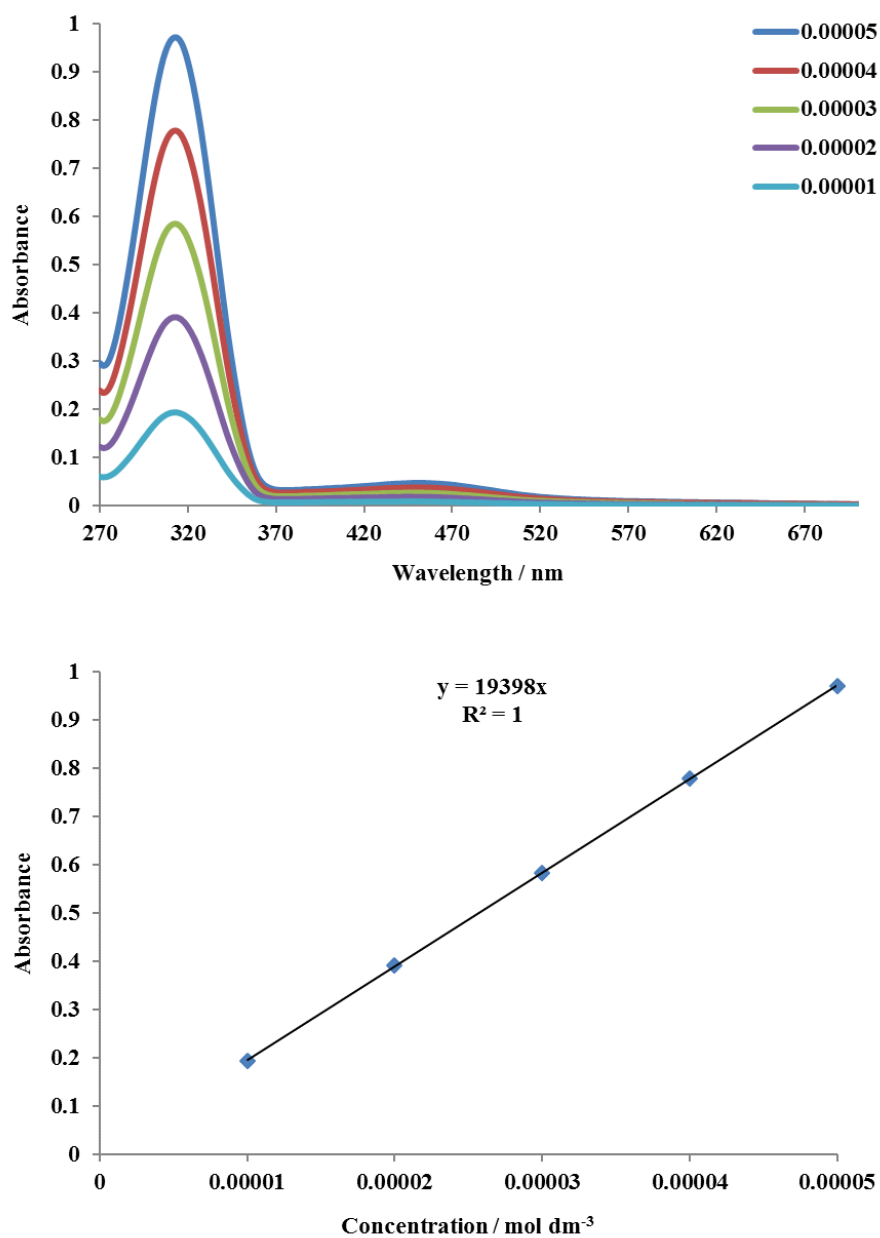
Figure 67 UV–visible spectroscopic analysis for compound **209**.

290

$y = 15639x$
$R^2 = 0.9996$
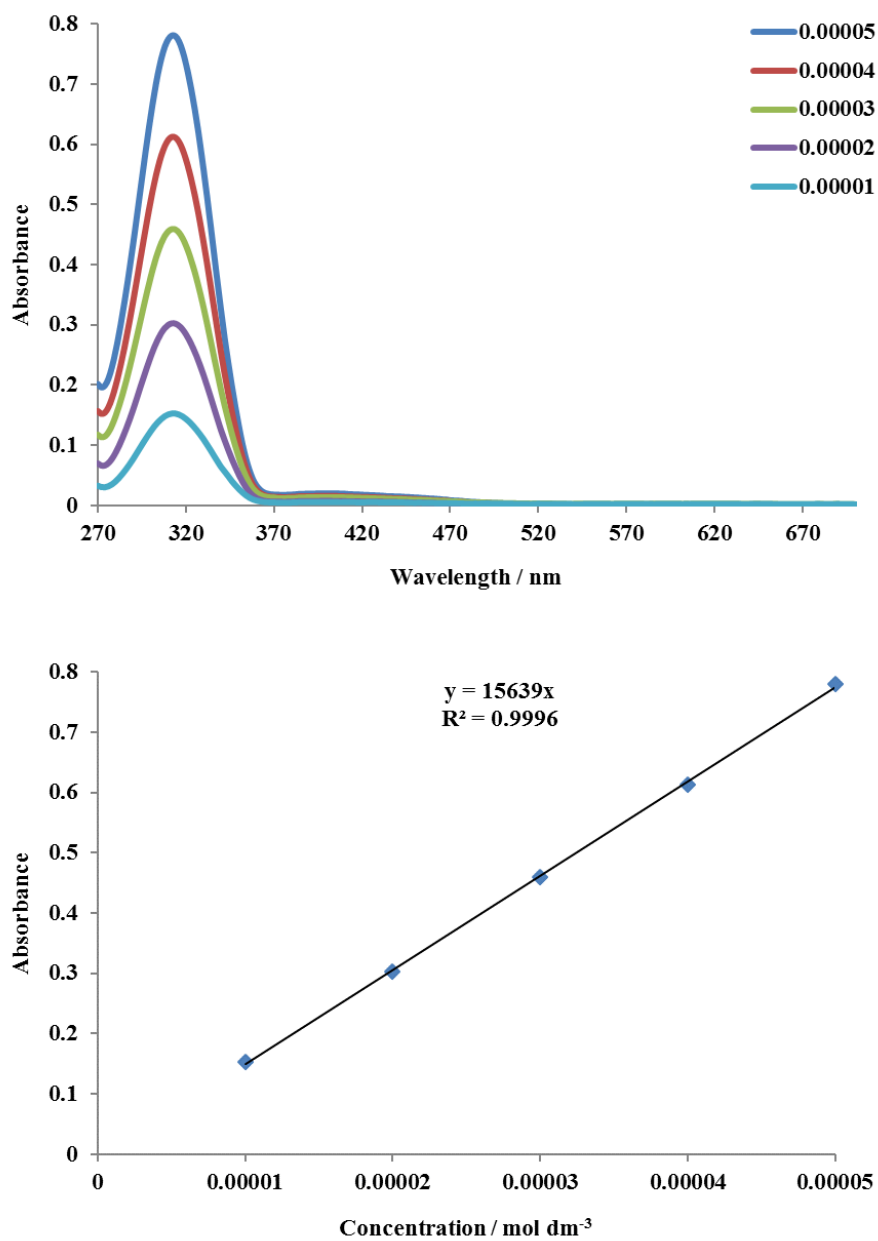
Figure 68 UV–visible spectroscopic analysis for compound **211**.

Appendix 4: HPLC Data

Arylation Products of 136

Method A
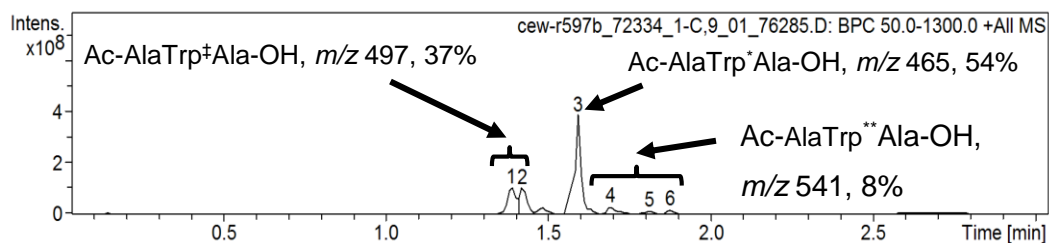
Figure 69 HPLC–ESI–MS chromatogram (BPC) of the crude reaction material (arylated tryptophan donated Trp*, diarylated tryptophans donated Trp**, dihydroxylated byproducts donated Trp‡).
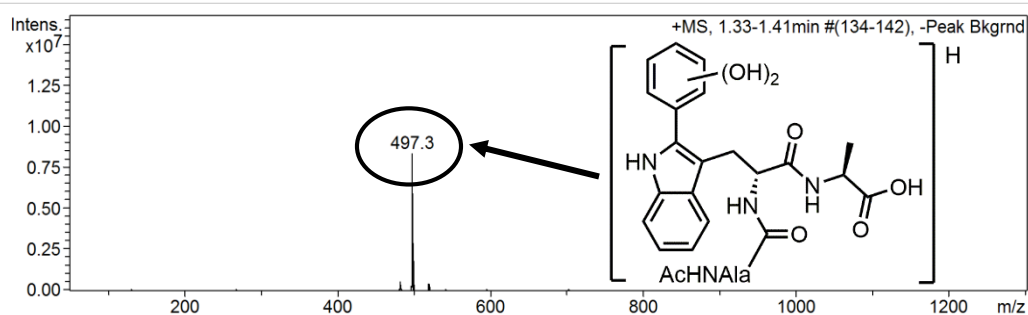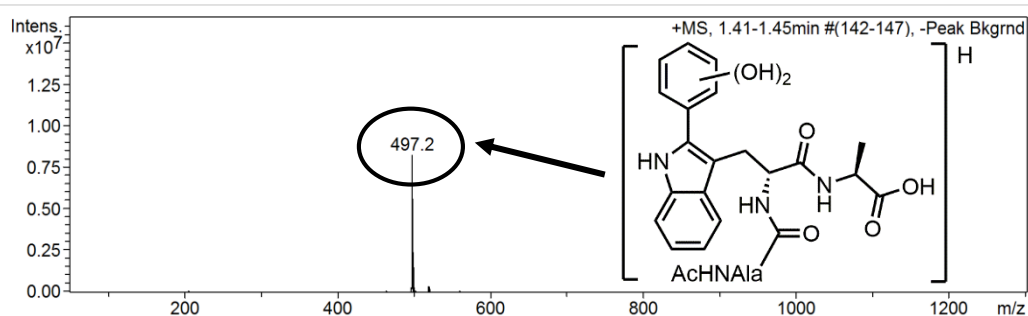
Figure 70 ESI–MS of dihydroxylated side products from arylation of **136**.
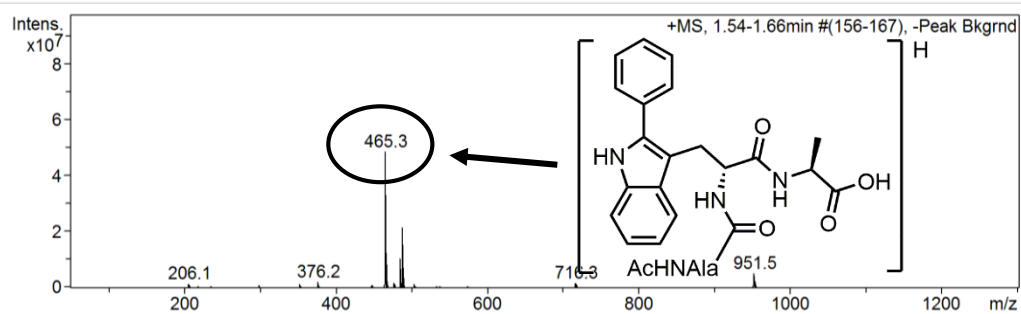
Figure 71 ESI–MS of arylation product **137**.
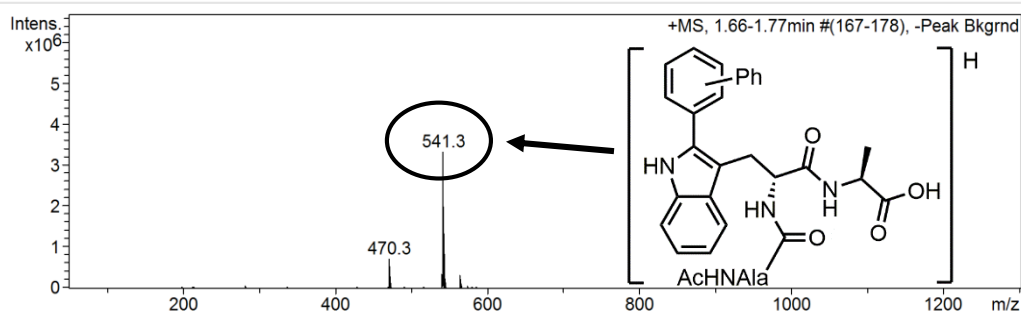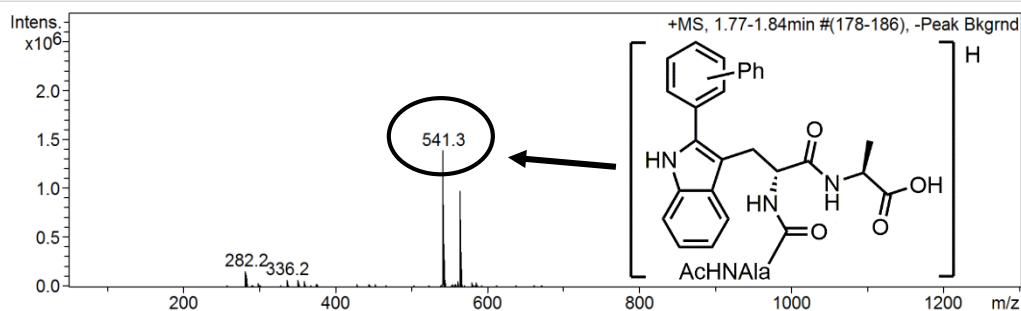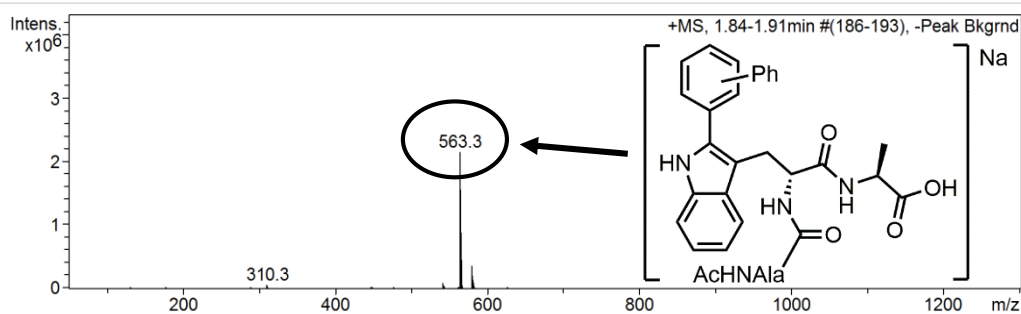
Figure 72 ESI–MS of diarylated side products from arylation of **136**.

Method B
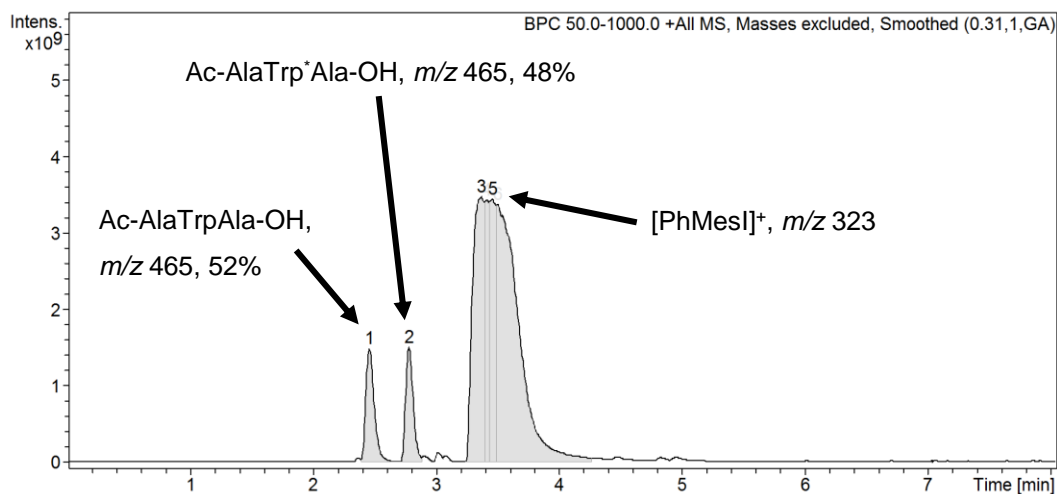
Figure 73 HPLC–ESI–MS chromatogram (BPC) of the crude reaction material (arylated tryptophan donated Trp*, starting material donated Trp).
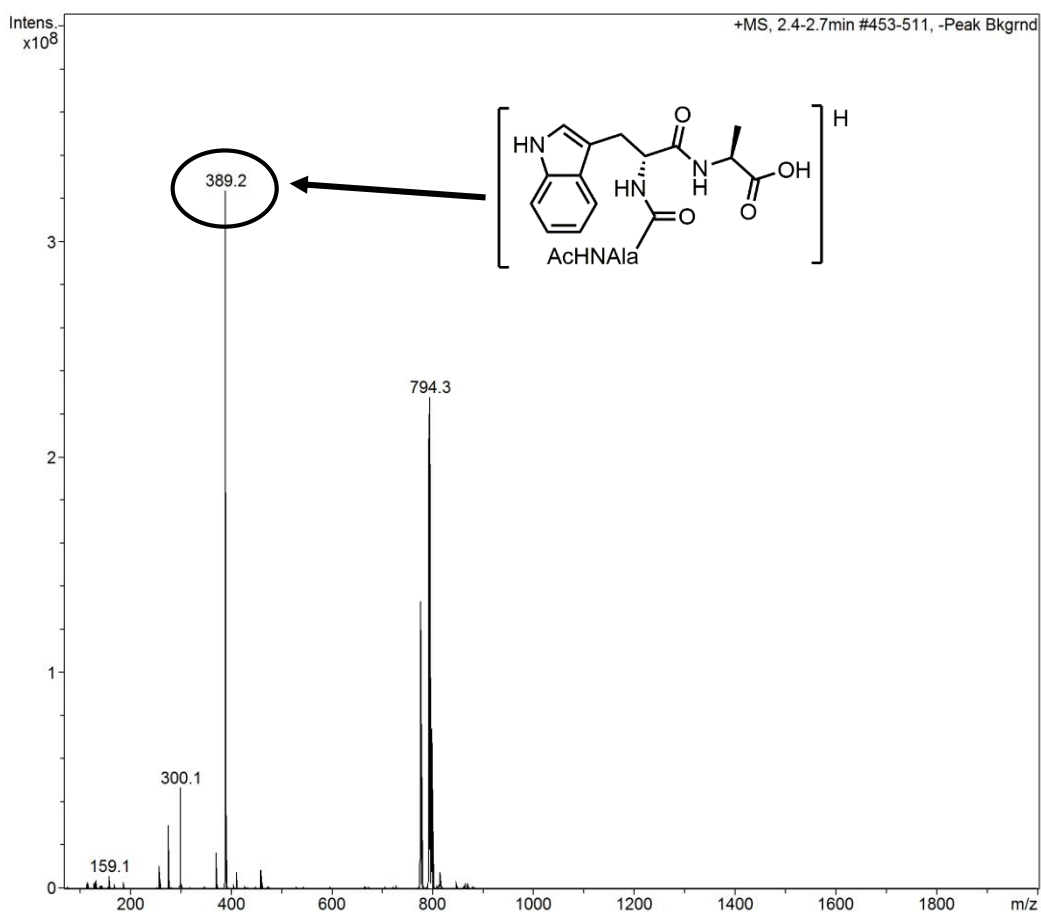
Figure 74 ESI–MS of starting material **136**.

Cmpd 2, 2.8 min
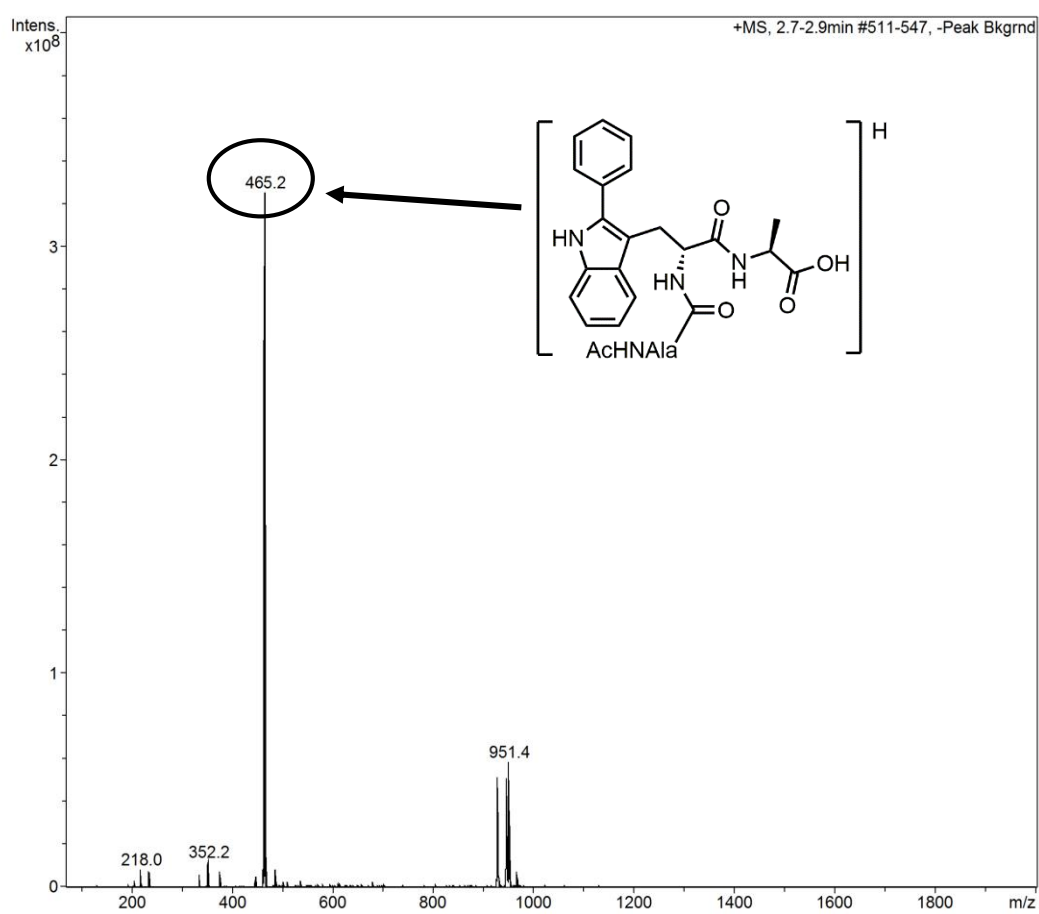
Figure 75 ESI–MS of arylation product **137**.

Cmpd 3, 3.4 min
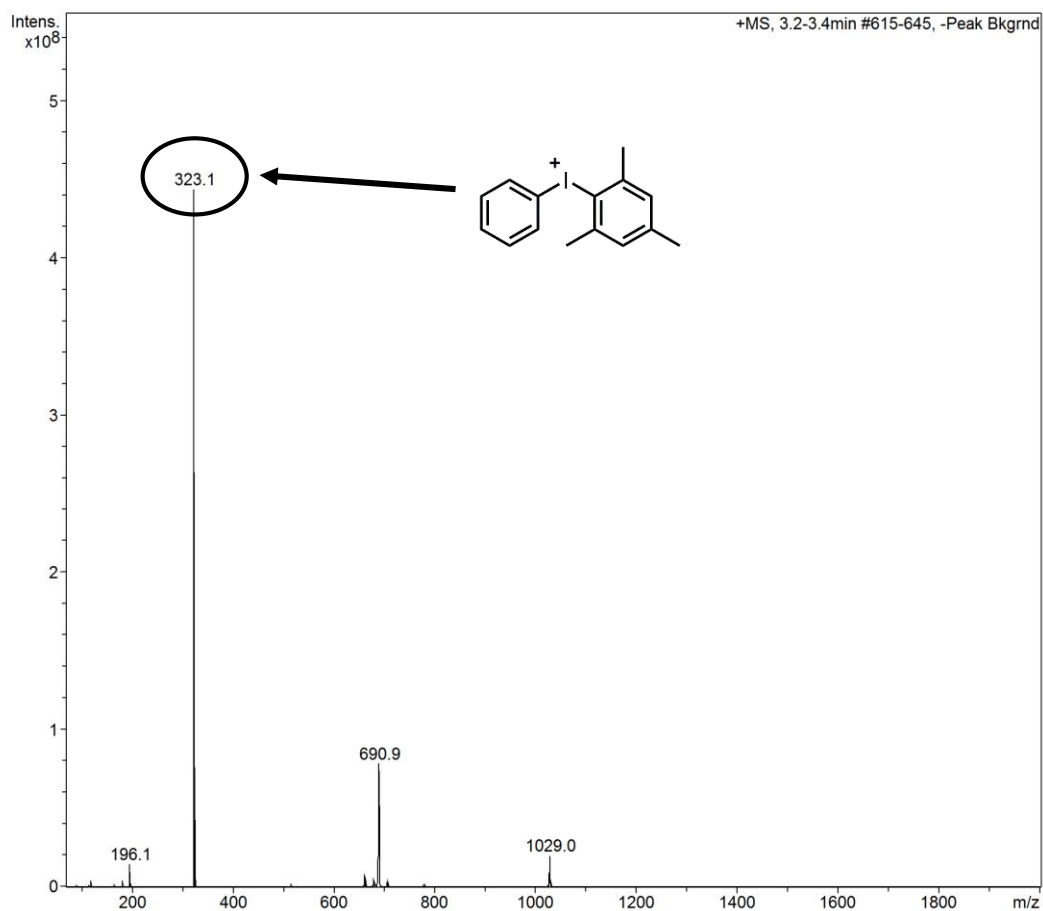
Figure 76 ESI–MS of starting material **140**.

Method C
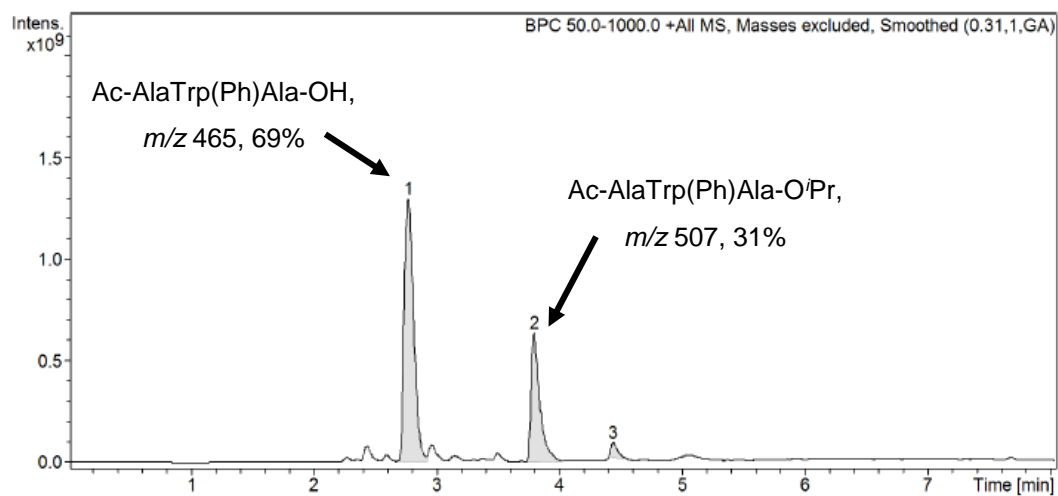
Figure 77 HPLC–ESI–MS chromatogram (BPC) of the crude reaction material.
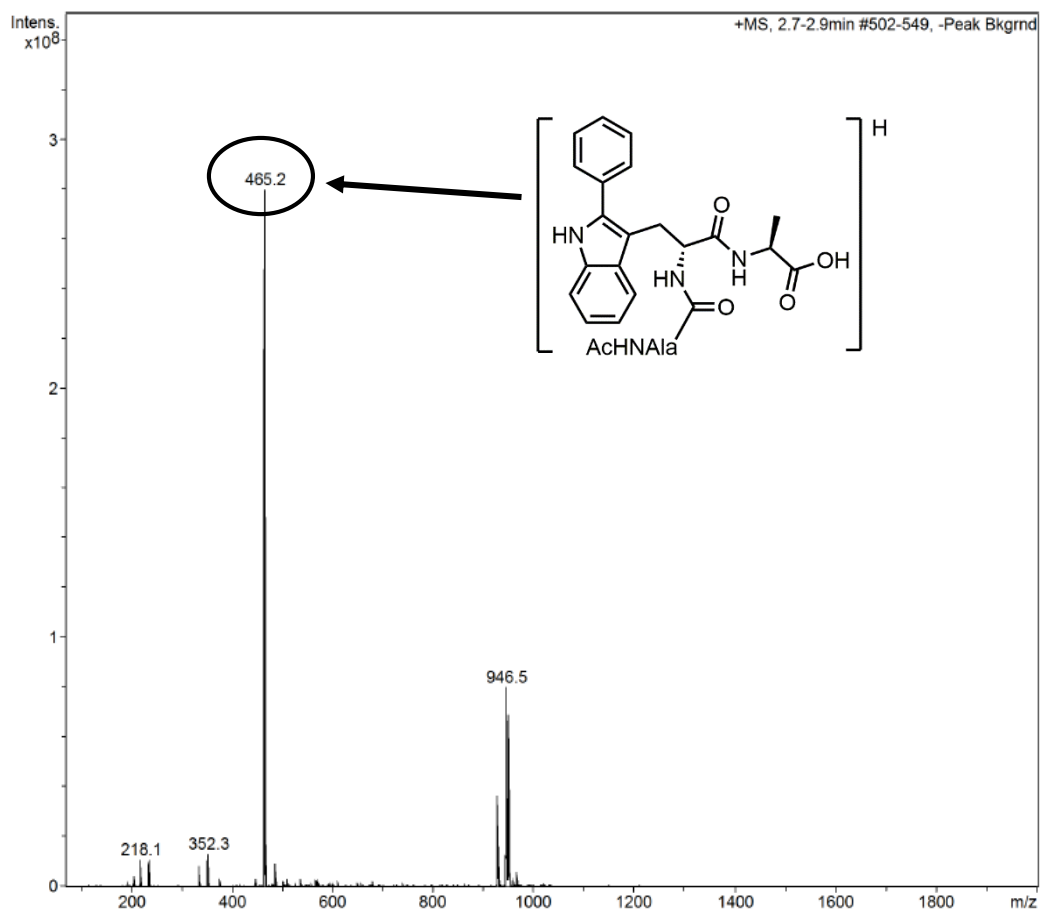
Figure 78 ESI–MS of arylation product **137**.
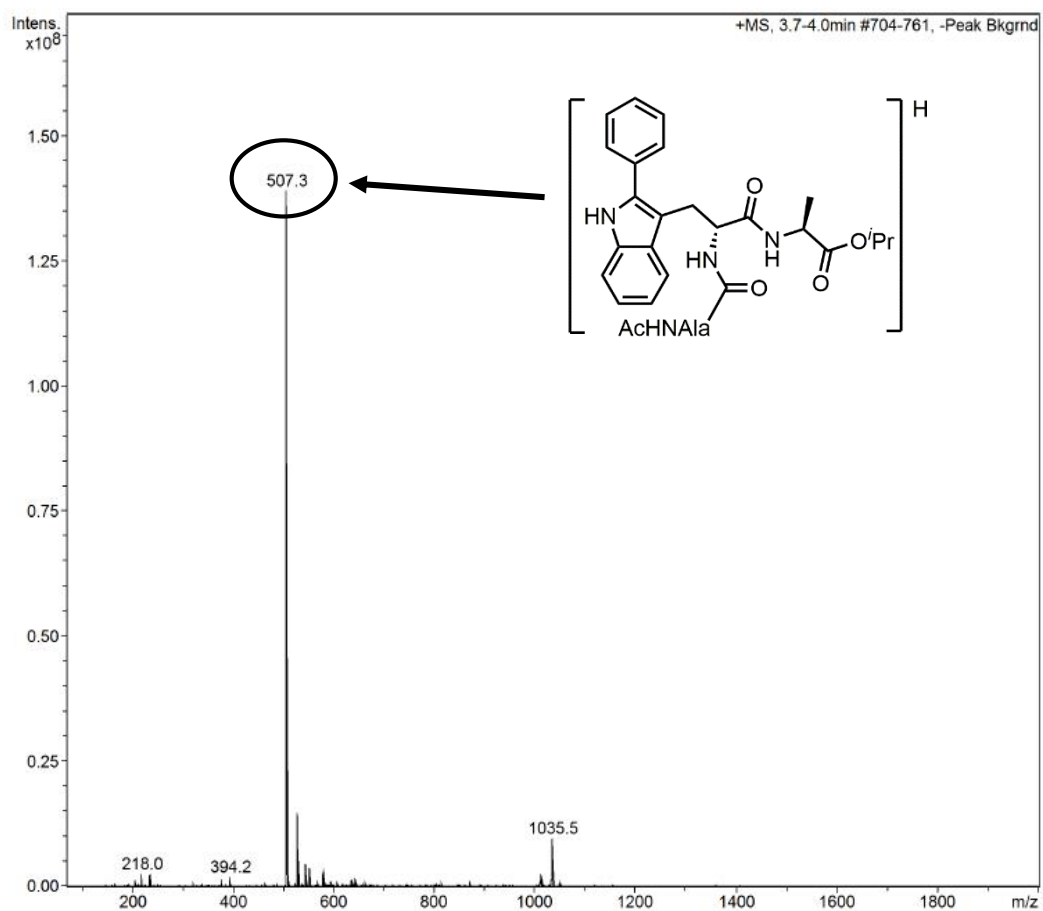
Figure 79 ESI–MS of *ⁱ*Pr-ester formed during workup from arylation product **137**.

Arylation Products of 138

Method A
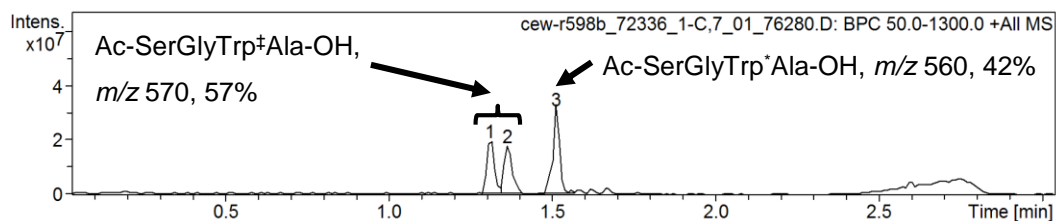
Figure 80 HPLC–ESI–MS chromatogram (BPC) of the crude reaction material (arylated tryptophan donated Trp*, dihydroxylated byproducts donated Trp‡).
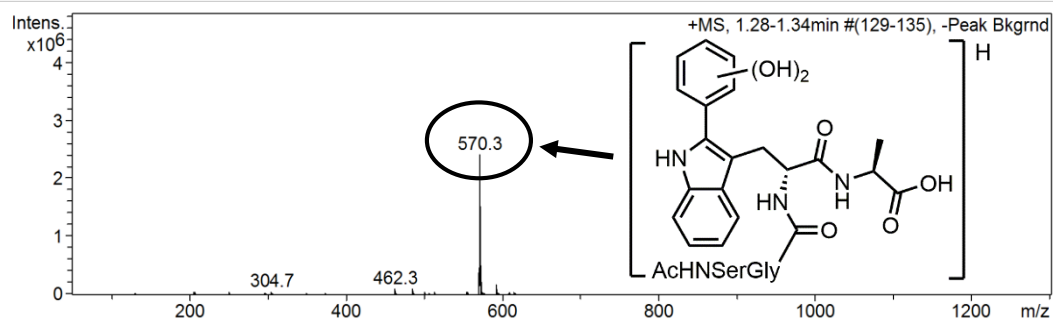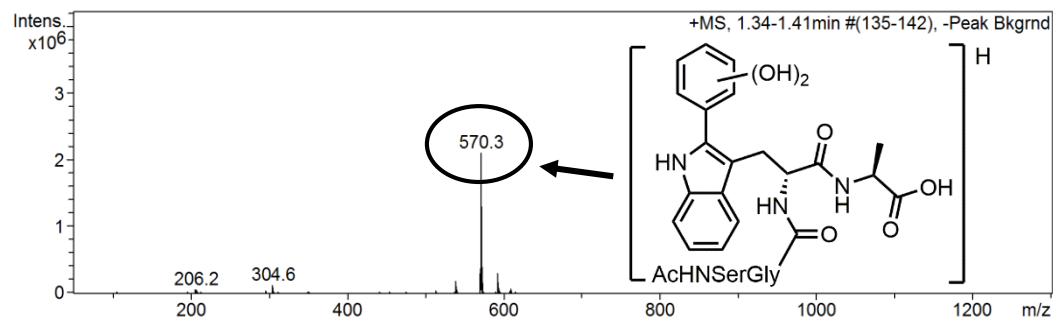
Figure 81 ESI–MS of dihydroxylated side products from arylation of **138**.
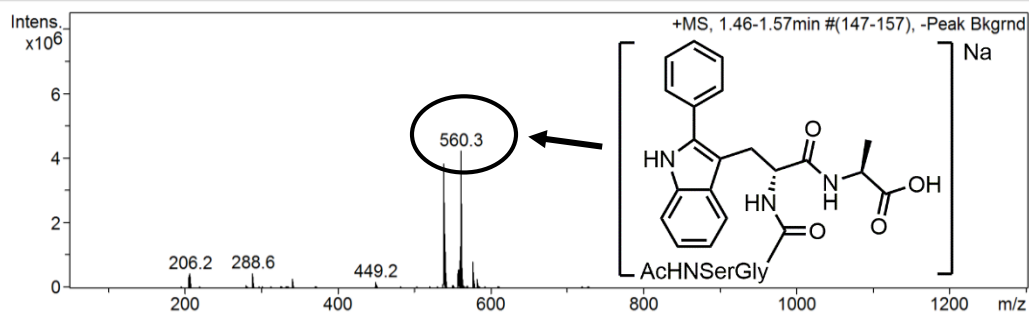
Figure 82 ESI–MS of arylation product **139**.

Method B
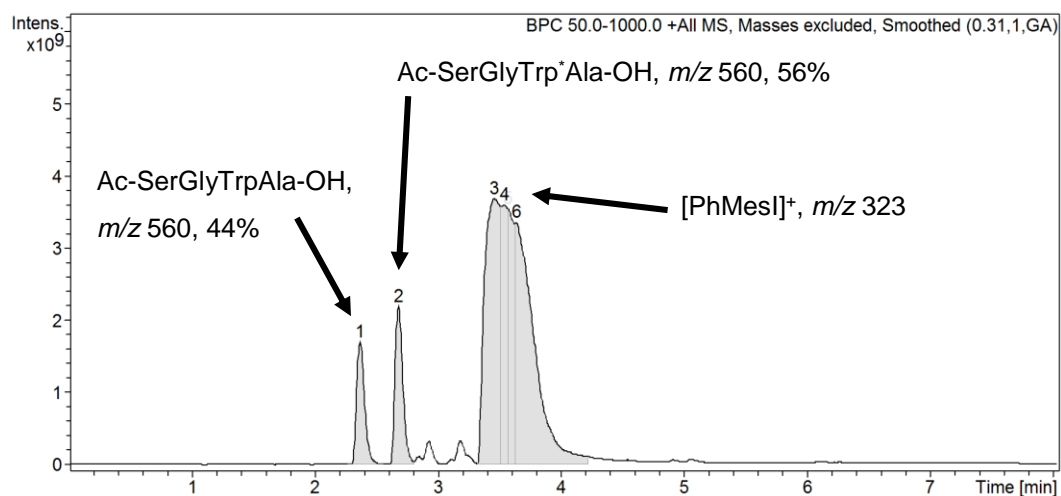
Figure 83 HPLC–ESI–MS chromatogram (BPC) of the crude reaction material (arylated tryptophan donated Trp*, starting material donated Trp).
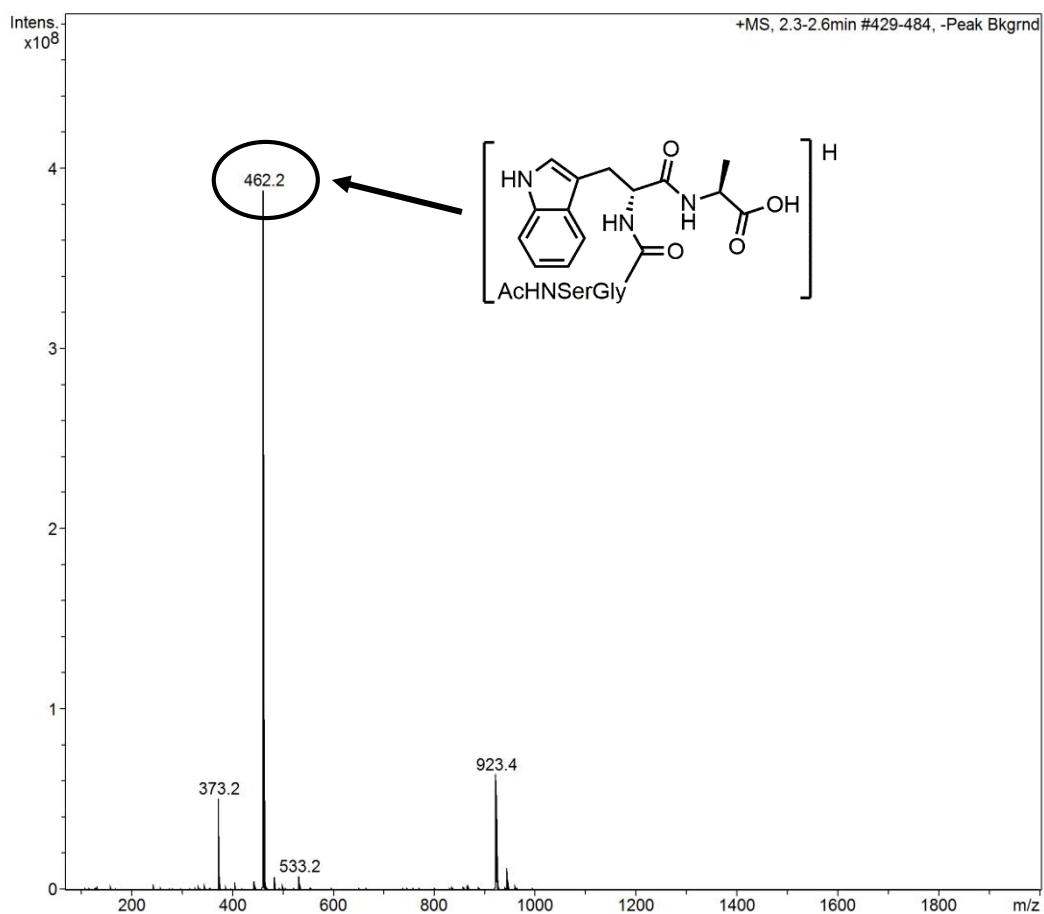
Figure 84 ESI–MS of starting material **138**.

Cmpd 2, 2.7 min
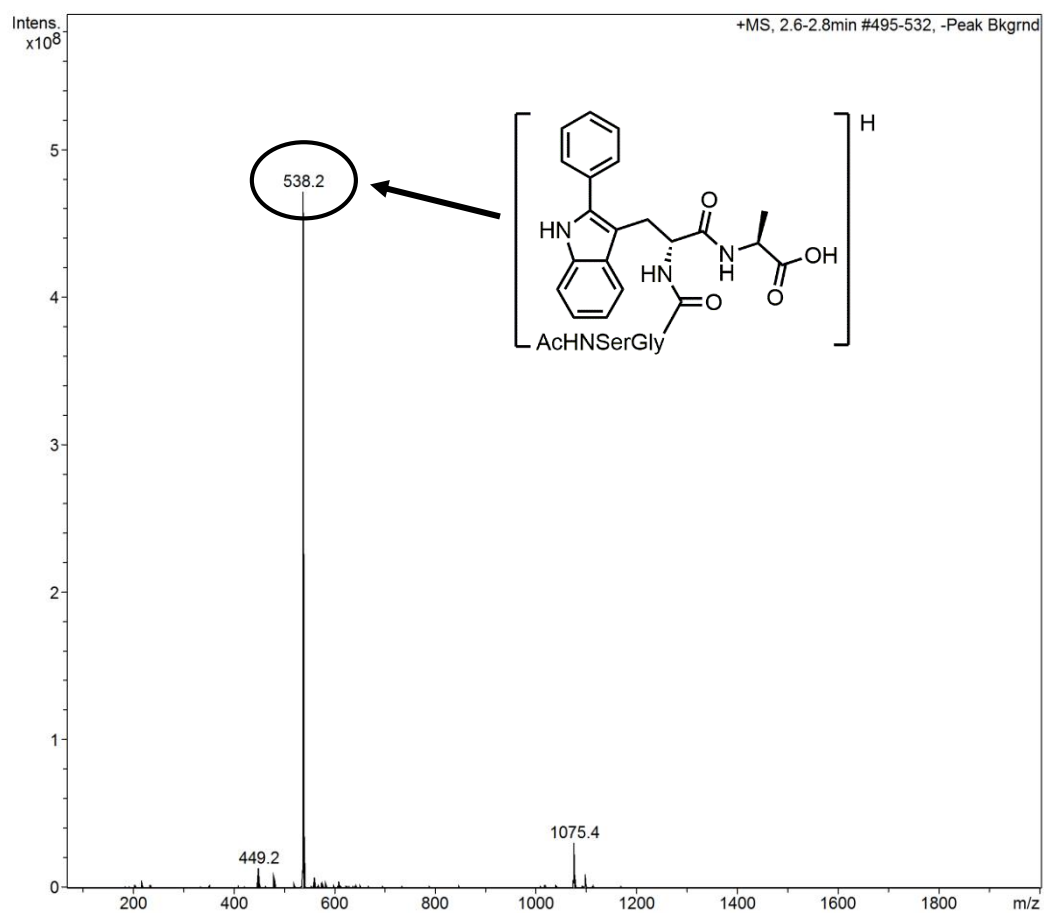
Figure 85 ESI–MS of arylation product **139**.

Cmpd 3, 3.5 min
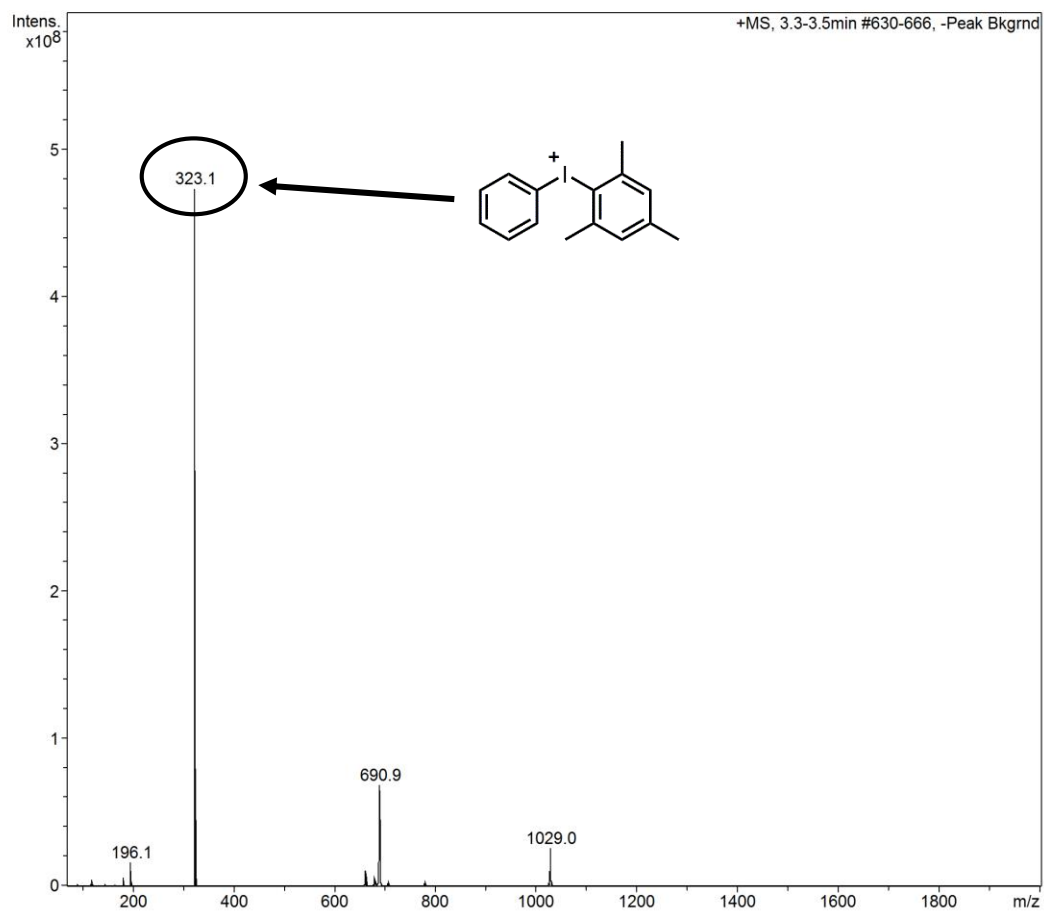
Figure 86 ESI–MS of starting material **140**.

Method C
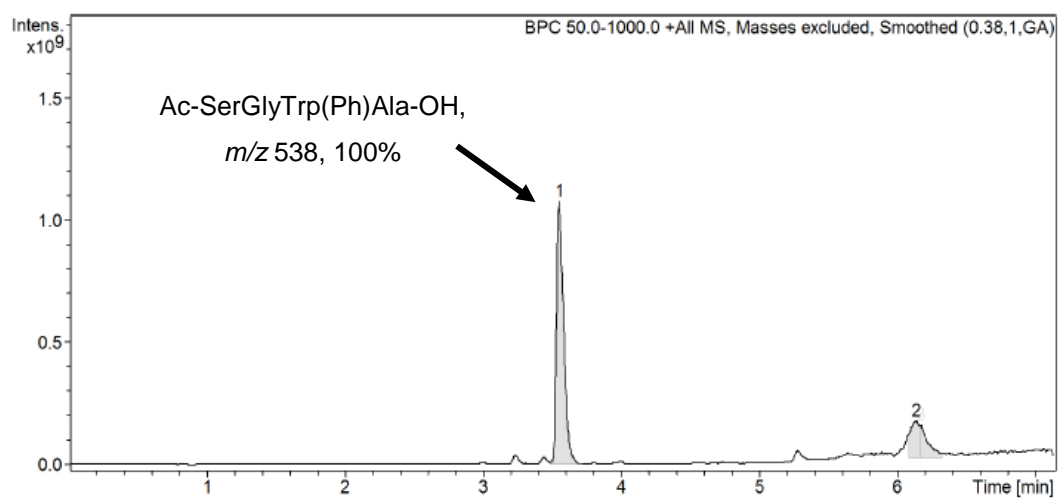
Figure 87 HPLC–ESI–MS chromatogram (BPC) of the crude reaction material.
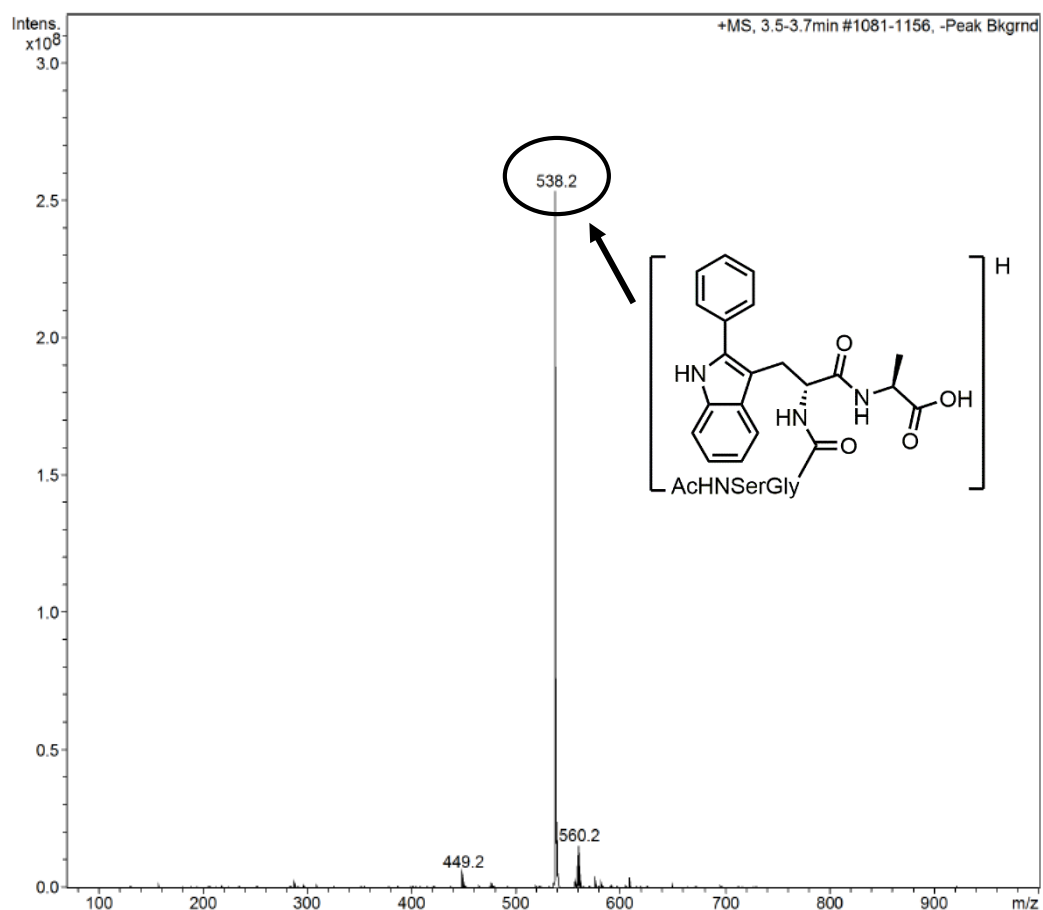
Figure 88 ESI–MS of arylation product **139**.

Appendix 5: GC Data

Calculations

Mesitylene Reference Solution

Maximum concentration of substrate in the reaction:

$$c_{max}\,(reaction) = \frac{0.6\,mmol}{3\,mL} = 0.2\,mmol\,mL^{-1}$$

For sampling a 30 uL aliquot is taken and diluted with 0.6 mL mesitylene standard. This gives a maximum substrate concentration in the GC sample of 0.0095 mmol mL⁻¹:

$$c_{max}\,(GC\,sample) = c_{max}\,(reaction) \cdot \frac{V\,(aliquot)}{V_{total}\,(GC\,sample)}$$

$$= 0.2\,mmol\,mL^{-1} \cdot \frac{0.03\,mL}{0.63\,mL} = 0.0096\,mmol\,mL^{-1}$$

0.6 mL of mesitylene reference solution should have the maximum substrate concentration:

$$n_{GC\,sample}(mesitylene) = c_{max}(GC\,sample) \cdot V_{total}(GC\,sample)$$

$$= 0.0095\,mmol\,mL^{-1} \cdot 0.63\,mL = 0.006\,mmol$$

$$V_{GC\,sample}(mesitylene) = \frac{M(mesitylene)}{\rho\,(mesitylene)} \cdot n(mesitylene)$$

$$= \frac{120.19\,g\,mol^{-1}}{0.8637\,g\,mL^{-1}} \cdot 0.006\,mmol = 0.835\,\mu L$$

$$V_{reference}(mesitylene) = \frac{V_{GC\,sample}(mesitylene)}{V_{mesitylene}(GC\,sample)} \cdot V(reference)$$

$$= \frac{0.835\,\mu L}{0.6\,mL} \cdot 100\,mL = 139\,\mu L$$

Calibration Solutions

Five solutions used at 100%, 80%, 60%, 40% and 20% concentrations of c_{max}(substrate). All solutions contain c(mesitylene) = 100% c_{max}(substrate), with V_{total} = 1 mL

Calculation of Conversion from Peak Area

To calculate the substrate concentration in the GC sample:

$$c(substrate) = \frac{^{av. \; peak \; area \; (substrate)}/_{av.peak \; are \; (standard)}}{RRF \; (substrate)} \cdot c(mesitylene)$$

To calculate the substrate concentration in the reaction solution:

$$c(substrate) = c_{GC \; sample}(substrate)$$

$$\cdot \frac{V_{total} \; (GC \; sample) \cdot \; ^{V_{total} \; (reaction)}/_{V_{GC \; sample} \; (substrate)}}{V_{total}(reaction)}$$

To convert substrate concentration into conversion:

$$n(substrate)\% = \frac{c_{reaction} \; (substrate)}{c_{max} \; (reaction)}$$

Calculation of Error

The maximum possible error is always accounted for. This is based on the maximum ratio of peak areas for three injections, as well as the standard error of the slope from the calibration curve:

$$c_{GC \; sample}(substrate)_{max}$$

$$= \frac{\max \left(^{peak \; area \; (substrate)}/_{peak \; area \; (standard)} \right)}{slope \; (RRF) \cdot (1 - standard \; error)}$$

$$\cdot \; c_{GC \; sample}(substrate)$$

Calibrations
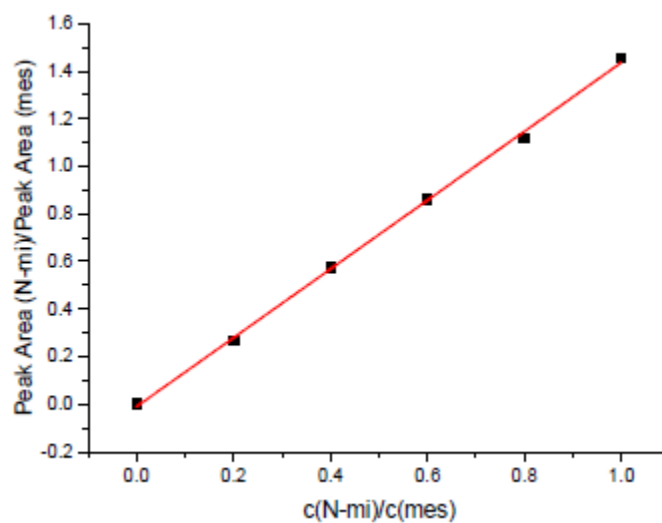
Equation	y = a + b*x		
Weight	No Weighting		
Residual Sum of Squares	0.00128		
Pearson's r	0.99956		
Adj. R-Square	0.99891		
		Value	Stand.Error
Peak Area	Intercept	-0.0098	0.01296
	Slope	**1.44528**	**0.0214**

Figure 89 Calibration plot to determine RRF for 1-methylindole **33**.
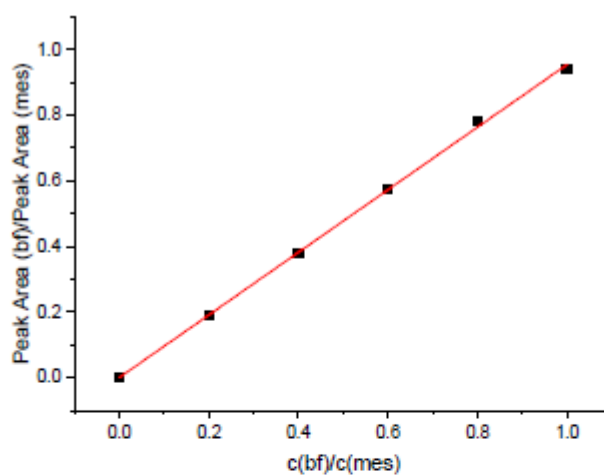
Equation	y = a + b*x	
Weight	No Weighting	
Residual Sum of Squares	4.03236E-4	
Pearson's r	0.99968	
Adj. R-Square	0.99921	
	Value	Stand.Error
	Intercept	-3.9E-4	0.00727
Peak Area	Slope	**0.95548**	**0.012**

Figure 90 Calibration plot to determine RRF for benzofuran **239**.
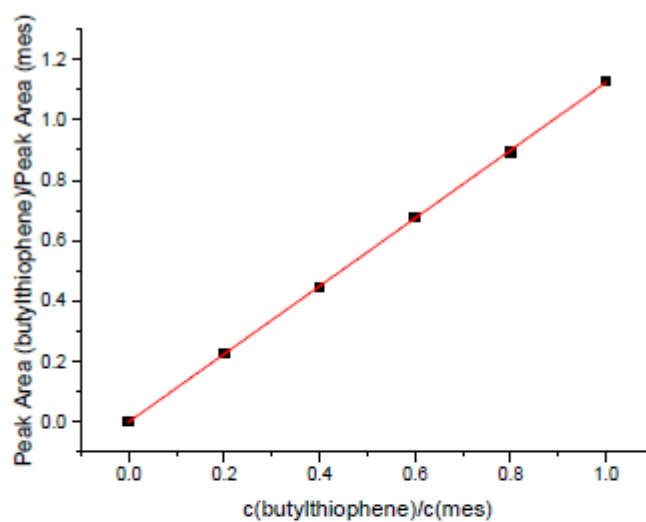
Equation	y = a + b*x		
Weight	No Weighting		
Residual Sum of Squares	7.47595E-5		
Pearson's r	0.99996		
Adj. R-Square	0.99989		
		Value	Stand.Error
Peak Area	Intercept	-7.77E-	0.00313
	Slope	**1.12519**	**0.00517**

Figure 91 Calibration plot to determine RRF for butylthiophene **241**.
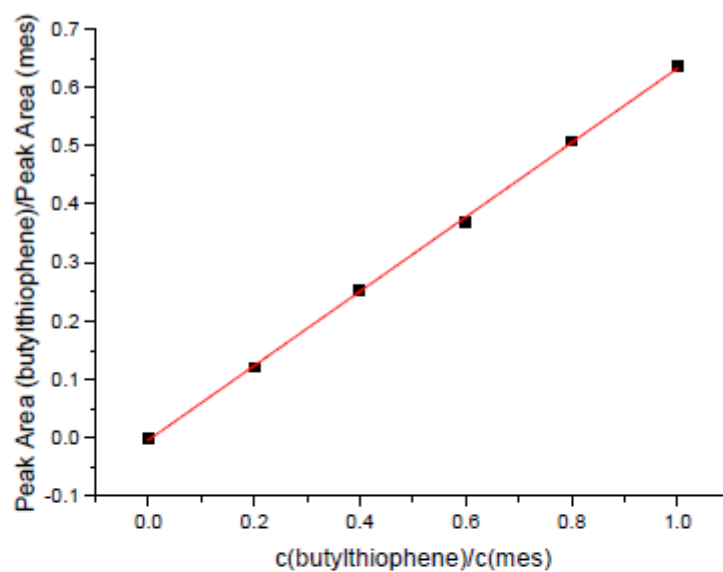
Equation	y = a + b*x	
Weight	No Weighting	
Residual Sum of Squares	1.24132E-4	
Pearson's r	0.99978	
Adj. R-Square	0.99945	
		Value	Stand.Error
Peak Area	Intercept	-0.0038	0.00403
	Slope	**0.63618**	**0.00666**

Figure 92 Calibration plot to determine RRF for butylfuran **243**.

Line Fitting
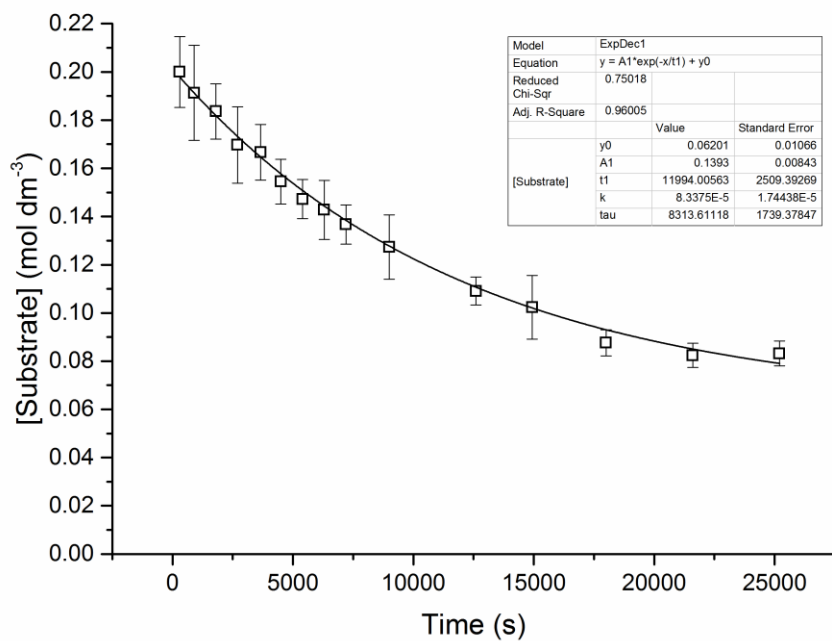
Figure 93 1st order exponential decay for arylation of 1-methylindole **33** with Pd/C.
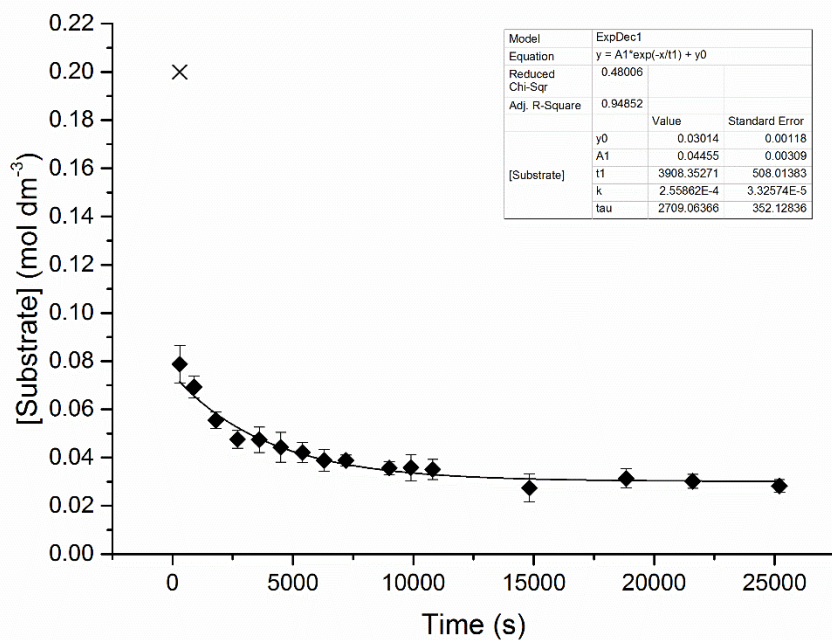
Figure 94 1st order exponential decay for arylation of 1-methylindole **33** with PVP–Pd **13**.

Model	ExpDec1	
Equation	y = A1*exp(-x/t1) + y0	
Reduced Chi-Sqr	0.09419	
Adj. R-Square	0.98299	
	Value	Standard Error
y0	0.10672	0.00348
A1	0.07681	0.00298
[Substrate] t1	10118.96592	1249.36258
k	9.88243E-5	1.22016E-5
tau	7013.9327	865.99215
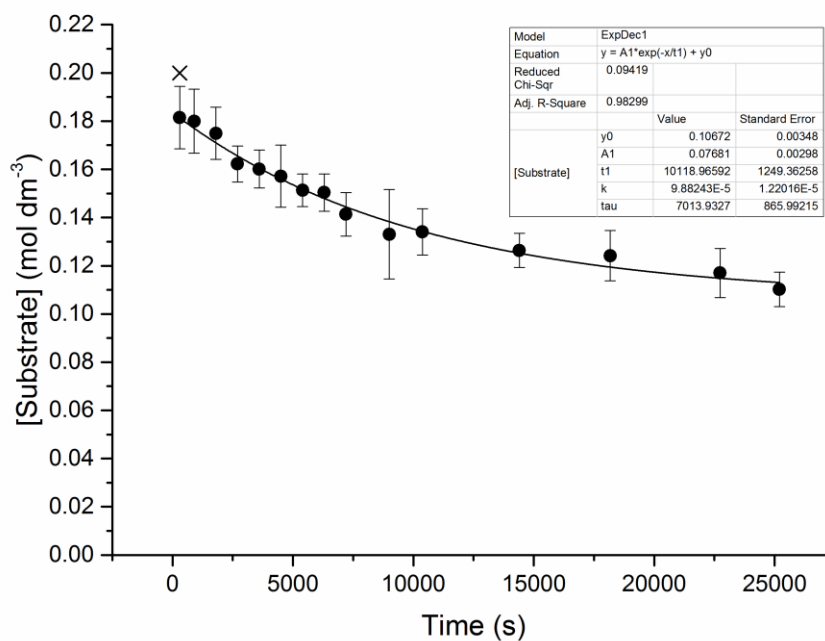
Figure 95 1st order exponential decay for arylation of 1-methylindole **33** with Pd(OAc)$_2$.

Model	ExpDec1	
Equation	y = A1*exp(-x/t1) + y0	
Reduced Chi-Sqr	1.40033	
Adj. R-Square	0.97687	
	Value	Standard Error
y0	0.06012	0.00396
A1	0.09407	0.00383
[Substrate] t1	9138.24228	1085.14397
k	1.0943E-4	1.29946E-5
tau	6334.14687	752.16449
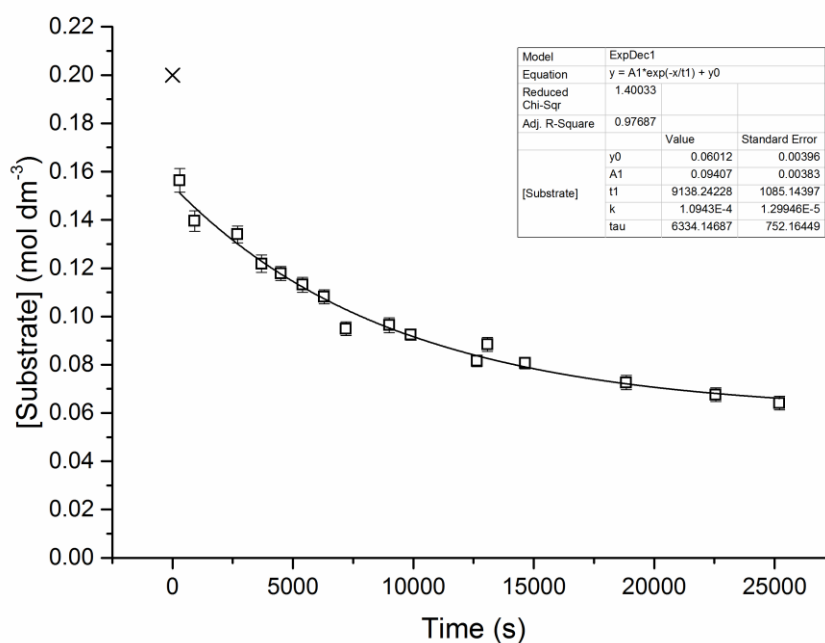
Figure 96 1st order exponential decay for arylation of benzofuran **239** with Pd/C.

311

Model	ExpDec1	
Equation	y = A1*exp(-x/t1) + y0	
Reduced Chi-Sqr	10.99631	
Adj. R-Square	0.98107	
	Value	Standard Error
y0	-0.2772	0.4116
A1	0.41323	0.40874
[Substrate] t1	95113.28663	109849.50235
k	1.05138E-5	1.21427E-5
tau	65927.50646	76141.87282
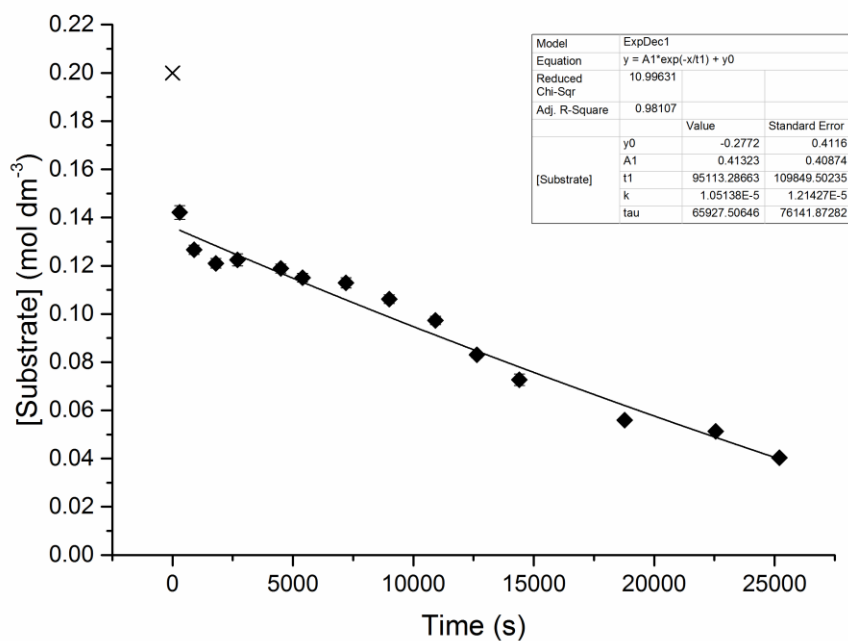
Figure 97 Exponential decay suggesting non-1st order kinetic profile for arylation of benzofuran **239** with PVP–Pd **13**.

Model	ExpDec1	
Equation	y = A1*exp(-x/t1) + y0	
Reduced Chi-Sqr	0.40485	
Adj. R-Square	0.98046	
	Value	Standard Error
y0	0.06523	0.00435
A1	0.12685	0.00472
[Substrate] t1	22324.56417	1873.29729
k	4.47937E-5	3.75873E-6
tau	15474.20871	1298.47074
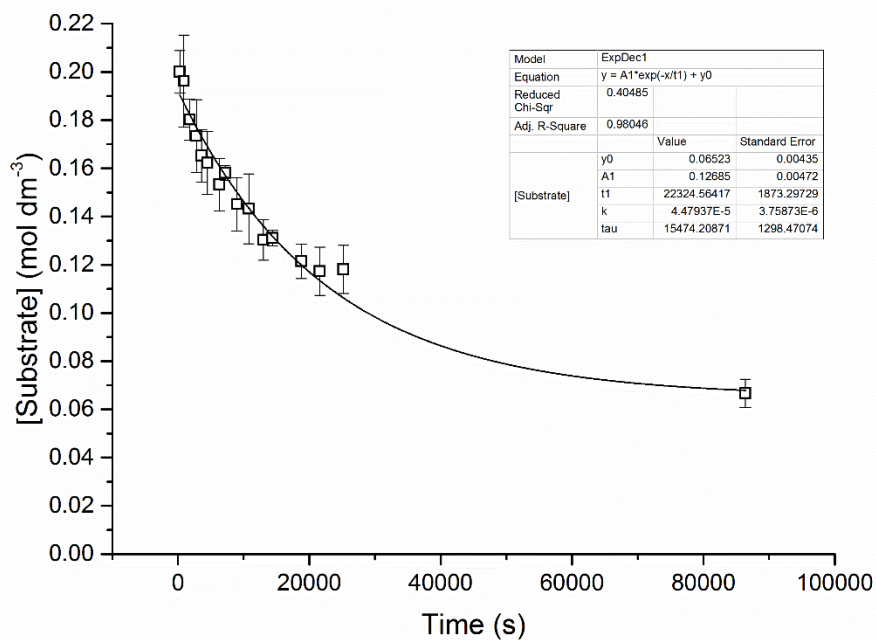
Figure 98 1st order exponential decay for arylation of butylthiophene **241** with Pd/C.

Model	ExpDec1	
Equation	y = A1*exp(-x/t1) + y0	
Reduced Chi-Sqr	6.43919	
Adj. R-Square	0.99625	
	Value	Standard Error
y0	-0.20069	0.15175
A1	0.36179	0.14969
[Substrate] t1	187799.47357	102143.53162
k	5.32483E-6	2.89616E-6
tau	130172.67562	70800.50095
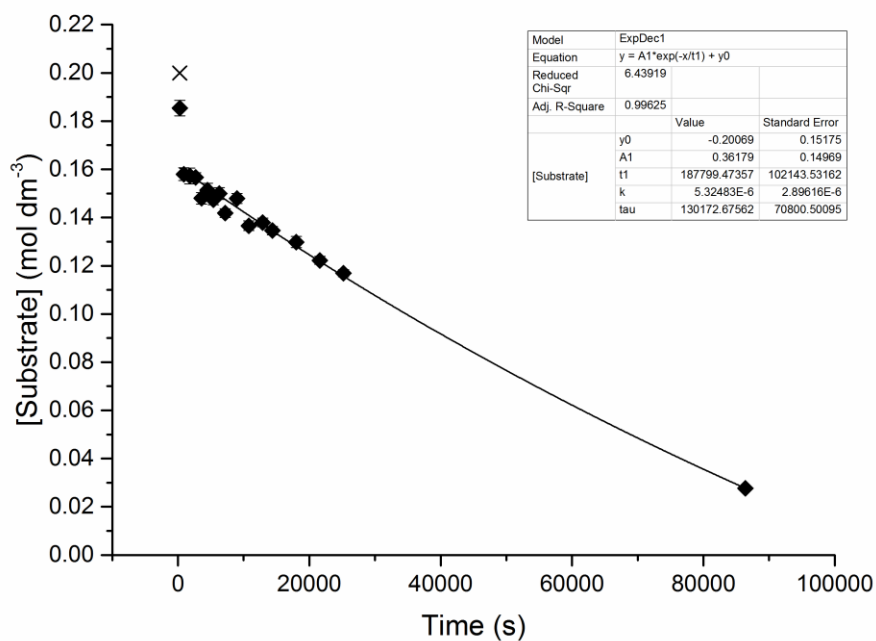
Figure 99 Exponential decay suggesting non-1st order kinetic profile for arylation of butylthiophene **241** with PVP–Pd **13**.

Model	ExpDec1	
Equation	y = A1*exp(-x/t1) + y0	
Reduced Chi-Sqr	2.92053	
Adj. R-Square	0.99036	
	Value	Standard Error
y0	-0.29133	0.31567
A1	0.43998	0.31427
[Substrate] t1	339098.69049	279012.65012
k	2.94899E-6	2.42645E-6
tau	235045.30125	193396.83177
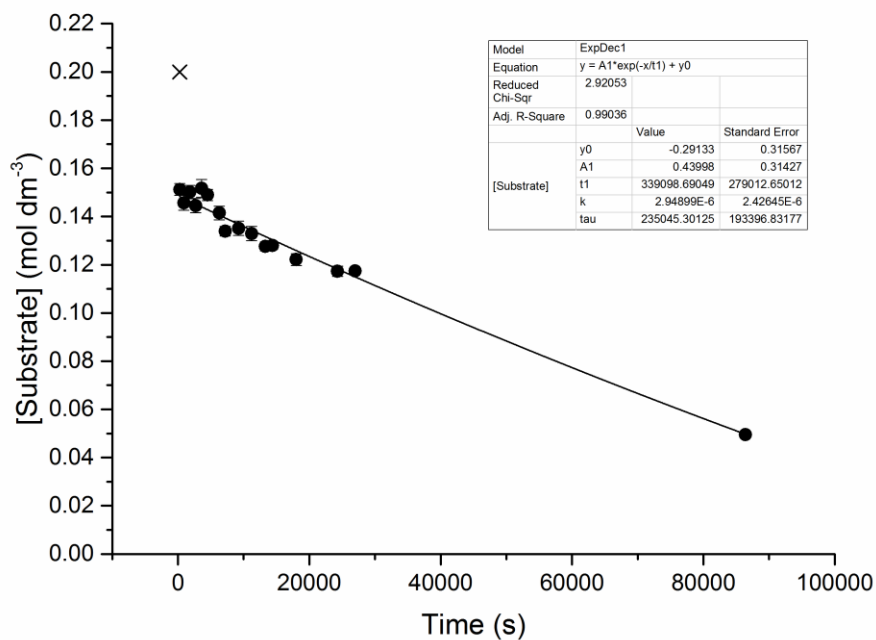
Figure 100 Exponential decay suggesting non-1st order kinetic profile for arylation of butylthiophene **241** with Pd(OAc)$_2$.

313
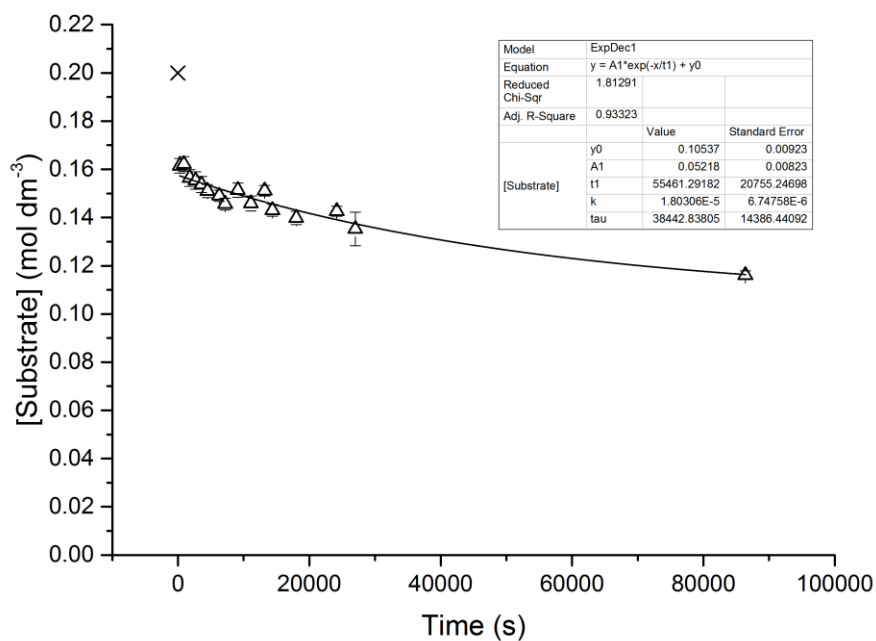
Figure 101 1st order exponential decay for arylation of butylthiophene **241** with Pd$_2$(dba)$_3$ **238**.
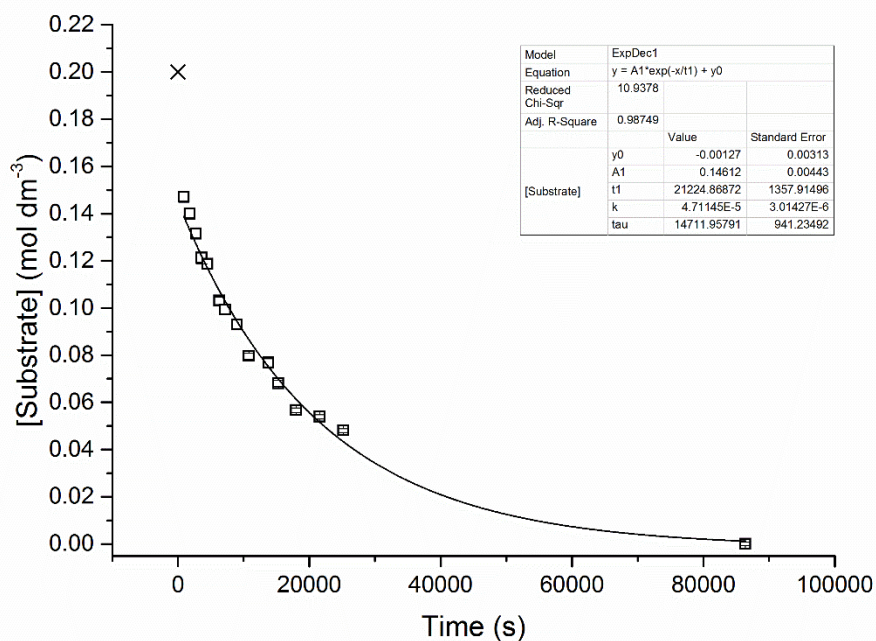
Figure 102 1st order exponential decay for arylation of butylfuran **243** with Pd/C.

Model	ExpDec1	
Equation	y = A1*exp(-x/t1) + y0	
Reduced Chi-Sqr	21.53669	
Adj. R-Square	0.97835	
	Value	Standard Error
y0	0.00817	0.00402
A1	0.15395	0.00592
[Substrate] t1	17732.59818	1370.95404
k	5.63933E-5	4.35992E-6
tau	12291.30043	950.27293
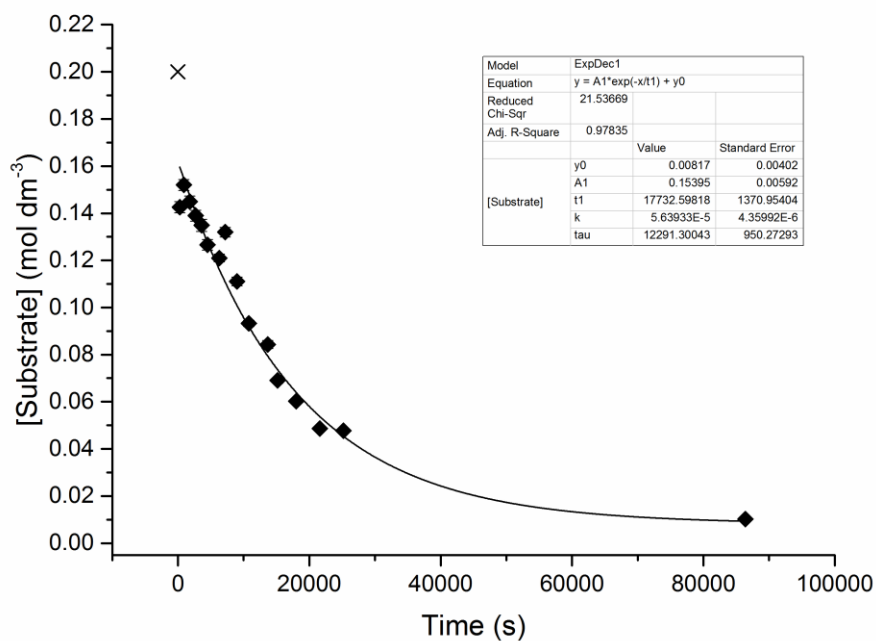
Figure 103 1st order exponential decay for arylation of butylfuran **243** with PVP–Pd **13**.

Model	ExpDec1	
Equation	y = A1*exp(-x/t1) + y0	
Reduced Chi-Sqr	6.26723	
Adj. R-Square	0.96461	
	Value	Standard Error
y0	0.06192	0.00569
A1	0.07253	0.00479
[Substrate] t1	38003.32805	9018.91388
k	2.63135E-5	6.24469E-6
tau	26341.89969	6251.43472
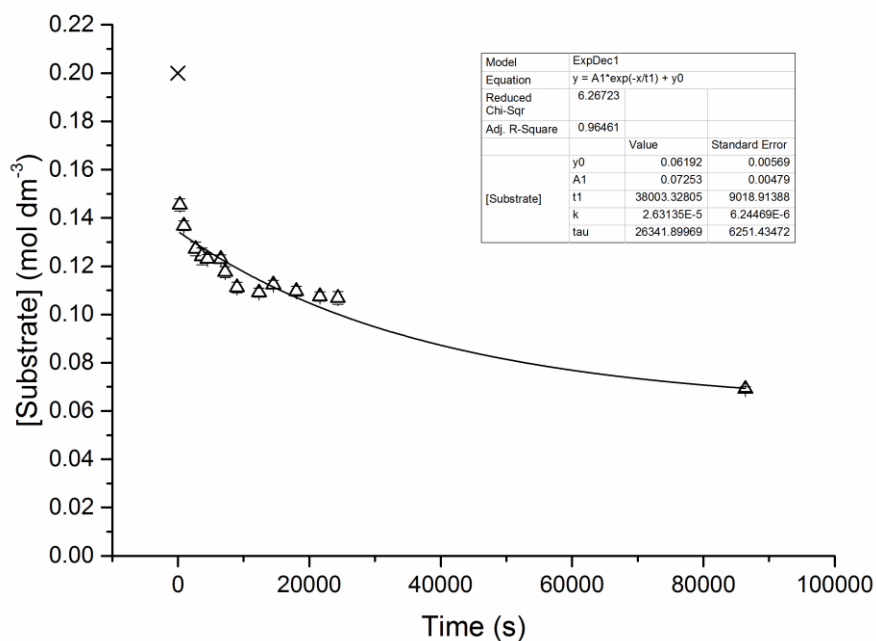
Figure 104 1st order exponential decay for arylation of butylfuran **243** with $Pd_2(dba)_3$ **238**.

Model	ExpDec1		
Equation	y = A1*exp(-x/t1) + y0		
Reduced Chi-Sqr	4.61548		
Adj. R-Square	0.98147		
		Value	Standard Error
	y0	0.0079	0.00335
	A1	0.12918	0.00453
Concentration	t1	8367.7427	795.70152
	k	1.19507E-4	1.13641E-5
	tau	5800.07726	551.53827
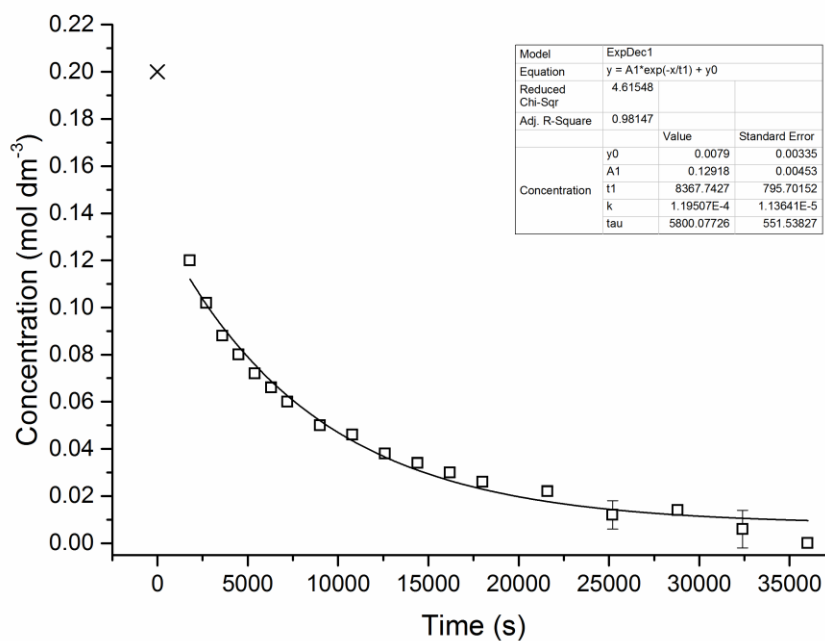
Figure 105 1st order exponential decay for arylation of butylfuran **243** with Pd/C at 70 °C.

Model	Logistic		
Equation	y = A2 + (A1-A2)/(1 + (x/x0)^p)		
Reduced Chi-Sqr	1.04557E-6		
Adj. R-Square	0.99841		
		Value	Standard Error
	A1	-3.4215	25.03511
	A2	0.20978	0.00356
	x0	16.24531	167.8137
Concentration	p	0.74567	0.13739
	EC20	2.53115	27.0031
	EC50	16.24531	167.8137
	EC80	104.26475	1041.80789
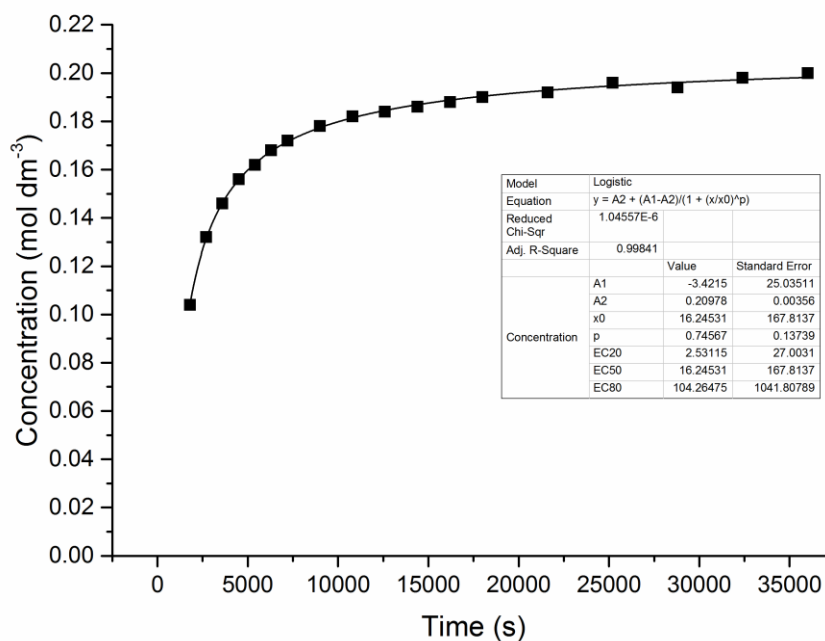
Figure 106 1st order logarithmic growth for 2-phenylbutylfuran **246** from reaction of butylfuran with Pd/C at 70 °C.

316

Appendix 6: ESI–MS Data for Pd$_x$(dba)$_y$ Clusters
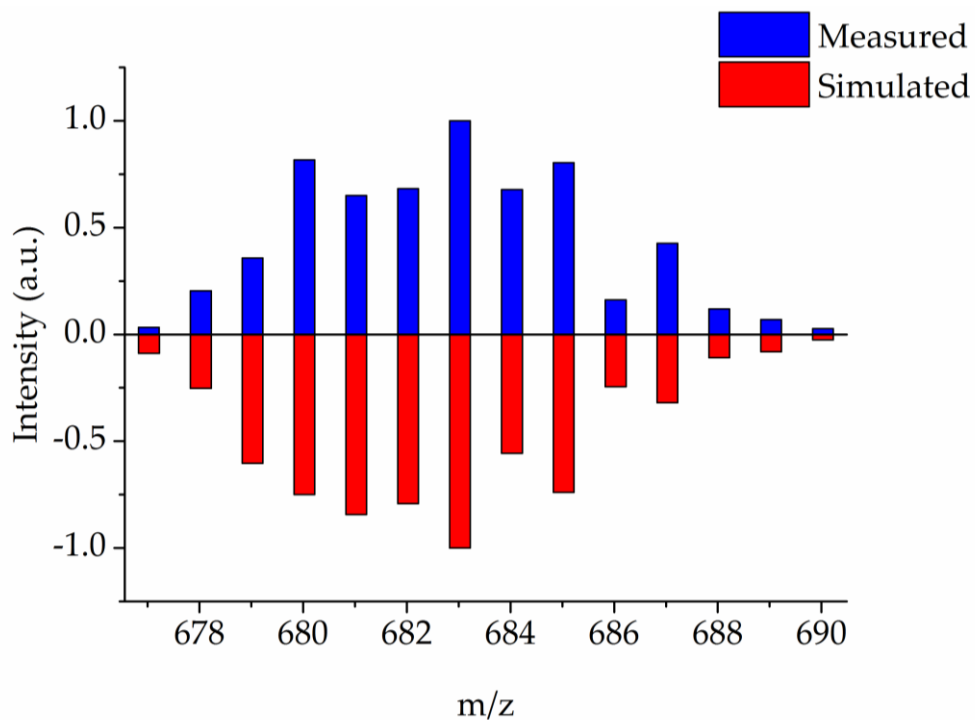
Figure 107 Measured vs. simulated mass values for [Pd$_2$(dba)$_2$H]$^+$ cluster.
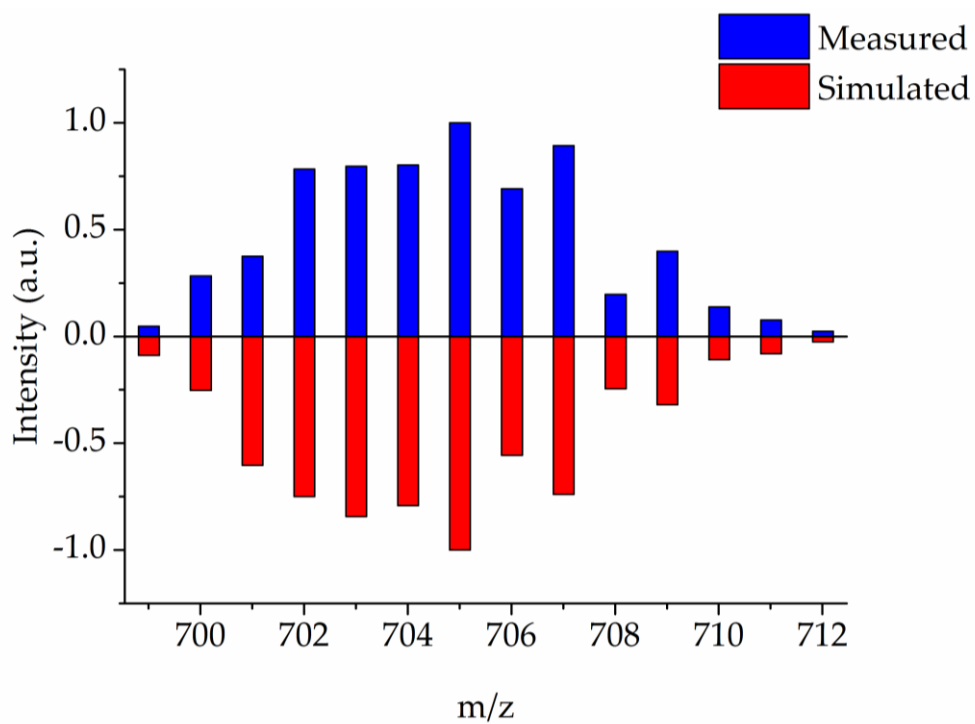
Figure 108 Measured vs. simulated mass values for [Pd$_2$(dba)$_2$Na]$^+$ cluster.
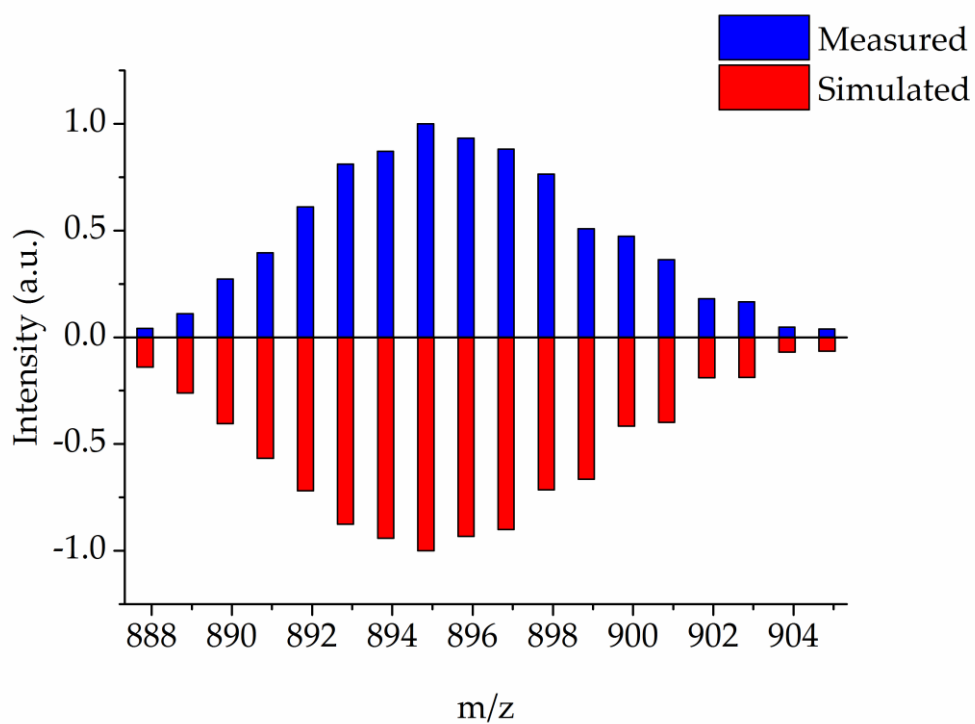
Figure 109 Measured vs. simulated mass values for [Pd$_4$(dba)$_2$H]$^+$ cluster.
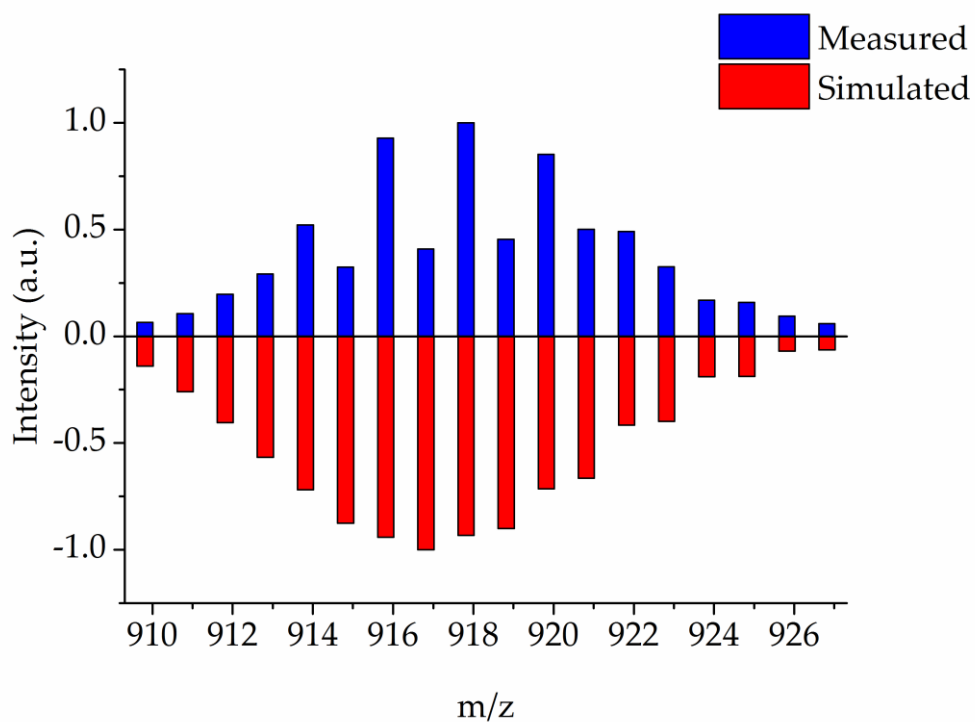
Figure 110 Measured vs. simulated mass values for [Pd$_4$(dba)$_2$Na]$^+$ cluster.
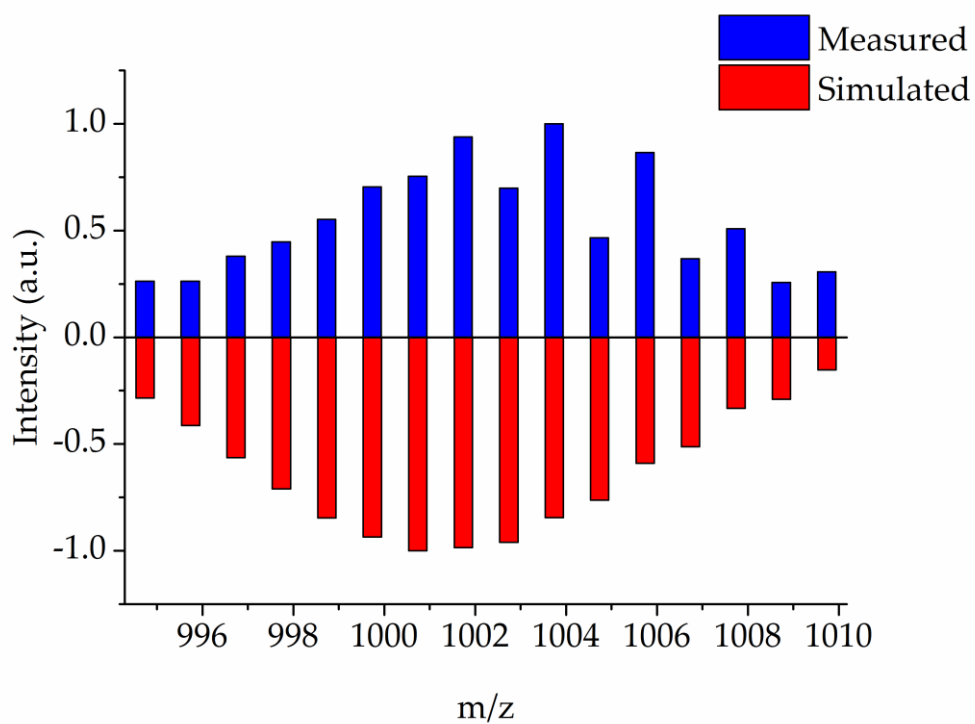
Figure 111 Measured vs. simulated mass values for [Pd$_5$(dba)$_2$H]$^+$ cluster.
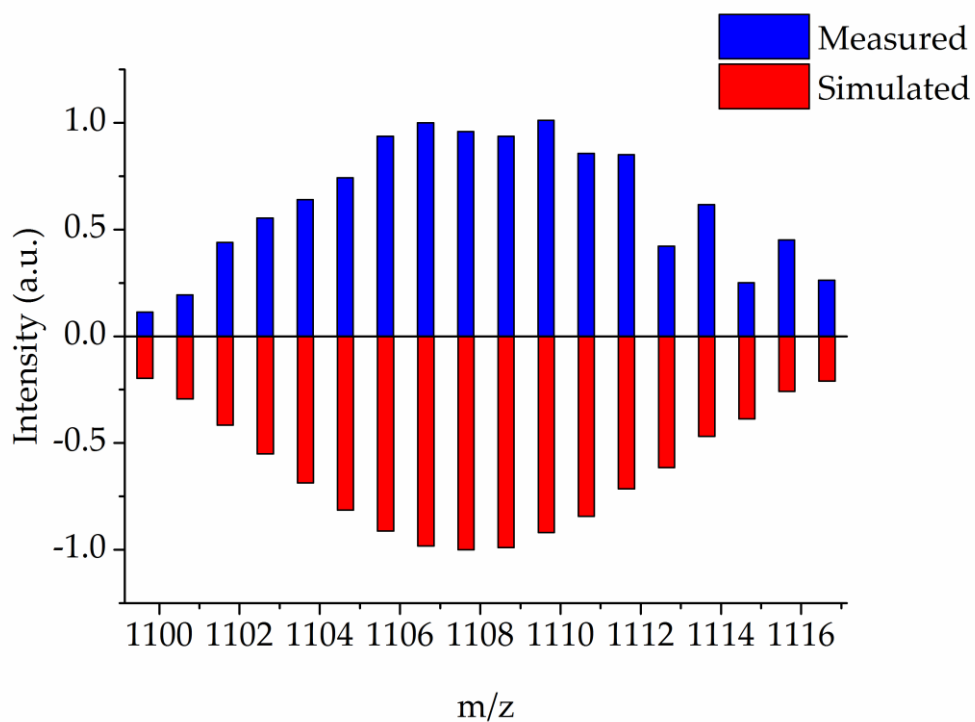
Figure 112 Measured vs. simulated mass values for [Pd$_6$(dba)$_2$H]$^+$ cluster.
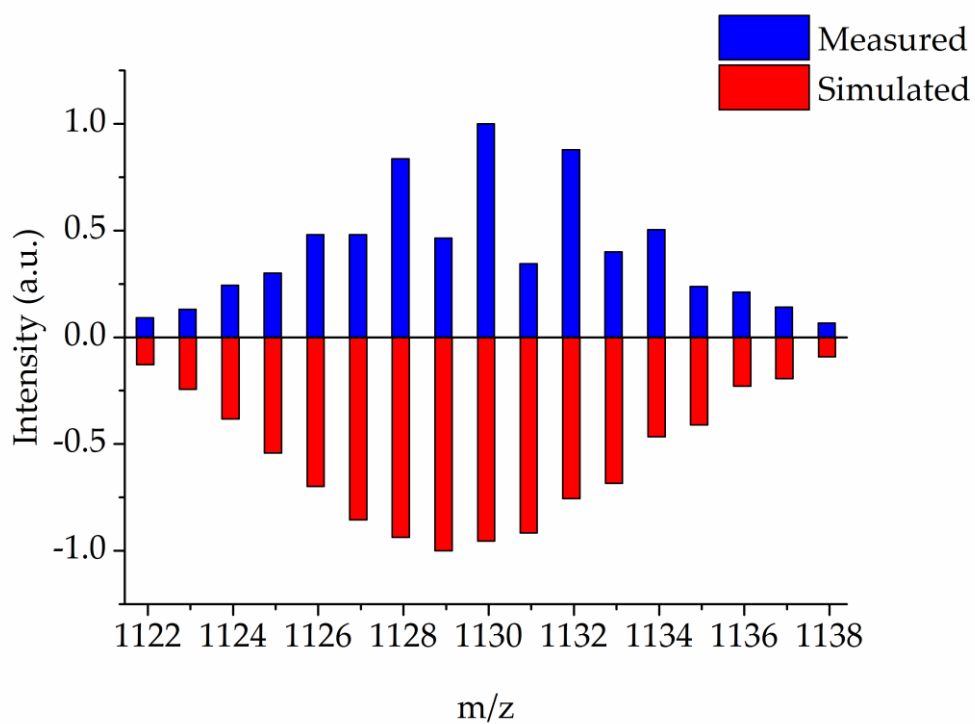
Figure 113 Measured vs. simulated mass values for [Pd$_4$(dba)$_3$H]$^+$ cluster.
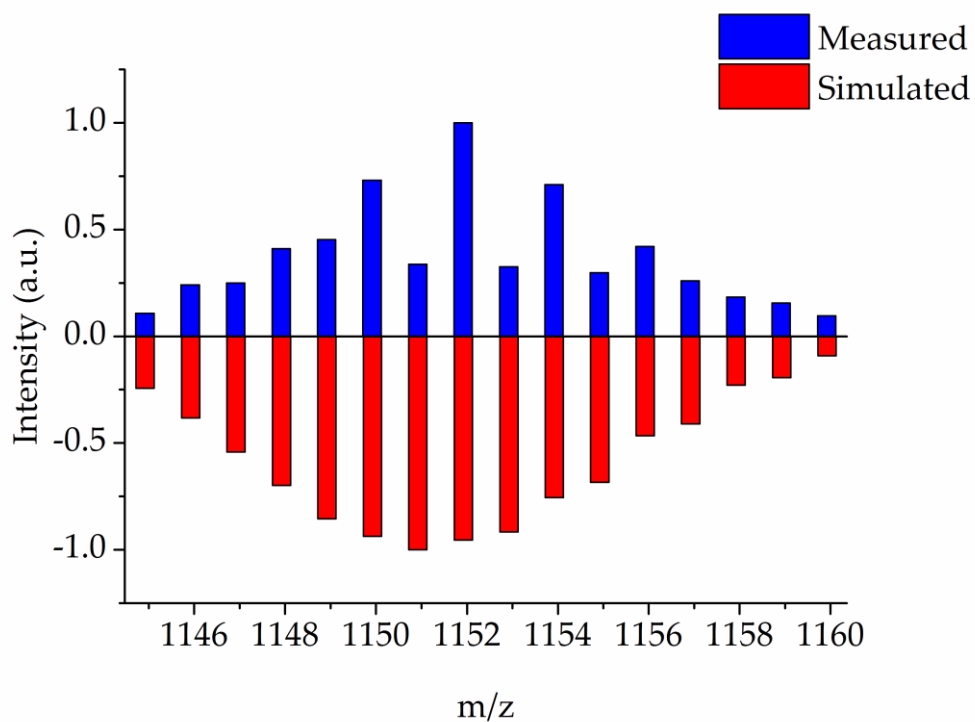
Figure 114 Measured vs. simulated mass values for [Pd$_4$(dba)$_3$Na]$^+$ cluster.
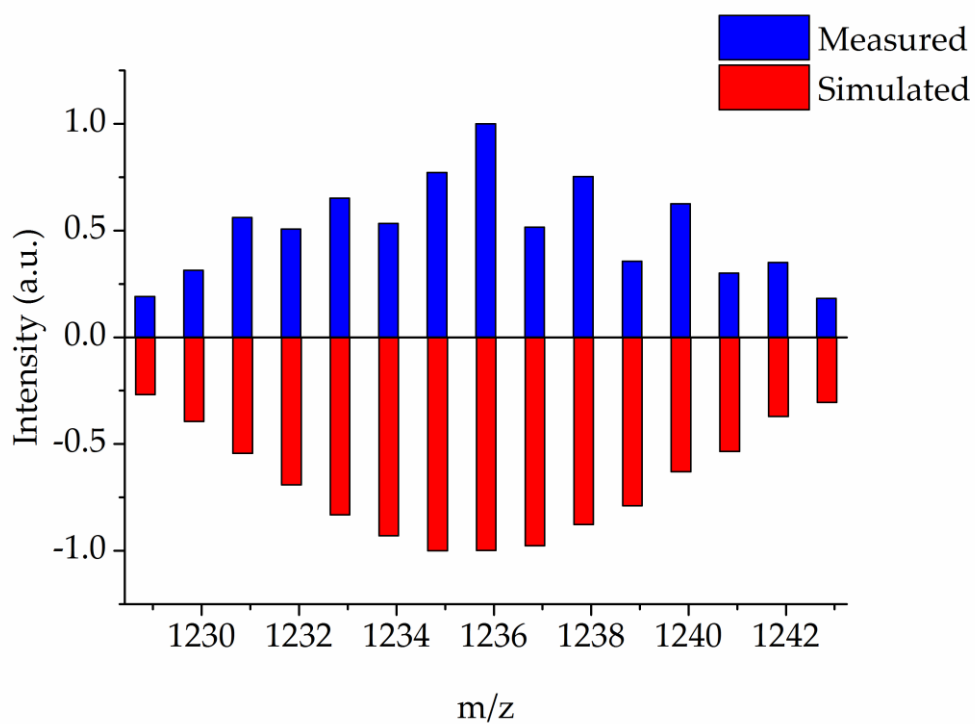
Figure 115 Measured vs. simulated mass values for $[Pd_5(dba)_3H]^+$ cluster.
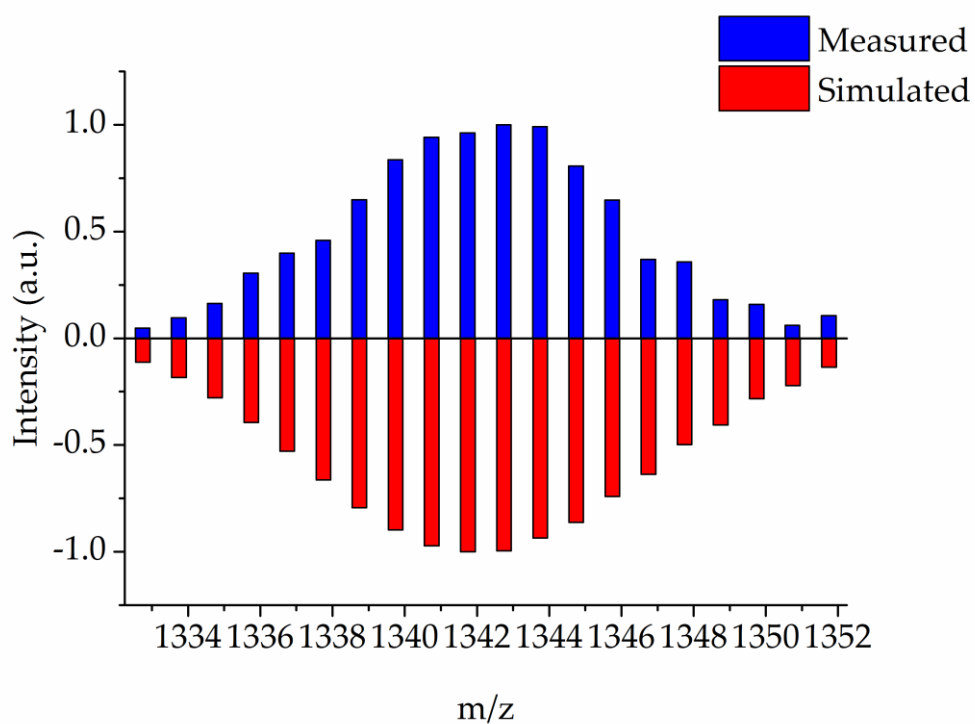
Figure 116 Measured vs. simulated mass values for $[Pd_6(dba)_3H]^+$ cluster.
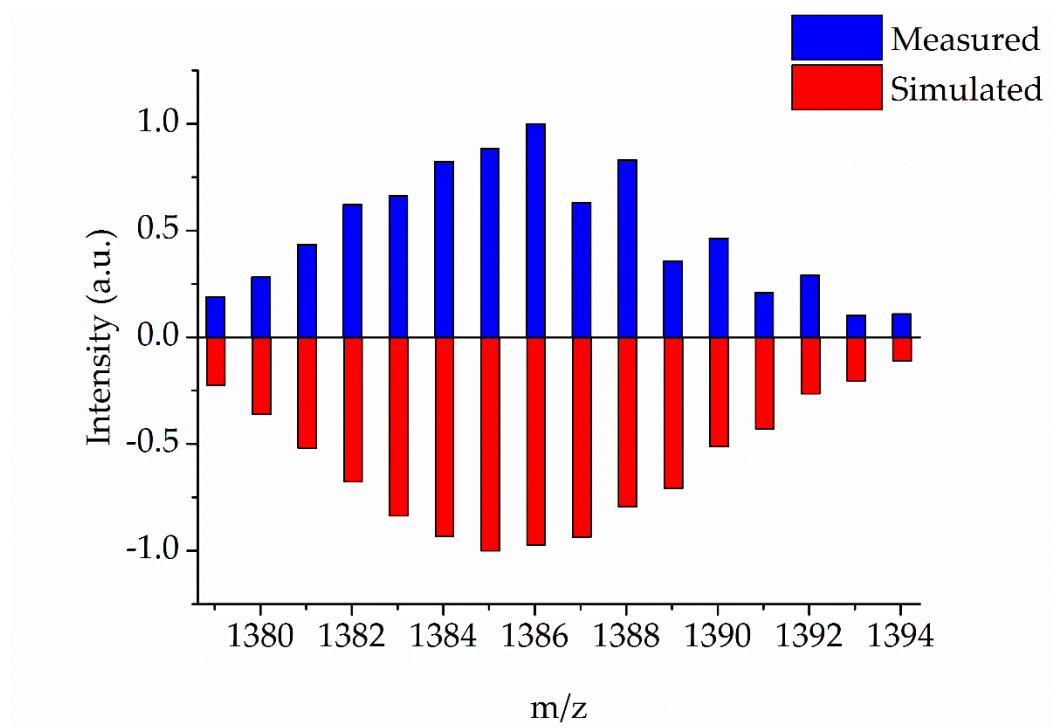
Figure 117 Measured vs. simulated mass values for [Pd$_4$(dba)$_4$Na]$^+$ cluster.
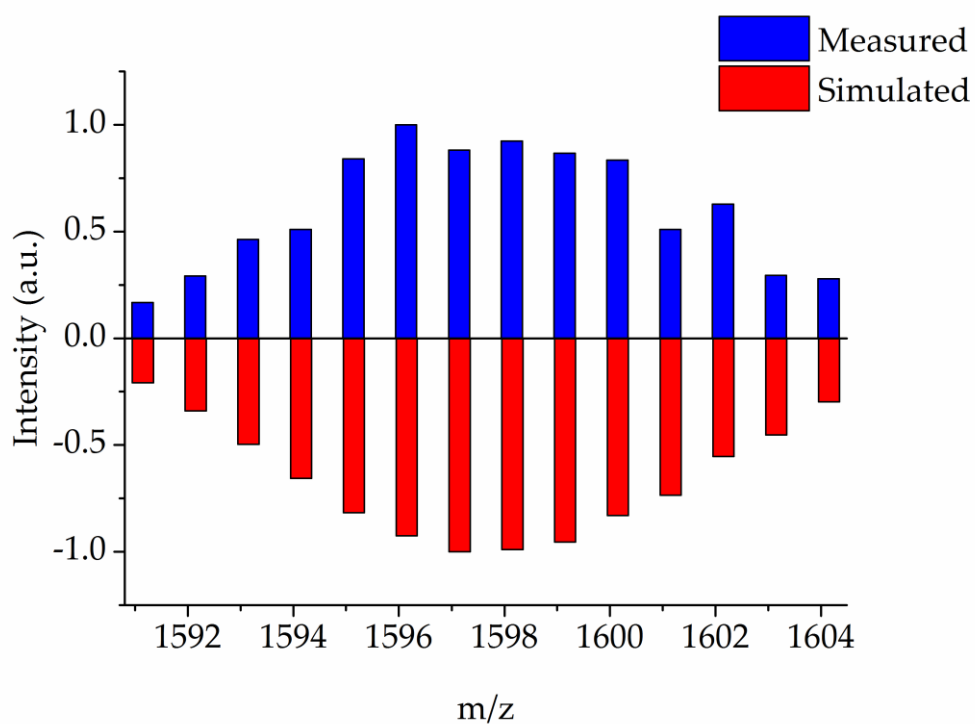
Figure 118 Measured vs. simulated mass values for [Pd$_4$(dba)$_5$H]$^+$ cluster.
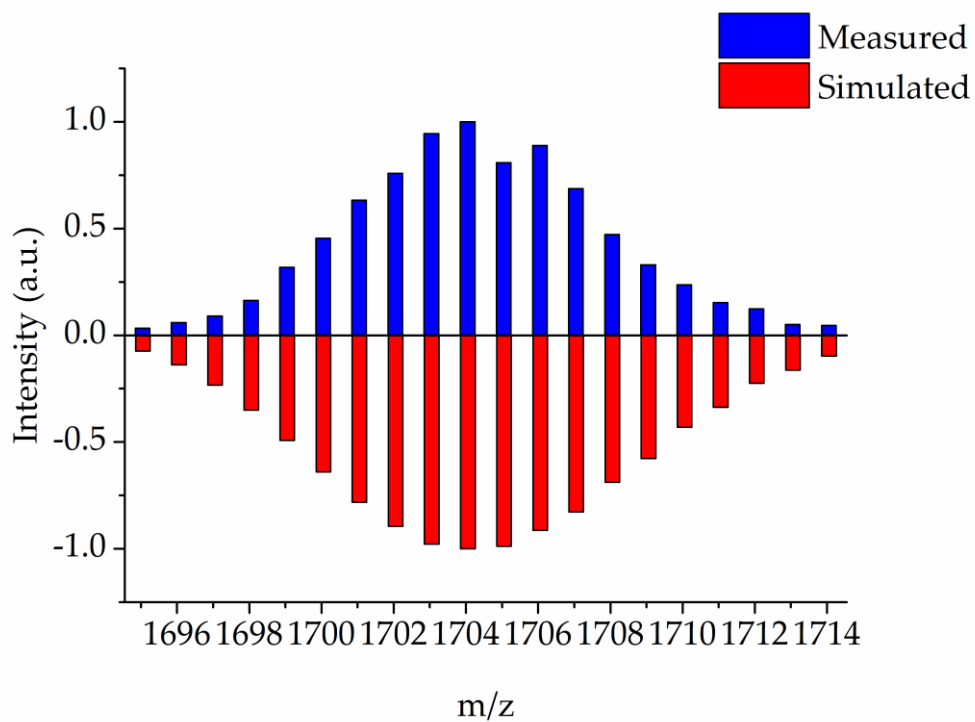
Figure 119 Measured vs. simulated mass values for $[Pd_5(dba)_5H]^+$ cluster.
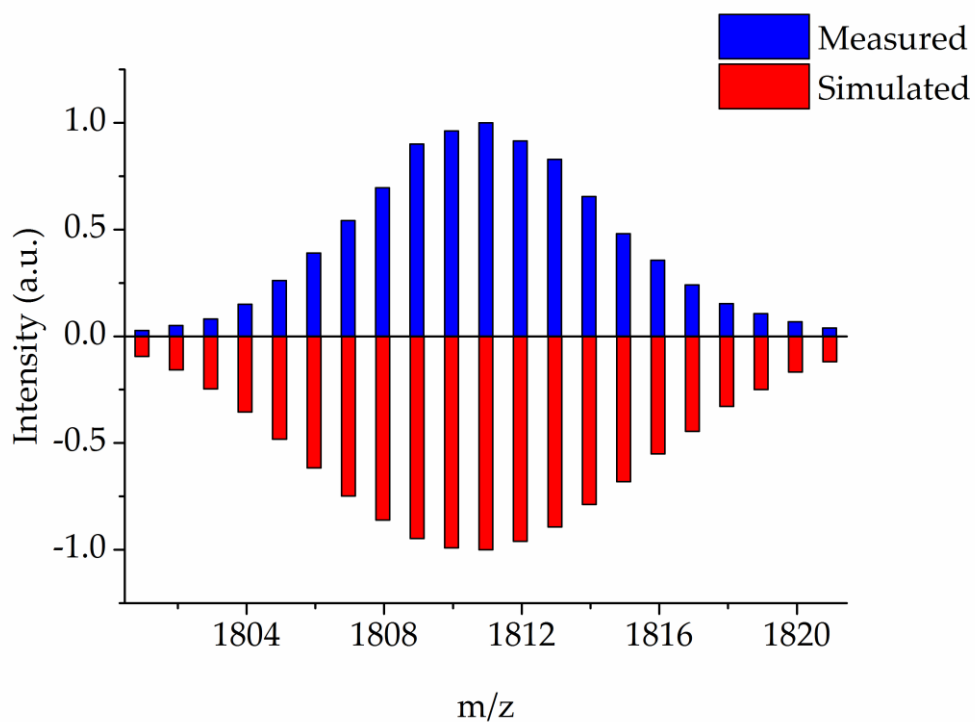
Figure 120 Measured vs. simulated mass values for $[Pd_6(dba)_5H]^+$ cluster.
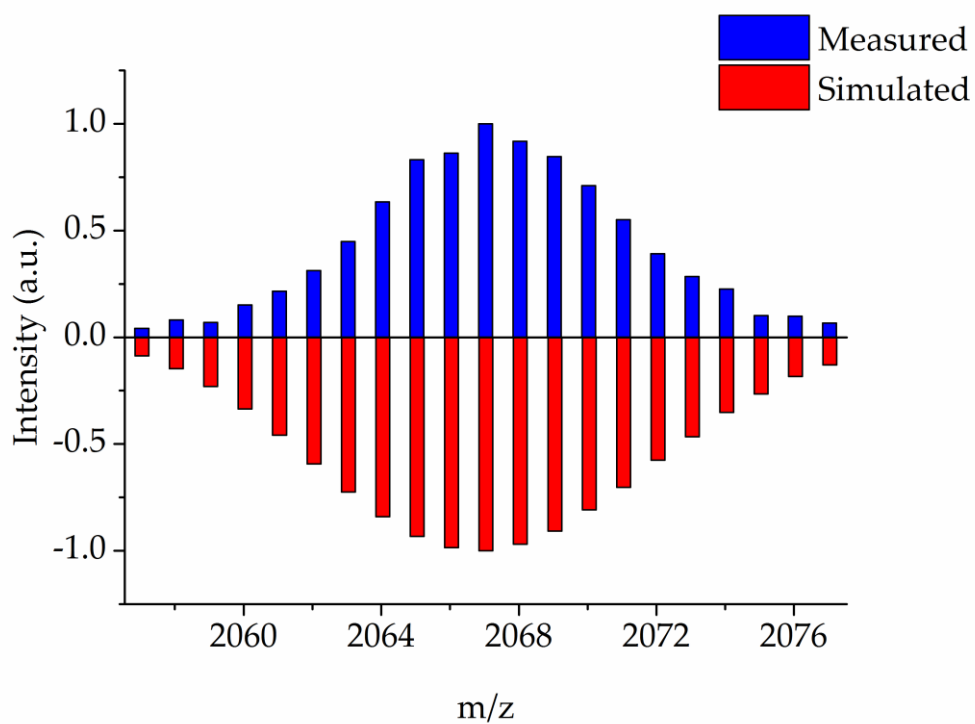
Figure 121 Measured vs. simulated mass values for [Pd$_6$(dba)$_6$Na]$^+$ cluster.
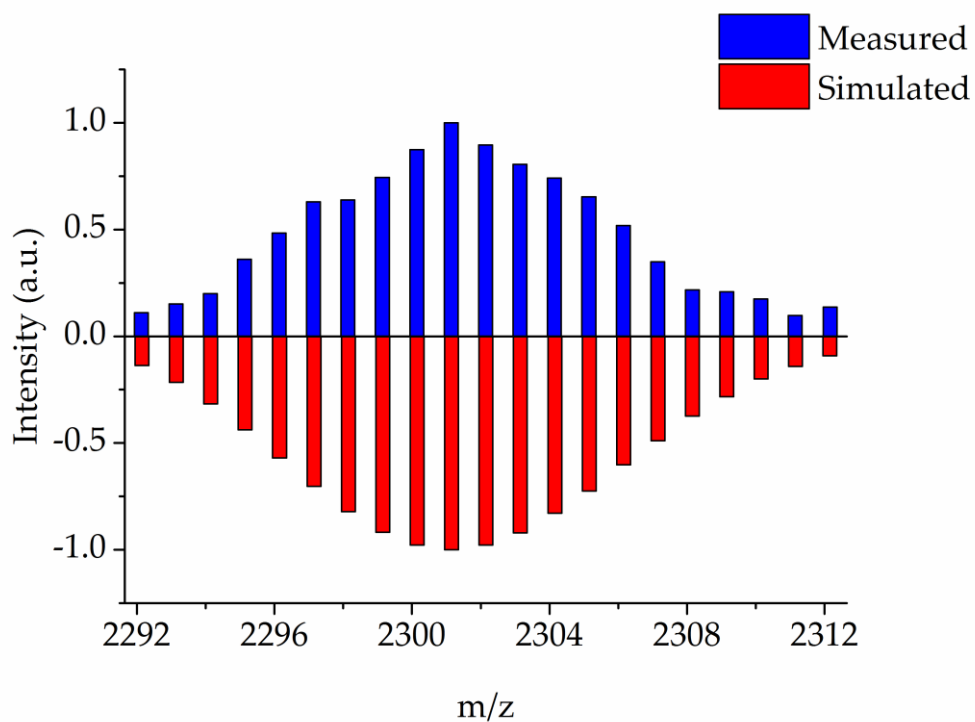
Figure 122 Measured vs. simulated mass values for [Pd$_6$(dba)$_7$Na]$^+$ cluster.
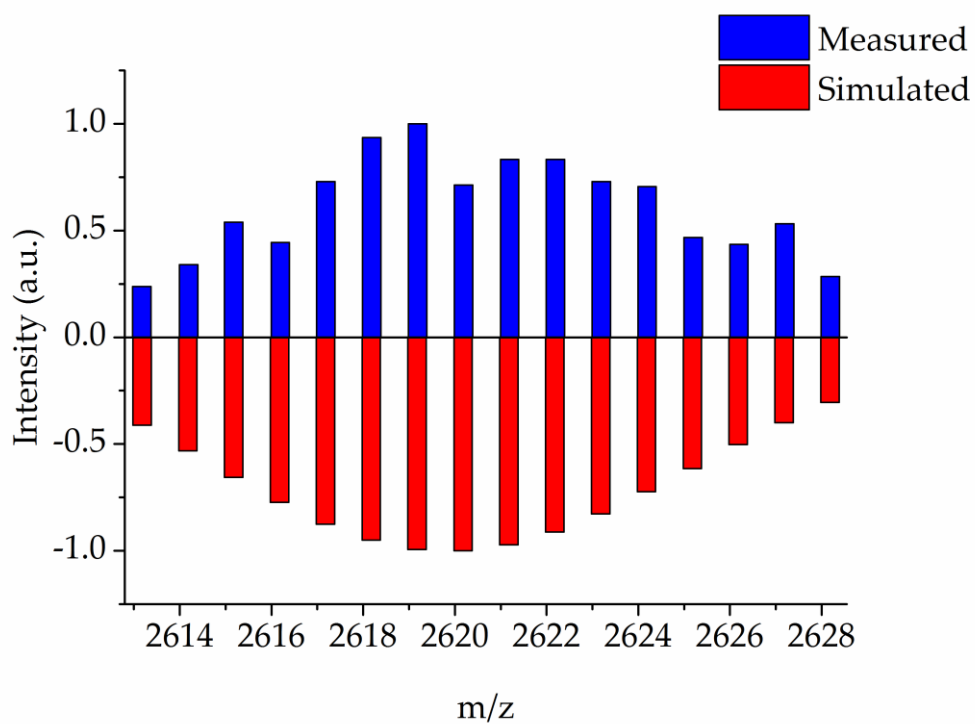
Figure 123 Measured vs. simulated mass values for [Pd$_7$(dba)$_8$H]$^+$ cluster.
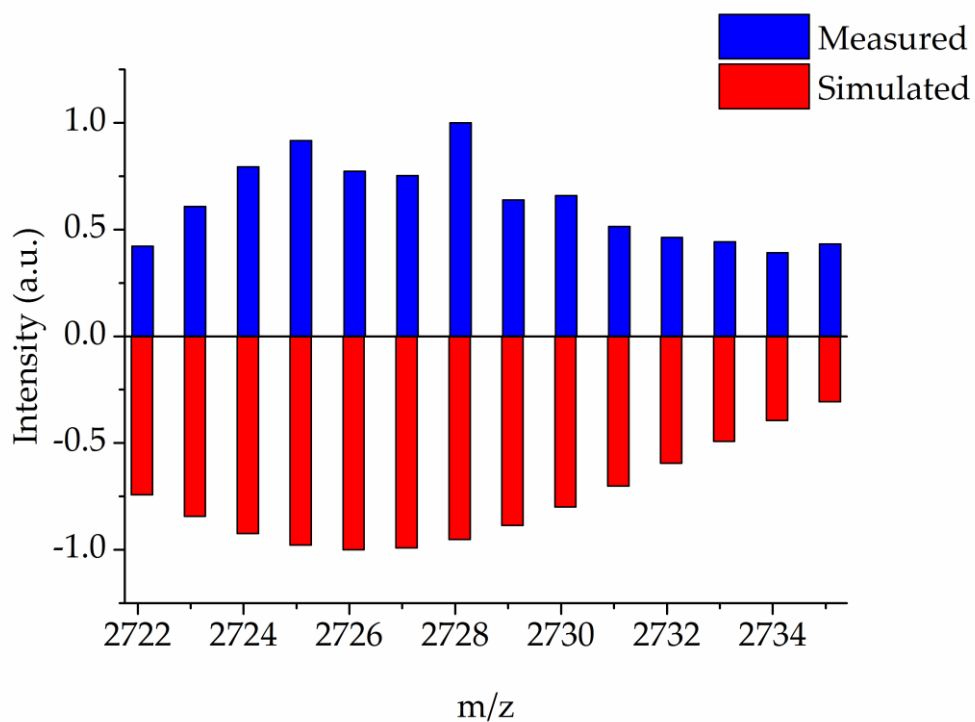
Figure 124 Measured vs. simulated mass values for [Pd$_8$(dba)$_8$H]$^+$ cluster.
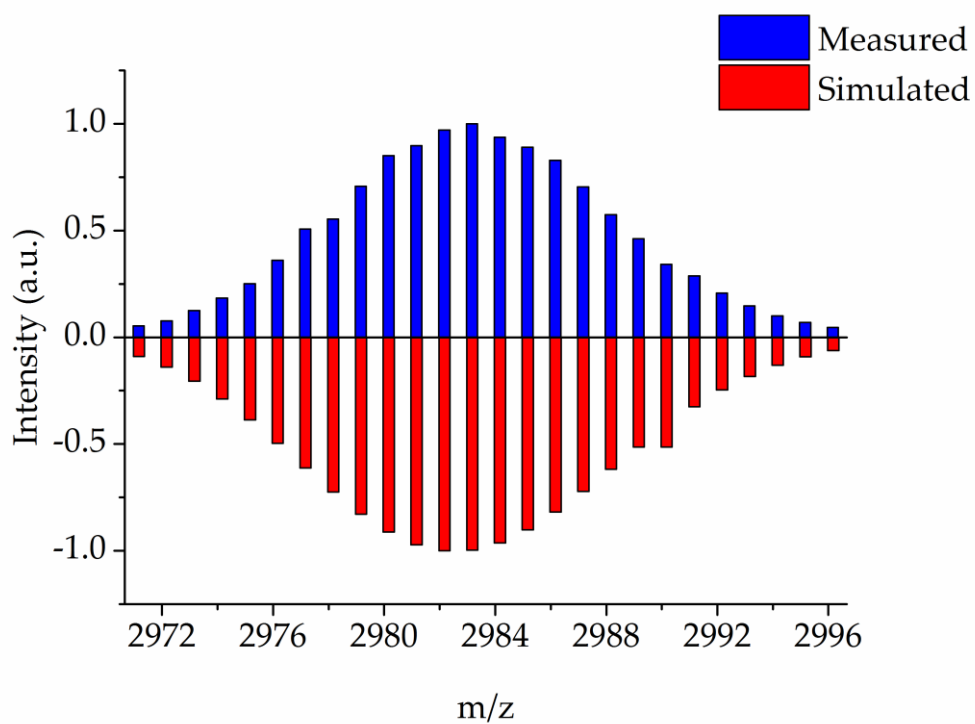
Figure 125 Measured vs. simulated mass values for [Pd$_8$(dba)$_9$Na]$^+$ cluster.
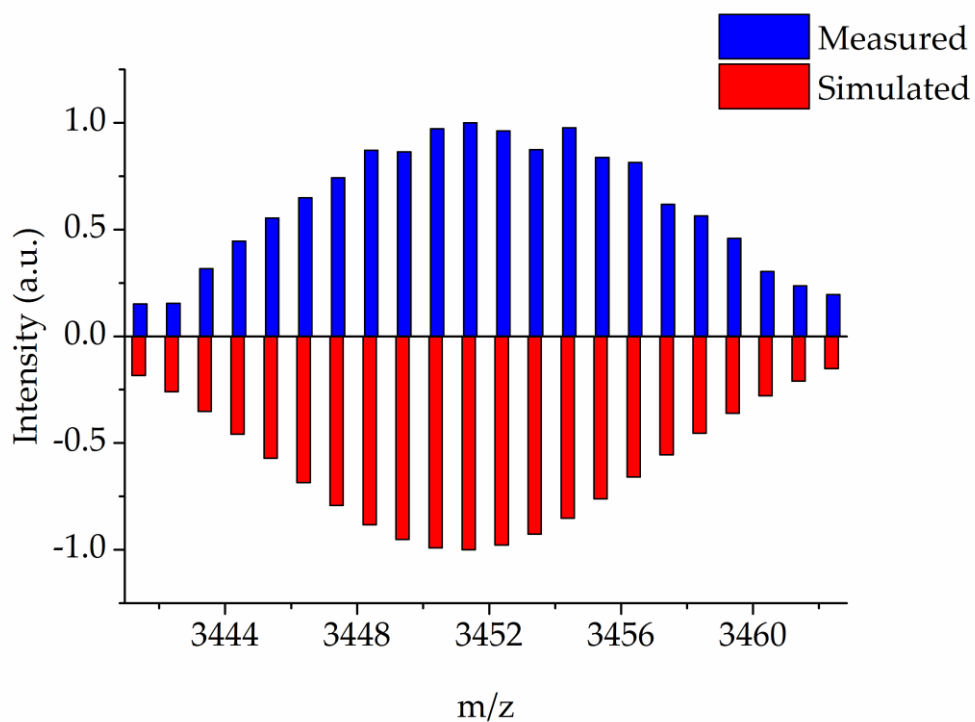
Figure 126 Measured vs. simulated mass values for [Pd$_8$(dba)$_{11}$Na]$^+$ cluster.

Appendix 7: NMR Spectra
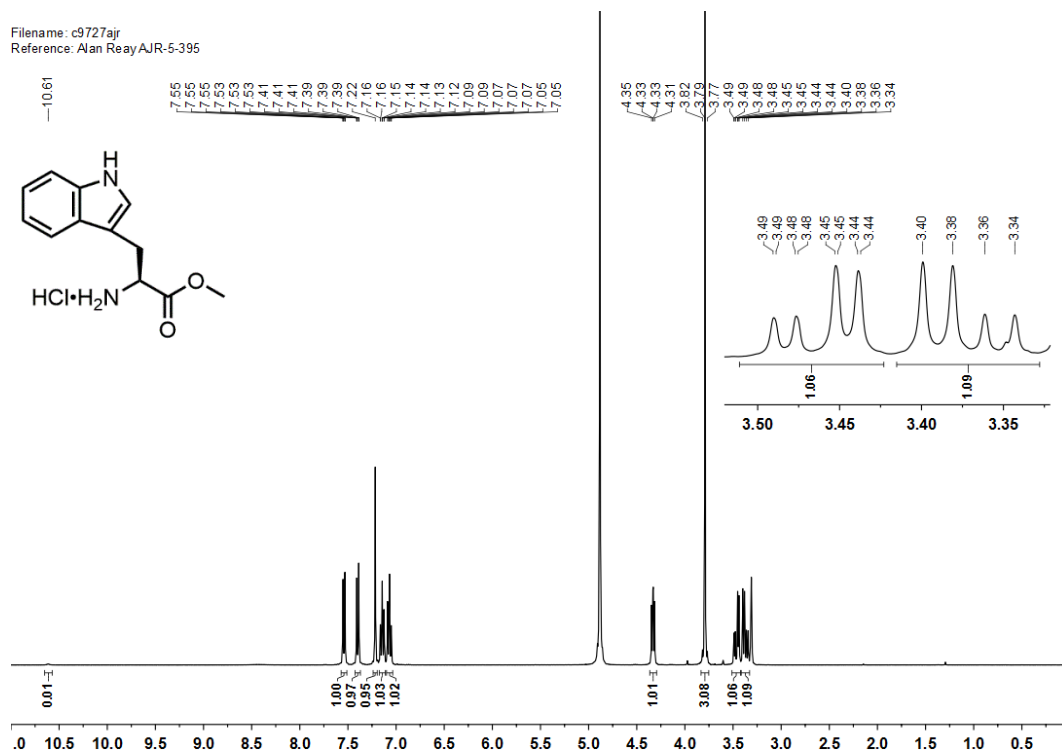
Figure 127 ^{1}H NMR spectrum of **135** (400 MHz, CD$_3$OD).
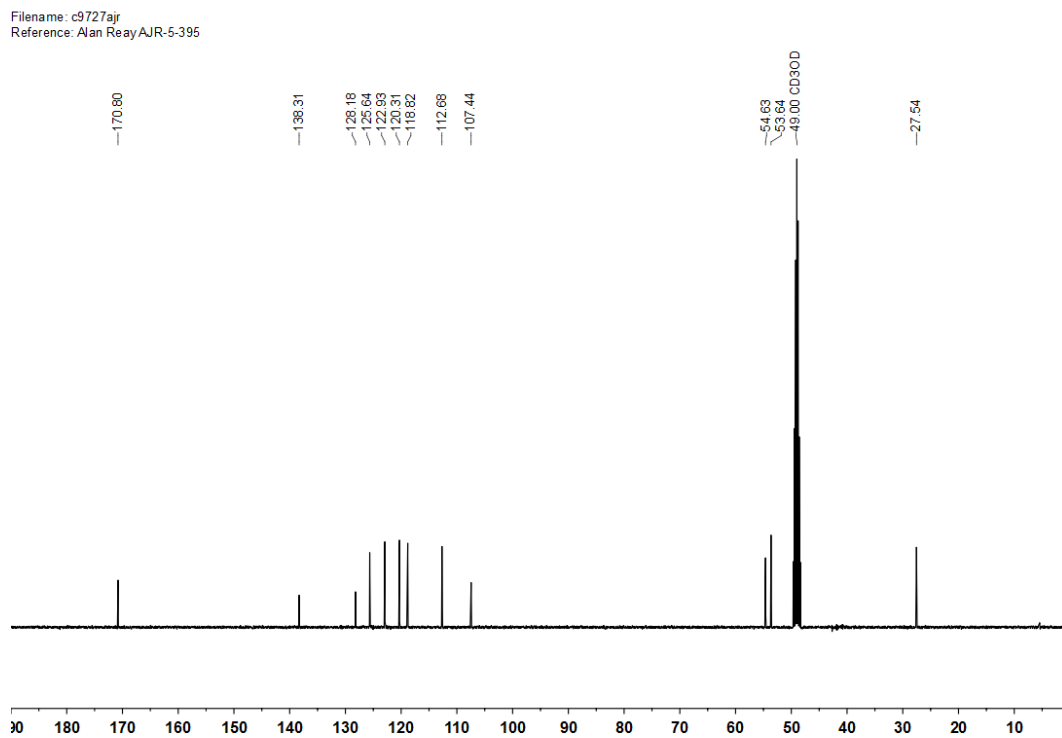
Figure 128 ^{13}C NMR spectrum of **135** (101 MHz, CD$_3$OD).
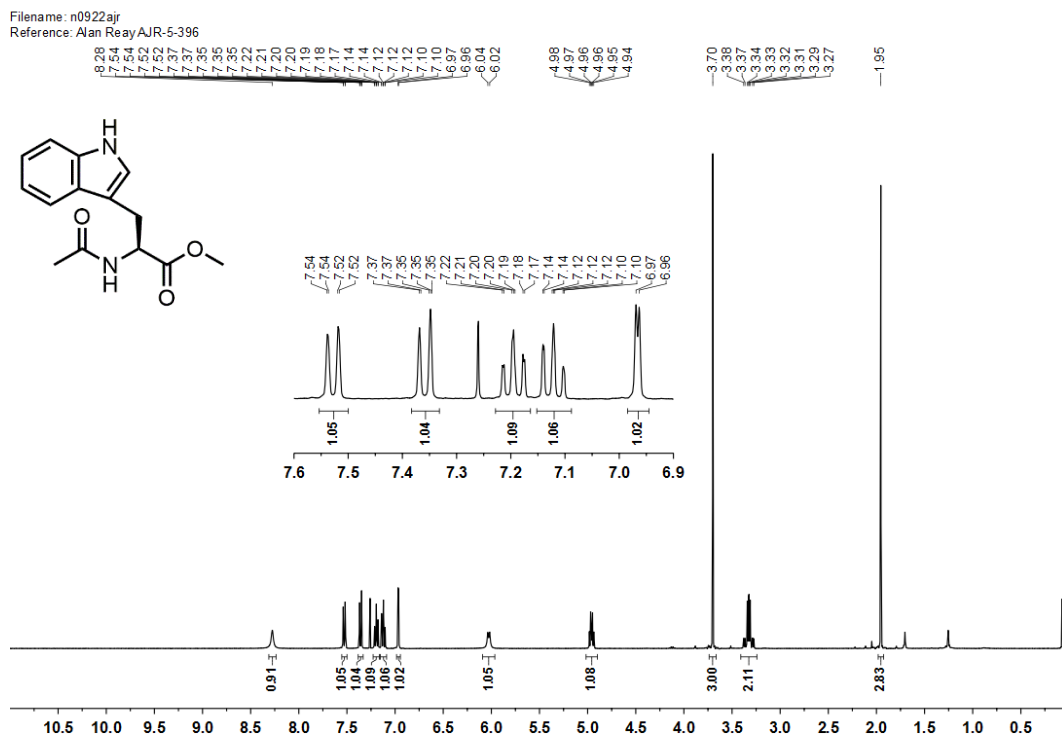
Figure 129 ^{1}H NMR spectrum of **74** (400 MHz, CDCl₃).
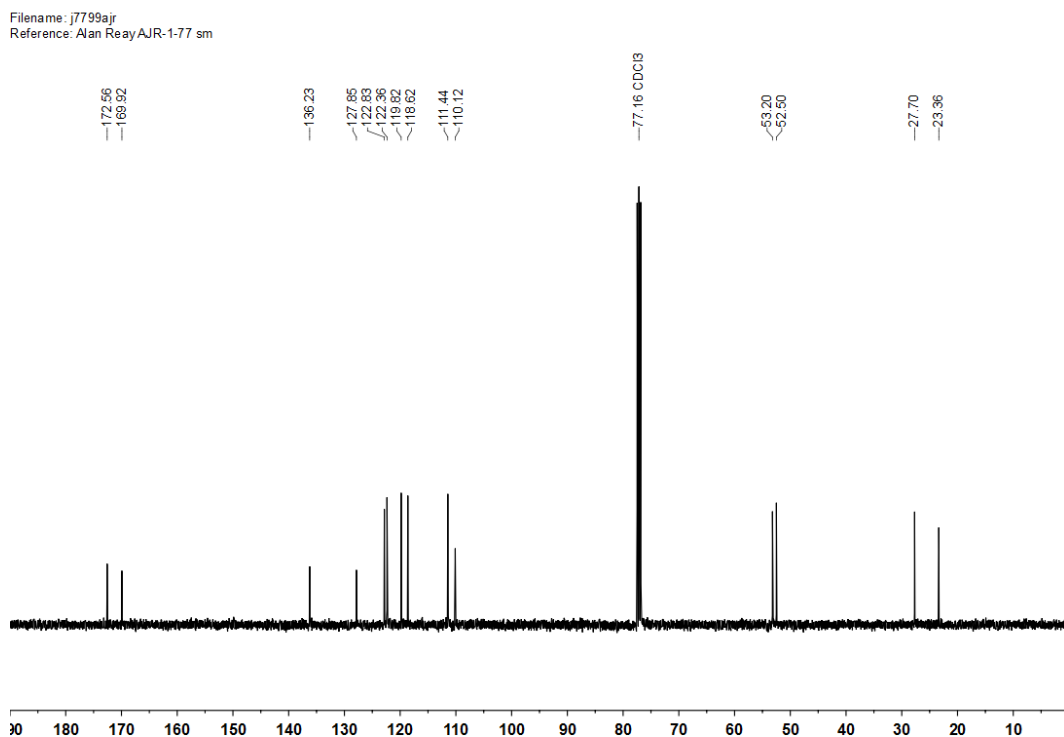
Figure 130 ^{13}C NMR spectrum of **74** (101 MHz, CDCl₃).
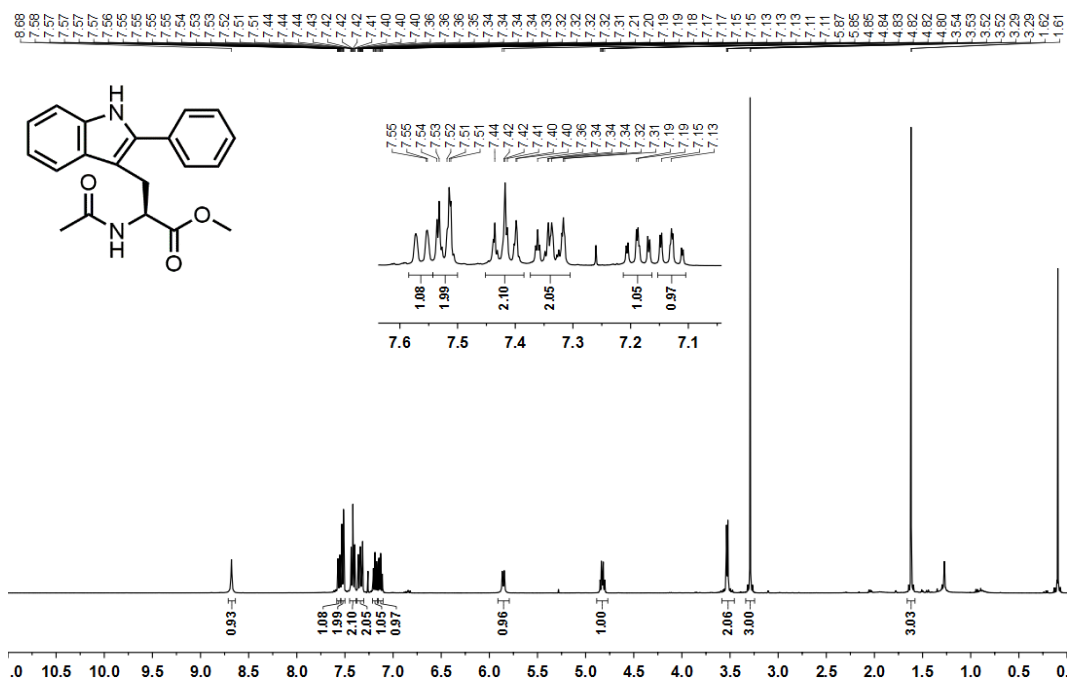
Figure 131 ^{1}H NMR spectrum of **75** (400 MHz, CDCl$_3$).
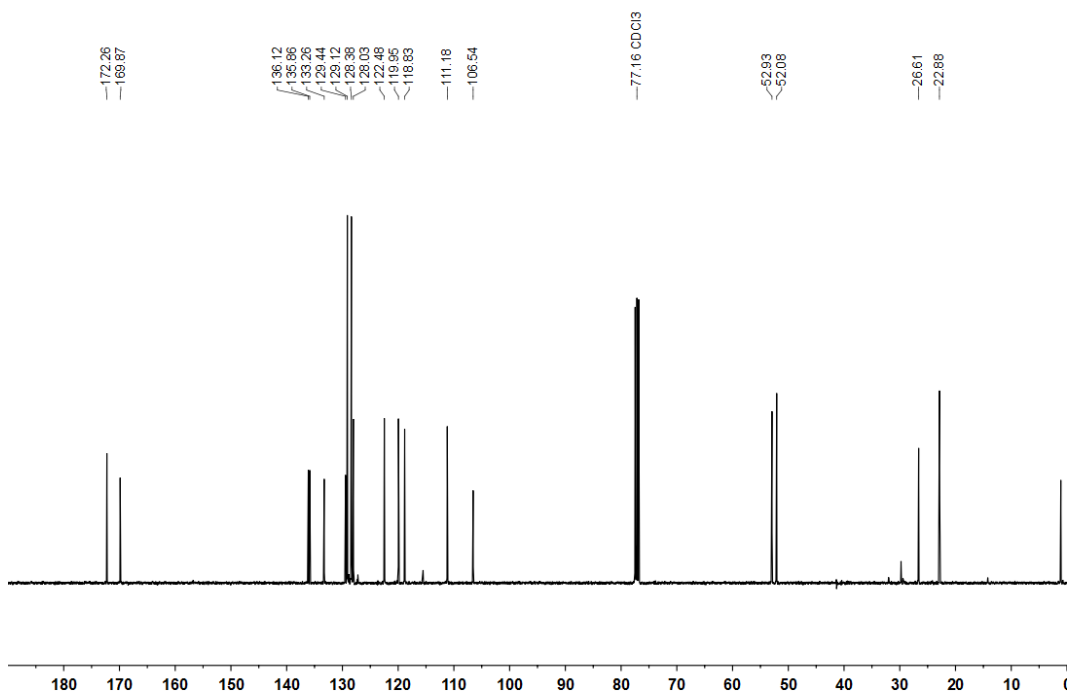
Figure 132 ^{13}C NMR spectrum of **75** (101 MHz, CDCl$_3$).

Filename: b8803ajr
Reference: Alan Reay AJR-2-153
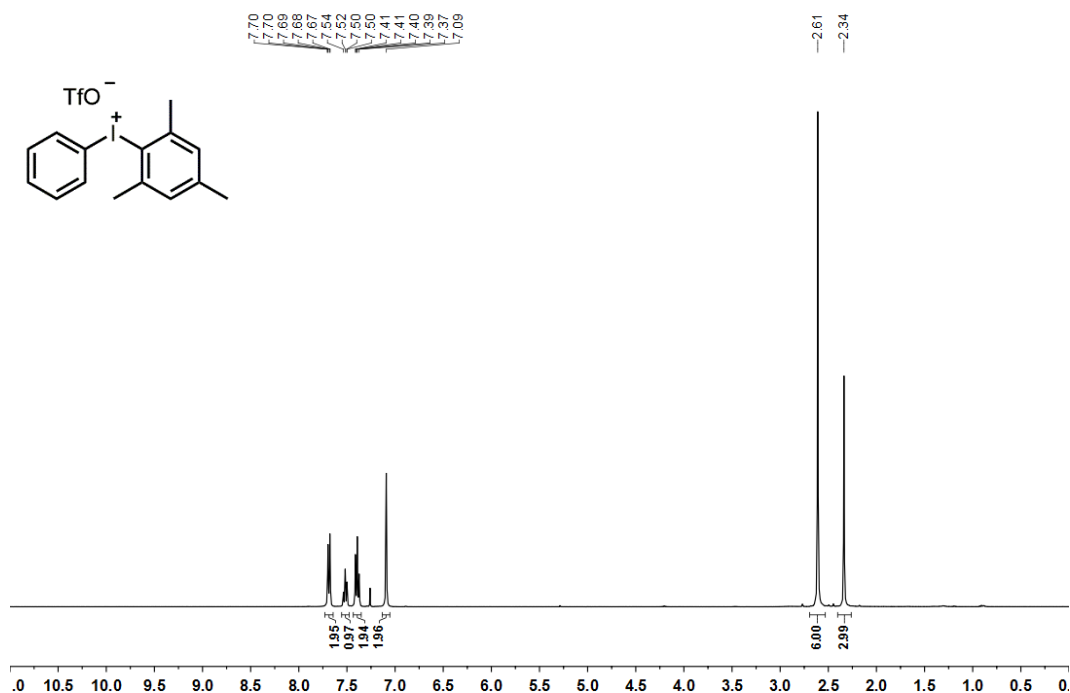
Figure 133 ^{1}H NMR spectrum of **140** (400 MHz, CDCl$_3$).

Filename: b8803ajr
Reference: Alan Reay AJR-2-153
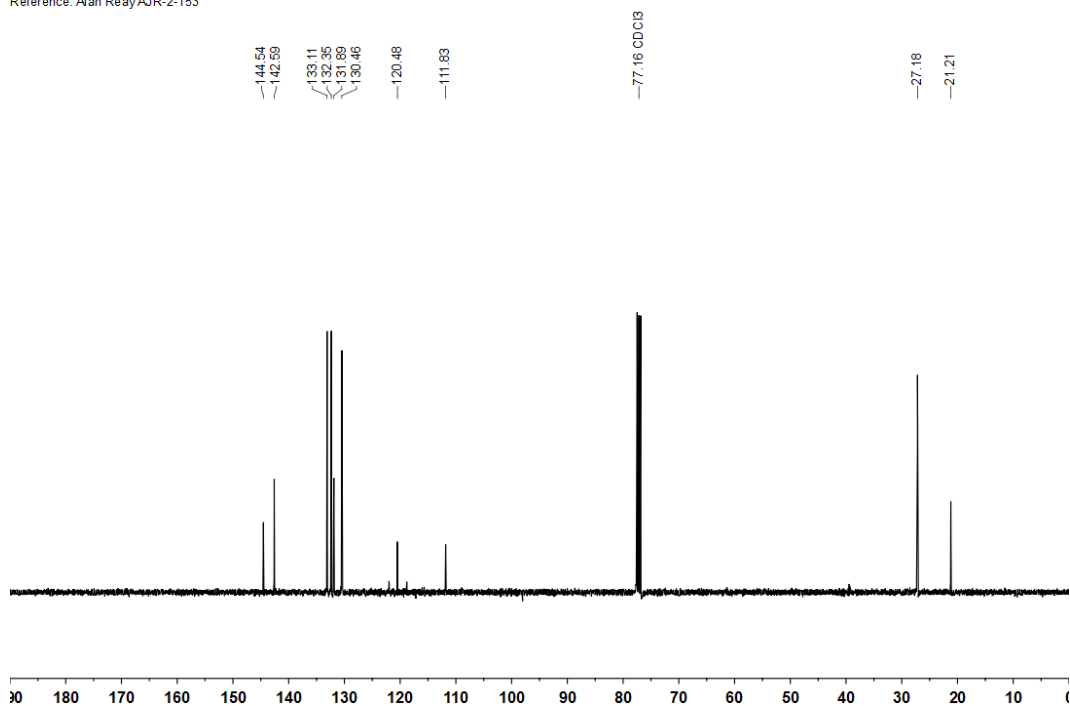
Figure 134 ^{13}C NMR spectrum of **140** (101 MHz, CDCl$_3$).

Filename: c4781ajr
Reference: Alan Reay AJR-4-318

—78.23
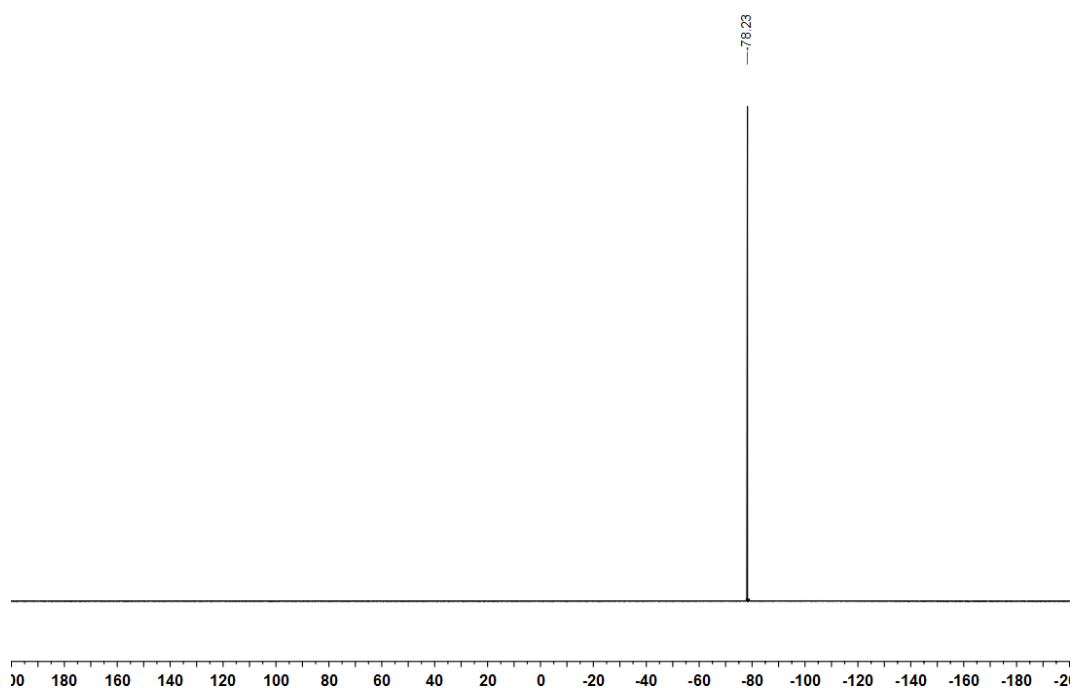
Figure 135 ^{19}F NMR spectrum of **140** (376 MHz, CDCl$_3$).
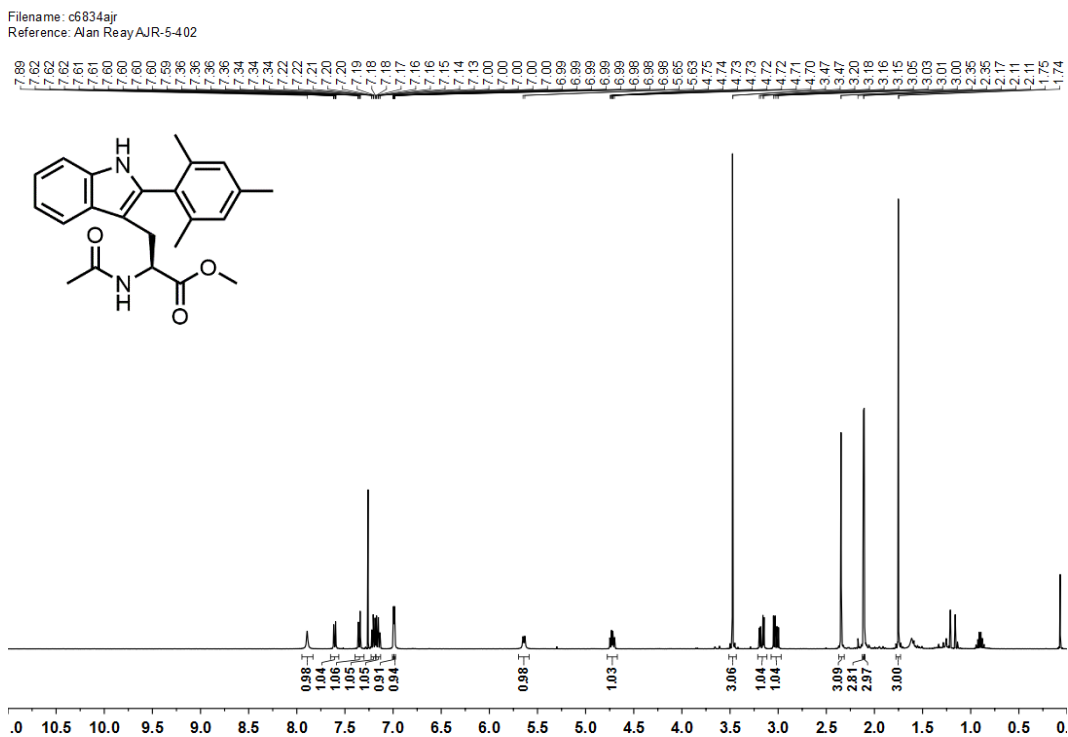
Figure 136 ^{1}H NMR spectrum of **142** (400 MHz, CDCl$_3$).
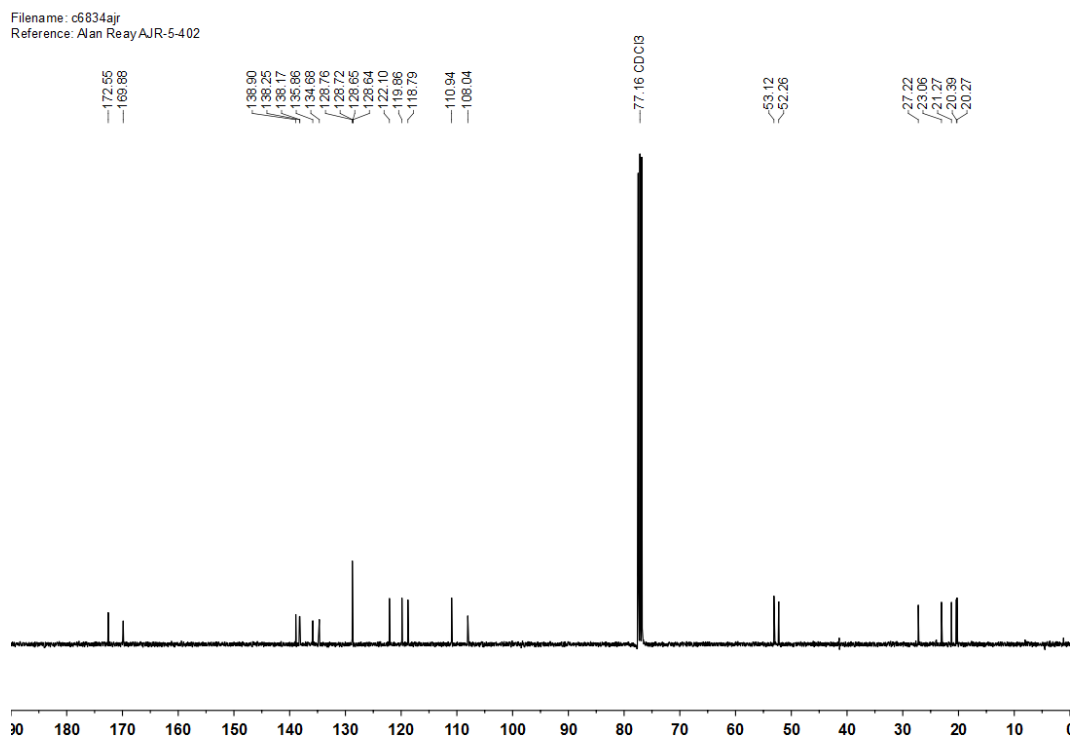
Figure 137 ^{13}C NMR spectrum of **142** (101 MHz, CDCl$_3$).
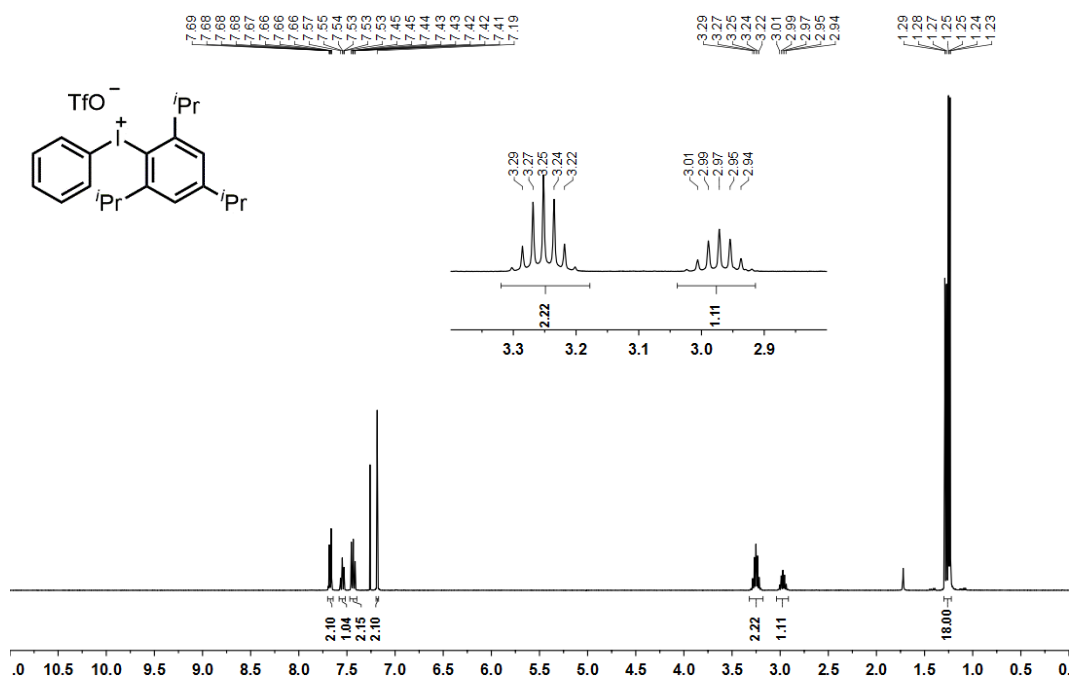
Figure 138 ^{1}H NMR spectrum of **143** (400 MHz, CDCl$_3$).
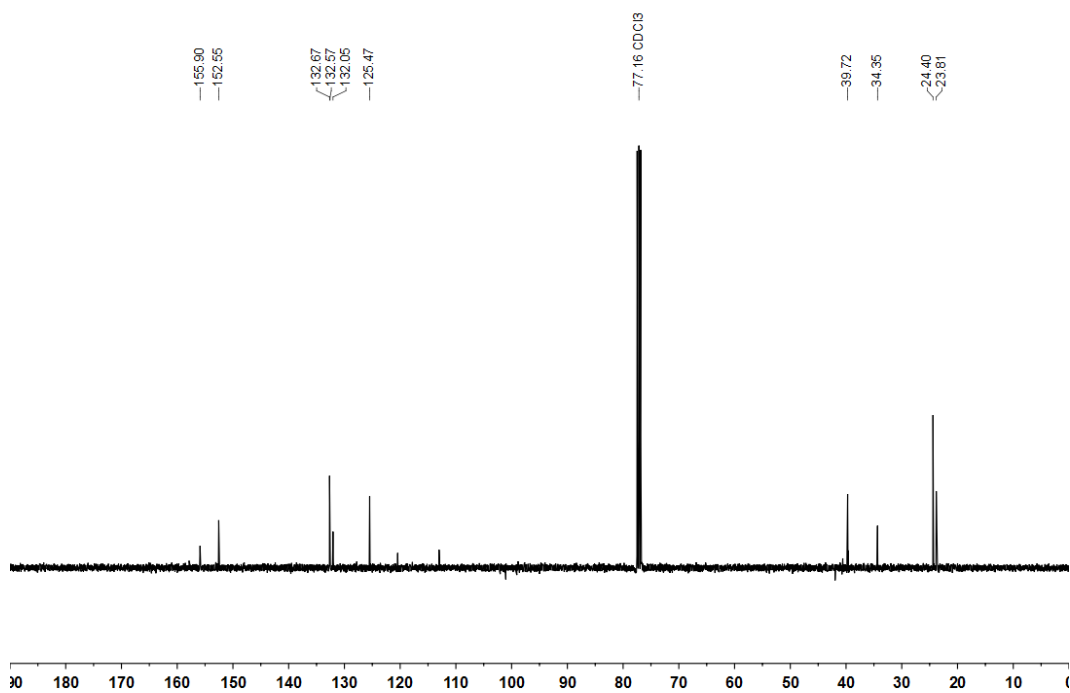
Figure 139 ^{13}C NMR spectrum of **143** (101 MHz, CDCl$_3$).

333

Figure 140 ^{1}H NMR spectrum of **144** (400 MHz, CDCl$_3$).

Figure 141 ^{13}C NMR spectrum of **144** (101 MHz, CDCl$_3$).

—1.97

120 110 100 90 80 70 60 50 40 30 20 10 0 -10 -20 -30 -40 -50 -60 -70 -80 -90 -100 -110 -120
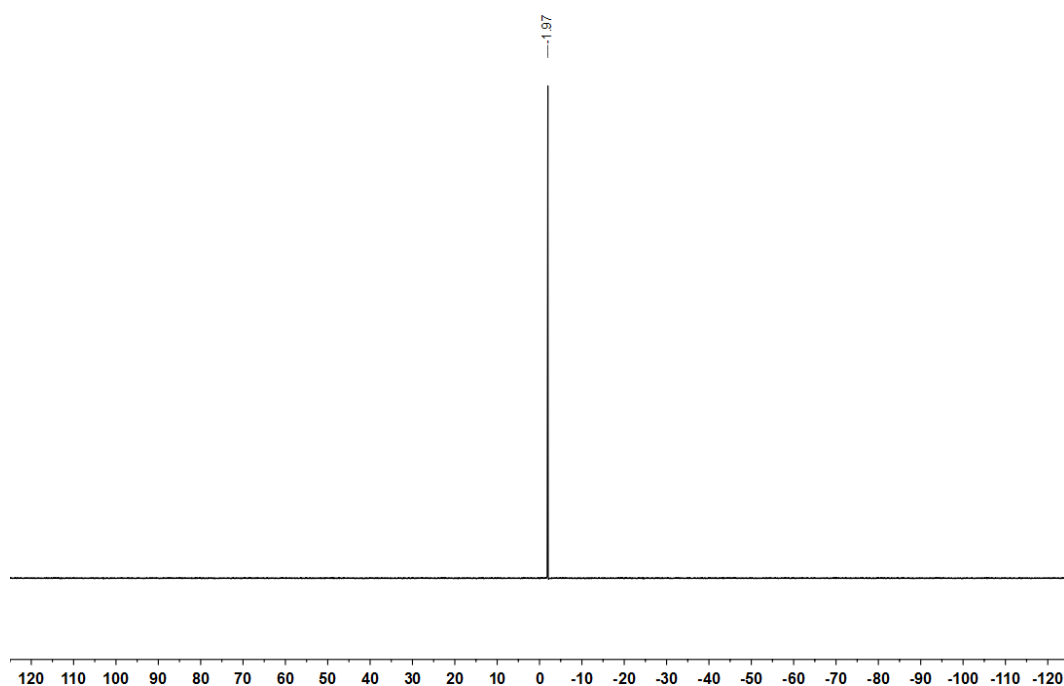
Figure 142 ^{11}B NMR spectrum of **144** (128 MHz, CDCl$_3$).

147.27
147.34

-147.20   -147.24   -147.28   -147.32   -147.36   -147.40
ppm

00 180 160 140 120 100 80 60 40 20 0 -20 -40 -60 -80 -100 -120 -140 -160 -180 -2
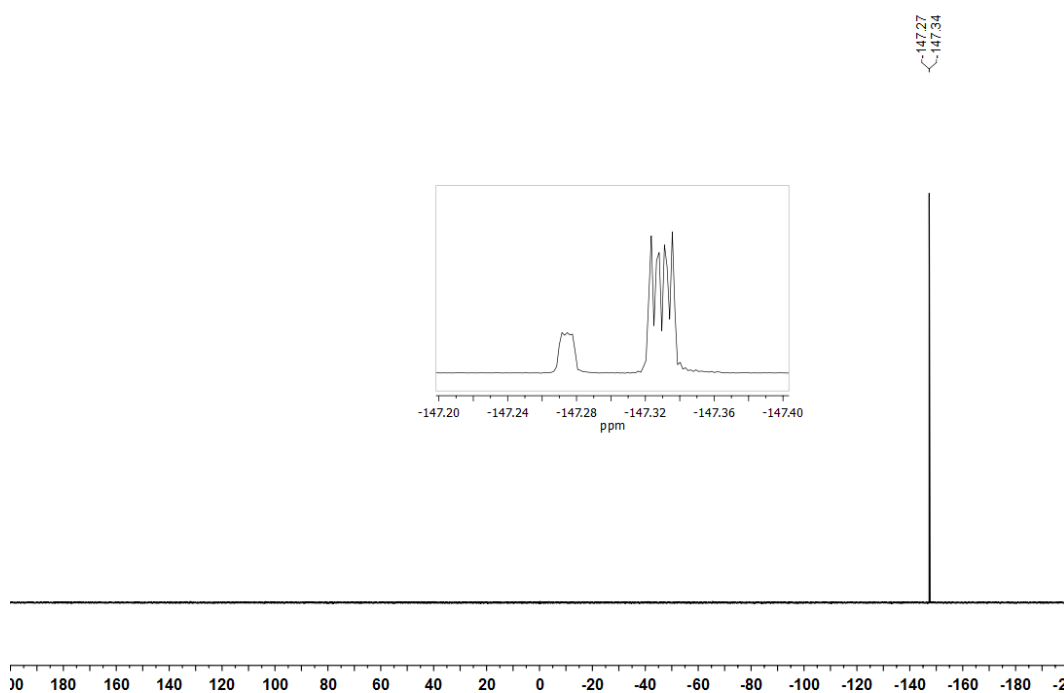
Figure 143 ^{19}F NMR spectrum of **144** (376 MHz, CDCl$_3$).
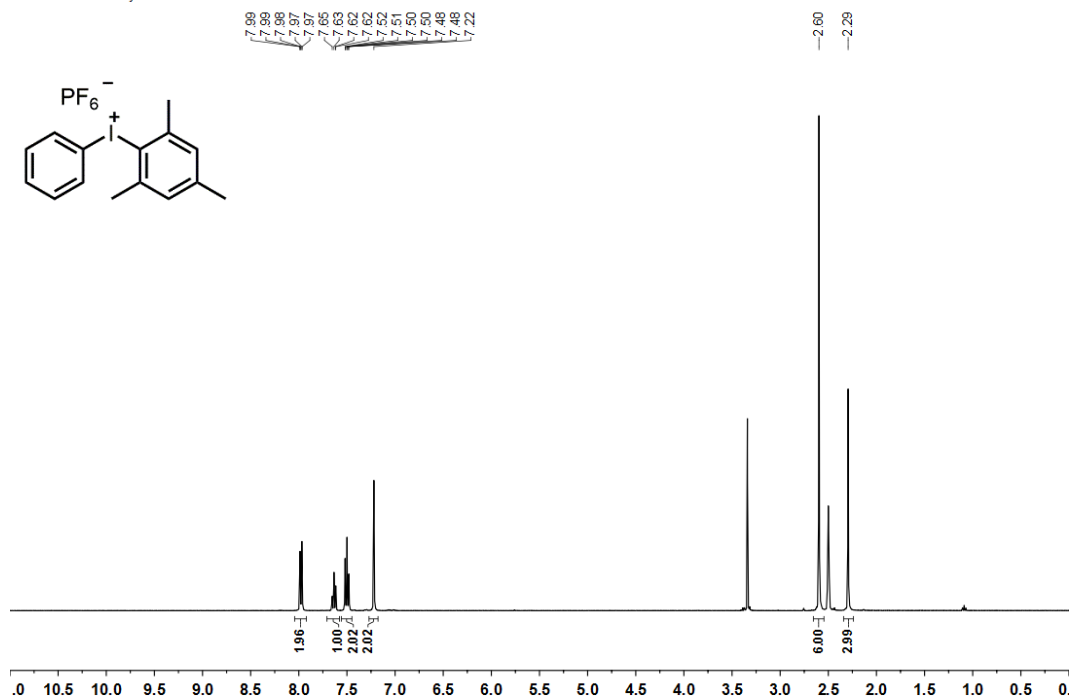
Figure 144 ^{1}H NMR spectrum of **145** (400 MHz, (CD$_3$)$_2$SO).
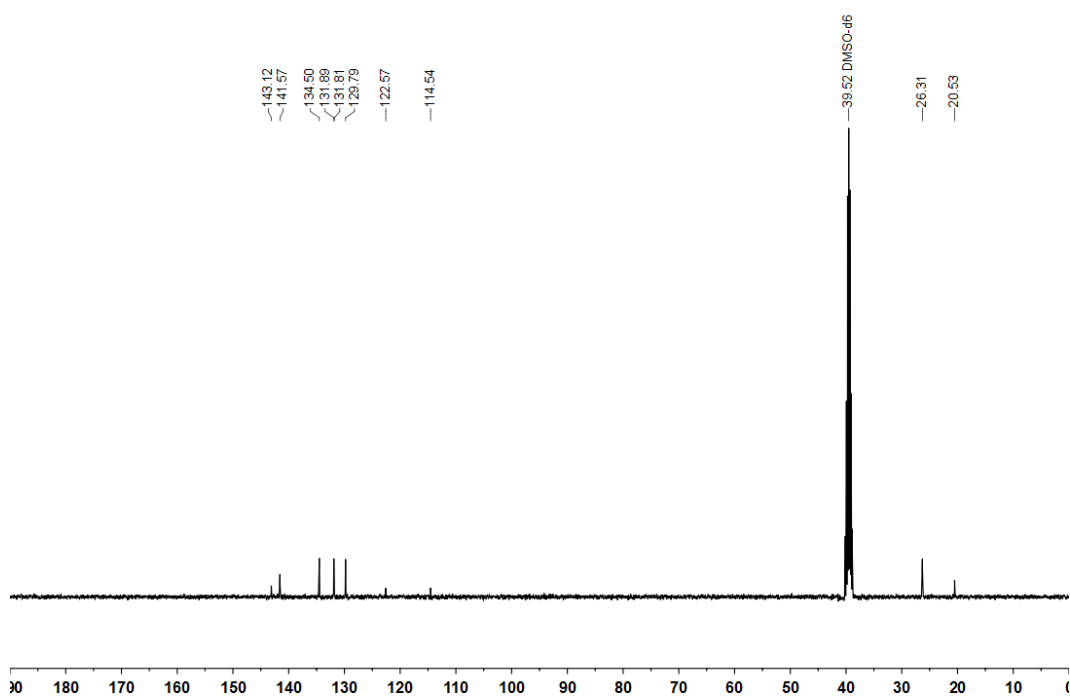
Figure 145 ^{13}C NMR spectrum of **145** (101 MHz, (CD$_3$)$_2$SO).

Filename: b9171ajr
Reference: Alan Reay AJR-2-163

69.07
70.96

180 160 140 120 100 80 60 40 20 0 -20 -40 -60 -80 -100 -120 -140 -160 -180 -2
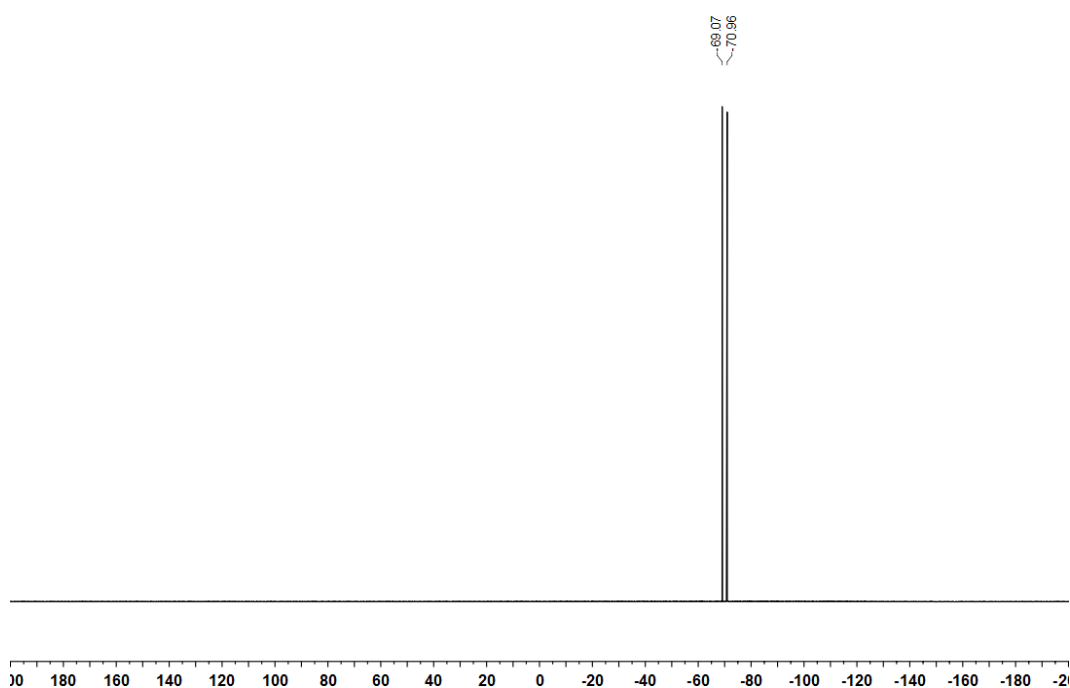
Figure 146 ^{19}F NMR spectrum of **145** (376 MHz, (CD$_3$)$_2$SO).

Filename: b9171ajr
Reference: Alan Reay AJR-2-163

130.39
134.79
139.18
143.58
147.97
152.37
156.76

300 250 200 150 100 50 0 -50 -100 -150 -200 -250 -300 -3
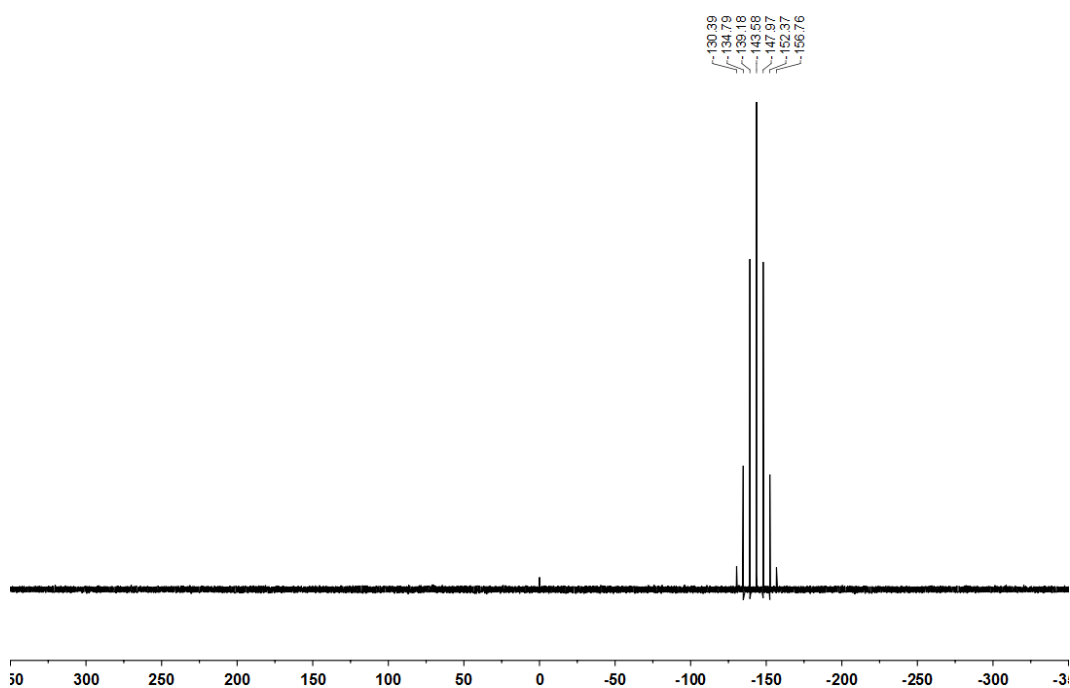
Figure 147 ^{31}P NMR spectrum of **145** (162 MHz, (CD$_3$)$_2$SO).

Figure 148 ^{1}H NMR spectrum of **146** (400 MHz, (CD$_3$)$_2$SO).

Figure 149 ^{13}C NMR spectrum of **146** (101 MHz, (CD$_3$)$_2$SO).

Filename: c4215ajr
Reference: Alan Reay AJR-4-338
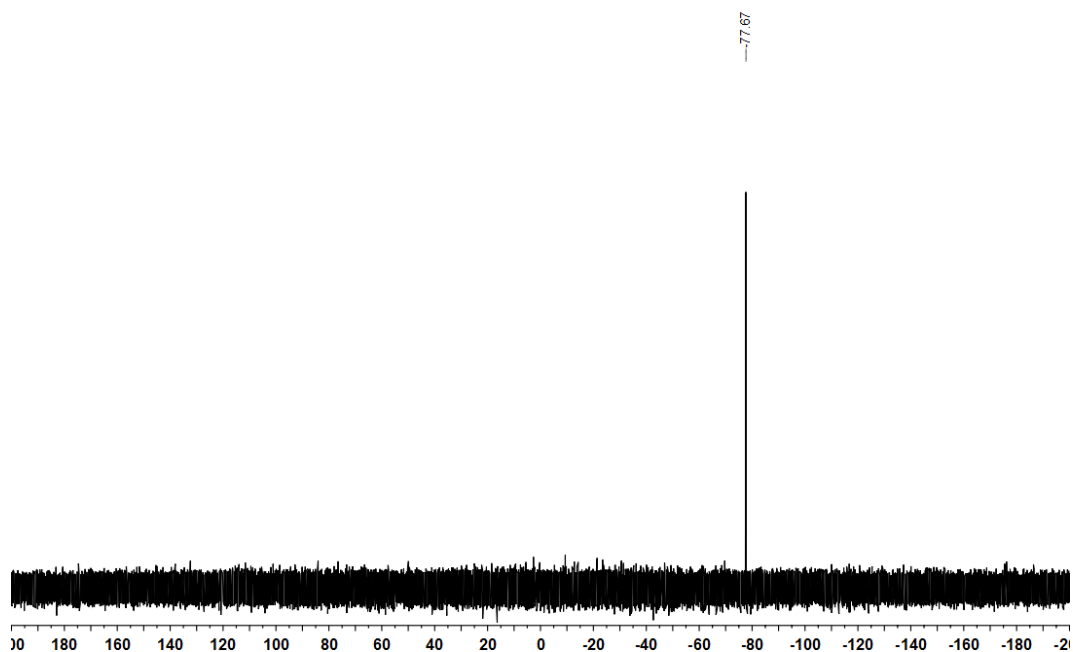
Figure 150 ^{19}F NMR spectrum of **146** (376 MHz, (CD$_3$)$_2$SO).

Filename: n3916ajr
Reference: Alan Reay AJR-5-433
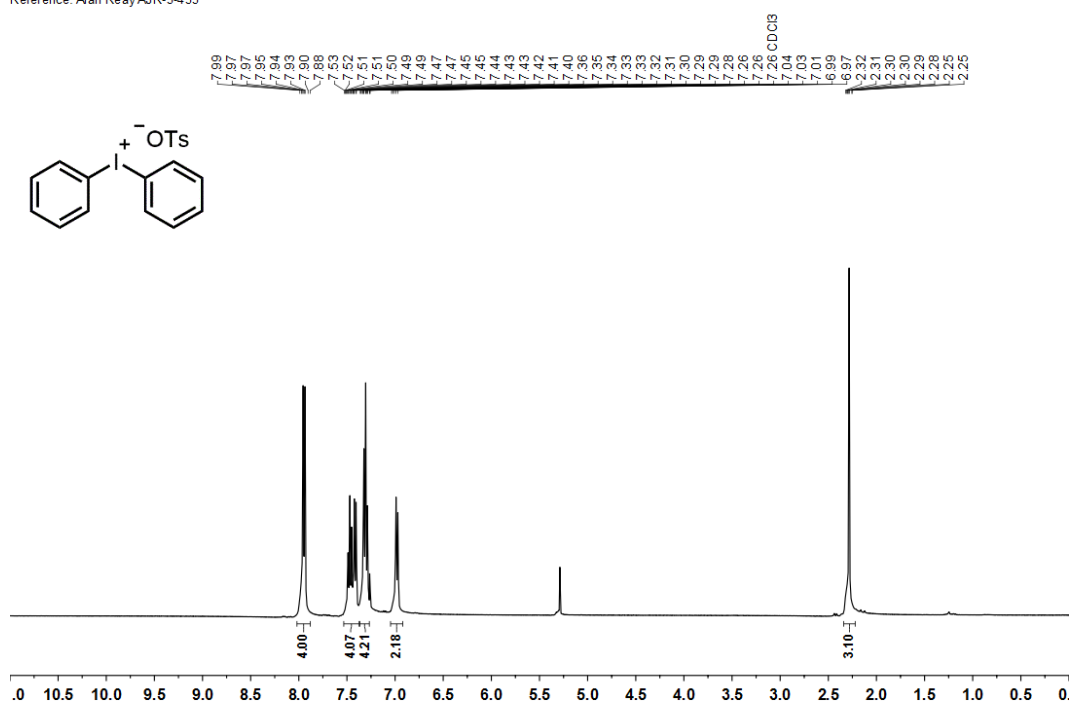
Figure 151 ^{1}H NMR spectrum of **132** (400 MHz, (CD$_3$)$_2$SO).

Filename: n3916ajr
Reference: Alan Reay AJR-5-433
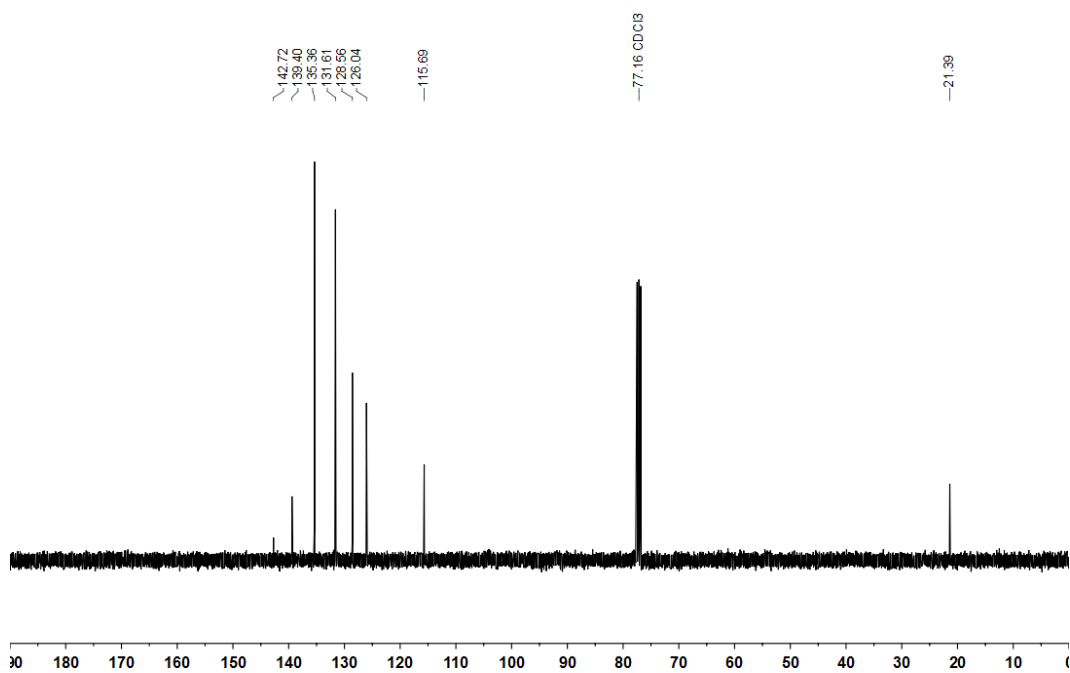
Figure 152 ^{13}C NMR spectrum of **132** (101 MHz, (CD$_3$)$_2$SO).
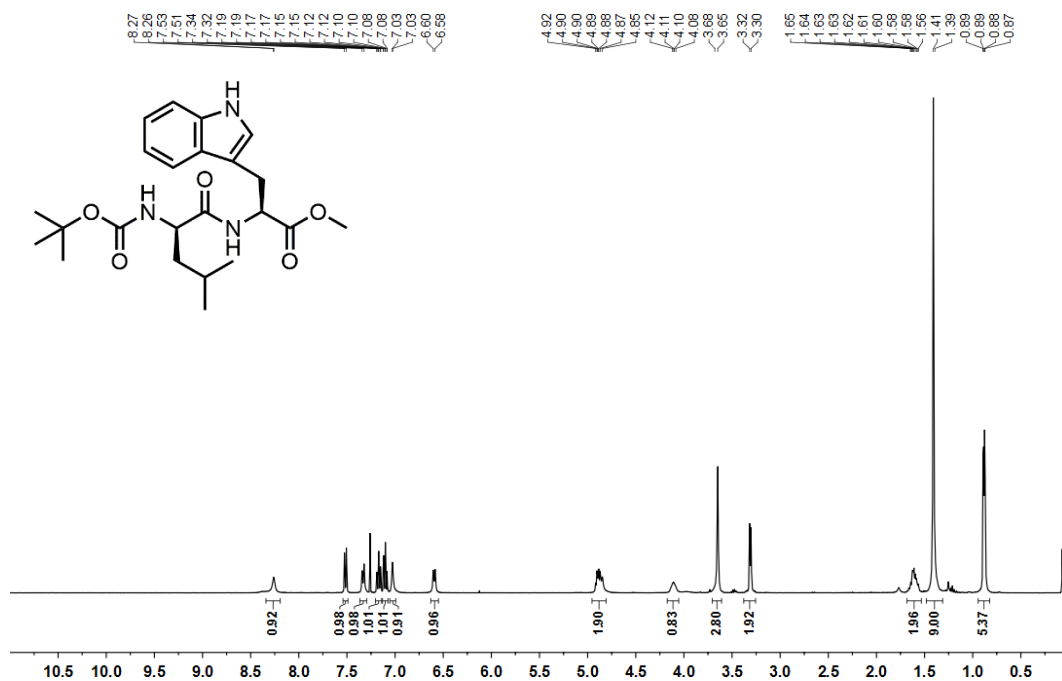
Figure 153 ^{1}H NMR spectrum of **149** (400 MHz, CDCl$_3$).
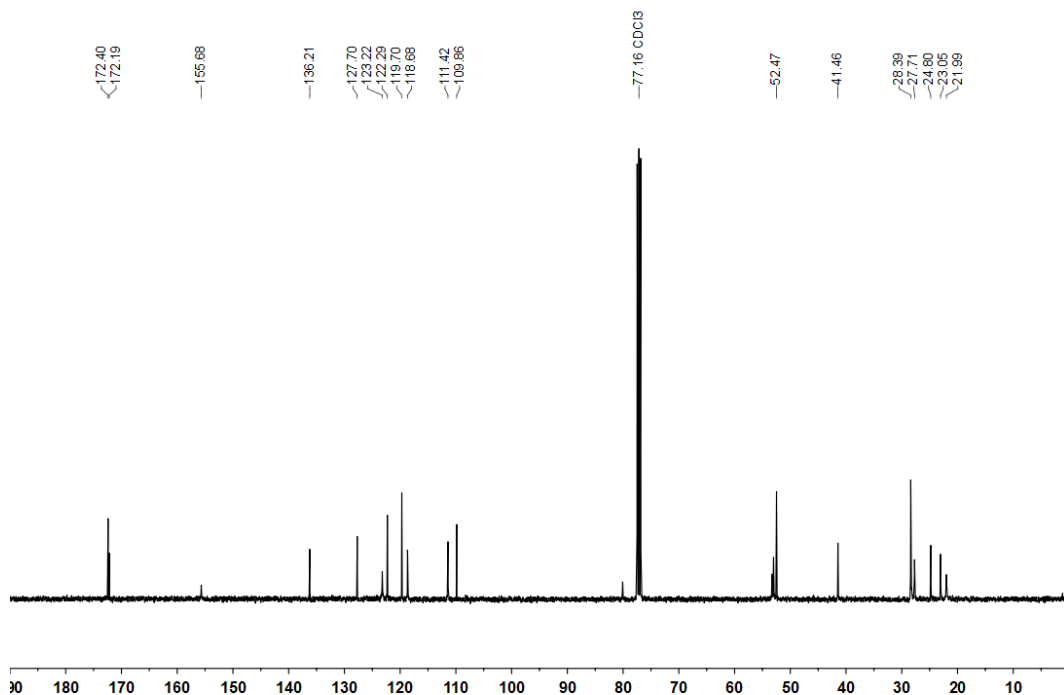
Figure 154 ^{13}C NMR spectrum of **149** (101 MHz, CDCl$_3$).
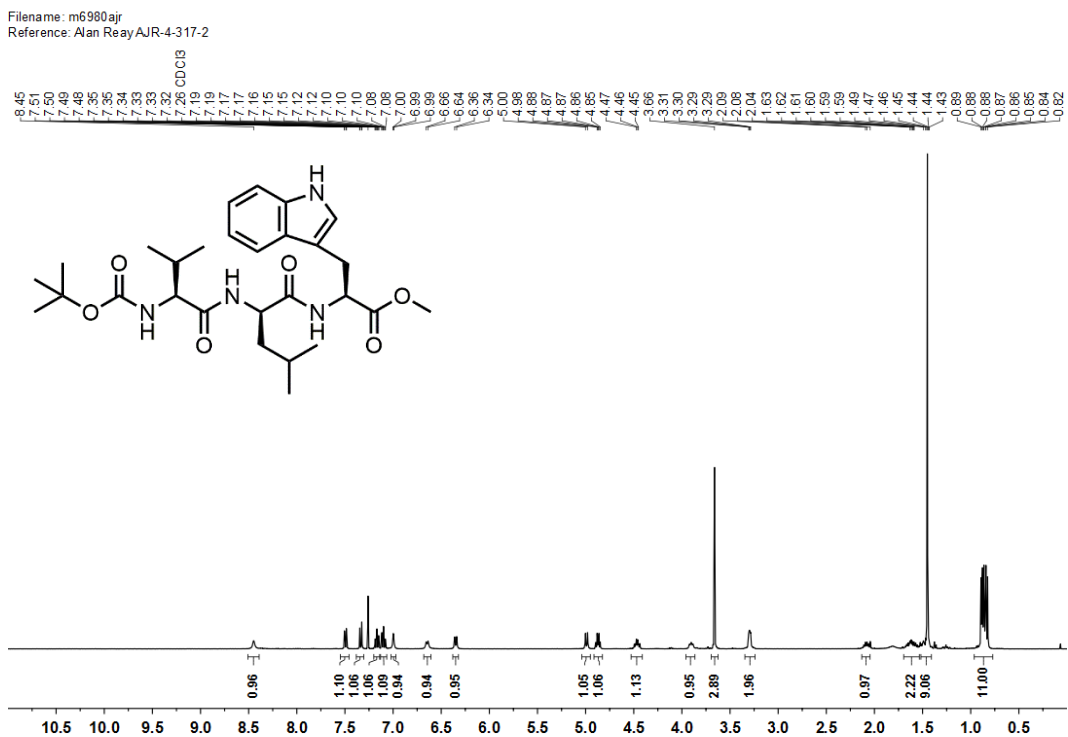
Figure 155 ^{1}H NMR spectrum of **152** (400 MHz, CDCl$_3$).
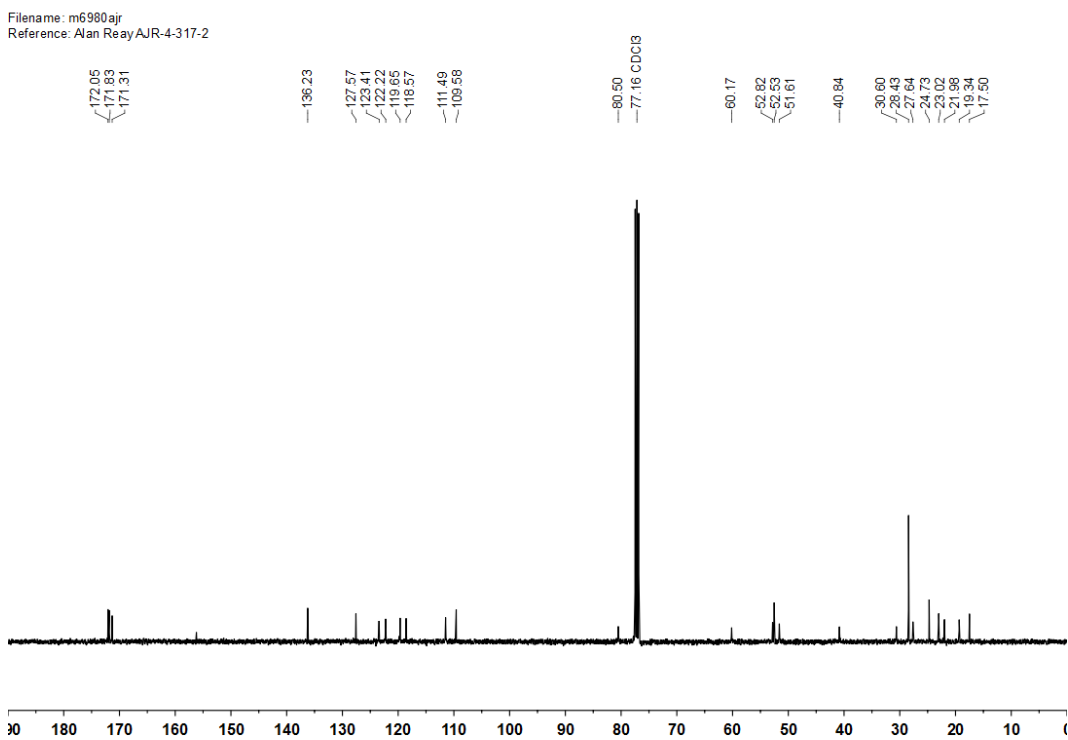
Figure 156 ^{13}C NMR spectrum of **152** (101 MHz, CDCl$_3$).
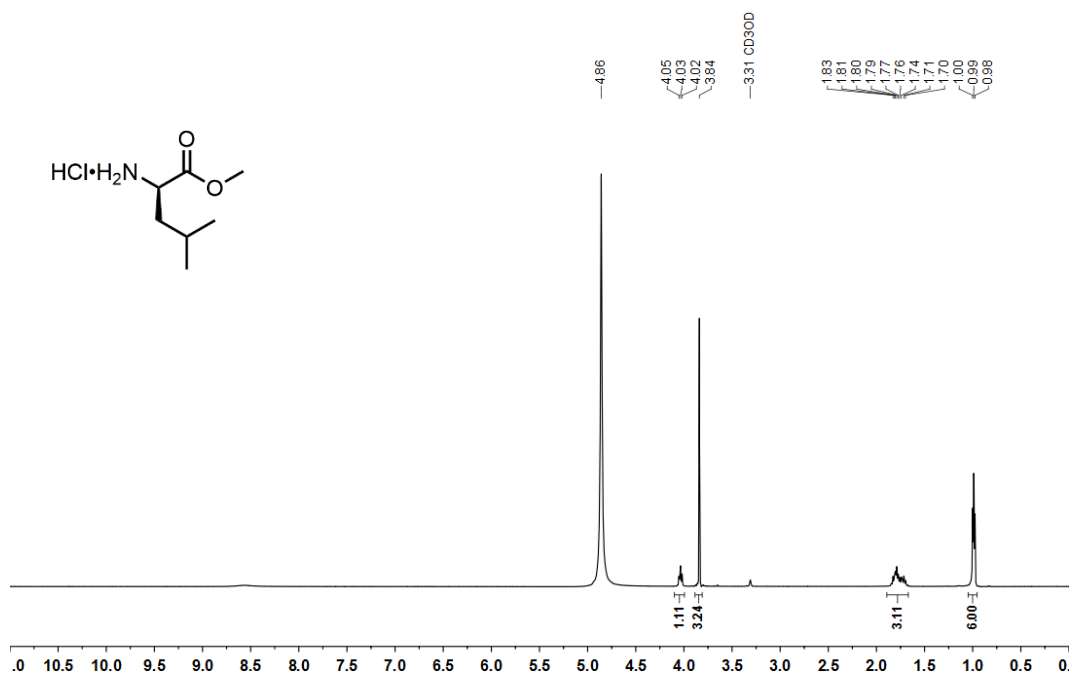
Figure 157 ^{1}H NMR spectrum of **155** (400 MHz, CD$_3$OD).
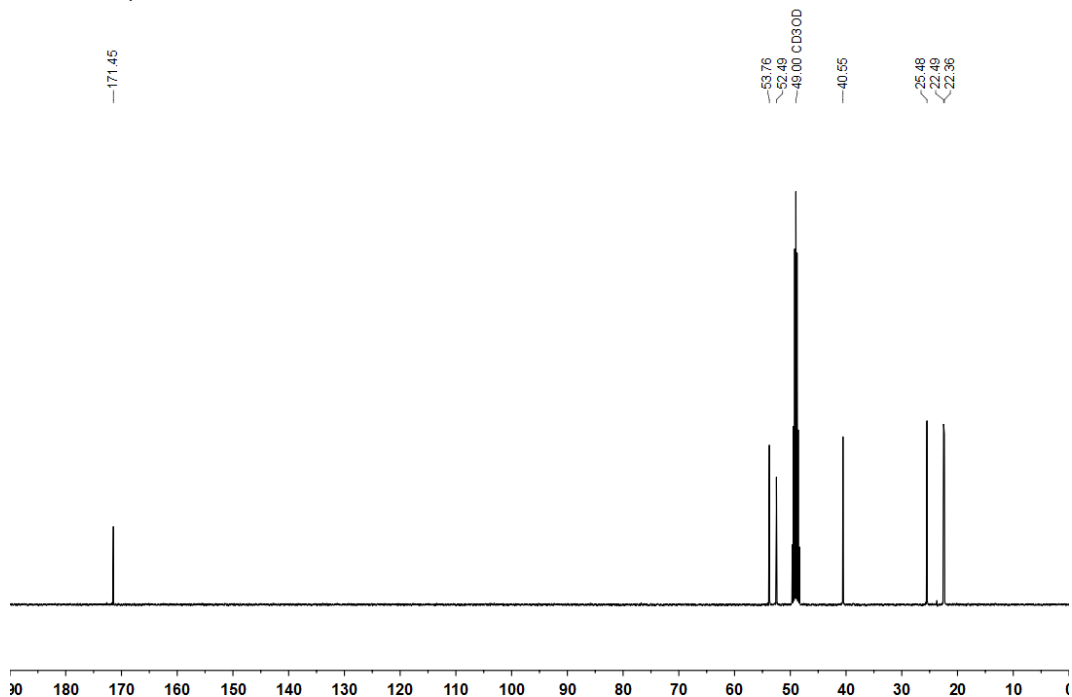
Figure 158 ^{13}C NMR spectrum of **155** (101 MHz, CD$_3$OD).
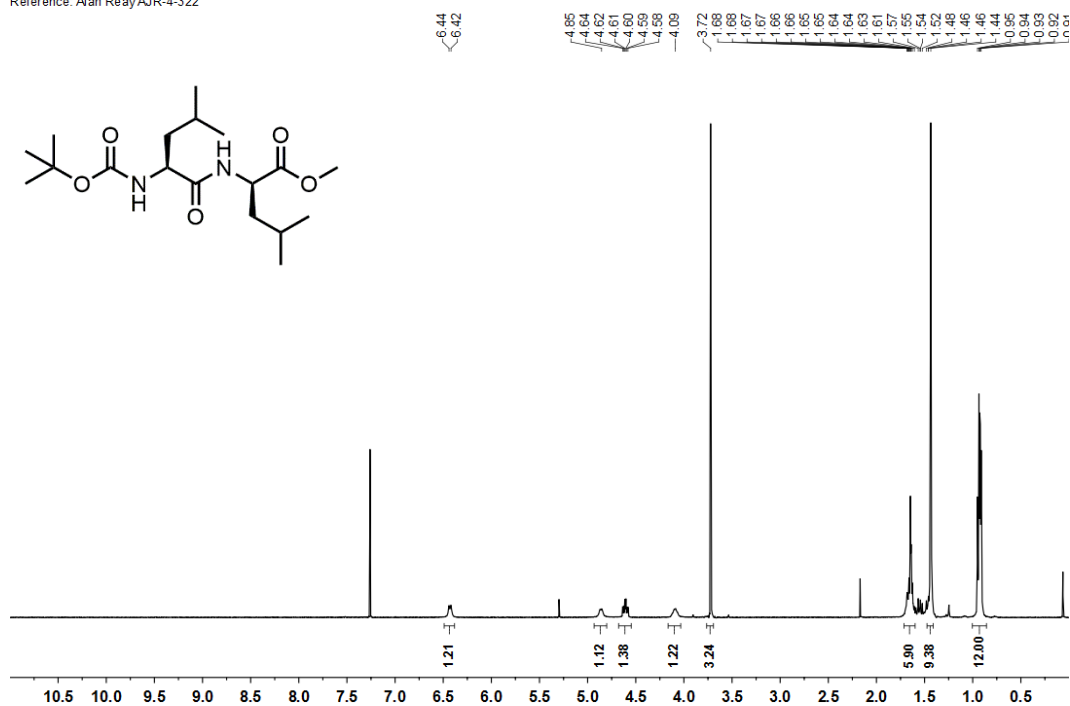
Figure 159 ^{1}H NMR spectrum of **156** (400 MHz, CDCl$_3$).
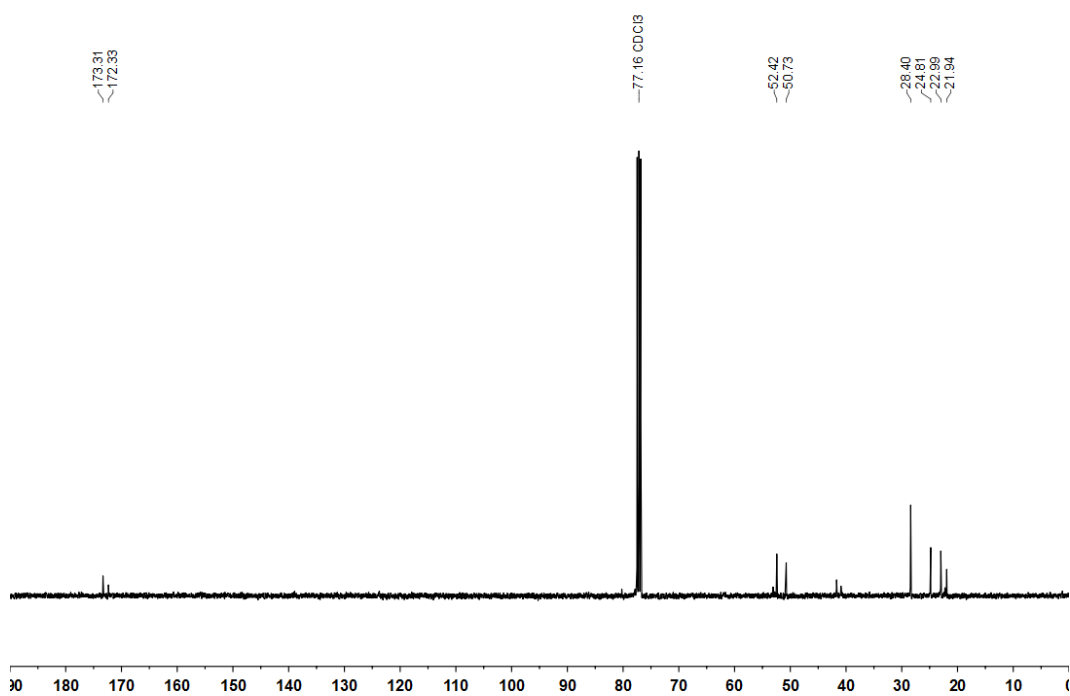
Figure 160 ^{13}C NMR spectrum of **156** (101 MHz, CDCl$_3$).
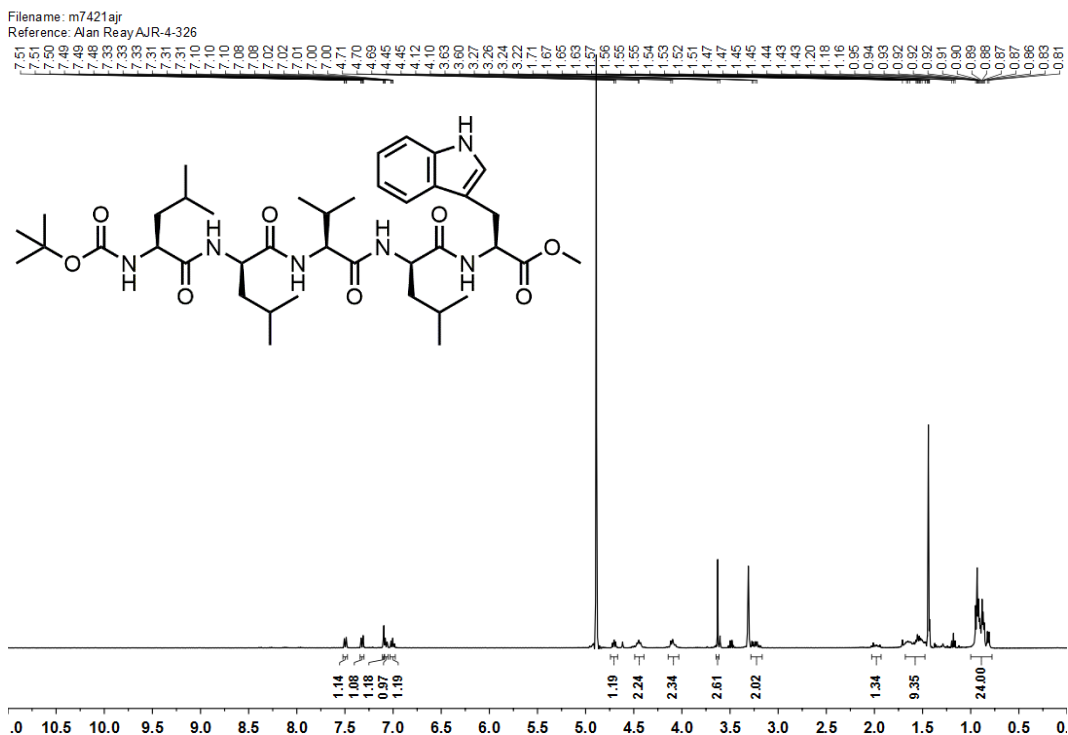
Figure 161 ^{1}H NMR spectrum of **158** (400 MHz, CDCl$_3$).
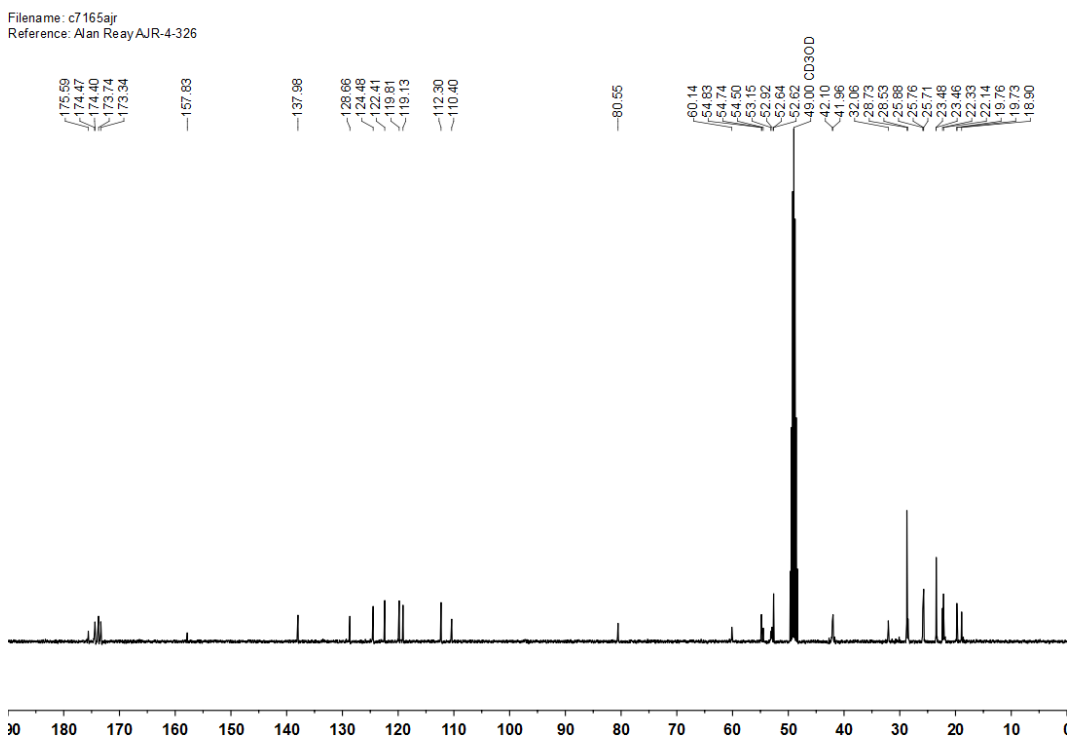
Figure 162 ^{13}C NMR spectrum of **158** (101 MHz, CDCl$_3$).

Figure 163 ^{1}H NMR spectrum of **160** (400 MHz, CDCl$_3$).
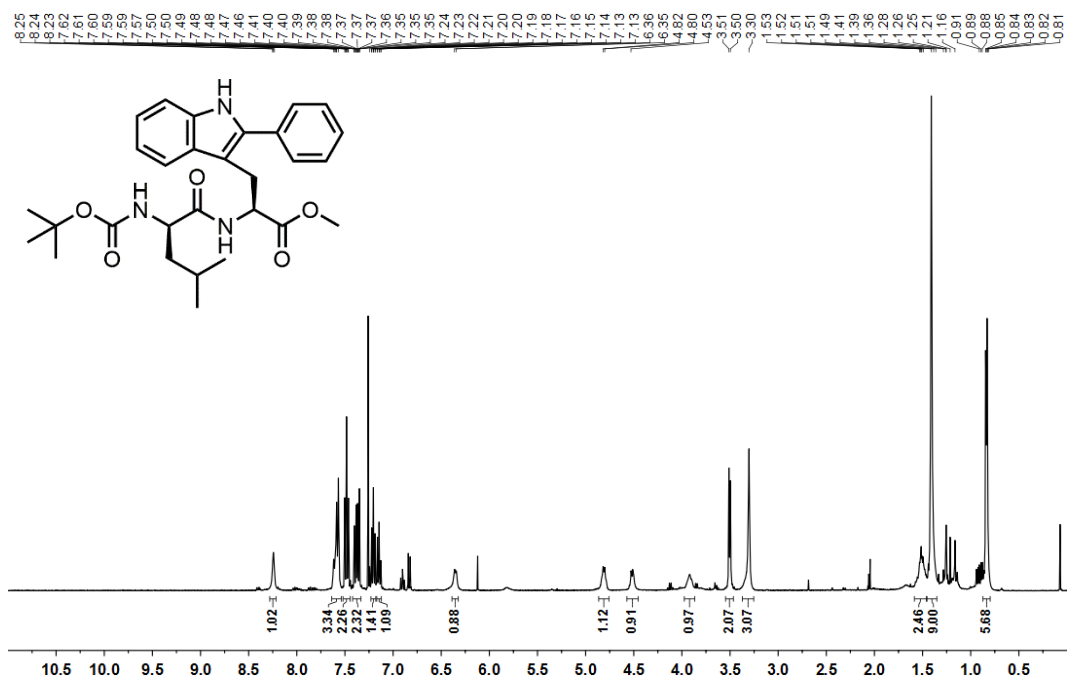
Figure 164 ^{13}C NMR spectrum of **160** (101 MHz, CDCl$_3$).
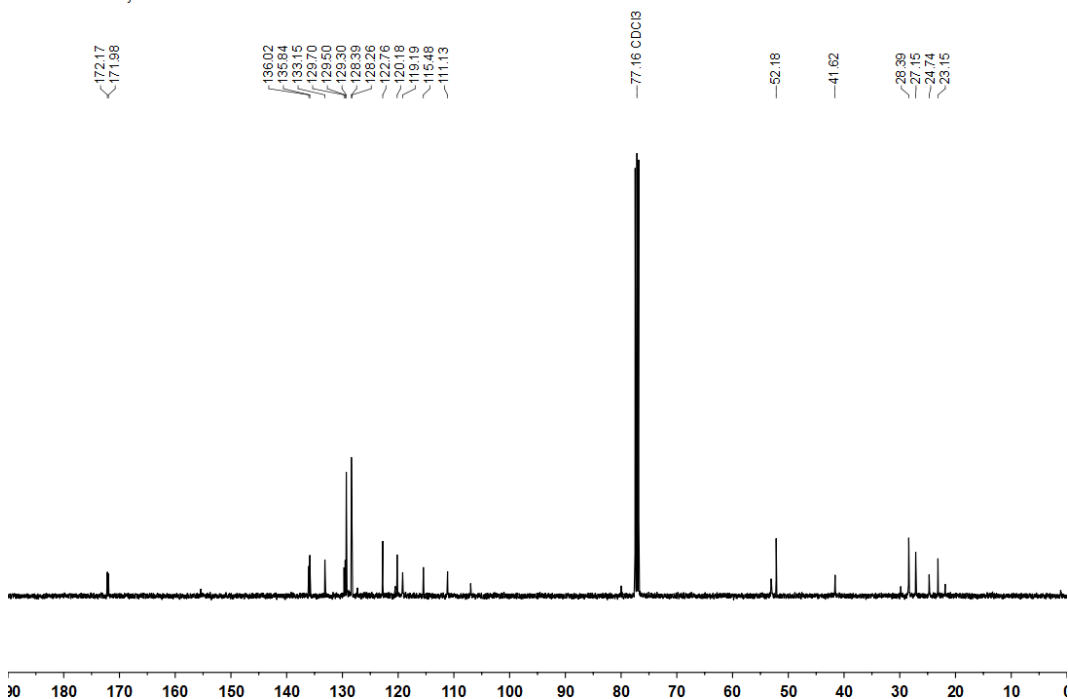
Filename: m8001ajr
Reference: Alan Reay AJR-4-337
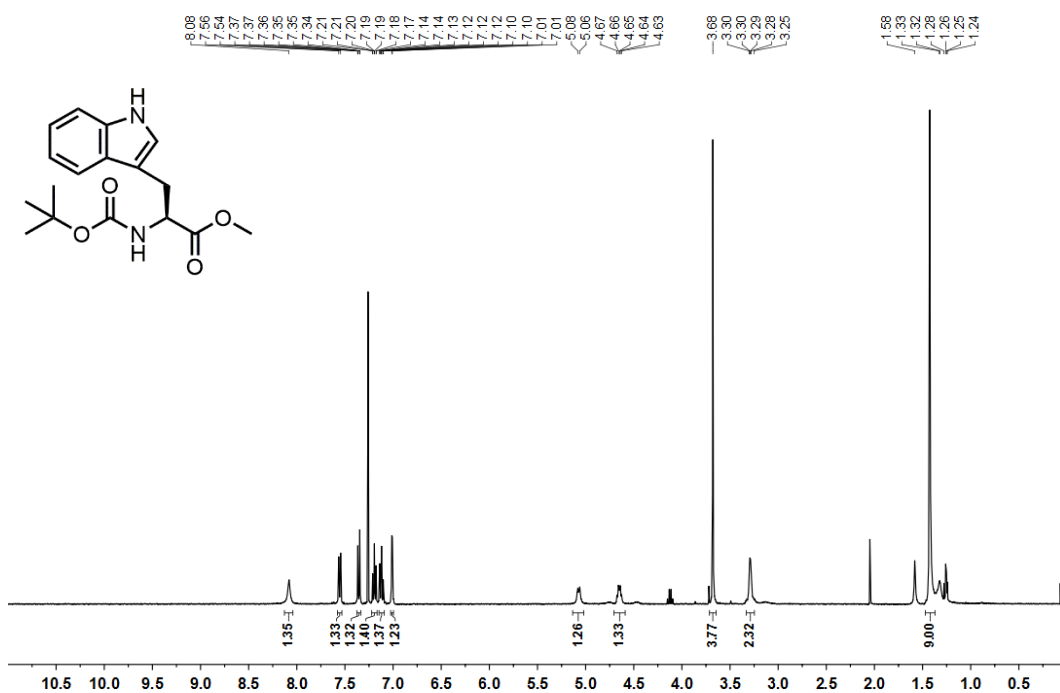
Figure 165 ¹H NMR spectrum of **161** (400 MHz, CDCl₃).

Filename: d0157ajr
Reference: Alan Reay AJR-5-423
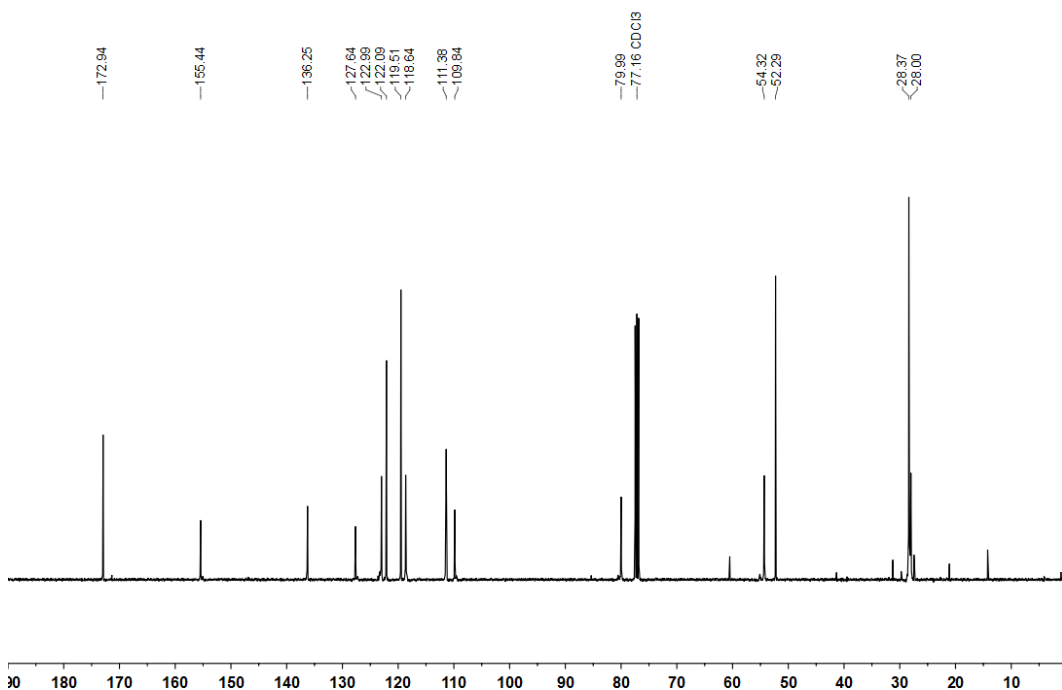
Figure 166 ¹³C NMR spectrum of **161** (101 MHz, CDCl₃).

347

Filename: m5769ajr
Reference: Alan Reay AJR-4-309

Figure 167 ^{1}H NMR spectrum of **163** (400 MHz, CD$_3$OD).

Filename: m5769ajr
Reference: Alan Reay AJR-4-309
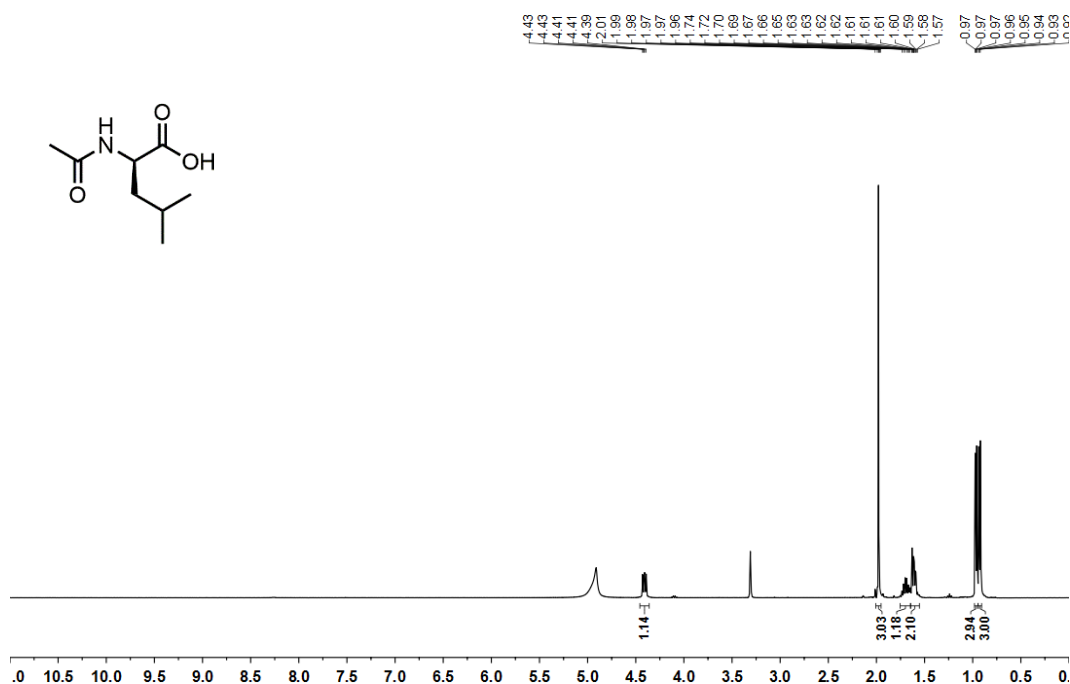
Figure 168 ^{13}C NMR spectrum of **163** (101 MHz, CD$_3$OD).
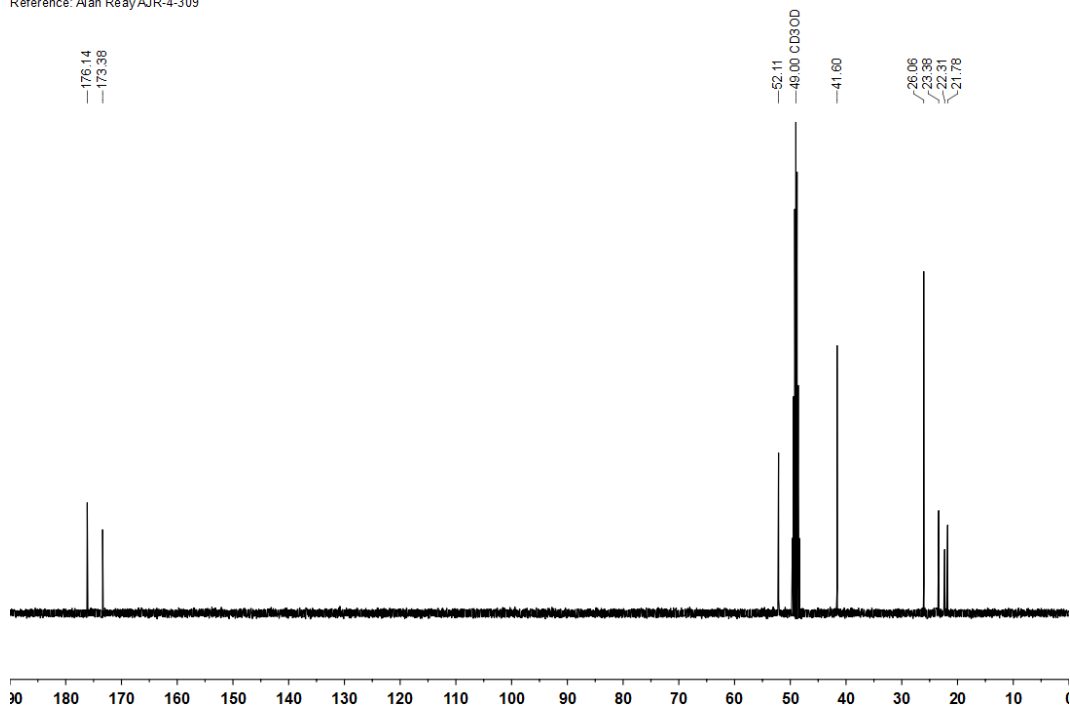
Filename: c4796ajr
Reference: Alan Reay AJR-4-343
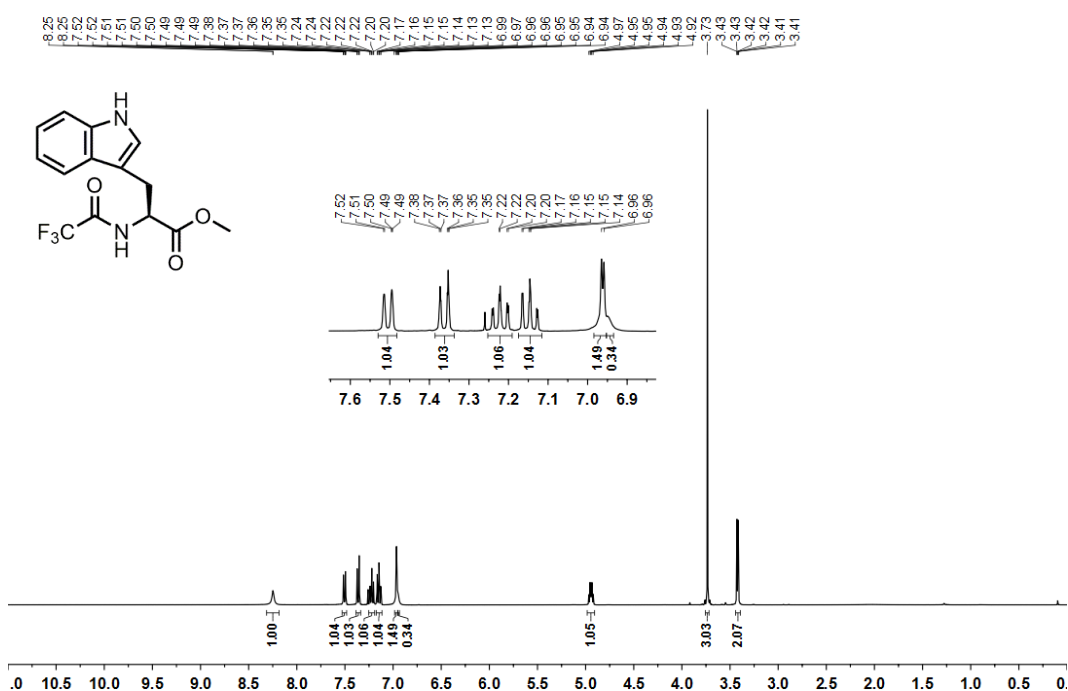
Figure 169 ^{1}H NMR spectrum of **92** (400 MHz, CDCl$_3$).

Filename: c4803ajr
Reference: Alan Reay AJR-4-343
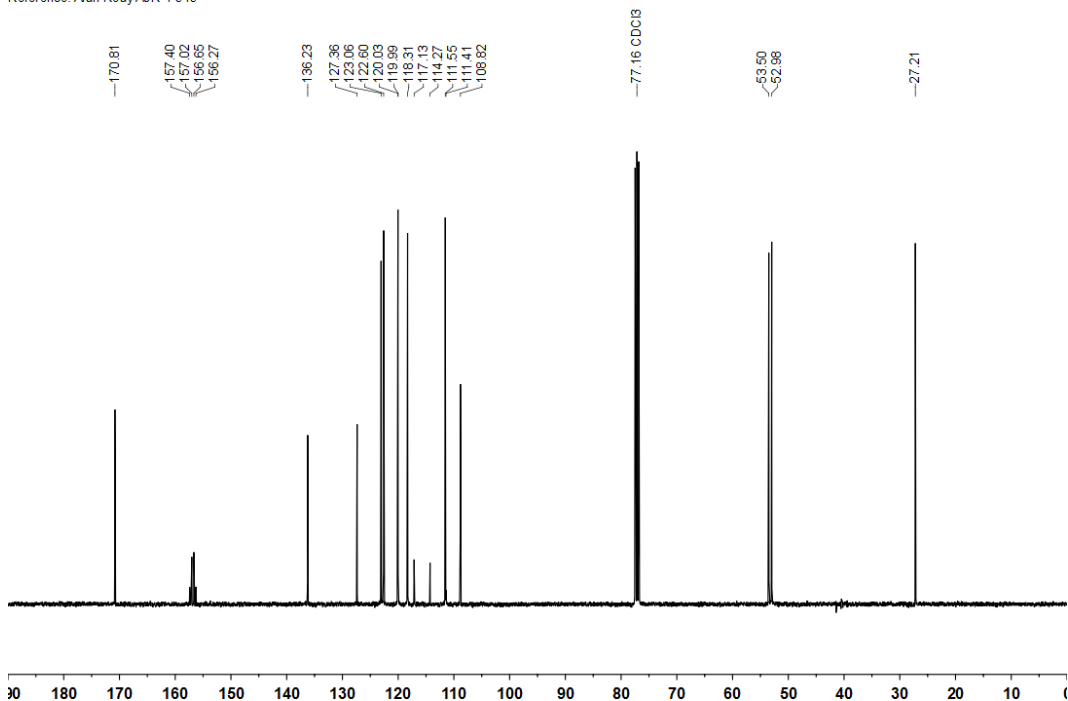
Figure 170 ^{13}C NMR spectrum of **92** (101 MHz, CDCl$_3$).

349
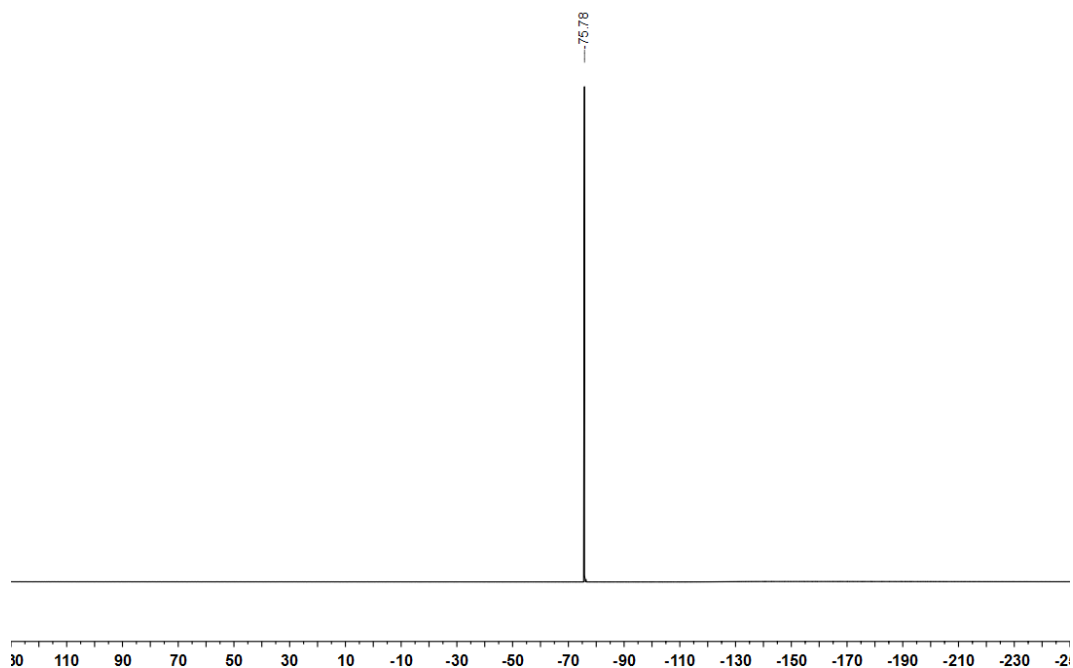
Figure 171 ^{19}F NMR spectrum of **92** (376 MHz, CDCl$_3$).

Figure 172 ^{1}H NMR spectrum of **166** (400 MHz, CDCl$_3$).

Figure 173 ^{13}C NMR spectrum of **166** (101 MHz, CDCl$_3$).

Filename: m7930ajr
Reference: Alan Reay AJR-4-334

—-77.04

80	110	90	70	50	30	10	-10	-30	-50	-70	-90	-110	-130	-150	-170	-190	-210	-230	-2	
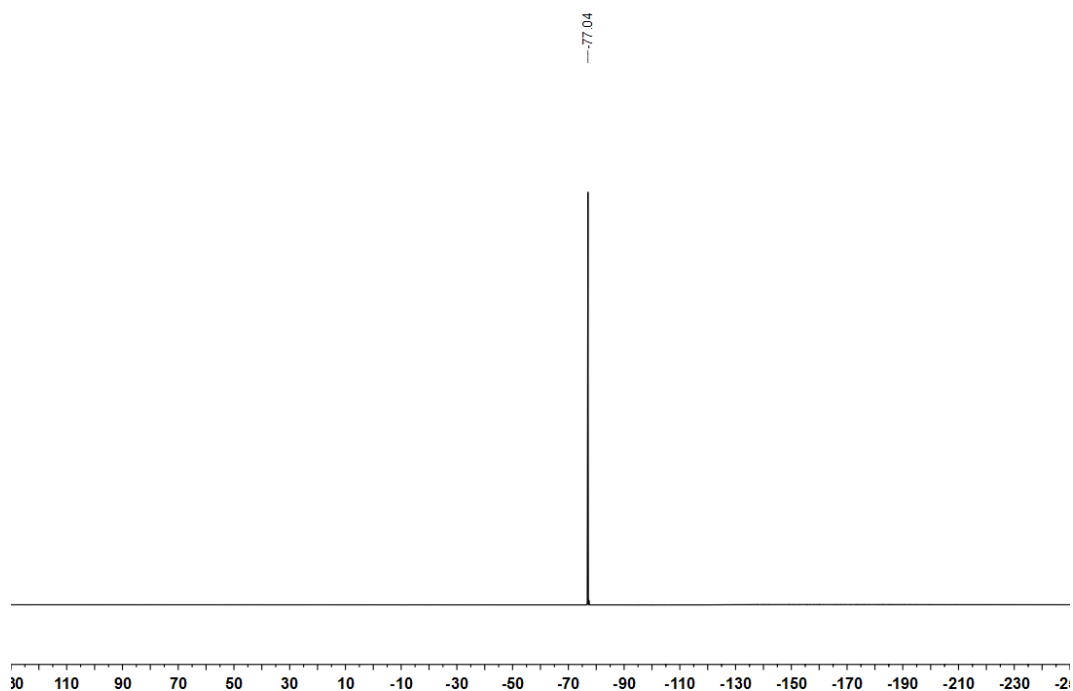
Figure 174 ^{19}F NMR spectrum of **166** (376 MHz, CDCl$_3$).

Figure 175 ^{1}H NMR spectrum of **167** (400 MHz, CDCl$_3$).

Figure 176 ^{13}C NMR spectrum of **167** (101 MHz, CDCl$_3$).

Filename: c4735ajr
Reference: Alan Reay AJR-4-344

—-75.57

| 180 | 160 | 140 | 120 | 100 | 80 | 60 | 40 | 20 | 0 | -20 | -40 | -60 | -80 | -100 | -120 | -140 | -160 | -180 |
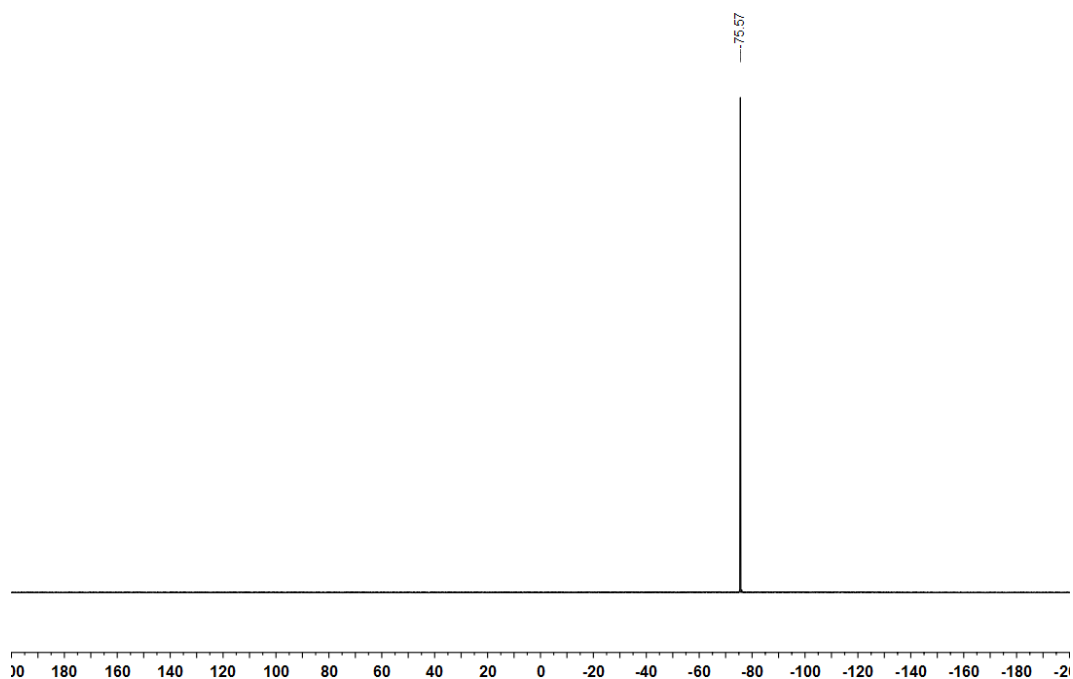
Figure 177 ^{19}F NMR spectrum of **167** (376 MHz, CDCl$_3$).

Figure 178 ^{1}H NMR spectrum of **169** (400 MHz, CD$_3$OD).

Figure 179 ^{13}C NMR spectrum of **169** (101 MHz, CD$_3$OD).

Filename: c4443ajr
Reference: Alan Reay AJR-4-342

—77.33

```
)0  180  160  140  120  100   80   60   40   20    0   -20  -40  -60  -80  -100 -120 -140 -160 -180  -2(
```
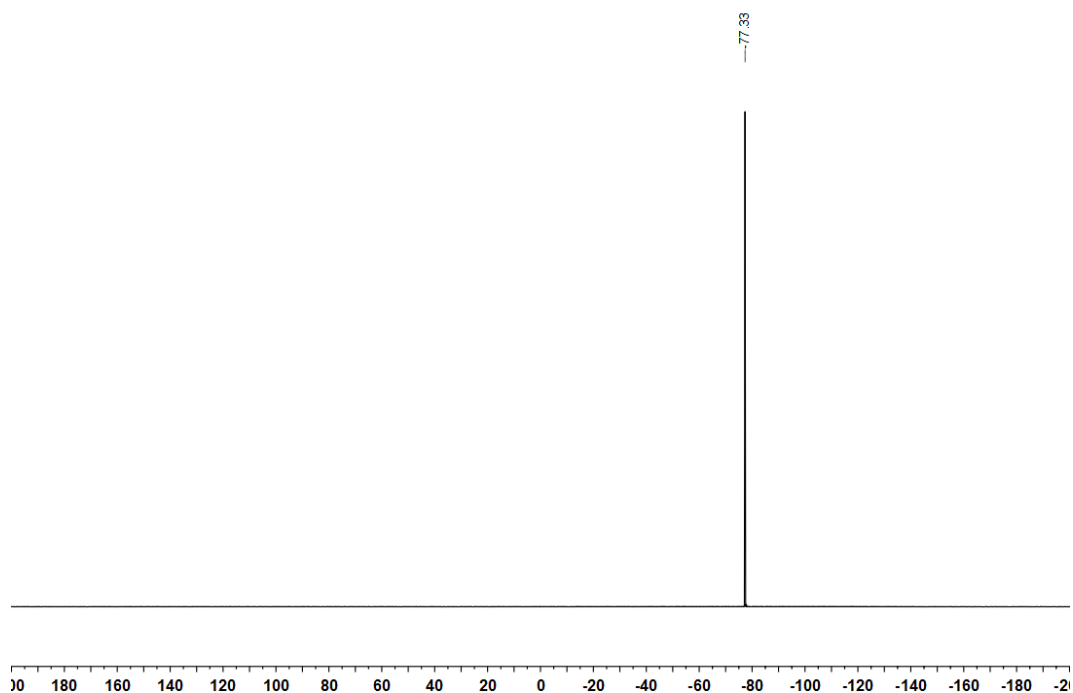
Figure 180 ^{19}F NMR spectrum of **169** (376 MHz, CDCl$_3$).

Figure 181 ^{1}H NMR spectrum of **170** (400 MHz, CDCl$_3$).

Figure 182 ^{13}C NMR spectrum of **170** (101 MHz, CDCl$_3$).

Filename: c4736ajr
Reference: Alan Reay AJR-4-345-1

—75.59

00	180	160	140	120	100	80	60	40	20	0	-20	-40	-60	-80	-100	-120	-140	-160	-180	-2
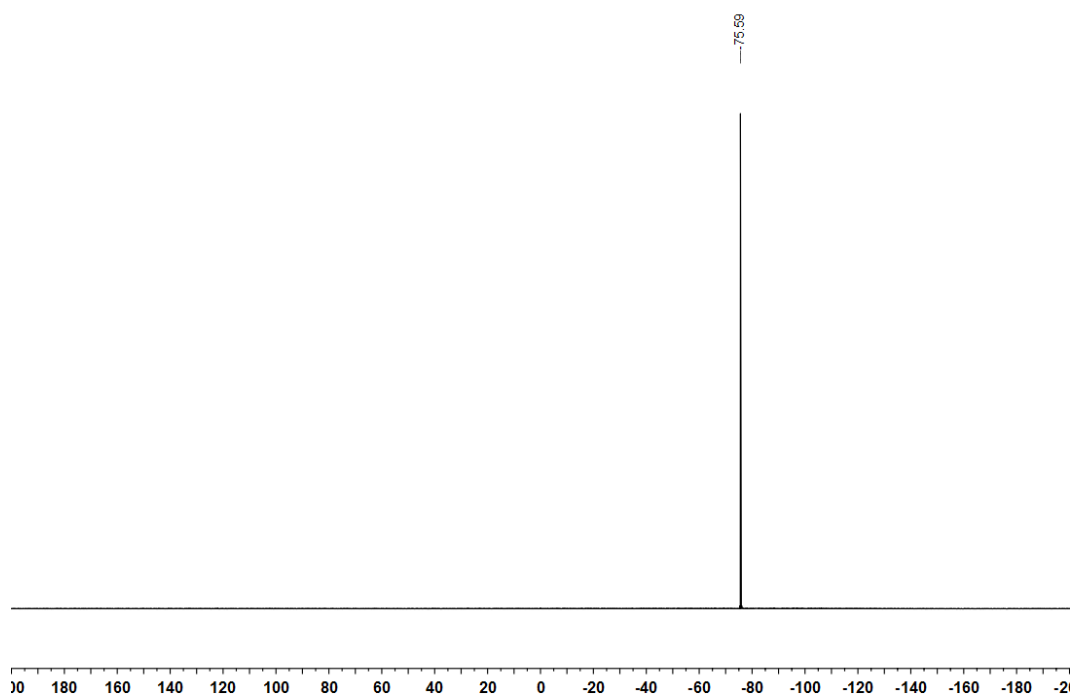
Figure 183 ^{19}F NMR spectrum of **170** (376 MHz, CDCl$_3$).

Figure 184 ^{1}H NMR spectrum of **171** (400 MHz, CDCl$_3$).

Figure 185 ^{13}C NMR spectrum of **171** (101 MHz, CDCl$_3$).

Filename: m8655ajr
Reference: Alan Reay AJR-4-346-2

—-75.88

| 150 | 130 | 110 | 90 | 70 | 50 | 30 | 10 | -10 | -30 | -50 | -70 | -90 | -110 | -130 | -150 | -170 | -190 | -210 | -230 | -2 |
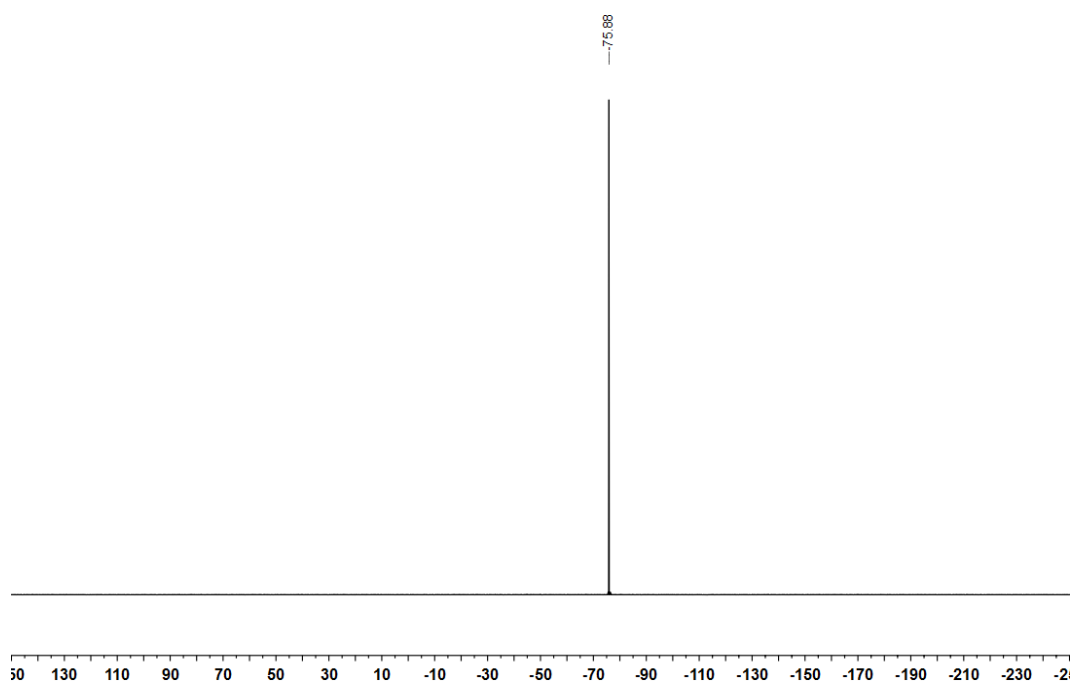
Figure 186 ^{19}F NMR spectrum of **171** (376 MHz, CDCl$_3$).

Figure 187 ^{1}H NMR spectrum of **172** (400 MHz, CDCl$_3$).

Figure 188 ^{13}C NMR spectrum of **172** (101 MHz, CDCl$_3$).

Filename: d0671ajr
Reference: Alan Reay AJR-5-427

—−75.73

00	180	160	140	120	100	80	60	40	20	0	-20	-40	-60	-80	-100	-120	-140	-160	-180	-2
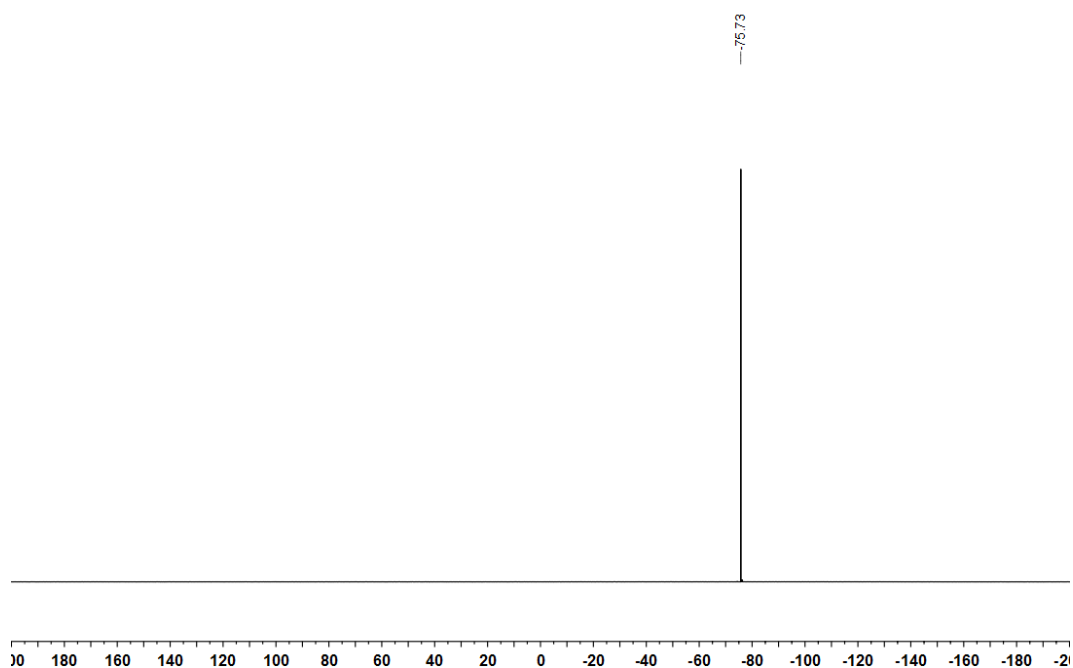
Figure 189 ^{19}F NMR spectrum of **172** (376 MHz, CDCl$_3$).

Figure 190 ^{1}H NMR spectrum of **173** (400 MHz, CDCl$_3$).

Figure 191 ^{13}C NMR spectrum of **173** (101 MHz, CDCl$_3$).
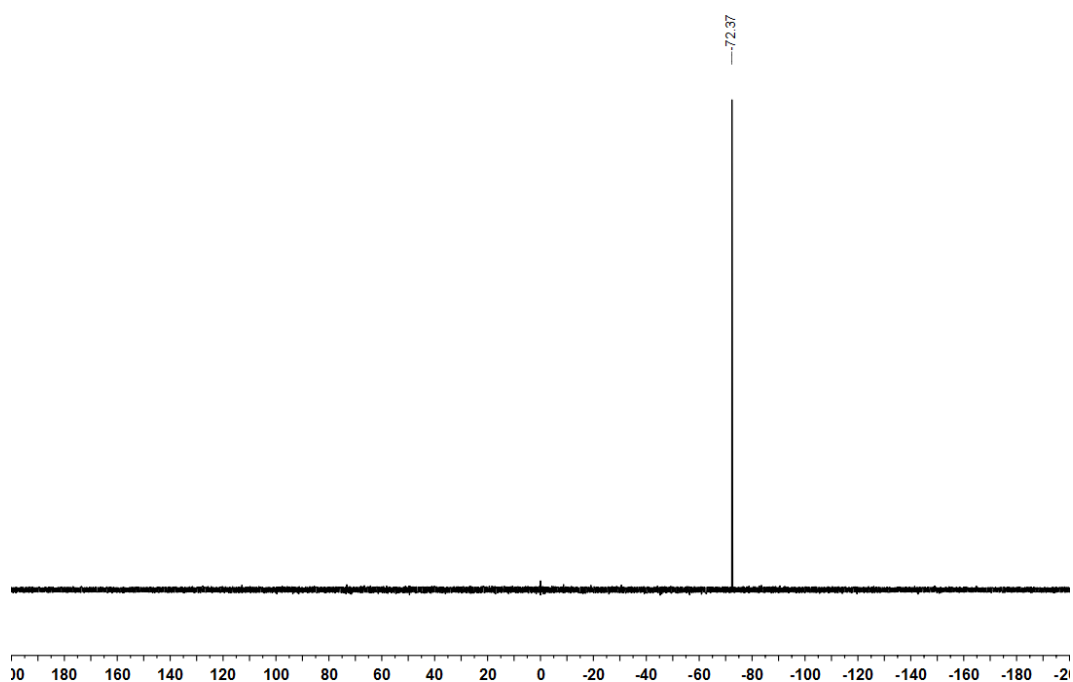
Figure 192 ^{19}F NMR spectrum of **173** (376 MHz, CDCl$_3$).

Figure 193 ^{1}H NMR spectrum of **174** (400 MHz, CDCl$_3$).
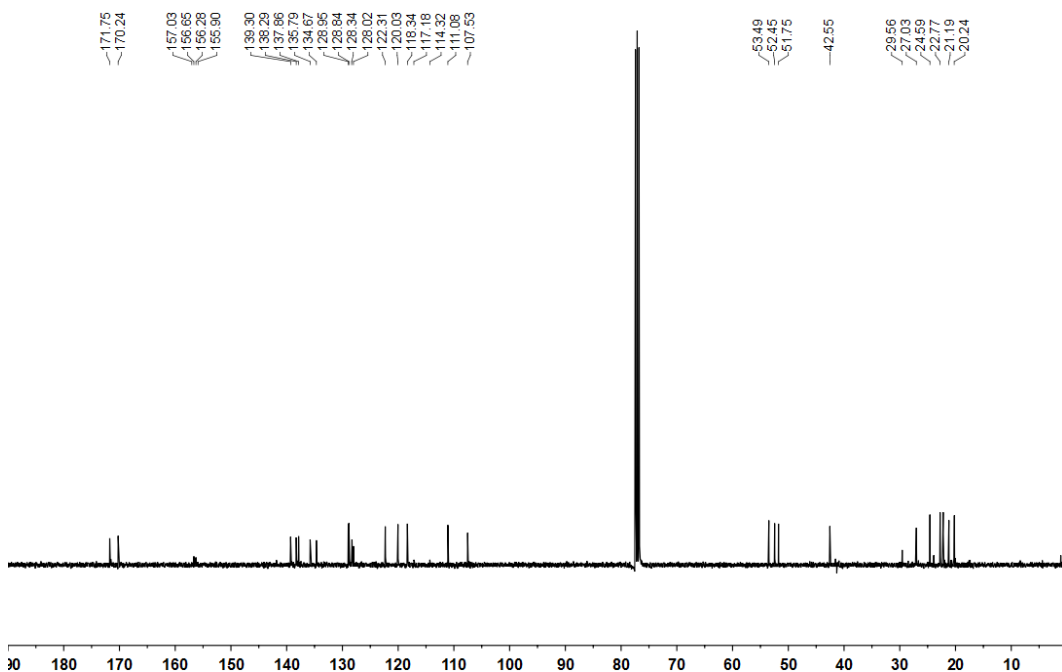
Figure 194 ^{13}C NMR spectrum of **174** (101 MHz, CDCl$_3$).

Filename: m8656ajr
Reference: Alan Reay AJR-4-348-1

—-75.76

| 50 | 130 | 110 | 90 | 70 | 50 | 30 | 10 | -10 | -30 | -50 | -70 | -90 | -110 | -130 | -150 | -170 | -190 | -210 | -230 | -2 |
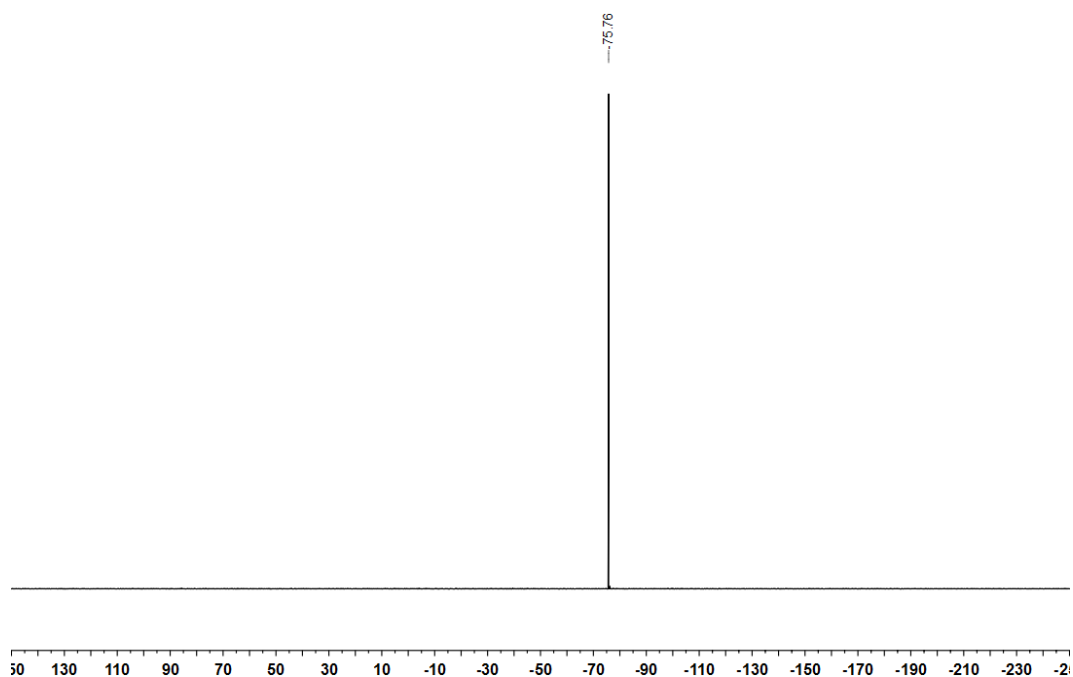
Figure 195 ^{19}F NMR spectrum of **174** (376 MHz, CDCl$_3$).

Filename: m8619ajr
Reference: Alan Reay AJR-4-349-2
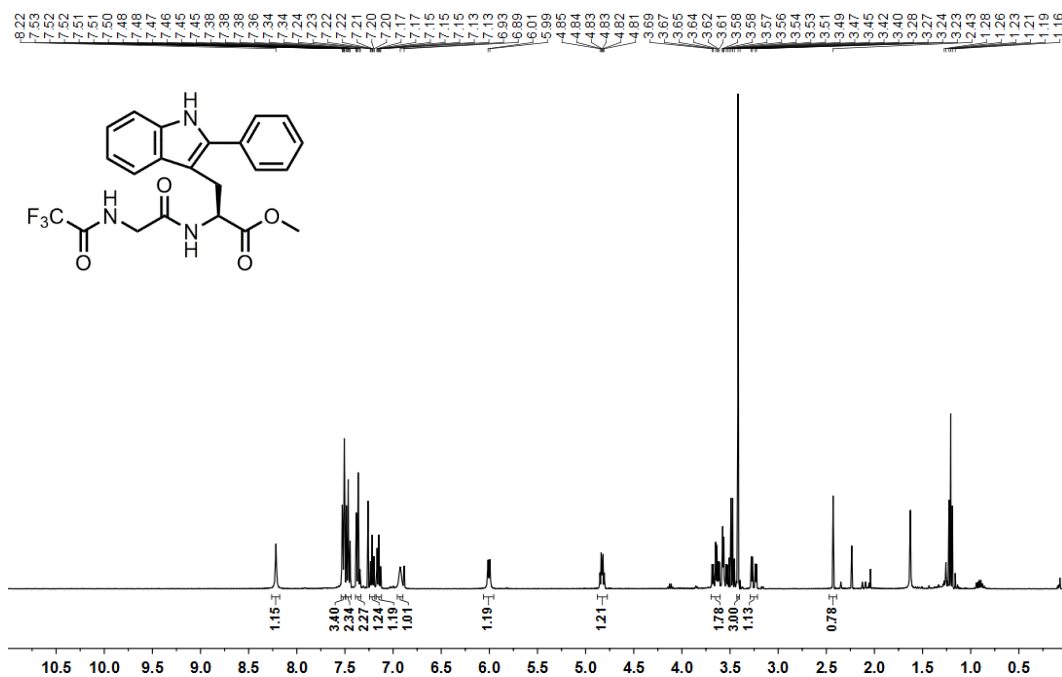
Figure 196 ^{1}H NMR spectrum of **175** (400 MHz, CDCl$_3$).

Filename: c7042ajr
Reference: Alan Reay AJR-4-349-2
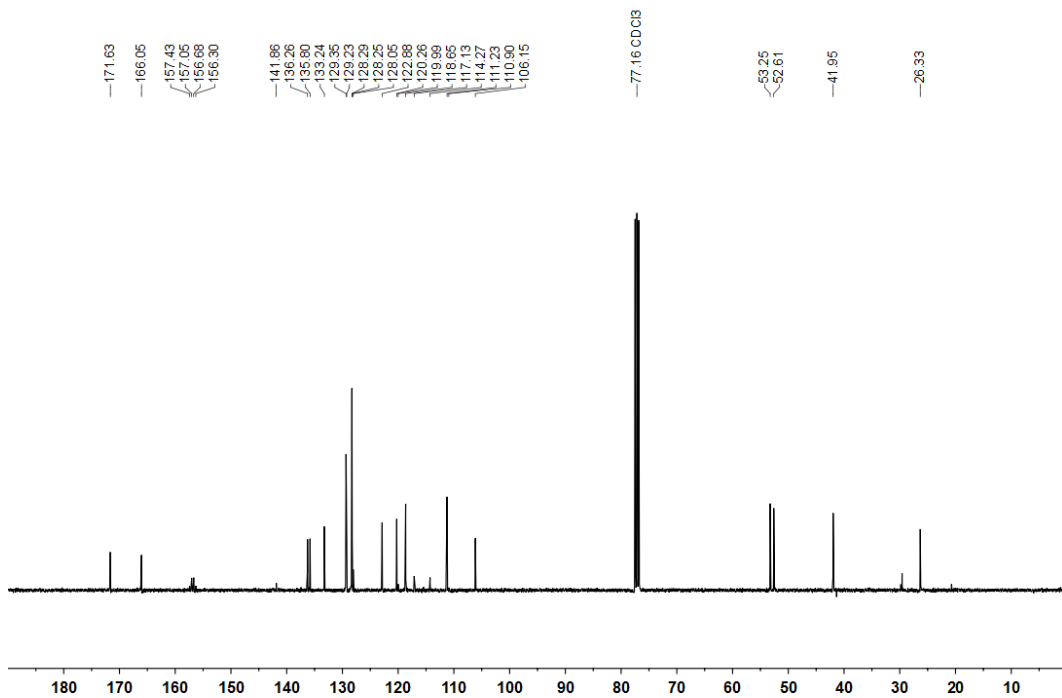
Figure 197 ^{13}C NMR spectrum of **175** (101 MHz, CDCl$_3$).

Filename: m8619ajr
Reference: Alan Reay AJR-4-349-2
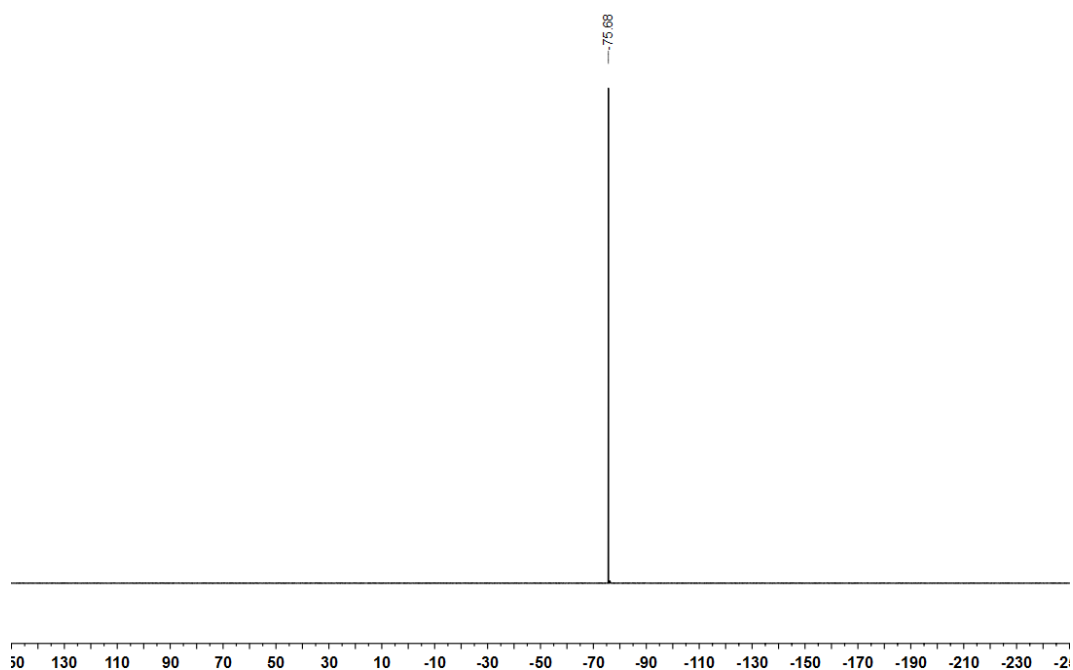
Figure 198 ^{19}F NMR spectrum of **175** (376 MHz, CDCl$_3$).

Filename: d0838ajr
Reference: Alan Reay AJR-5-429

Figure 199 ^{1}H NMR spectrum of **176** (400 MHz, CDCl$_3$).

Filename: d0838ajr
Reference: Alan Reay AJR-5-429

Figure 200 ^{13}C NMR spectrum of **176** (101 MHz, CDCl$_3$).

Filename: d0743ajr
Reference: Alan Reay AJR-5-429

—75.66

| | | | | | | | | | | | | | | | | | | | | |
|00|180|160|140|120|100|80|60|40|20|0|-20|-40|-60|-80|-100|-120|-140|-160|-180|-2|
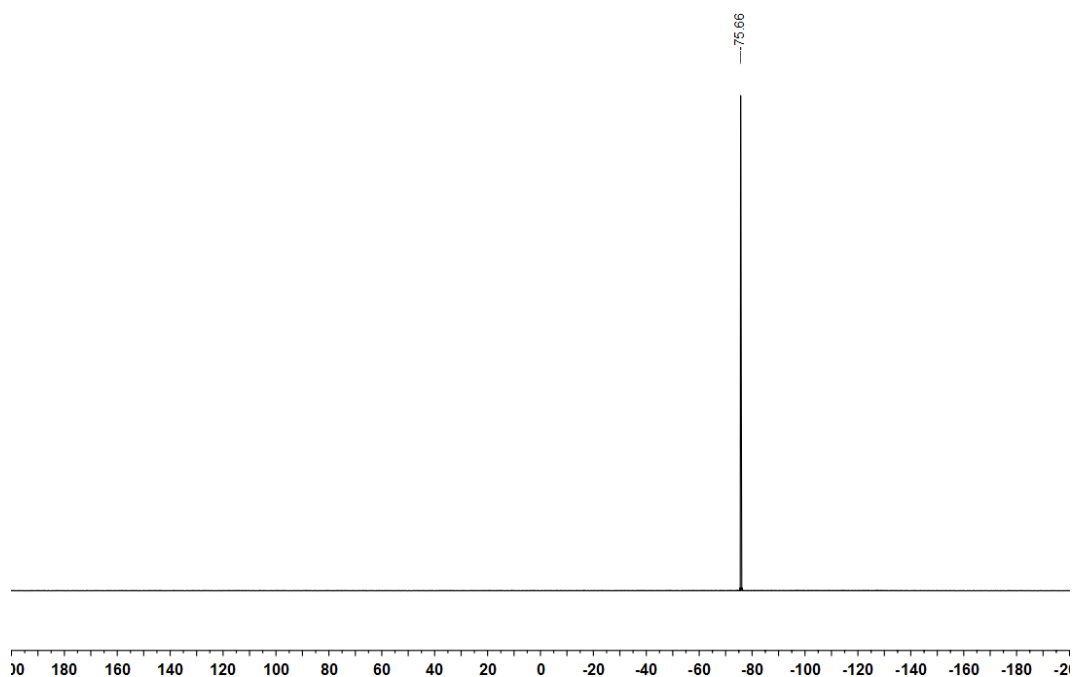
Figure 201 ^{19}F NMR spectrum of **176** (376 MHz, CDCl$_3$).
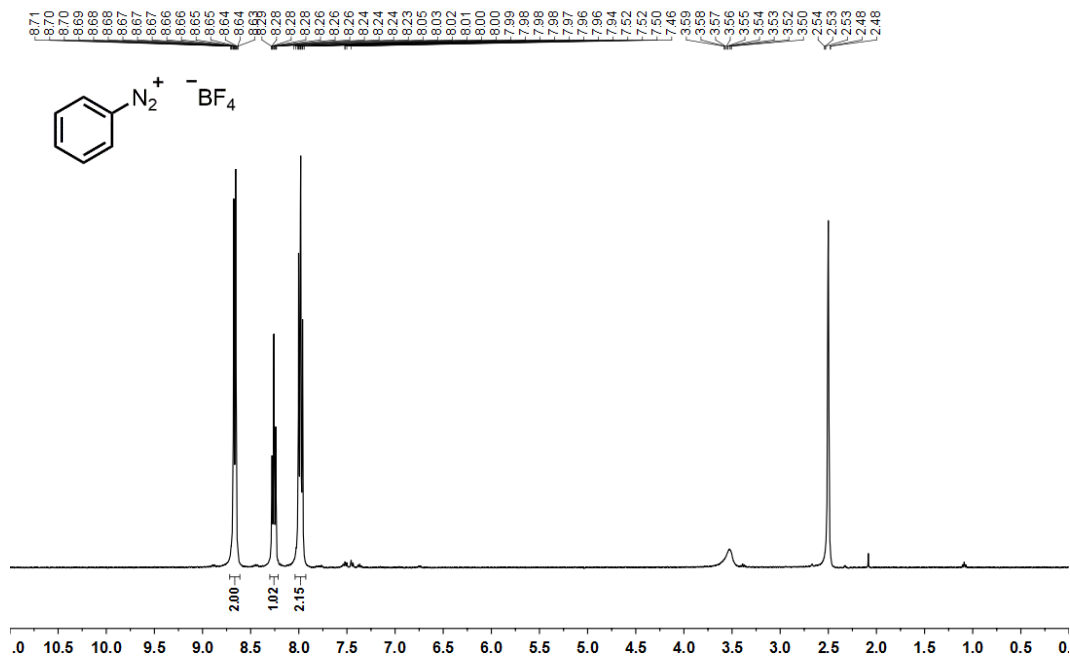
Figure 202 ^{1}H NMR spectrum of **48** (400 MHz, (CD$_3$)$_2$SO).
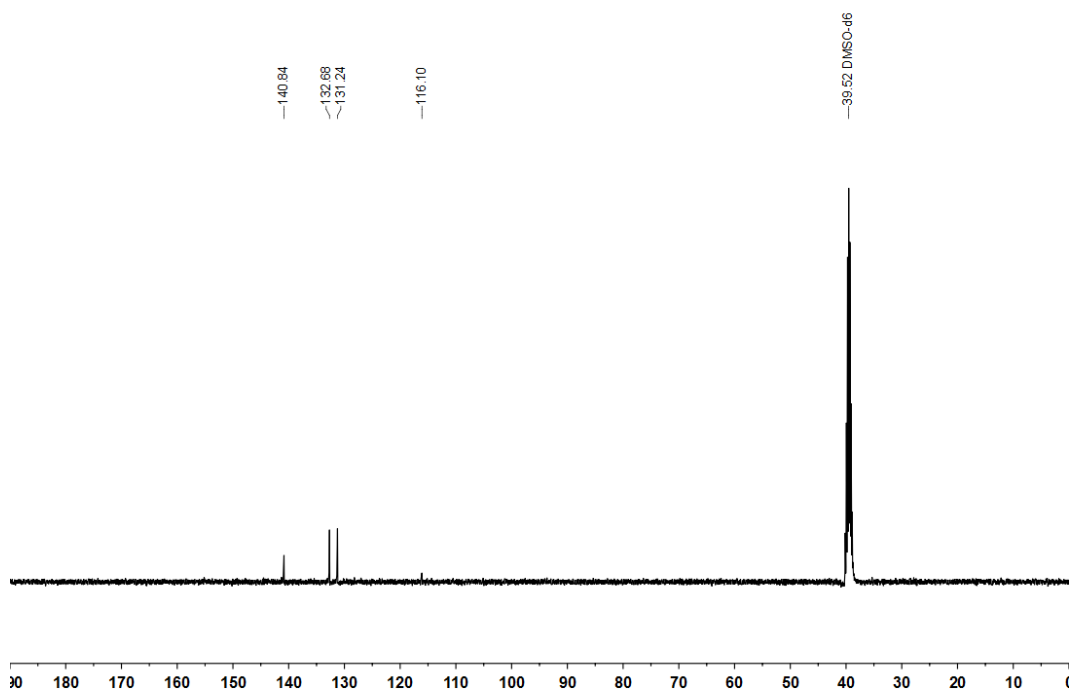
Figure 203 ^{13}C NMR spectrum of **48** (101 MHz, (CD$_3$)$_2$SO).

371

—2.26

120 110 100 90 80 70 60 50 40 30 20 10 0 -10 -20 -30 -40 -50 -60 -70 -80 -90 -100 -110 -120
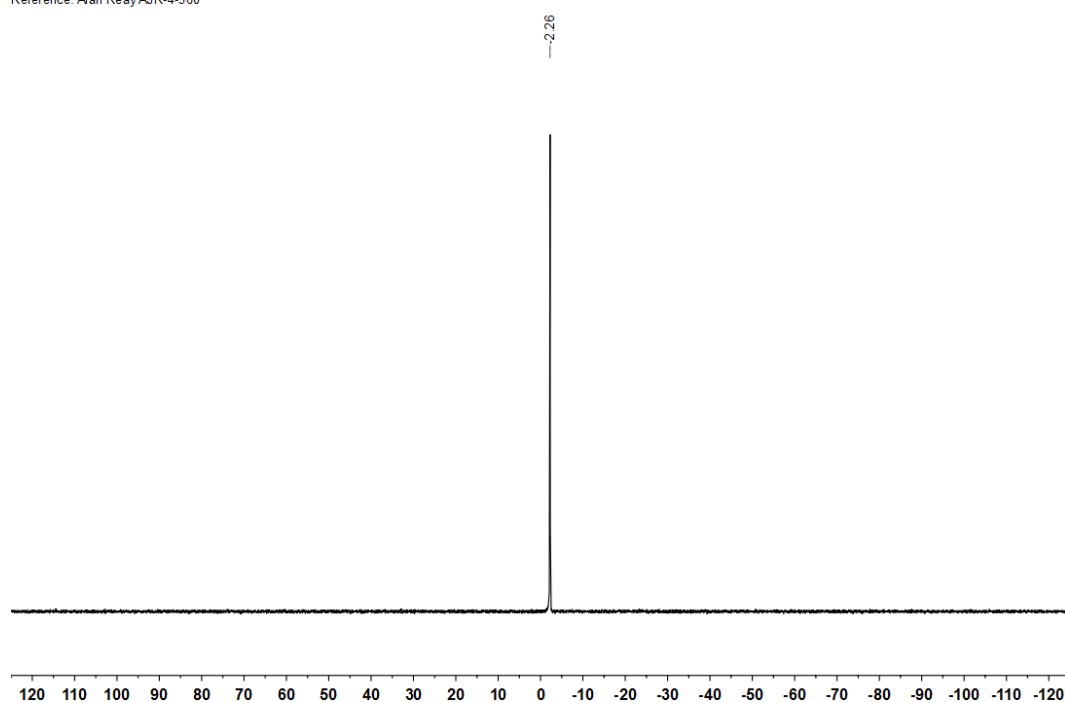
Figure 204 ^{11}B NMR spectrum of **48** (128 MHz, $(CD_3)_2SO$).

148.06
148.12

—148.06
—148.12

-147.9 -148.0 -148.1 -148.2 -148.3

00 180 160 140 120 100 80 60 40 20 0 -20 -40 -60 -80 -100 -120 -140 -160 -180 -2(
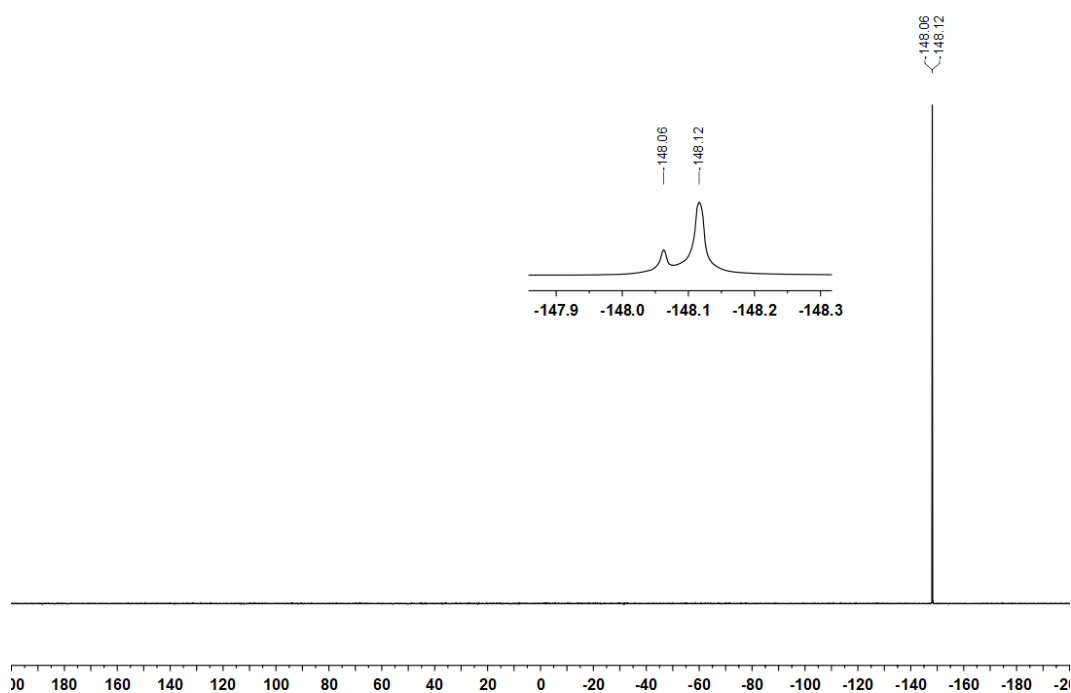
Figure 205 ^{19}F NMR spectrum of **48** (376 MHz, $(CD_3)_2SO$).
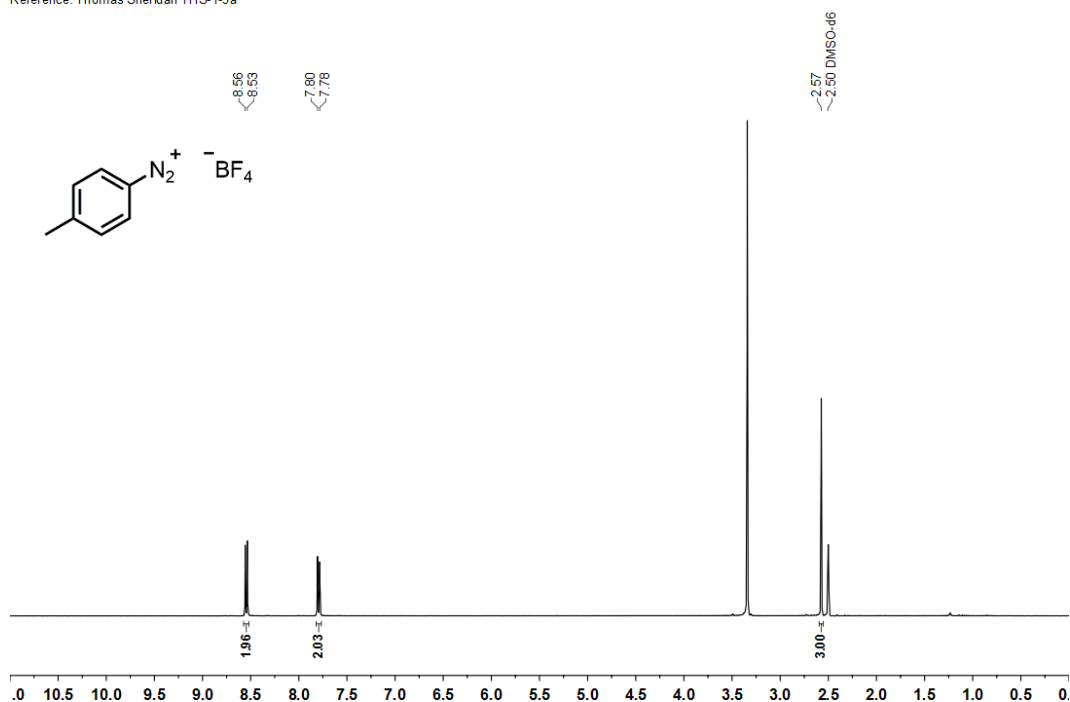
Figure 206 ^{1}H NMR spectrum of **192** (400 MHz, (CD$_3$)$_2$SO).
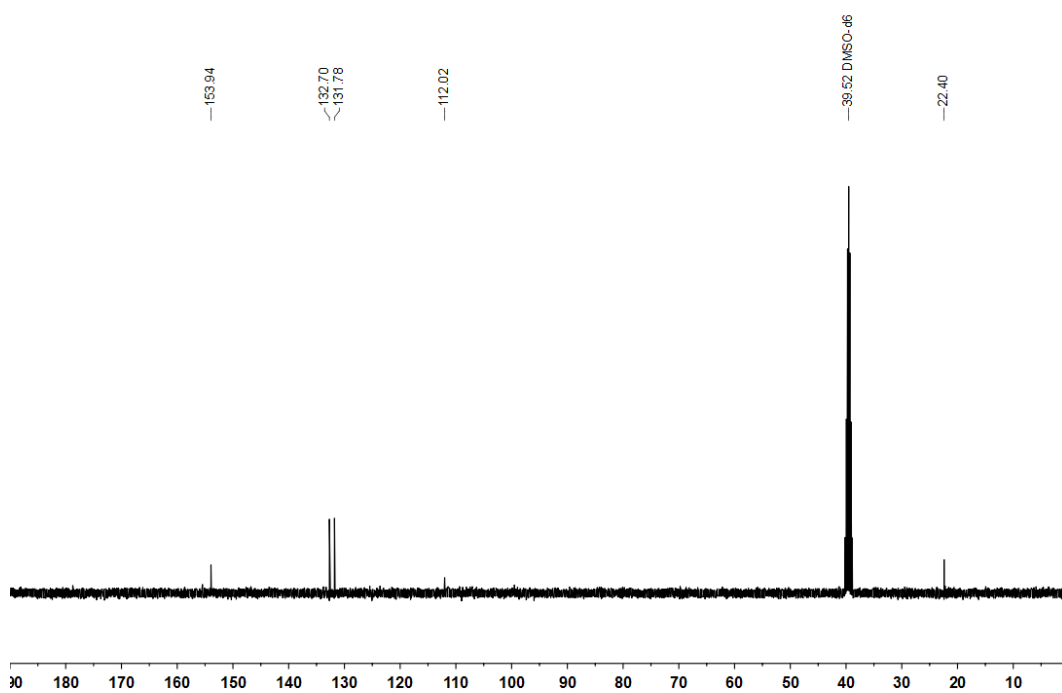
Figure 207 ^{13}C NMR spectrum of **192** (101 MHz, (CD$_3$)$_2$SO).

Filename: a3628ths
Reference: Thomas Sheridan THS-1-3a (boron)

—2.27
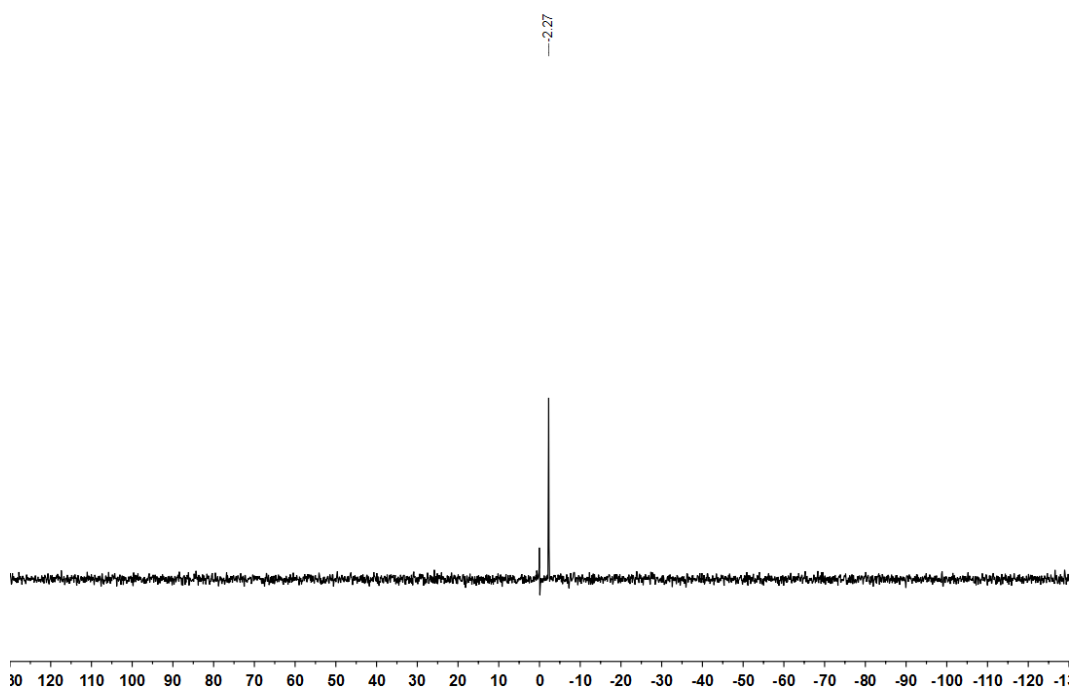
Figure 208 ^{11}B NMR spectrum of **192** (128 MHz, (CD$_3$)$_2$SO).

Filename: a3628ths
Reference: Thomas Sheridan THS-1-3a (Fluorine)

148.08
148.14
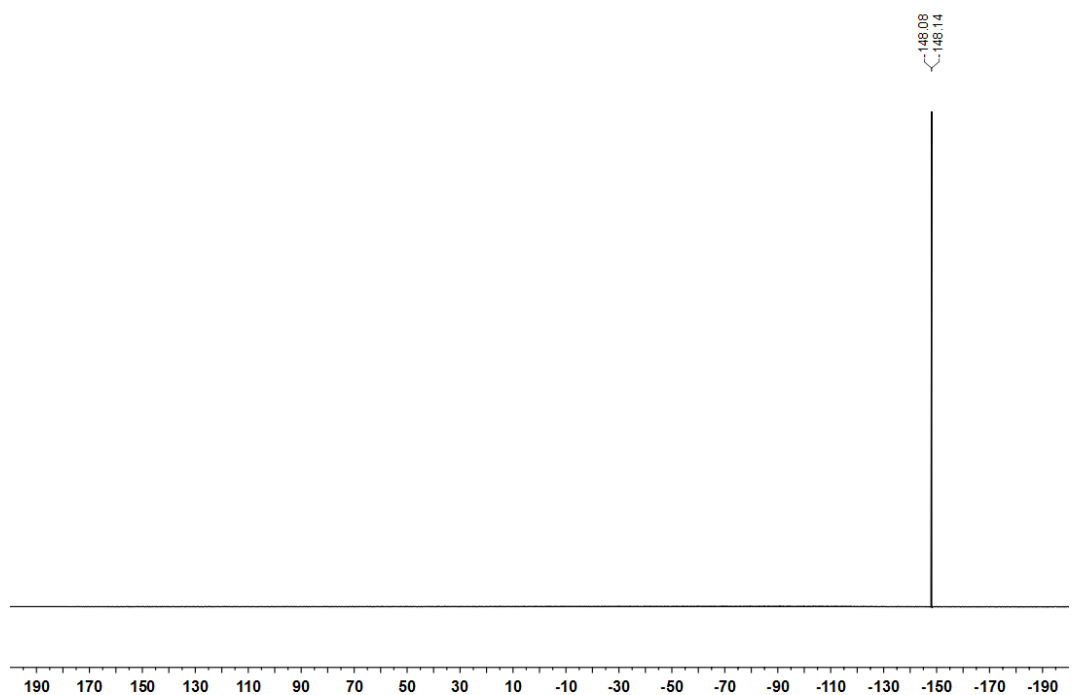
Figure 209 ^{19}F NMR spectrum of **192** (376 MHz, (CD$_3$)$_2$SO).

374
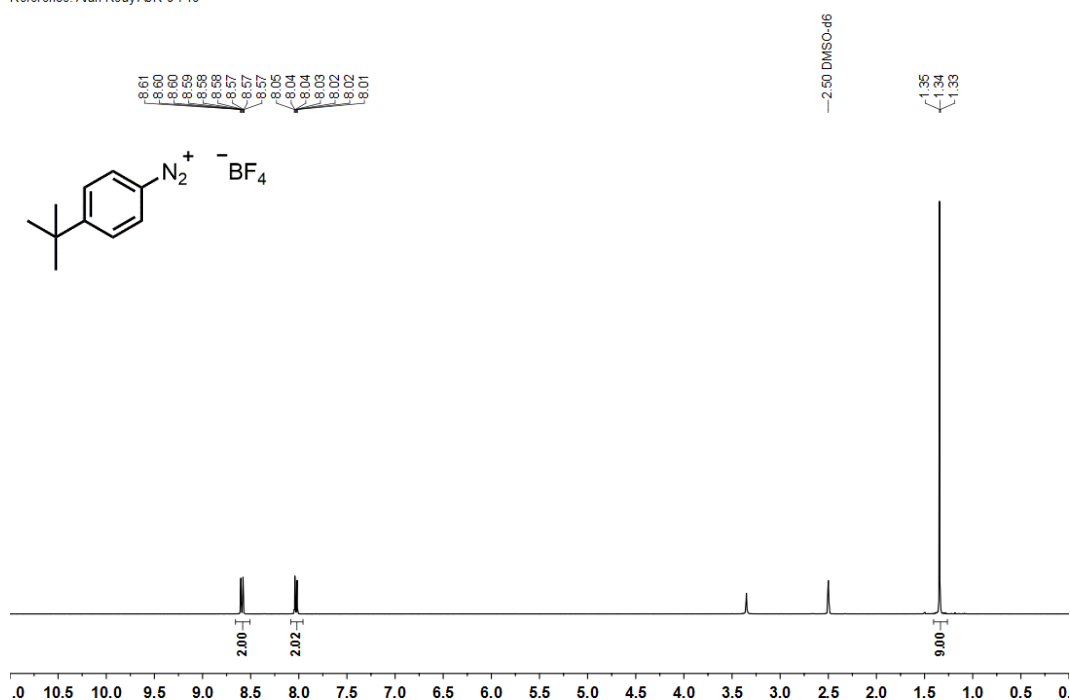
Figure 210 ^{1}H NMR spectrum of **193** (400 MHz, (CD$_3$)$_2$SO).
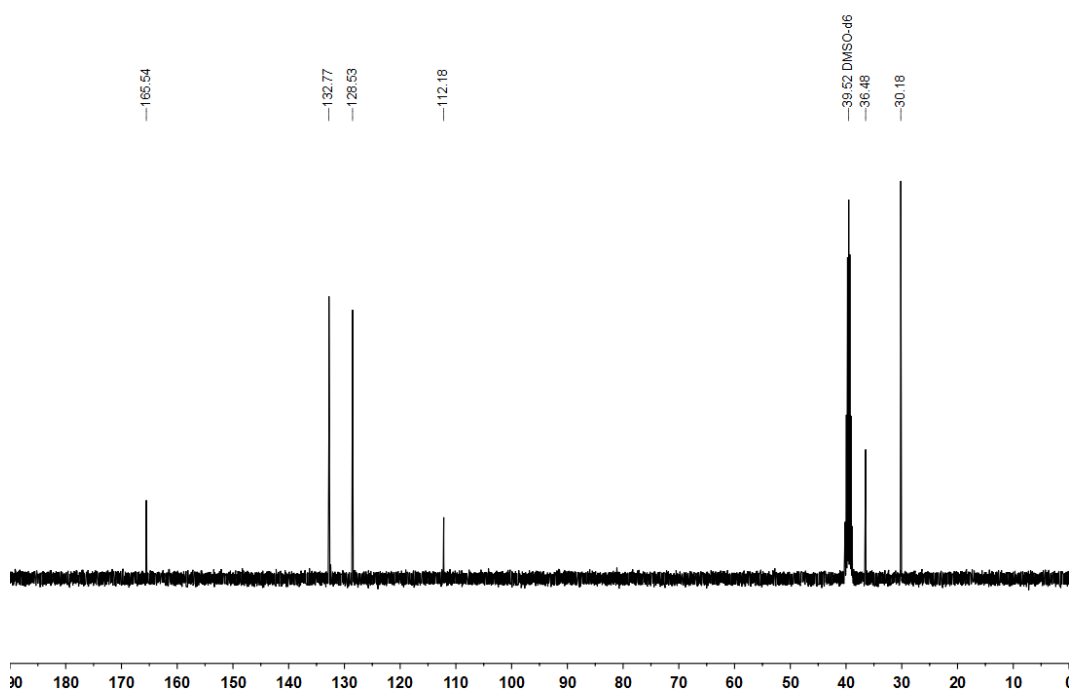
Figure 211 ^{13}C NMR spectrum of **193** (101 MHz, (CD$_3$)$_2$SO).

—2.27
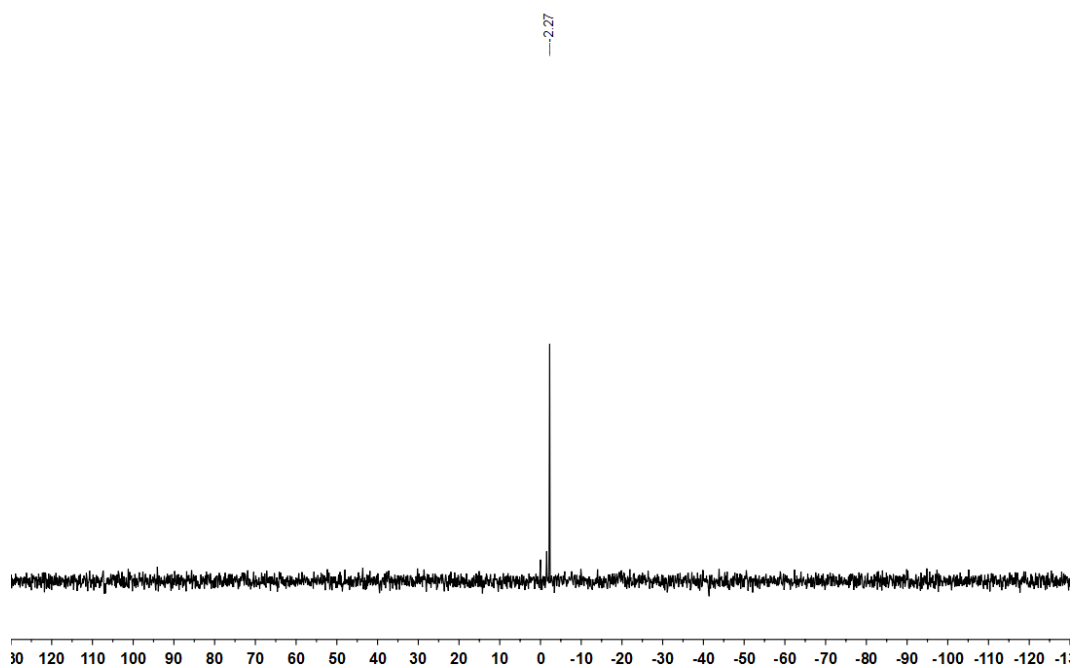
Figure 212 ^{11}B NMR spectrum of **193** (128 MHz, (CD$_3$)$_2$SO).

148.08
148.09
148.13
148.14
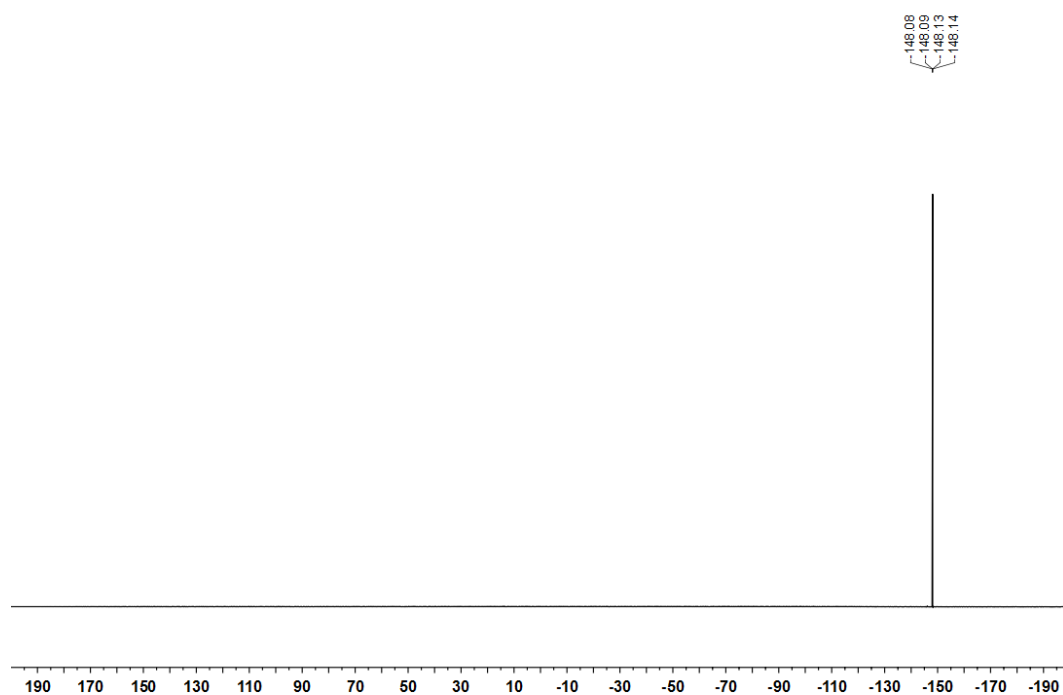
Figure 213 ^{19}F NMR spectrum of **193** (376 MHz, (CD$_3$)$_2$SO).
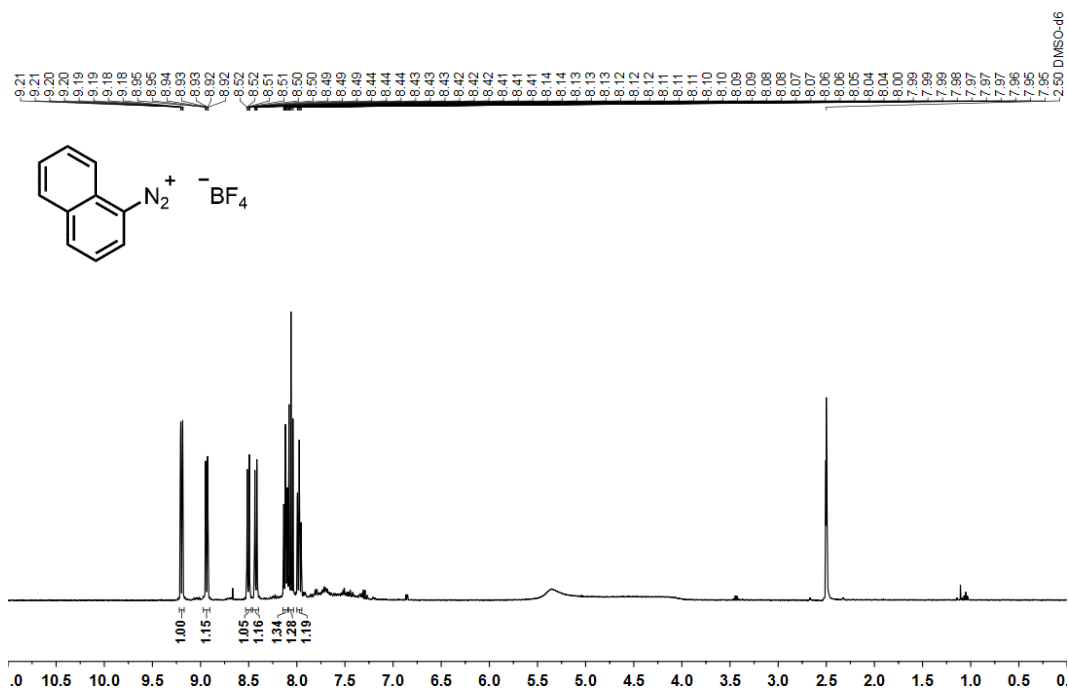
Figure 214 ^{1}H NMR spectrum of **194** (400 MHz, (CD$_3$)$_2$SO).
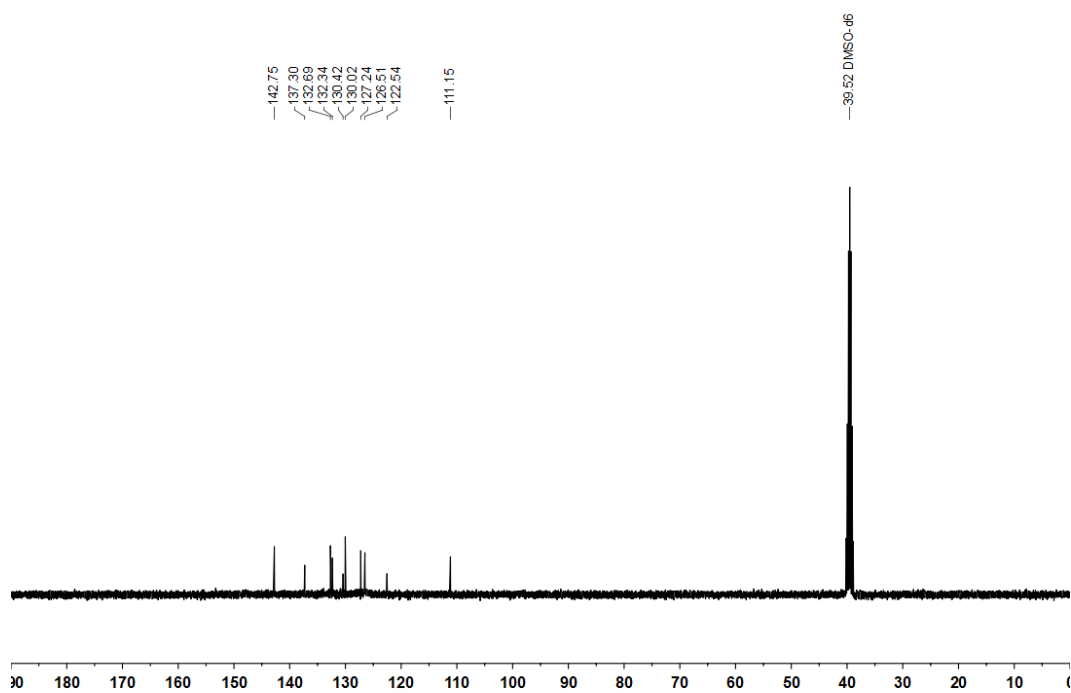
Figure 215 ^{13}C NMR spectrum of **194** (101 MHz, (CD$_3$)$_2$SO).
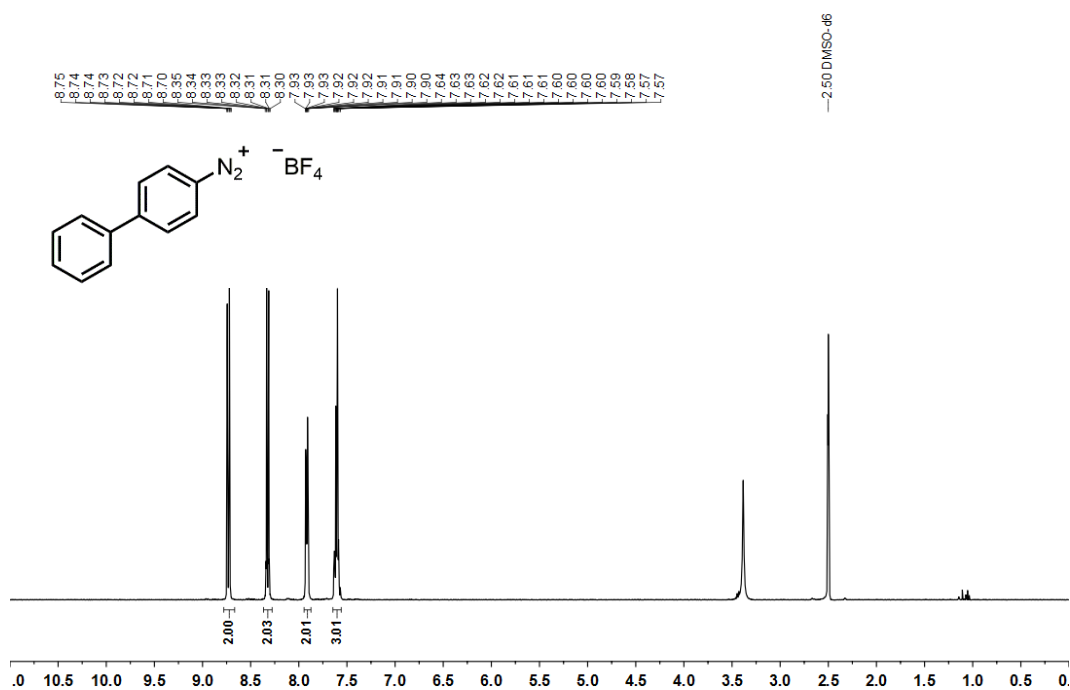
Figure 216 ^{1}H NMR spectrum of **195** (400 MHz, $(CD_3)_2SO$).
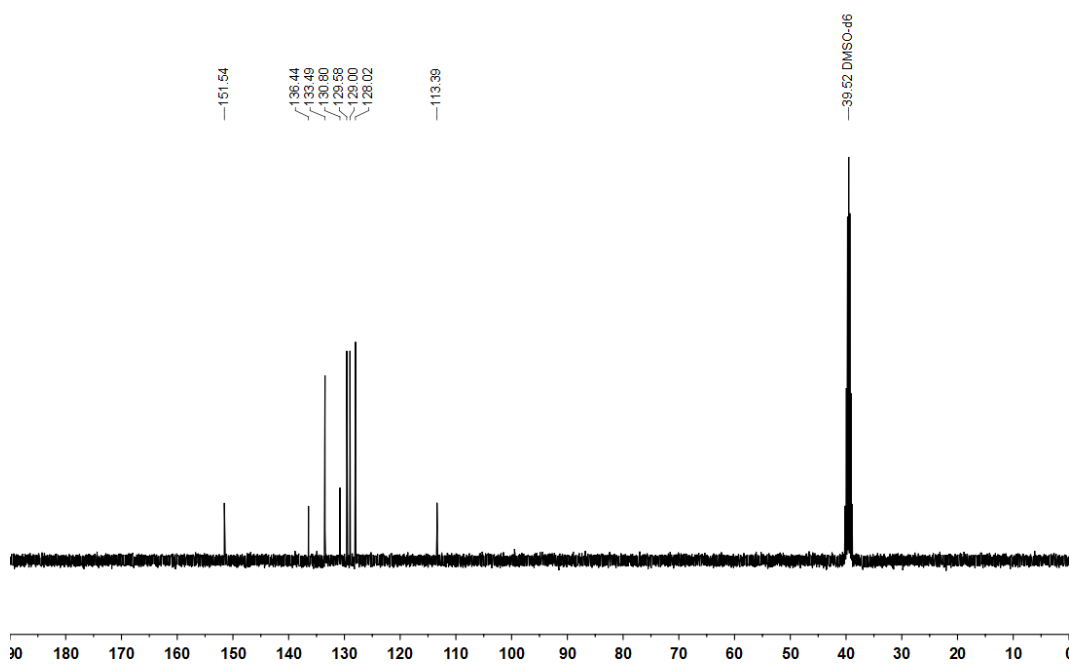
Figure 217 ^{13}C NMR spectrum of **195** (101 MHz, $(CD_3)_2SO$).
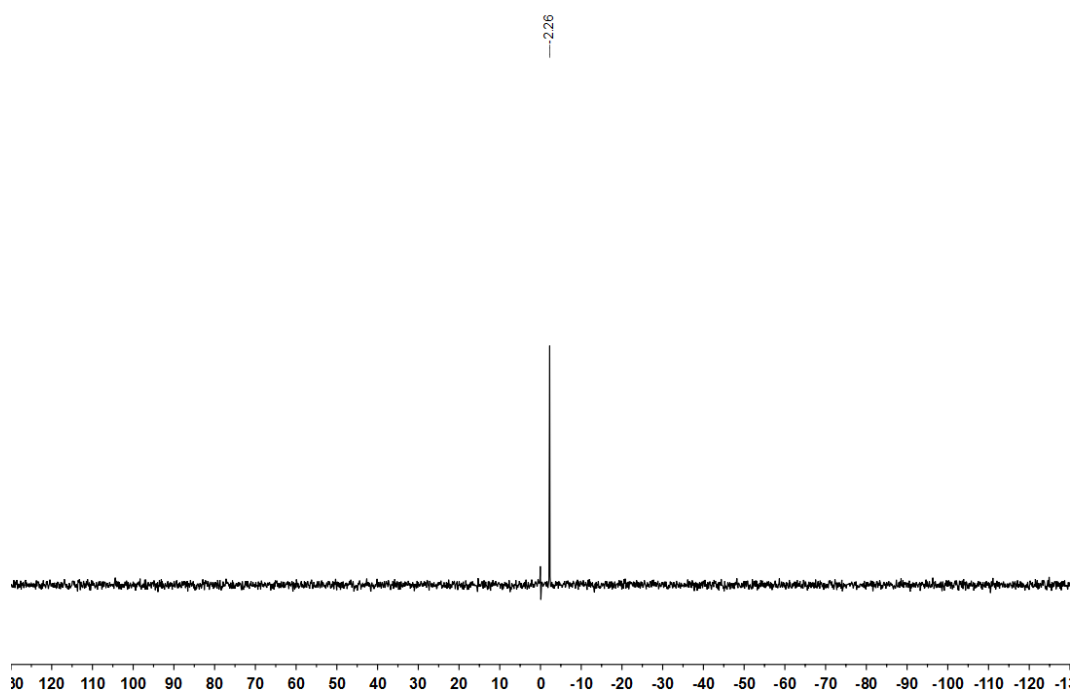
Figure 218 ^{11}B NMR spectrum of **195** (128 MHz, $(CD_3)_2SO$).
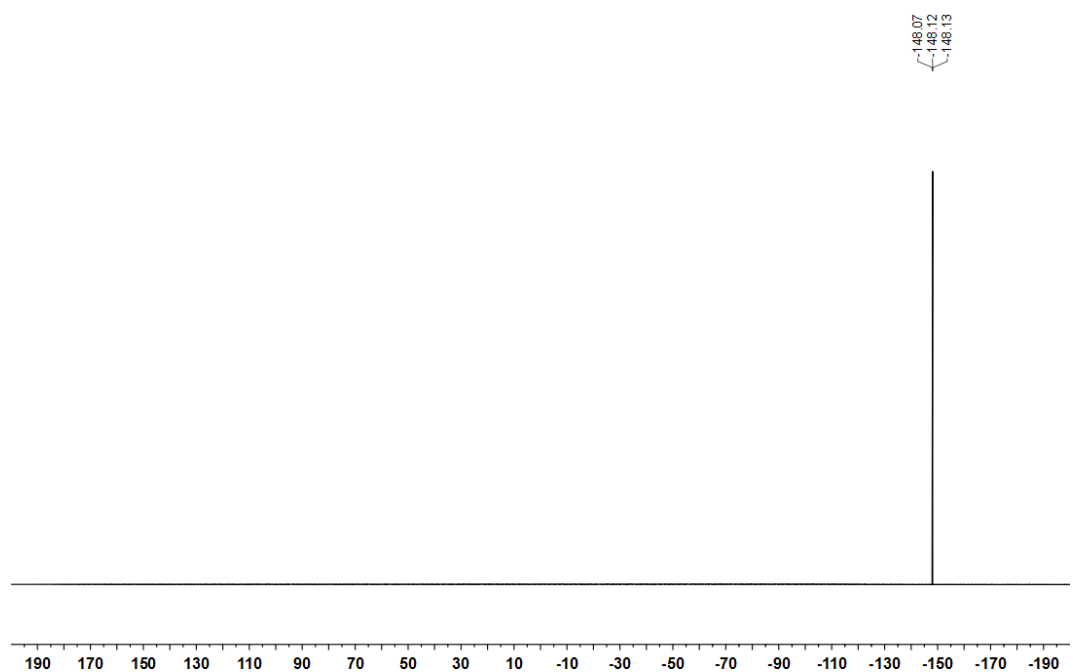
Figure 219 ^{19}F NMR spectrum of **195** (376 MHz, $(CD_3)_2SO$).
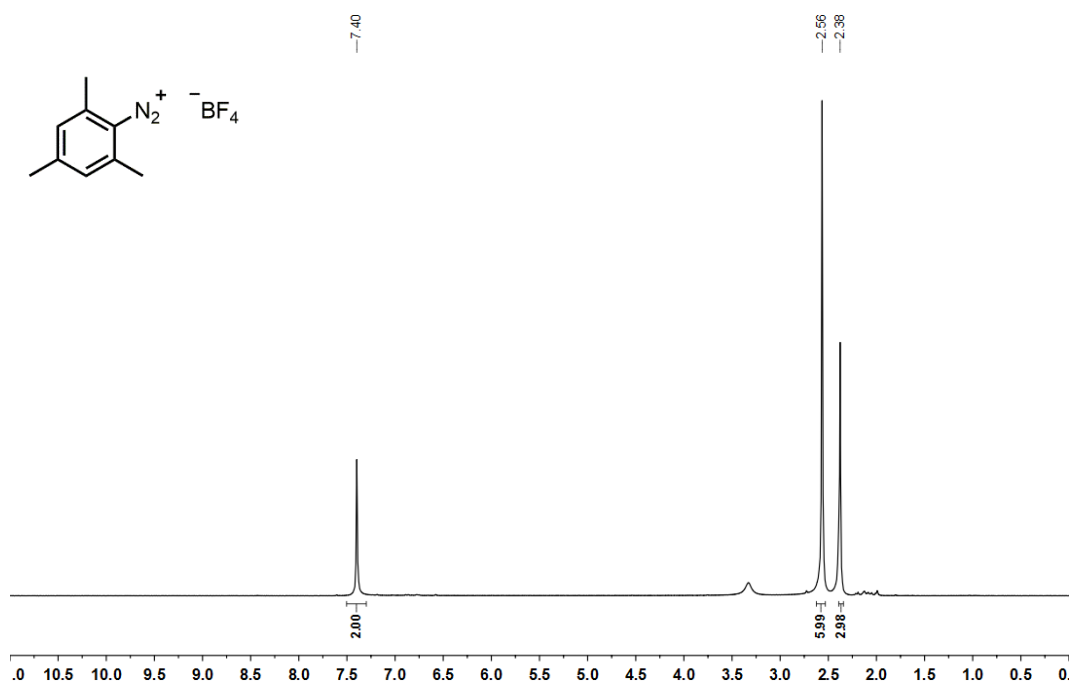
Figure 220 ^{1}H NMR spectrum of **196** (400 MHz, (CD$_3$)$_2$SO).
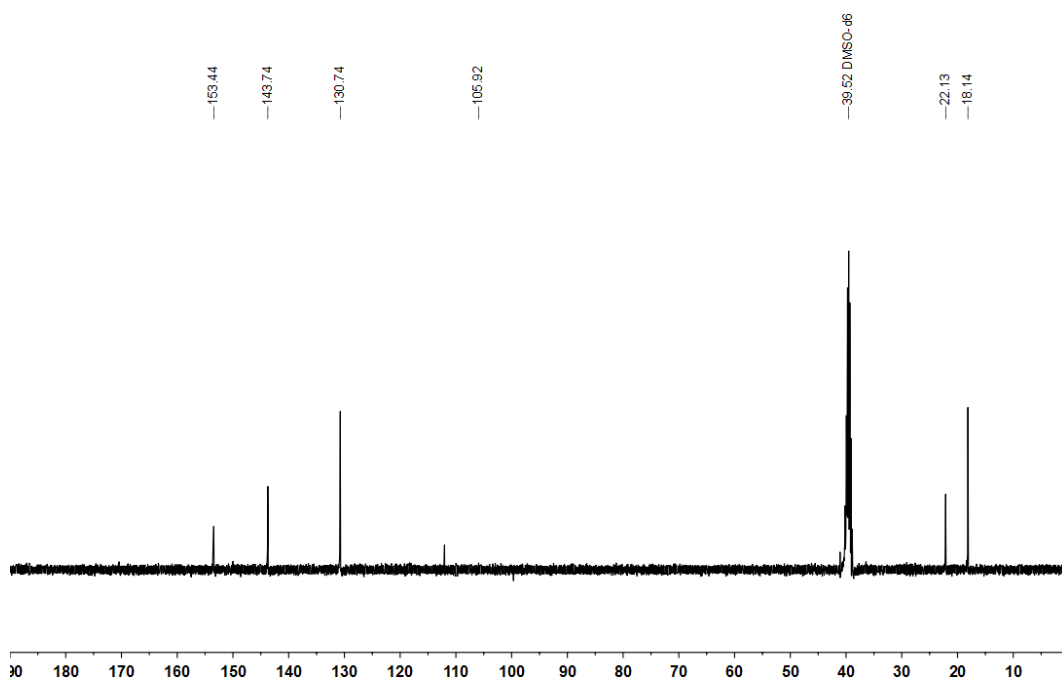
Figure 221 ^{13}C NMR spectrum of **196** (101 MHz, (CD$_3$)$_2$SO).

Filename: c5981ajr
Reference: Alan Reay AJR-5-376
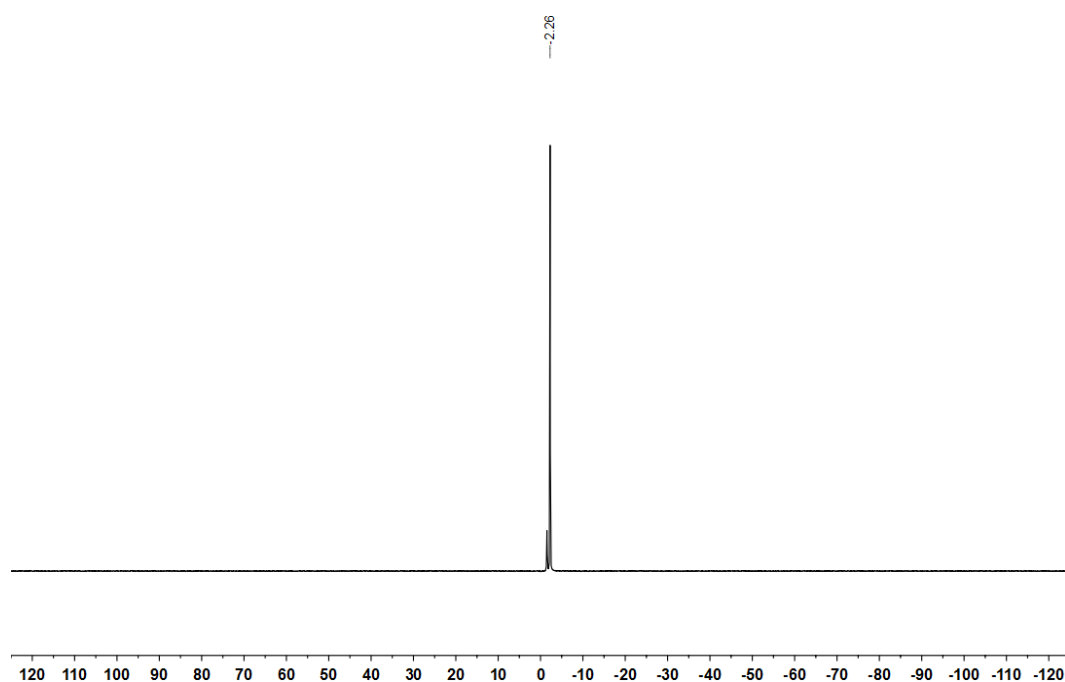
Figure 222 ^{11}B NMR spectrum of **196** (128 MHz, (CD$_3$)$_2$SO).

Filename: c5981ajr
Reference: Alan Reay AJR-5-376
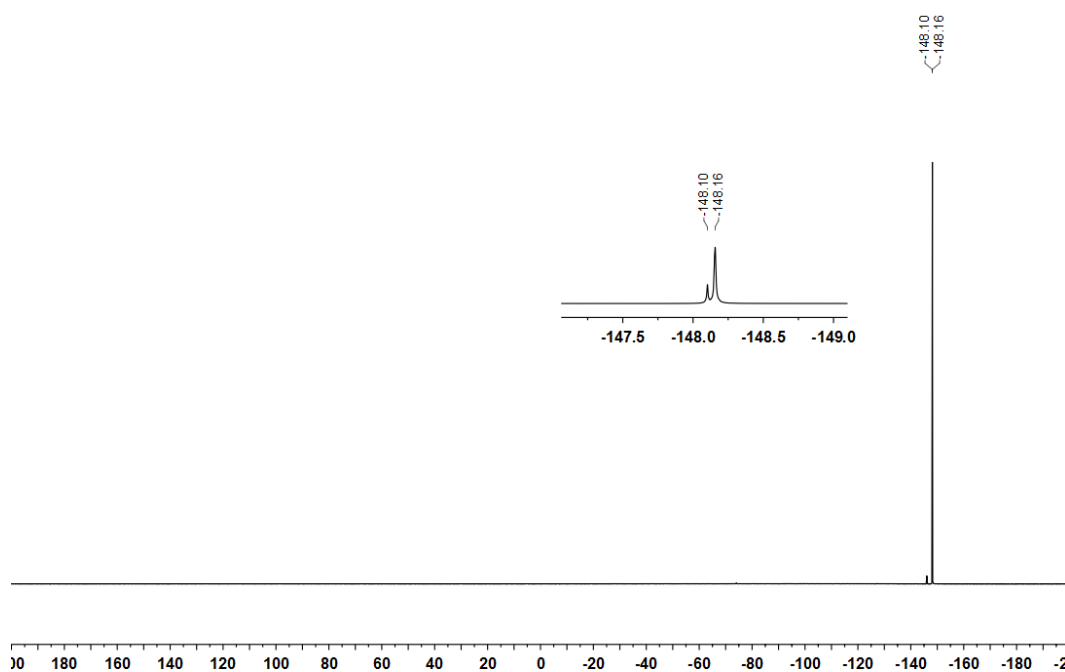
Figure 223 ^{19}F NMR spectrum of **196** (376 MHz, (CD$_3$)$_2$SO).

381
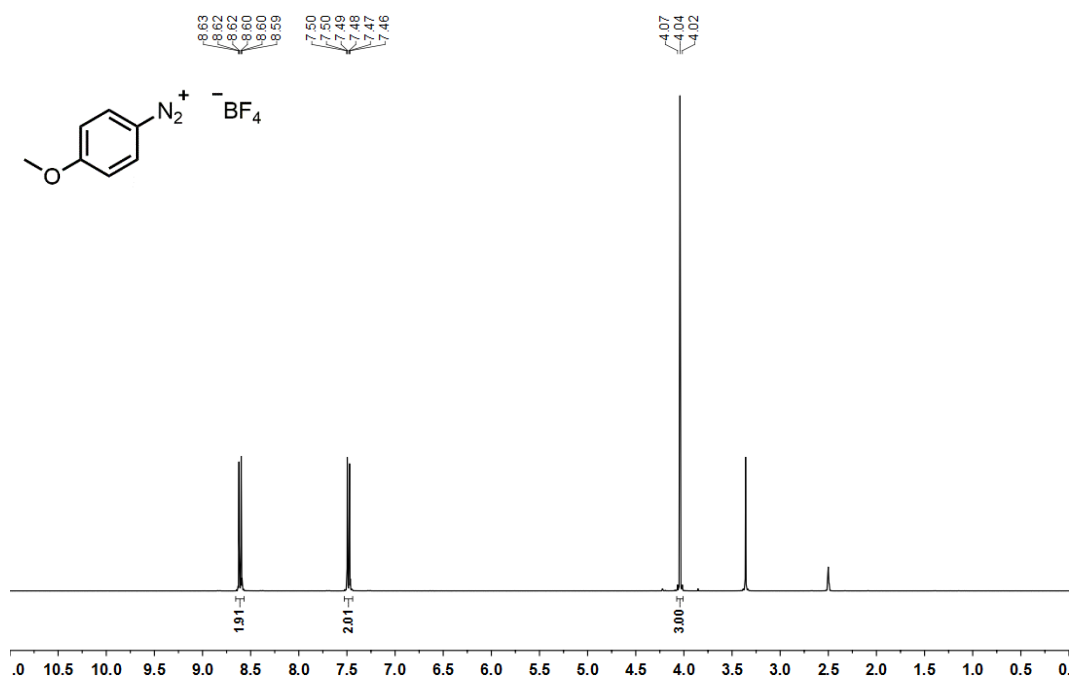
Figure 224 ^{1}H NMR spectrum of **197** (400 MHz, (CD$_3$)$_2$SO).
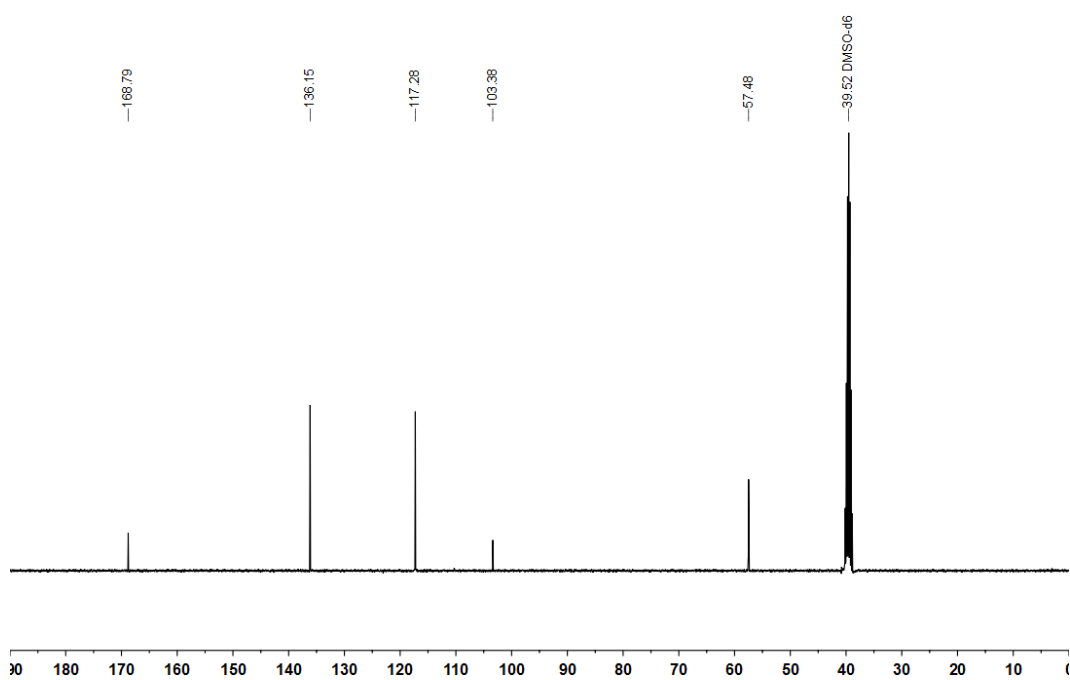
Figure 225 ^{13}C NMR spectrum of **197** (101 MHz, (CD$_3$)$_2$SO).

Filename: c6832ajr
Reference: Alan Reay AJR-5-406

—2.26

120 110 100 90 80 70 60 50 40 30 20 10 0 -10 -20 -30 -40 -50 -60 -70 -80 -90 -100 -110 -120
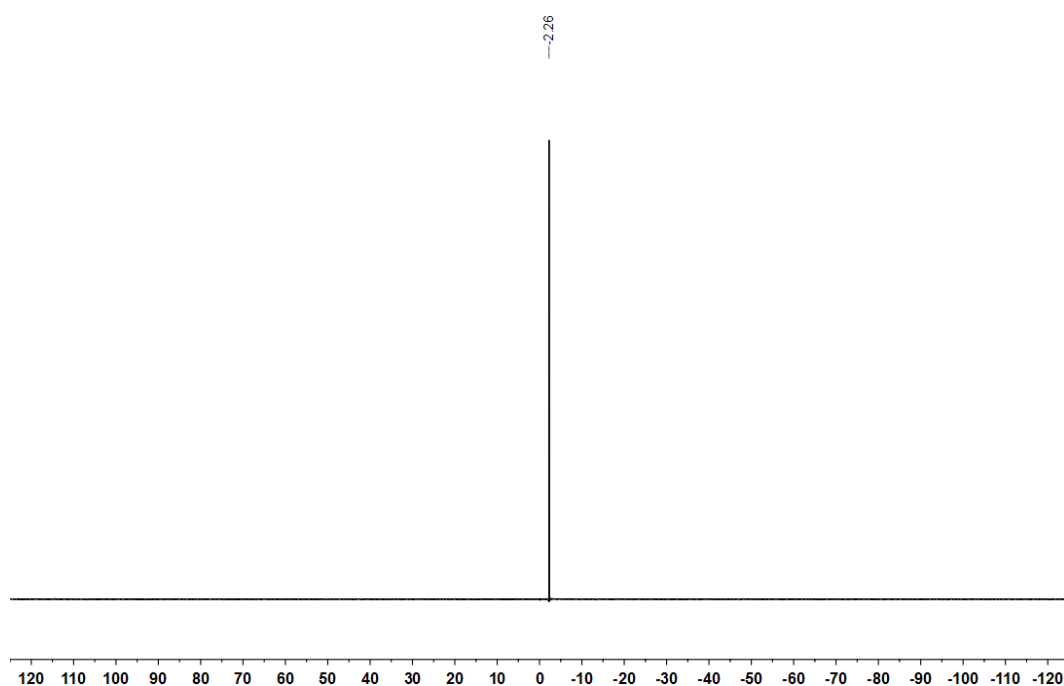
Figure 226 ^{11}B NMR spectrum of **197** (128 MHz, (CD$_3$)$_2$SO).

Filename: c6832ajr
Reference: Alan Reay AJR-5-406

—148.06
—148.12

—148.06
—148.12

-147.8   -148.0   -148.2   -148.4

00 180 160 140 120 100 80 60 40 20 0 -20 -40 -60 -80 -100 -120 -140 -160 -180 -20
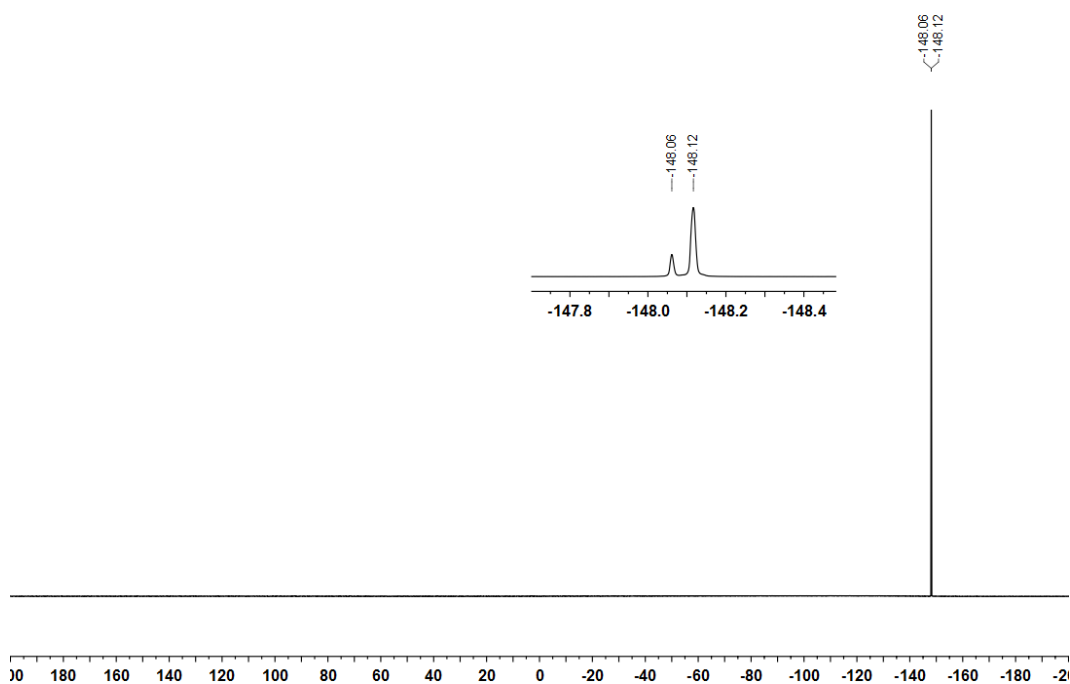
Figure 227 ^{19}F NMR spectrum of **197** (376 MHz, (CD$_3$)$_2$SO).
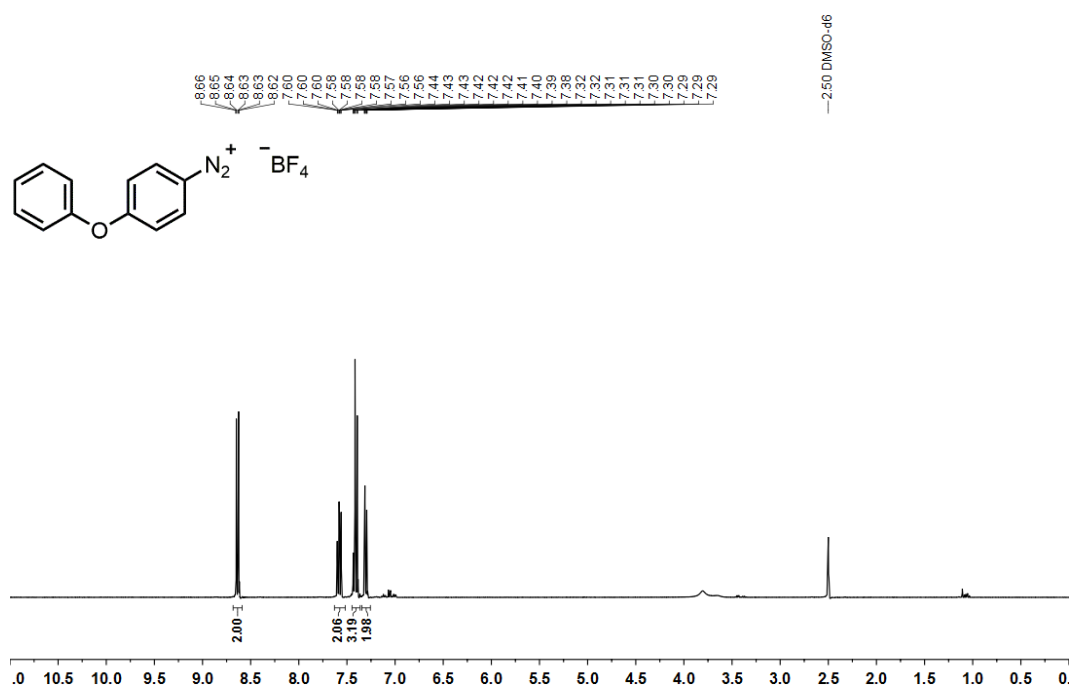
Figure 228 ^{1}H NMR spectrum of **198** (400 MHz, (CD$_3$)$_2$SO).
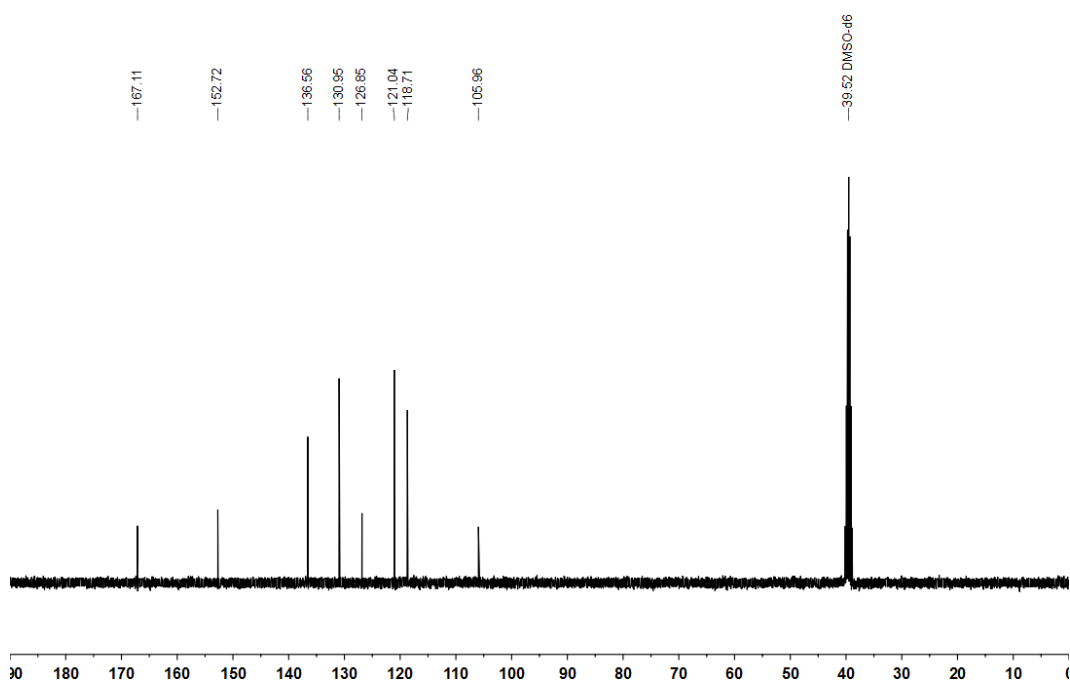
Figure 229 ^{13}C NMR spectrum of **198** (101 MHz, (CD$_3$)$_2$SO).

Filename: a3639ajr
Reference: Alan Reay AJR-8-722

—2.26
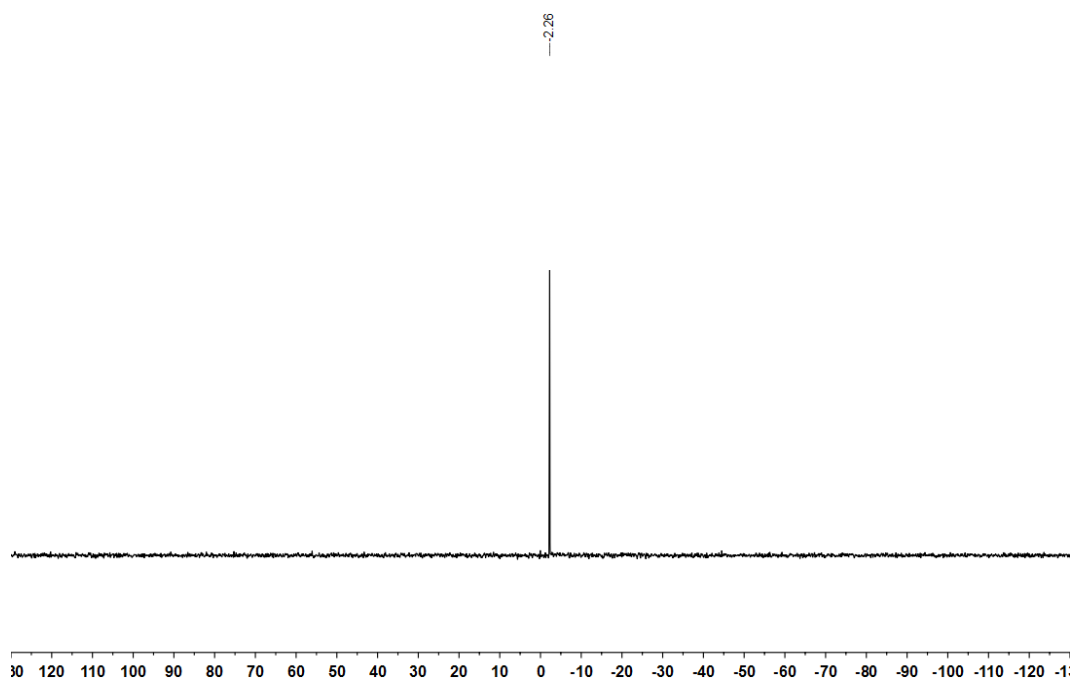
Figure 230 ^{11}B NMR spectrum of **198** (128 MHz, (CD$_3$)$_2$SO).

Filename: a3639ajr
Reference: Alan Reay AJR-8-722

148.07
148.12
148.12
148.13
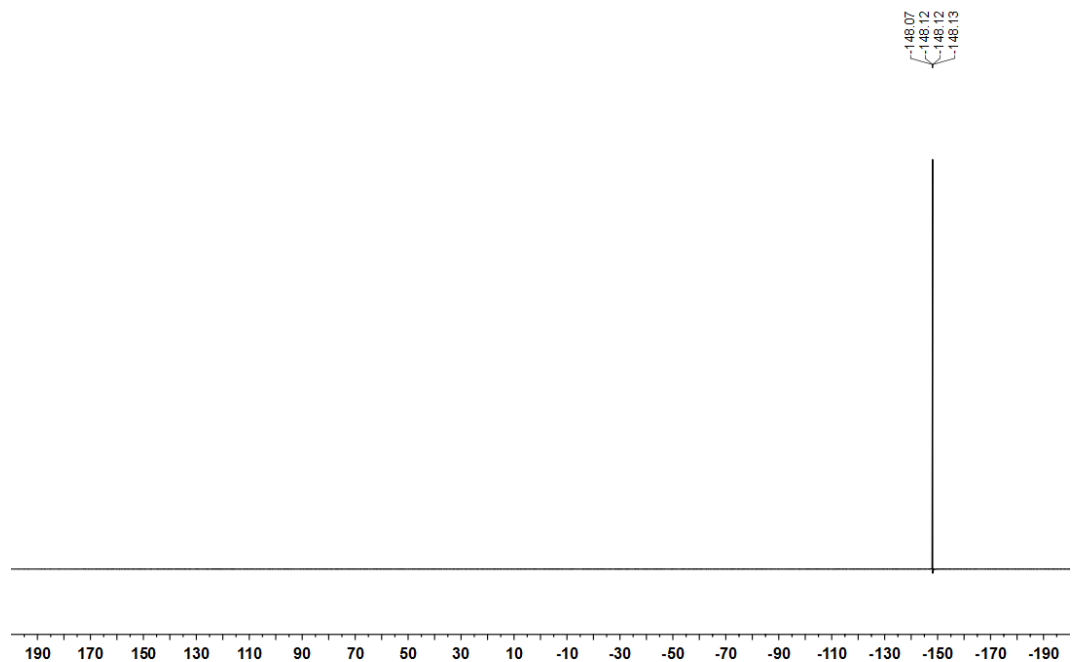
Figure 231 ^{19}F NMR spectrum of **198** (376 MHz, (CD$_3$)$_2$SO).
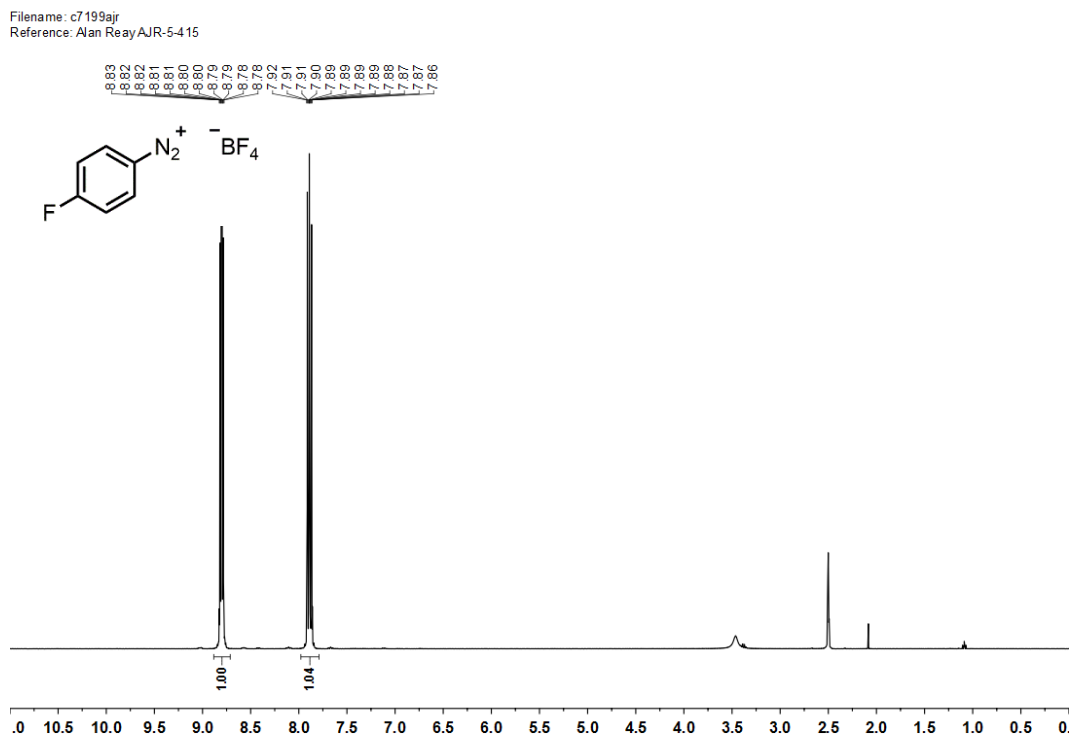
Figure 232 ^{1}H NMR spectrum of **199** (400 MHz, (CD$_3$)$_2$SO).
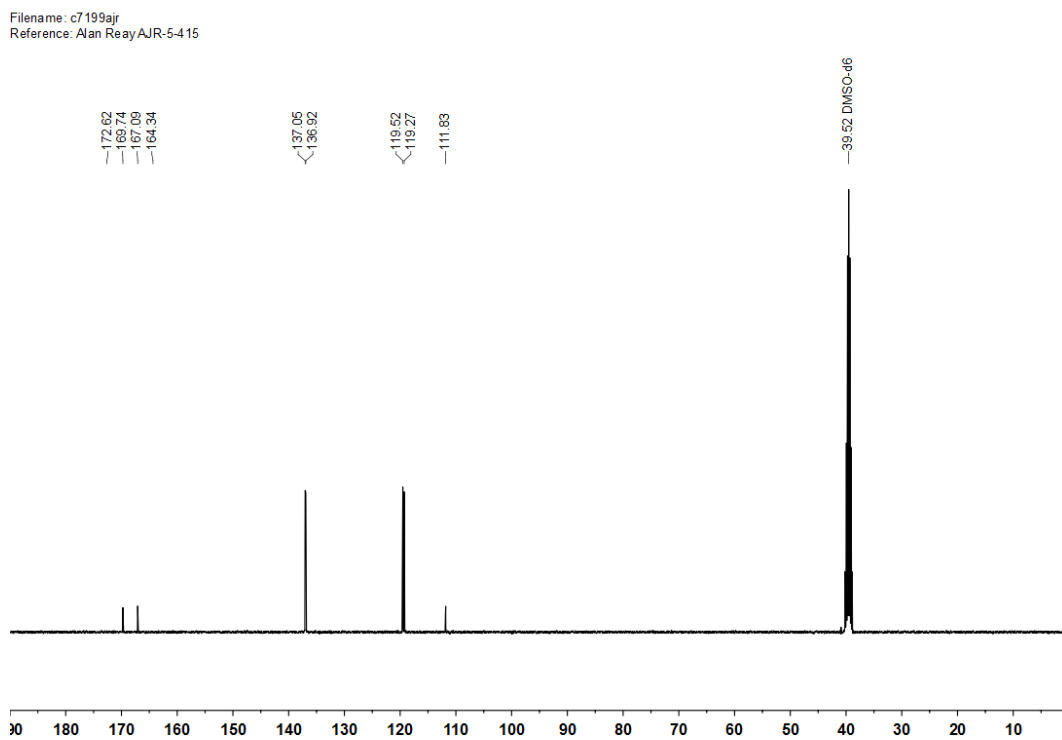
Figure 233 ^{13}C NMR spectrum of **199** (101 MHz, (CD$_3$)$_2$SO).
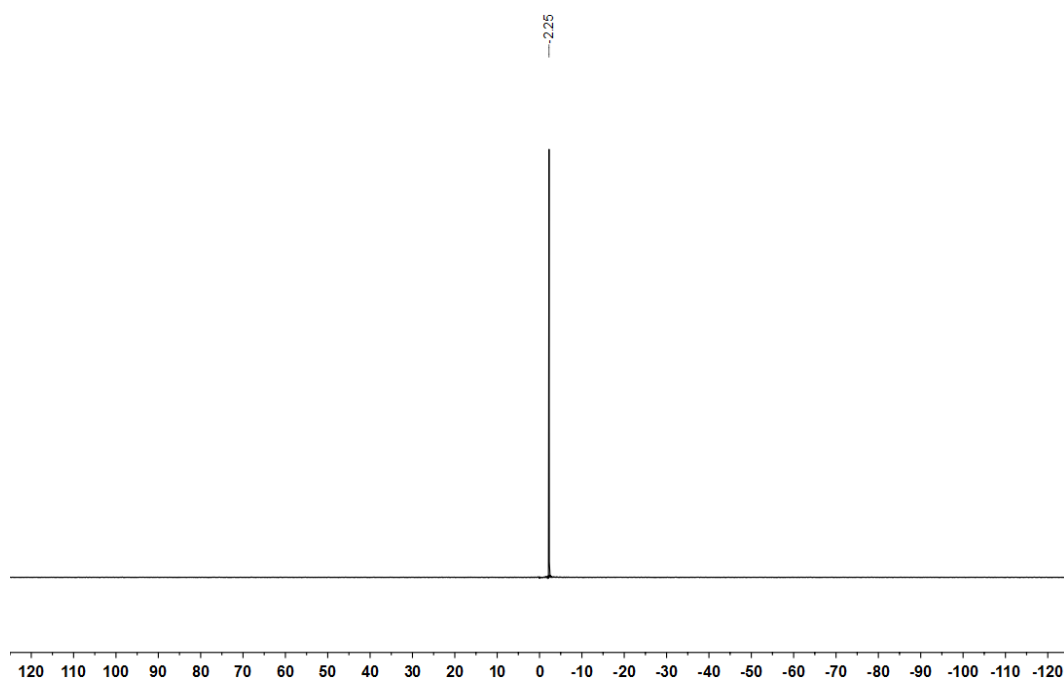
Figure 234 ^{11}B NMR spectrum of **199** (128 MHz, (CD$_3$)$_2$SO).
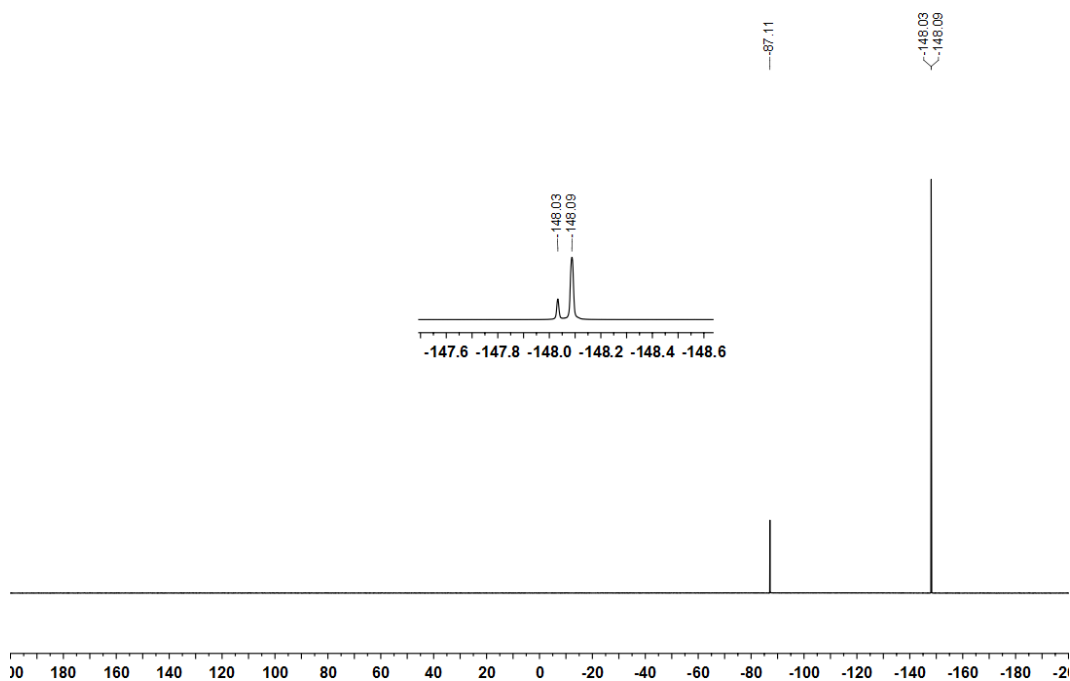
Figure 235 ^{19}F NMR spectrum of **199** (376 MHz, (CD$_3$)$_2$SO).
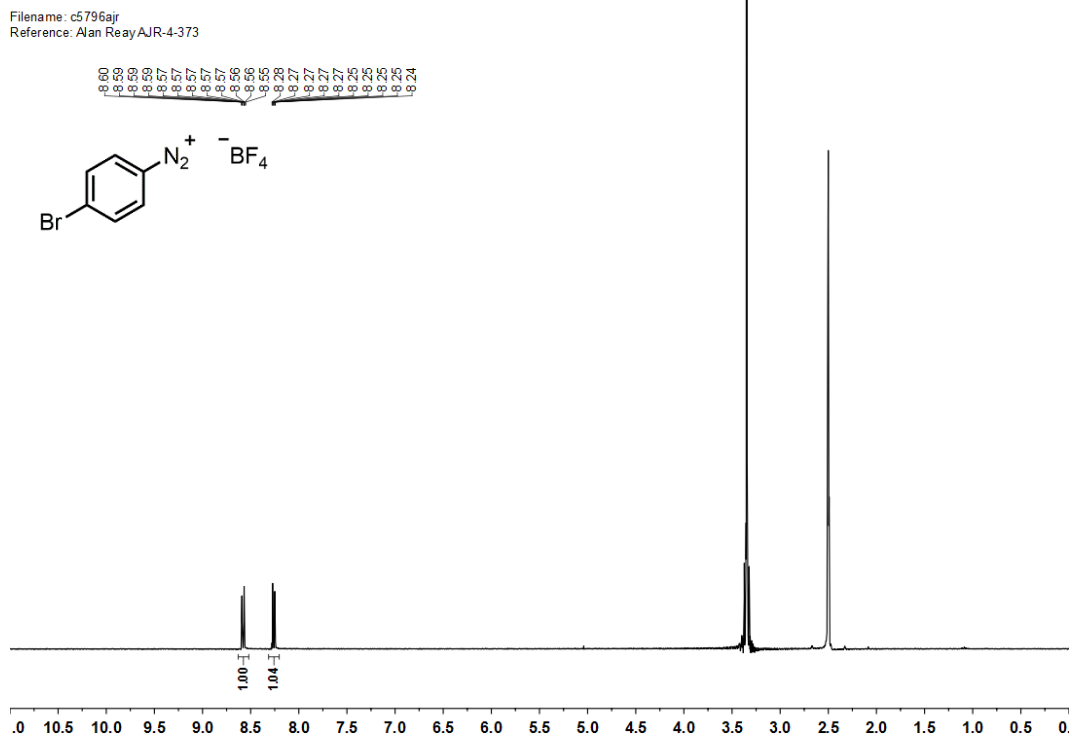
Figure 236 ^{1}H NMR spectrum of **200** (400 MHz, (CD$_3$)$_2$SO).
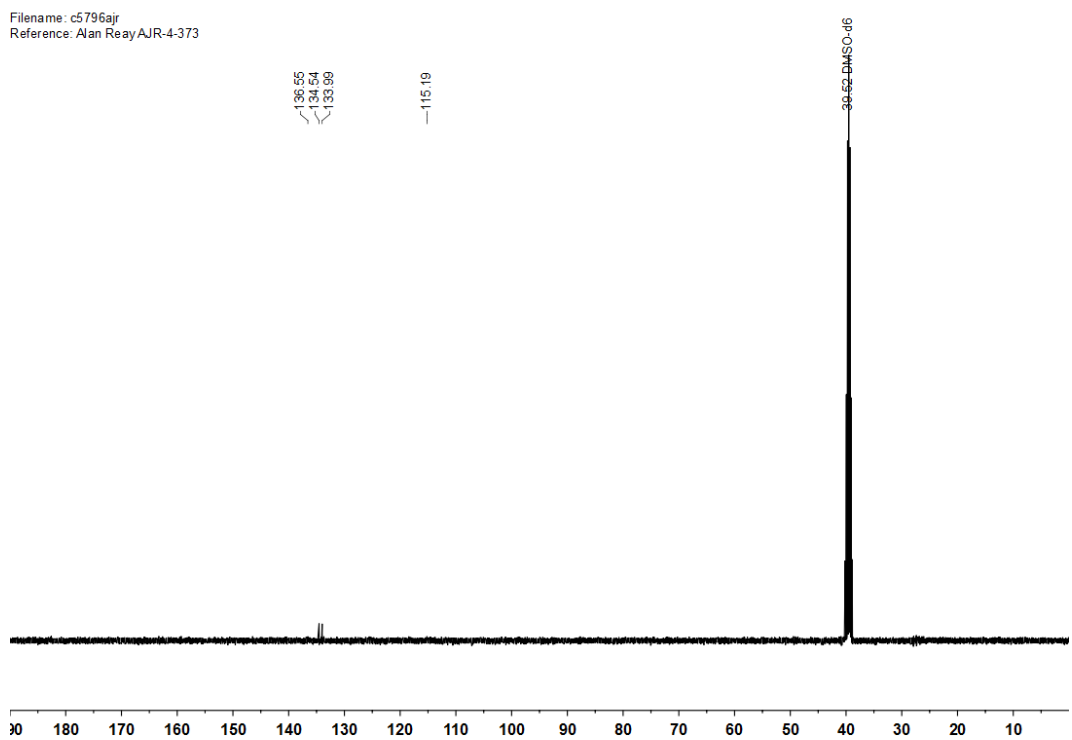
Figure 237 ^{13}C NMR spectrum of **200** (101 MHz, (CD$_3$)$_2$SO).
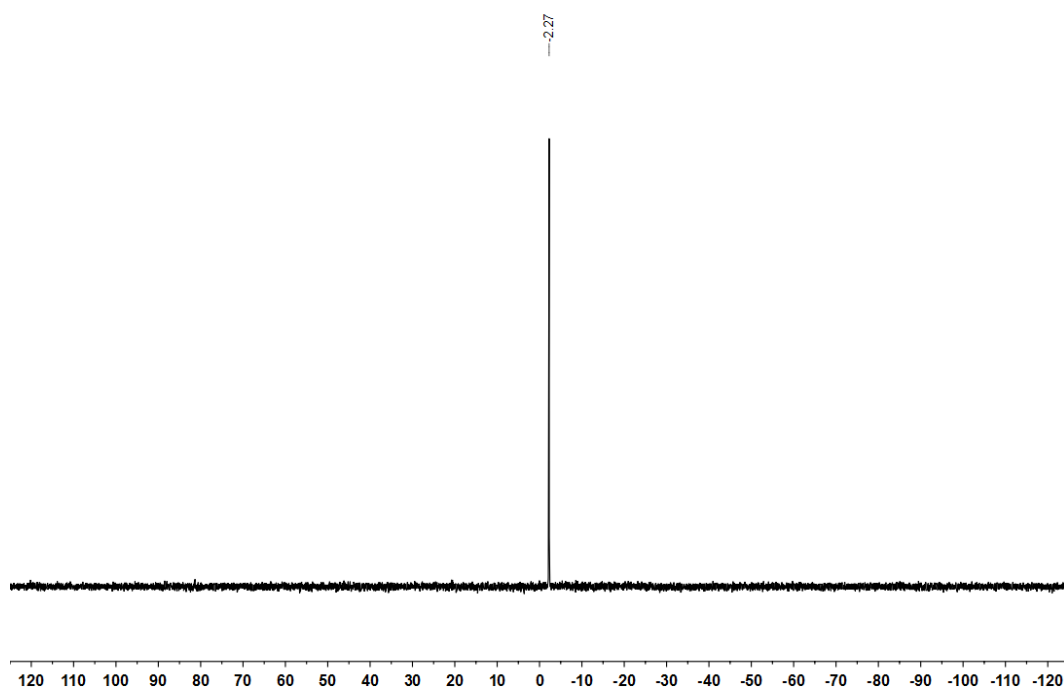
Figure 238 ^{11}B NMR spectrum of **200** (128 MHz, (CD$_3$)$_2$SO).
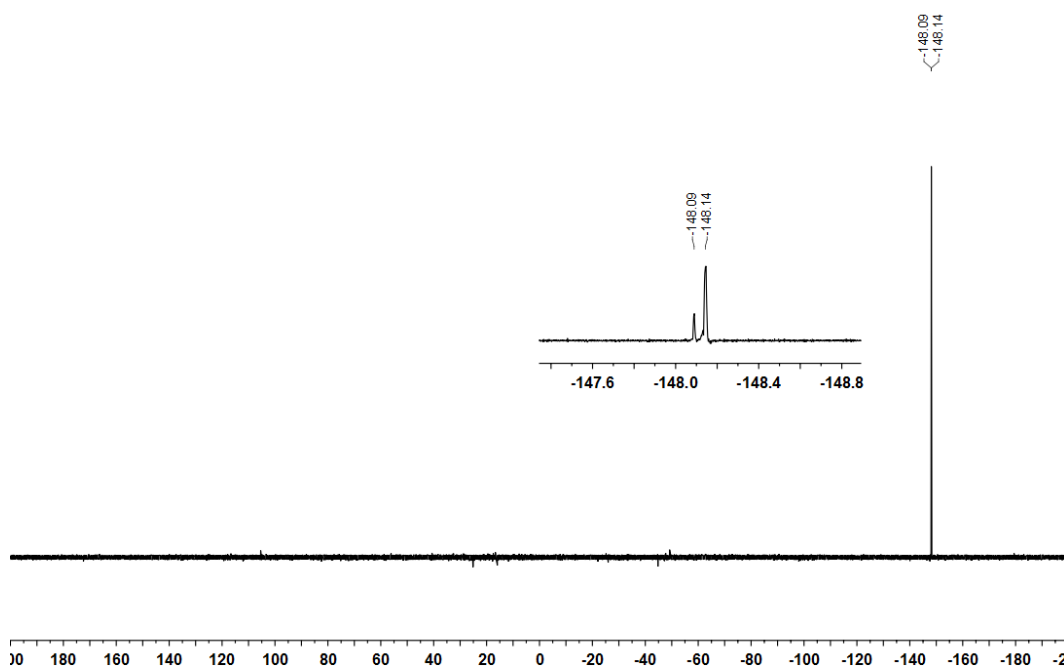
Figure 239 ^{19}F NMR spectrum of **200** (376 MHz, (CD$_3$)$_2$SO).
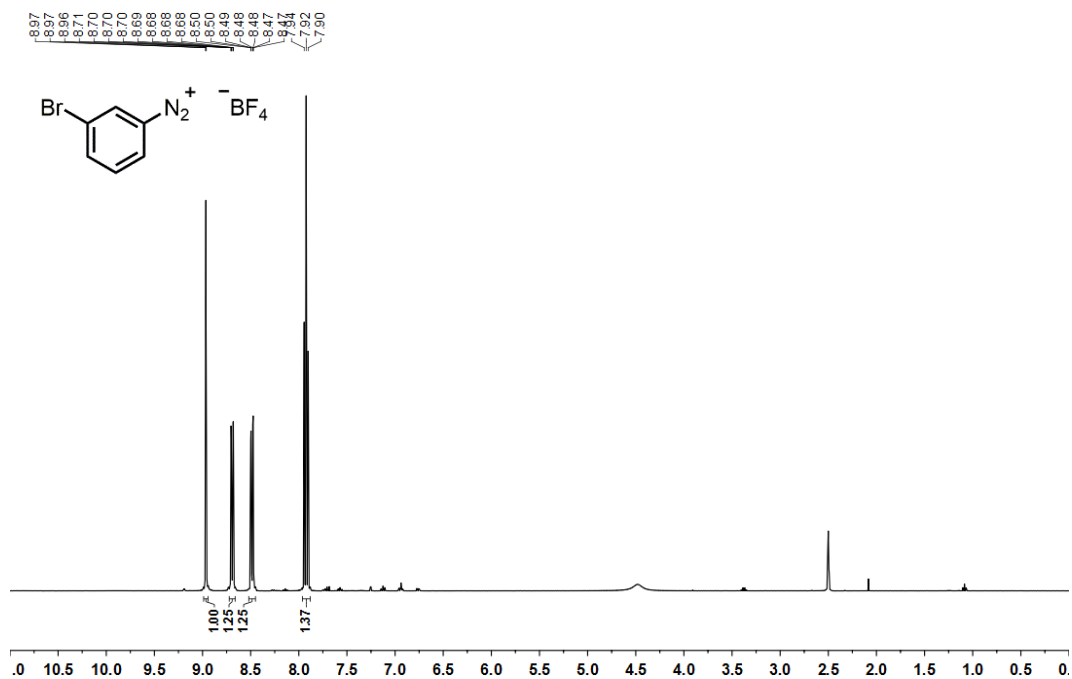
Figure 240 ^{1}H NMR spectrum of **201** (400 MHz, (CD$_3$)$_2$SO).
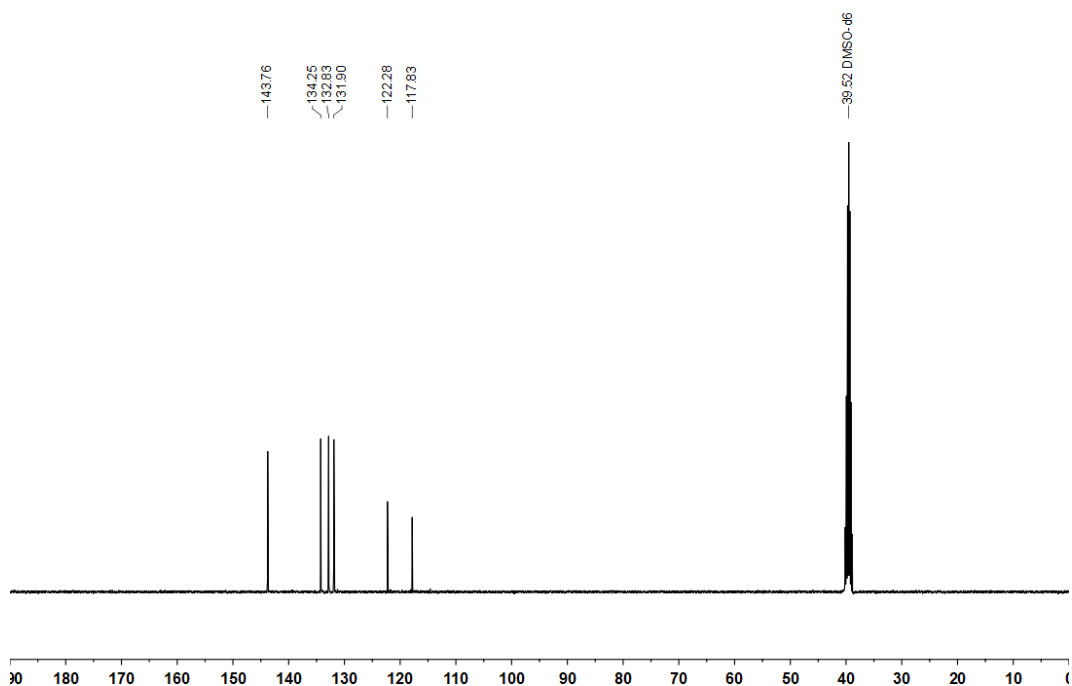
Figure 241 ^{13}C NMR spectrum of **201** (101 MHz, (CD$_3$)$_2$SO).

Filename: c6156ajr
Reference: Alan Reay AJR-5-390

—2.25

120 110 100 90 80 70 60 50 40 30 20 10 0 -10 -20 -30 -40 -50 -60 -70 -80 -90 -100 -110 -120
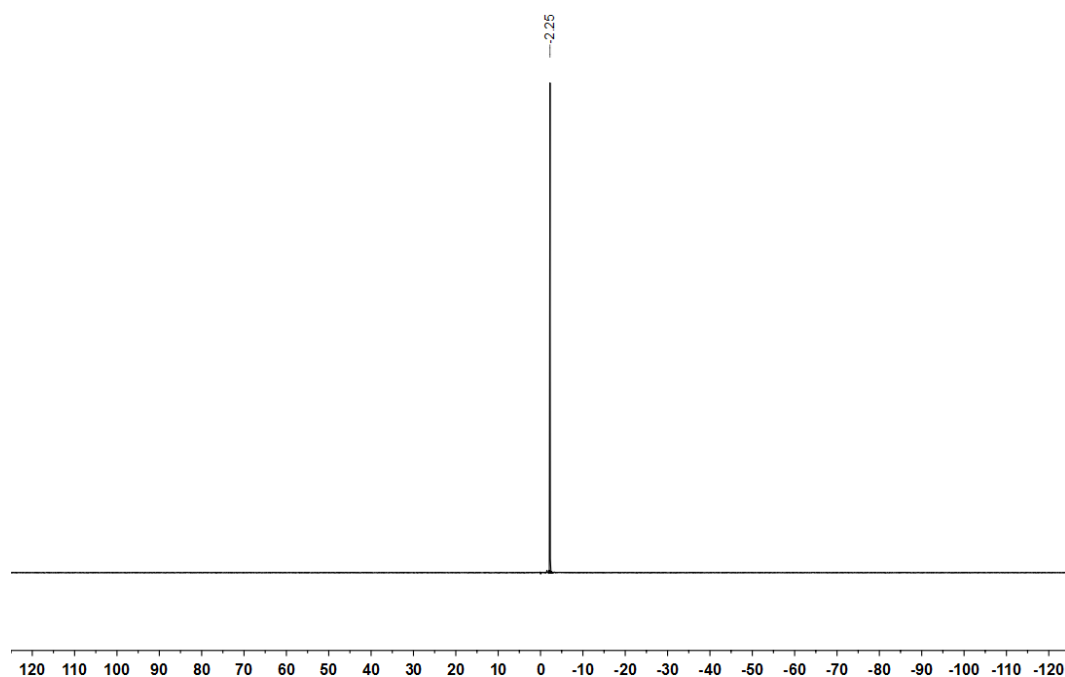
Figure 242 ^{11}B NMR spectrum of **201** (128 MHz, $(CD_3)_2SO$).

Filename: c6156ajr
Reference: Alan Reay AJR-5-390

-147.95
-148.01

-147.95
-148.01

-147.6 -147.8 -148.0 -148.2 -148.4

00 180 160 140 120 100 80 60 40 20 0 -20 -40 -60 -80 -100 -120 -140 -160 -180 -2
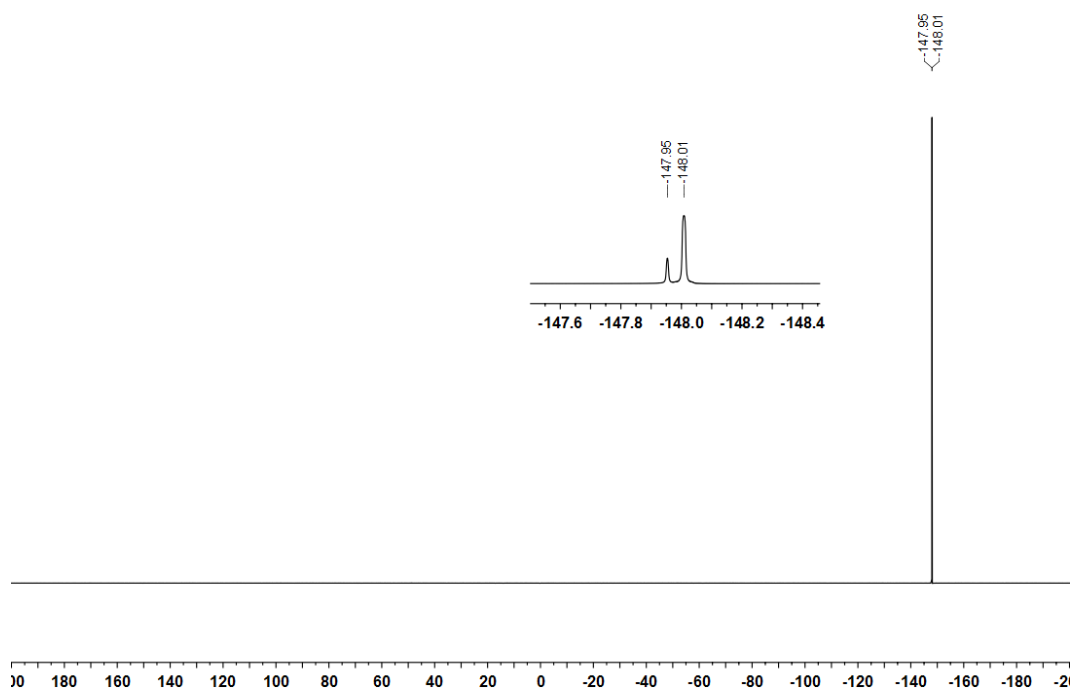
Figure 243 ^{19}F NMR spectrum of **201** (376 MHz, $(CD_3)_2SO$).
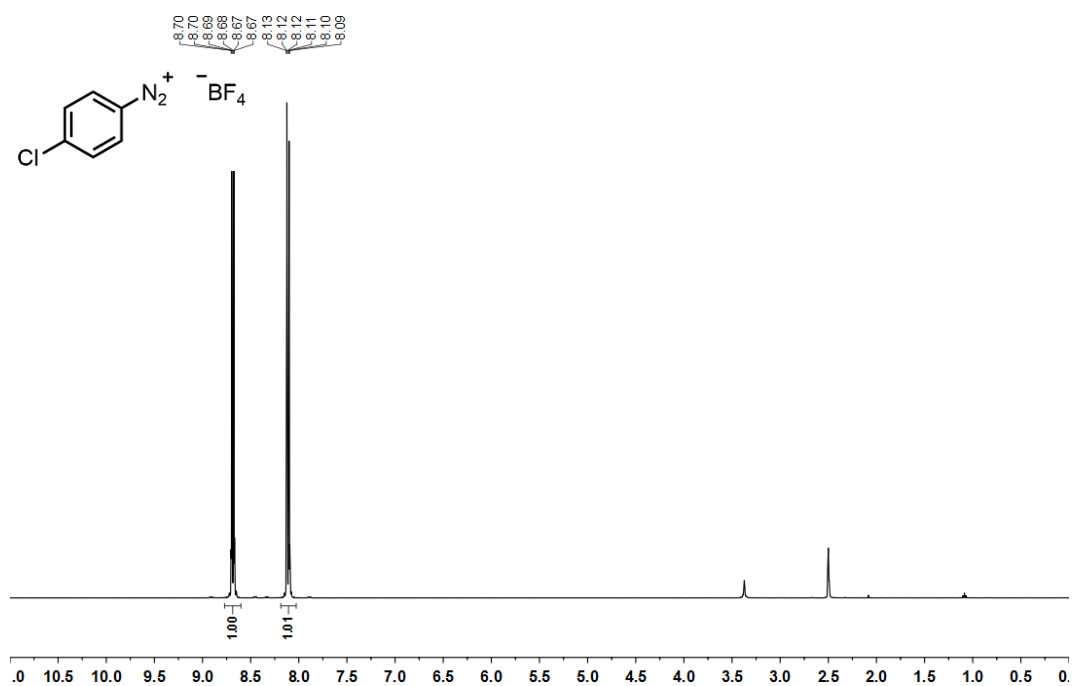
Figure 244 ^{1}H NMR spectrum of **202** (400 MHz, (CD$_3$)$_2$SO).
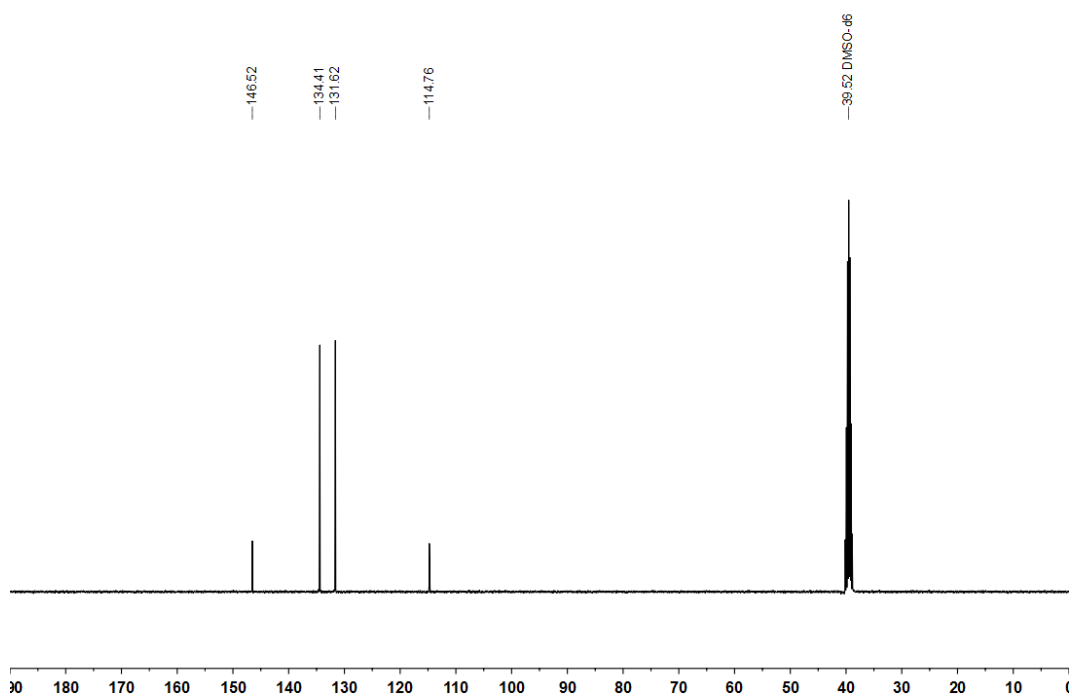
Figure 245 ^{13}C NMR spectrum of **202** (101 MHz, (CD$_3$)$_2$SO).

Filename: c5929ajr
Reference: Alan Reay AJR-5-375

−2.25

120 110 100 90 80 70 60 50 40 30 20 10 0 -10 -20 -30 -40 -50 -60 -70 -80 -90 -100 -110 -120
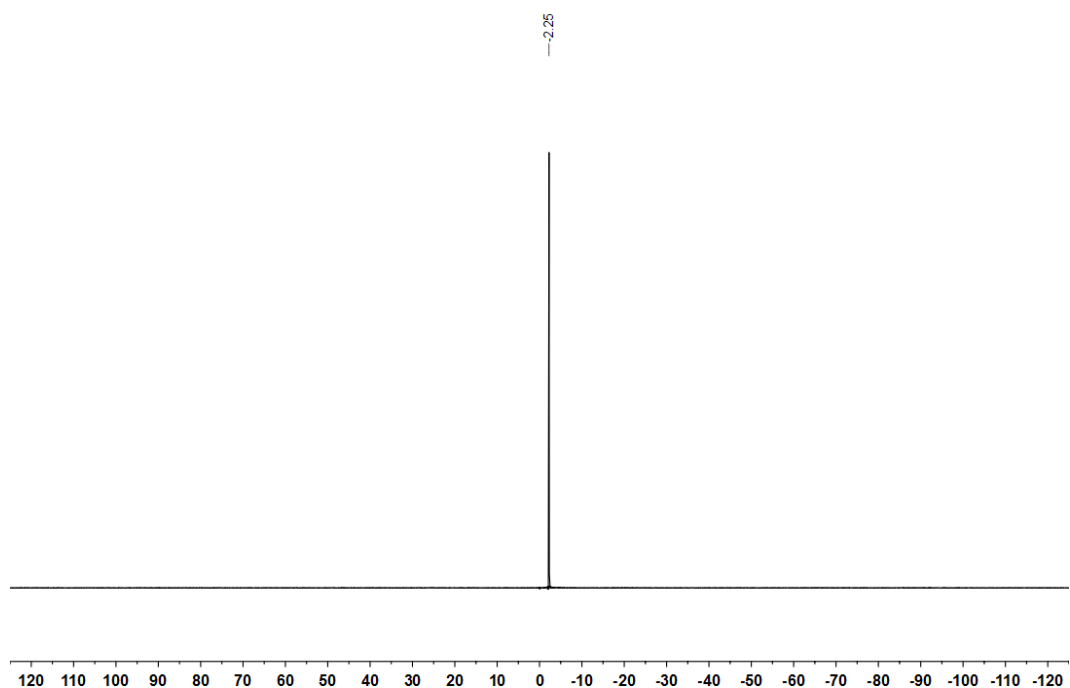
Figure 246 ^{11}B NMR spectrum of **202** (128 MHz, (CD$_3$)$_2$SO).

Filename: c5929ajr
Reference: Alan Reay AJR-5-375

147.99
148.04

147.99
148.04

-147.6   -147.8   -148.0   -148.2   -148.4

00 180 160 140 120 100 80 60 40 20 0 -20 -40 -60 -80 -100 -120 -140 -160 -180 -2
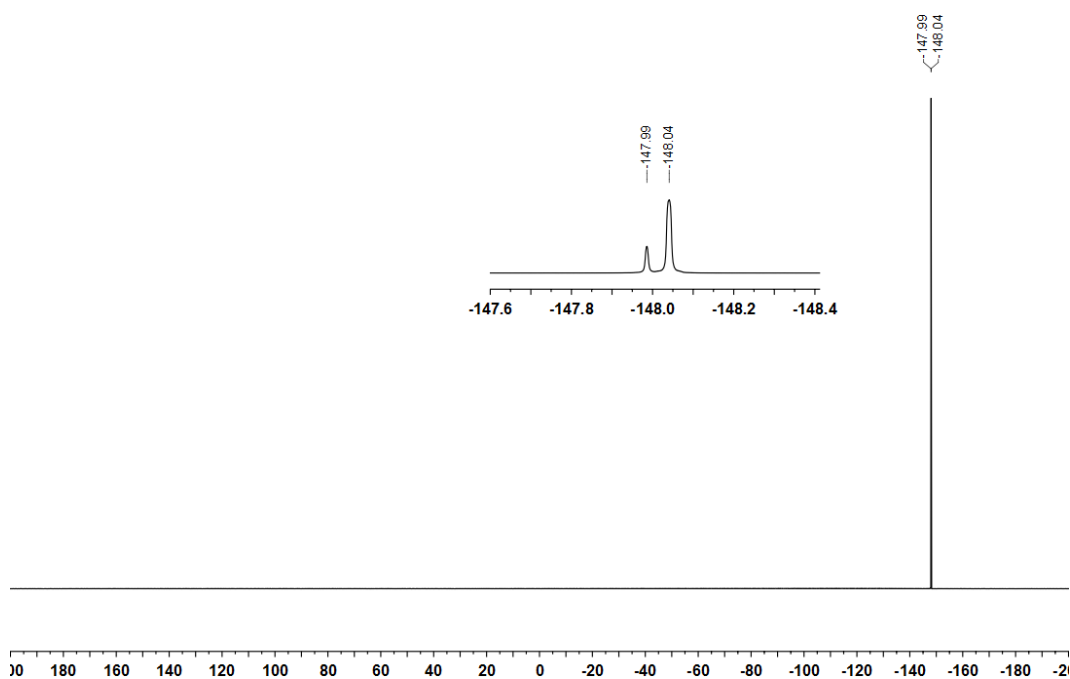
Figure 247 ^{19}F NMR spectrum of **202** (376 MHz, (CD$_3$)$_2$SO).
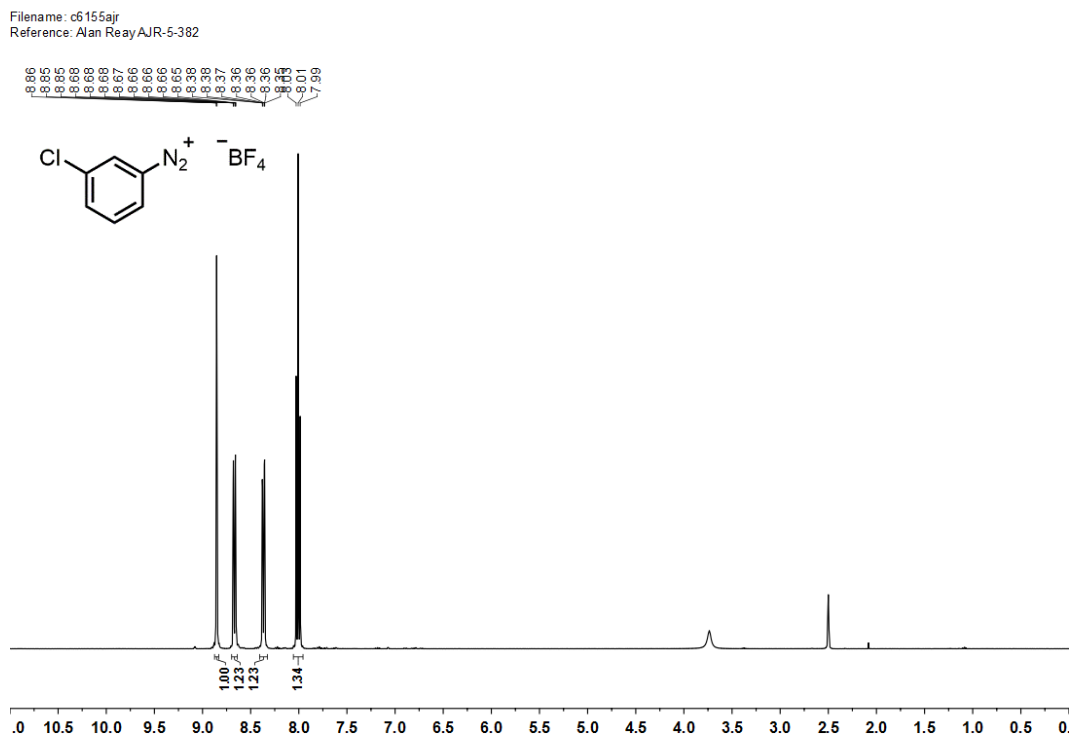
Figure 248 ^{1}H NMR spectrum of **203** (400 MHz, (CD$_3$)$_2$SO).
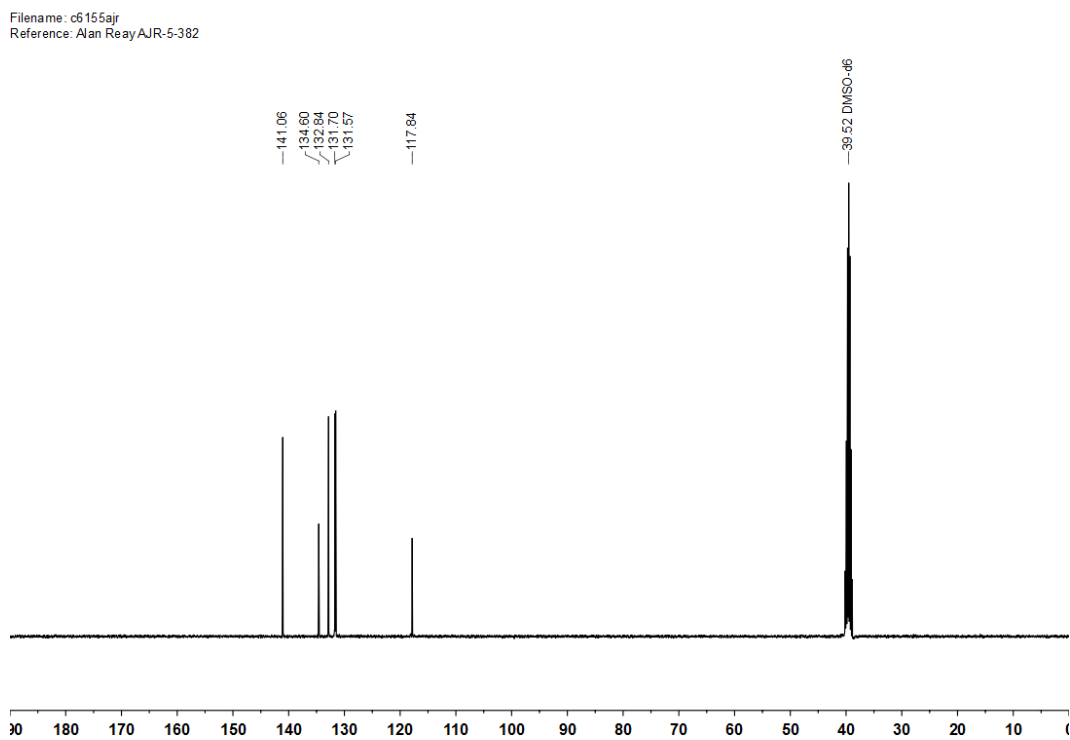
Figure 249 ^{13}C NMR spectrum of **203** (101 MHz, (CD$_3$)$_2$SO).

Filename: c6155ajr
Reference: Alan Reay AJR-5-382

—2.24

120 110 100 90 80 70 60 50 40 30 20 10 0 -10 -20 -30 -40 -50 -60 -70 -80 -90 -100 -110 -120
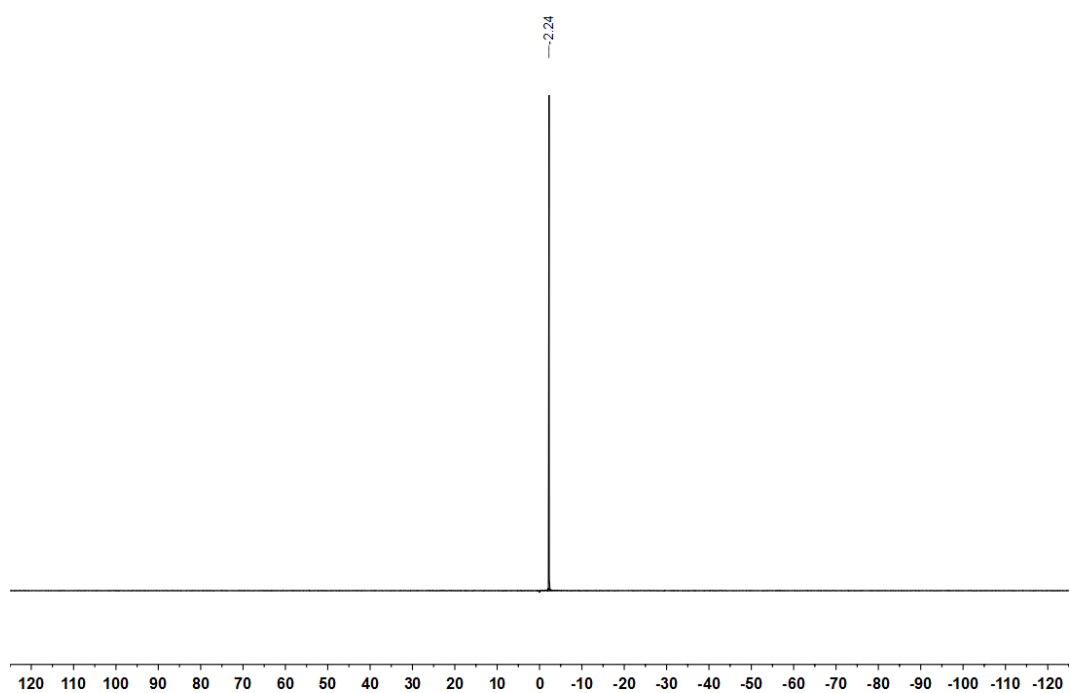
Figure 250 ^{11}B NMR spectrum of **203** (128 MHz, $(CD_3)_2SO$).

Filename: c6155ajr
Reference: Alan Reay AJR-5-382

147.94
147.99

147.94
147.99

-147.6   -147.8   -148.0   -148.2   -148.4

00 180 160 140 120 100 80 60 40 20 0 -20 -40 -60 -80 -100 -120 -140 -160 -180 -2(
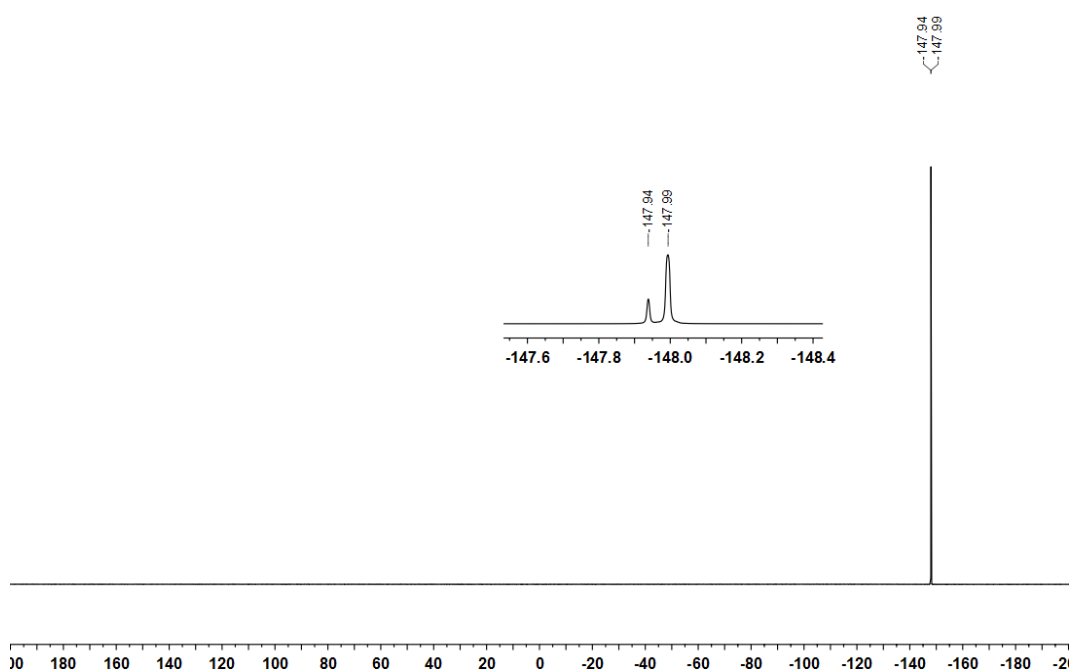
Figure 251 ^{19}F NMR spectrum of **203** (376 MHz, $(CD_3)_2SO$).

395
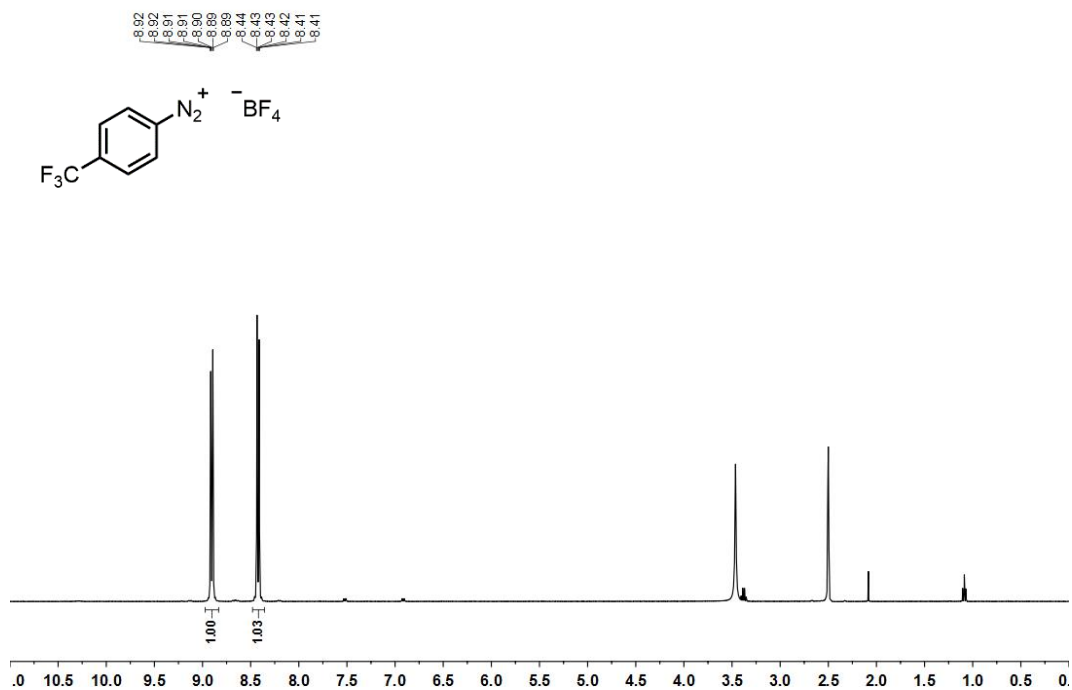
Figure 252 ^{1}H NMR spectrum of **54** (400 MHz, (CD$_3$)$_2$SO).
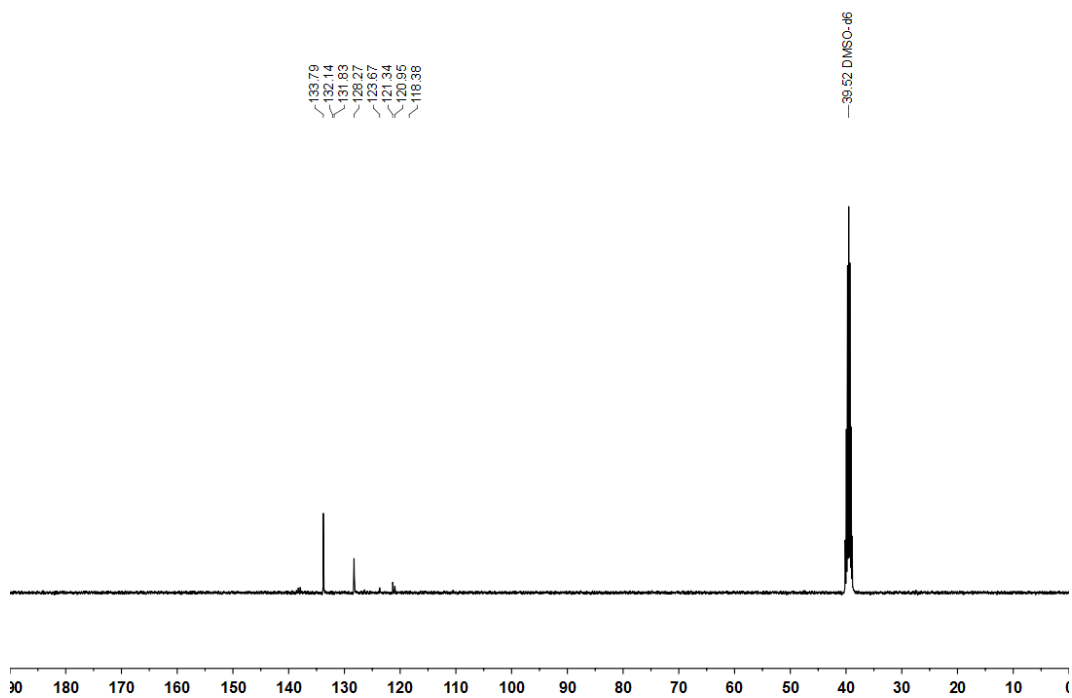
Figure 253 ^{13}C NMR spectrum of **54** (101 MHz, (CD$_3$)$_2$SO).

396
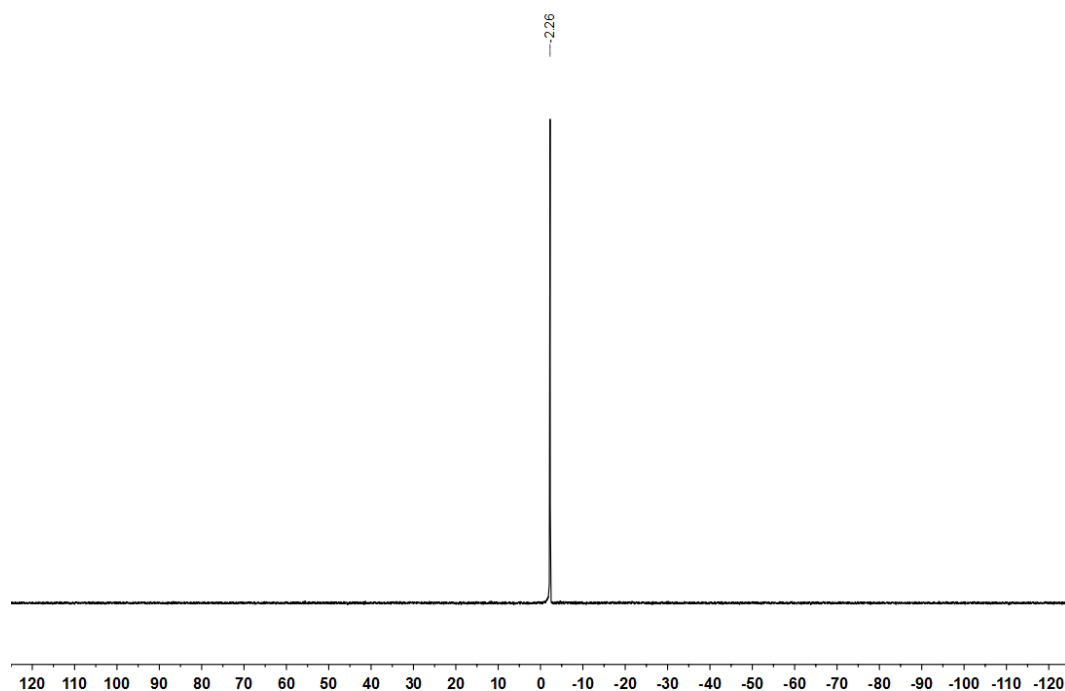
Figure 254 ^{11}B NMR spectrum of **54** (128 MHz, (CD$_3$)$_2$SO).
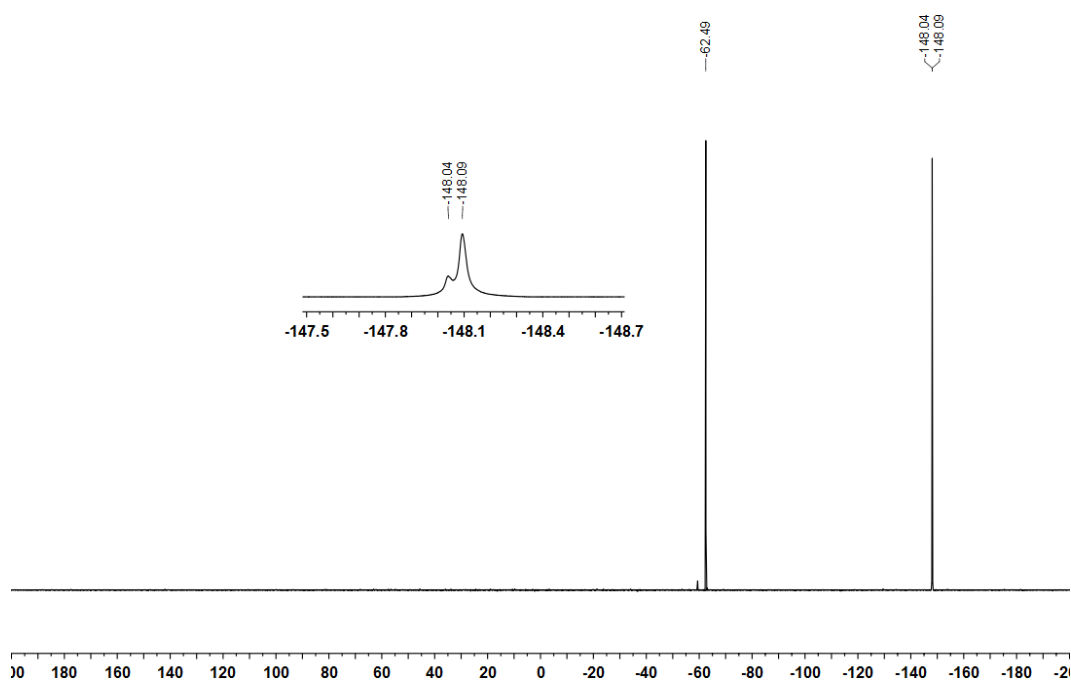
Figure 255 ^{19}F NMR spectrum of **54** (376 MHz, (CD$_3$)$_2$SO).

397
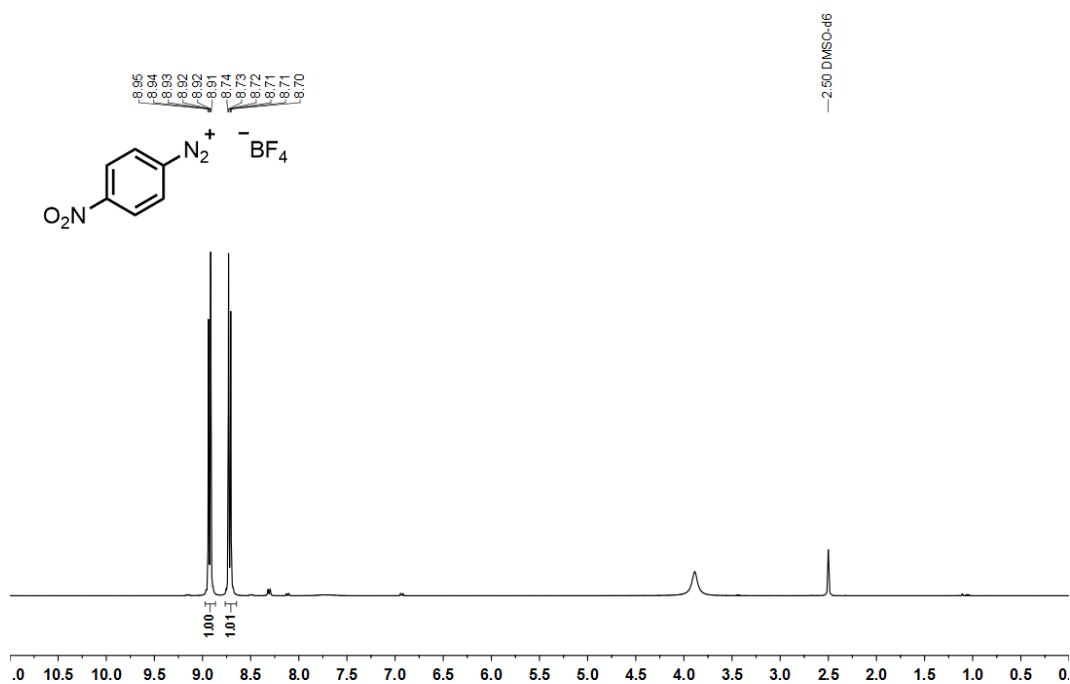
Figure 256 ^{1}H NMR spectrum of **204** (400 MHz, (CD$_3$)$_2$SO).
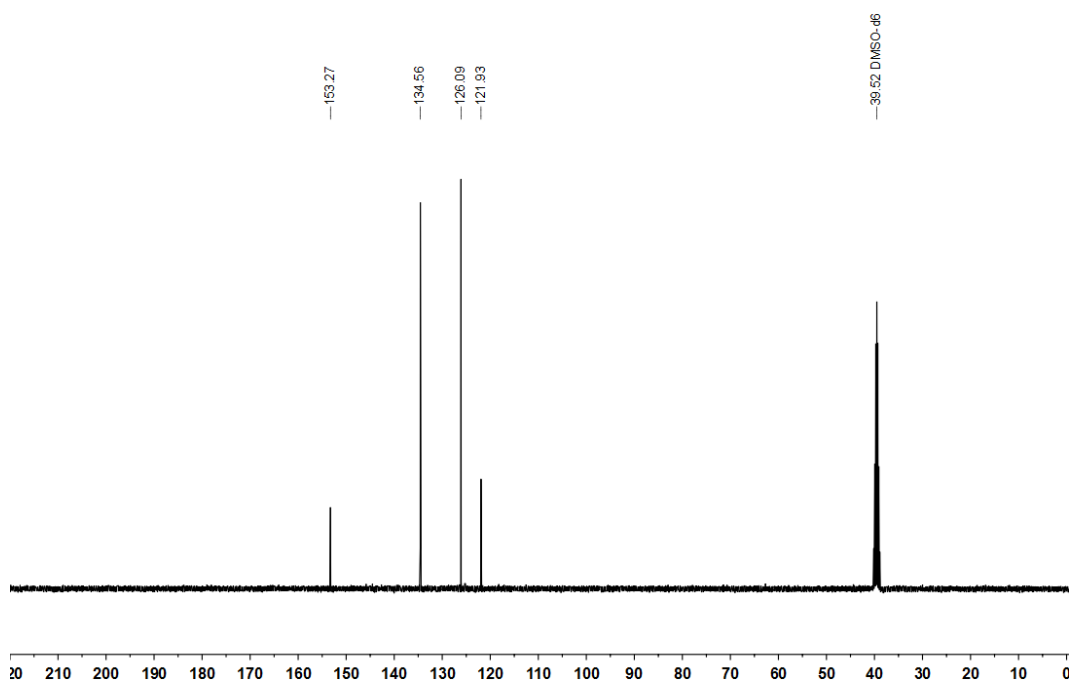
Figure 257 ^{13}C NMR spectrum of **204** (101 MHz, (CD$_3$)$_2$SO).

398
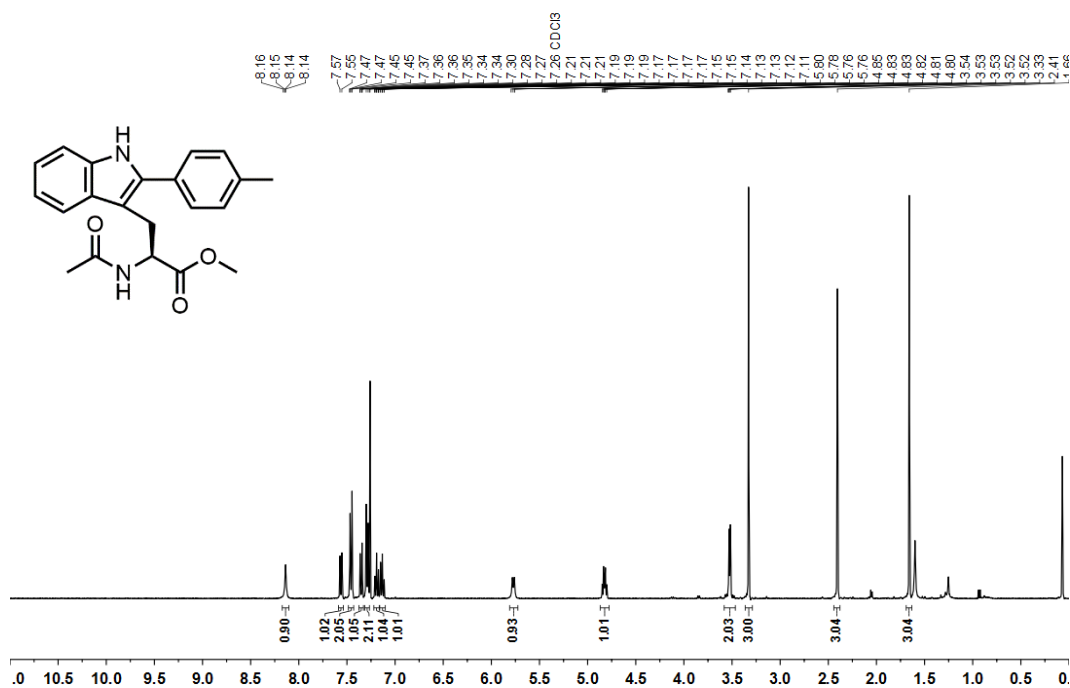
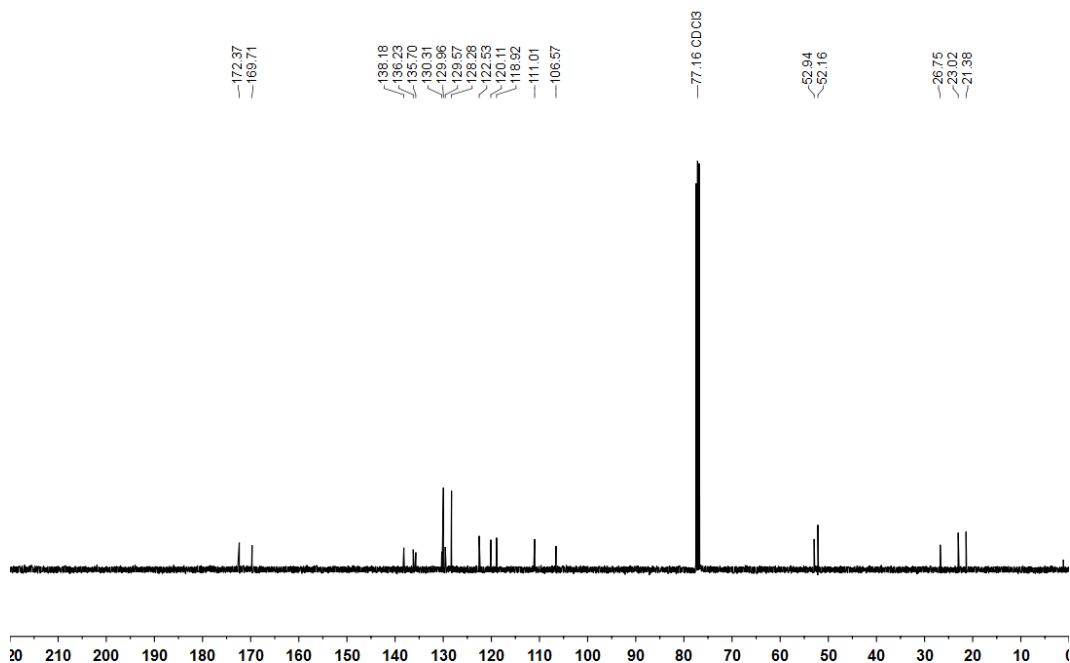**Figure 258** ^{1}H NMR spectrum of **76** (400 MHz, CDCl$_3$).

Figure 259 ^{13}C NMR spectrum of **76** (101 MHz, CDCl$_3$).

Filename: p6770ajr
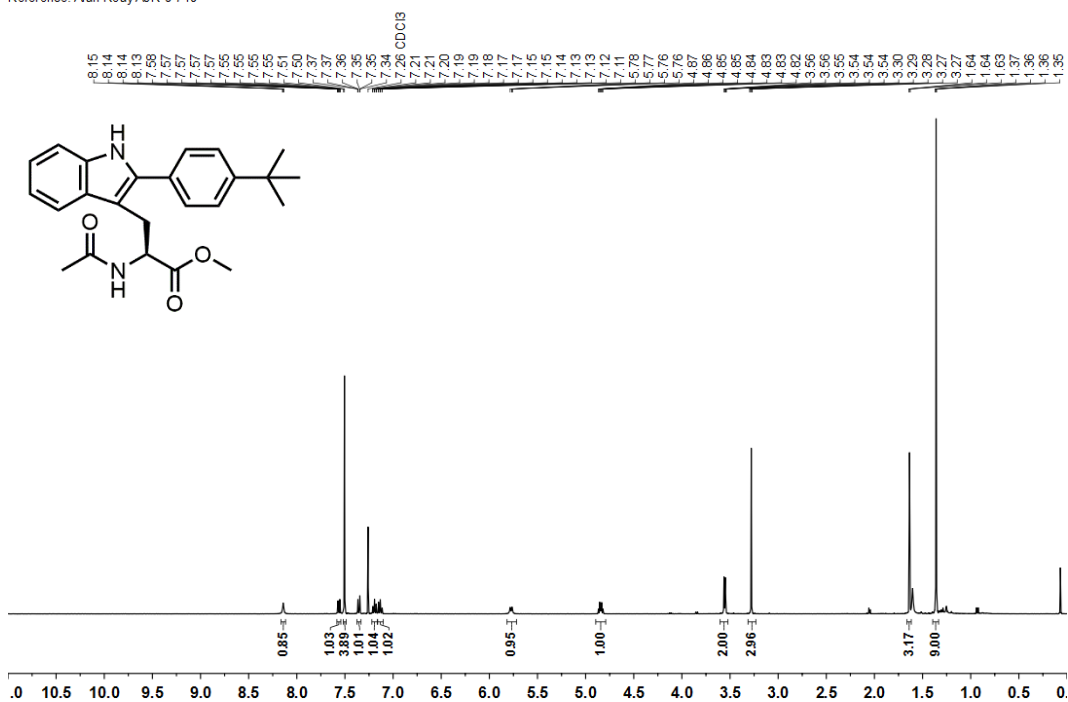Reference: Alan Reay AJR-8-718

Figure 260 ^{1}H NMR spectrum of **205** (400 MHz, CDCl$_3$).
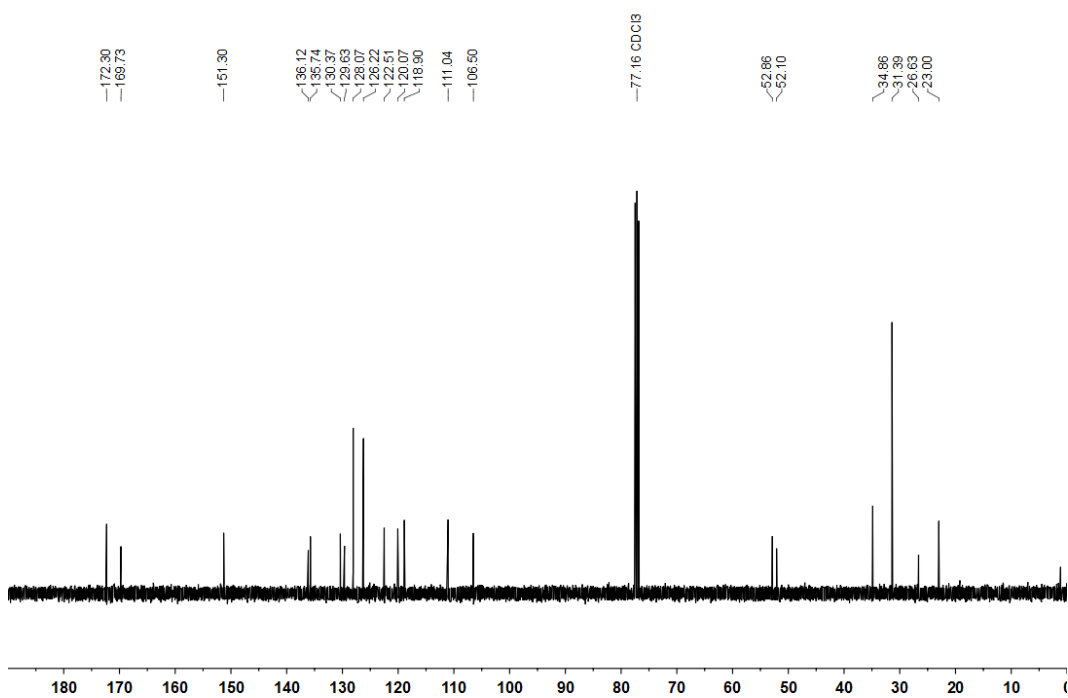
Filename: a3902ajr
Reference: Alan Reay AJR-8-718

Figure 261 ^{13}C NMR spectrum of **205** (101 MHz, CDCl$_3$).

Figure 262 ^{1}H NMR spectrum of **206** (400 MHz, CDCl$_3$).

Figure 263 ^{13}C NMR spectrum of **206** (101 MHz, CDCl$_3$).
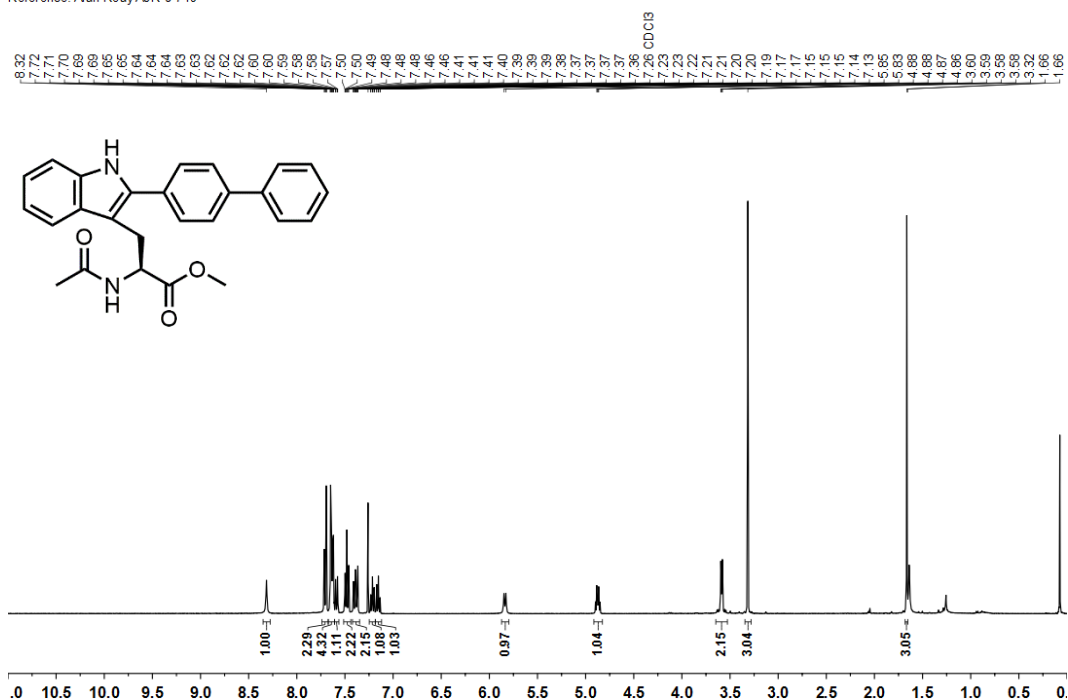
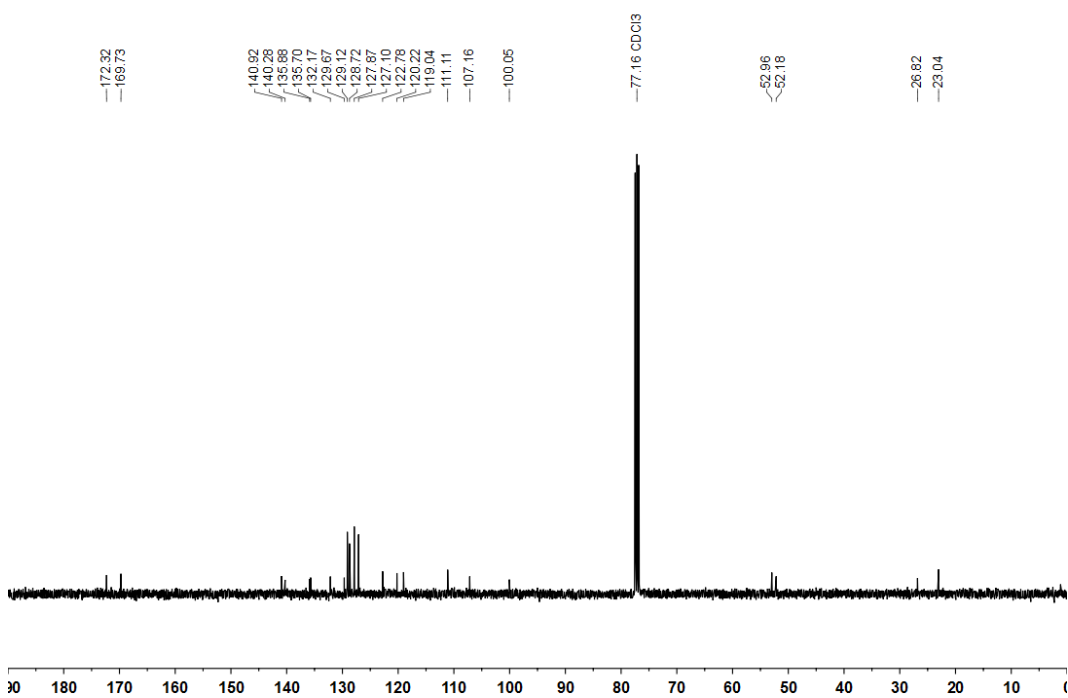**Figure 264** ¹H NMR spectrum of **207** (400 MHz, CDCl₃).

Figure 265 ¹³C NMR spectrum of **207** (101 MHz, CDCl₃).

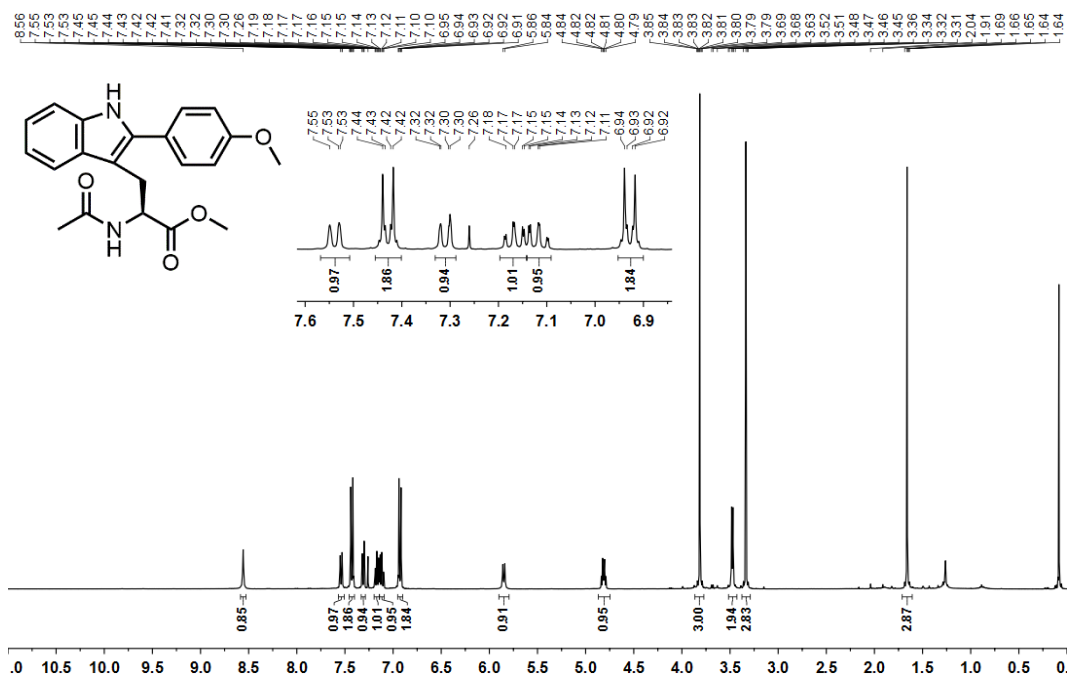Filename: d0742ajr
Reference: Alan Reay AJR-5-410

Figure 266 ^{1}H NMR spectrum of **77** (400 MHz, CDCl$_3$).

Filename: d0742ajr
Reference: Alan Reay AJR-5-410

Figure 267 ^{13}C NMR spectrum of **77** (101 MHz, CDCl$_3$).

Figure 268 [^1]H NMR spectrum of **208** (400 MHz, CDCl$_3$).
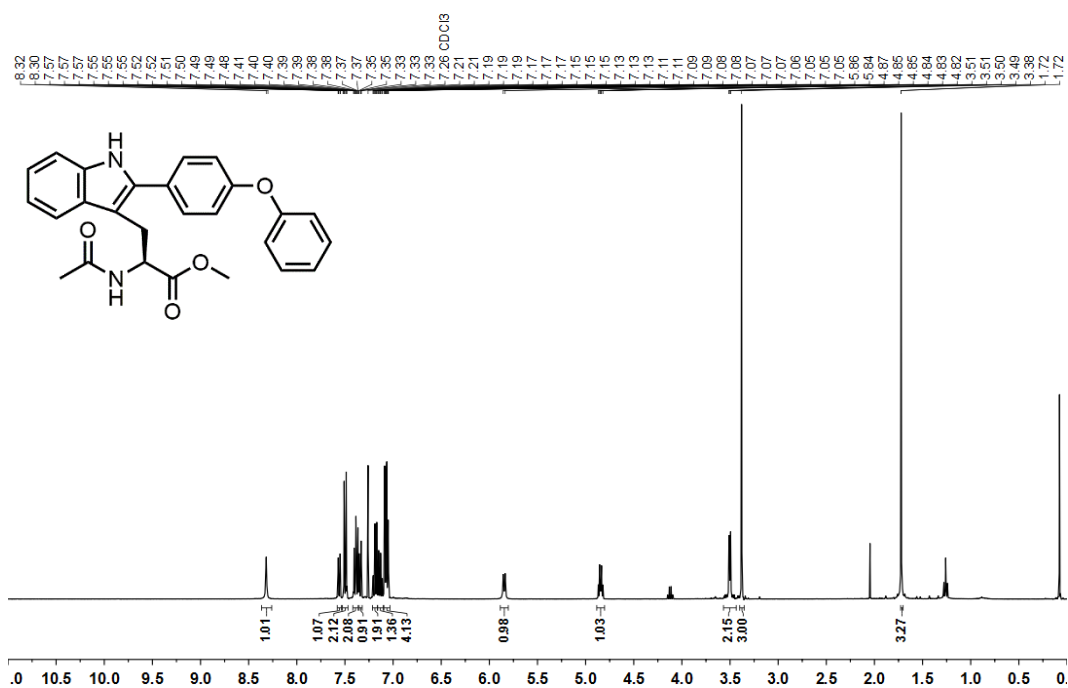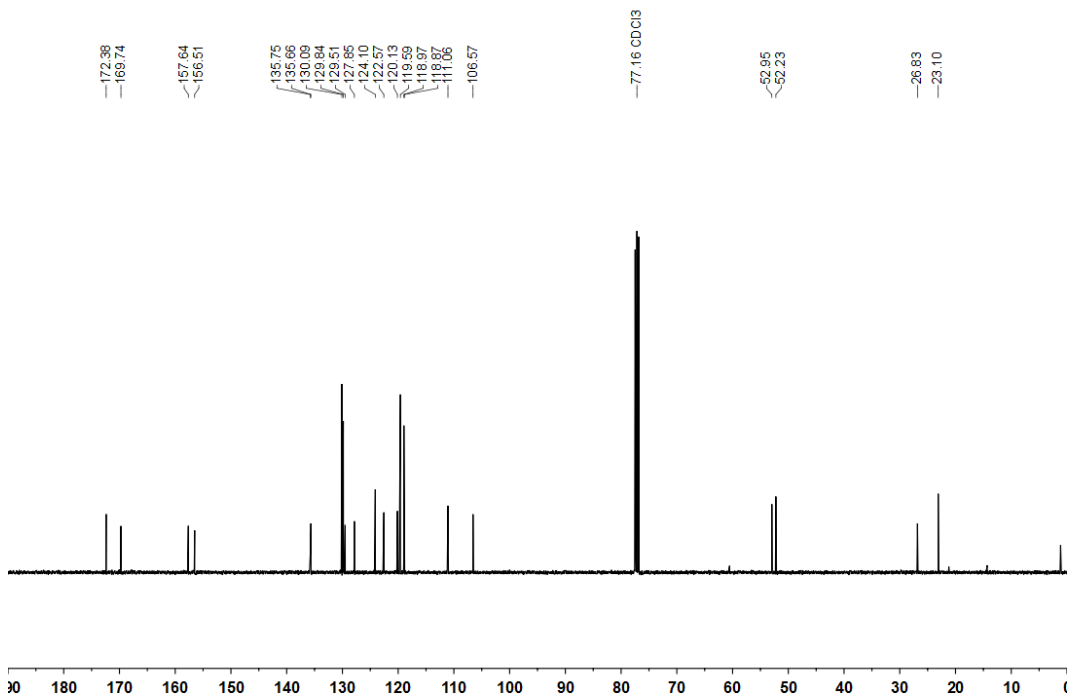
Figure 269 [^13]C NMR spectrum of **208** (101 MHz, CDCl$_3$).
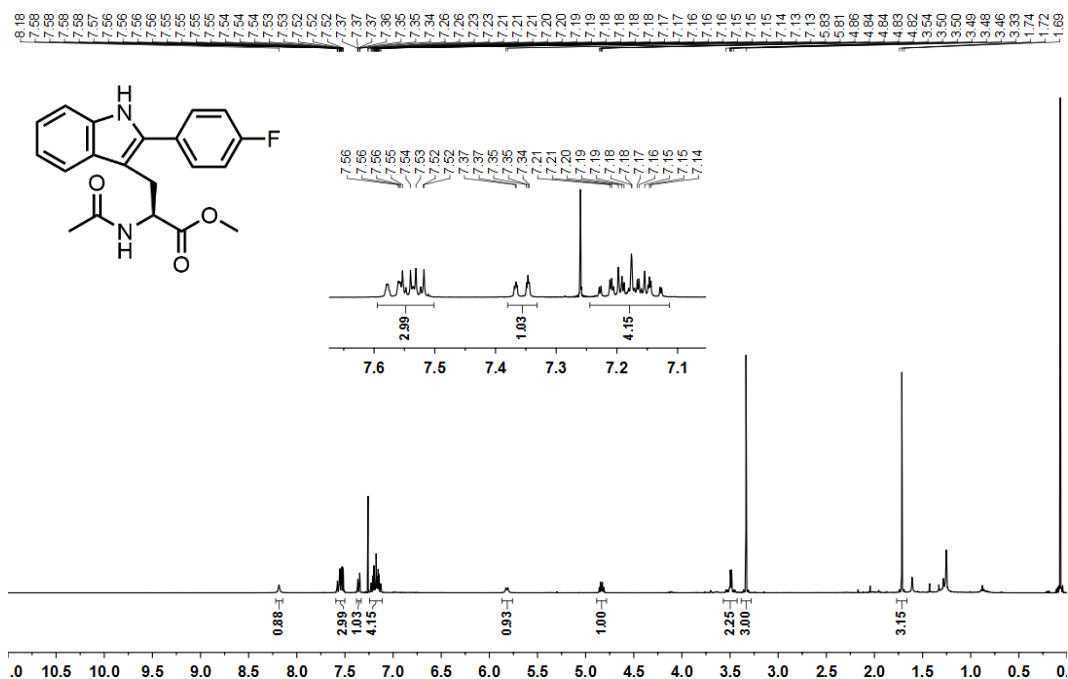
Figure 270 ^{1}H NMR spectrum of **120** (400 MHz, CDCl$_3$).
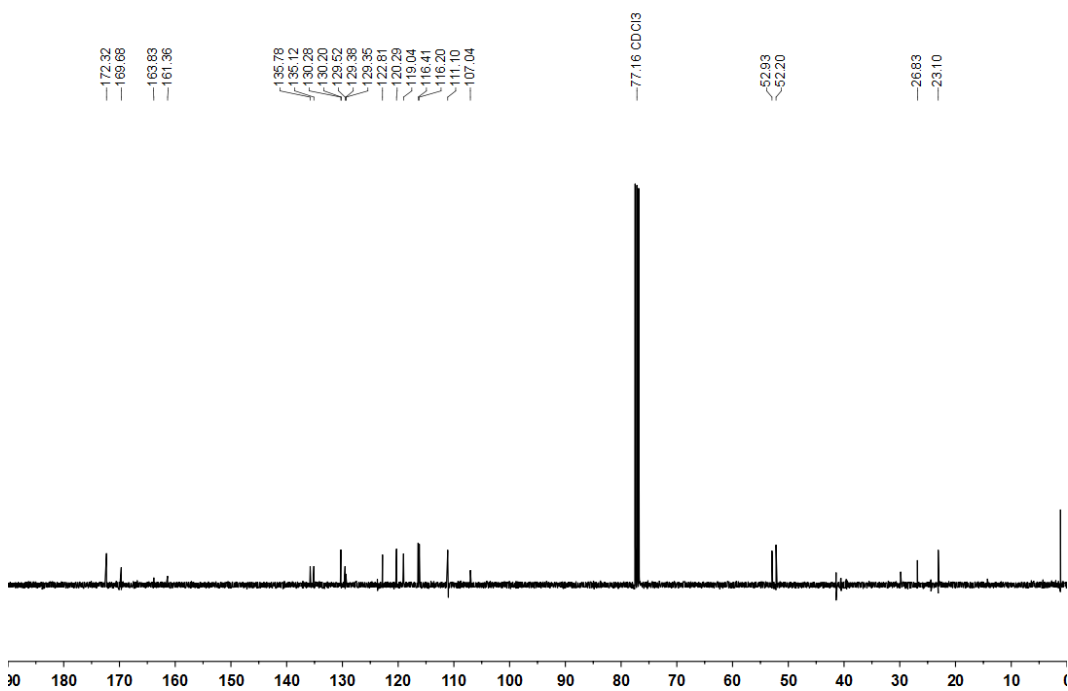
Figure 271 ^{13}C NMR spectrum of **120** (101 MHz, CDCl$_3$).
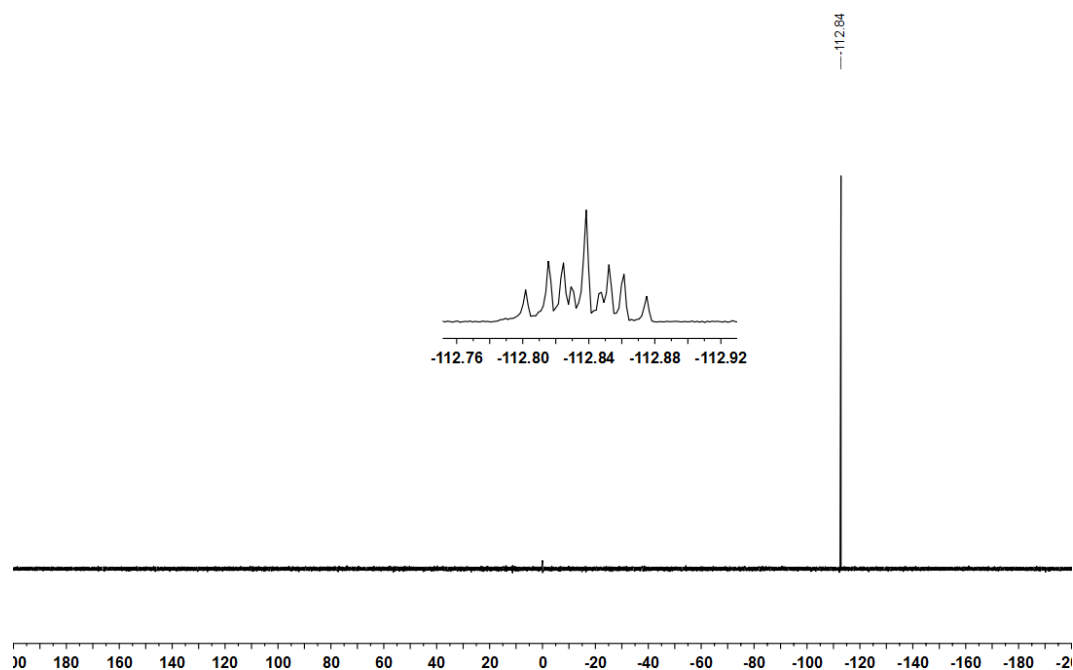
Figure 272 ^{19}F NMR spectrum of **120** (376 MHz, CDCl$_3$).

Filename: n1411ajr
Reference: Alan Reay AJR-5-401
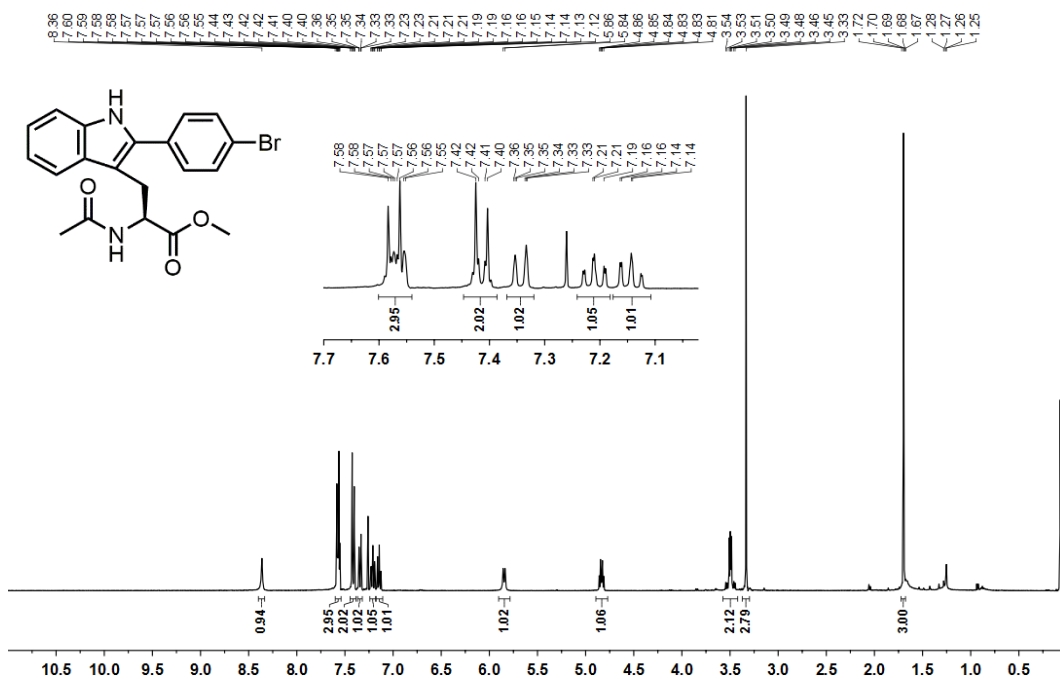
Figure 273 ^{1}H NMR spectrum of **79** (400 MHz, CDCl$_3$).
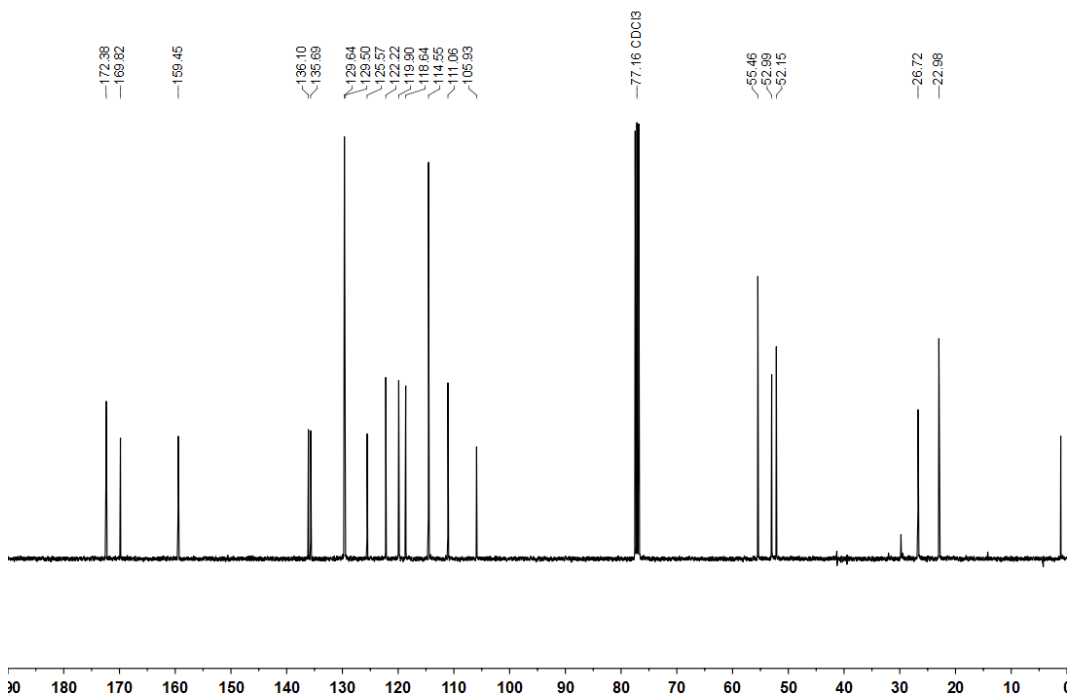
Filename: n1411ajr
Reference: Alan Reay AJR-5-401
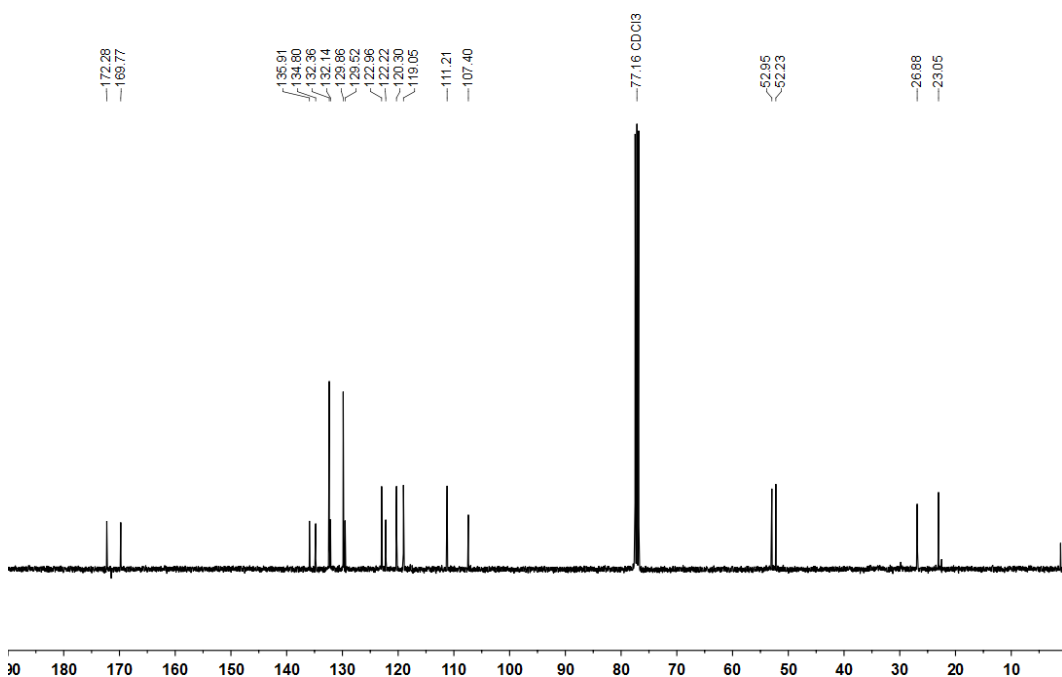
Figure 274 ^{13}C NMR spectrum of **79** (101 MHz, CDCl$_3$).

Figure 275 ^{1}H NMR spectrum of **209** (400 MHz, CDCl$_3$).

Figure 276 ^{13}C NMR spectrum of **209** (101 MHz, CDCl$_3$).

Figure 277 ^{1}H NMR spectrum of **210** (400 MHz, CDCl$_3$).

Figure 278 ^{13}C NMR spectrum of **210** (101 MHz, CDCl$_3$).
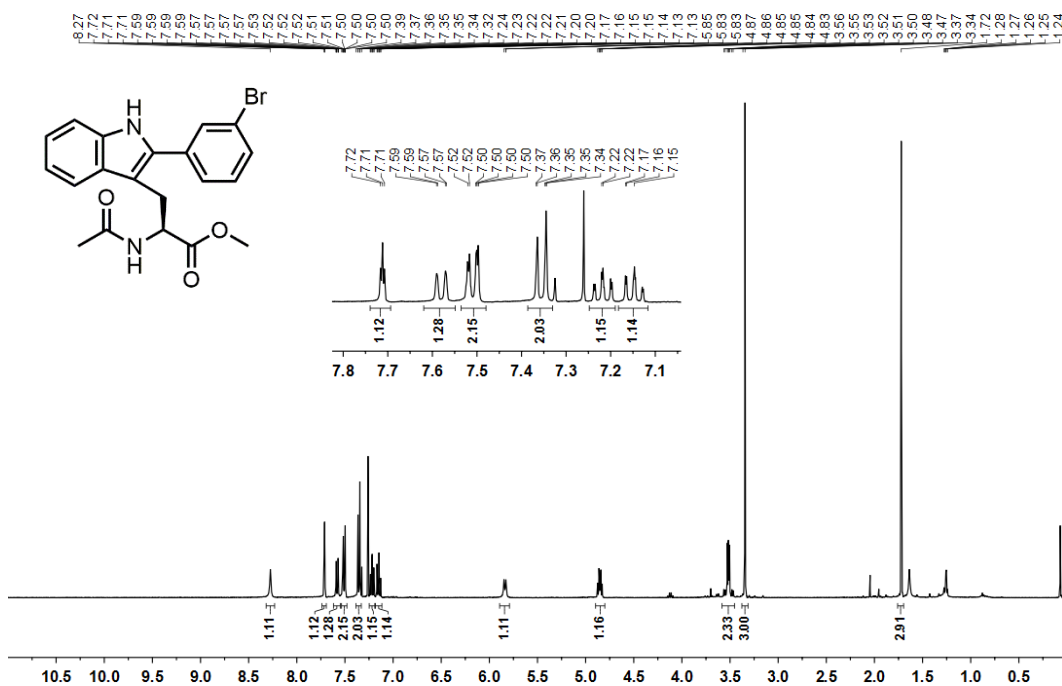
Filename: n1413ajr
Reference: Alan Reay AJR-5-408
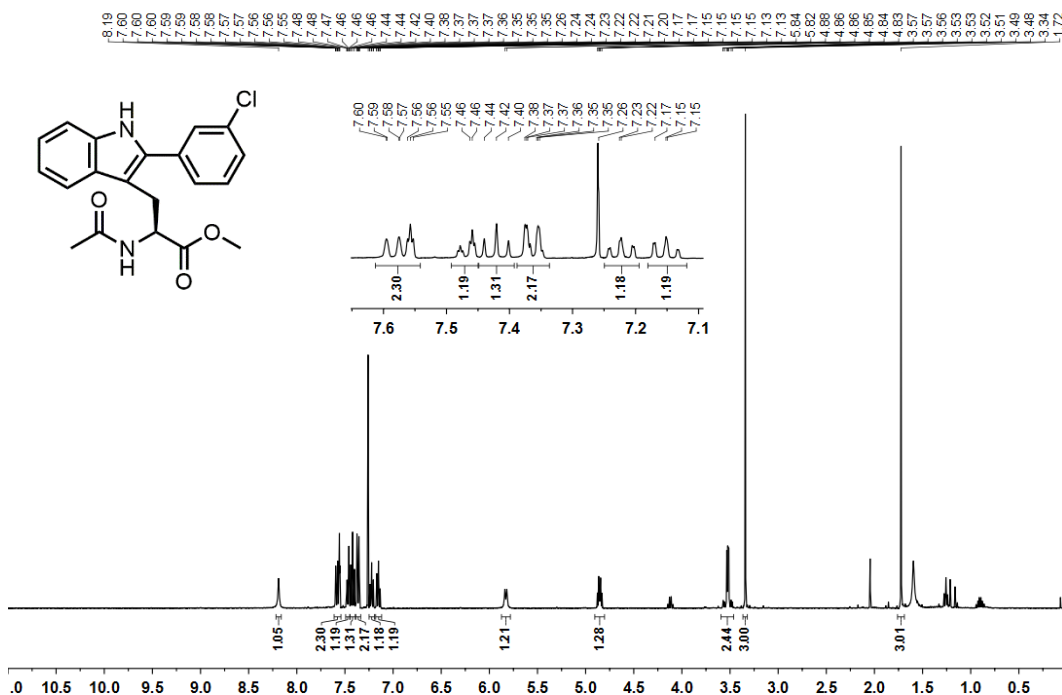
Figure 279 ^{1}H NMR spectrum of **211** (400 MHz, CDCl$_3$).

Filename: n1413ajr
Reference: Alan Reay AJR-5-408
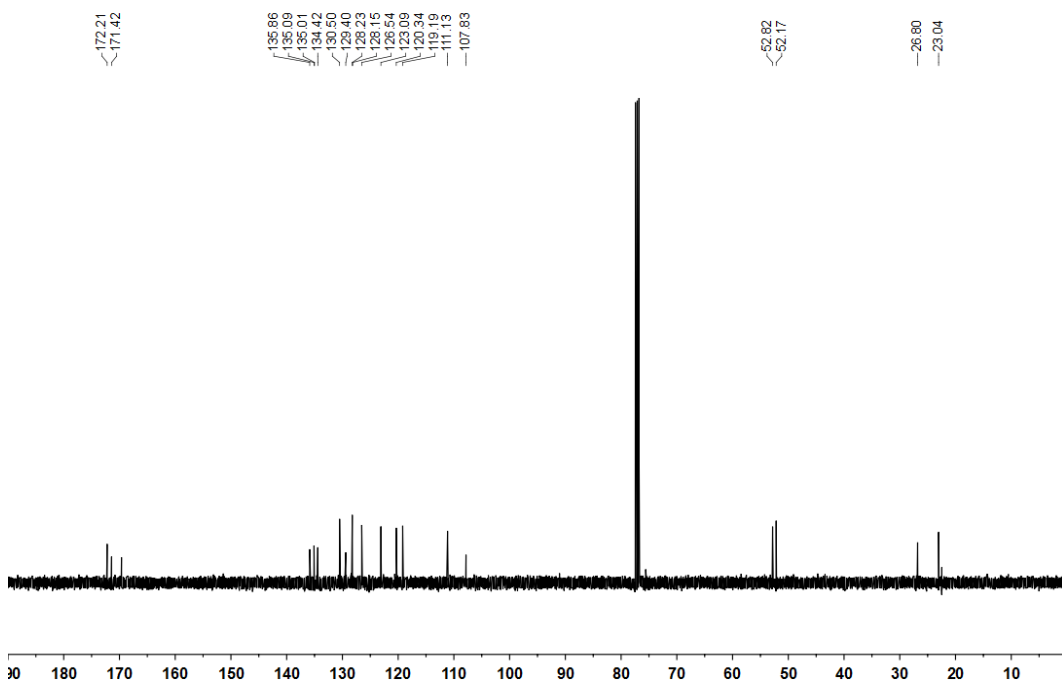
Figure 280 ^{13}C NMR spectrum of **211** (101 MHz, CDCl$_3$).

Filename: n7561ajr
Reference: Alan Reay AJR-6-532

7.73
7.73
7.72
7.71
7.70
7.26
7.25
7.24
7.24

3.31 CD3OD
2.60
2.58
2.57
2.55
2.54
2.53
2.51
2.38
2.06
2.05
2.03
2.02

TsO   OTs
  \   /
   Pd
  /   \
MeCN   MeCN

4.00
3.98

1.82
6.26
3.33

.0 10.5 10.0 9.5 9.0 8.5 8.0 7.5 7.0 6.5 6.0 5.5 5.0 4.5 4.0 3.5 3.0 2.5 2.0 1.5 1.0 0.5 0.
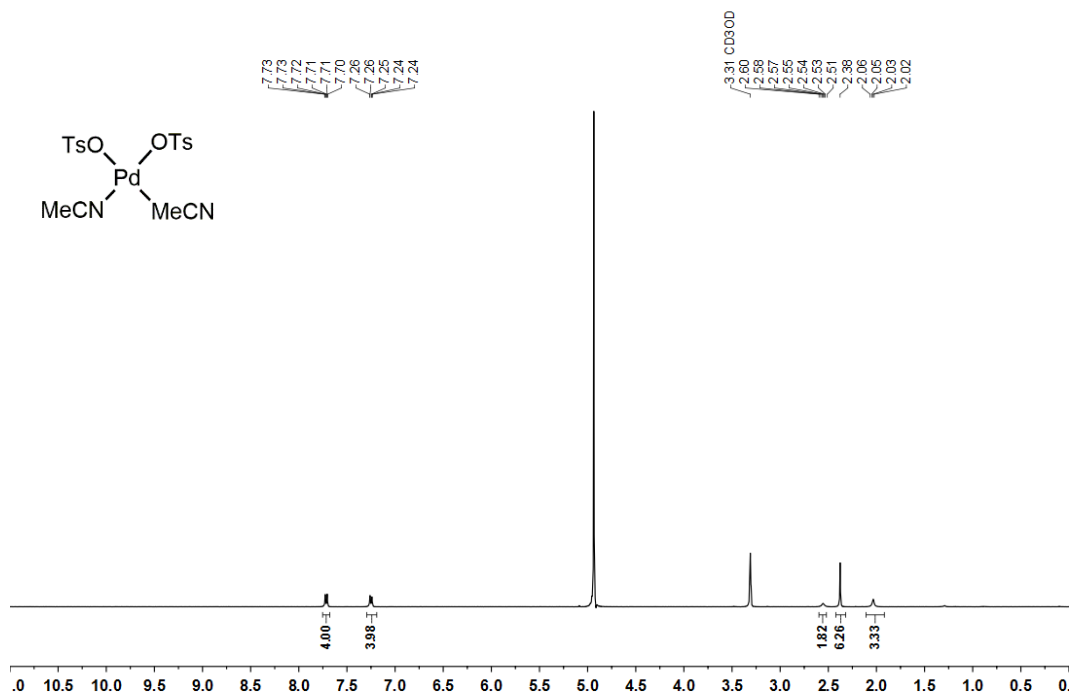
Figure 281 ^{1}H NMR spectrum of **215** (400 MHz, CD$_3$OD).

Filename: AJR-6-532 13C data (500 MHz).1.fid
Reference:

129.95
127.03

49.00 CD3OD

21.31

90 180 170 160 150 140 130 120 110 100 90 80 70 60 50 40 30 20 10 0
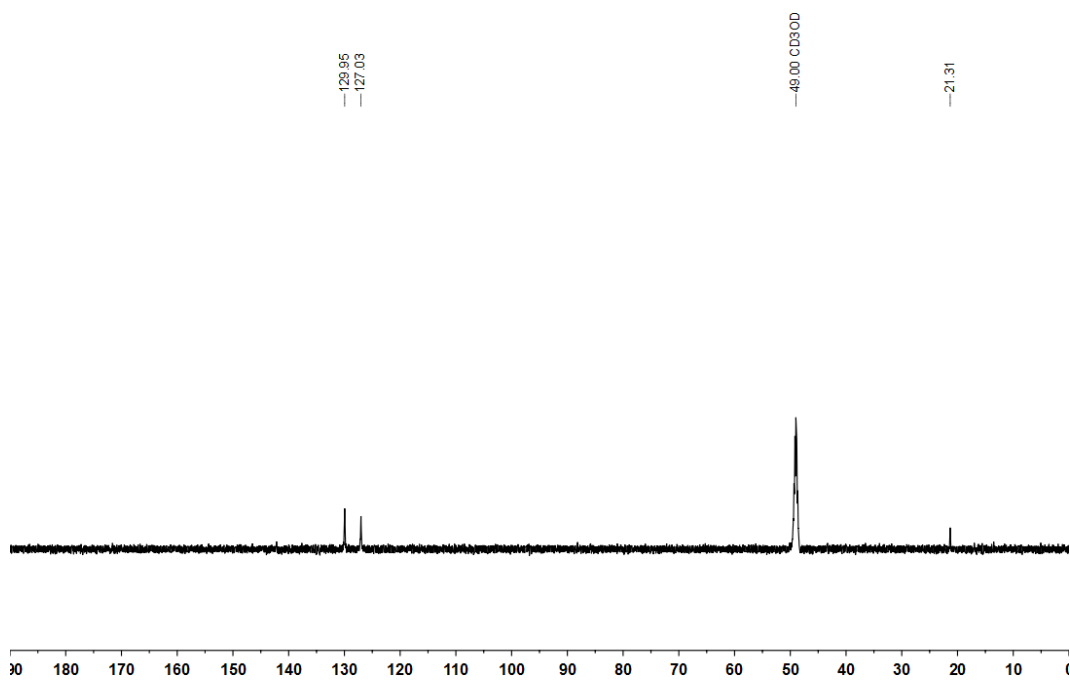
Figure 282 ^{13}C NMR spectrum of **215** (125 MHz, CD$_3$OD).
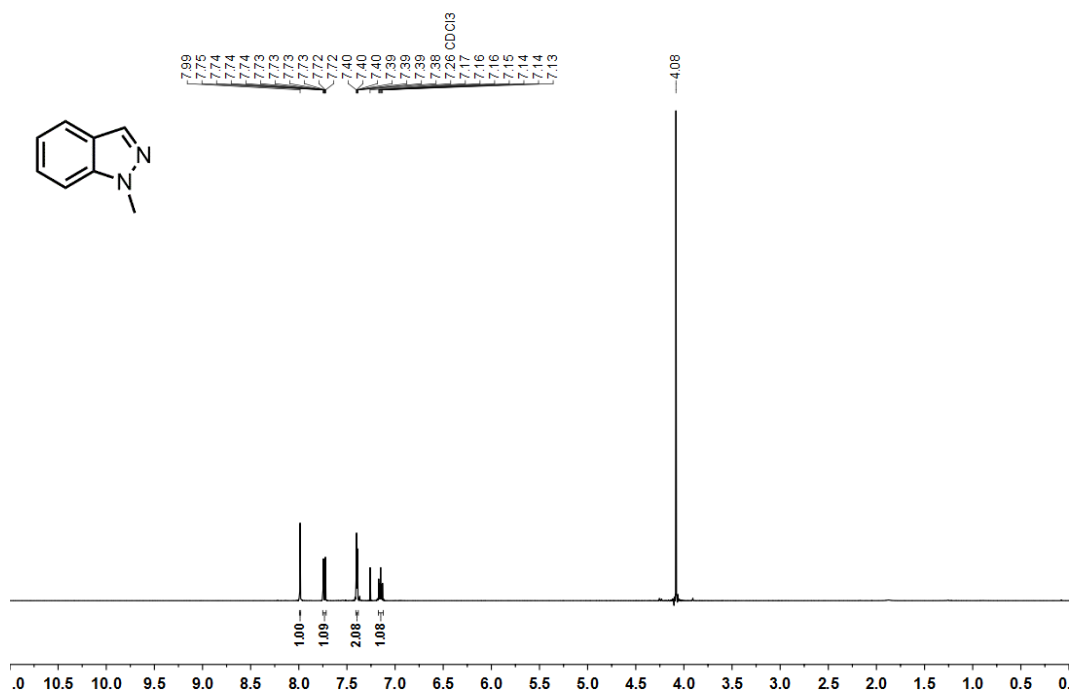
Figure 283 ^{1}H NMR spectrum of **224** (400 MHz, CDCl$_3$).
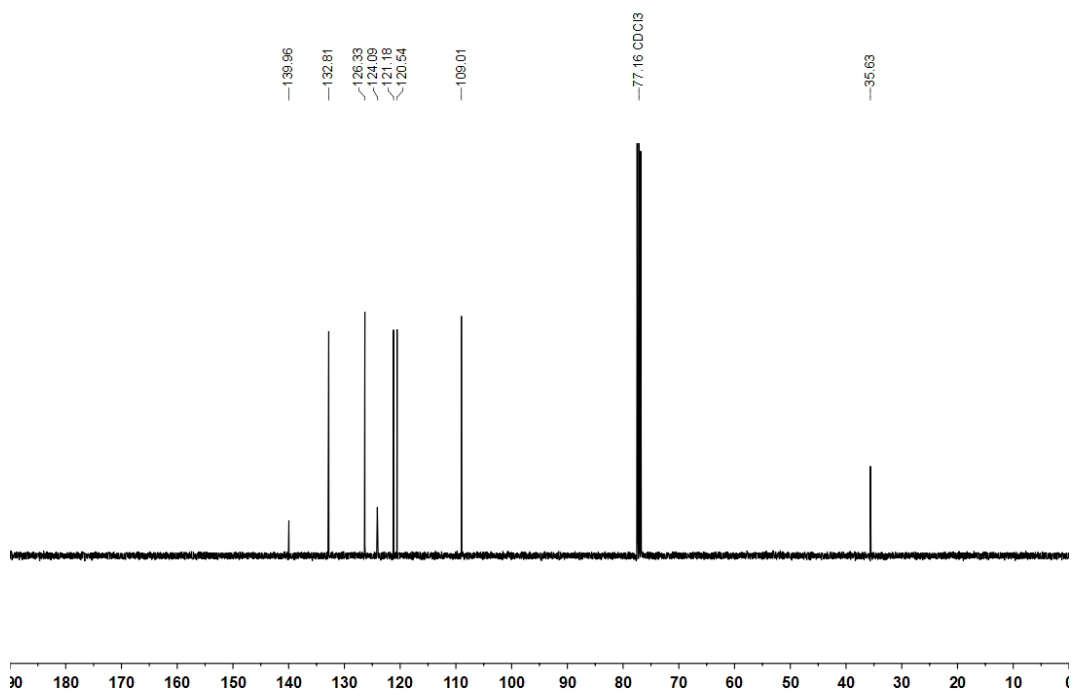
Figure 284 ^{13}C NMR spectrum of **224** (101 MHz, CDCl$_3$).

Filename: n5596ajr
Reference: Alan Reay AJR-6-480
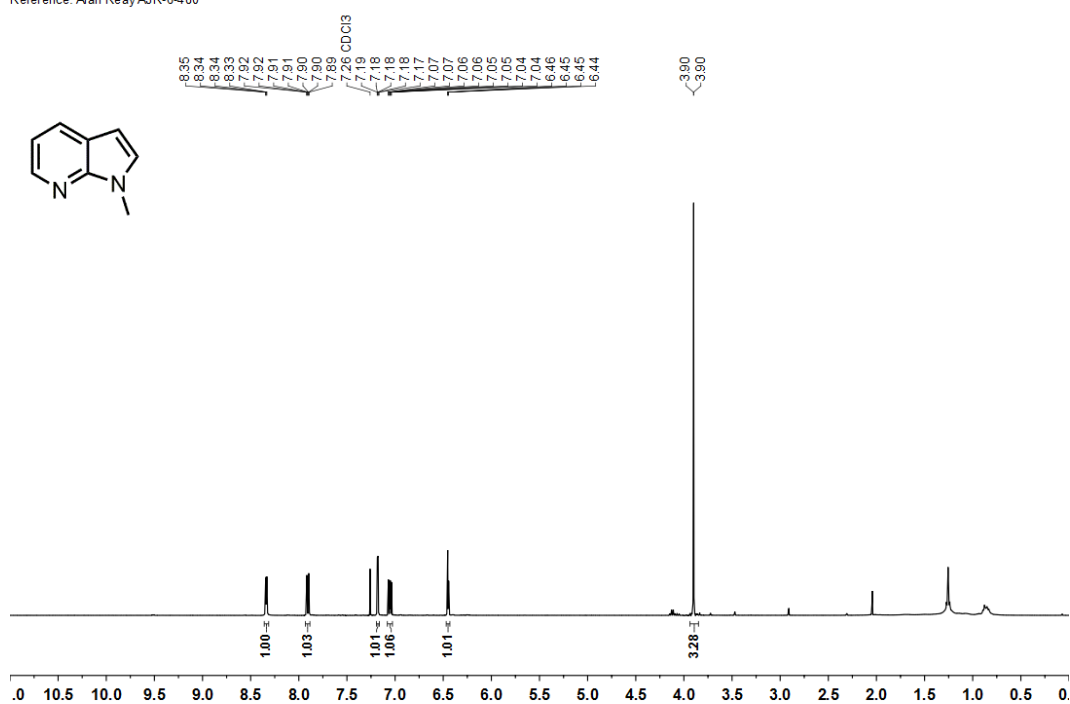
Figure 285 ^{1}H NMR spectrum of **231** (400 MHz, CDCl$_3$).

Filename: n5596ajr
Reference: Alan Reay AJR-6-480
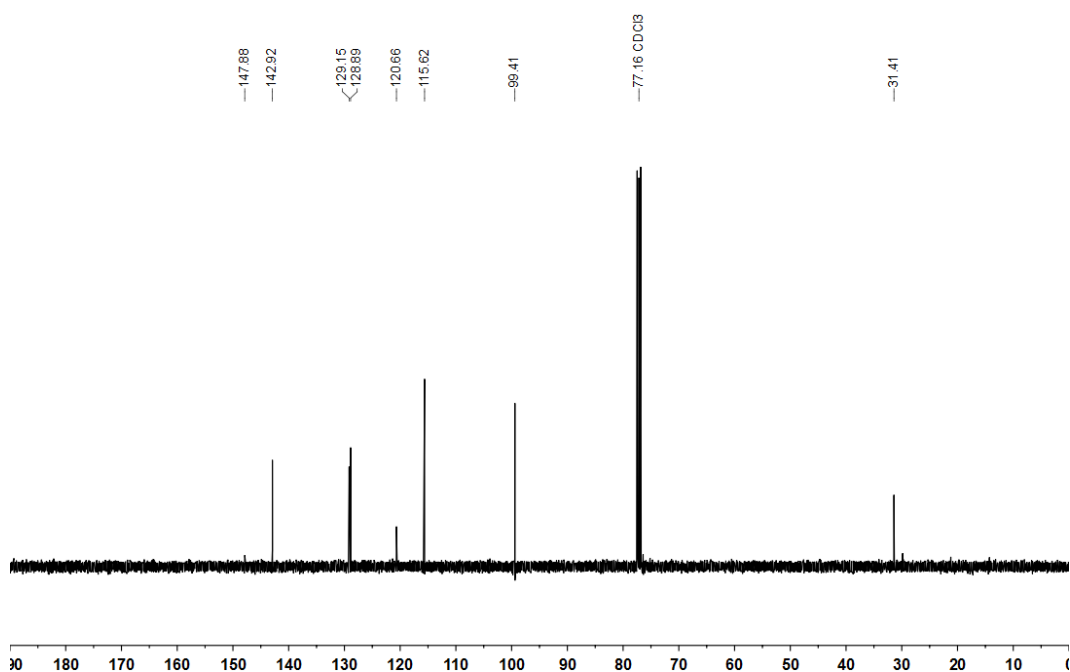
Figure 286 ^{13}C NMR spectrum of **231** (101 MHz, CDCl$_3$).

413
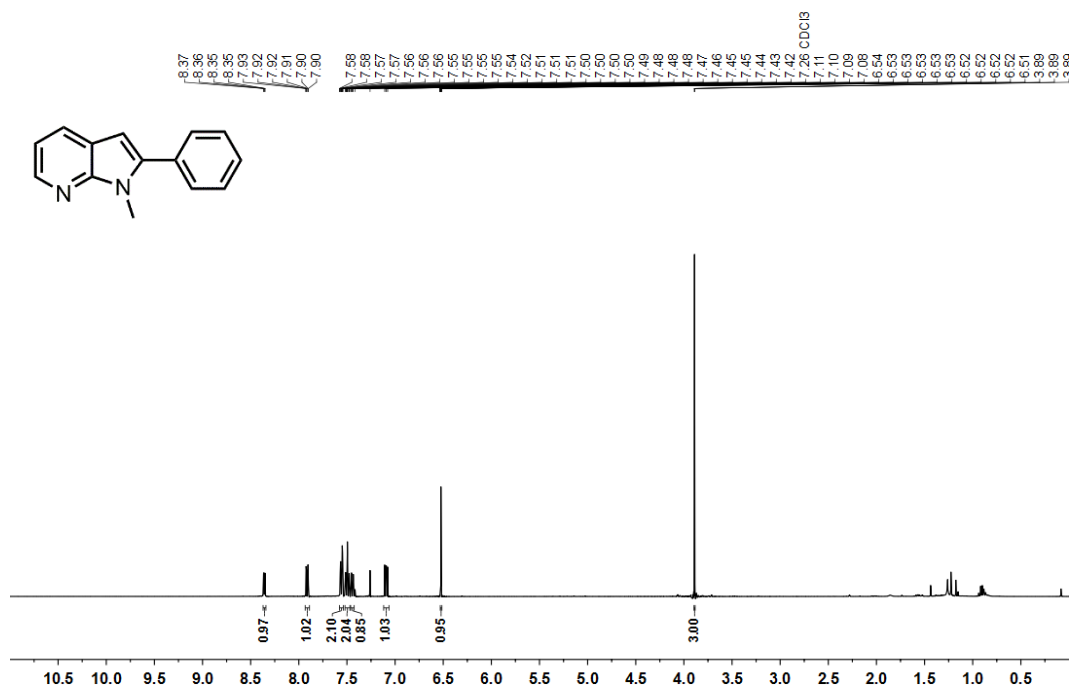
Figure 287 ^{1}H NMR spectrum of **232** (400 MHz, CDCl$_3$).
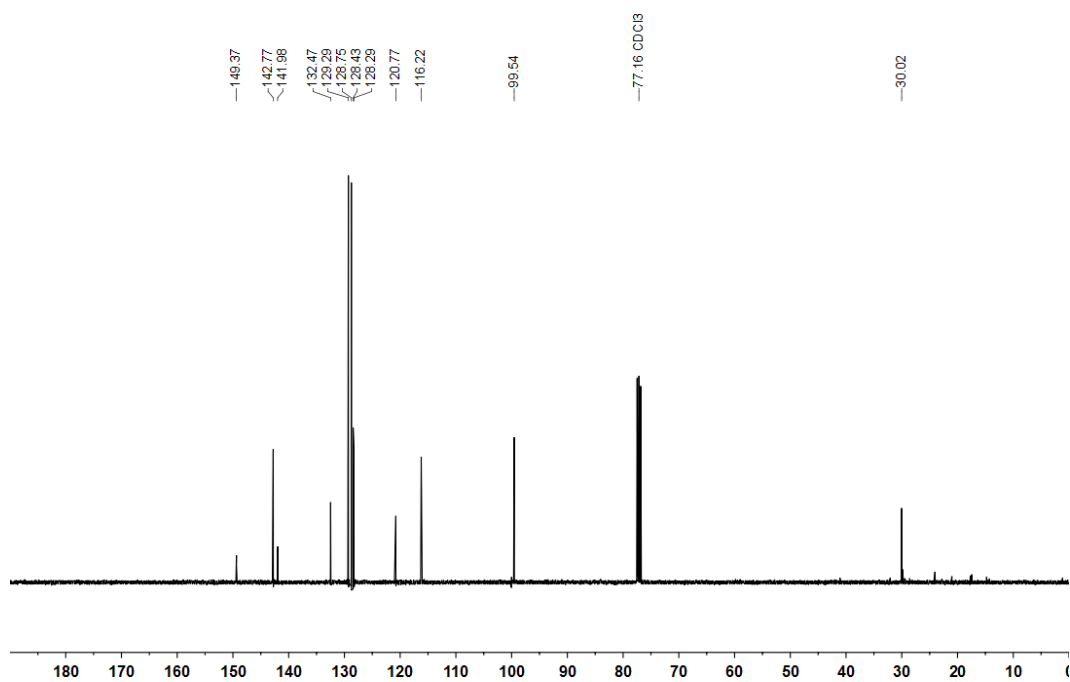
Figure 288 ^{13}C NMR spectrum of **232** (101 MHz, CDCl$_3$).

Filename: n5654ajr
Reference: Alan Reay AJR-6-486

Figure 289 ^{1}H NMR spectrum of **233** (400 MHz, (CD$_3$)$_2$SO).

Filename: n5801ajr
Reference: Alan Reay AJR-6-486

Figure 290 ^{13}C NMR spectrum of **233** (101 MHz, CDCl$_3$).
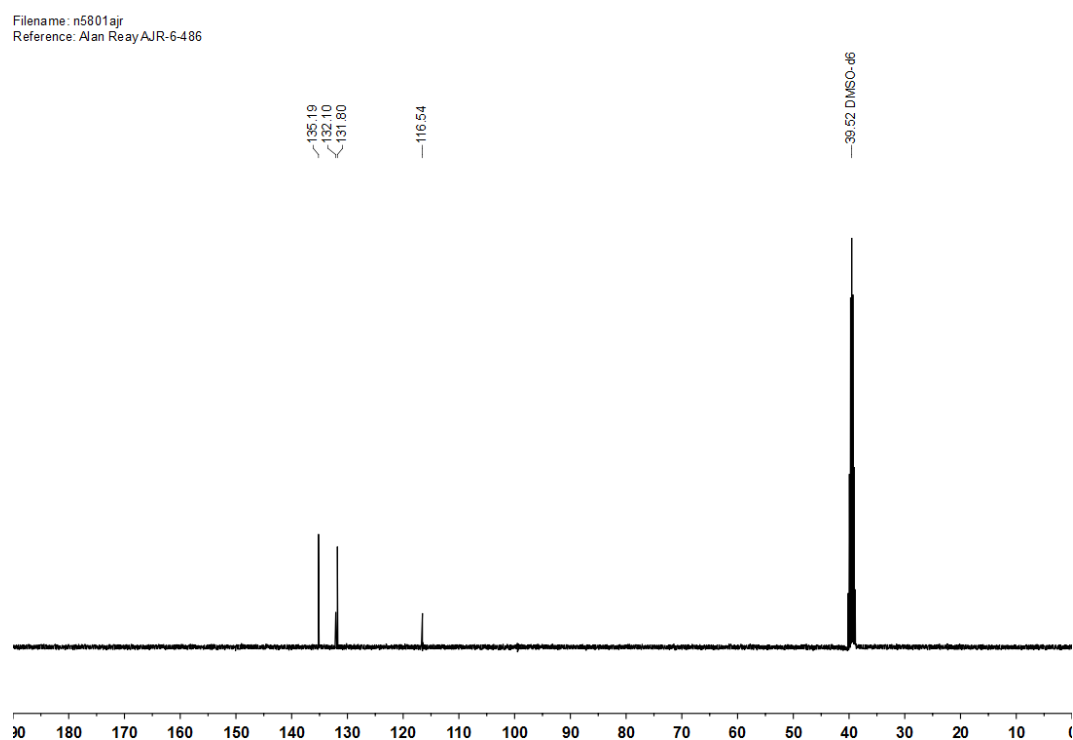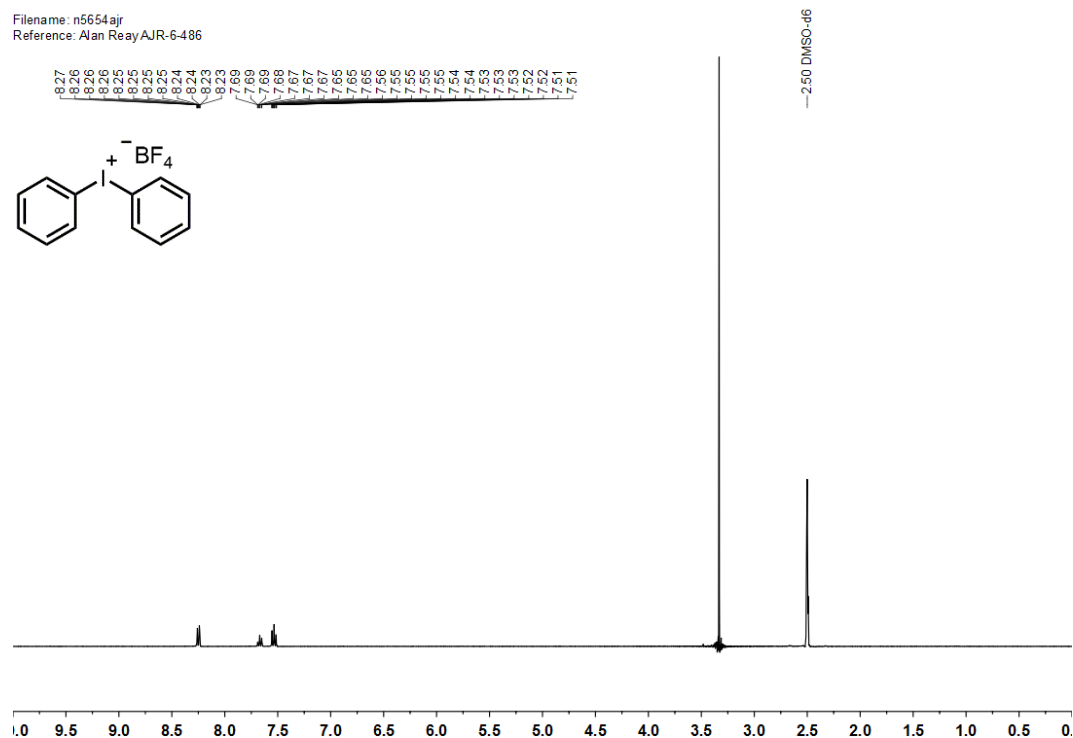
Filename: a0551ajr
Reference: Alan Reay AJR-7-641-2
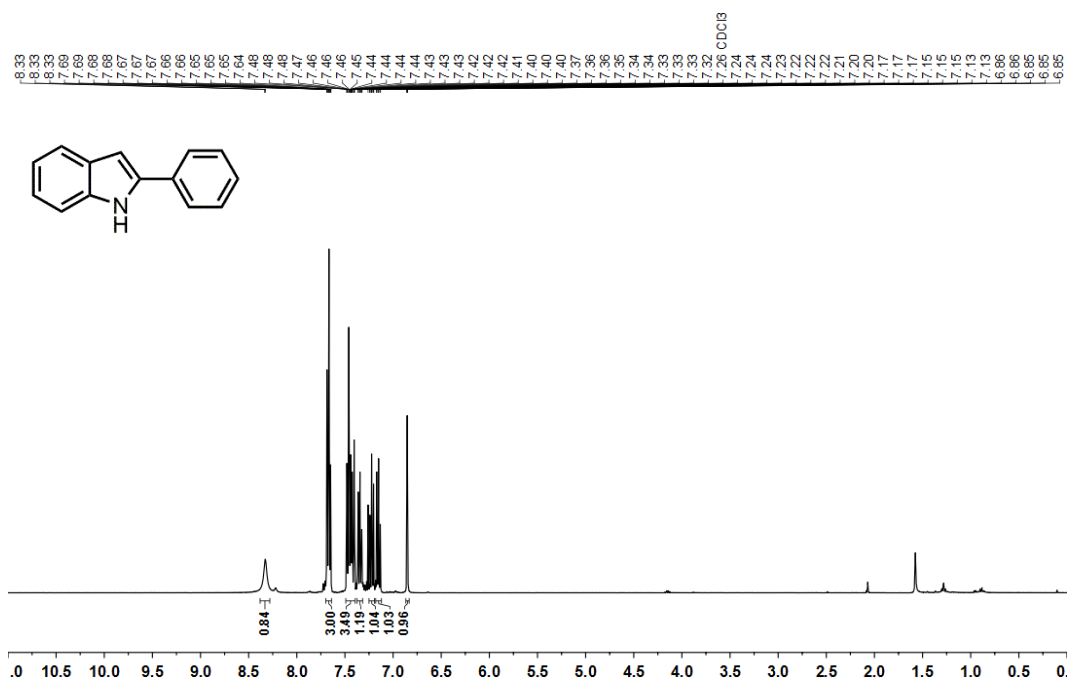
Figure 291 ^{1}H NMR spectrum of **234** (400 MHz, CDCl$_3$).

Filename: a0603ajr
Reference: Alan Reay AJR-7-641-2
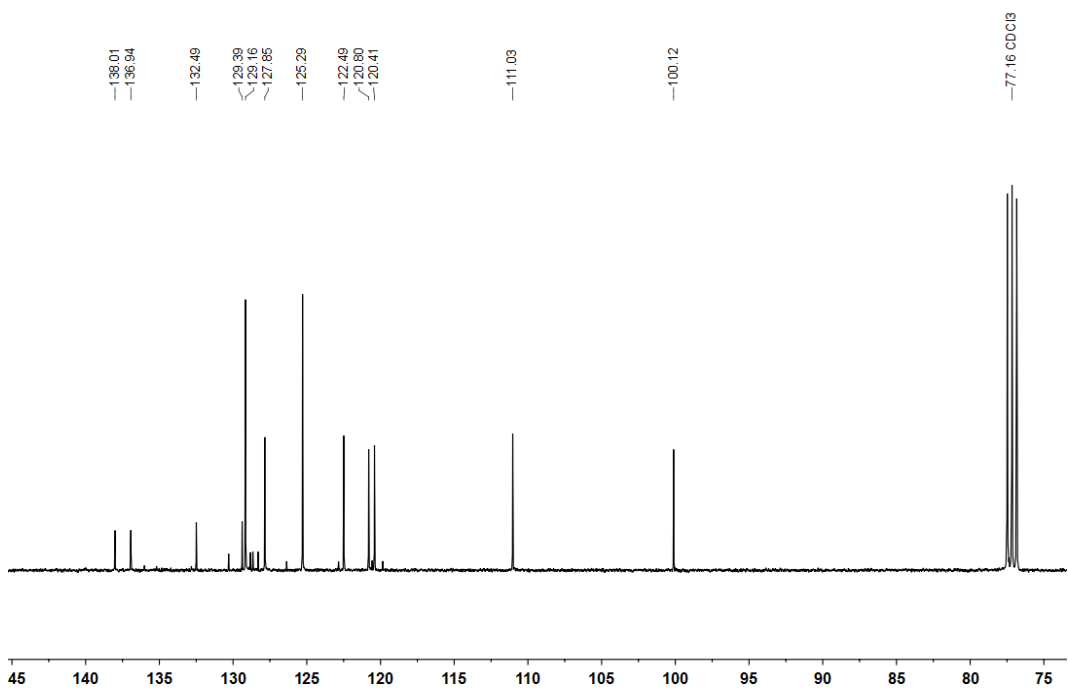
Figure 292 ^{13}C NMR spectrum of **234** (101 MHz, CDCl$_3$).

Figure 293 ^{1}H NMR spectrum of **38** (400 MHz, (CD$_3$)$_2$SO).

Figure 294 ^{13}C NMR spectrum of **38** (101 MHz, (CD$_3$)$_2$SO).

417

Filename: a4454ajr
Reference: Alan Reay AJR-8-726

—77.66

190 170 150 130 110 90 70 50 30 10 -10 -30 -50 -70 -90 -110 -130 -150 -170 -190
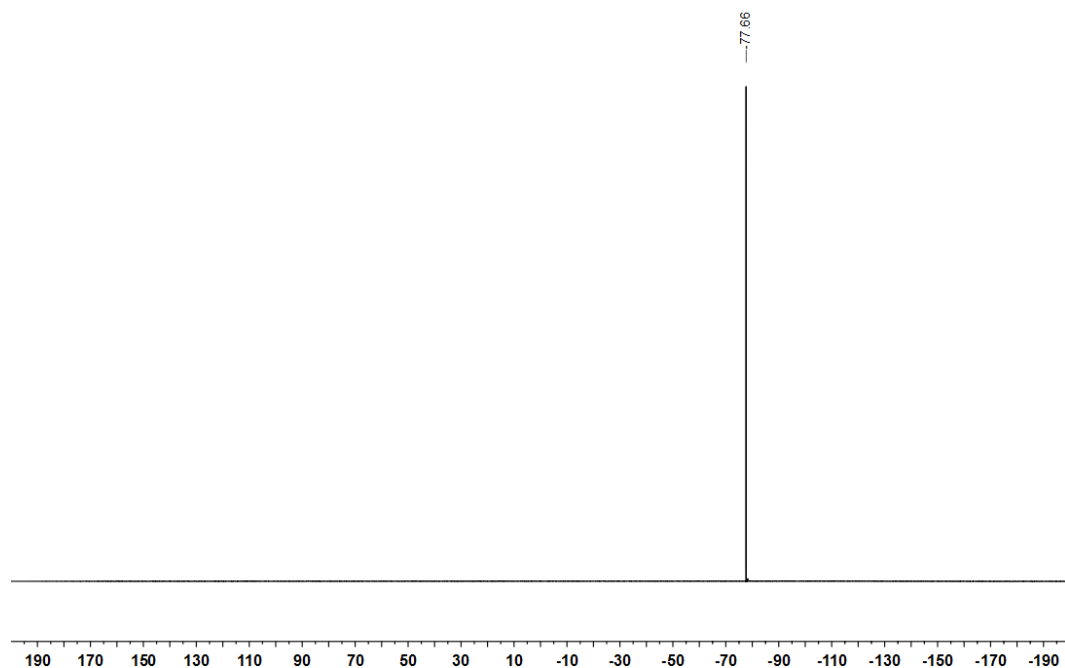
Figure 295 ^{19}F NMR spectrum of **38** (376 MHz, $(CD_3)_2SO$).
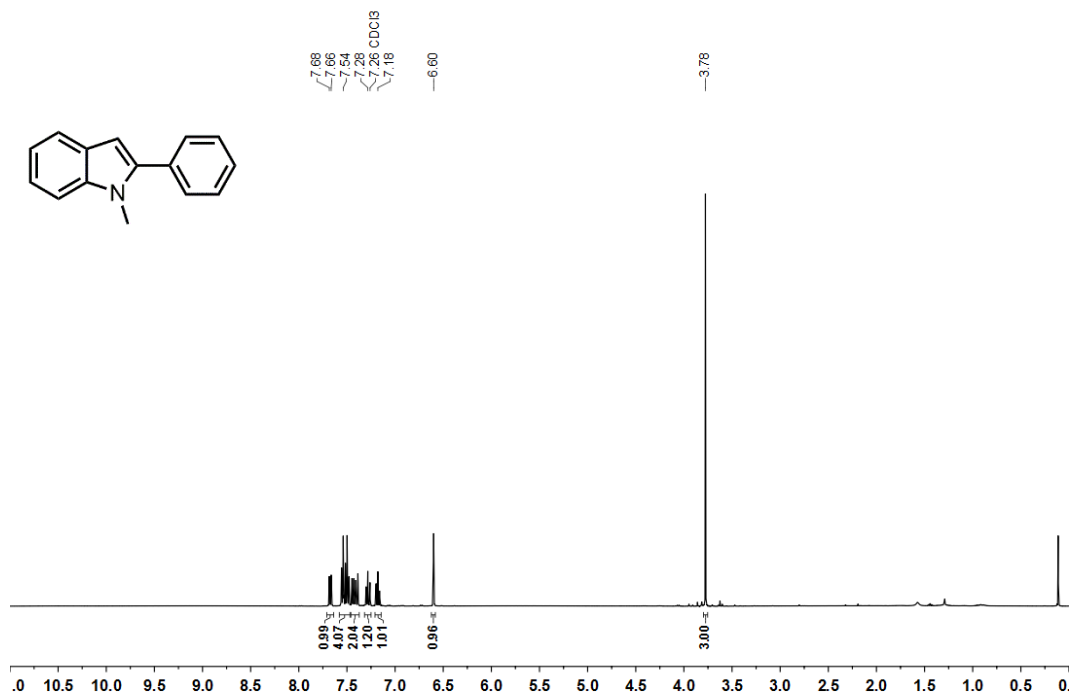
Figure 296 ^{1}H NMR spectrum of **34** (400 MHz, CDCl$_3$).
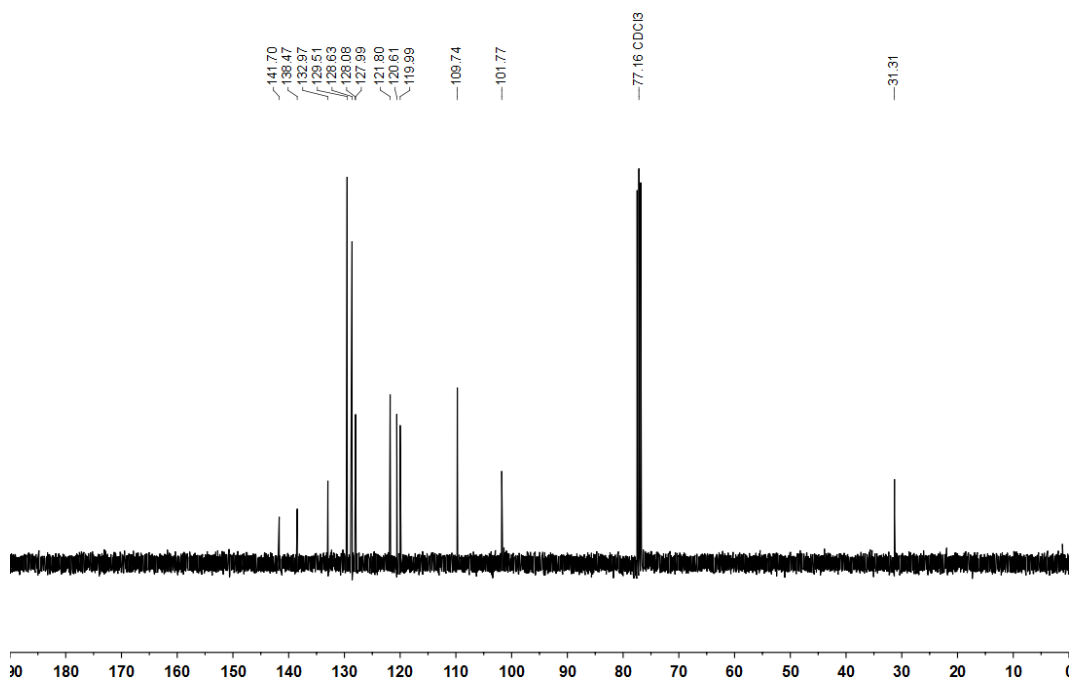
Figure 297 ^{13}C NMR spectrum of **34** (101 MHz, CDCl$_3$).
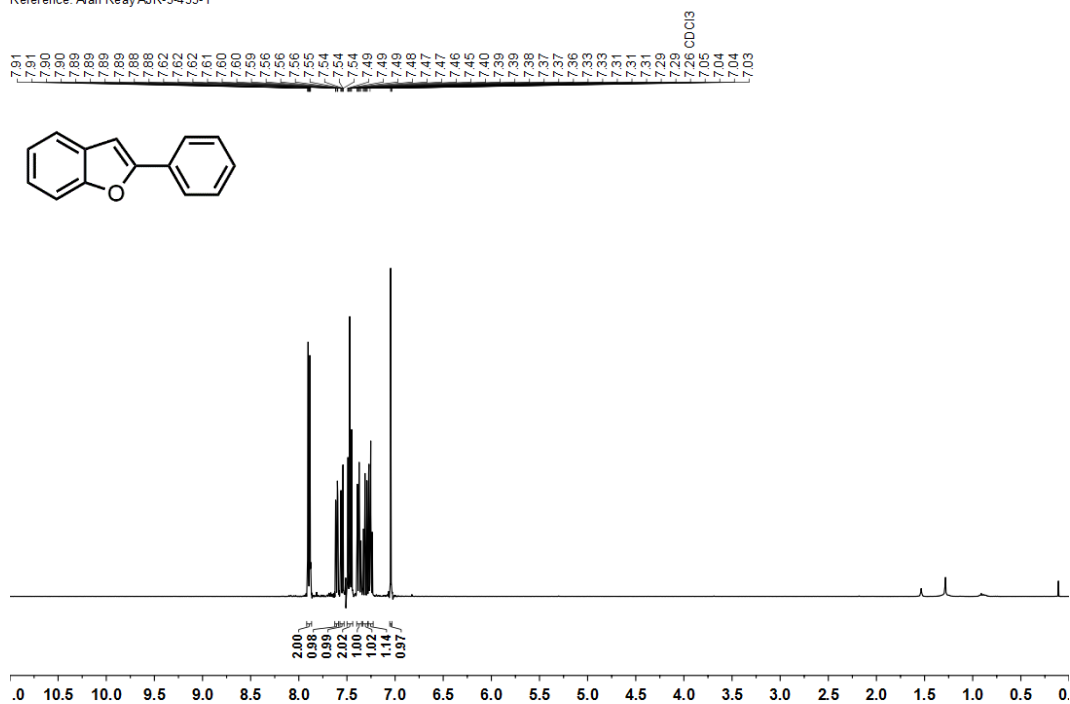
Figure 298 ^{1}H NMR spectrum of **240** (400 MHz, CDCl$_3$).
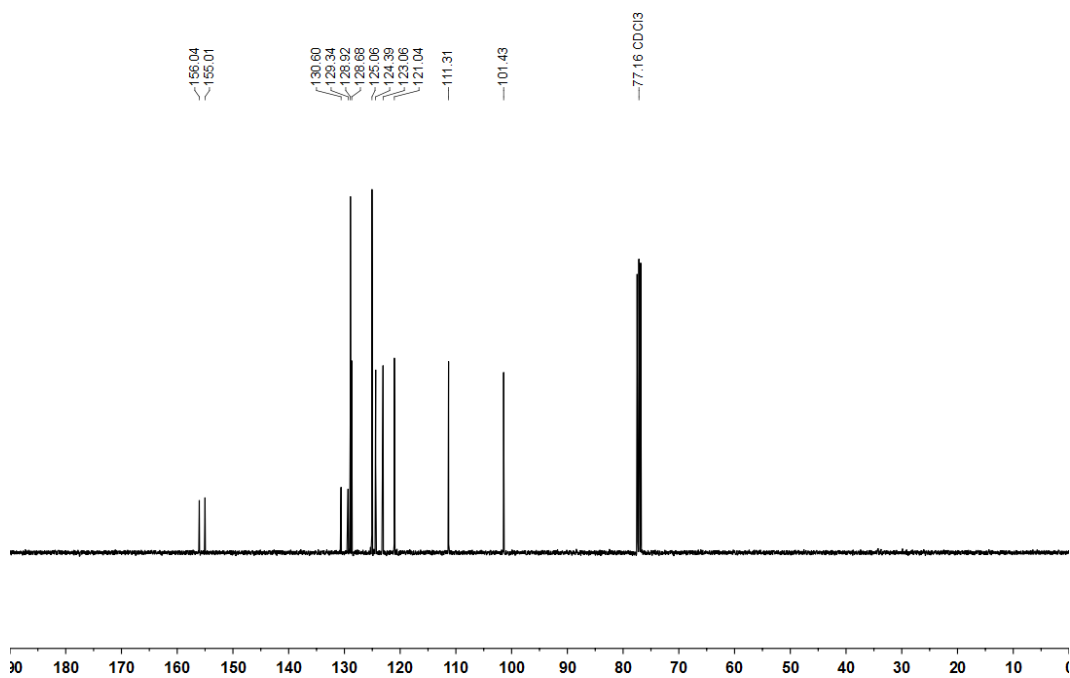
Figure 299 ^{13}C NMR spectrum of **240** (101 MHz, CDCl$_3$).
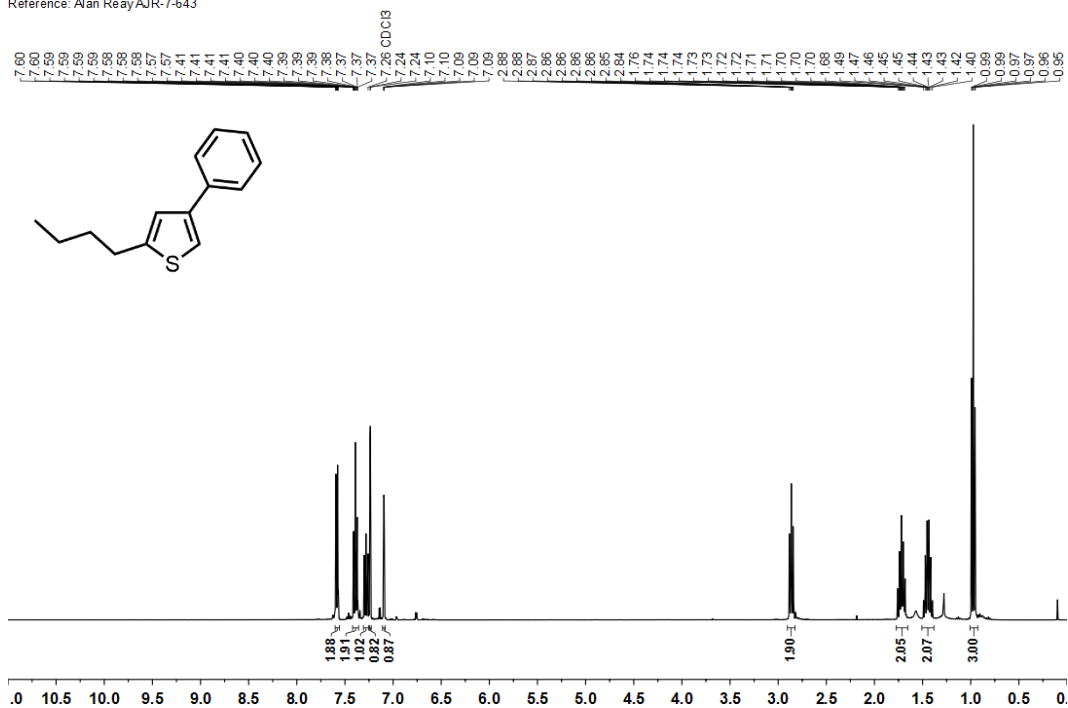
Figure 300 ^{1}H NMR spectrum of **242** (400 MHz, CDCl[3]).
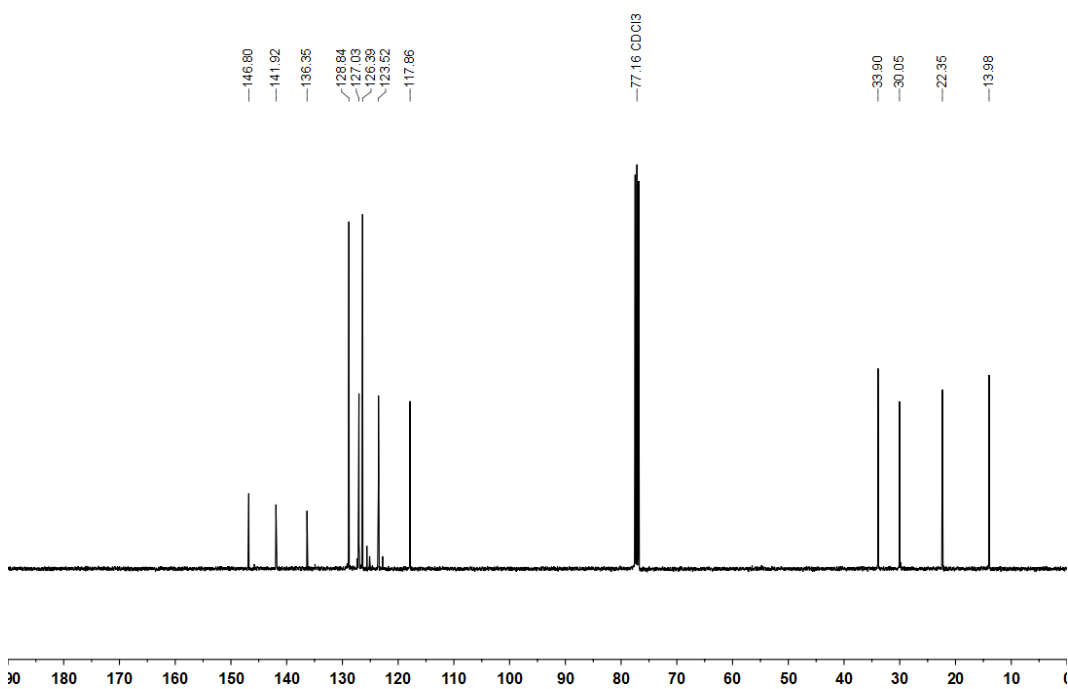
Figure 301 ^{13}C NMR spectrum of **242** (101 MHz, CDCl[3]).
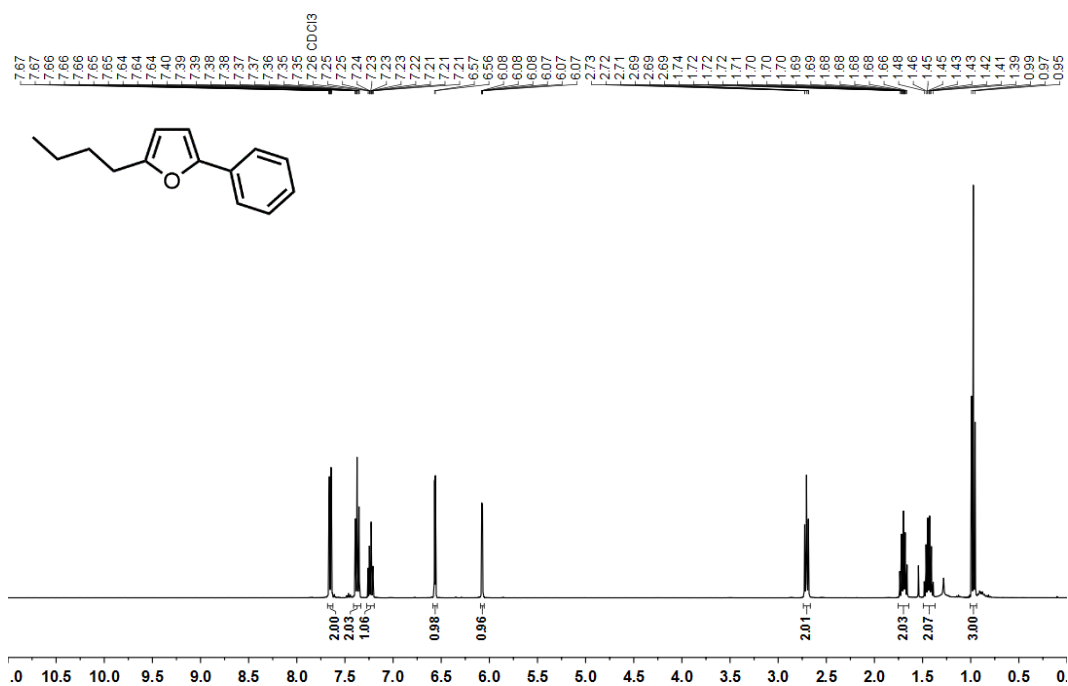
Figure 302 ^{1}H NMR spectrum of **246** (400 MHz, CDCl$_3$).
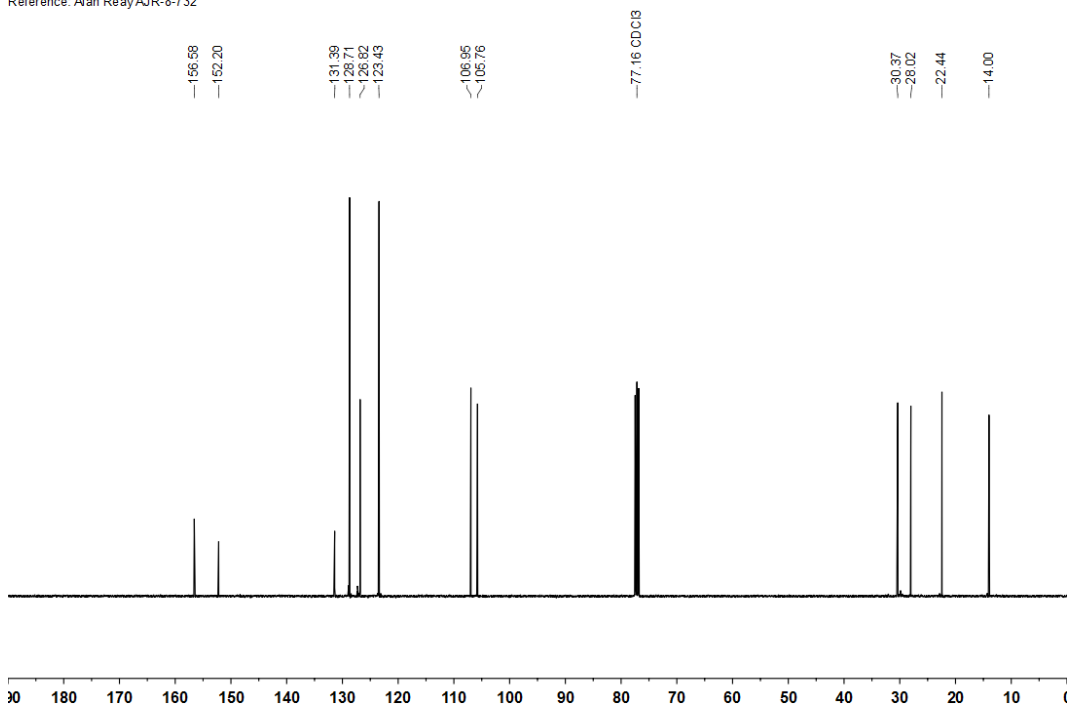
Figure 303 ^{13}C NMR spectrum of **246** (101 MHz, CDCl$_3$).
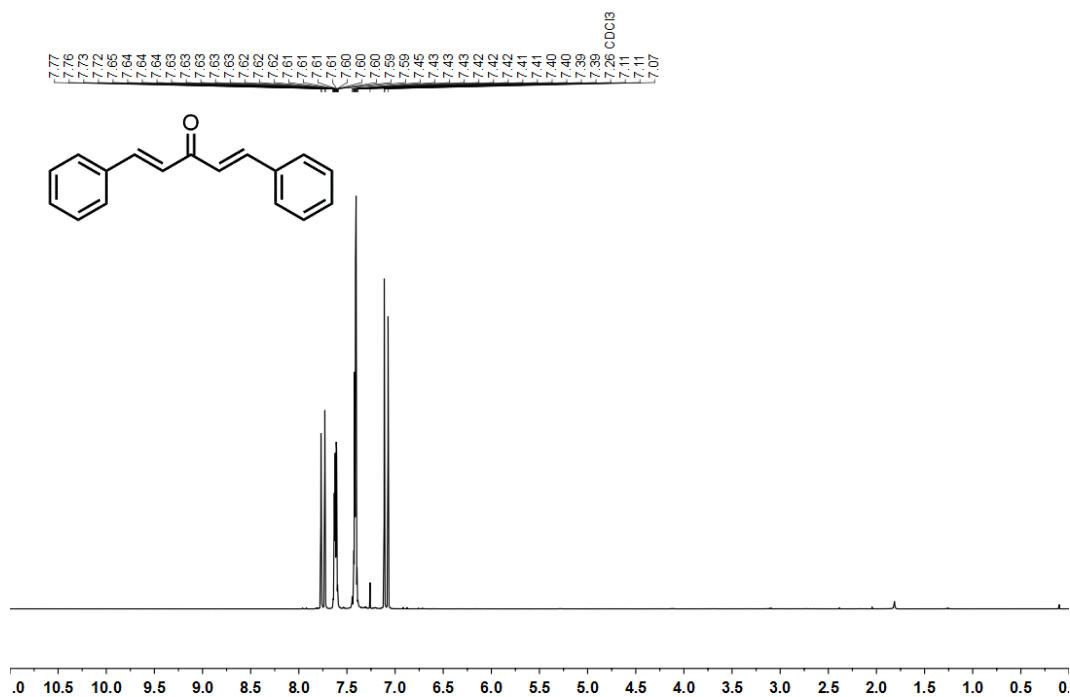
Figure 304 ^{1}H NMR spectrum of **247** (400 MHz, CDCl$_3$).
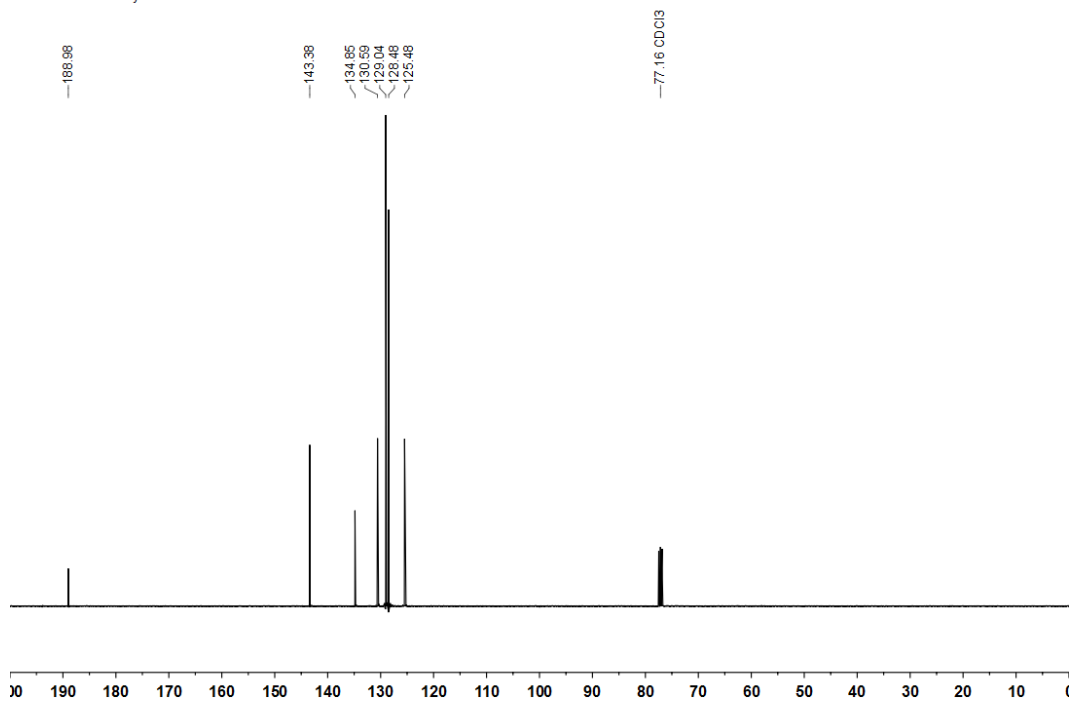
Figure 305 ^{13}C NMR spectrum of **247** (101 MHz, CDCl$_3$).

Major isomer

Minor isomer

Filename: AJR-4-335/128 scans
Reference: Pd2(dba)3.CHCl3 dry conditions
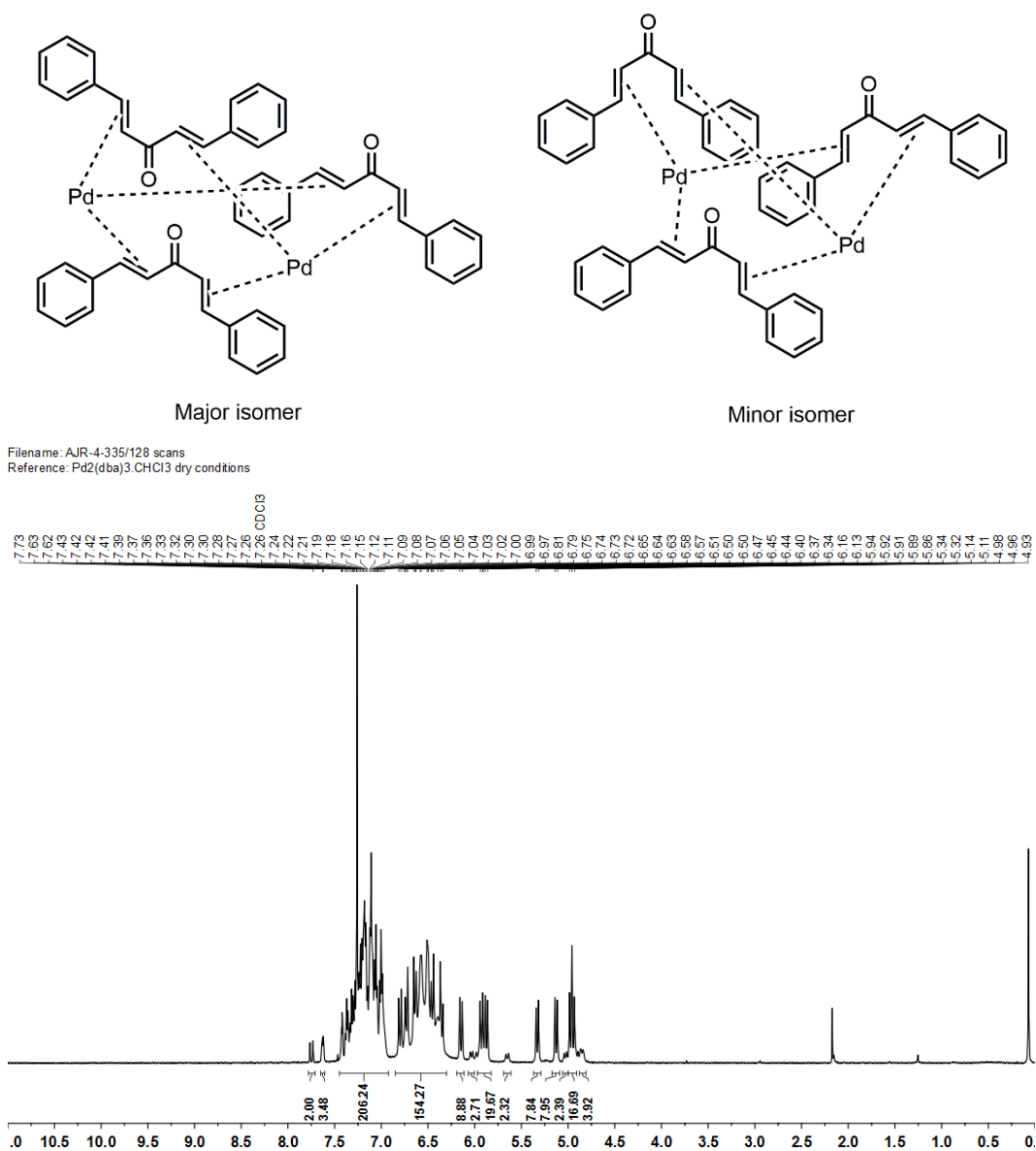
Figure 306 ^{1}H NMR spectrum of **238** (500 MHz, CDCl$_3$).
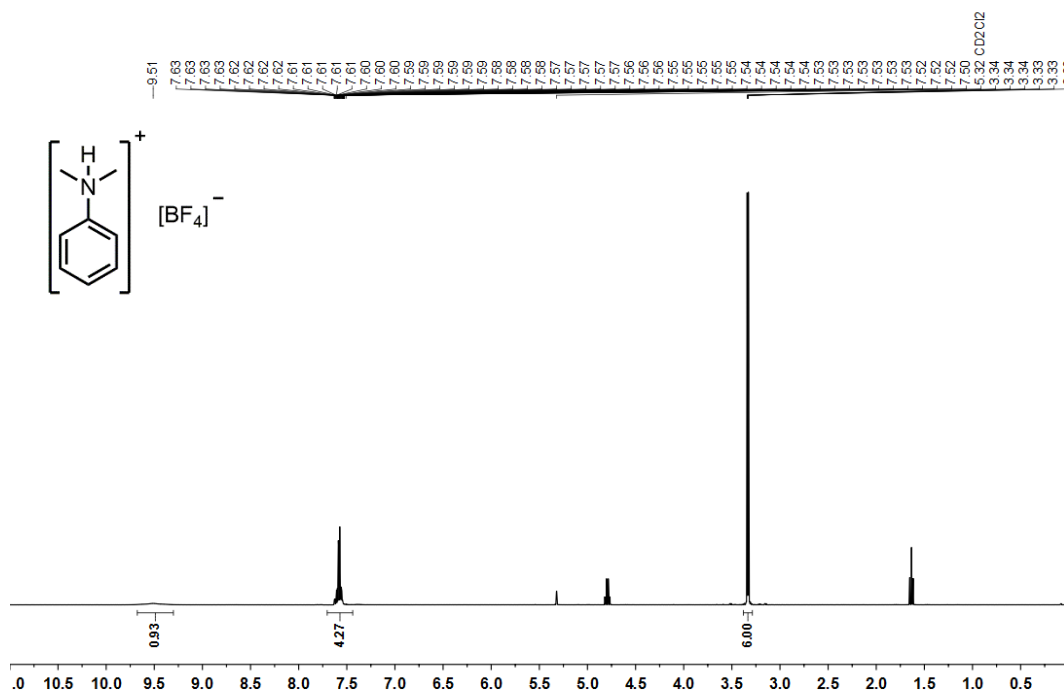
Figure 307 ^{1}H NMR spectrum of **252** (400 MHz, CD$_2$Cl$_2$).
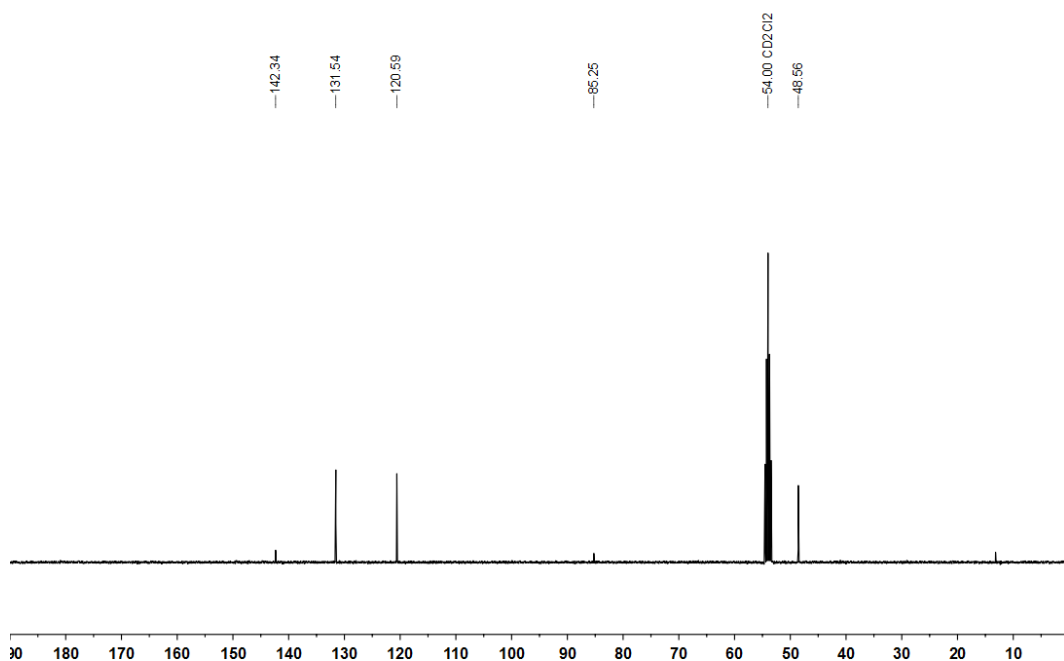
Figure 308 ^{13}C NMR spectrum of **252** (101 MHz, CD$_2$Cl$_2$).

Filename: a1279ajr
Reference: Alan Reay AJR-7-680

—1.91
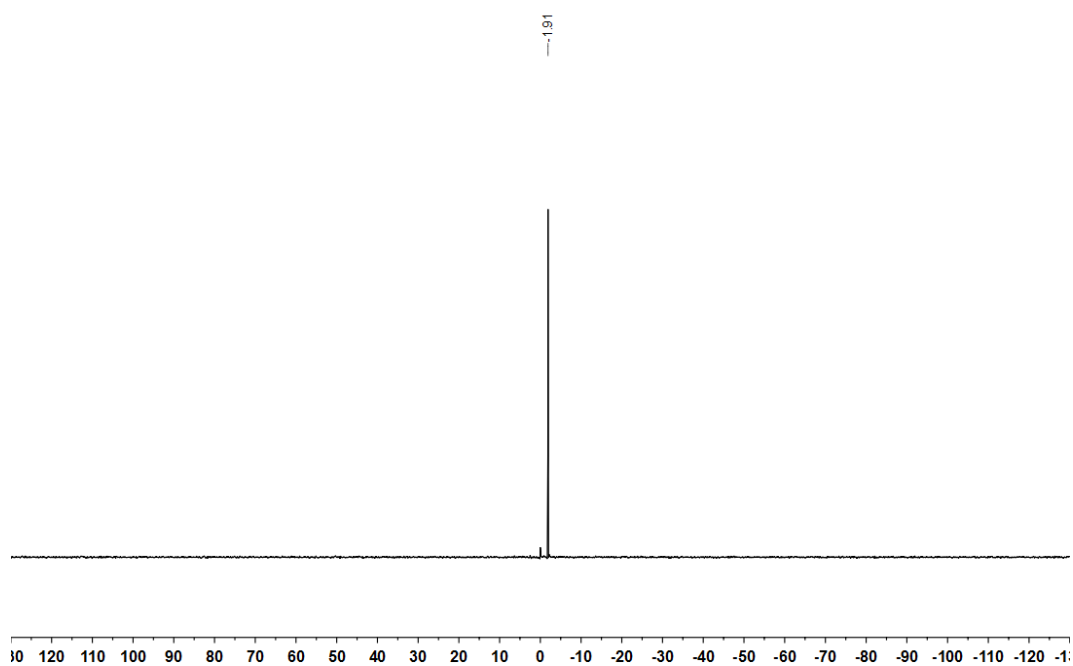
Figure 309 ^{11}B NMR spectrum of **252** (128 MHz, CD$_2$Cl$_2$).

Filename: a1279ajr
Reference: Alan Reay AJR-7-680

—151.02
—151.02

1.00
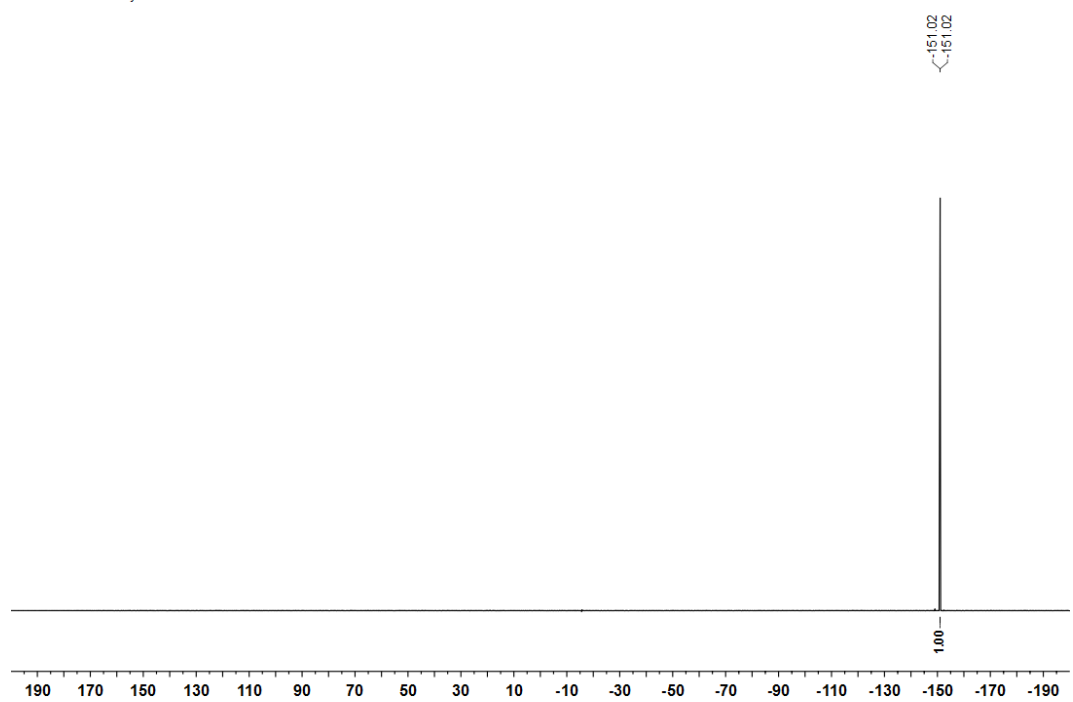
Figure 310 ^{11}B NMR spectrum of **252** (376 MHz, CD$_2$Cl$_2$).

426

Abbreviations

Ac	acetyl
AE	atom economy
AMLA	ambiphilic metal–ligand activation
aq.	aqueous
Ar	arene
ATR	attenuated total reflectance
Bn	benzyl
Boc	*tert*-butoxycarbonyl
B.P.	boiling point
bpy	2,2′-bipyridine
Bu	butyl
Bz	benzoyl
C, *c*.	concentration
cat.	catalyst, catalytic
CMD	concerted metalation deprotonation
conv.	Conversion
CPBA	chloroperbenzoicacid
Cy	cyclohexyl
dba	dibenzylideneacetone
DCE	1,2-dichloroethane
DCM	dichloromethane
dec.	decomposition
DEPBT	3-(Diethoxyphosphoryloxy)-1,2,3-benzotriazin-4-(3*H*)-one

DFT	density functional theory
DIPEA	*N*, *N*-di-*iso*-propylethylamine
DME	dimethyl ether
DMEDA	*N*,*N*′-dimethylethylenediamine
DMF	dimethylformamide
DMSO	dimethylsulfoxide
DOSY	diffusion-ordered NMR spectroscopy
dtbpy	2,6-di-*tert*-butylpyridine
EI	electron ionisation
eq.	equivalents
ESI	electrospray ionisation
Et	ethyl
EXAFS	extended X-ray absorption fine structure spectroscopy
FMoc	fluorenylmethyloxycarbonyl
FT	Fourier transform
FWHM	full-width at half-maximum
GC	gas chromatography
HPLC	high performance liquid chromatography
HR	high resolution
Hz	hertz
i-	*iso-*
ICR	ion cyclotron resonance
IPE	di-*iso*-propylether
IR	infrared

L	ligand
LIFDI	liquid introduced field desorption ionisation
lit.	literature
m-	*meta-*
M	mol dm^{-3}
Me	methyl
Mes	mesityl, 1,3,5-trimethylphenyl
MHz	megahertz
MI	mass intensity
M.P.	melting point
Ms	methanesulfonic, methanesulfonyl
MS	mass spectrometry
Mw	molecular weight
NBS	*N*-bromosuccinamide
NMP	*N*-methyl-2-pyrrolidone
NMR	nuclear magnetic resonance
OE	optimum efficiency
p-	*para-*
PdNPs	palladium nanoparticles
Ph	phenyl
pin	pinacol ester
Piv	pivaloyl
ppm	parts per million
Pr	propyl

PVP	(poly)vinylpyrrolidone
pyr.	pyridine
quant.	quantitative yield
R_f	retention factor
RME	reaction mass efficiency
RT	at ambient temperature
SEM	2-trimethylsilylethoxymethyl
t-	*tertiary*
TBS	*tert*-butyldimethylsilyl
TBTU	*O*-(Benzotriazol-1-yl)-*N*,*N*,*N*′,*N*′-tetramethyluronium tetrafluoroborate
TEM	transmission electron microscopy
Tf	triflic, trifluoromethanesulfonic
Tfa	trifluoroacetyl
TFA	trifluoroacetic acid
THF	tetrahydrofuran
TLC	thin layer chromatography
TOF	turnover frequency
Tol	tolyl, *p*-methylphenyl
TPPTS	3,3′,3″-phosphanetriyltris(benzenesulfonic acid) trisodium
Ts	tosyl
UV	ultraviolet
V	volts
VT	variable temperature

W	watts
w.r.t.	with respect to
X	leaving group
XAS	X-ray absorption spectroscopy
XPhos	2-dicyclohexylphosphino-2′,4′,6′-tri-*iso*-propylbiphenyl
XPS	X-ray photoelectron spectroscopy

References

(1)   Kambe, N.; Iwasaki, T.; Terao, J. *Chem. Soc. Rev.* **2011**, *40*, 4937-4947.

(2)   Nicolaou, K. C.; Bulger, P. G.; Sarlah, D. *Angew. Chem. Int. Ed.* **2005**, *44*, 4442-4489.

(3)   Johansson Seechurn, C. C. C.; Kitching, M. O.; Colacot, T. J.; Snieckus, V. *Angew. Chem. Int. Ed.* **2012**, *51*, 5062-5085.

(4)   Heck, R. F.; Nolley, J. P. *J. Org. Chem.* **1972**, *37*, 2320-2322.

(5)   Mizoroki, T.; Mori, K.; Ozaki, A. *Bull. Chem. Soc. Jpn.* **1971**, *44*, 581-581.

(6)   Milstein, D.; Stille, J. K. *J. Am. Chem. Soc.* **1978**, *100*, 3636-3638.

(7)   Milstein, D.; Stille, J. K. *J. Am. Chem. Soc.* **1979**, *101*, 4992-4998.

(8)   Stille, J. K. *Angew. Chem. Int. Ed.* **1986**, *25*, 508-524.

(9)   Miyaura, N.; Suzuki, A. *J. Chem. Soc., Chem. Commun.* **1979**, 866-867.

(10)   Miyaura, N.; Yamada, K.; Suzuki, A. *Tetrahedron Lett.* **1979**, *20*, 3437-3440.

(11)   Sonogashira, K.; Tohda, Y.; Hagihara, N. *Tetrahedron Lett.* **1975**, *16*, 4467-4470.

(12)   Tamao, K.; Sumitani, K.; Kumada, M. *J. Am. Chem. Soc.* **1972**, *94*, 4374-4376.

(13)   Corriu, R. J. P.; Masse, J. P. *J. Chem. Soc., Chem. Commun.* **1972**, 144a-144a.

(14)   Hiyama, T.; Obayashi, M.; Mori, I.; Nozaki, H. *J. Org. Chem.* **1983**, *48*, 912-914.

(15)   Negishi, E.; King, A. O.; Okukado, N. *J. Org. Chem.* **1977**, *42*, 1821-1823.

(16)   Danishefsky, S. J.; Masters, J. J.; Young, W. B.; Link, J. T.; Snyder, L. B.; Magee, T. V.; Jung, D. K.; Isaacs, R. C. A.; Bornmann, W. G.; Alaimo, C. A.; Coburn, C. A.; Di Grandi, M. J. *J. Am. Chem. Soc.* **1996**, *118*, 2843-2859.

(17)   Garg, N. K.; Caspi, D. D.; Stoltz, B. M. *J. Am. Chem. Soc.* **2004**, *126*, 9552-9553.

(18)   Bajwa, S. E.; Storr, T. E.; Hatcher, L. E.; Williams, T. J.; Baumann, C. G.; Whitwood, A. C.; Allan, D. R.; Teat, S. J.; Raithby, P. R.; Fairlamb, I. J. S. *Chem. Sci.* **2012**, *3*, 1656-1661.

(19)   Carole, W. A.; Bradley, J.; Sarwar, M.; Colacot, T. J. *Org. Lett.* **2015**, *17*, 5472-5475.

(20)   Reay, A. J.; Fairlamb, I. J. S. *Chem. Commun.* **2015**, *51*, 16289-16307.

(21)   de Vries, A. H. M.; Mulders, J. M. C. A.; Mommers, J. H. M.; Henderickx, H. J. W.; de Vries, J. G. *Org. Lett.* **2003**, *5*, 3285-3288.

(22)   Reetz, M. T.; de Vries, J. G. *Chem. Commun.* **2004**, 1559-1563.

(23)   Zhao, F.; Bhanage, B. M.; Shirai, M.; Arai, M. *Chem. Eur. J.* **2000**, *6*, 843-848.

(24)   Brazier, J. B.; Nguyen, B. N.; Adrio, L. A.; Barreiro, E. M.; Leong, W. P.; Newton, M. A.; Figueroa, S. J. A.; Hellgardt, K.; Hii, K. K. M. *Catal. Today* **2014**, *229*, 95-103.

(25)   Cassol, C. C.; Umpierre, A. P.; Machado, G.; Wolke, S. I.; Dupont, J. *J. Am. Chem. Soc.* **2005**, *127*, 3298-3299.

(26)   Thathagar, M. B.; ten Elshof, J. E.; Rothenberg, G. *Angew. Chem. Int. Ed.* **2006**, *45*, 2886-2890.

(27)   Gaikwad, A. V.; Rothenberg, G. *Phys. Chem. Chem. Phys.* **2006**, *8*, 3669-3675.

(28)   Reimann, S.; Stötzel, J.; Frahm, R.; Kleist, W.; Grunwaldt, J.-D.; Baiker, A. *J. Am. Chem. Soc.* **2011**, *133*, 3921-3930.

(29)   Teranishi, T.; Miyake, M. *Chem. Mater.* **1998**, *10*, 594-600.

(30)   Le Bars, J.; Specht, U.; Bradley, J. S.; Blackmond, D. G. *Langmuir* **1999**, *15*, 7621-7625.

(31)   Koczkur, K. M.; Mourdikoudis, S.; Polavarapu, L.; Skrabalak, S. E. *Dalton Trans.* **2015**, *44*, 17883-17905.

(32)   Ellis, P. J.; Fairlamb, I. J. S.; Hackett, S. F. J.; Wilson, K.; Lee, A. F. *Angew. Chem. Int. Ed.* **2010**, *49*, 1820-1824.

(33)   Lee, A. F.; Ellis, P. J.; Fairlamb, I. J. S.; Wilson, K. *Dalton Trans.* **2010**, *39*, 10473-10482.

(34)   Widegren, J. A.; Bennett, M. A.; Finke, R. G. *J. Am. Chem. Soc.* **2003**, *125*, 10301-10310.

(35)   Widegren, J. A.; Finke, R. G. *J. Mol. Catal. A: Chem.* **2003**, *198*, 317-341.

(36)   Knight, W. D.; Clemenger, K.; de Heer, W. A.; Saunders, W. A.; Chou, M. Y.; Cohen, M. L. *Phys. Rev. Lett.* **1984**, *52*, 2141-2143.

(37)   Blaser, H.-U.; Indolese, A.; Schnyder, A.; Steiner, H.; Studer, M. *J. Mol. Catal. A: Chem.* **2001**, *173*, 3-18.

(38)   Yin, L.; Liebscher, J. *Chem. Rev.* **2007**, *107*, 133-173.

(39)   Molnár, Á. *Chem. Rev.* **2011**, *111*, 2251-2320.

(40)   Balanta, A.; Godard, C.; Claver, C. *Chem. Soc. Rev.* **2011**, *40*, 4973-4985.

(41)   Ackermann, L.; Vicente, R.; Kapdi, A. R. *Angew. Chem. Int. Ed.* **2009**, *48*, 9792-9826.

(42)   Yamaguchi, J.; Yamaguchi, A. D.; Itami, K. *Angew. Chem. Int. Ed.* **2012**, *51*, 8960-9009.

(43)   Wang, J.; Rosingana, M.; Watson, D. J.; Dowdy, E. D.; Discordia, R. P.; Soundarajan, N.; Li, W.-S. *Tetrahedron Lett.* **2001**, *42*, 8935-8937.

(44)   Chaumontet, M.; Piccardi, R.; Audic, N.; Hitce, J.; Peglion, J.-L.; Clot, E.; Baudoin, O. *J. Am. Chem. Soc.* **2008**, *130*, 15157-15166.

(45)   Chaumontet, M.; Piccardi, R.; Baudoin, O. *Angew. Chem. Int. Ed.* **2009**, *48*, 179-182.

(46)   Lafrance, M.; Rowley, C. N.; Woo, T. K.; Fagnou, K. *J. Am. Chem. Soc.* **2006**, *128*, 8754-8756.

(47)   Davies, D. L.; Donald, S. M. A.; Macgregor, S. A. *J. Am. Chem. Soc.* **2005**, *127*, 13754-13755.

(48)   Storr, T. E.; Firth, A. G.; Wilson, K.; Darley, K.; Baumann, C. G.; Fairlamb, I. J. S. *Tetrahedron* **2008**, *64*, 6125-6137.

(49)   Storr, T. E.; Baumann, C. G.; Thatcher, R. J.; De Ornellas, S.; Whitwood, A. C.; Fairlamb, I. J. S. *J. Org. Chem.* **2009**, *74*, 5810-5821.

(50)   Adrio, L. A.; Nguyen, B. N.; Guilera, G.; Livingston, A. G.; Hii, K. K. *Catal. Sci. Tech.* **2012**, *2*, 316-323.

(51)   Djakovitch, L.; Wagner, M.; Hartung, C. G.; Beller, M.; Koehler, K. *J. Mol. Catal. A: Chem.* **2004**, *219*, 121-130.

(52)   Raluy, E.; Favier, I.; Lopez-Vinasco, A. M.; Pradel, C.; Martin, E.; Madec, D.; Teuma, E.; Gómez, M. *Phys. Chem. Chem. Phys.* **2011**, *13*, 13579-13584.

(53)   Adak, L.; Bhadra, S.; Ranu, B. C. *Tetrahedron Lett.* **2010**, *51*, 3811-3814.

(54)   Saha, D.; Adak, L.; Ranu, B. C. *Tetrahedron Lett.* **2010**, *51*, 5624-5627.

(55)   Ehlers, P.; Petrosyan, A.; Baumgard, J.; Jopp, S.; Steinfeld, N.; Ghochikyan, T. V.; Saghyan, A. S.; Fischer, C.; Langer, P. *ChemCatChem* **2013**, *5*, 2504-2511.

(56)   Nassar-Hardy, L.; Deraedt, C.; Fouquet, E.; Felpin, F.-X. *Eur. J. Org. Chem.* **2011**, *2011*, 4616-4622.

(57)   Baumann, C. G.; De Ornellas, S.; Reeds, J. P.; Storr, T. E.; Williams, T. J.; Fairlamb, I. J. S. *Tetrahedron* **2014**, *70*, 6174-6187.

(58)   Williams, T. J.; Fairlamb, I. J. S. *Tetrahedron Lett.* **2013**, *54*, 2906-2908.

(59)   Hyotanishi, M.; Isomura, Y.; Yamamoto, H.; Kawasaki, H.; Obora, Y. *Chem. Commun.* **2011**, *47*, 5750-5752.

(60)   Yano, H.; Nakajima, Y.; Obora, Y. *J. Organomet. Chem.* **2013**, *745–746*, 258-261.

(61)   Chiba, M.; Thanh, M. N.; Hasegawa, Y.; Obora, Y.; Kawasaki, H.; Yonezawa, T. *J. Mater. Chem. C* **2015**, *3*, 514-520.

(62)   Sahnoun, S.; Messaoudi, S.; Peyrat, J.-F.; Brion, J.-D.; Alami, M. *Tetrahedron Lett.* **2008**, *49*, 7279-7283.

(63)   Sahnoun, S.; Messaoudi, S.; Brion, J.-D.; Alami, M. *Org. Biomol. Chem.* **2009**, *7*, 4271-4278.

(64)   Parisien, M.; Valette, D.; Fagnou, K. *J. Org. Chem.* **2005**, *70*, 7578-7584.

(65)   Djakovitch, L.; Felpin, F.-X. *ChemCatChem* **2014**, *6*, 2175-2187.

(66)   Cano, R.; Schmidt, A. F.; McGlacken, G. P. *Chem. Sci.* **2015**, *6*, 5338-5346.

(67)   Deprez, N. R.; Sanford, M. S. *Inorg. Chem.* **2007**, *46*, 1924-1935.

(68)   Zhdankin, V. V.; Stang, P. J. *Chem. Rev.* **2008**, *108*, 5299-5358.

(69)   Merritt, E. A.; Olofsson, B. *Angew. Chem. Int. Ed.* **2009**, *48*, 9052-9070.

(70)   Yoshimura, A.; Zhdankin, V. V. *Chem. Rev.* **2016**.

(71)   Lancer, K. M.; Wiegand, G. H. *J. Org. Chem.* **1976**, *41*, 3360-3364.

(72)   Pinto de Magalhães, H.; Lüthi, H. P.; Togni, A. *J. Org. Chem.* **2014**, *79*, 8374-8382.

(73)   Cook, A. K.; Emmert, M. H.; Sanford, M. S. *Org. Lett.* **2013**, *15*, 5428-5431.

(74)   Gou, Q.; Zhang, Z.-F.; Liu, Z.-C.; Qin, J. *J. Org. Chem.* **2015**, *80*, 3176-3186.

(75)   Tanabe, K.; Taniguchi, A.; Matsumoto, T.; Oisaki, K.; Sohma, Y.; Kanai, M. *Chem. Sci.* **2014**, *5*, 2747-2753.

(76)   Bumagin, N. A.; Luzikova, E. V.; Sukhomlinova, L. I.; Tolstoya, T. P.; Beletskaya, I. P. *Russ. Chem. Bull.* **1995**, *44*, 385-386.

(77)   Kalyani, D.; Deprez, N. R.; Desai, L. V.; Sanford, M. S. *J. Am. Chem. Soc.* **2005**, *127*, 7330-7331.

(78)   Deprez, N. R.; Sanford, M. S. *J. Am. Chem. Soc.* **2009**, *131*, 11234-11241.

(79)   Powers, D. C.; Lee, E.; Ariafard, A.; Sanford, M. S.; Yates, B. F.; Canty, A. J.; Ritter, T. *J. Am. Chem. Soc.* **2012**, *134*, 12002-12009.

(80)   Neufeldt, S. R.; Sanford, M. S. *Adv. Synth. Catal.* **2012**, *354*, 3517-3522.

(81)   Deprez, N. R.; Kalyani, D.; Krause, A.; Sanford, M. S. *J. Am. Chem. Soc.* **2006**, *128*, 4972-4973.

(82)   Daugulis, O.; Zaitsev, V. G. *Angew. Chem. Int. Ed.* **2005**, *44*, 4046-4048.

(83) Xiao, B.; Fu, Y.; Xu, J.; Gong, T.-J.; Dai, J.-J.; Yi, J.; Liu, L. *J. Am. Chem. Soc.* **2010**, *132*, 468-469.

(84) Storr, T. E.; Greaney, M. F. *Org. Lett.* **2013**, *15*, 1410-1413.

(85) Modha, S. G.; Greaney, M. F. *J. Am. Chem. Soc.* **2015**, *137*, 1416-1419.

(86) Kumar Muthyala, M.; Choudhary, S.; Pandey, K.; Shelke, G. M.; Jha, M.; Kumar, A. *Eur. J. Org. Chem.* **2014**, *2014*, 2365-2370.

(87) Huang, X.; Zhu, Q.; Xu, Y. *Synth. Commun.* **2001**, *31*, 2823-2828.

(88) Edwards, R.; de Vries, W.; Westwell, A. D.; Daniels, S.; Wirth, T. *Eur. J. Org. Chem.* **2015**, *2015*, 6909-6916.

(89) Mo, F.; Dong, G.; Zhang, Y.; Wang, J. *Org. Biomol. Chem.* **2013**, *11*, 1582-1593.

(90) Wu, X.-F.; Neumann, H.; Beller, M. *Chem. Commun.* **2011**, *47*, 7959-7961.

(91) Bonin, H.; Fouquet, E.; Felpin, F.-X. *Adv. Synth. Catal.* **2011**, *353*, 3063-3084.

(92) Felpin, F.-X.; Miqueu, K.; Sotiropoulos, J.-M.; Fouquet, E.; Ibarguren, O.; Laudien, J. *Chem. Eur. J.* **2010**, *16*, 5191-5204.

(93) Taylor, J. G.; Moro, A. V.; Correia, C. R. D. *Eur. J. Org. Chem.* **2011**, *2011*, 1403-1428.

(94) Kutonova, K. V.; Trusova, M. E.; Stankevich, A. V.; Postnikov, P. S.; Filimonov, V. D. *Beilstein J. Org. Chem.* **2015**, *11*, 358-362.

(95) Kikukawa, K.; Matsuda, T. *Chem. Lett.* **1977**, *6*, 159-162.

(96) Saini, V.; Liao, L.; Wang, Q.; Jana, R.; Sigman, M. S. *Org. Lett.* **2013**, *15*, 5008-5011.

(97) Li, X.; Yan, X.-Y.; Chang, H.-H.; Wang, L.-C.; Zhang, Y.; Chen, W.-W.; Li, Y.-W.; Wei, W.-L. *Org. Biomol. Chem.* **2012**, *10*, 495-497.

(98) Li, X.; Wang, L.-C.; Chang, H.-H.; Zhang, C.-X.; Wei, W.-L. *Appl. Catal., A* **2013**, *462–463*, 15-22.

(99)   Li, X.; Zhu, T.; Shao, Z.; Li, Y.; Chang, H.; Gao, W.; Zhang, Y.; Wei, W. *Tetrahedron* **2016**, *72*, 69-75.

(100)   Nicewicz, D. A.; MacMillan, D. W. C. *Science* **2008**, *322*, 77-80.

(101)   Kalyani, D.; McMurtrey, K. B.; Neufeldt, S. R.; Sanford, M. S. *J. Am. Chem. Soc.* **2011**, *133*, 18566-18569.

(102)   Biajoli, A. F. P.; da Penha, E. T.; Correia, C. R. D. *RSC Adv.* **2012**, *2*, 11930-11935.

(103)   Zhao, J.; Zhang, Y.; Cheng, K. *J. Org. Chem.* **2008**, *73*, 7428-7431.

(104)   Oger, N.; Le Grognec, E.; Felpin, F.-X. *J. Org. Chem.* **2014**, *79*, 8255-8262.

(105)   Deadman, B. J.; Collins, S. G.; Maguire, A. R. *Chem. Eur. J.* **2015**, *21*, 2298-2308.

(106)   Oger, N.; d'Halluin, M.; Le Grognec, E.; Felpin, F.-X. *Org. Process Res. Dev.* **2014**, *18*, 1786-1801.

(107)   Joncour, R.; Susperregui, N.; Pinaud, N.; Miqueu, K.; Fouquet, E.; Sotiropoulos, J.-M.; Felpin, F.-X. *Chem. Eur. J.* **2013**, *19*, 9291-9296.

(108)   Oger, N.; Le Callonnec, F.; Jacquemin, D.; Fouquet, E.; Le Grognec, E.; Felpin, F.-X. *Adv. Synth. Catal.* **2014**, *356*, 1065-1071.

(109)   Vivian, J. T.; Callis, P. R. *Biophys. J.* **2001**, *80*, 2093-2109.

(110)   Kolundzic, F.; Noshi, M. N.; Tjandra, M.; Movassaghi, M.; Miller, S. J. *J. Am. Chem. Soc.* **2011**, *133*, 9104-9111.

(111)   Colletti, S. L.; Li, C.; Fisher, M. H.; Wyvratt, M. J.; Meinke, P. T. *Tetrahedron Lett.* **2000**, *41*, 7825-7829.

(112)   Roy, A. D.; Goss, R. J. M.; Wagner, G. K.; Winn, M. *Chem. Commun.* **2008**, 4831-4833.

(113)   Lebrasseur, N.; Larrosa, I. *J. Am. Chem. Soc.* **2008**, *130*, 2926-2927.

(114)   Ruiz-Rodríguez, J.; Albericio, F.; Lavilla, R. *Chem. Eur. J.* **2010**, *16*, 1124-1127.

(115)   Preciado, S.; Mendive-Tapia, L.; Albericio, F.; Lavilla, R. *J. Org. Chem.* **2013**, *78*, 8129-8135.

(116)   Preciado, S.; Mendive-Tapia, L.; Torres-Garcia, C.; Zamudio-Vazquez, R.; Soto-Cerrato, V.; Perez-Tomas, R.; Albericio, F.; Nicolas, E.; Lavilla, R. *Med. Chem. Comm.* **2013**, *4*, 1171-1174.

(117)   Mendive-Tapia, L.; Preciado, S.; Garcia, J.; Ramon, R.; Kielland, N.; Albericio, F.; Lavilla, R. *Nat. Commun.* **2015**, *6*, 1-9.

(118)   Dong, H.; Limberakis, C.; Liras, S.; Price, D.; James, K. *Chem. Commun.* **2012**, *48*, 11644-11646.

(119)   Williams, T. J.; Reay, A. J.; Whitwood, A. C.; Fairlamb, I. J. S. *Chem. Commun.* **2014**, *50*, 3052-3054.

(120)   Zhu, Y.; Bauer, M.; Ackermann, L. *Chem. Eur. J.* **2015**, *21*, 9980-9983.

(121)   Evans, E. F.; Lewis, N. J.; Kapfer, I.; Macdonald, G.; Taylor, R. J. K. *Synth. Commun.* **1997**, *27*, 1819-1825.

(122)   Borsook, H.; Thimann, K. V. *J. Biol. Chem.* **1932**, *98*, 671–705.

(123)   Nascimento, O. R.; Costa-Filho, A. J.; De Morais, D. I.; Ellena, J.; Delboni, L. F. *Inorg. Chim. Acta* **2001**, *312*, 133-138.

(124)   Phipps, R. J.; Grimster, N. P.; Gaunt, M. J. *J. Am. Chem. Soc.* **2008**, *130*, 8172-8174.

(125)   Zhu, Y.; Bauer, M.; Ploog, J.; Ackermann, L. *Chem. Eur. J.* **2014**, *20*, 13099-13102.

(126)   Rodriguez, R. A.; Pan, P.-S.; Pan, C.-M.; Ravula, S.; Lapera, S.; Singh, E. K.; Styers, T. J.; Brown, J. D.; Cajica, J.; Parry, E.; Otrubova, K.; McAlpine, S. R. *J. Org. Chem.* **2007**, *72*, 1980-2002.

(127)   Sorokina, Y. M.; Sladkova, A. A.; Popova, L. A.; Shadyro, O. I.; Knizhnikov, V. A. *Russ. J. Org. Chem.* **2012**, *48*, 1297-1301.

(128)   Notte, G. T.; Sammakia, T. *J. Am. Chem. Soc.* **2006**, *128*, 4230-4231.

(129)   Xia, Z.; Zhu, Q. *Org. Lett.* **2013**, *15*, 4110-4113.

(130)   Matheis, C.; Jouvin, K.; Goossen, L. J. *Org. Lett.* **2014**, *16*, 5984-5987.

(131)   Hammarback, L. A. *M.Chem. Research Report*, University of York, United Kingdom, 2015.

(132)   Sheridan, T. H. *M.Chem. Research Report*, University of York, United Kingdom, 2016.

(133)   Rauf, W.; Thompson, A. L.; Brown, J. M. *Dalton Trans.* **2010**, *39*, 10414-10421.

(134)   Bedford, R. B.; Haddow, M. F.; Mitchell, C. J.; Webster, R. L. *Angew. Chem. Int. Ed.* **2011**, *50*, 5524-5527.

(135)   McElroy, C. R.; Constantinou, A.; Jones, L. C.; Summerton, L.; Clark, J. H. *Green. Chem.* **2015**, *17*, 3111-3121.

(136)   Prat, D.; Wells, A.; Hayler, J.; Sneddon, H.; McElroy, C. R.; Abou-Shehada, S.; Dunn, P. J. *Green. Chem.* **2016**, *18*, 288-296.

(137)   Reay, A. J.; Williams, T. J.; Fairlamb, I. J. S. *Org. Biomol. Chem.* **2015**, *13*, 8298-8309.

(138)   Hunt, A. J.; Farmer, T. J.; Clark, J. H. In *Element Recovery and Sustainability*; Hunt, A. J., Ed.; RSC Publishing: Cambridge, UK, 2013, pp 1–28.

(139)   Cahiez, G.; Duplais, C.; Buendia, J. *Chem. Rev.* **2009**, *109*, 1434-1476.

(140)   Khusnutdinov, R. I.; Bayguzina, A. R.; Dzhemilev, U. M. *Russ. J. Org. Chem.* **2012**, *48*, 309-348.

(141)   Correa, A.; Garcia Mancheno, O.; Bolm, C. *Chem. Soc. Rev.* **2008**, *37*, 1108-1117.

(142)   Bauer, I.; Knölker, H.-J. *Chem. Rev.* **2015**, *115*, 3170-3387.

(143)   Cahiez, G.; Moyeux, A. *Chem. Rev.* **2010**, *110*, 1435-1462.

(144)   Gao, K.; Yoshikai, N. *Acc. Chem. Res.* **2014**, *47*, 1208-1219.

(145)   Ackermann, L. *J. Org. Chem.* **2014**, *79*, 8948-8954.

(146)   Collins, G.; Schmidt, M.; McGlacken, G. P.; O'Dwyer, C.; Holmes, J. D. *J. Phys. Chem. C* **2014**, *118*, 6522-6530.

(147)   Tang, D.-T. D.; Collins, K. D.; Glorius, F. *J. Am. Chem. Soc.* **2013**, *135*, 7450-7453.

(148) Tang, D.-T. D.; Collins, K. D.; Ernst, J. B.; Glorius, F. *Angew. Chem. Int. Ed.* **2014**, *53*, 1809-1813.

(149) Collins, K. D.; Honeker, R.; Vasquez-Cespedes, S.; Tang, D.-T. D.; Glorius, F. *Chem. Sci.* **2015**, *6*, 1816-1824.

(150) Taylor, R. D.; MacCoss, M.; Lawson, A. D. G. *J. Med. Chem.* **2014**, *57*, 5845-5859.

(151) Ben-Yahia, A.; Naas, M.; El Kazzouli, S.; Essassi, E. M.; Guillaumet, G. *Eur. J. Org. Chem.* **2012**, *2012*, 7075-7081.

(152) Naas, M.; El Kazzouli, S. d.; Essassi, E. M.; Bousmina, M.; Guillaumet, G. *J. Org. Chem.* **2014**, *79*, 7286-7293.

(153) Unsinn, A.; Knochel, P. *Chem. Commun.* **2012**, *48*, 2680-2682.

(154) Kannaboina, P.; Anilkumar, K.; Aravinda, S.; Vishwakarma, R. A.; Das, P. *Org. Lett.* **2013**, *15*, 5718-5721.

(155) Bielawski, M.; Aili, D.; Olofsson, B. *J. Org. Chem.* **2008**, *73*, 4602-4607.

(156) Ronson, T. O., Ph.D. Thesis, University of York, United Kingdom, 2015.

(157) Crabtree, R. H. *Chem. Rev.* **2012**, *112*, 1536-1554.

(158) Crabtree, R. H. *Chem. Rev.* **2015**, *115*, 127-150.

(159) Mower, M. P.; Blackmond, D. G. *J. Am. Chem. Soc.* **2015**, *137*, 2386-2391.

(160) Herbert, T. A. *M.Chem. Research Report*, University of York, United Kingdom, 2012.

(161) Pridgen, L. N.; Jones, S. S. *J. Org. Chem.* **1982**, *47*, 1590-1592.

(162) Wakioka, M.; Nakamura, Y.; Wang, Q.; Ozawa, F. *Organometallics* **2012**, *31*, 4810-4816.

(163) Fairlamb, I. J. S. *Org. Biomol. Chem.* **2008**, *6*, 3645-3656.

(164) Macé, Y.; Kapdi, A. R.; Fairlamb, I. J. S.; Jutand, A. *Organometallics* **2006**, *25*, 1795-1800.

(165) Amatore, C.; Jutand, A.; Khalil, F.; M'Barki, M. A.; Mottier, L. *Organometallics* **1993**, *12*, 3168-3178.

(166) Takahashi, Y.; Ito, T.; Sakai, S.; Ishii, Y. *J. Chem. Soc. D* **1970**, 1065-1066.

(167) Mazza, M. C.; Pierpont, C. G. *Inorg. Chem.* **1973**, *12*, 2955-2959.

(168) Ukai, T.; Kawazura, H.; Ishii, Y.; Bonnet, J. J.; Ibers, J. A. *J. Organomet. Chem.* **1974**, *65*, 253-266.

(169) Tanaka, H.; Kawazura, H. *Bull. Chem. Soc. Jpn.* **1980**, *53*, 1743-1744.

(170) Zalesskiy, S. S.; Ananikov, V. P. *Organometallics* **2012**, *31*, 2302-2309.

(171) Burrows, A. D.; Mingos, D. M. P.; Menzer, S.; Vilar, R.; Williams, D. J. *J. Chem. Soc., Dalton Trans.* **1995**, 2107-2108.

(172) Kawazura, H.; Tanaka, H.; Yamada, K.-i.; Takahashi, T.; Ishii, Y. *Bull. Chem. Soc. Jpn.* **1978**, *51*, 3466-3470.

(173) Kapdi, A. R.; Whitwood, A. C.; Williamson, D. C.; Lynam, J. M.; Burns, M. J.; Williams, T. J.; Reay, A. J.; Holmes, J.; Fairlamb, I. J. S. *J. Am. Chem. Soc.* **2013**, *135*, 8388-8399.

(174) Pentsak, E. O.; Kashin, A. S.; Polynski, M. V.; Kvashnina, K. O.; Glatzel, P.; Ananikov, V. P. *Chem. Sci.* **2015**, *6*, 3302-3313.

(175) Yuan, X.; Yan, N.; Katsyuba, S. A.; Zvereva, E. E.; Kou, Y.; Dyson, P. J. *Phys. Chem. Chem. Phys.* **2012**, *14*, 6026-6033.

(176) Heard, C. J., Ph.D. Thesis, University of Birmingham, United Kingdom, 2014.

(177) Musaev, D. G.; Figg, T. M.; Kaledin, A. L. *Chem. Soc. Rev.* **2014**.

(178) Loach, R. P.; Fenton, O. S.; Amaike, K.; Siegel, D. S.; Ozkal, E.; Movassaghi, M. *J. Org. Chem.* **2014**, *79*, 11254-11263.

(179) Marson, C. M. *Chem. Soc. Rev.* **2011**, *40*, 5514-5533.

(180) Pitt, W. R.; Parry, D. M.; Perry, B. G.; Groom, C. R. *J. Med. Chem.* **2009**, *52*, 2952-2963.

(181)   Crespo-Quesada, M.; Yarulin, A.; Jin, M.; Xia, Y.; Kiwi-Minsker, L. *J. Am. Chem. Soc.* **2011**, *133*, 12787-12794.

(182)   Zang, W.; Li, G.; Wang, L.; Zhang, X. *Catal. Sci. Tech.* **2015**, *5*, 2532-2553.

(183)   Long, R.; Rao, Z.; Mao, K.; Li, Y.; Zhang, C.; Liu, Q.; Wang, C.; Li, Z.-Y.; Wu, X.; Xiong, Y. *Angew. Chem. Int. Ed.* **2015**, *54*, 2425-2430.

(184)   Tao, A. R.; Habas, S.; Yang, P. *Small* **2008**, *4*, 310-325.

(185)   Xia, Y.; Xiong, Y.; Lim, B.; Skrabalak, S. E. *Angew. Chem. Int. Ed.* **2009**, *48*, 60-103.

(186)   Jia, C.-J.; Schuth, F. *Phys. Chem. Chem. Phys.* **2011**, *13*, 2457-2487.

(187)   Xia, Y.; Xia, X.; Peng, H.-C. *J. Am. Chem. Soc.* **2015**, *137*, 7947-7966.

(188)   Lim, B.; Jiang, M.; Tao, J.; Camargo, P. H. C.; Zhu, Y.; Xia, Y. *Adv. Funct. Mater.* **2009**, *19*, 189-200.

(189)   Collins, G.; Schmidt, M.; O'Dwyer, C.; Holmes, J. D.; McGlacken, G. P. *Angew. Chem. Int. Ed.* **2014**, *53*, 4142-4145.

(190)   Dolomanov, O. V.; Bourhis, L. J.; Gildea, R. J.; Howard, J. A. K.; Puschmann, H. *J. Appl. Crystallogr.* **2009**, *42*, 339-341.

(191)   Palatinus, L.; Chapuis, G. *J. Appl. Crystallogr.* **2007**, *40*, 786-790.

(192)   Palatinus, L.; van der Lee, A. *J. Appl. Crystallogr.* **2008**, *41*, 975-984.

(193)   Palatinus, L.; Prathapa, S. J.; van Smaalen, S. *J. Appl. Crystallogr.* **2012**, *45*, 575-580.

(194)   Sheldrick, G. *Acta Crystallogr., Sect. A* **2008**, *64*, 112-122.

(195)   Appleton, D. R.; Babcock, R. C.; Copp, B. R. *Tetrahedron* **2001**, *57*, 10181-10189.

(196)   Angelini, E.; Balsamini, C.; Bartoccini, F.; Lucarini, S.; Piersanti, G. *J. Org. Chem.* **2008**, *73*, 5654-5657.

(197)   Kitamura, T.; Matsuyuki, J.-i.; Taniguchi, H. *Synthesis* **1994**, *1994*, 147-148.

(198)   Zhu, S.; MacMillan, D. W. C. *J. Am. Chem. Soc.* **2012**, *134*, 10815-10818.

(199)   Petersen, T. B.; Khan, R.; Olofsson, B. *Org. Lett.* **2011**, *13*, 3462-3465.

(200)   Kakinuma, Y.; Moriyama, K.; Togo, H. *Synthesis* **2013**, *45*, 183-188.

(201)   Jeong, Y.-C.; Moloney, M. G. *Synlett* **2009**, *2009*, 2487-2491.

(202)   Cardillo, G.; Gentilucci, L.; Tomasini, C.; Tomasoni, L. *Tetrahedron: Asymmetry* **1995**, *6*, 1947-1955.

(203)   Sato, K.; Kozikowski, A. P. *Tetrahedron Lett.* **1989**, *30*, 4073-4076.

(204)   Calmes, M.; Daunis, J.; Jacquier, R.; Verducci, J. *Tetrahedron* **1987**, *43*, 2285-2292.

(205)   Stadler, P. A. *Helv. Chim. Acta* **1978**, *61*, 1675-1681.

(206)   Gellerman, G.; Rudi, A.; Kashman, Y. *Tetrahedron* **1994**, *50*, 12959-12972.

(207)   Otani, T. T.; Briley, M. R. *J. Pharm. Sci.* **1979**, *68*, 496-499.

(208)   Turner, R. A.; Hauksson, N. E.; Gipe, J. H.; Lokey, R. S. *Org. Lett.* **2013**, *15*, 5012-5015.

(209)   Steglich, W.; Hinze, S. *Synthesis* **1976**, *1976*, 399-401.

(210)   Naturale, G.; Lamblin, M.; Commandeur, C.; Felpin, F.-X.; Dessolin, J. *Eur. J. Org. Chem.* **2012**, *2012*, 5774-5788.

(211)   Kieffer, M. E.; Repka, L. M.; Reisman, S. E. *J. Am. Chem. Soc.* **2012**, *134*, 5131-5137.

(212)   Erb, W.; Hellal, A.; Albini, M.; Rouden, J.; Blanchet, J. *Chem. Eur. J.* **2014**, *20*, 6608-6612.

(213)   Hanson, P.; Jones, J. R.; Taylor, A. B.; Walton, P. H.; Timms, A. W. *J. Chem. Soc., Perkin Trans. 2* **2002**, 1135-1150.

(214)   Bahr, J. L.; Yang, J.; Kosynkin, D. V.; Bronikowski, M. J.; Smalley, R. E.; Tour, J. M. *J. Am. Chem. Soc.* **2001**, *123*, 6536-6542.

(215)   Becker, B. C.; Adams, R. *J. Am. Chem. Soc.* **1932**, *54*, 2973-2982.

(216)   Tang, Z. Y.; Zhang, Y.; Wang, T.; Wang, W. *Synlett* **2010**, *2010*, 804-808.

(217)   Southam, R. M.; Whiting, M. C. *J. Chem. Soc., Perkin Trans. 2* **1982**, 597-603.

(218)   Shu, X.-z.; Zhang, M.; He, Y.; Frei, H.; Toste, F. D. *J. Am. Chem. Soc.* **2014**, *136*, 5844-5847.

(219)   Chaudhuri, A.; Loughlin, J. A.; Romsted, L. S.; Yao, J. *J. Am. Chem. Soc.* **1993**, *115*, 8351-8361.

(220)   Kuokkanen, T.; Palokangas, J.; Talvensaari, M. *J. Phys. Org. Chem.* **2000**, *13*, 452-460.

(221)   Yang, H.-H.; McCreery, R. L. *Anal. Chem.* **1999**, *71*, 4081-4087.

(222)   Drent, E.; Van Broekhoven, J. A. M.; Doyle, M. J. *J. Organomet. Chem.* **1991**, *417*, 235-251.

(223)   Ren, K.; Malpert, J. H.; Gu, H.; Li, H.; Neckers, D. C. *Tetrahedron* **2002**, *58*, 5267-5273.

(224)   Stang, P. J.; Zhdankin, V. V.; Tykwinski, R.; Zefirov, N. S. *Tetrahedron Lett.* **1991**, *32*, 7497-7498.

(225)   Prasad, B.; Sreenivas, B. Y.; Krishna, G. R.; Kapavarapu, R.; Pal, M. *Chem. Commun.* **2013**, *49*, 6716-6718.